Application of a New Approach Methodology (NAM)-based Strategy for Genotoxicity Assessment of Data-poor Compounds

By

Anne-Marie Fortin

Thesis submitted in partial fulfillment of the requirements for the degree of

Master of Science

In

Biology

With a specialization in

Environmental and Chemical Toxicology

University of Ottawa
Ottawa, ON

Abstract

The conventional battery for genotoxicity testing is not well-suited to assessing the large number of chemicals needing evaluation. Traditional *in vitro* tests lack throughput capacity, provide little mechanistic information, and have poor specificity in predicting *in vivo* genotoxicity. The Health Canada GeneTox21 research program is developing a multi-endpoint platform for modernized *in vitro* genotoxicity assessment. The GeneTox21 assays include the TGx-DDI transcriptomic biomarker (i.e., 64-gene expression signature to identify DNA damage-inducing (DDI) substances), the MicroFlow® assay (i.e., a flow cytometry-based micronucleus (MN) test), and the MultiFlow® assay (i.e., a multiplexed flow cytometry-based reporter assay that yields mechanism-of-action (MoA) information). As part of GeneTox21 development, the objective of this study was to investigate the utility of the TGx-DDI transcriptomic biomarker, multiplexed with the MicroFlow® and MultiFlow® assays, as an integrated testing strategy for screening data-poor substances prioritized by Health Canada's New Substances Assessment and Control Bureau. Human lymphoblastoid TK6 cells were exposed to 3 control and 10 data-poor substances, using a 6-point concentration range. Cells were exposed for 4 hours with or without exogenous metabolic activation. Gene expression profiling was conducted using the targeted TempO-Seq™ assay, and the TGx-DDI classifier was applied to the dataset. Classifications were compared with those based on the MicroFlow® and MultiFlow® assays. Benchmark Concentration (BMC) modeling was used for potency ranking. The results of the integrated hazard calls indicate that five data-poor compounds are genotoxic *in vitro*, causing DNA damage via a clastogenic MoA, and one is positive via a pan-genotoxic MoA. Two compounds are likely irrelevant positives in the MN test; two are considered possibly

genotoxic causing DNA damage via an ambiguous MoA. From quantitative analyses of concentration-response data, we observed nearly identical potency rankings for each assay with two main potency groups being observed. This ranking was maintained when all endpoint BMCs were converted into a single score using the Toxicological Prioritization (ToxPi) approach. Overall, this study contributes to the establishment of a modernized approach for effective genotoxicity assessment and chemical prioritization for further regulatory scrutiny. We conclude that integration of the TGx-DDI biomarker with other GeneTox21 assays is an effective NAM-based strategy for genotoxicity assessment of data-poor compounds.

Acknowledgements

I'd like to first thank my two amazing supervisors Dr. Paul White and Dr. Carole Yauk! I joined Dr. White's lab at Health Canada as an undergraduate co-op student and was first introduced to the exciting field of genetic toxicology! I quickly became very interested and asked to continue on for my undergraduate thesis, and later, graduate work. When I heard Dr. Carole Yauk was moving from Heath Canada to start up her new lab at the University of Ottawa, I knew it would be a great opportunity to further explore toxicogenomics and asked to be one of her first uOttawa students! Turns out I couldn't have asked for a better supervisorial team! Thank you both for all your support and guidance throughout these last couple years. Between COVID-19, lab closures, and procurement delays you have always been so supportive and encouraged me every step of the way. You have both helped me grow in my career by enhancing my critical thinking skills and improving my science communication. Thank you for everything! I'd like to also thank my thesis committee members Dr. Laurie Chan and Dr. Iain Lambert for their support and guidance throughout this project.

In addition, I'd like to thank all of the collaborators at Health Canada without whom this work would not have been possible! On the bioinformatics team, Dr. Matthew Meier and Andrew Williams – thank you for all the work you've done on this project and for always being open to answer all my questions when I had them! Thank you to the Health Canada biologists Julie Buick and Andrea Rowan-Carroll for taking time out of their busy schedules to help and train me in the lab for TGx-DDI sample preparation and sequencing. Thank you to Health Canada biologist Hannah Battaion for all your help with the flow cytometer – and for all the hours spent discussing and troubleshooting our way through the issues with it, I couldn't have

done it without you. I'd also like to thank the additional co-authors that have contributed to the manuscript and many posters/presentations for all their feedback: Dr. Alexandra Long, Joleen Hannah, Dr. Julie Cox, and Claire Pinsonnault.

A big thank you to all the wonderful graduate students I've met and worked with along the way! Elizabeth Huliganga, Tatiana Kozbenko and I started this journey in September 2020 together; thank you both for your support throughout the years and I can't wait to see what GReAT things you accomplish next! To Annette Dodge, Emmanuelle Monniez, Geronimo Parodi-Matteo and David Shuster – I've loved getting to know you all and I wish you all the best of luck finishing your degrees!

Thank you to my wonderful family, including my parents Jean-Pierre and Catherine, sister Claire, and grandmother (aka Nana), for all your support and encouragement during this process! You patiently listened to my frustrations when experiments weren't going as planned, and celebrated with me when I completed my research goals (even if you didn't fully understand what I was saying haha)! Everything I've accomplished is because of you all, and I couldn't have done it without you! With all of you on my side I know I can do anything I set my mind to. Thank you for everything.

Finally, I'd like to thank my amazing partner Jake. Thank you for always being there during my roller-coaster of emotions over the past two years. For making me laugh and cheering me up when I felt down, encouraging me, and celebrating my accomplishments! I can't wait to see what new adventures we have moving forward in this new chapter.

Table of Contents

List of Figures

Chapter 1

Chapter 2

Chapter 3

List of Tables

Chapter 1

Chapter 2

List of Abbreviations

2-DC	2-Dimentional hierarchical clustering
3Rs	Replacement, Reduction, Refinement
ADI	Acceptable Daily Intake
AIC	Akaike Information Criterion
AOP	Adverse Outcome Pathway
BMC	Benchmark concentration
BMCL	Benchmark concentration lower confidence limit
BMCU	Benchmark concentration upper confidence limit
BMDS	Benchmark Dose Software
BMR	Benchmark response
BT	1,2,4-benzenetriol
CA	Chromosomal aberrations
CCCP	Carbonyl cyanide m-chlorphenyl hydrazone
CEPA	Canadian Environmental Protection Act
CHO	Chinese hamster ovary
DDI	DNA damage-inducing
DDR	DNA damage response
DEGs	Differentially expressed genes
DMANN	D-mannitol
DMBA	7,12-dimethylbenz[*a*]anthracene

DO	Detector oligos
DSB	Double strand breaks
DSL	Domestic Substances List
EHSRB	Environmental Health Science and Research Bureau
EMA	Ethidium monoazide bromide
EPA	Environmental Protection Agency
EPEG	Etoposide
ER	Endoplasmic reticulum
eSTAR	Emerging Systems Toxicology for the Assessment of Risk
EU	European Union
EURL-ECVAM	European Union Reference Laboratory and the European Centre for the Validation of Alternative Methods
FC	Fold change
FCM	Flow-cytometric method
FDA	U.S. Food and Drug Administration
FISH	Fluorescence *in situ* hybridization
GEF	Global Evaluation Factor
GEO	Gene Expression Omnibus
ɣH2AX	Phosphorylated histone H2A family member X
HBGV	Health-Based Guidance Values
HDACi	Histone deacetylase inhibition
HESI	Health and Environmental Sciences Institute

hprt	Hypoxanthine-guanine phosphoribosyl transferase
HTT	High-throughput transcriptomics
HTTK	High-throughput toxicokinetics
ICATM	International Cooperation on Alternative Test Methods
ICCVAM	Interagency Coordinating Committee on the Validation of Alternative Methods
ICH	International Council for Harmonization
IVIVE	*In vitro* to *in vivo* extrapolation
JaCVAM	Japanese Center for the Validation of Alternative Methods
MCF	Mean channel fluorescence
MN	Micronuclei
MoA	Mechanism of Action
NAMs	New Approach Methodologies
NCBI	National Centre for Biotechnology Information
NGS	Next generation sequencing
NICEATM	National Toxicology Program Interagency Center for the Evaluation of Alternative Toxicological Methods
NOAEL	No-observed-adverse-effect level
NSACB	New Substances Assessment and Control Bureau
NSC	Nearest shrunken centroid
NSC-PA	Nearest shrunken centroid probability analysis
NSNR	New Substances Notification Regulations

NTP	National Toxicology Program
OECD	Organisation for Economic Co-operation and Development
p-H3	Phosphorylated histone H3
PAH	Polycyclic aromatic hydrocarbon
PCA	Principal component analysis
POD	Point-of-departure
PSL	Priority Substances List
QSAR	Quantitative Structure-Activity Relationships
REACH	Registration, Evaluation and Authorization of Chemicals
RIVM	The Dutch National Institute for Public Health and the Environment
RNC	Relative nuclei count
RS	Relative survival
TempO-Seq	Templated oligo assay with sequencing readout
TG	Test guideline
TGR	Transgenic rodent
TGx	Toxicogenomics
tk	Thymidine kinase
TK6	Human lymphoblastoid TK6
ToxPi	Toxicological Prioritization
TSCA	Toxic Substances Control Act
WOE	Weight of evidence
xprt	Xanthine-guanine phosphoribosyl transferase

Statement of Contributions

Chapter 2: Application of a New Approach Methodology (NAM)-based Strategy for Genotoxicity Assessment of Data-poor Compounds

Target Journal: Frontiers in Toxicology

Authors: Anne-Marie Fortin[1], Alexandra S. Long[2], Andrew Williams[3], Matthew Meier[3], Julie Cox[4], Claire Pinsonnault[5], Carole Yauk[1], Paul A. White[3]

Affiliations:

[1]Department of Biology, University of Ottawa, Ottawa, Canada,
[2]Existing Substances and Risk Assessment Bureau, Health Canada, Ottawa, Canada
[3]Environmental Health Science and Research Bureau, Health Canada, Ottawa, Canada,
[4]Bureau of Gastroenterology, Infection and Viral Diseases, Health Canada, Ottawa, Canada,
[5]New Substances Assessment and Control Bureau, Health Canada, Ottawa

Study Design……	Anne-Marie Fortin Paul A. White Carole Yauk Julie Cox Alexandra S. Long
Manuscript Preparation……	Anne-Marie Fortin Carole Yauk Paul A. White
Data Analysis……	Anne-Marie Fortin Andrew Williams Matthew Meier
GeneTox21 Research Program……	Paul A. White Alexandra S. Long Julie Cox
Data-poor test chemical prioritization……	Claire Pinsonnault Alexandra S. Long

Chapter One

1.1 Toxicity testing and data-poor chemicals

Toxicology is the scientific study of the harmful effects of chemical agents in biological systems; it is considered a relatively modern inter-disciplinary science that has evolved to combine the knowledge and techniques from all scientific branches (i.e., biological, physical, chemical, and environmental) (Still et al., 2020). The importance of toxicological research became increasingly clear following the Second World War, which triggered an exponential expansion in the development and production of new chemicals for medicinal treatments, industrial/agricultural use, or household and/or personal products to improve day-to-day life (Still et al., 2020). Today, this expansion has continued with thousands of chemicals in use every day. An analysis of 22 chemical inventories from 19 countries estimated a staggering 350,000 chemicals and mixtures of chemicals registered for production and use (Wang et al., 2020). Thus, toxicological evaluations are an essential element of public and environmental health protection to reduce and/or manage the risk of chemical exposure and prevent potential adverse effects.

From the Canadian perspective, the landmark *Canadian Environmental Protection Act* (CEPA) was passed in 1988 by the Government of Canada to address the potentially dangerous exposures to chemicals in commerce that may have immediate or long-term harmful effects on the environment or human health (Government of Canada, 1999). As part of the act, the government is responsible for maintaining the Domestic Substances List (DSL) that catalogues the over 23,000 existing chemicals that are currently used, manufactured, or imported into Canada (Government of Canada, 2019). This involves the categorization and screening of existing substances for potential exposure to Canadians, inherent toxicity, and persistence.

Chemicals of concern are placed on a Priority Substances List (PSL) for a more comprehensive assessment (Government of Canada, 2019). In addition to the thousands of existing chemicals on the DSL, every year there are hundreds of notifications for new substances entering the Canadian marketplace. Under CEPA's New Substances Notification Regulations (NSNR) new substances imported or manufactured to Canada (including those that undertake a "Significant New Activity") require a notification that provides the necessary health toxicity information (Environment Canada, 2006). Since the DSL's creation, over 5,000 new substances have been added. However, there is still an immense backlog of legacy chemicals requiring toxicological evaluation by Canadian regulators as well as regulatory bodies worldwide (USNRC, 2007; Schoeters, 2010; Barton-Maclaren et al., 2017; Council of Canadian Academies, 2017). Moreover, one of the main challenges is that there is a remarkably large majority of chemicals that are known as "data-poor", with very limited or no toxicological data available (Barton-Maclaren et al., 2017; Health Canada, 2021).

1.2 The importance of DNA damage and genotoxicity testing

Environmental chemicals can induce genetic damage potentially leading to the manifestation of debilitating adverse health outcomes. This includes short-term effects (i.e., anemia, immunosuppression), or long-term diseases such as cancer and other degenerative conditions (i.e., accelerated aging, cardiovascular or neurogenerative diseases) (National Academies Press (US), 2014; OECD, 2017). The accumulation of DNA damage in germ cells has been associated with infertility, spontaneous abortions, or heritable mutations that are passed down to subsequent generations (Aitken and De Iuliis, 2007; Yauk et al., 2015). In somatic cells, genetic damage/alterations can trigger carcinogenesis (i.e., transformation of healthy cells into cancer cells), a multi-step process characterized by the accumulation of genetic mutations resulting in abnormal cell division and malignancy (Phillips and Arlt, 2009). About 5 to 10% of cancers are hereditary. The remaining cancers result from the accumulation of mutations throughout a person's lifetime (Weston and Harris, 2003; Pecorino, 2015). Tumor initiation due to mutagenesis and genome instability can be attributed to both internal (spontaneous) or external (environmental) factors (Weston and Harris, 2003; Friedberg et al., 2004; Warshawsky, 2005). Exogenous environmental chemicals (e.g., polycyclic aromatic hydrocarbons (PAHs)) and physical agents (e.g., ultraviolet light and ɣ-radiation) have been associated to the etiology of human cancer (Clancy, 2008; Basu, 2018). Due to the mechanistic association between DNA damage and the potential consequential adverse health effects such as cancer, degenerative conditions, as well as heritable genetic diseases, genotoxicity testing is a crucial component of chemical safety assessments.

The overarching goal of genotoxicity testing is to determine if a chemical exposure can cause adverse genetic effects such as mutations and/or chromosomal abnormalities. Mutations, defined as irreversible changes in the DNA sequence of an organism, can include events such as point mutations (i.e., nucleotide substitutions) or small insertions and deletions (i.e., indels). Chromosomal abnormalities can be structural (i.e., chromosomal insertions, deletions, or rearrangements that form via breakage); or numerical (i.e., changes in chromosome number). To study these endpoints a battery of tests are used, as no one assay can provide the necessary information for all endpoints (Thybaud et al., 2007; OECD, 2017). The Organisation for Economic Co-operation and Development (OECD) publishes internationally standardized test guidelines (TGs) for assessing genotoxicity (OECD, 2017). Organizations such as the International Council for Harmonisation (ICH) of Technical Requirements for Pharmaceuticals for Human Use, as well as government regulatory bodies (i.e., Government of Canada, and the United States Food and Drug Administration (FDA)), leverage OECD TGs to produce guidance documents that define accepted genetic toxicology test batteries (USFDA, 2002; Environment Canada, 2006; ICH, 2011). Generally, the current genotoxicity test battery involves the use of at least 2 or 3 *in vitro* tests carried out in bacteria or cultured animal cells. Typically, this involves:

(1) Tests for gene mutations

a. TG 471, *in vitro* bacterial reverse mutation test (i.e., Ames test). The test is performed in specific strains of *Salmonella typhimurium* and/or *Escherichia coli* containing mutated histidine or tryptophan biosynthesis genes that inhibit growth. Exposure to mutagens may induce a reversion (i.e., a second

mutation) that will restore biosynthesis and consequently permit prototrophic growth (OECD, 2017).

b. TG 476/490, *in vitro* mammalian cell gene mutation assays. TG 476 identifies substances that induce mutations in the *hprt* (hypoxanthine-guanine phosphoribosyl transferase) or *xprt* (xanthine-guanine phosphoribosyl transferase) genes. These assays are most commonly performed in Chinese hamster ovary cell lines (CHO, CHL, and V79), L5178Y mouse lymphoma cells, TK6 human lymphoblastoid cells, or AS52 cells (*xprt* only). TG 490 identifies substances that induce mutations in the thymidine kinase (*tk*) gene. This test is most commonly performed in L5178Y mouse lymphoma or human lymphoblastoid TK6 cell lines (OECD, 2017).

(2) Tests for chromosomal aberrations (CA)

a. TG 473, *in vitro* mammalian chromosomal aberration test. Performed in established cells lines (i.e., CHO, CHL, V79, TK6) or primary cells, induced CAs are observed via microscopy in arrested metaphase following chemical exposure. Fluorescence *in situ* hybridization (FISH) can be applied for further visualization of chromosome damage (OECD, 2017).

b. TG 487 *in vitro* mammalian cell micronucleus test. Micronuclei (MN) are small nuclei-like structures that are formed when whole chromosomes or fragments fail to align and segregate properly during mitosis. These structures persist into interphase and are not immediately reincorporated into the primary nucleus (Krupina et al., 2021). Thus, this assay can detect

both structural and numerical chromosome abnormalities. MN can be detected by microscopy, or more recently by automation via flow cytometry or image analysis. Additional mechanistic information can be provided via FISH or centromere staining. The test can be conducted in established cell lines (CHO, CHL, V79, L5178Y, TK6) (OECD, 2017).

It is often required that *in vitro* genotoxicity tests are conducted with an exogenous source of metabolic activation (i.e., rat liver S9 fractions) as most *in vitro* models cannot entirely simulate *in vivo* mammalian hepatic metabolism (OECD, 2017). This is important, as some non-genotoxic chemicals can be converted or activated into DNA damaging products or by-products by a series of metabolic pathways (Bartsch et al., 1982).

Finally, depending on the results obtained and decision-making context, one or more *in vivo* tests may also be required (Thybaud et al., 2007; OECD, 2017). *In vivo* tests study similar mutational and chromosomal endpoints. For example, the transgenic rodent (TGR) somatic and germ cell gene mutation assay (TG 488) identifies substances that induce mutations in transgenic reporter genes and can detect mutants in virtually all tissue types. Similarly, chromosome damage can be detected by the *in vivo* CA test (TG 475) in bone marrow cells; or via the *in vivo* micronucleus test (TG 474) in erythroblasts/mature red blood cells from peripheral blood or bone marrow (OECD, 2017).

1.3 Limitations of current genotoxicity test strategies

As outlined by Krewski et al. 2010, there has been increased global pressure to modernize toxicology-testing strategies to meet a growing number of demands. First, there is an urgent need to evaluate the toxicity of the existing (data-poor) chemicals and to generate toxicity data for new chemicals/materials (e.g., nanomaterials) as they emerge. To do this, new methods are needed to reduce the time and cost of toxicological assessment. Second, more detailed mechanistic information is required to better predict potential adverse effects and evaluate potential toxicity to the most vulnerable members of the population for human health risk assessment and regulatory decision making (Krewski et al., 2010, 2020). Third, and arguably one of the biggest challenges with the existing test battery, is the emerging policies that call for the elimination of animal testing in certain sectors. This is especially relevant for cosmetics where jurisdictions such as the European Union (EU) enacted the 7th amendment to the Cosmetics Directive, banning the use of *in vivo* genotoxicity endpoints (Pfuhler et al., 2014). Thus, when applying the conventional test battery, positive *in vitro* genotoxic calls cannot be followed-up with *in vivo* assays. These regulations stem from ethical perspectives such as the 3Rs model by Russel and Burch for the "Replacement, Reduction, Refinement (less pain and distress)" in animal test strategies (Russell and Burch, 1960). This perspective is echoed in the U.S. Toxic Substances Control Act (TSCA), which was recently amended by the *Frank R. Lautenberg Chemical Safety for the 21st Century Act* to direct the Environmental Protection Agency (EPA) to "reduce and replace the use of vertebrate animals in the testing of chemical substances or mixtures; and promote the development and incorporation of alternative test strategies"(Frank R. Lautenberg Chemical Safety for the 21st Century Act, 2014). Moreover, in

Canada, the Minister of Health's current mandate letter states a commitment to introduce legislation to end toxicity testing on animals (Office of the Prime Minister, 2021). Thus, in light of these demands, there is an urgent need for efficient and effective test strategies that apply animal-free methods for genotoxicity assessment of new and existing chemicals (Krewski et al., 2020).

The problem is that, due to a number of limitations, the traditional test battery for *in vitro* genotoxicity testing is not well-suited to meet the demands described above (Corvi and Madia, 2017; Krewski et al., 2020). The conventional *in vitro* tests are generally laborious and lower-throughput. Additionally, *in vitro* genotoxicity tests in mammalian cells have a remarkably limited ability to predict effects manifested *in vivo*, often reporting irrelevant positives that do not pose an appreciable mutagenic risk to humans (Kirkland et al., 2006, 2007; Thybaud et al., 2007; Nesslany, 2017). In fact, it was reported that 75-95% of non-carcinogens were positive in at least one *in vitro* genotoxicity assay (Kirkland et al., 2006). This low specificity results in a large number of problematic positives that are subjected to unnecessary, costly, and time-consuming *in vivo* follow-up. Or, in cases where *in vivo* follow-up testing is not feasible due to costs or regulations, potentially safe products or drugs may be excluded from the development pipeline (Li et al., 2019). More specifically, traditional *in vitro* genotoxicity assays may provide misleading results due to cellular endpoints that are induced by chemical stressors not primarily attacking DNA, or as a result of high cytotoxicity (Li et al., 2017). Thus, elucidating the underlying mechanism of action (MoA) of genotoxic chemicals has been widely acknowledged as essential for identifying potentially irrelevant positives and informing the biological relevance to human health (Kirkland et al., 2007; Guyton et al., 2009; Dearfield et al.,

2011). Understanding the mechanism underlying *in vitro* responses can increase overall confidence in the result by providing information relating to a substance's (or its metabolites) ability to interact with genetic material, and/or its associated cell division apparatus (Thybaud et al., 2007). Ultimately, this has led to an ongoing paradigm shift in (geno)toxicity testing to modernize and develop new *in vitro* or *in silico* tools for chemical hazard assessment (Krewski et al., 2020).

1.4 New Approach Methodologies

To address the major challenges described above, global efforts have focussed on the development and validation of alternative *in vitro* and *in silico* genotoxicity testing tools that are higher throughput and provide mechanistic insights to modernize toxicity testing (USNRC, 2007; Firestone et al., 2010). In light of this, integrated data streams from higher-throughput methodologies are being applied for chemical screening, prioritization, and risk assessment. This includes New Approach Methodologies (NAMs), defined broadly as *in silico, in chemico* and *in vitro* assays, that are higher-throughput and avoid the use of animals to identify chemical hazards (Pfuhler et al., 2014; ECHA, 2016; Kavlock et al., 2018). In the last few decades, several national organizations have been created to support the development and promotion of NAM-based strategies to modernize chemical risk assessment. Notably, the European Union Reference Laboratory for Alternatives to Animal Testing (EURL-ECVAM); the U.S. National Toxicology Program Interagency Center for the Evaluation of Alternative Toxicological Methods (NICEATM), the U.S. Interagency Coordinating Committee on the Validation of Alternative Methods (ICCVAM), and the Japanese Center for the Validation of Alternative Methods (JaCVAM). Additionally, these organizations, including Health Canada, are part of the International Cooperation on Alternative Test Methods (ICATM), established in 2009, to support international cooperation, transparency, and harmonization of alternative methods (Barroso et al., 2016).

Overall, the modernization of genotoxicity testing through the development of NAM-based strategies will ultimately improve the efficacy of the chemical assessment process,

reduce animal use in line with the 3Rs-philosophy, and improve the relevance of risk assessment for human health risk assessment and regulatory decision-making.

1.4.1 Transitioning from hazard identification to quantitative understanding in genetic toxicology

The assessment of chemical genotoxicity for regulatory evaluations and decision-making traditionally provides purely qualitative, dichotomous hazard classifications, e.g., classifying chemicals as either genotoxic or non-genotoxic. Recently, there has been a shift toward quantitative analyses of genotoxicity concentration-response data to estimate points of departure (POD) values (White et al., 2020). For a given chemical, a POD represents the point on a concentration-response curve that corresponds to a no-effect or low-effect level. PODs are an essential metric for risk characterization; essentially, a quantitative starting point for later extrapolation and analyses (Edler, 2014; USNRC, 2014b). This includes deriving Health-Based Guidance Values (HBGVs), e.g., acceptable daily intake (ADI), defined as the maximum exposure to a substance that is not expected to result in an appreciable adverse human effect. However, converting *in vitro* derived PODs to equivalent *in vivo* PODs is not straightforward and is reliant on various toxicokinetic factors including protein binding, bioavailability, and clearance from the body (Bell et al., 2018). Therefore, high-throughput toxicokinetic and *in vitro* to *in vivo* extrapolation (IVIVE) models are essential for the incorporation of *in vitro* data into risk assessment activities.

Historically, the no-observed-adverse-effect level (NOAEL) approach was applied to determine PODs from concentration-response data. However, a more advanced approach, i.e., the Benchmark Concentration (BMC) approach (Crump, 1984), has now become the preferred

method for many regulatory agencies (Food and Agriculture Organization of the United Nations and World Health Organization, 2020).

1.4.1.1 Benchmark Concentration (BMC) Modeling

By fitting mathematical models to the data, the BMC approach, as summarized in Figure 1, aims to determine the concentration required to elicit a predefined change in response in relation to background (the Benchmark Response – BMR).

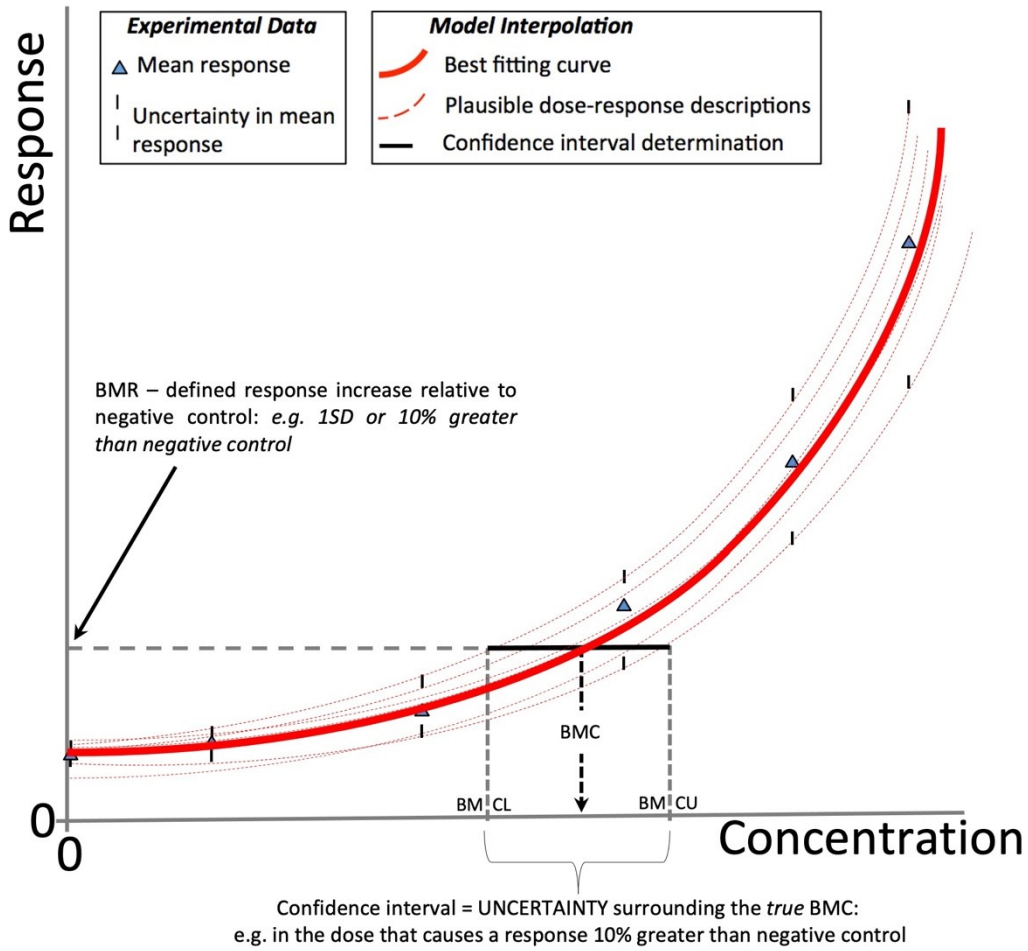

Figure 2: Visual representation of the Benchmark Concentration (BMC) approach. BMCL and BMCU represent the lower and upper confidence limits (i.e., uncertainty) of the BMC. Figure prepared by John W. Wills, used with permission.

Statistical uncertainty in the BMC is denoted as the upper and lower confidence limits (Edler, 2014). The comparison of BMCs enables potency rankings of genotoxic chemicals, i.e., the lower the BMC, the more potent the chemical. In human health risk assessment, the BMC (or the BMCL for a more conservative approach) determined from *in vivo* concentration-response data can be used as the POD for the derivation of HBGVs (Food and Agriculture Organization of the United Nations and World Health Organization, 2020). BMC modeling of concentration-response data can be conducted with freely-available tools. Currently, two software packages are commonly used for BMC analysis: 1) the U.S. EPA's Benchmark Dose Software (BMDS) (Davis et al., 2011) or 2) the PROAST R package developed by The Dutch National Institute for Public Health and the Environment (RIVM) (Varewyck and Verbeke, 2017; Slob, 2018).

1.5 The application of toxicogenomics (TGx) for toxicity testing and risk assessment

Toxicogenomics (TGx), the application of "omic" (e.g., genomic, transcriptomic, proteomic, metabolomic) technologies to toxicology, can complement conventional toxicology approaches by providing a comprehensive overview of the cellular responses following chemical exposure (Guyton et al., 2009; Krewski et al., 2020). Following treatment, one of the earliest quantifiable effects in toxicological response is the alteration of gene expression, i.e., mRNA levels. Thus, global transcriptional profiling can identify early molecular markers of toxicological effects. The analysis of affected genes and/or pathways can provide mechanistic insights, enabling disease phenotype predictions earlier than conventional toxicity cellular endpoints (Thomas et al., 2013; Farmahin et al., 2017; Yauk et al., 2019).

1.5.1 Transcriptomic biomarkers for chemical risk assessment

One challenge hindering the use of transcriptomic data in risk assessment and regulatory decision-making is the lack of standardization in data generation and interpretation. Harmonized strategies in study design, exposure conditions, data analysis, and data interpretation are needed to ensure accurate and reproducible outcomes (Kinaret et al., 2020). Although global transcriptomic profiling following chemical exposure provides a rich source of information, it can be somewhat complicated and time-consuming to mine for a MoA. Probing transcriptomic data for validated biomarkers can quickly and objectively inform the mechanism of a substance or predict toxicological properties. Biomarkers are gene sets that exhibit characteristic and reproducible responses following exposures to chemicals with a specific MoA

or causing a certain toxicity (Li et al., 2019). Therefore, the application of TGx biomarkers to regulatory assessments can provide an efficient and standardized approach to evaluate the toxicity of a chemical.

1.5.1.1 The TGx-DDI transcriptomic biomarker

To explore the use of a TGx approach to genotoxicity testing, Li et al. (2015) developed the TGx-DDI transcriptomic biomarker. TGx-DDI uses changes in the expression of 64 genes to classify chemical substances as DNA damage-inducing (DDI) or non-DDI following *in vitro* exposure of cultured mammalian cells. The 64 genes were identified from whole genome transcriptional profiles of TK6 human lymphoblastoid cells exposed to a reference set of 28 chemical agents with well characterized MoAs, covering a wide range of known DDI (e.g., DNA alkylation) and non-DDI (e.g., endoplasmic reticulum (ER) stress) mechanisms (Li et al., 2019). Expression profiles were generated using Agilent gene expression DNA microarrays and compiled into a database for analysis. The nearest shrunken centroid (NSC) method was applied to the database to identify a biomarker capable of discriminating between DDI and non-DDI agents. The result was a 64-gene transcriptomic biomarker named TGx-DDI (Cho et al., 2019; Li et al., 2019). The transcriptomic response of the 64 genes is typically visualized in a heatmap that shows clear differences in the profiles of DDI and non-DDI agents (Figure 2).

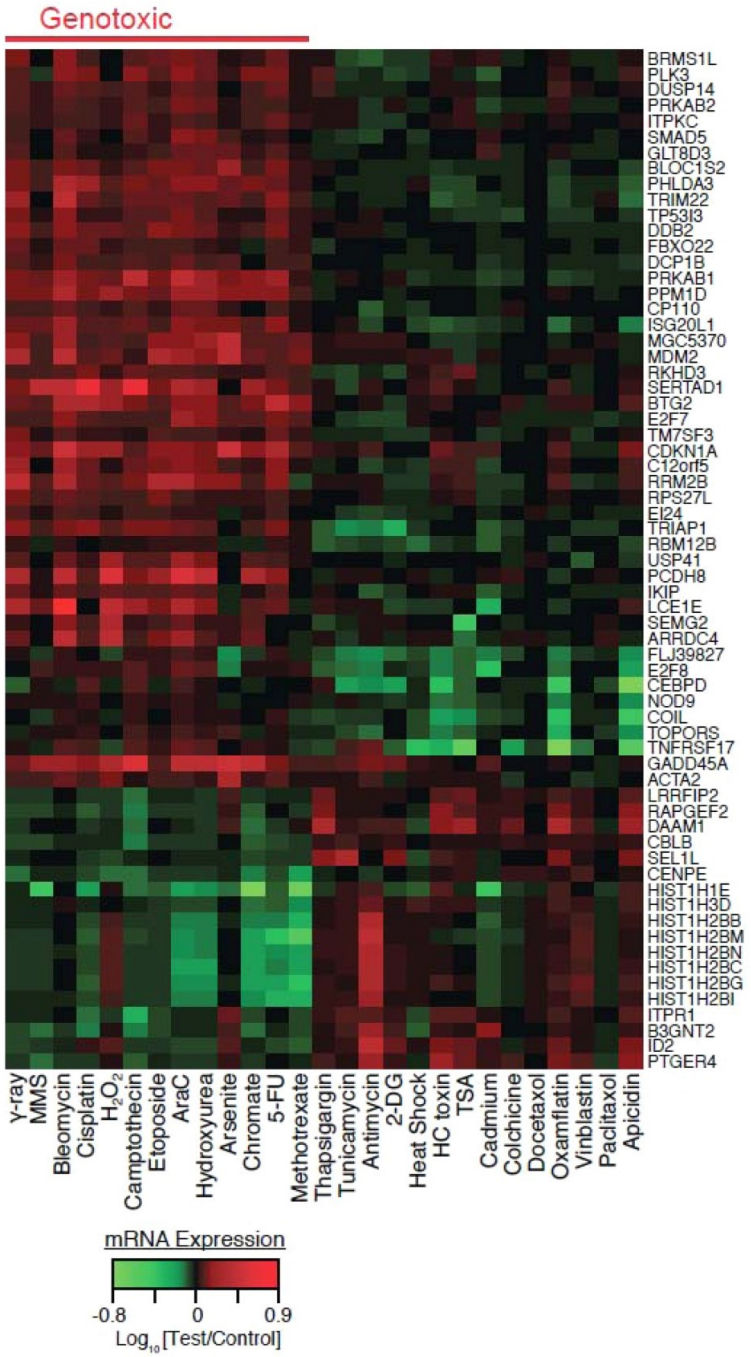

Figure 3: Heatmap of the TGx-DDI 64-gene biomarker used to discriminate DDI from non-DDI reference agents (from Li et al. 2015). The color scale indicates the gene expression fold-changes relative to control: up-regulated genes are shown in red, down-regulated genes are shown in green, and genes with no change are shown in black.

Pathway analysis revealed the top two pathways enriched in the TGx-DDI gene set relate to p53 signaling and cell cycle regulation (see Supplementary Table I) (Corton et al., 2019; Li et al., 2019). Upon sensing DNA damage, an elaborate DNA damage response (DDR) network is triggered, of which the transcription factor p53 plays an important role. In response to DNA damage, the p53 protein is phosphorylated and translocated to the nucleus to mediate the transcriptional activation of several genes involved in cell-cycle arrest, apoptosis, DNA repair, and metabolic regulation (Lakin and Jackson, 1999). Thus, p53 and its mediated DDR genes are key markers to detect induced DNA damage following chemical exposure.

To derive an overall classification call (i.e., DDI or non-DDI) for each test chemical a three-pronged statistical analysis of the TGx-DDI biomarker genes is performed (Li et al., 2017). An example of the three-pronged approach is shown in Figure 3, which shows the classification results for the test chemical disperse orange (Buick et al., 2017). Each analysis compares the responses of the TGx-DDI biomarker genes induced by each experimental sample (i.e., each non-cytotoxic concentration per compound) to the responses of the training set compounds with known DDI and non-DDI mechanisms. The three-pronged approach is comprised of: (1) a Nearest Shrunken Centroids Probability Analysis (NSC-PA), which assigns calls based on the probability that class membership of the centroids was >0.90. (2) a Principal Component Analysis (PCA), where the first principal component separates all DDI and non-DDI agents, and (3) 2-Dimentional Hierarchical Clustering (2-DC), which relies on the average linkage with Euclidian distances. For a conservative approach, a chemical is classified as DDI if there is at least one positive call in any of the three analyses; or a non-DDI call if this criterion is not met (Li et al., 2017, 2019).

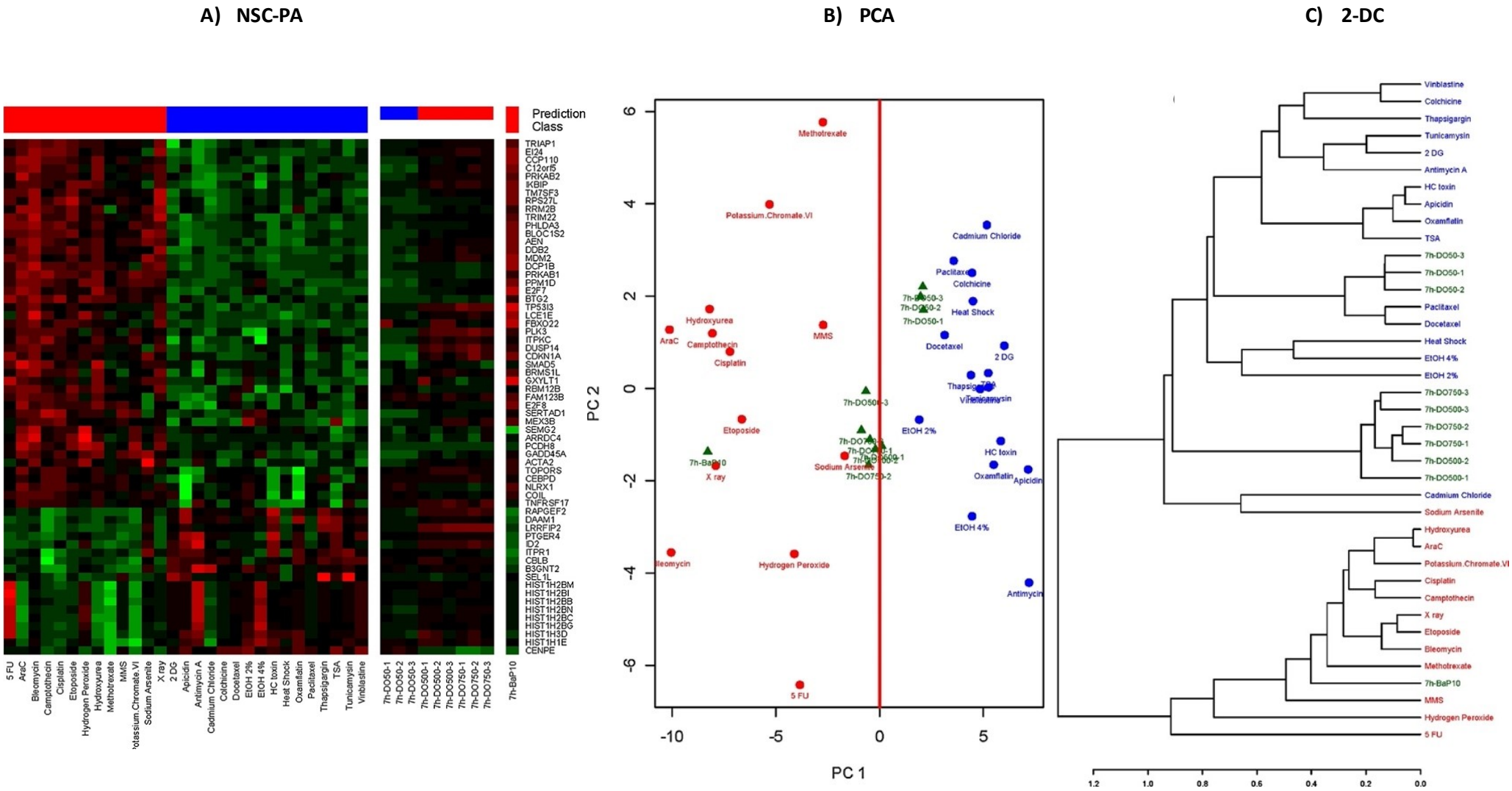

Figure 4: Example of the three-pronged statistical approach for TGx-DDI biomarker analysis following exposure to disperse orange (50, 500 and 750 µg/mL) (from Buick et al. 2017). (a) The left heat map shows the reference chemicals used to generate the biomarker. The heatmap on the right shows the biomarker responses to the test chemicals and control. The Nearest Shrunken Centroids (NSC) classification probabilities for all treatment conditions are shown using red (DDI) and blue (non-DDI) bars above each heat map. (b and c) Principal Component Analysis (PCA) (left) and hierarchical clustering (right) using the TGx-DDI biomarker. Genotoxic reference chemicals are shown in red text, non-genotoxic reference chemicals are shown in blue text, and test agents are shown in green text. The line drawn on the PCA plot and the main branch on the de ndogram divides the DDI and non-DDI agents and was used to classify the test compounds under investigation. The overall call for disperse orange was DDI. The mid and high concentrations were classified as DDI in the NSC-PA and PCA analyses; however, all concentrations were non-DDI for the 2-DC analysis.

Following TGx-DDI development, the biomarker was validated as a robust genotoxicity hazard assessment tool by a working group within the Health and Environmental Sciences Institute's (HESI) Emerging Systems Toxicology for the Assessment of Risk (eSTAR) Committee. Specifically, Li et al. (2017) tested 45 diverse chemicals belonging to five classes of genotoxic phenotypes. TGx-DDI correctly classified the vast majority of the chemicals in the validation study, and correctly-classified 9 of 10 chemicals as non-DDI that had been previously defined as irrelevant positives (Li et al., 2017, 2019). Several subsequent studies showed that TGx-DDI can be expanded to different cell lines (Buick et al., 2020) (e.g., HepaRG™) and is applicable to various gene expression measurement platforms that allow for higher-throughput screening (e.g., qRT-PCR, nCounter, and TempO-Seq™) (Cho et al., 2019; Li et al., 2019). In addition to validation work, the TGx-DDI biomarker has been investigated for its utility in regulatory decision-making. Moffat et al. (2015) used the TGx-DDI biomarker in parallel with *in vivo* rodent studies to support weight of evidence (WOE) approaches in Health Canada's risk assessment of benzo[*a*]pyrene (Moffat et al., 2015). Buick et al. (2017) used the TGx-DDI biomarker in parallel with the *in vitro* micronucleus test. The results identified both disperse orange and 1,2,4-benzenetriol, two chemicals of regulatory interest at Health Canada, as genotoxic and DDI; and provided key information on their potency relative to each other and the reference compounds (Buick et al., 2017). Although these case studies show promise that the TGx-DDI biomarker can provide significant value to existing genotoxicity approaches, more work is required to explore the utility of its incorporation into new genetic toxicity assessment platforms such as GeneTox21 (see section 1.7) and determine the most effective way to integrate this assay within the existing genotoxicity testing battery.

1.5.2 Quantitative Transcriptomics

In addition to applying transcriptomic biomarkers for hazard identification, many studies have established that BMC values derived from transcriptomic data correlate well with those derived from *in vivo* apical endpoints (Thomas et al., 2011, 2013; Farmahin et al., 2017). Software tools have been developed to perform BMC analyses on genomic data. Developed via a collaboration involving the US Environmental Protection Agency, the National Toxicology Program, Health Canada, and Sciome, the BMDExpress2.2 software facilitates BMC modeling of differential gene expression data while combining functional classification analysis (Yang et al., 2007).

The application of quantitative modeling to global gene expression data is challenging due to the complex nature of the datasets. There is currently limited consensus regarding the best approaches to derive a meaningful transcriptomic POD (Farmahin et al., 2017). For example, Thomas et al. 2011 selected the BMCL of the most sensitive pathway/cellular biological process for establishment of a POD (Thomas et al., 2011). However, as discussed by Moffat et al. (2015), this approach may be unnecessarily conservative, as it may not relate to the underlying mechanism of an adverse effect. Instead, they proposed an alternative approach of selecting the lowest BMCL from a pathway known to be associated with a preliminary MoA (Moffat et al., 2015). In an attempt to determine best practices, Farmahin et al. (2017) investigated 11 different approaches to derive transcriptomic PODs for chemical risk assessment. Their results showed that all of the proposed approaches produced transcriptional BMCs within a 10-fold range of those derived from apical endpoints. They concluded that approaches based on a summary metric of the BMCs for the most robustly responsive genes

provided a reasonable estimate of the concentration where effects in longer-term rodent studies began to occur (Farmahin et al., 2017). The US National Toxicology Program (NTP) convened an expert panel to produce best practices including the use of rigorous filtering criteria to remove false positives and for deriving a transcriptomic POD that is based on the lowest median gene set (e.g., pathway) BMCs (USNTP, 2018).

In the case of the TGx-DDI biomarker, the aforementioned case study by Buick et al. (2017) derived the median TGx-DDI gene BMCs for the compounds disperse orange, 1,2,4-benzenetriol (BT) and BaP. The results revealed comparable BMCs for micronucleus frequency and the median TGx-DDI BMC. BMC modeling facilitated potency assessment and confirmed that BT is more potent than DO (Buick et al., 2017). However, more research is required to permit an assessment of the regulatory utility of the TGx-DDI approach.

1.5.3 TempO-Seq™

Today, transcriptomic methodologies are available that are relatively high-throughput and cost-efficient, making it feasible to screen large numbers of substances in a single experiment (Liu et al., 2019). Notably, the targeted sequencing assay TempO-Seq™ (templated oligo assay with sequencing readout) is the main transcriptomic technology being used by programs such as ToxCast at the U.S. EPA for screening environmental chemicals (Harrill et al., 2021). Similarly, this technology is applied in this thesis.

Developed by BioSpyder Technologies Inc., TempO-Seq™ uses precisely designed detector oligos (DO) to target and monitor whole transcriptomes with thousands of target genes and isotypes in a high-throughput multiplexed format. Moreover, the assay can directly target the

RNA from the crude cell lysate, thus avoiding the need for RNA purification or reverse transcription (Yeakley et al., 2017; Bio-Spyder, 2020). As shown in Figure 4, the workflow proceeds as follows: 1) unique DO pairs anneal to their adjacent target sequences of the RNAs to be monitored; 2) excess mis-hybridized or unhybridized DOs are removed enzymatically; 3) the properly hybridized DO pairs are then ligated; 4) using primer binding sequences that are present in all the DOs, ligated DO pairs are amplified and barcoded according to sample identity and pooled into a single library for sequencing with Illumina Next Generation Sequencing (NGS) to count the number of ligated DO sequences per sample (Bio-Spyder, 2020).

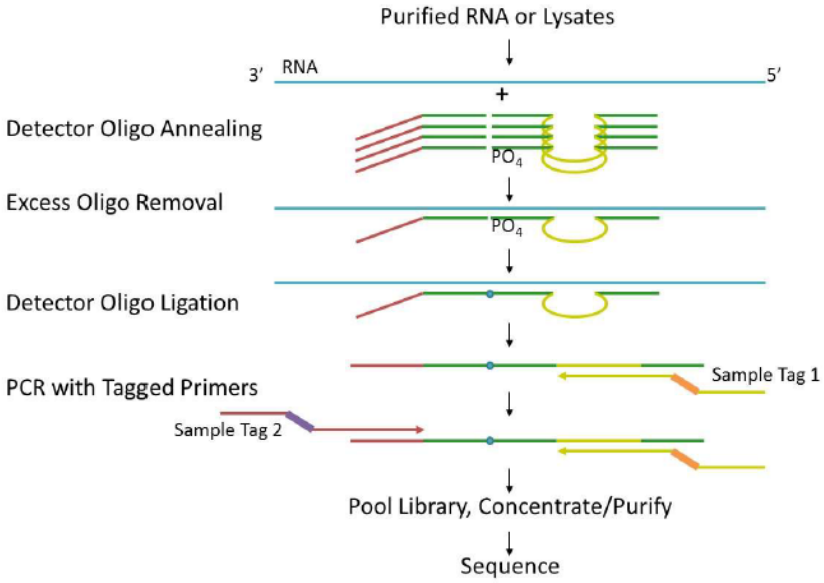

Figure 5: Overview of TempO-Seq™ Assay Principles. Detector oglios (DOs) hybridize to the RNA targets to be measured. Excess or mis-hybridized DOs are removed via enzymatic digestion and subsequently DO pairs are ligated together. Using primer binding sequences common to all DOs, the ligated DOs are amplified by PCR and labelled with unique sample IDs. The PCR products are pooled, purified and sequenced on an Illumina NGS system. From the TempO-Seq™ Assay User Guide. Presented with permission from BioSpyder Technologies Inc..

Despite increasing efficiencies through the use of Tempo-Seq™, performing whole transcriptome analyses on many samples (e.g., multiple concentrations per test compound) still poses a large financial burden and consumes bioinformatic resources. To further lower costs and support high-throughput transcriptomics, the TempO-Seq™ S1500+ gene set was developed in collaboration with the U.S. Tox21 Program (Mav et al., 2018). The goal was to characterize an optimal transcriptome subset of "sentinel genes" that are representative of all known canonical pathways across the human genome and are capable of predicting the expression changes of unmeasured genes for the remainder of the transcriptome (Mav et al., 2018). The S1500+ set comprises 2739 genes that embody biological diversity, thus allowing high-content, lower cost, screening while providing maximal mechanistic information for toxicological analyses (Mav et al., 2018).

1.6 Flow cytometry-based approaches for genotoxicity testing

Various biotechnology companies have sought to develop *in vitro* genotoxicity assays to address the shortcoming of currently availably OECD-approved tests. For example, Litron Laboratories applies flow cytometry techniques to solve challenging problems in (geno)toxicology including low throughput capacity, scalability, low specificity, and a paucity of MoA information (Litron Laboratories, 2013). Their commercially available kits for genotoxicity testing have grown in popularity due to their standardized operating procedures, analysis templates, and demonstrated assay performance in interlaboratory validation studies.

1.6.1 The *in vitro* MicroFlow® assay

To modernize the OECD TG 487 *in vitro* micronucleus test, Litron Laboratories aimed to automate the scoring of MN via flow cytometry to reduce costs, enhance throughout, and limit subjectivity (Bryce et al., 2008). As depicted in Figure 5, the *in vitro* MicroFlow® assay utilizes two fluorescent dyes for MN scoring. The first step is an ethidium monoazide bromide (EMA) staining that identifies the chromatin of necrotic and apoptotic (mid-late stages) cells. Following cell lysis, where the cytoplasmic membranes are digested, the suspended free nuclei and MN are then incubated with pan-nucleic acid dye SYTOX Green and RNase (Avlasevich et al., 2006; Bryce et al., 2008). The double stained SYTOX/EMA necrotic chromatin can thus be differentiated from healthy SYTOX nuclei/MN and removed from subsequent scoring. Moreover, the addition of latex counting beads allows for inherent cytotoxicity and relative survival measurements by applying nuclei-to-bead ratios (Bryce et al., 2013).

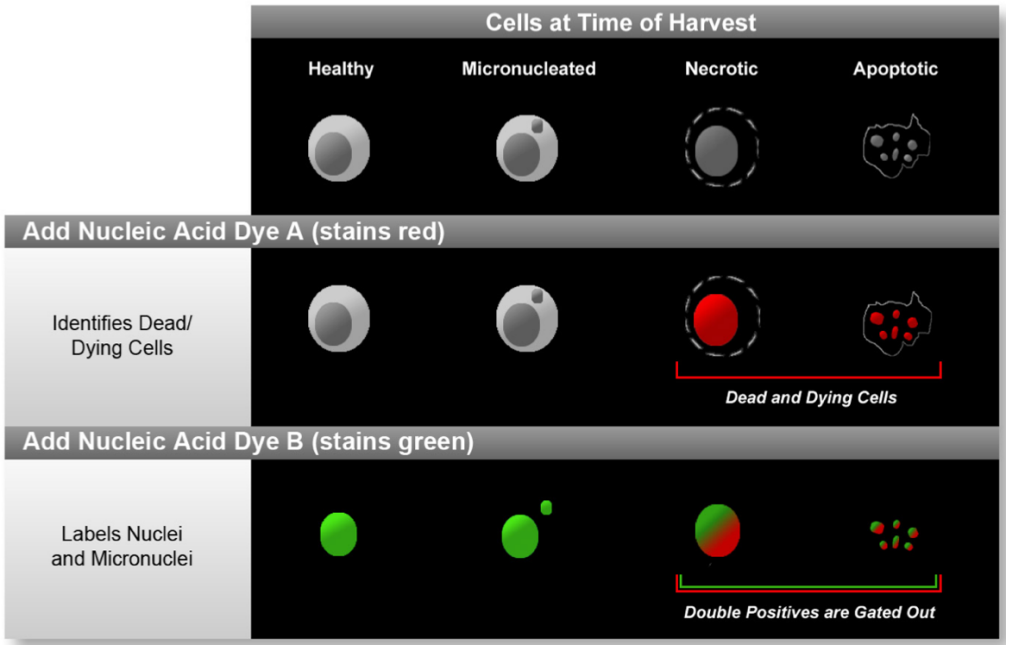

Figure 6: Differential staining applied in the in vitro MicroFlow® assay for MN scoring. Presented with permission from Litron Laboratories.

Multiple studies, including an interlaboratory transferability study (Bryce et al., 2008), show that data derived from this flow-cytometric method (FCM) corresponded closely to traditional microscopy-based measurements in both mouse lymphoma L5178Y and human TK6 cells (Avlasevich et al., 2006; Bryce et al., 2007, 2008). Importantly, this FCM scoring method has now been included as part of OECD TG 487 as an analysis technique (OECD, 2016a). More recently, Bryce et al. developed and validated a miniaturized version of the *in vitro* MicroFlow®, where the FCM scoring approach is combined with assay treatment and processing in microtiter plates (Bryce et al., 2010, 2013). Expansion to 96-well plates allows for a higher-throughput format to study multiple compounds simultaneously with concentration-response analyses

(Bryce et al., 2010). The *in vitro* MicroFlow® assay has now been applied in many genotoxicity studies to assess the chromosome damage induced by tested chemicals.

1.6.2 The MultiFlow® DNA Damage assay

Following the development of the *in vitro* MicroFlow® assay, Bryce et al. hypothesized that the MN analysis would benefit from the measurement of alternative genotoxicity biomarkers to differentiate MN induction due to clastogenic, aneugenic or irrelevant MoAs (Bryce et al., 2014). Clastogenicity is characterized by chromosomal insertions, deletions, or rearrangements that form via breakage (i.e., stand breaks). Aneugenicity is characterized by the induction of changes in chromosome number that differs from a multiple of the haploid complement. Differentiating irrelevant MoAs is especially important to improve the specificity of the *in vitro* micronucleus assay, which can often produce positive results with non-genotoxicants (Kirkland et al., 2006, 2007). Questionable positives could thus be followed-up with an additional assay to confirm genotoxicity and identify a likely MoA. The result was the MultiFlow® DNA Damage Assay, a novel flow-cytometric add-and-read test that uses multiplexed biomarkers to classify genotoxic activity and MoA. Figure 6 demonstrates the principle and workflow for the assay. Human lymphoblastoid TK6 cells are exposed to various concentrations of test substance for 4h and 24h. Following the exposures, cells are lysed and multiplexed with fluorescent DNA damage and polyploidization biomarkers, and analyzed using flow-cytometry (Dertinger et al., 2019).

The assay simultaneously measures the following reporter endpoints:

- *Phosphorylation of H2AX at serine 139 (γH2AX)*: γH2AX is a sensitive DNA damage marker for double strand breaks (DSB) (Sharma et al., 2012; Wilde et al., 2017; Dertinger et al., 2019). Following DSBs, histone H2AX is phosphorylated on serine 139 generating γH2AX and initiating a signaling pathway that spreads the DNA damage signal along the chromatin recruiting other proteins in the DDR. This results in the nuclear translocation of repair proteins and formation of localized foci at the sites of DSBs (Sharma et al., 2012). It is well documented that clastogens have frequently been observed to induce amplification of γH2AX (e.g., etoposide, mitomycin C) (Mah et al., 2010; Wilde et al., 2017).
- *Phosphorylation of histone H3 at serine 10 (pH3):* Phosphorylation of histone H3 (p-H3) is used to identify mitotic cells. During mitosis histone H3 becomes phosphorylated on serine 10 by Aurora kinase B, which triggers the packing of DNA into chromatin. Certain aneugens (e.g., vinblastine, colchicine) disrupt mitotic spindle assembly and induce mitotic arrest resulting in an increased proportion of mitotic cells (Wilde et al., 2017).
- *Nuclear p53:* The phosphoprotein p53 is a well-known transcriptional regulator with a key function in response to genotoxic stress (Wilde et al., 2017). Following DNA damage, the p53 protein is activated and translocated to the nucleus where it stimulates transcription of other proteins to facilitate DNA repair, cell cycle arrest or apoptosis (Zerdoumi et al., 2015).
- *Polyploidization:* Polyploidization is measured by quantifying DNA-associated fluorescence that corresponds to the frequency of 8n and greater DNA content in nuclei

(Dertinger et al., 2019). Polyploidization arises from cell division (i.e., cytokinesis) failure resulting in an extra set of chromosomes. Polyploidy has been proposed to be an important developmental step contributing to aneuploidy (Davoli and de Lange, 2011).

- *Nuclei Count:* Nuclei counts are determined to provide information about treatment-related cytotoxicity using a known concentration of latex spheres (i.e., counting beads).

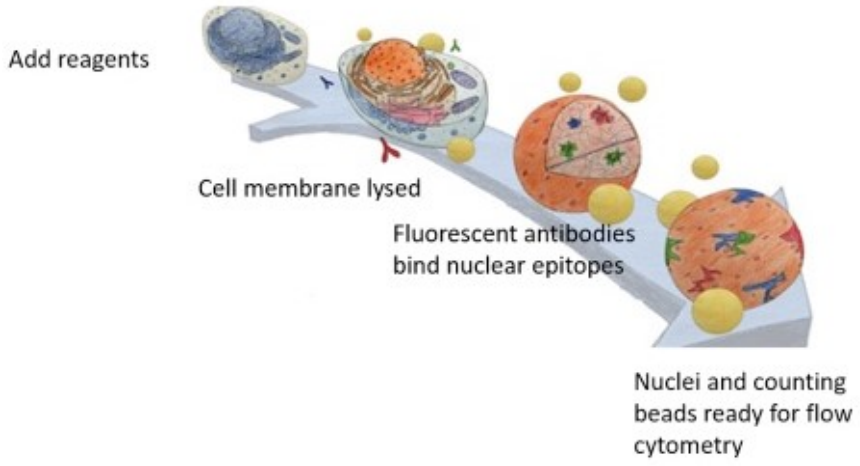

Figure 7: Overview of MultiFlow® Workflow. After 4h or 24h of chemical exposure, TK6 cells are treated with complete labelling solution containing nuclei release reagent, counting beads, and fluorescent antibodies that bind to various DNA damage and polyploidization biomarkers. After 30-minute incubation, cells are analyzed via flow cytometry. Presented with permission from Litron Laboratories.

To classify the test substance, flow cytometry results are analyzed using Global Evaluation Factors (GEF). GEFs represent the threshold at which an increase in biomarker response, represented as a fold change from the solvent control, is significant. The GEFs for each biomarker were generated from a multi-laboratory study that pooled together the aggregate fold-increase response data of various chemicals (Bryce et al., 2017). The data were

applied to a partition platform to calculate the threshold values that best constituted a biologically significant response (Bryce et al., 2017). In applying the GEFs for classification, if the GEFs of aneugenic- or clastogenic-sensitive biomarkers in two consecutive concentrations are exceeded or met, the test substance is classified as either a clastogen or aneugen (Bryce et al., 2017). Non-responsive substances are classified as non-genotoxicants. They include cytotoxicants causing secondary genotoxicity effects known to trigger misleading positive results. An interlaboratory study by Bryce et al. (2013) showed promising results; pooling the results of 231 experiments from multiple laboratories and comparing assay concordance to *a priori* MoA classifications revealed that the assay's sensitivity and specificity was greater or equal to 92% (Bryce et al., 2017). Overall, existing studies suggest that the MultiFlow® DNA Damage assay is an efficient and transferable multiplexed assay for modernized genotoxicity assessment.

1.7 GeneTox21

In light of the effort to modernize the current genotoxicity testing paradigm, Health Canada is developing the GeneTox21 assessment platform (Felter et al., 2021). The goal of the GeneTox21 research program is to establish and evaluate an integrated, higher throughput, and multiplexed platform for *in vitro* genetic toxicity assessment of new and existing chemicals. GeneTox21 incorporates six modernized *in vitro* assays, a brief overview of each assay and their respective endpoints are summarized in Table 1.

Table 1: Overview of the six assays comprising the GeneTox21 platform.

GeneTox 21 Assay	Endpoint
In vitro TGR[1]	Mutation
Ames II[2]	Mutation
Comet Chip[3]	DNA strand breaks
Micronucleus[3]	Chromosomal abnormality
MultiFlow[3]	Genetic damage reporter
TGx-DDI[3]	Genetic damage reporter

[1]Muta™Mouse *FE1 cells,* [2]*Salmonella typhimurium* TA98 and TAmix cells, [3]Human lymphoblastoid TK6 cells

The TGR mutation assay (i.e., an *in vitro* version of the *in vivo* TG 488) is conducted in FE1 epithelial cells derived from Muta™Mouse lung. The FE1 cells contain a retrievable λgt10lacZ shuttle vector with a lacZ transgene for mutation scoring (Maertens et al., 2017). The Ames II assay is a modified bacterial reverse mutation assay (TG 471) (OECD, 2020) in a higher-throughput liquid microtiter plate format (Flückiger-Isler et al., 2004). The modernized assay applies a set of six *S. typhimurium* strains (TA98 and TAMix (TA7001-TA7006 strains) (Gee et al., 1994). Individually designed, each strain of the TAMix can only revert back to wild-type via one

specific base-pair substitution; TA98 detects frameshift mutations (Flückiger-Isler et al., 2004). Thus, the assay provides detailed mutagenic information in one culture. The CometChip® is a higher-throughput (i.e., 96-well format) version of the well-established single cell gel electrophoresis assay (i.e., the comet assay) that detects DNA strand breaks by measuring electrophoretic DNA migration (Ge et al., 2014). The extent of migration from the nucleus (i.e., "the comet tail") is proportional to the amount of DNA damage (Ge et al., 2014). The remaining GeneTox 21 assays, the micronucleus, MultiFlow®, and TGx-DDI assays have been discussed in detail in previous sections (see Section 1.6 Flow-Cytometry Based Methods and Section 1.5.1.1 TGx-DDI).

To evaluate the GeneTox21 assessment platform, a set of 35 reference compounds was judiciously selected in consultation with a Research Advisory Committee (see Supplementary Table II). To ensure a robust assessment platform, the reference compounds selected span four categories: 1) compounds that are expected to test positive *in vitro*, 2) compounds that are expected to test negative *in vitro*, 3) compounds that frequently test positive *in vitro* despite being negative *in vivo* (i.e., irrelevant positives), and 4) compounds that are Ames negative despite being positive *in vivo* and/or *in vitro*. The compounds and categorization selected were also influenced by the EURL-ECVAM recommended lists of genotoxic and non-genotoxic chemicals for assessment of the performance of new or improved genotoxicity tests (Kirkland et al., 2008, 2016).

To evaluate the utility of the GeneTox21 assessment platform to address key data gaps, 20 chemicals that have been flagged as data-poor by Health Canada's New Substances Assessment and Control Bureau (NSACB) are also being examined as part of the GeneTox21 platform

evaluation (see Supplementary Table III). These data-poor compounds were flagged by regulatory partners as having carcinogenicity/genotoxicity structural alerts using the OECD Quantitative Structure-Activity Relationships (QSAR) Toolbox (Dimitrov et al., 2016).

Chemical evaluation with the GeneTox21 program generates large amounts of data; therefore, computational and informatics tools are being developed and repurposed to consolidate, visualize, analyze and interpret the multiplexed data. For example, the Toxicological Prioritization (ToxPi) software (Reif et al., 2013; Marvel et al., 2018) was designed as a prioritization support tool that integrates multiple sources of evidence, derives graphically-displayed profiles, and provides an accompanying single score to rank compounds under consideration (USNRC, 2014a). Collectively, the analyses and interpretation will enable effective prioritization of compounds for risk assessment and regulatory decision making. Overall, the GeneTox21 assessment platform generates multiplexed data for the genotoxicity assessment of new and existing chemicals. The program integrates both qualitative and quantitative genotoxicity results for a comprehensive evaluation that enables tiered screening and prioritization for risk assessment activities.

1.5.1 Implementation of the GeneTox21 platform

Published case-studies have explored the integration of select GeneTox21 assays to assess the genotoxicity of prototypical compounds with promising results (Buick et al., 2020, 2021; Smart et al., 2020; Avlasevich et al., 2021). For example, Buick et al. applied TGx-DDI in parallel with the MicroFlow® assay in HepaRG cells (Buick et al., 2020). As shown in Table 2, the pairing of the TGx-DDI and MicroFlow® assays correctly classified all five DDI and non-DDI

agents. Notably, colchicine, a known aneugenic agent, yielded the expected results: a significant increase in %MN, and a non-DDI call. MN induction can occur from direct DNA damage (i.e., clastogenicity) or mechanisms effecting cell division/mitotic machinery leading to aneuploidy (i.e., aneugenicity) (Luzhna et al., 2013). These results indicate that the MN induction observed by colchicine may not be occurring through direct DNA damage, therefore suggesting an aneugenic mechanism (Buick et al., 2020).

Table 2: MN frequency and TGx-DDI classification for test chemicals examined by Buick et al. (2020).

Test Chemical	MN Induction			Overall TGx-DDI Classification		
	Low	Mid	High	Low	Mid	High
DDI Chemicals						
Aflatoxin B1	+	+	+	Non-DDI	DDI	DDI
Cisplatin	-	+	+	Non-DDI	Non-DDI	DDI
Etoposide	+	+	+	DDI	DDI	DDI
Methyl methanesulfonate	-	+	+	Non-DDI	DDI	DDI
2-Nitrofluorene	-	+	+	Non-DDI	DDI	DDI
Non-DDI Chemicals						
Ampicillin Trihydrate	-	-	-	Non-DDI	Non-DDI	Non-DDI
Colchicine	-	+	+	Non-DDI	Non-DDI	Non-DDI
2-Deoxy-D-Glucose	-	-	-	Non-DDI	Non-DDI	Non-DDI
Sodium Ascorbate	-	-	-	Non-DDI	Non-DDI	Non-DDI
Sodium Chloride	-	-	-	Non-DDI	Non-DDI	Non-DDI

Low, mid, and high concentrations were selected for each compound. For MN results, a "+" sign indicates a statistically-significant induction of MN and at least a two-fold change over vehicle controls. If this criteria was not met a "-" sign is denoted. For TGx-DDI results, an overall call of DDI indicates that at least one of three statistical analyses classified the test compound as DDI. If this criteria was not met the overall call is denoted as non-DDI. (Buick et al., 2020).

More recently the TGx-DDI transcriptomic biomarker was paired with the high-throughput CometChip® in HepaRG cells to achieve similar classification accuracy and mechanistic insight for 12 reference compounds (Buick et al., 2021).

Avlasevich et al. (2021) evaluated the performance of a combining the *in vitro* MicroFlow® and MultiFlow® genotoxicity endpoints (Avlasevich et al., 2021). Human TK6 cells

were exposed to 32 chemicals with known genotoxic MoAs with and without phenobarbital-induced rat liver S9 resulting in 64 *a priori* calls (32 chemicals x 2 metabolic conditions). Notably, the results demonstrated that in isolation, the MN endpoint displayed poor specificity for non-genotoxicants, correctly classifying only 15/22 (68%) according to their *a priori* expectations. When followed-up with analysis of the MultiFlow® endpoints to confirm the apparent MN response, the specificity greatly improved; 21/22 (95%) non-genotoxicants were classified according to their *a priori* expectations (Avlasevich et al., 2021).

These case-studies demonstrate that integrating several genotoxicity endpoints provides a more accurate hazard assessment, with a limited number of irrelevant positives. Therefore, in this thesis, we explore whether a combination of the three assays (i.e., the integration of transcriptomic and flow-cytometry based genotoxicity endpoints) constitutes an efficient approach to obtain information on the genotoxicity and mechanism of action of data-poor chemicals.

1.8 Objectives

The overarching objective of this thesis is to investigate the utility of the TGx-DDI transcriptomic biomarker, multiplexed with additional GeneTox21 assays (i.e., the *in vitro* MicroFlow® assay and the MultiFlow® DNA damage assay), as a NAMs-based, integrated testing strategy for assessing the genotoxicity of select data-poor compounds prioritized by Health Canada's New Substances Assessment and Control Bureau (NSACB). The study has four main objectives:

1) Use the TGx-DDI biomarker to evaluate the genotoxicity of data-poor NSACB compounds.
2) Apply the *in vitro* MicroFlow® assay and the MultiFlow® DNA Damage assay to evaluate the genotoxicity of the data-poor NSACB compounds. The MicroFlow® assay will assess chromosome damage, whereas the MultiFlow® assay will provide insight into MoA.
3) Compare the hazard calls and BMC-derived potency rankings of the data-poor compounds and evaluate the complementarity of these GeneTox21 assays.
4) Adapt an integrated data analysis tool (i.e., ToxPi) for the interpretation and visualization of the results obtained using these, multiplexed GeneTox21 endpoints.

Incorporation of the TGx-DDI transcriptomic biomarker into a novel integrated genotoxicity testing strategy will address the urgent need for effective, efficient, and mechanism-based assessment strategies of data-poor compounds. This thesis will also provide insight into the potential hazard of these data-poor, prioritized chemicals, providing regulators with the information required to protect the health of Canadians.

1.9 References

Aitken, R. J., and De Iuliis, G. N. (2007). Origins and consequences of DNA damage in male germ cells. *Reprod. Biomed. Online* 14, 727–733. doi: 10.1016/S1472-6483(10)60676-1.

Avlasevich, S. L., Bryce, S. M., Cairns, S. E., and Dertinger, S. D. (2006). In vitro micronucleus scoring by flow cytometry: Differential staining of micronuclei versus apoptotic and necrotic chromatin enhances assay reliability. *Environ. Mol. Mutagen.* 47, 56–66. doi: 10.1002/em.20170.

Avlasevich, S., Pellegrin, T., Godse, M., Bryce, S., Bemis, J., Bajorski, P., et al. (2021). Biomarkers of DNA damage response improve in vitro micronucleus assays by revealing genotoxic mode of action and reducing the occurrence of irrelevant positive results. *Mutagenesis* 36, 407–418. doi: 10.1093/MUTAGE/GEAB039.

Barroso, J., Ahn, I. Y., Caldeira, C., Carmichael, P. L., Casey, W., Coecke, S., et al. (2016). "International harmonization and cooperation in the validation of alternative methods," in *Advances in Experimental Medicine and Biology* (Springer New York LLC), 343–386. doi: 10.1007/978-3-319-33826-2_14.

Barton-Maclaren, T. S., Westphal, M., Sarwar, E., Mattison, D., Chiu, W. A., Dix, D., et al. (2017). Challenges and opportunities in the risk assessment of existing substances in Canada: Lessons learned from the international community. *Int. J. Risk Assess. Manag.* 20, 261–283. doi: 10.1504/IJRAM.2017.082569.

Bartsch, H., Kuroki, T., Roberfroid, M., and Malaveille, C. (1982). Metabolic activation systems in vitro for carcinogen/mutagen screening tests. *Chem. Mutagen.* Vol. 7, 95–161. doi: 10.1007/978-1-4615-6625-0_3.

Basu, A. K. (2018). DNA damage, mutagenesis and cancer. *Int. J. Mol. Sci.* 19. doi: 10.3390/ijms19040970.

Bell, S. M., Chang, X., Wambaugh, J. F., Allen, D. G., Bartels, M., Brouwer, K. L. R., et al. (2018). In vitro to in vivo extrapolation for high throughput prioritization and decision making. *Toxicol. Vitr.* 47, 213–227. doi: 10.1016/j.tiv.2017.11.016.

Bryce, S. M., Avlasevich, S. L., Bemis, J. C., Lukamowicz, M., Elhajouji, A., Van Goethem, F., et al. (2008). Interlaboratory evaluation of a flow cytometric, high content in vitro micronucleus assay. *Mutat. Res. - Genet. Toxicol. Environ. Mutagen.* 650, 181–195. doi: 10.1016/j.mrgentox.2007.11.006.

Bryce, S. M., Avlasevich, S. L., Bemis, J. C., Phonethepswath, S., and Dertinger, S. D. (2010). Miniaturized flow cytometric in vitro micronucleus assay represents an efficient tool for comprehensively characterizing genotoxicity dose-response relationships. *Mutat. Res. - Genet. Toxicol. Environ. Mutagen.* 703, 191–199. doi: 10.1016/j.mrgentox.2010.08.020.

Bryce, S. M., Avlasevich, S. L., Bemis, J. C., Tate, M., Walmsley, R. M., Saad, F., et al. (2013). Flow cytometric 96-well microplate-based in vitro micronucleus assay with human TK6 cells: Protocol optimization and transferability assessment. *Environ. Mol. Mutagen.* 54, 180–194. doi: 10.1002/em.21760.

Bryce, S. M., Bemis, J. C., Avlasevich, S. L., and Dertinger, S. D. (2007). In vitro micronucleus assay scored by flow cytometry provides a comprehensive evaluation of cytogenetic damage and cytotoxicity. *Mutat. Res.* 630, 78. doi: 10.1016/J.MRGENTOX.2007.03.002.

Bryce, S. M., Bemis, J. C., Mereness, J. A., Spellman, R. A., Moss, J., Dickinson, D., et al. (2014).

Interpreting in vitro micronucleus positive results: Simple biomarker matrix discriminates clastogens, aneugens, and misleading positive agents. *Environ. Mol. Mutagen.* 55, 542–555. doi: 10.1002/em.21868.

Bryce, S. M., Bernacki, D. T., Bemis, J. C., Spellman, R. A., Engel, M. E., Schuler, M., et al. (2017). Interlaboratory evaluation of a multiplexed high information content in vitro genotoxicity assay. *Environ. Mol. Mutagen.* 58, 146–161. doi: 10.1002/EM.22083.

Buick, J. K., Williams, A., Gagné, R., Swartz, C. D., Recio, L., Ferguson, S. S., et al. (2020). Flow cytometric micronucleus assay and TGx-DDI transcriptomic biomarker analysis of ten genotoxic and non-genotoxic chemicals in human HepaRG™ cells. *Genes Environ.* 42, 5. doi: 10.1186/s41021-019-0139-2.

Buick, J. K., Williams, A., Kuo, B., Wills, J. W., Swartz, C. D., Recio, L., et al. (2017). Integration of the TGx-28.65 genomic biomarker with the flow cytometry micronucleus test to assess the genotoxicity of disperse orange and 1,2,4-benzenetriol in human TK6 cells. *Mutat. Res. - Fundam. Mol. Mech. Mutagen.* 806, 51–62. doi: 10.1016/j.mrfmmm.2017.09.002.

Buick, J. K., Williams, A., Meier, M. J., Swartz, C. D., Recio, L., Gagné, R., et al. (2021). A Modern Genotoxicity Testing Paradigm: Integration of the High-Throughput CometChip® and the TGx-DDI Transcriptomic Biomarker in Human HepaRG™ Cell Cultures. *Front. Public Heal.* 9, 1144.

Cho, E., Buick, J. K., Williams, A., Chen, R., Li, H. H., Corton, J. C., et al. (2019). Assessment of the performance of the TGx-DDI biomarker to detect DNA damage-inducing agents using quantitative RT-PCR in TK6 cells. *Environ. Mol. Mutagen.* 60, 122–133. doi: 10.1002/em.22257.

Clancy, S. (2008). DNA damage & repair: mechanisms for maintaining DNA integrity. *Nat. Educ.* 1, 103. Available at: https://www.nature.com/scitable/topicpage/dna-damage-repair-mechanisms-for-maintaining-dna-344/.

Corton, C. J., Witt, K. L., and Yauk, C. L. (2019). Identification of p53 Activators in a Human Microarray Compendium. *Chem. Res. Toxicol.* 32, 1748–1759. doi: 10.1021/acs.chemrestox.9b00052.

Corvi, R., and Madia, F. (2017). In vitro genotoxicity testing–Can the performance be enhanced? *Food Chem. Toxicol.* 106, 600–608. doi: 10.1016/j.fct.2016.08.024.

Council of Canadian Academies (2017). Integrating emerging technologies into chemical safety assessment: Progress since the 2012 report of the expert panel on the integrated testing of pesticides. *Int. J. Risk Assess. Manag.* 20, 46–58. doi: 10.1504/IJRAM.2017.082559.

Crump, K. (1984). A new method for determining allowable daily intakes. *Fundam. Appl. Toxicol.* 4, 854–871. doi: 10.1016/0272-0590(84)90107-6.

Davis, J. A., Gift, J. S., and Zhao, Q. J. (2011). Introduction to benchmark dose methods and U.S. EPA's benchmark dose software (BMDS) version 2.1.1. *Toxicol. Appl. Pharmacol.* 254, 181–191. doi: 10.1016/j.taap.2010.10.016.

Davoli, T., and de Lange, T. (2011). The Causes and Consequences of Polyploidy in Normal Development and Cancer. *Annu. Rev. Cell Dev. Biol.* 27, 585–610. doi: 10.1146/annurev-cellbio-092910-154234.

Dearfield, K. L., Thybaud, V., Cimino, M. C., Custer, L., Czich, A., Harvey, J. S., et al. (2011). Follow-up actions from positive results of in vitro genetic toxicity testing. *Environ. Mol. Mutagen.* 52, 177–204. doi: 10.1002/em.20617.

Dertinger, S. D., Kraynak, A. R., Wheeldon, R. P., Bernacki, D. T., Bryce, S. M., Hall, N., et al. (2019). Predictions of genotoxic potential, mode of action, molecular targets, and potency via a tiered multiflow® assay data analysis strategy. *Environ. Mol. Mutagen.* 60, 513–533. doi: 10.1002/em.22274.

Dimitrov, S. D., Diderich, R., Sobanski, T., Pavlov, T. S., Chankov, G. V., Chapkanov, A. S., et al. (2016). QSAR Toolbox – workflow and major functionalities. *SAR QSAR Environ. Res.* 27, 203–219. doi: 10.1080/1062936X.2015.1136680.

ECHA (2016). *New approach methodologies in regulatory science : proceedings of a scientific workshop : Helsinki, 19-20 April 2016*. European Chemicals Agency.

Edler, L. (2014). "Benchmark dose in regulatory toxicology," in *Regulatory Toxicology* (Springer Berlin Heidelberg), 359–375. doi: 10.1007/978-3-642-35374-1_93.

Environment Canada (2006). *Guidelines for the notification and testing of new substances : chemicals and polymers : pursuant to section 69 of the Canadian Environmental Protection Act, 1999.* Govt. of Canada.

Farmahin, R., Williams, A., Kuo, B., Chepelev, N. L., Thomas, R. S., Barton-Maclaren, T. S., et al. (2017). Recommended approaches in the application of toxicogenomics to derive points of departure for chemical risk assessment. *Arch. Toxicol.* 91, 2045–2065. doi: 10.1007/s00204-016-1886-5.

Felter, S. P., Bhat, V. S., Botham, P. A., Bussard, D. A., Casey, W., Hayes, A. W., et al. (2021). Assessing chemical carcinogenicity: hazard identification, classification, and risk assessment. Insight from a Toxicology Forum state-of-the-science workshop. *Crit. Rev. Toxicol.* 51, 653–694. doi: 10.1080/10408444.2021.2003295.

Firestone, M., Kavlock, R., Zenick, H., and Kramer, M. (2010). The U.S. environmental protection agency strategic plan for evaluating the toxicity of chemicals. *J Toxicol Env. Heal. B Crit Rev.* 13, 139–162. doi: 10.1080/10937404.2010.483178.

Flückiger-Isler, S., Baumeister, M., Braun, K., Gervais, V., Hasler-Nguyen, N., Reimann, R., et al. (2004). Assessment of the performance of the Ames II™ assay: A collaborative study with 19 coded compounds. *Mutat. Res. - Genet. Toxicol. Environ. Mutagen.* 558, 181–197. doi: 10.1016/j.mrgentox.2003.12.001.

Food and Agriculture Organization of the United Nations, and World Health Organization (2020). "Chapter 5 Dose-response assessment and derivation of health-based guidance values Second edition (2020)," in *Environmental Health Criteria 240 Principles and Methods for the Risk Assessment of Chemicals in Food* (World Health Organization). [Accessed September 13, 2022].

Frank R. Lautenberg Chemical Safety for the 21st Century Act (2014). Available at: https://www.congress.gov/114/plaws/publ182/PLAW-114publ182.pdf [Accessed July 13, 2022].

Friedberg, E. C., McDaniel, L. D., and Schultz, R. A. (2004). The role of endogenous and exogenous DNA damage and mutagenesis. *Curr. Opin. Genet. Dev.* 14, 5–10. doi: 10.1016/j.gde.2003.11.001.

Ge, J., Prasongtanakij, S., Wood, D. K., Weingeist, D. M., Fessler, J., Navasummrit, P., et al. (2014). Cometchip: A high-throughput 96-well platform for measuring DNA damage in microarrayed human cells. *J. Vis. Exp.*, e50607. doi: 10.3791/50607.

Gee, P., Maron, D. M., and Ames, B. N. (1994). Detection and classification of mutagens: A set

of base-specific Salmonella tester strains. *Proc. Natl. Acad. Sci. U. S. A.* 91, 11606–11610. doi: 10.1073/pnas.91.24.11606.

Government of Canada (1999). Canadian Environmental Protection Act, 1999. Available at: https://laws-lois.justice.gc.ca/eng/acts/c-15.31/ [Accessed July 7, 2022].

Government of Canada (2019). Guide to understanding the Canadian Environmental Protection Act: Chapter 9. Available at: https://www.canada.ca/en/environment-climate-change/services/canadian-environmental-protection-act-registry/publications/guide-to-understanding/chapter-9.html [Accessed July 7, 2022].

Guyton, K. Z., Kyle, A. D., Aubrecht, J., Cogliano, V. J., Eastmond, D. A., Jackson, M., et al. (2009). Improving prediction of chemical carcinogenicity by considering multiple mechanisms and applying toxicogenomic approaches. *Mutat. Res. - Rev. Mutat. Res.* 681, 230–240. doi: 10.1016/j.mrrev.2008.10.001.

Harrill, J. A., Everett, L. J., Haggard, D. E., Sheffield, T., Bundy, J. L., Willis, C. M., et al. (2021). High-Throughput Transcriptomics Platform for Screening Environmental Chemicals. *Toxicol. Sci.* 181, 68–89. doi: 10.1093/toxsci/kfab009.

Health Canada (2021). Chemicals Management Plan Science Committee background paper: Evolution of the Existing Substances Risk Assessment Program under the Canadian Environmental Protection Act, 1999 and considerations looking forward Chemicals Management Plan (CMP) Science Com. Available at: https://www.canada.ca/en/health-canada/services/chemical-substances/chemicals-management-plan/science-committee/meeting-records-reports/background-paper-evolution-existing-substances-risk-assessment-program-canadian-environmental-protection-act-1999.html [Accessed May 26, 2022].

ICH (2011). Guidance on Genotoxicity Testing and Data Interpretation for Pharmaceuticals Intended for Human Use S2(R1).

Kavlock, R. J., Bahadori, T., Barton-Maclaren, T. S., Gwinn, M. R., Rasenberg, M., and Thomas, R. S. (2018). Accelerating the Pace of Chemical Risk Assessment. *Chem. Res. Toxicol.* 31, 287–290. doi: 10.1021/acs.chemrestox.7b00339.

Kinaret, P. A. S., Serra, A., Federico, A., Kohonen, P., Nymark, P., Liampa, I., et al. (2020). Transcriptomics in toxicogenomics, part i: Experimental design, technologies, publicly available data, and regulatory aspects. *Nanomaterials* 10, 750. doi: 10.3390/nano10040750.

Kirkland, D., Aardema, M., Müller, L., and Hayashi, M. (2006). Evaluation of the ability of a battery of three in vitro genotoxicity tests to discriminate rodent carcinogens and non-carcinogens. II. Further analysis of mammalian cell results, relative predictivity and tumour profiles. *Mutat. Res. - Genet. Toxicol. Environ. Mutagen.* 608, 29–42. doi: 10.1016/j.mrgentox.2006.04.017.

Kirkland, D., Kasper, P., Martus, H. J., Müller, L., van Benthem, J., Madia, F., et al. (2016). Updated recommended lists of genotoxic and non-genotoxic chemicals for assessment of the performance of new or improved genotoxicity tests. *Mutat. Res. Toxicol. Environ. Mutagen.* 795, 7–30.

Kirkland, D., Kasper, P., Müller, L., Corvi, R., and Speit, G. (2008). Recommended lists of genotoxic and non-genotoxic chemicals for assessment of the performance of new or improved genotoxicity tests: A follow-up to an ECVAM workshop. *Mutat. Res. - Genet.*

Toxicol. Environ. Mutagen. 653, 99–108. doi: 10.1016/j.mrgentox.2008.03.008.
Kirkland, D., Pfuhler, S., Tweats, D., Aardema, M., Corvi, R., Darroudi, F., et al. (2007). How to reduce false positive results when undertaking in vitro genotoxicity testing and thus avoid unnecessary follow-up animal tests: Report of an ECVAM Workshop. *Mutat. Res. - Genet. Toxicol. Environ. Mutagen.* 628, 31–55. doi: 10.1016/j.mrgentox.2006.11.008.
Krewski, D., Acosta, D., Andersen, M., Anderson, H., Bailar, J. C., Boekelheide, K., et al. (2010). Toxicity testing in the 21st century: A vision and a strategy. *J. Toxicol. Environ. Heal. - Part B Crit. Rev.* 13, 51–138. doi: 10.1080/10937404.2010.483176.
Krewski, D., Andersen, M. E., Tyshenko, M. G., Krishnan, K., Hartung, T., Boekelheide, K., et al. (2020). Toxicity testing in the 21st century: progress in the past decade and future perspectives. *Arch. Toxicol.* 94, 3. doi: 10.1007/s00204-019-02613-4.
Krupina, K., Goginashvili, A., and Cleveland, D. W. (2021). Causes and consequences of micronuclei. *Curr. Opin. Cell Biol.* 70, 91–99. doi: 10.1016/j.ceb.2021.01.004.
Lakin, N. D., and Jackson, S. P. (1999). Regulation of p53 in response to DNA damage. *Oncogene* 18, 7644–7655. doi: 10.1038/sj.onc.1203015.
Li, H.-H., Yauk, C. L., Chen, R., Hyduke, D. R., Williams, A., Frötschl, R., et al. (2019). TGx-DDI, a Transcriptomic Biomarker for Genotoxicity Hazard Assessment of Pharmaceuticals and Environmental Chemicals. *Front. Big Data* 2, 36. doi: 10.3389/fdata.2019.00036.
Li, H. H., Chen, R., Hyduke, D. R., Williams, A., Frötschl, R., Ellinger-Ziegelbauer, H., et al. (2017). Development and validation of a high-throughput transcriptomic biomarker to address 21st century genetic toxicology needs. *Proc. Natl. Acad. Sci. U. S. A.* 114, E10881–E10889. doi: 10.1073/pnas.1714109114.
Litron Laboratories (2013). Litron Laboratories. Available at: https://litronlabs.com/ [Accessed December 5, 2019].
Liu, Z., Huang, R., Roberts, R., and Tong, W. (2019). Toxicogenomics: A 2020 Vision. *Trends Pharmacol. Sci.* 40, 92–103. doi: 10.1016/j.tips.2018.12.001.
Luzhna, L., Kathiria, P., and Kovalchuk, O. (2013). Micronuclei in genotoxicity assessment: From genetics to epigenetics and beyond. *Front. Genet.* 4, 131. doi: 10.3389/fgene.2013.00131.
Maertens, R. M., Long, A. S., and White, P. A. (2017). Performance of the in vitro transgene mutation assay in MutaMouse FE1 cells: Evaluation of nine misleading ("False") positive chemicals. *Environ. Mol. Mutagen.* 58, 582–591. doi: 10.1002/em.22125.
Mah, L. J., El-Osta, A., and Karagiannis, T. C. (2010). γh2AX: A sensitive molecular marker of DNA damage and repair. *Leukemia* 24, 679–686. doi: 10.1038/leu.2010.6.
Marvel, S. W., To, K., Grimm, F. A., Wright, F. A., Rusyn, I., and Reif, D. M. (2018). ToxPi Graphical User Interface 2.0: Dynamic exploration, visualization, and sharing of integrated data models. *BMC Bioinformatics* 19, 1–7. doi: 10.1186/S12859-018-2089-2/FIGURES/3.
Mav, D., Shah, R. R., Howard, B. E., Auerbach, S. S., Bushel, P. R., Collins, J. B., et al. (2018). A hybrid gene selection approach to create the S1500+ targeted gene sets for use in high-throughput transcriptomics. *PLoS One* 13, e0191105. doi: 10.1371/journal.pone.0191105.
Moffat, I., Chepelev, N. L., Labib, S., Bourdon-Lacombe, J., Kuo, B., Buick, J. K., et al. (2015). Comparison of toxicogenomics and traditional approaches to inform mode of action and points of departure in human health risk assessment of benzo[a]pyrene in drinking water. *Crit. Rev. Toxicol.* 45, 1–43. doi: 10.3109/10408444.2014.973934.
National Academies Press (US) (2014). "Environmental Health Risks of Chemicals in Our Society:

Workshop Summary.," in *Roundtable on Environmental Health Sciences, Research, and Medicine; Board of Population Health and Public Health Practice; Institute of Medicine.* Available at: https://www.ncbi.nlm.nih.gov/books/NBK268889/.

Nesslany, F. (2017). The current limitations of in vitro genotoxicity testing and their relevance to the in vivo situation. *Food Chem. Toxicol.* 106, 609–615. doi: https://doi.org/10.1016/j.fct.2016.08.035.

OECD (2016). "Test No. 487: In Vitro Mammalian Cell Micronucleus Test" in *OECD Guidelines for the Testing of Chemicals* (Paris: OECD Publishing) doi: 10.1787/9789264264861-en.

OECD (2017). "No.238: Overview of the set of OECD Genetic Toxicology Test Guidelines and updates performed in 2014-2015," in *OECD Series on Testing and Assessment* (Paris: OECD Publishing), 1–70.

OECD (2020). "Test No. 471: Bacterial Reverse Mutation Test" in *OECD Guidelines for the Testing of Chemicals* (Paris: OECD Publishing) https://doi.org/10.1787/9789264071247-en.

Office of the Prime Minister (2021). Minister of Health Mandate Letter. Available at: https://pm.gc.ca/en/mandate-letters/2021/12/16/minister-health-mandate-letter [Accessed September 23, 2022].

Pecorino, L. (2015). *Molecular Biology of Cancer, Mechanisms, Targets, and Therapeutics: Biology, Molecular biology*. 3rd Editio. Oxford University Press.

Pfuhler, S., Fautz, R., Ouedraogo, G., Latil, A., Kenny, J., Moore, C., et al. (2014). The Cosmetics Europe strategy for animal-free genotoxicity testing: Project status up-date. *Toxicol. Vitr.* 28, 18–23. doi: 10.1016/j.tiv.2013.06.004.

Phillips, D. H., and Arlt, V. M. (2009). "Genotoxicity: damage to DNA and its consequences.," in *Molecular, Clinical and Environmental Toxicology Volume 1: Molecular Toxicology* (Birkhäuser Basel), 87–110. doi: 10.1007/978-3-7643-8336-7_4.

Reif, D. M., Sypa, M., Lock, E. F., Wright, F. A., Wilson, A., Cathey, T., et al. (2013). ToxPi GUI: an interactive visualization tool for transparent integration of data from diverse sources of evidence. *Bioinformatics* 29, 402. doi: 10.1093/BIOINFORMATICS/BTS686.

Russell, W. M. S., and Burch, R. L. (1960). The Principles of Humane Experimental Technique. *Med. J. Aust.* 1, 500–500. doi: 10.5694/j.1326-5377.1960.tb73127.x.

Schoeters, G. (2010). The REACH perspective: Toward a new concept of toxicity testing. *J. Toxicol. Environ. Heal. - Part B Crit. Rev.* 13, 232–241. doi: 10.1080/10937404.2010.483938.

Sharma, A., Singh, K., and Almasan, A. (2012). Histone H2AX phosphorylation: A marker for DNA damage. *Methods Mol. Biol.* 920, 613–626. doi: 10.1007/978-1-61779-998-3_40.

Slob, W. (2018). Joint project on Benchmark Dose modelling with RIVM. *EFSA Support. Publ.* 15, 1497E. doi: 10.2903/sp.efsa.2018.en-1497.

Smart, D. J., Helbling, F. R., Verardo, M., Huber, A., McHugh, D., and Vanscheeuwijck, P. (2020). Development of an integrated assay in human TK6 cells to permit comprehensive genotoxicity analysis in vitro. *Mutat. Res. Toxicol. Environ. Mutagen.* 849, 503129.

Still, K. R., Watson, K. D., and Wexler, P. (2020). "History of toxicology," in *Information Resources in Toxicology* (Academic Press), 11–32. doi: 10.1016/b978-0-12-813724-6.00002-5.

Thomas, R. R., Wesselkamper, S. C., Wang, N. C. Y., Zhao, J. J., Petersen, D. D., Lambert, J. C., et al. (2013). Temporal concordance between apical and transcriptional points of departure

for chemical risk assessment. *Toxicol. Sci.* 134, 180–194. doi: 10.1093/toxsci/kft094.
Thomas, R. S., Clewell, H. J., Allen, B. C., Wesselkamper, S. C., Wang, N. C. Y., Lambert, J. C., et al. (2011). Application of transcriptional benchmark dose values in quantitative cancer and noncancer risk assessment. *Toxicol. Sci.* 120, 194–205. doi: 10.1093/toxsci/kfq355.
Thybaud, V., Aardema, M., Clements, J., Dearfield, K., Galloway, S., Hayashi, M., et al. (2007). Strategy for genotoxicity testing: Hazard identification and risk assessment in relation to in vitro testing. *Mutat. Res. - Genet. Toxicol. Environ. Mutagen.* 627, 41–58. doi: 10.1016/j.mrgentox.2006.10.003.
USFDA (2002). Preparation of Food Contact Notifications for Food Contact Substances (Toxicology Recommendations): Guidance for Industry. Available at: https://www.fda.gov/regulatory-information/search-fda-guidance-documents/guidance-industry-preparation-food-contact-substance-notifications-toxicology-recommendations#:~:text=Guidance%20for%20Industry%3A%20Preparation%20of%20Food%20Contact%20Substance,Drug%20Administration%20%28FDA%20or%20we%29%20on%20this%20topic. [Accessed July 12, 2022].
USNRC (2007). *Toxicity testing in the 21st century: A vision and a strategy*. Washingon, DC: National Academies Press doi: 10.17226/11970.
USNRC (2014a). "Appendix C Toxicological Priority Index (ToxPi)," in *A Framework to Guide Selection of Chemical Alternatives* (Washington, DC: The National Academies Press). doi: https://doi.org/10.17226/18872.
USNRC (2014b). "Derivation of Toxicity Values," in *Review of EPA's Integrated Risk Information System (IRIS) Process* (Washingon, DC: National Academies Press), 110–134. doi: 10.17226/18764.
USNTP (2018). *Research Report on National Toxicology Program Approach to Genomic Dose-Response Modeling*. Durham, NC: National Toxicology Program Available at: https://www.ncbi.nlm.nih.gov/books/NBK531562/.
Varewyck, M., and Verbeke, T. (2017). Software for benchmark dose modelling. *EFSA Support. Publ.* 14, 1170E. doi: 10.2903/sp.efsa.2017.en-1170.
Wang, Z., Walker, G. W., Muir, D. C. G., and Nagatani-Yoshida, K. (2020). Toward a Global Understanding of Chemical Pollution: A First Comprehensive Analysis of National and Regional Chemical Inventories. *Environ. Sci. Technol.* 54, 2575–2584.
Warshawsky, D. (2005). "Chapter 1 Carcinogens and Mutagens," in *Molecular Carcinogenesis and the Molecular Biology of Human Cancer* (Taylor & Francis), 17–40. doi: 10.1201/9780203503430-5.
Weston, A., and Harris, C. C. (2003). *Multistage Carcinogenesis*. , eds. D. Kufe, R. Pollock, and R. Weichselbaum Hamilton (ON): BC Decker Available at: https://www.ncbi.nlm.nih.gov/books/NBK13982/ [Accessed February 9, 2021].
White, P. A., Long, A. S., and Johnson, G. E. (2020). Quantitative Interpretation of Genetic Toxicity Dose-Response Data for Risk Assessment and Regulatory Decision-Making: Current Status and Emerging Priorities. *Environ. Mol. Mutagen.* 61, 66–83. doi: 10.1002/em.22351.
Wilde, S., Dambowsky, M., Hempt, C., Sutter, A., and Queisser, N. (2017). Classification of in vitro genotoxicants using a novel multiplexed biomarker assay compared to the flow cytometric micronucleus test. *Environ. Mol. Mutagen.* 58, 662–677. doi: 10.1002/em.22130.

Yang, L., Allen, B. C., and Thomas, R. S. (2007). BMDExpress: A software tool for the benchmark dose analyses of genomic data. *BMC Genomics* 8, 1–8. doi: 10.1186/1471-2164-8-387.

Yauk, C. L., Aardema, M. J., Benthem, J. van, Bishop, J. B., Dearfield, K. L., DeMarini, D. M., et al. (2015). Approaches for identifying germ cell mutagens: Report of the 2013 IWGT workshop on germ cell assays. *Mutat. Res. - Genet. Toxicol. Environ. Mutagen.* 783, 36–54. doi: 10.1016/j.mrgentox.2015.01.008.

Yauk, C. L., Cheung, C., Barton-Maclaren, T. S., Boucher, S., Bourdon-Lacombe, J., Chauhan, V., et al. (2019). Toxicogenomic applications in risk assessment at Health Canada. *Curr. Opin. Toxicol.* 18, 34–45. doi: 10.1016/j.cotox.2019.02.005.

Yeakley, J. M., Shepard, P. J., Goyena, D. E., VanSteenhouse, H. C., McComb, J. D., and Seligmann, B. E. (2017). A trichostatin A expression signature identified by TempO-Seq targeted whole transcriptome profiling. *PLoS One* 12, e0178302. doi: 10.1371/journal.pone.0178302.

Zerdoumi, Y., Kasper, E., Soubigou, F., Adriouch, S., Bougeard, G., Frebourg, T., et al. (2015). A new genotoxicity assay based on p53 target gene induction. *Mutat. Res. - Genet. Toxicol. Environ. Mutagen.* 789–790, 28–35. doi: 10.1016/j.mrgentox.2015.05.010.

Chapter Two

2.1 Introduction

There is an urgent need to improve the efficiency and predictivity of the existing toxicology testing paradigms to address the immense backlog of chemicals requiring evaluation by regulatory bodies worldwide (USNRC, 2007; Schoeters, 2010; Barton-Maclaren et al., 2017; Council of Canadian Academies, 2017). One of the main challenges is the large number of chemicals with no or very limited experimental toxicology data, known as "data-poor compounds" (Barton-Maclaren et al., 2017; Health Canada, 2021). To address the paucity of experimental data, integrated data streams from higher-throughput methodologies are being applied for chemical prioritization and risk assessment. This includes New Approach Methodologies (NAMs), defined broadly as *in silico, in chemico* and *in vitro* assays, that avoid the use of animals to identify chemical hazards (ECHA, 2016; Kavlock et al., 2018). NAMs seek to modernize traditional toxicology testing strategies by addressing the current limitations with conventional assays to accelerate the pace of hazard assessment and reduce reliance on animal tests that are time-consuming and resource-intensive (Pfuhler et al., 2014; Kavlock et al., 2018).

Genotoxicity testing is a critical component of all chemical safety assessments. Chemicals that induce genetic damage may cause long-term adverse health outcomes including cancer, heritable genetic disorders, and other degenerative conditions (Phillips and Arlt, 2009; Heflich et al., 2020). The conventional genotoxicity test battery generally includes a bacterial reverse mutation test (i.e., Ames test) and an *in vitro* mammalian cell chromosome damage test and/or mutation assay (ICH, 1998; USFDA, 2007; OECD, 2017). Depending on the results obtained and decision-making context, one or more *in vivo* tests may also be required (ICH, 1998; Thybaud et al., 2007; OECD, 2017). However, this test battery is not well suited to assessing the large

number of data-poor chemicals needing evaluation. Most of the *in vitro* tests used are generally lower-throughput, provide little mechanistic information, and have a limited ability to predict effects *in vivo*. Chromosome damage assays, in particular, often yield positive calls for chemicals that do not pose an appreciable carcinogenic risk to humans; these hazard calls can lead to unnecessary, costly, and time-consuming *in vivo* follow-up (Kirkland et al., 2006, 2007; Thybaud et al., 2007; Nesslany, 2017). Thus, in recent years there have been efforts to develop modernized *in vitro* genotoxicity testing tools that address these limitations. To meet this demand, toxicogenomic (TGx) and flow cytometric-based approaches have been developed for high-throughput assessment of DNA damage in human relevant models.

Transcriptional profiling can identify early molecular markers of toxicological mechanism of action (MoA) and/or effects (Thomas et al., 2013; Farmahin et al., 2017; Yauk et al., 2019). Since analysis of the large data sets produced by transcriptomics is complex, transcriptomic biomarkers have been developed to more efficiently and objectively predict toxicity from these data (Krewski et al., 2020). For example, Li et al. (2015) developed the TGx-DDI transcriptomic biomarker. The TGx-DDI biomarker is comprised of 64 genes; it is used to classify chemicals as DNA damage-inducing (DDI) or non-DDI by analyzing changes in gene expression following *in vitro* exposure of cultured mammalian cells. The 64 genes were identified from gene expression profiles of human TK6 cells exposed to a reference set of 28 chemical agents spanning a wide range of known DDI and non-DDI mechanisms (Li et al., 2015). The biomarker has been extensively validated and confirmed to be amenable to use with numerous gene expression technologies (Li et al., 2017; Cho et al., 2019; Buick et al., 2021). A variety of proof-of-concept studies have shown its potential utility for hazard identification, chemical prioritization, and

potency comparisons (Buick et al., 2015, 2020, 2021; Moffat et al., 2015; Li et al., 2017, 2019; Cho et al., 2019).

A series of miniaturized flow cytometry-based assays have been developed by Bryce et al. (Bryce et al., 2008, 2010, 2013, 2014, 2016, 2017) to accelerate *in vitro* genotoxicity testing. The *in vitro* MicroFlow® assay applies an automated approach to score micronuclei (MN) to identify chromosomal damage induced by chemicals (Bryce et al., 2008, 2010, 2013). This approach has been thoroughly validated and is now part of existing test guidelines (i.e., TG 487) as an option for MN scoring (OECD, 2017). The MultiFlow® DNA Damage assay uses several multiplexed biomarker responses to further classify genotoxic activity based on the mechanism. This includes the measurement of: phosphorylation of histone H2AX (ɣH2AX), which is indicative of DNA double strand breaks; phosphorylation of histone H3 (p-H3) to identify mitotic cells; nuclear p53 localization to identify DNA damage responses; and the frequency of 8n DNA content to detect polyploidization (Bryce et al., 2014, 2016, 2017). Responses in specific MultiFlow® biomarkers can classify genotoxic agents into two main MoAs: (1) clastogenicity, which is characterized by chromosomal insertions, deletions, or rearrangements that form via breakage (i.e., DNA double stand breaks); or (2) aneugenicity, which characterized by the induction of changes in chromosome number that differs from a multiple of the haploid complement.

Published case-studies have explored the integration of the aforementioned assays to assess the genotoxicity of prototypical compounds with promising results (Buick et al., 2020; Smart et al., 2020; Avlasevich et al., 2021). Buick et al. 2020 applied the TGx-DDI biomarker in parallel with the MicroFlow® assay in HepaRG™ cells (Buick et al., 2020). Avlasevich et al.

(2021) evaluated the performance of the *in vitro* MicroFlow® and MultiFlow® genotoxicity endpoints (Avlasevich et al., 2021). These case-studies demonstrate that integrating several *in vitro* genotoxicity assays provides a more robust and accurate hazard assessment, with a limited number of irrelevant positives. As such, all three assays have been incorporated into the GeneTox21 research program at Health Canada to establish an effective animal-free platform for genotoxicity assessment (Felter et al., 2021).

Herein we explore the utility of the TGx-DDI transcriptomic biomarker, multiplexed with the *in vitro* MicroFlow® assay and the MultiFlow® DNA damage assay, as a NAM-based integrated test strategy for assessing the genotoxicity of data-poor compounds prioritized by Health Canada's New Substances Assessment and Control Bureau (NSACB). The data-poor compounds were flagged by regulatory partners as having carcinogenicity/genotoxicity structural alerts using the Organisation for Economic Co-operation and Development (OECD) Quantitative Structure-Activity Relationships (QSAR) Toolbox (Dimitrov et al., 2016). Human lymphoblastoid TK6 cells were exposed to ten NSACB data-poor substances in conjunction with two positive and one negative control chemicals: etoposide (EPEG), 7,12-dimethylbenz[*a*]anthracene (DMBA), and D-mannitol (DMANN), respectively. Cells were exposed with or without exogenous metabolic activation (i.e., rat liver S9) to a range of concentrations. Gene expression profiling was conducted using the targeted TempO-Seq™ assay (Yeakley et al., 2017; Mav et al., 2018) and the TGx-DDI classifier was applied to the dataset. Classifications were compared with those based on the MicroFlow® and MultiFlow® assays. Benchmark Concentration (BMC) modeling of the genotoxicity endpoints was used to rank the test chemicals by their potencies. The Toxicological Prioritization (ToxPi) software (Reif

et al., 2013; Marvel et al., 2018) was used to integrate the multiplexed endpoint BMCs and create a visual toxicological profile. Overall, we demonstrate how this novel NAM-based *in vitro* testing strategy provides a robust and efficient approach to identify genotoxic data-poor substances and assess potency for further prioritization.

2.2 Methods and Materials

2.2.1 Chemicals Investigated

Test chemical information (including the solvent control) and their respective abbreviations, CAS No., and source are presented in Table 1.

Table 1: Information on test chemicals used in this study.

Chemical	Abbreviation	CAS No.	Source
methanone, (2-amino-5-chlorophenyl)	NSACB 1	719-59-5	Sigma-Aldrich (Oakville, ON)
2-amino-4-methylphenol	NSACB 2	95-84-1	Sigma-Aldrich (Oakville, ON)
3,5-dimethylpyrazole-1-methanol	NSACB 3	85264-33-1	Sigma-Aldrich (Oakville, ON)
3-diethylaminophenol	NSACB 4	91-68-9	Sigma-Aldrich (Oakville, ON)
2,6-diaminopyridine	NSACB 5	141-86-6	Sigma-Aldrich (Oakville, ON)
2-methoxy-4-nitrophenol	NSACB 6	3251-56-7	Sigma-Aldrich (Oakville, ON)
2-[(3-amino-4-methoxyphenyl)amino]ethanol	NSACB 7	83763-47-7	Best of Chemicals (BOC) Sciences (Shirley, NY)
2-[(4-methyl-2-nitrophenyl)amino]ethanol	NSACB 8	100418-33-5	Toronto Research Chemicals Inc (North York, ON)
4-[(3-hydroxypropyl)amino]-3-nitrophenol	NSACB 9	92952-81-3	Toronto Research Chemicals Inc (North York, ON)
1-(1-methyl-2-propoxyethoxy)-2-propanol	NSACB 10	29911-27-1	Sigma-Aldrich (Oakville, ON)
7,12-dimethylbenz[*a*]anthracene	DMBA	57-97-6	Sigma-Aldrich (Oakville, ON)
etoposide	EPEG	33419-42-0	Sigma-Aldrich (Oakville, ON)
D-mannitol	DMANN	69-65-8	Sigma-Aldrich (Oakville, ON)
dimethyl sulfoxide	DMSO	67-85-5	Sigma-Aldrich (Oakville, ON)

2.2.2 Cell Culture

All experiments were performed with human lymphoblastoid TK6 (IVTG strain) cells (#13051501) purchased from Sigma-Aldrich (Oakville, ON). Cells were grown in RPMI1640 cell culture medium (ThermoFisher Scientific, Ottawa, ON) supplemented with 10% horse serum (ThermoFisher Scientific, Ottawa, ON), 2 mM L-Glutamine (ThermoFisher Scientific, Ottawa, ON), 1.8 mM sodium pyruvate (ThermoFisher Scientific, Ottawa, ON), and 100 U/mL of

penicillin and streptomycin (ThermoFisher Scientific, Ottawa, ON). Cells were incubated at 37°C with 5% CO_2 and maintained below $1x10^6$/mL and >90% viability.

2.2.3 Viability Assessment

The cell density was adjusted to 1.5 x 10^5/mL, aliquoted in 96-well plates (100 µL/well), and exposed to 1 µL of test chemical (1% v/v) solubilized in DMSO at a range of concentrations. For test chemicals requiring metabolic activation the medium was supplemented with 10 µL of 5% S9 Mix (0.5% v/v) containing Aroclor-1254 Induced Mutazyme® (Moltox, Boone, NC). Treated cells were then incubated at 37°C with 5% CO_2 for 4h. Cells were collected via centrifugation at 300 x g for 5 minutes, washed with PBS, resuspended in fresh media, and incubated at 37°C with 5% CO_2 for 20h. The viable cell count was quantified via propidium iodide fluorescence analysis with the Miltenyi Biotec MACSQuant ® Analyzer 10 flow cytometer with integrated 96-well MiniSampler device. Instrument settings: autolabel PI.
The fluidics parameters were as follows: sample volume of 100 µL at a medium mix rate, followed by a sample uptake volume of 25 µL analyzed at a medium flow rate. The screen mode was used to rinse the probe between samples. Top concentrations were selected (Table 2) up to 10 mM or lower due to solubility (OECD, 2016b). If cytotoxic, top concentrations were selected for each assay that induce: approximately 40% viability (i.e., 60% cytotoxicity) for the TGx-DDI assay and *in vitro* MicroFlow® assay (Bryce et al., 2008; OECD, 2016b), and 20% viability (i.e., 80% cytotoxicity) for the MultiFlow® DNA Damage assay (Bryce et al., 2016).

Table 2: Experimental information for the data-poor chemicals and controls used in this study.

Chemical	S9 Condition	TGx-DDI* Lowest-Highest Concentration 6 conc. (half-log spacing)	MultiFlow/MicroFlow* Lowest-Highest Concentration 10 conc. (half-log spacing)
NSACB 1	-S9	24 – 135 µM	16.9 – 382 µM
	+S9	16.9 – 95.5 µM	11.9 – 270 µM
NSACB 2	-S9	-	39 – 884 µM
	+S9	28 – 156µM	39 – 884 µM
NSACB 3	-S9	-	46 – 884 µM
	+S9	12 – 65 µM	8 –185 µM
NSABC 4	-S9	-	55 – 1250 µM
	+S9	55 – 10 µM	78 – 1768 µM
NSACB 5	-S9	-	442 – 10000 µM
	+S9	884 – 5000 µM	442 – 10000 µM
NSACB 6	-S9	-	442 – 10000 µM
	+S9	884 – 5000 µM	442 – 10000 µM
NSACB 7	-S9	6 – 35 µM	6.3 – 142 µM
	+S9	17.7 – 100.1 µM	17.7 – 400 µM
NSACB 8	-S9	221 – 1250 µM	156.3 – 3536 µM
	+S9	221 – 1250 µM	156.3 – 3536 µM
NSACB 9	-S9	417 – 2356 µM	295 – 6665 µM
	+S9	460 – 2600 µM	295 – 6665 µM
NSACB 10	-S9	1768 – 10000 µM	442 – 10000 µM
	+S9	1768 – 10000 µM	442 – 10000 µM
EPEG	-S9	0.028 – 0.16 µM	0.028 – 0.63 µM
	+S9	-	0.028 – 0.63 µM
DMBA	-S9	-	33 – 750 µM
	+S9	0.73 – 4.1 µM	1.04 – 23.4 µM
DMANN	-S9	1768 – 10000 µM	442 – 10000 µM
	+S9	1768 – 10000 µM	442 – 10000 µM

*Concentrations with <20% viability for MultiFlow® and <40% viability for TGx-DDI and MicroFlow® assays were excluded from analysis

2.2.4 Exposure for TGx-DDI Assay

The cell density was adjusted to 1.5 x 10^5/mL, aliquoted in 96-well plates (100 µL/well), and exposed to 1 µL of test chemical (1% v/v) solubilized in DMSO in a six-point concentration range on a half-log distribution scale in duplicate (Table 2). Six DMSO solvent controls were included per plate. For test chemicals requiring metabolic activation, the medium was supplemented with 10 µL of 5% S9 Mix (0.5% v/v) containing Aroclor-1254 Induced Mutazyme® (Moltox, Boone, NC). Treated cells were incubated at 37°C with 5% CO_2 for 4H. Cells were

collected via centrifugation at 300 x g for 5 minutes, washed with PBS, and resuspended in 1X TempO-Seq™ Enhanced Lysis buffer in PBS (40 µL/well) (BioSpyder Technologies, Carlsbad, CA, USA). If treated with 0.5% rat liver S9, cells were collected via centrifugation at 300 x g for 5 minutes, washed with PBS, resuspended in fresh media, and incubated at 37°C with 5% CO_2 for a 3h recovery period. Following incubation, cells were collected, washed, and resuspended in 1X TempO-Seq™ Enhanced Lysis buffer in PBS (40 µL/well) (BioSpyder Technologies, Carlsbad, CA, USA) and frozen at -80°C.

2.2.5 TempO-Seq™, Library Purification and Sequencing

The TempO-Seq™ Human Surrogate+Tox Panel (S1500+) v2.0 (BioSpyder Technologies, Carlsbad, CA, USA) assay was completed following the manufacturer's instructions in a 96-well plate format. Each 96-well plate included three assay controls in duplicate: a negative no-cell lysate (1X TempO-Seq™ Enhanced Lysis buffer only), Human Reference Total RNA (Takara Bio, CA, USA), and Human Brain Reference Total RNA (Takara Bio, CA, USA). Briefly, for each treatment, 2 µL of cell lysate in 1X TempO-Seq™ Enhanced Lysis buffer was hybridized to the Human S1500+ Surrogate detector oligo (DO) probe mix (V2.0), incubated at 70°C for 10 minutes, then ramped down to 45°C over 50 minutes (0.5°C/minute). A nuclease digestion followed to remove excess or incorrectly bound DOs at 37°C for 1 hour. The bound DO pairs were then ligated together at 37°C for 1 hour and 15 minutes at 80°C to generate templates for amplification. A 10 µL aliquot of amplification template was transferred to its respective well in the TempO-Seq™ PCR Pre-Mix and Primers plate and amplified on the CFX96 thermocycler (Bio-Rad, Mississauga, ON, Canada) with the following program: 37°C for 10 min, 95°C for 1

min; 25 cycles of 95°C for 10 sec, 65°C for 30 sec, 68°C for 30 sec; 68°C for 2 min. For library building and purification, three 96-well plates (288 sample libraries) were pooled together (5 µL per sample) and purified using the Macherey-Nagel NucleoSpin® Gel and PCR Cleanup Kit (Clontech Laboratories Inc., Bethlehem, PA, USA) with the adjustments specified by the TempO-Seq™ Assay User Guide. The pooled purified TempO-Seq™ libraries were then diluted, quantified, and assessed for quality using the Agilent High Sensitivity D1000 TapeStation (Agilent Technologies, Santa Clara, CA, USA) and the qPCR KAPA Library Quantification Kit (Universal qPCR Master Mix) for Illumina NextSeq 500. Samples were sequenced on a total of two NextSeq® 500/550 High Output (75-cycle) flow cells using an Illumina NextSeq® 500 Sequencing Platform (Illumina, San Diego, CA, USA). A separate pool was completed for a fourth plate and an additional 96 sample libraries were added to the sequencing data for subsequent analysis.

2.2.6 Sequencing Data Preprocessing and Alignment

Sequencing data are accessible in the National Centre for Biotechnology Information (NCBI) Gene Expression Omnibus (GEO) database under accession number GSE213454. Briefly, bcl2fastq (v2.20.0.422) was applied to demultiplex the raw sequencing data and assign each data set to its respective sample files. The data were trimmed using fastp (v0.20.0). Leveraging the BioSpyder TempO-SeqR v3.0 analysis pipeline, the resulting FASTQ files were aligned to the reference sequences for the TempO-Seq™ Human Surrogate+Tox Panel (S1500+) v2.0 probes producing a table of counts per probe per sample. A study-wide quality control analysis pipeline

adapted from Harrill et al. (2021) was applied to the count matrix; 7/276 samples (i.e., S1_pool2, S2_pool2, S31, S79, S95_pool2, S109, S119) were removed due to low quality.

2.2.7 Statistical Analyses for TGx-DDI Classification

The count matrix underwent log2(CPM + 1) normalization to account for read-depth variability between samples. TGx-DDI genes with multiple probes were averaged. For each compound, sample replicates were averaged and the log2 fold changes were estimated for each concentration. Samples that were cytotoxic (viability < 40%), or did not achieve a minimum read depth, were removed from the analysis.

Detailed information regarding the TGx-DDI classification statistical analyses has been described previously (Yauk et al., 2016; Buick et al., 2017, 2021). Briefly, to classify chemicals as DDI or non-DDI, a three-pronged statistical approach was applied. Each analysis compares the sample biomarker responses to those of training set compounds with known DDI and non-DDI mechanisms. The three analyses are listed below:

(1) The Nearest Shrunken Centroids Probability Analysis (NSC-PA) method was conducted (Tibshirani et al., 2002) using the pamr function in R. This summarized the training dataset by calculating a standardized centroid (SC) for the DDI and non-DDI chemicals in the training set. The SC represents the average expression for each gene in a class relative to its within-class standard deviation. To create the NSC, the SCs were shrunken in the direction of the overall centroid. To classify each concentration for each chemical, the expression profiles were compared to the training set NSCs (Li et al., 2017) and assigned to a class (DDI or non-DDI)

based on the probability that class membership was >0.90 (else it was not classifiable). This analysis was visualized as a heatmap.

(2) Principal Component Analysis (PCA) was conducted using the prcomp() function in R (Venables and Ripley, 2002). The PCA estimated the principal components (PC) of the training set data and the PCA loadings were applied to the experimental samples. The sample and training set data were visualized in a scatterplot. Chemical concentrations with a negative PC1 were classified as DDI and with a positive PC1 were classified as non-DDI.

(3) 2-Dimentional hierarchical clustering (2-DC) based on average linkage with Euclidean distances (Becker et al., 1990) was generated for the training set and experimental data using the hclust function in R. Clustering on the main branch with non-DDI agents or on the main branch with DDI agents led to non-DDI or DDI calls for those chemical concentrations, respectively. If the sample was on a branch outside the main DDI and non-DDI clusters, that concentration could not be classified.

If a chemical had a positive call in one of the three statistical analyses (NSC-PA, PCA, 2-DC) at any concentration, the overall call assigned was DDI. Conversely, if none of the three analyses produced a positive call, the overall call assigned was non-DDI.

2.2.8 Exposure for the MultiFlow and MicroFlow Assays

The cell density was adjusted to 2.0 x 10^5/mL and cells were aliquoted in 96-well plates (200 µL/well). Cells were exposed to 2 µL of solubilized test chemical (1% v/v) in a ten-point concentration range on a half-log distribution scale in duplicate (Table 2). All chemicals were also tested in the presence of S9 applying the conditions described previously. Treated cells

were incubated at 37°C with 5% CO_2 for 4H. At the 4H timepoint, aliquots of cells were collected for the MultiFlow® DNA Damage assay (Litron Laboratories, Rochester, NY, USA). The remaining cells were collected via centrifugation at 300 x g for 5 minutes, washed with PBS, resuspended in fresh media, and incubated at 37°C with 5% CO_2. These cells were incubated for an additional 20h for the second time point of the MultiFlow® DNA Damage assay and for the *in vitro* MicroFlow® assay (Litron Laboratories, Rochester, NY, USA).

2.2.9 In Vitro MicroFlow® Assay Processing and Analysis

At 24-hours post-exposure cells were collected via centrifugation at 300 x g for 6 minutes. The supernatant was carefully removed and freshly prepared Complete Nucleic Acid Dye A (50 µL/well) was added. The plate was then placed under a visible light source on ice for 30 minutes. 1X Buffer Solution (150 µL/well) was added, cells were collected via centrifugation at 300 x g for six minutes, and the supernatant was carefully removed. Cells were resuspended in Complete Lysis Solution 1 (100 µL/well), mixed thoroughly, and incubated at room temperature for 1 hour. Completed Lysis Solution 2 was added (100 µL/well) and the plate was rocked gently to mix. The plate was then analyzed via flow cytometry with the Miltenyi Biotec MACSQuant® Analyzer 10 flow cytometer with an integrated 96-well MiniSampler. The mixing and fluidics parameters were as follows: sample mixing of 50 µL at a medium mix rate, followed by a sample uptake volume of 50 µL that was analyzed at a medium flow rate. The fast mode was used to rinse the probe between samples. Instrument settings followed instructions stated in the MicroFlow® MicroNucleus Analysis kit (In Vitro, 96 well) (Litron Laboratories, Rochester, NY) to detect fluorochromes SYTOX Green® in the FITC channel and ethidium monoazide (EMA),

in the PerCP-Cy5.5 channel. An analysis stop gate of 5,000 EMA-negative nuclei per well was applied.

The *in vitro* MicroFlow® results were analyzed using the analysis template provided by Litron Laboratories (Rochester, NY). The % MN was calculated using the count of MN events relative to the count of nucleated events. Results for graphical and statistical representations were expressed as a relative fold-change from the average plate-specific DMSO solvent control normalized to 1.

$$\% \, MN = \frac{MN \; Events}{Nucleated \; Events} \; x \; 100$$

Cytotoxicity was determined using the Relative Survival (RS) equation. Treatments with RS values less than 40% and %EMA-positive nuclei values greater than 4-fold over solvent controls were removed from analysis.

$$RS = \frac{Nuclei \; in \; treated \; culture/mL}{Nuclei \; in \; mean \; sovent \; control/mL} \; x \; 100$$

$$Fold \; EMA = \frac{\% \; Apoptotic/Necrotic}{Mean \; \% \; Apoptotic/Necrotic \; of \; solvent \; controls} \; x \; 100$$

A positive call was indicated by a 2.50-fold increase in %MN and a statistically significant ($p < 0.05$) %MN increase relative to solvent controls in at least one non-cytotoxic concentration (Avlasevich et al., 2021). Statistical significance was determined using a Poisson regression with a Holm-Sidak multiple correction procedure.

2.2.10 MultiFlow DNA Damage Assay Processing and Analysis

At 4H and 24H sampling times, fresh complete labeling solution was prepared; solution containing nuclei release solution, DNA stain, RNase solution, γH2AX Alex Fluor® 647, phosphor-histone antibody PE, and p53 antibody conjugated to fluorescein isothiocyanate (FITC) (Litron Laboratories, Rochester, NY) was added (50 µL/well) to a fresh 96-well plate. Treated cells were gently resuspended and 25 µL/well was mixed thoroughly with the labeling solution. The plate was incubated for 30 minutes at room temperature shielded from light. The cells were then analyzed via flow cytometry with the Miltenyi Biotec MACSQuant® Analyzer 10 flow cytometer with an integrated 96-well MiniSampler. Instrument settings followed the MultiFlow® Smart Start Guide (Litron Laboratories, Rochester, NY) to detect fluorescence emissions from fluorochromes FITC (in the B1 channel), PE (in the B2 channel), propidium iodide (in the B3 channel) and Alexa Fluor® 647 (in the R1 channel). The mixing and fluidics parameters were as follows: sample mixing of 40 µL at a medium mix rate, followed by a sample uptake volume of 20 µL, which was analyzed at a medium flow rate. The fast mode was used to rinse the probe between samples (Bernacki et al., 2016; Bryce et al., 2016).

The MultiFlow ® DNA Damage assay results were analyzed using the analysis template provided by Litron Laboratories (Rochester, NY). The γH2AX and p53 endpoints were measured based on their median fluorescence intensity (i.e., mean channel fluorescence or MCF) relative to the DMSO solvent control. The p-H3 and polyploidy endpoints were measured based on their frequencies among all events (i.e., all 2n-4n and polyploidy (8n) DNA content). The equations for calculating γH2AX shift, nuclear p53 shift, % polyploidy, and % p-H3 positive events are shown below. Results for graphical and statistical representations were expressed as a relative

fold-change from the average plate-specific DMSO solvent control normalized to 1 (Bernacki et al., 2016; Bryce et al., 2016).

$$\gamma H2AX\ shift = \frac{MCF\ of\ treated\ culture}{Mean\ MCF\ of\ solvent\ control}$$

$$Nuclear\ p53\ shift\ = \frac{MCF\ of\ treated\ culture}{Mean\ MCF\ of\ solvent\ control}$$

$$\%\ Polyploidy = \frac{\#\ events\ polyploidy\ (8n)\ DNA\ content}{\#\ events\ 2n, 4n\ and\ polyploidy\ DNA\ content}\ x\ 100$$

$$\%\ pH3\ events = \frac{\#\ events\ pH3\ positive\ 4n\ and\ greater\ DNA\ content}{\#\ events\ 2n, 4n\ and\ polyploidy\ DNA\ content}\ x\ 100$$

Latex microspheres were used as counting beads to determine nuclear density. Cytotoxicity was determined using the Relative Nuclei Count (RNC) equation, with cytotoxicity = 100% - RNC at 24H (Bernacki et al., 2016; Bryce et al., 2016):

$$RNC = \frac{Density\ of\ nuclei\ in\ treated\ culture}{Density\ of\ nuclei\ in\ mean\ sovent\ control}\ x\ 100$$

Litron developed Global Evaluation Factors (GEF) to identify a biologically significant increase in select biomarker levels. The determined GEFs, expressed as fold-change (FC) increase over solvent control, are as follows:

- For clastogenic biomarkers: 4H γH2AX, 1.51 FC; 24H γH2AX, 2.11 FC; 4H p53, 1.40 FC; 24H p53, 1.45 FC.

- For aneugenic biomarkers: 4H p-H3, 1.71 FC; 24H p-H3, 1.52 FC; 24H polyploidy, 5.86 FC; 24H p53, 1.45 FC.

A clastogenic or aneugenic call required two successive concentrations that met or exceeded the GEFs in at least 2 of the 4 respective MoA biomarkers. Chemicals that met or exceeded two GEFs in a single non-cytotoxic concentration were designated as "weak" responses. In cases where both clastogen and aneugen biomarkers exceeded the GEF the MoA was considered pan-genotoxic. In cases where less than two biomarkers met the GEFs, the call was non-genotoxic. Exposure concentrations that resulted in greater than 80% cytotoxicity were excluded from MoA classification.

2.2.11 Benchmark Concentration Modeling of TGx-DDI Biomarker Genes

Gene expression data were used for BMC modeling as described by Buick et al. (2021). Briefly, the counts() function in the DESeq2 R package was applied to convert the normalized read counts into log2. Groups where N = 1 were removed and filtered to exclude probes with fewer than 5 reads. The log2 transformed data were run with the BMDExpress V2.3 software following the guidelines outlined by the US National Toxicology Program (NTP) Approach to Genomic Dose-Response Modeling report (USNTP, 2018). The log2 data were prefiltered using a Williams Trend Test applying a permutation p-value cutoff < 0.05 with 500 permutations and linear FC of ≥ 1.5. The pre-filtered data were analyzed using EPA BMDS parametric models to derive BMCs. This included: the Exponential 2, 3, 4 & 5 models, Linear, 2° Polynomial, and the Restricted Power (≥ 1). The benchmark response factor (BMR) was set to 1 standard deviation. The "Best BMC" was selected based on the best-fit model (i.e., model with the lowest Akaike

Information Criterion (AIC)). The upper (BMCU) and lower (BMCL) 95% confidence limits of the BMCs were calculated. The calculated gene BMCs were filtered and removed if: the model fit was insufficient (p-value < 0.1), BMC/BMCL ratio ≥ 20, BMCU/BMC ≥ 20, and a BMCU/BMCL ≥ 40. Applying a bootstrapping method described in detail by Buick et al. (2021), the median BMC of the TGx-DDI biomarker genes was derived to represent an overall TGx-DDI BMC for each compound. 95% confidence intervals were calculated from the bootstrapped distribution of the BMC median.

2.2.12 Benchmark Concentration Modeling of MultiFlow and MicroFlow Endpoints

BMC modeling was done on test chemicals with positive MultiFlow® and/or MicroFlow® calls. The modeling was performed with the PROAST R package (V70.3) developed by the RIVM (i.e., Dutch National Institute for Public Health and the Environment). To model the continuous concentration-response data, a single 5-parameter exponential model ($y=a*[c^{(1-\exp(-x/b)^d)}]$) was applied (White et al., 2020). For the MicroFlow® assay, the % induction of MN relative to test chemical concentration was modeled; a BMR of 1.0 (i.e., 100% increase in response relative to control) was applied (Long et al., 2018; White et al., 2020; Avlasevich et al., 2021). For the MultiFlow assay, the FC in response for each biomarker (e.g., 4H and 24H p53; 4H and 24H γH2AX) relative to test chemical concentration was modeled. A BMR of 0.5 (i.e., 50% increase) was applied (Avlasevich et al., 2021). The lowest BMC of the MultiFlow biomarkers was selected as the overall BMC.

2.2.12 ToxPi Visualization

The calculated endpoint BMCs were integrated and converted into a single visual profile for each compound using the Toxicological Prioritization Index (ToxPi) software (v2.3) (Reif et al., 2013; Marvel et al., 2018). The BMC, BMCL, and BMCU values for each compound were formatted in Excel using the templates provided by ToxPi and saved as a comma-separated value (csv) file. A value of 10,000 µM (i.e., 10 mM) was entered when an infinite upper confidence interval or a BMC could not be calculated for a particular endpoint; or if a calculated BMC value was greater than the actual top passing/valid concentration. Differential weighting was assigned to the slices. TGx-DDI and MN were assigned 1/3 of the profile each; the four p53 and γH2AX timepoints were assigned 1/12 of the profile each to make up 1/3. The BMCL and BMCU values were assigned to their respective slices and were $-\log_{10}$ transformed. The ToxPi analysis was run to derive ToxPi scores. First, the BMCL and BMCU values for each endpoint were summed and transformed into a single slice score for each compound. This was achieved by normalizing the summed BMC values to a [0,1] interval by dividing by the slice maximum (USNRC, 2014a). Thus, in this case, values closer to 1 (i.e., maximum unit score) denoted a higher potency. Alternatively, values closer to 0 (closer to the origin) denoted a lower potency; and values that did not extend from the origin were denoted as inactive. The overall ToxPi score was calculated by combining all weighted slice scores for each compound and the 95% confidence intervals were calculated. The ToxPi hierarchical clustering algorithm was applied to cluster like-chemical ToxPi profiles. ToxPi analysis figures (i.e., profiles, rank plot, and hierarchical clustering) were downloaded.

2.3 Results

Human lymphoblastoid TK6 cells were exposed to ten data-poor chemicals across a range of concentrations alongside solvent controls, as well as three reference control chemicals. Genotoxicity was assessed using three *in vitro* assays: 1) the TGx-DDI transcriptomic biomarker, 2) the *in vitro* MicroFlow® assay, and 3) the MultiFlow® DNA Damage assay. Potency ranking for chemical prioritization was conducted on chemicals with positive hazard flags using BMC modeling and compared across the assays. A single genotoxicological profile integrating all endpoint BMCs was created.

Prior to assessing genotoxicity, concentration ranges were identified using viability studies +/- S9 to select top concentrations for each assay. Cell viability was quantified at 24 hours via propidium iodide fluorescence analysis (Supplementary Figure I). Both positive controls, EPEG and DMBA, caused a decline in viability; whereas, the negative control, DMANN, showed no decrease in viability. NSACB chemicals #1-9 caused concentration-dependent decreases in viability both +/- S9. NSACB #10 did not impact viability up to the highest concentration of 10 mM.

2.3.1 TGx-DDI Biomarker Classification

To classify test compounds as DDI or non-DDI using the TGx-DDI biomarker, transcriptional profiles were generated using TempO-Seq™ S1500+ sequencing. A trio of independent statistical analyses, 2-DC, PCA, and NSC-PA, were used to derive the overall TGx-DDI classifications (Figure 1; Supplementary Figure II; Supplementary Figure III). To ensure a conservative assessment of genotoxic potential, if one of the analyses classified a test article as

DDI, the overall call given was DDI. The biomarker correctly classified the three control chemicals: DMBA and EPEG were classified as DDI; the negative control DMANN was classified as non-DDI.

Eight out of ten NSACB compounds were identified as DDI, with varying potencies. NSACB compounds #5 and #7 showed the strongest responses. The trio of statistical analyses identified NSACB #5 as DDI across all concentrations (2-DC was inconclusive at the highest four concentrations); and NSACB #7 was DDI across all concentrations except the lowest. The strength of this response can be visualized in Figure 1, i.e., when comparing the similarity of the heatmaps of NSACB #5 and #7 to those DDI compounds in the training set. NSACB #9 had a moderate DDI response; the 2-DC statistical analysis identified #9 as DDI for the majority of concentrations, but the NSC-PA and PCA analyses only identified this compound as DDI at the highest non-cytotoxic concentration. NSACB compounds #1, 2, 3, 4, and 8 were also classified as DDI. However, these were considered weaker DDI responses as these compounds were only positive at the highest non-cytotoxic concentrations and the DDI calls were not consistent across the statistical analyses (with the exception of #3). NSACB compounds #6 and 10 were classified as non-DDI; all three analyses yielded non-DDI calls across all concentrations.

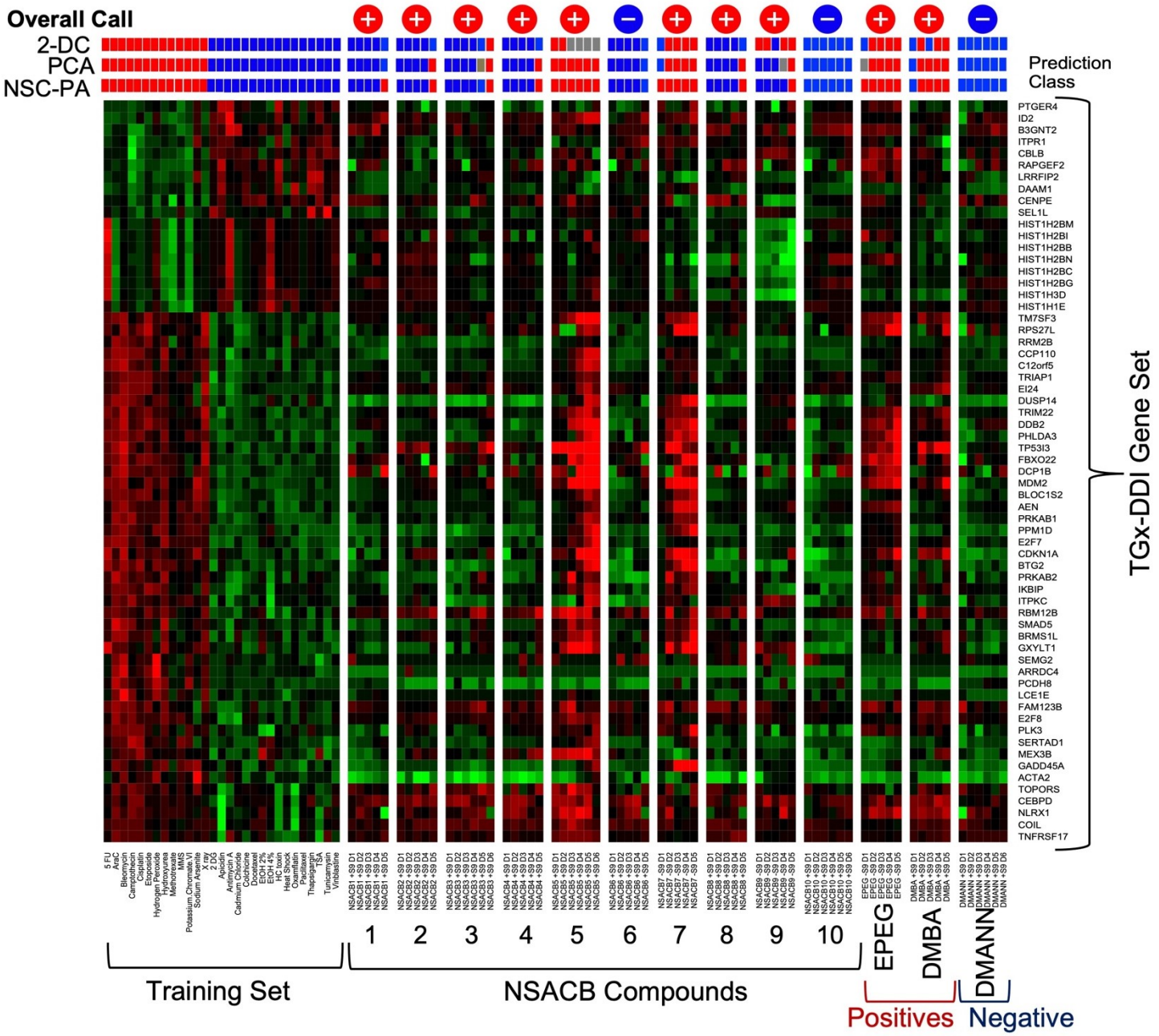

Figure 1: TGx-DDI classification of NSACB data-poor compounds. The heatmap on the left depicts the 28 reference chemicals used as a training set to generate the biomarker. The color scale indicates the average gene expression fold changes of two replicates relative to solvent control: up-regulated genes are shown in red, down-regulated genes are shown in green, genes with no change are shown in black. Three analyses: (1) 2-dimensional hierarchical clustering (2-DC), (2) principal component analysis (PCA), and (3) nearest shrunken centroid probability analysis (NSC-PA) were used to determine classification probabilities shown for all treatment conditions using red (DDI), blue (non-DDI), and grey (inconclusive) boxes. The overall calls are also shown at the top of each column: "+" signifies a positive DDI call, "-" signifies a non-DDI call. D1 represents the lowest concentration tested, D6 the highest. Cytotoxic concentrations (< 40% relative survival) were removed from the analysis. Presented -S9 condition for #7, 9, EPEG. Presented +S9 condition for #1, 2, 3, 4, 5, 6, 8, 10, DMBA, DMANN.

2.3.2 In vitro MicroFlow® Assay Classification

Chromosome damage was assessed using the *in vitro* MicroFlow® assay for the test chemicals (Figure 2, Supplementary Figure IV). A positive result was designated by at least one concentration that induced >2.5 FC in %MN and was statistically significant ($p < 0.05$) compared to vehicle controls. Both positive controls, EPEG and DMBA, exhibited significant fold-increases in %MN, whereas this was not observed with the negative control DMANN (Supplementary Figure IV).

All ten NSACB chemicals met the classification criteria for a positive call in at least one S9 condition. The majority were positive -S9, but #8 and #10 only tested positive in +S9 conditions. NSACB #1, 5, 6, 7, 8, and 9 showed a robust fold-increase in %MN with a clear concentration-response relationship. NSACB #2 and #3 displayed variable responses with a significant increase observed only at the highest concentration. NSACB #4 and #10 exhibited a concentration-response pattern at the lowest concentrations before decreasing or plateauing at the higher concentrations.

2.3.3 MultiFlow® DNA Damage Assay Classification

To provide insight into the MoA, the test compounds were assessed with the MultiFlow® assay. The assay data were visualized using radar plots that depict the FCs in the MultiFlow® biomarkers following chemical exposure (Figure 3, Supplementary Figure V). If a test chemical induced a significant increase in two out of four clastogen-specific biomarkers (i.e., 4H and 24H p53, and γH2AX) in at least one concentration, a clastogenic MoA was predicted. Similarly, significant responses in two out of four aneugen-specific biomarkers (4H p-

H3, 24H p53, p-H3, and polyploidy) predicted an aneugenic MoA. If both of these criteria were met, a pan-genotoxic MoA was predicted. If none of these criteria were met the chemical was classified as non-genotoxic.

The control chemicals responded as expected (Supplementary Figure V). Positive controls, EPEG and DMBA, had concentration-dependent increases in the clastogen biomarkers: 4H p53, 24H p53, and 4H γH2AX for EPEG; 4H and 24H γH2AX for DMBA.

In total, six of the ten NSACB compounds were classified as genotoxic using the MultiFlow® assay. NSACB compounds #2, 3, 5, 7, and 9 exhibited concentration-dependent increases in MultiFlow® clastogen-specific biomarkers and were classified as clastogens (Figure 3). NSACB #3, 5, and 7 induced responses in 4H p53 and 4H γH2AX; NSACB #2 induced responses in 4H γH2AX and 24H p53; and NSACB #9 induced responses in 4H and 24H γH2AX. NSACB #2, 5, and 9 had the most robust increases, whereas NSACB #3 and 7 had more moderate responses. NSACB #4 was the only test chemical classified as a pan-genotoxicant. This compound displayed significant increases in clastogen biomarkers 4H p53 and γH2AX, as well as aneugen marker 4H p-H3 and pan-genotoxic marker 24H p53. The remaining compounds, NSACB #1, 6, 8, and 10 were classified as non-genotoxic. Three of the non-genotoxic compounds (#1, 6, and 10) had a moderate to robust response increase in one of the aneugenic biomarkers (i.e., 4H p53) in more than one concentration. However, without an increase in any other biomarker, an aneugenic call could not be made.

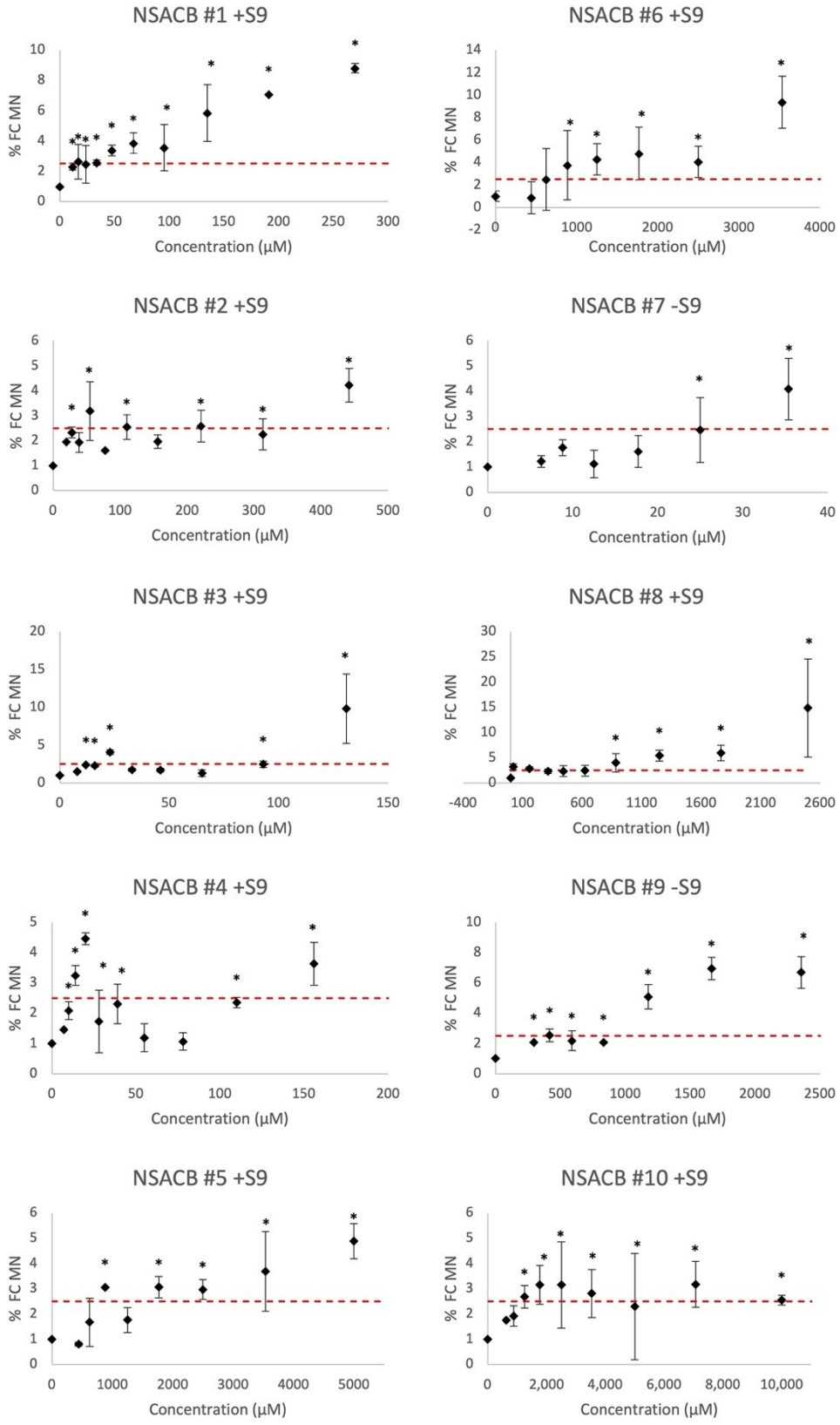

Figure 2: In vitro MicroFlow® assay results for ten NSACB data-poor substances (#1-10). Fold-increase in % micronucleus (MN) compared to vehicle control is depicted by black diamonds. The dashed red line shows the 2.5-fold threshold required in %MN to yield a positive classification. Statistically significant increases ($p < 0.05$) are designated by an asterisk (*). Cytotoxic concentrations (<40% viability) were removed from the analysis. Error bars denote standard deviation from mean. N=2.

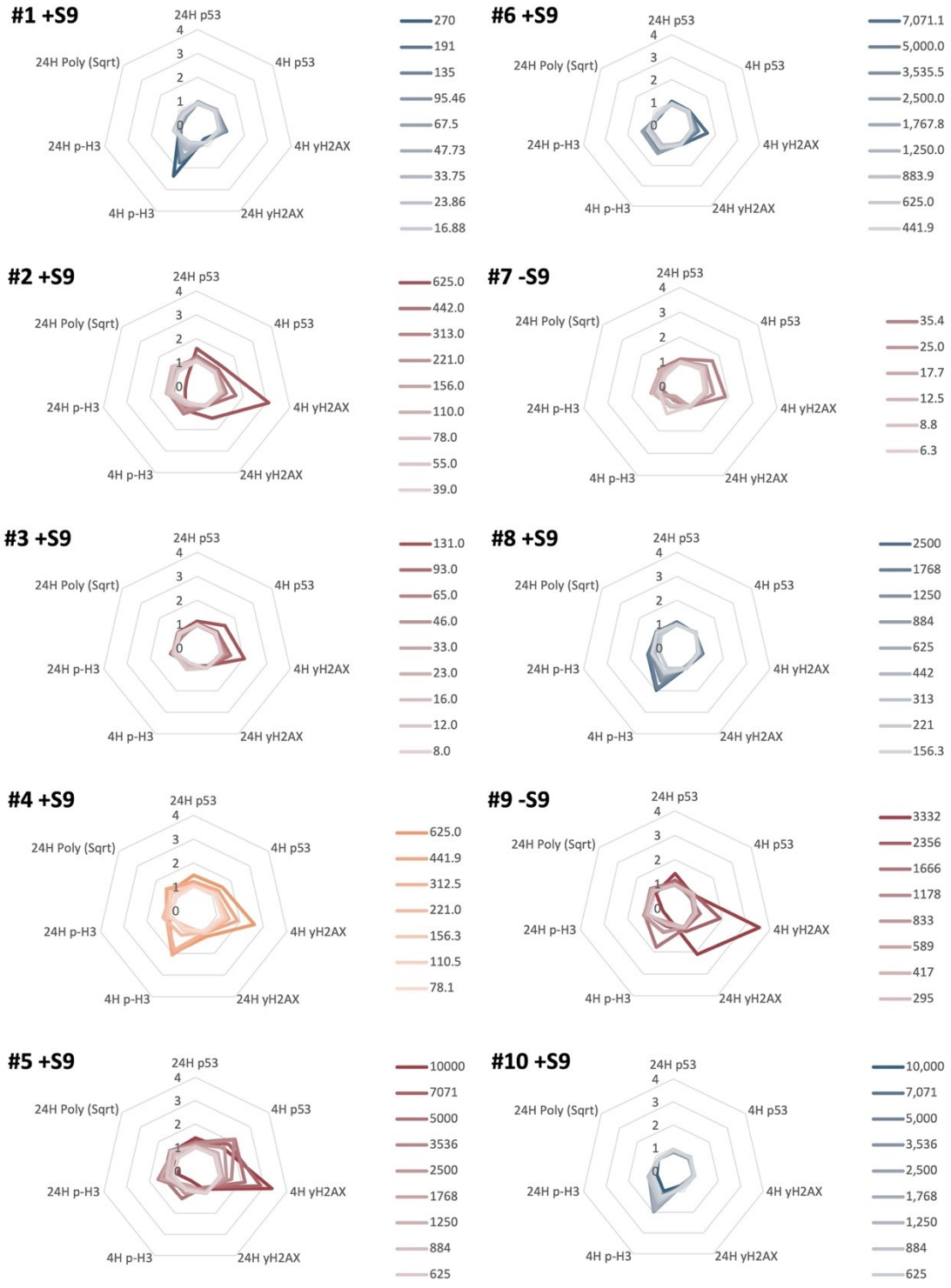

Figure 3: MultiFlow® DNA Damage assay classification results for ten NSACB data-poor substances (#1-10). Each radar plot shows the seven biomarkers predicting the predominant mode of action (MoA) for each chemical. Clastogen MoA biomarkers are on the right of each radar plot: 4H p53, 4H γH2AX, 24H p53, and 24H γH2AX. Aneugen MoA biomarkers are on the left of each radar plot: 4H p-H3, 24H p-H3, 24H Polyploidy, and 24H p53. The biomarker data are expressed as a fold-increase over the mean solvent control for each non-cytotoxic concentration (<20% viability) represented by lines with different colour intensities (as shown in the legend). The line colour in each plot represents the classification call: clastogens are red, non-genotoxicants are blue, and pan-genotoxicants are orange. Chemicals meeting or exceeding the Global Evaluation Factors (GEFs) in at least one concentration in two MoA-specific biomarkers were classified as aneugenic or clastogenic, or classified as pan-genotoxic if both the aneugen and clastogen criteria were met.

2.3.4 Summary of Hazard Calls

An overview of the TGx-DDI, MicroFlow®, and MultiFlow® classification calls for the test chemicals is depicted in Table 3. The control chemicals performed as expected. EPEG and DMBA were positive across all three assays; DMANN tested negative in all three assays. For the data-poor compounds, eight out of ten (NSACB #1, 2, 3, 4, 5, 7, 8 and 9) were classified as DDI by the TGx-DDI transcriptomic biomarker in at least one S9 condition. In contrast, all ten NSACB compounds were positive for MN induction. Using MultiFlow®, five were identified as clastogens and one was identified as a pan-genotoxicant in at least one S9 condition.

Overall, six compounds, NSACB #2, 3, 4, 5, 7, and 9, were positive in all three assays. NSACB #1 and #8 were positive in the TGx-DDI and MicroFlow® assays, but were identified as non-genotoxicants by the MultiFlow® assay. The remaining compounds, NSACB #6 and #10, only tested positive in the MicroFlow® assay, and were classified as non-DDI and non-genotoxicants by the TGx-DDI and MultiFlow® assays, respectively.

Table 3: Summary classifications for the ten data-poor compounds and control chemicals.

		#1	#2	#3	#4	#5	#6	#7	#8	#9	#10	EPEG	DMBA	DMANN
TGx-DDI	-S9	-						+	-	+	-	+		-
	+S9	+	+	+	+	+	-	+	+	+	-		+	-
MicroFlow®	-S9	+	+	+	+	+	+	+	-	+	-	+	+	-
	+S9	+	+	+	+	+	+	+	+	+	+	+	+	-*
MultiFlow®	-S9	-	-	+ C	+ C	+ C	-	+ C	-	+ C	-	+ C	-	-
	+S9	-	+ C	+ C	+ C/A	+ C	-	+ C	-	+ C	-	+ C	+ C	-

*Data Leveraged from Litron Laboratories. The classifications are as follows for each assay: red boxes with a "+" signify a positive call, blue boxes with a "-" signify a negative call, and dark grey boxes were not tested. For the MultiFlow® DNA Damage assay C = clastogen, A = aneugen, C/A = pan-genotoxicant.

2.3.5 Independent BMC Analysis of TGx-DDI Biomarker Genes, MicroFlow® and MultiFlow® Assay Endpoints

In addition to hazard calls, quantitative analyses of genotoxicity data can be applied for chemical potency ranking and subsequent prioritization. To assess the relative potency of the NSACB compounds with positive hazard flags, we conducted BMC modeling to derive BMC values for the TGx-DDI biomarker gene set, and the MicroFlow® and MultiFlow® assay endpoints (Supplementary Figure VI). To evaluate the consistency of the potency rankings derived from each assay, the NSACB compounds with concordant positive hazard calls (i.e., #2, 3, 4, 5, 7 and 9) were compared (Figure 4A-C). The most to least potent chemicals based on the TGx-DDI BMC ranking was (Figure 4A): EPEG (lowest median gene BMC) > DMBA > NSACB 7 > NSACB 4 > NSACB 2 > NSACB 3 > NSACB 9 > NSACB 5 (greatest median gene BMC). Two main potency groups for the NSACB compounds can be observed. The first group, NSACB #7, 4, 3, and 2, have confidence intervals that overlap and are thus considered equipotent. The second group, NSACB #9 and #5, also have confidence intervals that overlap and are also considered equipotent, but are in a distinct, less potent, group from NSACB #7, 4, 3 and 2.

MicroFlow® BMC analysis yielded a highly similar potency ranking (Figure 4B): EPEG > DMBA > NSACB 7 > NSACB 3 > NSACB 4 > NSACB 2 > NSACB 9 > NSACB 5. However, due to the overlapping confidence intervals, all the data-poor compounds are considered equipotent to one another.

Finally, MultiFlow® BMCs were evaluated and the lowest BMC of clastogen biomarkers selected as the point of departure (Figure 4C). This analysis revealed the following potency ranking: EPEG > DMBA > NSACB 7 > NSACB 3 > NSACB 4 > NSACB 2 > NSACB 9 > NSACB 5.

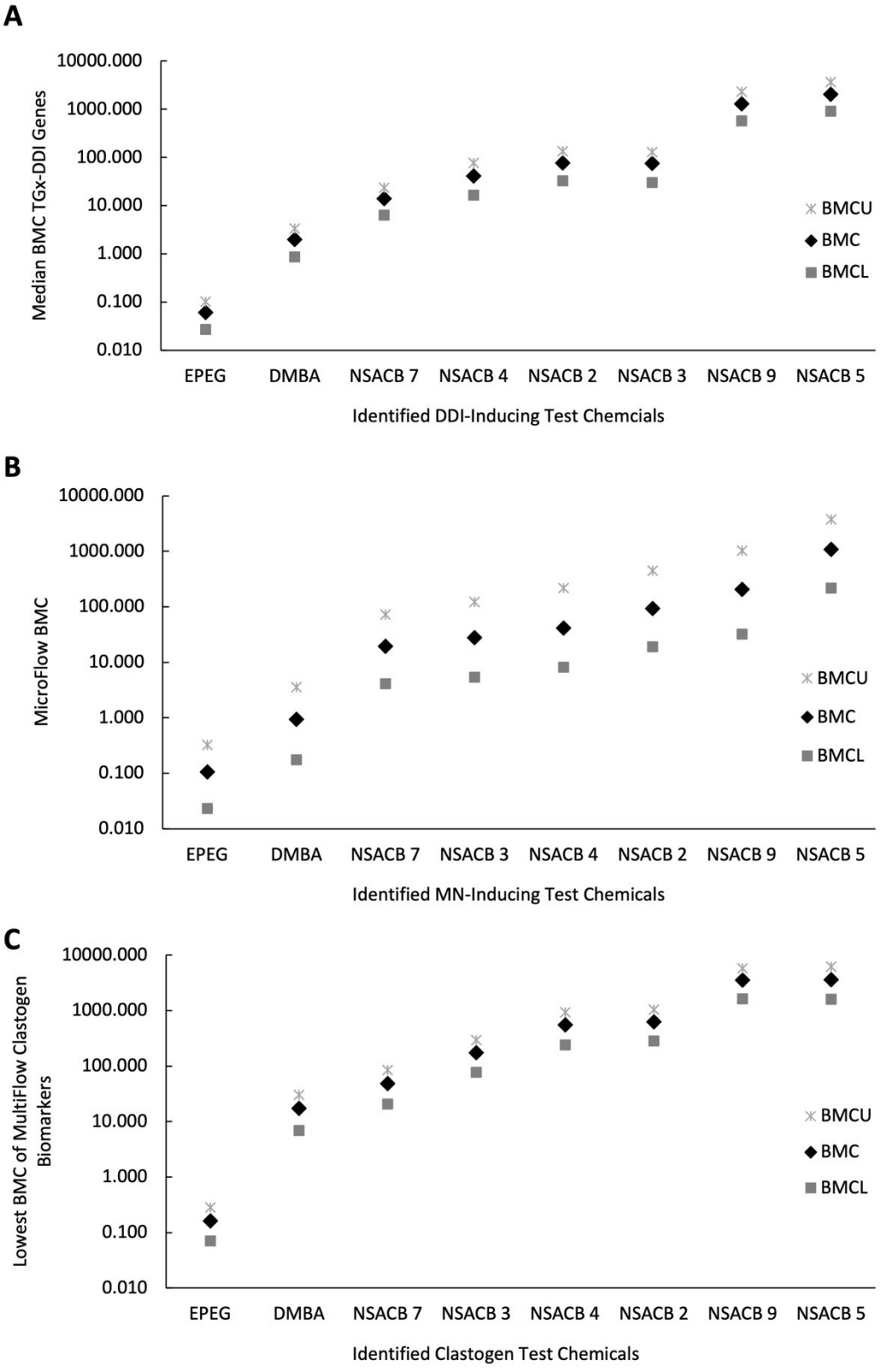

Figure 4: ***Comparison of potency rankings derived from each assay based on the respective Benchmark Concentrations (BMCs) for the NSACB compounds with concordant positive hazard flags.*** (A) The potency ranking from the TGx-DDI transcriptomic biomarker based on *the bootstrapped* median gene BMC, (B) the ranking from the *in vitro* MicroFlow® assay, and (C) the potency ranking from MultiFlow® assay based on the lowest clastogen biomarker BMC.

As with TGx-DDI, two distinct potency groups can be observed for the data-poor compounds. (1) NSACB #7, 3, 4, and 2 make up one equipotent group, and (2) NSABC #9 and 5 make up a distinct, less potent, group. Overall, BMC modeling of the endpoints in the proposed *in vitro* testing strategy yielded nearly identical potency rankings for the genotoxic NSACB compounds.

2.3.6 Integration of concentration-response data for a singular chemical prioritization strategy

The ToxPi software was used to integrate all endpoint BMC metrics into a single score; the scores were subsequently used to rank the NSACB compounds and visualize mechanistic information regarding their genotoxic hazards (Figure 5; Supplementary Figure VII). With respect to the latter, the analyses generated toxicological profile graphics for each compound. The endpoints are represented by the coloured pie slices; the radius of each slice denotes the relative effect size expressed as -log10 BMC. Thus, a lower endpoint BMC, which reflects higher potency, is indicated by greater protrusion from the origin. To compare to the independent endpoint BMC rankings displayed in Figure 4, the compounds with concordant positive hazard flags were first ranked based on their overall ToxPi scores for all endpoints (Figure 5a). The greater the overall ToxPi score, the more potent the compound. In this case, the most potent to least potent ranking was: EPEG > DMBA > NSACB 7 > NSACB 4 > NSACB 2 > NSACB 3 > NSACB 9 > NSACB 5. More specifically, based on the presented ToxPi profile (Figure 5a), EPEG is the most potent for five of the six endpoints examined: TGx-DDI, MN, 4H ɣH2AX, 24H p53 and 4H p53. In contrast, except for a small 4H p53 slice, NSACB #5 had almost no slices protruding from the centre. The majority of the compounds, with the exception of NSACB #4, 2, and 9, lacked a 24H ɣH2AX slice. Comparisons of multiplexed ToxPi profiles (Figure 5b) showed that compounds #7,

3, 4, and 2 clustered together on a single branch; NSACB #9 and 5 clustered separately. This clustering is similar to the potency groupings observed in Figures 4A and 4C.

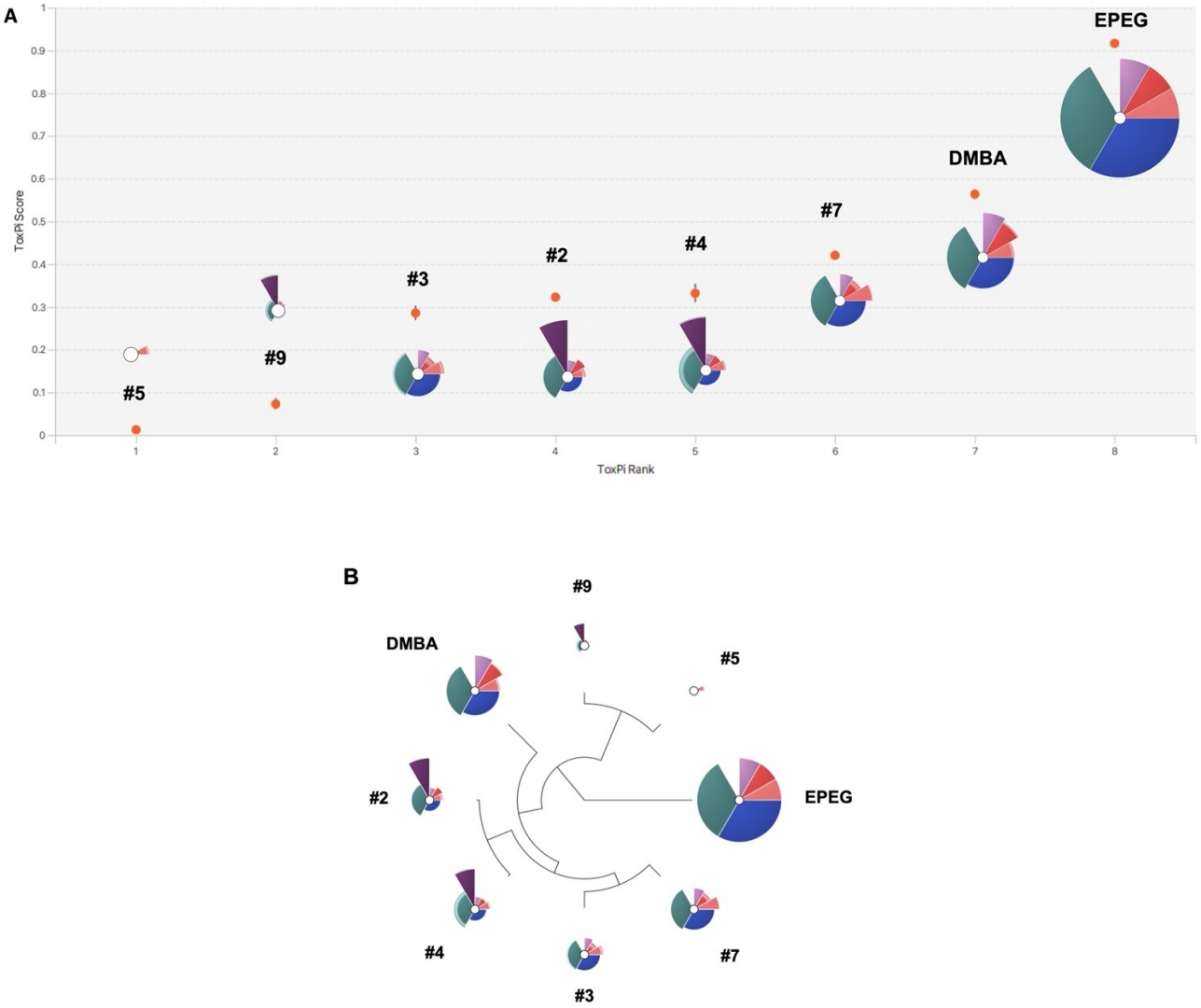

Figure 5: ToxPi visualization of multiplexed BMCs for the NSACB compounds with concordant positive hazard flags. (A) ToxPi score rankings and profiles for the data-poor compounds. For the ToxPi profiles, the distance of each slice from the origin indicates the slice score and endpoint potency (i.e., -log10 BMC). Slices represent the following endpoints: teal is TGx-DDI BMC, blue is MicroFlow® BMC, pink and purple are the MultiFlow® BMCs (i.e., dark pink is 24H p53, light pink is 4H p53, dark purple is 24H γH2AX, light purple is 4H γH2AX). Lower and upper bound confidence intervals are indicated by lighter shaded areas at the periphery of each slice. The width of each slice indicates the assigned endpoint weight. The TGx-DDI, MicroFlow®, and combined MultiFlow® endpoints each represent 1/3 of the profile. (B) Hierarchical clustering of the ToxPi profiles. The ToxPi algorithm groups substances with similar toxicological profiles.

An additional ToxPi analysis was conducted for all NSACB compounds (Supplementary Figure VII), including those with discordant results (i.e., #1, 6, 8 and 10). In this case, the most potent to least potent ranking was: EPEG > DMBA > NSACB 7 > NSACB 4 > NSACB 1 > NSACB 2 > NSACB 3 > NSACB 8 > NSACB 9 > NSACB 6 > NSACB 5 > NSACB 10. The ToxPi profile of compound #1 clustered with #7, 3, 4 and 2, while the profiles of compounds #6, 8 and 10 clustered with #9 and 5.

2.4 Discussion

TGx biomarkers are envisioned to provide a powerful NAM for modernizing toxicological testing by enabling rapid extraction of mechanistic information from data-rich transcriptomic datasets (Li et al., 2017). Preliminary data support that pairing TGx biomarkers, such as TGx-DDI, with additional markers of DNA damage (e.g., *in vitro* MN assay and high-throughput CometChip®) is a highly effective approach for accurate and efficient genotoxicity assessment (Buick et al., 2017, 2020, 2021). Flow-cytometry based assays have been developed to detect and quantify increases in markers of genotoxicity (i.e., MN, p53, ɣH2AX, p-H3, polyploidy). The integrated analysis of these endpoints has demonstrated efficacy in enhanced genotoxicity assessment (Smart et al., 2020; Avlasevich et al., 2021). Herein we combined the TGx-DDI transcriptomic biomarker in high-throughput format with the MicroFlow® and MultiFlow® DNA damage assays to explore application as an integrated test strategy for genotoxicity assessment of data-poor compounds. Human-relevant TK6 human lymphoblastoid cells were exposed to 10 data-poor test chemicals prioritized by Health Canada's NSACB in conjunction with 3 control chemicals. We established hazard calls and potency ranking for each assay and then explored concordance and integration of the tests. Our results indicate that all ten NSACB compounds were positive in at least one assay. Six NSACB compounds (#2, 3, 4, 5, 7, and 9) had concordant results between all three assays, and four were discordant. NSACB #1 and #8 were positive in the TGx-DDI and MicroFlow® assays, but were identified as non-genotoxicants by the MultiFlow® assay. NSACB #6 and #10 tested positive only in the MicroFlow® assay and were classified as non-DDI and non-genotoxicants by the TGx-DDI and MultiFlow® assays. Though

providing critical insight individually, our work demonstrates the value of integrating these assays to strengthen confidence in hazard identification and chemical potency ranking.

To establish that the assays were performing as expected, the results of three reference control chemicals were examined. EPEG was identified as positive by the TGx-DDI biomarker, had significant concentration-dependent fold-increases in MN, and induced the clastogen biomarkers 4H/24H p53 and 4H γH2AX. As a topoisomerase II inhibitor, EPEG inhibits DNA synthesis and causes double-strand breaks (Montecucco et al., 2015). Thus, the results obtained by the test strategy were in line with expectations. Similarly, the positive control chemical DMBA displayed a strong TGx-DDI response, MN induction, and increases in the clastogen biomarkers 4H and 24H γH2AX. DMBA is metabolized into 3,4-diol-1,2-epoxide that reacts with DNA to form bulky adducts (RamaKrishna et al., 1992); DMBA has been shown to induce chromosome damage *in vitro* (Matsushima et al., 1999; Von Der Hude et al., 2000) and *in vivo* (De Boeck et al., 2005). In contrast, the negative control, DMANN, did not yield any positive calls in any of the assays. It is well established that DMANN is non-genotoxic; and it is a negative control for assessing the performance of new or improved genotoxicity tests (Kirkland et al., 2016).

We then explored the hazard calls made for the data-poor NSACB compounds. Eight out of ten (NSACB #1, 2, 3, 4, 5, 7, 8, and 9) were classified as DDI; all ten were positive for MN induction; five were identified as clastogens (NSACB #2, 3, 5, 7, 9); and one was identified as a pan-genotoxicant (NSACB #4) in at least one S9 condition. Six of our data-poor compounds (NSACB #2, 3, 4, 5, 7, and 9) had concordant results; i.e., DDI, MN inducing, and clastogenic calls for the TGx-DDI, MicroFlow®, MultiFlow® assays, respectively. Thus, we conclude that these

compounds are genotoxic *in vitro*, causing DNA damage via a clastogenic MoA. Although these are data-poor compounds, there are a few supporting reports for these findings. For example, NSACB #7 caused a statistically significant and biologically relevant increase in the frequency of %MN +S9 (OECD 487) and an equivocal result -S9 (SCCS, 2006). Similarly, we observed a notably stronger %MN frequency in the +S9 condition at the highest concentration (Supplemental Figure IV). NSACB #5 and 7 were positive in previous studies using the *in vitro* mammalian chromosome aberration test (OECD 473) (SCCS, 2007, 2013). NSACB #5 was clastogenic following a short-term treatment +S9 (6h) and after continuous treatment -S9 (24h) (SCCS, 2013). This aligns with our MultiFlow® results showing a strong response in clastogen-related biomarkers in both S9 conditions for multiple concentrations (i.e., 4H ɣH2AX, 4H p53). NSACB #9 induced structural chromosome aberrations in the presence of S9 and the results were equivocal -S9 (SCCS, 2007). In our MultiFlow® results, we observed strong fold-increases in clastogenic biomarkers 4H and 24H ɣH2AX in both S9 conditions. The European Commission report also noted for NSACB #9 that there was no increase in the frequency of polyploidy metaphase in both S9 conditions; however, one experiment out of two did show an increase in the rate of endomitotic metaphase in multiple concentrations +S9 (SCCS, 2007). With endomitosis, cells can enter mitosis but the division of chromosomes is not followed by cytokinesis (i.e., no dissolution of the nuclear membrane) resulting in an increased number of chromosomes in the cell (Vitrat et al., 1998). Interestingly, we observed a significant increase in p-H3 (i.e., an aneugenic marker for mitotic delay) in a single concentration. However, it was only observed in the -S9 condition and no other aneugenic biomarkers were significantly increased. Overall, our results contribute to the weight-of-evidence for the genotoxicity of

these compounds and provide new evidence for those where little toxicological data, if any, exist. Therefore, we recommend that these compounds be prioritized for further regulatory scrutiny.

Conversely, there were four instances of discordant test results across the three assays. Two compounds, NSACB #6 and #10, were identified as non-DDI by TGx-DDI but yielded positive results in the MN test (NSACB #10 +S9 only, NSACB #6 -S9 and +S9). Since MN can occur from mechanisms affecting cell division/mitotic machinery leading to aneuploidy (i.e., aneugen) (Luzhna et al., 2013), we speculated that these compounds may be aneugens. An example of this is colchicine, a known aneugenic agent, which is positive for MN but negative (non-DDI) by TGx-DDI (Buick et al., 2020). An advantage of integrating the MultiFlow® assay into the test strategy is that it can differentiate clastogenic from aneugenic mechanisms. The MultiFlow® assay classified both NSACB #6 and #10 as non-genotoxicants. Thus, the MultiFlow® results suggest that NSACB #6 and #10 are likely irrelevant positives in the MN test. It is well established that genotoxicity tests in mammalian cells have low specificity in predicting genotoxic effects manifested *in vivo*, often reporting irrelevant positives that do not pose an appreciable mutagenic risk in humans (Kirkland et al., 2007; Guyton et al., 2009; Dearfield et al., 2011). Indeed, Kirkland et al. determined that mammalian *in vitro* chromosome damage tests in particular had specificity for carcinogenicity of < 45% (Kirkland et al., 2005, 2006). This could be due to several factors. For one, cellular endpoints can be induced from chemical stressors not primarily attacking DNA (i.e., non-genotoxic mechanisms) or from cytotoxicity. At high concentrations, some chemical agents induce mammalian cell death. This can cause DNA degradation and fragmentation as a result of cellular metabolism, and not as a direct DNA-

damaging mechanism of the chemical agents themselves (Williams et al., 1974); thus, these chemicals produce an irrelevant positive genotoxicity call. Known cytotoxicants such as carbonyl cyanide m-chlorphenyl hydrazone (CCCP) induce MN in the MicroFlow® assay, but have been correctly classified as non-genotoxicants by the MultiFlow® assay (Avlasevich et al., 2021). Moreover, the TGx-DDI transcriptomic biomarker was originally designed to provide biological relevance as a complement to positive chromosome damage assay results by identifying changes in gene expression that predict a DDI mechanism (Li et al., 2017). In subsequent works, Li et al. have demonstrated the utility of the biomarker for this purpose, i.e., classifying 90% (i.e., 9 out of 10) irrelevant positives identified in *in vitro* chromosome damage assays (Li et al., 2017). Therefore, it is plausible from our results that NSACB #6 and #10 are irrelevant positives operating either as cytotoxicants (i.e., NSACB #6 was cytotoxic) or via non-genotoxic mechanisms.

The last two compounds, NSACB #1 and #8, were identified as weakly DDI by TGx-DDI (both in +S9 conditions only) and MN-inducing by MicroFlow® (#1 in both S9 conditions, #8 only +S9). However, they were both also identified as non-genotoxicants by the MultiFlow® assay. Given that both the TGx-DDI biomarker and MultiFlow® assay are DNA damage reporter assays that rely on transcriptional and cellular changes in DNA damage response pathways (i.e., p53 and related genes), we expected to see a high correlation in hazard calls between these two assays. Of the 13 test chemicals, 11 (i.e., 85%) had concordant calls between these two assays; NSACB #1 and #8 are the only two where this was not the case. However, it is important to note the weakness of the DDI calls for these two compounds. NSACB #1 had one DDI call at the highest concentration in the NSC-PA only. NSACB #8 had two DDI calls at the highest

concentration by NSC-PA and PCA. In addition, the PCA call was visibly borderline, with the concentration grouping with the training set DDI compounds just left of the classification line on the PCA plot (Supplementary Figure III-K). Moreover, in both cases the highest concentration analyzed was very close to the viability threshold of 40% (i.e., 43% for NSACB #1 +S9, and 46% for NSACB #8); thus, high cytotoxicity could be leading to a misclassification. Alternatively, the discordant results between TGx-DDI and MultiFlow® could be due to different assay sensitivities. Nonetheless, both compounds induced strong concentration-dependent increases in %MN. Therefore, although these results are somewhat ambiguous, in order to be conservative further analyses should be considered to explore their DDI potential. This could include mutagenicity testing *in vitro*; alternatively, their transcriptomic profiles could be examined for further mechanistic insights. One advantage of the TGx-DDI assay is that the transcriptomic dataset is not limited to the 64 biomarker genes; there are additional expression data for remaining the approximately 2500 genes in the TempO-Seq™ S1500+ set (Mav et al., 2018). Thus, applying high-throughput transcriptomic test strategies, such as the one developed by Harrill et al., could also be used to identify biological perturbations via pathway analyses and derive transcriptional biological pathway altering concentrations (BPACs) (Harrill et al., 2021) to provide more insight into the toxicity of NSACB compounds #1 and #8.

In addition to determining qualitative genotoxicity calls (i.e., hazard identification), there has been a growing momentum in quantitative analyses of genotoxicity concentration-response data to derive potency metrics for potency ranking and regulatory decision-making (Johnson et al., 2014; MacGregor et al., 2015; White et al., 2020). BMC modeling aims to determine the concentration required to elicit a predefined change in response in relation to

background. Herein, we investigated the consistency of potency rankings based on BMC analysis across these *in vitro* assays. In order to directly compare the rankings we limited our analysis to the six compounds and two controls that were positive across all three assays. First, we derived an overall BMC for the TGx-DDI biomarker by calculating a bootstrap BMC confidence interval. Previous work has established that transcriptomic BMC values correlate well with those from apical endpoints *in vivo* (Thomas et al., 2011, 2013; Farmahin et al., 2017). Moreover, as shown by Buick et al., the bootstrap median BMC enables more biomarker genes to be modeled, allows for the generation of 95% confidence intervals, and resulted in identical potency rankings between TGx-DDI and the *in vitro* high-throughput comet assay (Buick et al., 2021). Second, to calculate an overall MultiFlow® BMC, the four clastogen biomarkers (i.e., 4H/24H p53, 4H/24H γH2AX) were modeled for each compound. The biomarker with the lowest BMC was selected as the BMC for potency ranking since this would represent the most sensitive, and thus, conservative, endpoint. Using this approach, the potency ranking for all the assays were nearly identical. The only exception was NSACB #3, which was slightly more potent in the TGx-DDI assay, surpassing NSACB #4 and #2. However, the confidence intervals overlapped for these three compounds and thus they are considered equipotent. Two main potency groups (i.e., NSACB #7, 4, 2, 3 and NSACB # 9, 5) were observed for both the TGx-DDI and MultiFlow® chemical rankings. For MicroFlow®, the confidence intervals were larger resulting in one equipotent group encompassing all data-poor compounds. Overall, independent quantitative analyses derived concordant potency rankings and groupings across the assays.

As modernized *in vitro* test strategies are being developed and applied for qualitative and quantitative analysis there is a growing need to supplement this work with new approaches that combine and interpret the large amounts of data generated for decision making. Prioritization software tools, such as ToxPi, that combine results from multiple data streams and reduce it to one metric have been used for this purpose. Avlasevich et al. (2021) explored the integration of quantitative BMC modeling with the ToxPi software to combine and visualize concentration-response data from MultiFlow® and MicroFlow® endpoints to derive a unitless ToxPi score for a singular chemical prioritization strategy. We applied a similar approach to our genotoxicity assessment by aggregating all endpoint BMC metrics into ToxPi scores to rank the NSACB compounds and visualize their genotoxic hazards. To adequately compare to the individual assay potency rankings, only the concordant positive compounds were modeled (Figure 5). Remarkably, we observed a highly similar ToxPi pattern to the individual assay potency rankings. EPEG and DMBA were the most potent and the NSACB compound rankings were identical to the TGx-DDI assay ranking. It is important to note that we eliminated the 24H γH2AX endpoint for many compounds. This is due to a lack of a robust response in this endpoint resulting in an incalculable BMC or infinite BMCU; thus, for a meaningful ToxPi score comparison it is important to have a set of chemicals that elicit robust responses for each endpoint.

It is important to highlight one major caveat with the ToxPi approach. For each analysis, the ToxPi scores are derived as a relative comparison of the compounds in the dataset. Thus, each score is only meaningful in the context in which it was produced (USNRC, 2014a). Consequently, comparing ToxPi scores from separate analyses with different sets of compounds

would be misleading; a new analysis would need to be completed with all the compounds in question to accurately compare their potencies.

For the test strategy investigated in this study to be applied for further screening of data-poor compounds, it will first be essential to establish scientific confidence in this NAM-based approach for regulatory acceptance. Increasing numbers of new testing methods are being developed to improve chemical (geno)toxicological assessment; however, there is a growing bottleneck when it comes to implementation of these methods for risk assessment activities. Traditional validation processes, including the OECD Guidance Document (OECD GD 34) on the Validation and International Acceptance of New or Updated Test Methods for Hazard Assessment (OECD, 2005) can be time-consuming and complicated to navigate. Thus, there is growing recognition that updated frameworks, such as the ones described by van der Zalm et al. (2022) and Parish et al. (2020), are urgently needed to increase confidence in NAMs, thereby supporting accelerated regulatory uptake that is nevertheless aligned with the key principles employed for traditional validations (Parish et al., 2020; van der Zalm et al., 2022). As such, in this case study we have defined and demonstrated the context-of-use for the proposed NAM as the screening of data-poor compounds for genotoxicity hazard identification and prioritization. Future work will need to conduct technical characterization to assess the performance (i.e., accuracy) and reproducibility of the multiplexed NAM, as well as to establish human relevance of the endpoints examined (e.g., endpoints relevant to adverse outcome pathways (AOPs)). Performance studies are underway within the GeneTox21 research program to evaluate the proposed NAM (in addition to three other modernized *in vitro* assays) with four classes of reference compounds with diverse mechanisms.

In summary, this study demonstrates that the integration of an established transcriptomic (i.e., TGx-DDI transcriptomic biomarker) and two flow cytometry-based assays (MultiFlow® DNA Damage Assay and *in vitro* MicroFlow®) enabled an effective assessment of genotoxicity and revealed detailed mechanistic insights for ten data-poor compounds that were prioritized for evaluation by *in silico* screening. Moreover, comparison of BMC values derived from modeling concentration-response data enabled potency ranking of these compounds for further prioritization. Ultimately, this work applies a modernized approach for effective genotoxicity assessment, including chemical prioritization for further regulatory scrutiny; and importantly; the research contributes to the establishment of a confidence framework for the adoption and implementation of multiplexed NAMs for chemicals safety assessment. In addition, the considerable genotoxicity data generated in this study will provide regulators with crucial information regarding the hazard of these data-poor NSACB compounds.

2.5 References

Avlasevich, S., Pellegrin, T., Godse, M., Bryce, S., Bemis, J., Bajorski, P., et al. (2021). Biomarkers of DNA damage response improve in vitro micronucleus assays by revealing genotoxic mode of action and reducing the occurrence of irrelevant positive results. *Mutagenesis* 36, 407–418. doi: 10.1093/MUTAGE/GEAB039.

Barton-Maclaren, T. S., Westphal, M., Sarwar, E., Mattison, D., Chiu, W. A., Dix, D., et al. (2017). Challenges and opportunities in the risk assessment of existing substances in Canada: Lessons learned from the international community. *Int. J. Risk Assess. Manag.* 20, 261–283. doi: 10.1504/IJRAM.2017.082569.

Becker, R. A., Chambers, J. M., and Wilks, A. R. (1990). The New S Language, A Programming Environment for Data Analysis and Graphics. *Econ. J.* 100, 650. doi: 10.2307/2234167.

Bernacki, D. T., Bryce, S. M., Bemis, J. C., Kirkland, D., and Dertinger, S. D. (2016). γH2AX and p53 responses in TK6 cells discriminate promutagens and nongenotoxicants in the presence of rat liver S9. *Environ. Mol. Mutagen.* 57, 546–558. doi: 10.1002/em.22028.

Bryce, S. M., Avlasevich, S. L., Bemis, J. C., Lukamowicz, M., Elhajouji, A., Van Goethem, F., et al. (2008). Interlaboratory evaluation of a flow cytometric, high content in vitro micronucleus assay. *Mutat. Res. - Genet. Toxicol. Environ. Mutagen.* 650, 181–195. doi: 10.1016/j.mrgentox.2007.11.006.

Bryce, S. M., Avlasevich, S. L., Bemis, J. C., Phonethepswath, S., and Dertinger, S. D. (2010). Miniaturized flow cytometric in vitro micronucleus assay represents an efficient tool for comprehensively characterizing genotoxicity dose-response relationships. *Mutat. Res. - Genet. Toxicol. Environ. Mutagen.* 703, 191–199. doi: 10.1016/j.mrgentox.2010.08.020.

Bryce, S. M., Avlasevich, S. L., Bemis, J. C., Tate, M., Walmsley, R. M., Saad, F., et al. (2013). Flow cytometric 96-well microplate-based in vitro micronucleus assay with human TK6 cells: Protocol optimization and transferability assessment. *Environ. Mol. Mutagen.* 54, 180–194. doi: 10.1002/em.21760.

Bryce, S. M., Bemis, J. C., Mereness, J. A., Spellman, R. A., Moss, J., Dickinson, D., et al. (2014). Interpreting in vitro micronucleus positive results: Simple biomarker matrix discriminates clastogens, aneugens, and misleading positive agents. *Environ. Mol. Mutagen.* 55, 542–555. doi: 10.1002/em.21868.

Bryce, S. M., Bernacki, D. T., Bemis, J. C., and Dertinger, S. D. (2016). Genotoxic mode of action predictions from a multiplexed flow cytometric assay and a machine learning approach. *Environ. Mol. Mutagen.* 57, 171–189. doi: 10.1002/em.21996.

Bryce, S. M., Bernacki, D. T., Bemis, J. C., Spellman, R. A., Engel, M. E., Schuler, M., et al. (2017). Interlaboratory evaluation of a multiplexed high information content in vitro genotoxicity assay. *Environ. Mol. Mutagen.* 58, 146–161. doi: 10.1002/EM.22083.

Buick, J. K., Moffat, I., Williams, A., Swartz, C. D., Recio, L., Hyduke, D. R., et al. (2015). Integration of metabolic activation with a predictive toxicogenomics signature to classify genotoxic versus nongenotoxic chemicals in human TK6 cells. *Environ. Mol. Mutagen.* 56, 520–534. doi: 10.1002/em.21940.

Buick, J. K., Williams, A., Gagné, R., Swartz, C. D., Recio, L., Ferguson, S. S., et al. (2020). Flow cytometric micronucleus assay and TGx-DDI transcriptomic biomarker analysis of ten

genotoxic and non-genotoxic chemicals in human HepaRG™ cells. *Genes Environ.* 42, 5. doi: 10.1186/s41021-019-0139-2.

Buick, J. K., Williams, A., Kuo, B., Wills, J. W., Swartz, C. D., Recio, L., et al. (2017). Integration of the TGx-28.65 genomic biomarker with the flow cytometry micronucleus test to assess the genotoxicity of disperse orange and 1,2,4-benzenetriol in human TK6 cells. *Mutat. Res. - Fundam. Mol. Mech. Mutagen.* 806, 51–62. doi: 10.1016/j.mrfmmm.2017.09.002.

Buick, J. K., Williams, A., Meier, M. J., Swartz, C. D., Recio, L., Gagné, R., et al. (2021). A Modern Genotoxicity Testing Paradigm: Integration of the High-Throughput CometChip® and the TGx-DDI Transcriptomic Biomarker in Human HepaRG™ Cell Cultures. *Front. Public Heal.* 9, 1144.

Cho, E., Buick, J. K., Williams, A., Chen, R., Li, H. H., Corton, J. C., et al. (2019). Assessment of the performance of the TGx-DDI biomarker to detect DNA damage-inducing agents using quantitative RT-PCR in TK6 cells. *Environ. Mol. Mutagen.* 60, 122–133. doi: 10.1002/em.22257.

Council of Canadian Academies (2017). Integrating emerging technologies into chemical safety assessment: Progress since the 2012 report of the expert panel on the integrated testing of pesticides. *Int. J. Risk Assess. Manag.* 20, 46–58. doi: 10.1504/IJRAM.2017.082559.

De Boeck, M., Van Der Leede, B. J., Van Goethem, F., De Smedt, A., Steemans, M., Lampo, A., et al. (2005). Flow cytometric analysis of micronucleated reticulocytes: Time- and dose-dependent response of known mutagens in mice, using multiple blood sampling. *Environ. Mol. Mutagen.* 46, 30–42. doi: 10.1002/em.20127.

Dearfield, K. L., Thybaud, V., Cimino, M. C., Custer, L., Czich, A., Harvey, J. S., et al. (2011). Follow-up actions from positive results of in vitro genetic toxicity testing. *Environ. Mol. Mutagen.* 52, 177–204. doi: 10.1002/em.20617.

Dimitrov, S. D., Diderich, R., Sobanski, T., Pavlov, T. S., Chankov, G. V., Chapkanov, A. S., et al. (2016). QSAR Toolbox – workflow and major functionalities. *SAR QSAR Environ. Res.* 27, 203–219. doi: 10.1080/1062936X.2015.1136680.

ECHA (2016). *New approach methodologies in regulatory science : proceedings of a scientific workshop : Helsinki, 19-20 April 2016*. European Chemicals Agency.

Farmahin, R., Williams, A., Kuo, B., Chepelev, N. L., Thomas, R. S., Barton-Maclaren, T. S., et al. (2017). Recommended approaches in the application of toxicogenomics to derive points of departure for chemical risk assessment. *Arch. Toxicol.* 91, 2045–2065. doi: 10.1007/s00204-016-1886-5.

Felter, S. P., Bhat, V. S., Botham, P. A., Bussard, D. A., Casey, W., Hayes, A. W., et al. (2021). Assessing chemical carcinogenicity: hazard identification, classification, and risk assessment. Insight from a Toxicology Forum state-of-the-science workshop. *Crit. Rev. Toxicol.* 51, 653–694. doi: 10.1080/10408444.2021.2003295.

Guyton, K. Z., Kyle, A. D., Aubrecht, J., Cogliano, V. J., Eastmond, D. A., Jackson, M., et al. (2009). Improving prediction of chemical carcinogenicity by considering multiple mechanisms and applying toxicogenomic approaches. *Mutat. Res. - Rev. Mutat. Res.* 681, 230–240. doi: 10.1016/j.mrrev.2008.10.001.

Harrill, J. A., Everett, L. J., Haggard, D. E., Sheffield, T., Bundy, J. L., Willis, C. M., et al. (2021). High-Throughput Transcriptomics Platform for Screening Environmental Chemicals. *Toxicol. Sci.* 181, 68–89. doi: 10.1093/toxsci/kfab009.

Health Canada (2021). Chemicals Management Plan Science Committee background paper: Evolution of the Existing Substances Risk Assessment Program under the Canadian Environmental Protection Act, 1999 and considerations looking forward Chemicals Management Plan (CMP) Science Com. Available at: https://www.canada.ca/en/health-canada/services/chemical-substances/chemicals-management-plan/science-committee/meeting-records-reports/background-paper-evolution-existing-substances-risk-assessment-program-canadian-environmental-protection-act-1999.html [Accessed May 26, 2022].

Heflich, R. H., Johnson, G. E., Zeller, A., Marchetti, F., Douglas, G. R., Witt, K. L., et al. (2020). Mutation as a Toxicological Endpoint for Regulatory Decision-Making. *Environ. Mol. Mutagen.* 61, 34–41. doi: 10.1002/em.22338.

ICH (1998). *Genotoxicity: A Standard Battery for Genotoxicity Testing of Pharmaceuticals (ICH Topic S2B)*. International Conference on Harmonisation of Technical Requirements for Registration of Pharmaceuticals for Human Use.

Johnson, G. E., Soeteman-Hernández, L. G., Gollapudi, B. B., Bodger, O. G., Dearfield, K. L., Heflich, R. H., et al. (2014). Derivation of point of departure (PoD) estimates in genetic toxicology studies and their potential applications in risk assessment. *Environ. Mol. Mutagen.* 55, 609–623. doi: 10.1002/em.21870.

Kavlock, R. J., Bahadori, T., Barton-Maclaren, T. S., Gwinn, M. R., Rasenberg, M., and Thomas, R. S. (2018). Accelerating the Pace of Chemical Risk Assessment. *Chem. Res. Toxicol.* 31, 287–290. doi: 10.1021/acs.chemrestox.7b00339.

Kirkland, D., Aardema, M., Henderson, L., and Müller, L. (2005). Evaluation of the ability of a battery of three in vitro genotoxicity tests to discriminate rodent carcinogens and non-carcinogens: I. Sensitivity, specificity and relative predictivity. *Mutat. Res. - Genet. Toxicol. Environ. Mutagen.* 584, 1–256. doi: 10.1016/j.mrgentox.2005.02.004.

Kirkland, D., Aardema, M., Müller, L., and Hayashi, M. (2006). Evaluation of the ability of a battery of three in vitro genotoxicity tests to discriminate rodent carcinogens and non-carcinogens. II. Further analysis of mammalian cell results, relative predictivity and tumour profiles. *Mutat. Res. - Genet. Toxicol. Environ. Mutagen.* 608, 29–42. doi: 10.1016/j.mrgentox.2006.04.017.

Kirkland, D., Kasper, P., Martus, H. J., Müller, L., van Benthem, J., Madia, F., et al. (2016). Updated recommended lists of genotoxic and non-genotoxic chemicals for assessment of the performance of new or improved genotoxicity tests. *Mutat. Res. Toxicol. Environ. Mutagen.* 795, 7–30.

Kirkland, D., Pfuhler, S., Tweats, D., Aardema, M., Corvi, R., Darroudi, F., et al. (2007). How to reduce false positive results when undertaking in vitro genotoxicity testing and thus avoid unnecessary follow-up animal tests: Report of an ECVAM Workshop. *Mutat. Res. - Genet. Toxicol. Environ. Mutagen.* 628, 31–55. doi: 10.1016/j.mrgentox.2006.11.008.

Krewski, D., Andersen, M. E., Tyshenko, M. G., Krishnan, K., Hartung, T., Boekelheide, K., et al. (2020). Toxicity testing in the 21st century: progress in the past decade and future perspectives. *Arch. Toxicol.* 94, 3. doi: 10.1007/s00204-019-02613-4.

Li, H.-H., Hyduke, D. R., Chen, R., Heard, P., Yauk, C. L., Aubrecht, J., et al. (2015). Development of a toxicogenomics signature for genotoxicity using a dose-optimization and informatics strategy in human cells. *Environ. Mol. Mutagen.* 56, 505–519. doi: 10.1002/em.21941.

Li, H.-H., Yauk, C. L., Chen, R., Hyduke, D. R., Williams, A., Frötschl, R., et al. (2019). TGx-DDI, a Transcriptomic Biomarker for Genotoxicity Hazard Assessment of Pharmaceuticals and Environmental Chemicals. *Front. Big Data* 2, 36. doi: 10.3389/fdata.2019.00036.

Li, H. H., Chen, R., Hyduke, D. R., Williams, A., Frötschl, R., Ellinger-Ziegelbauer, H., et al. (2017). Development and validation of a high-throughput transcriptomic biomarker to address 21st century genetic toxicology needs. *Proc. Natl. Acad. Sci. U. S. A.* 114, E10881–E10889. doi: 10.1073/pnas.1714109114.

Long, A. S., Wills, J. W., Krolak, D., Guo, M., Dertinger, S. D., Arlt, V. M., et al. (2018). Benchmark dose analyses of multiple genetic toxicity endpoints permit robust, cross-tissue comparisons of MutaMouse responses to orally delivered benzo[a]pyrene. *Arch. Toxicol.* 92, 967. doi: 10.1007/S00204-017-2099-2.

Luzhna, L., Kathiria, P., and Kovalchuk, O. (2013). Micronuclei in genotoxicity assessment: From genetics to epigenetics and beyond. *Front. Genet.* 4, 131. doi: 10.3389/fgene.2013.00131.

MacGregor, J. T., Frötschl, R., White, P. A., Crump, K. S., Eastmond, D. A., Fukushima, S., et al. (2015). IWGT report on quantitative approaches to genotoxicity risk assessment II. Use of point-of-departure (PoD) metrics in defining acceptable exposure limits and assessing human risk. *Mutat. Res. - Genet. Toxicol. Environ. Mutagen.* 783, 66–78. doi: 10.1016/j.mrgentox.2014.10.008.

Marvel, S. W., To, K., Grimm, F. A., Wright, F. A., Rusyn, I., and Reif, D. M. (2018). ToxPi Graphical User Interface 2.0: Dynamic exploration, visualization, and sharing of integrated data models. *BMC Bioinformatics* 19, 1–7. doi: 10.1186/S12859-018-2089-2/FIGURES/3.

Matsushima, T., Hayashi, M., Matsuoka, A., Ishidate, M., Miura, K. F., Shimizu, H., et al. (1999). Validation study of the in vitro micronucleus test in a Chinese hamster lung cell line (CHL/IU). *Mutagenesis* 14, 569–580. doi: 10.1093/mutage/14.6.569.

Mav, D., Shah, R. R., Howard, B. E., Auerbach, S. S., Bushel, P. R., Collins, J. B., et al. (2018). A hybrid gene selection approach to create the S1500+ targeted gene sets for use in high-throughput transcriptomics. *PLoS One* 13, e0191105. doi: 10.1371/journal.pone.0191105.

Moffat, I., Chepelev, N. L., Labib, S., Bourdon-Lacombe, J., Kuo, B., Buick, J. K., et al. (2015). Comparison of toxicogenomics and traditional approaches to inform mode of action and points of departure in human health risk assessment of benzo[a]pyrene in drinking water. *Crit. Rev. Toxicol.* 45, 1–43. doi: 10.3109/10408444.2014.973934.

Montecucco, A., Zanetta, F., and Biamonti, G. (2015). Molecular mechanisms of etoposide. *EXCLI J.* 14, 95–108. doi: 10.17179/excli2014-561.

Nesslany, F. (2017). The current limitations of in vitro genotoxicity testing and their relevance to the in vivo situation. *Food Chem. Toxicol.* 106, 609–615. doi: https://doi.org/10.1016/j.fct.2016.08.035.

OECD (2005). "No. 34: Guidance document on the validation and international acceptance of new or updated test methods for hazard assessment," in *OECD Series on Testing and Assessment* (Paris: OECD Publishing), 1–96.

OECD (2016). "Test No. 487: In Vitro Mammalian Cell Micronucleus Test," in *OECD Guidelines for the Testing of Chemicals* (Paris: OECD Publishing). doi: https://doi.org/10.1787/9789264264861-en.

OECD (2017). "No.238: Overview of the set of OECD Genetic Toxicology Test Guidelines and updates performed in 2014-2015," in *OECD Series on Testing and Assessment* (Paris: OECD

Publishing), 1–70.
Parish, S. T., Aschner, M., Casey, W., Corvaro, M., Embry, M. R., Fitzpatrick, S., et al. (2020). An evaluation framework for new approach methodologies (NAMs) for human health safety assessment. *Regul. Toxicol. Pharmacol.* 112, 104592. doi: 10.1016/j.yrtph.2020.104592.
Pfuhler, S., Fautz, R., Ouedraogo, G., Latil, A., Kenny, J., Moore, C., et al. (2014). The Cosmetics Europe strategy for animal-free genotoxicity testing: Project status up-date. *Toxicol. Vitr.* 28, 18–23. doi: 10.1016/j.tiv.2013.06.004.
Phillips, D. H., and Arlt, V. M. (2009). "Genotoxicity: damage to DNA and its consequences.," in *Molecular, Clinical and Environmental Toxicology Volume 1: Molecular Toxicology* (Birkhäuser Basel), 87–110. doi: 10.1007/978-3-7643-8336-7_4.
RamaKrishna, N. V. S., Devanesan, P. D., Rogan, E. G., Cavalieri, E. L., Jeong, H., Jankowiak, R., et al. (1992). Mechanism of Metabolic Activation of the Potent Carcinogen 7,12-Dimethylbenz[a]anthracene. *Chem. Res. Toxicol.* 5, 220–226. doi: 10.1021/tx00026a011.
Reif, D. M., Sypa, M., Lock, E. F., Wright, F. A., Wilson, A., Cathey, T., et al. (2013). ToxPi GUI: an interactive visualization tool for transparent integration of data from diverse sources of evidence. *Bioinformatics* 29, 402. doi: 10.1093/BIOINFORMATICS/BTS686.
SCCS (2006). *Opinion of the Scientific Committee on Consumer Products on 2-Amino-4-hydroxethylamino-anisole sulfate COLIPA N° A84*. European Commission Health & Consumer Protection Directorate-General.
SCCS (2007). *Opinion of the Scientific Committee on Consumer Products on 4-Hydroxypropylamino-3-nitrophenol COLIPA N° B100*. European Commission Health & Consumer Protection Directorate-General.
SCCS (2013). *Opinion of the Scientific Committee on Consumer Safety on 2,6-Diaminopyridine COLIPA N°A136*. European Commission Health & Consumer Protection Directorate-General doi: 10.2772/51143.
Schoeters, G. (2010). The REACH perspective: Toward a new concept of toxicity testing. *J. Toxicol. Environ. Heal. - Part B Crit. Rev.* 13, 232–241. doi: 10.1080/10937404.2010.483938.
Smart, D. J., Helbling, F. R., Verardo, M., Huber, A., McHugh, D., and Vanscheeuwijck, P. (2020). Development of an integrated assay in human TK6 cells to permit comprehensive genotoxicity analysis in vitro. *Mutat. Res. Toxicol. Environ. Mutagen.* 849, 503129.
Thomas, R. R., Wesselkamper, S. C., Wang, N. C. Y., Zhao, J. J., Petersen, D. D., Lambert, J. C., et al. (2013). Temporal concordance between apical and transcriptional points of departure for chemical risk assessment. *Toxicol. Sci.* 134, 180–194. doi: 10.1093/toxsci/kft094.
Thomas, R. S., Clewell, H. J., Allen, B. C., Wesselkamper, S. C., Wang, N. C. Y., Lambert, J. C., et al. (2011). Application of transcriptional benchmark dose values in quantitative cancer and noncancer risk assessment. *Toxicol. Sci.* 120, 194–205. doi: 10.1093/toxsci/kfq355.
Thybaud, V., Aardema, M., Clements, J., Dearfield, K., Galloway, S., Hayashi, M., et al. (2007). Strategy for genotoxicity testing: Hazard identification and risk assessment in relation to in vitro testing. *Mutat. Res. - Genet. Toxicol. Environ. Mutagen.* 627, 41–58. doi: 10.1016/j.mrgentox.2006.10.003.
Tibshirani, R., Hastie, T., Narasimhan, B., and Chu, G. (2002). Diagnosis of multiple cancer types by shrunken centroids of gene expression. *Proc. Natl. Acad. Sci. U. S. A.* 99, 6567–6572. doi: 10.1073/pnas.082099299.

USFDA (2007). "Short-Term Tests for Genetic Toxicity," in *Guidance for Industry and Other Stakeholders Toxicological Principles for the Safety Assessment of Food Ingredients Redbook 2000* (Rockville, MD: United States Food and Drug Administration), 55–58. Available at: https://www.fda.gov/regulatory-information/search-fda-guidance-documents/redbook-2000-ivc1-short-term-tests-genetic-toxicity.

USNRC (2007). *Toxicity testing in the 21st century: A vision and a strategy*. Washingon, DC: National Academies Press doi: 10.17226/11970.

USNRC (2014). "Appendix C Toxicological Priority Index (ToxPi)," in *A Framework to Guide Selection of Chemical Alternatives* (Washington, DC: The National Academies Press). doi: https://doi.org/10.17226/18872.

USNTP (2018). *Research Report on National Toxicology Program Approach to Genomic Dose-Response Modeling*. Durham, NC: National Toxicology Program Available at: https://www.ncbi.nlm.nih.gov/books/NBK531562/.

van der Zalm, A. J., Barroso, J., Browne, P., Casey, W., Gordon, J., Henry, T. R., et al. (2022). A framework for establishing scientific confidence in new approach methodologies. *Arch. Toxicol.* 1, 1–15. doi: 10.1007/s00204-022-03365-4.

Venables, W. N., and Ripley, B. D. (2002). *Modern Applied Statistics with S*. New York, NY: Springer New York doi: 10.1007/978-0-387-21706-2.

Vitrat, N., Cohen-Solal, K., Pique, C., Le Couedic, J. P., Norol, F., Larsen, A. K., et al. (1998). Endomitosis of human megakaryocytes are due to abortive mitosis. *Blood* 91, 3711–3723. doi: 10.1182/blood.v91.10.3711.

Von Der Hude, W., Kalweit, S., Engelhardt, G., McKiernan, S., Kasper, P., Slacik-Erben, R., et al. (2000). In vitro micronucleus assay with Chinese hamster V79 cells - Results of a collaborative study with in situ exposure to 26 chemical substances. *Mutat. Res. - Genet. Toxicol. Environ. Mutagen.* 468, 137–163. doi: 10.1016/S1383-5718(00)00045-0.

White, P. A., Long, A. S., and Johnson, G. E. (2020). Quantitative Interpretation of Genetic Toxicity Dose-Response Data for Risk Assessment and Regulatory Decision-Making: Current Status and Emerging Priorities. *Environ. Mol. Mutagen.* 61, 66–83. doi: 10.1002/em.22351.

Williams, J. R., Little, J. B., and Shipley, W. U. (1974). Association of mammalian cell death with a specific endonucleolytic degradation of DNA. *Nature* 252, 754–755. doi: 10.1038/252754a0.

Yauk, C. L., Buick, J. K., Williams, A., Swartz, C. D., Recio, L., Li, H. H., et al. (2016). Application of the TGx-28.65 transcriptomic biomarker to classify genotoxic and non-genotoxic chemicals in human TK6 cells in the presence of rat liver S9. *Environ. Mol. Mutagen.* 57, 243–260. doi: 10.1002/em.22004.

Yauk, C. L., Cheung, C., Barton-Maclaren, T. S., Boucher, S., Bourdon-Lacombe, J., Chauhan, V., et al. (2019). Toxicogenomic applications in risk assessment at Health Canada. *Curr. Opin. Toxicol.* 18, 34–45. doi: 10.1016/j.cotox.2019.02.005.

Yeakley, J. M., Shepard, P. J., Goyena, D. E., VanSteenhouse, H. C., McComb, J. D., and Seligmann, B. E. (2017). A trichostatin A expression signature identified by TempO-Seq targeted whole transcriptome profiling. *PLoS One* 12, e0178302. doi: 10.1371/journal.pone.0178302.

Chapter Three

3.1 Summary of Study Outcomes

There is an urgent need to address the immense backlog of environmental chemicals requiring evaluation by regulatory bodies worldwide. Consequently, there exists a large number of data-poor compounds with very little to no experimental toxicology data (Barton-Maclaren et al., 2017). The conventional test battery for genotoxicity testing is not amenable to assessing the large numbers of chemicals that require evaluation in an effective or efficient manner (Kirkland et al., 2007; Thybaud et al., 2007; Nesslany, 2017). Thus, developing NAM-based genotoxicity test strategies are essential for modernizing genotoxicity testing for 21st-centrury needs (Krewski et al., 2010, 2020).

The overarching objective of this thesis was to investigate the utility of the TGx-DDI transcriptomic biomarker, multiplexed with alternative assays part of the GeneTox21 research program (i.e., the *in vitro* MicroFlow® assay and the MultiFlow® DNA damage assay), as a NAM-based, integrated testing strategy for assessing the genotoxicity of select data-poor compounds prioritized by Health Canada's New Substances Assessment and Control Bureau (NSACB). Human lymphoblastoid TK6 cells were exposed to ten NSACB data-poor substances in conjunction with three reference controls. The data-poor compounds were flagged by regulatory partners as having carcinogenicity/genotoxicity structural alerts using the OECD QSAR Toolbox. Cells were exposed for 4 hours with or without exogenous metabolic activation (i.e., rat liver S9) to a range of concentrations. Genotoxicity classifications were compared between the TGx-DDI, the MicroFlow®, and MultiFlow® assays. BMC modeling of the genotoxicity endpoints was used to rank the test chemicals by their potencies. The ToxPi

software (Reif et al., 2013; Marvel et al., 2018) was applied to integrate the multiplexed endpoint BMCs to create a visual toxicological profile for chemical prioritization.

Overall, applying this integrated test strategy we identified all ten data-poor compounds as positive in at least one assay. Six compounds had concordant positive results in the TGx-DDI, MicroFlow®, and MultiFlow® assays. Two compounds were only positive in the MicroFlow® assay. The remaining two compounds were positive in the TGx-DDI and MicroFlow® assays but negative in MultiFlow®. As discussed herein, the integration of these assays provided a complementary approach to support hazard calls with detailed mechanistic insights; this approach enabled a more wholistic view of genotoxicity than each assay could provide individually. Moreover, when applying quantitative analyses of concentration-response data, we observed nearly identical potency rankings derived from each individual assay. Remarkably, this ranking was maintained when all the endpoint BMCs were converted into a single score using ToxPi, also enabling the visualization of each endpoint and their respective potencies. The major thesis objectives, their respective outcomes, contributions to scientific knowledge, as well as future steps, are discussed below.

3.2 Fulfillment of Thesis Objectives

Objective 1: Use of the TGx-DDI transcriptomic biomarker to evaluate the genotoxicity of data-poor NSACB compounds.

Outcome: The TGx-DDI classification was completed for the test chemicals using the established three-pronged statistical approach. For the data-poor substances, eight out of ten NSACB compounds were identified as DDI based on the overall call, with varying degrees of potency. NSACB compounds #5 and #7 displayed the strongest DDI responses, NSACB #9 had a moderate DDI response, and NSACB #1, 2, 3, 4, and 8 displayed weak DDI responses. The remaining two compounds NSACB #6 and #10 were identified as non-DDI.

Objective 2: Apply the in vitro MicroFlow® assay and the MultiFlow® DNA Damage assay to evaluate the genotoxicity of the data-poor NSACB compounds.

Outcome: The *in vitro* MicroFlow® assay identified all ten NSACB compounds as MN-inducing in at least one S9 condition. In contrast, for the MultiFlow® assay, only five NSACB compounds were identified as clastogens (#2, 3, 5, 7, and 9), and one compound was identified as pan-genotoxic (#4). The remaining four compounds (#1, 6, 8, and 10) were classified as non-genotoxic.

Objective 3: Compare the hazard calls and potency ranking of the data-poor compounds and evaluate the complementarity of these GeneTox21 assays.

Outcome: When all the data from Objectives 1 and 2 are taken together, important mechanistic insights can be derived for the data-poor compounds assessed in this study. The

complementarity of the combined endpoints is highlighted in the tiered interpretation strategy in Figure 1. In Tier 1, the MicroFlow® assay is applied to identify chromosome damaging agents (i.e., MN-inducing). This is followed up by the TGx-DDI transcriptomic biomarker in Tier 2, which classifies a compound as DDI or non-DDI; thus, the combination of Tier 1 and Tier 2 can differentiate between DDI and non-DDI mechanisms leading to increases in MN frequency. Tier 3, the MultiFlow® assay, can identify clastogens, aneugens, pan-genotoxicants (i.e., mutagens) or non-genotoxicants. Therefore, the combination of Tiers 2 and 3 can determine if a DDI call may be the result of a clastogenic or pan-genotoxic/mutagenic mechanism. The inclusion of Tier 3 for a positive MN assay paired with a non-DDI TGx-DDI call can clarify whether this discrepancy is the result of an aneugenic response or if it is a likely irrelevant positive in regards to the MicroFlow® assay.

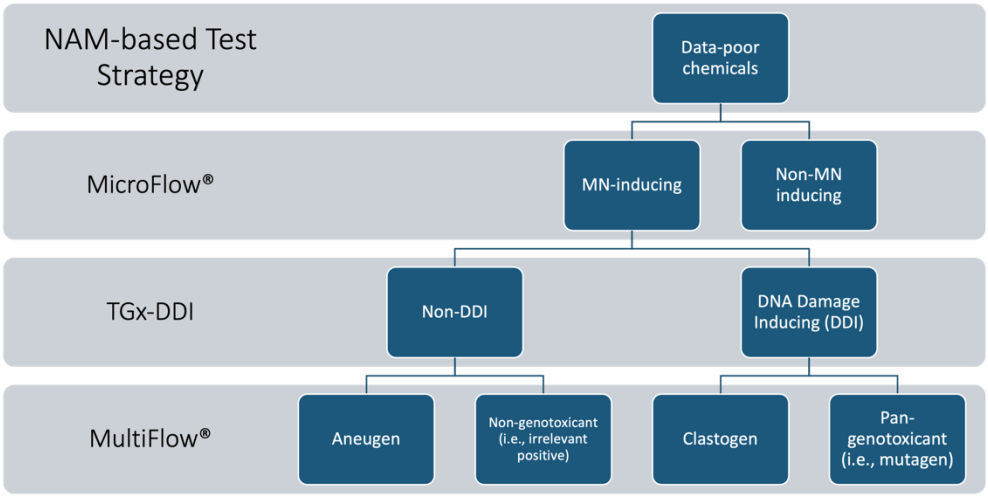

Figure 8: Tiered Interpretation Scheme for Suggested NAM-based Test Strategy for Assessing the Genotoxicity of Data-poor Compounds. The complementary approach applies: (1) the *in vitro* MicroFlow® assay to identify chromosome damaging agents; (2) the TGx-DDI transcriptomic biomarker to classify positive MicroFlow data as operating either via a DNA damage inducing (DDI) or non-DDI mechanism; the (3) MultiFlow® DNA Damage assay to identify clastogens or pan-genotoxic/mutagenic responses, as well to determine if a non-DDI TGx-DDI call may be the result of an aneugenic response or suggesting the compound is non-genotoxic (i.e., signifying a potentially irrelevant positive).

In this study, the integrated hazard calls suggest strongly that compounds #2, 3, 5, 7, and 9 are genotoxic *in vitro*, causing DNA damage via a clastogenic MoA; #4 via a pan-genotoxic MoA. Moreover, compounds #6 and #10 are likely irrelevant positives in the MN test yielding non-DDI and non-genotoxic calls by the TGx-DDI and MultiFlow® assays, respectively. Finally, compounds #1 and 8 are considered possibly genotoxic *in vitro* causing DNA damage with an ambiguous MoA. The significant increases in MN frequency, borderline results from TGx-DDI, and non-genotoxic calls by MultiFlow® suggest that these compounds should undergo further study to confirm genotoxicity (i.e., mutagenicity testing *in vitro*).

In addition to hazard calls, the compounds with concordant results in all three assays underwent quantitative BMC modeling to compare the consistency of potency rankings derived from each individual assay. From this work, we observed nearly identical rankings for the TGx-DDI and MultiFlow® assays. In addition, two main potency groups were observed in both assays: (1) NSACB #7, 3, 4, and 2; and (2) NSACB #9 and 5. Moreover, the MicroFlow® potency ranking was also identical to the MultiFlow® assay. However, in this case, the compounds did not form distinct potency groups due to the larger confidence intervals. Overall, independent BMC modeling for each respective assay revealed nearly identical potency rankings for the test chemicals.

Objective 4: Develop and/or adapt an integrated data analysis tool for the interpretation and visualization of the results obtained using the aforementioned, multiplexed GeneTox21 endpoints.

Outcome: The ToxPi software was applied to combine and visualize the concentration-response data to generate a singular chemical prioritization strategy. Using ToxPi all endpoint BMC metrics were integrated into a single unitless score to rank the NSACB compounds from most potent to least potent: NSACB 7 > NSACB 4 > NSACB 2 > NSACB 3 > NSACB 9 > NSACB 5. Remarkably, the outcome of this work was a highly similar pattern to the individual assay rankings (Objective 3). In addition, this approach enabled the visualization of genotoxic hazards in the form of a single toxicological profile enabling the scrutinizing of MoA groupings. Overall, the ToxPi approach provided an effective visual representation of each chemical's toxicological profile while simultaneously ranking the compounds based on the integrated endpoint BMCs.

3.3 Contribution to Scientific Knowledge

The objectives investigated in this study, and their respective outcomes discussed above, contribute to the advancement of scientific knowledge in the area of NAM-based genotoxicity testing. First, this study generated novel genotoxicity data for prioritized data-poor compounds (i.e., NSACB #1-10). This information will provide our collaborators at the NSACB of Health Canada with crucial information regarding the hazard of these compounds and contribute to the weight-of-evidence assessment.

Although previous work has shown that combinations of the TGx-DDI, MicroFlow®, and MultiFlow® endpoints are effective for genotoxicity assessment, this study is the first to integrate the endpoints of all three assays for a highly complementary approach that delivers detailed mechanistic insights (as highlighted by the data interpretation scheme presented in Figure 1). Moreover, this case-study greatly advances the validation efforts for the TGx-DDI biomarker, which is currently undergoing review by the US FDA's formal regulatory biomarker qualification program (Li et al., 2019), by demonstrating its regulatory utility in the decision-making of data-poor compounds. Secondly, our work demonstrates, for the first time, the consistency of the potency rankings derived from the three assays; thus, supporting their use in such applications. Finally, this study highlights the utility of ToxPi for an integrated quantitative assessment of potency to derive a singular prioritization strategy for further follow-up testing.

3.3 Future Directions

This thesis leaves some intriguing questions and perspectives for future work. The first would be to expand on the additional TGx data generated in this study. The TGx-DDI transcriptomic biomarker addresses several of the limitations of the existing *in vitro* genotoxicity test guidelines. In order to derive the TGx-DDI results, transcriptomic profiles are developed for each experimental sample; thus, the analysis yields data-rich lists of differentially expressed genes (DEGs) for each treatment condition. In this study, this would include data on the 2739 genes that are part of the TempO-Seq™ S1500+ set (Mav et al., 2018). Therefore, the remaining non-TGx-DDI genes could be explored in more detail to probe for other potential hazards. This could be accomplished by applying HTT test strategies, such as the one developed by Harrill et al., to identify biological perturbations by performing pathway analyses and deriving transcriptional biological pathway altering concentrations (BPACs) (Harrill et al., 2021). This could be especially useful for the NSACB compounds that had equivocal results and would contribute to the weight-of-evidence for those identified as genotoxic. In addition, a recent case study extrapolating the S1500+ expression values to the entire transcriptome following tunicamycin exposure resulted in an increase of the number of significant genes, correctly identified tunicamycin-related functional pathways, and improved overall biological interpretations (Mav et al., 2020). Applying a similar approach to the existing S1500+ data for the NSACB compounds would facilitate a more detailed, high-throughput, whole transcriptomic analysis to derive further mechanistic insights.

Another advantage to the TGx approach is that once the transcriptomic data are generated they can be subsequently analyzed with additional biomarkers probing alternative MoAs. One

example is the 81-gene TGx-HDACi transcriptomic biomarker, which was developed to identify epigenotoxicants that act via a histone deacetylase inhibition (HDACi) mechanism (Cho et al., 2021). In fact, the transcriptomic data generated for the NSACB compounds were analyzed with the TGx-HDACi biomarker (data not shown). Although all the compounds were HDACi negative, it does highlight the utility of a TGx approach for retrospective analysis. Moreover, these transcriptomic profiles can join the compendium of toxicological data to develop and validate new transcriptomic biomarkers.

A second area to follow-up from this work would be to compare the results for the data-poor compounds to the remaining GeneTox21 assays. Mutagenicity, in particular, would be an interesting endpoint to add to the existing test strategy. Genotoxicity is a broader term than mutagenicity; not all genotoxic compounds are mutagens, but all mutagens are genotoxic. The test strategy discussed herein suggests strongly that NSACB compounds #2, 3, 4, 5, 7, and 9 are chromosome and DNA damage inducing, but do we also see an increase in mutation frequency by the Ames II assay or *in vitro* TGR assay? Would the DDI or clastogen calls be consistent with an increase in strand breaks detected via CometChip®? Could the other GeneTox21 endpoints clarify ambiguous test results (i.e., NSACB #1 and #8)? On the other hand, is there a better combination of assays for accurate genotoxicity assessment? These are all questions likely to be explored with future studies as part of the GeneTox21 platform implementation.

Thirdly, there are still many compounds in commercial use that are considered data-poor. Further collaboration with Health Canada's NSACB or the Existing Substances Risk Assessment Bureau would be useful to: 1) screen data-poor compounds with the test strategy to assess genotoxicity, DNA damage, and predict a likely MoA; and 2) prioritize these data-poor

compounds for further scrutiny by incorporating qualitative and quantitative toxicity data. This would yield new experimental data for regulators to apply in their risk assessment and decision-making activities. However, as discussed in Chapter 2, it will first be essential to establish scientific confidence in this NAM-based strategy for regulatory acceptance. This will involve performance evaluation studies, which are underway within the GeneTox21 program, and harnessing modernized frameworks (van der Zalm et al., 2022) that facilitate use in regulatory decision-making.

The quantitative genotoxicity assessments completed in this work highlight some of the challenges encountered when deriving meaningful overall BMC values that integrate several metrics. In the context of transcriptomics, work has shown that BMCs derived from transcriptomic data sets correlate well to those derived from apical endpoints (i.e., DNA strand breaks, chromosomal abnormalities, or mutations) (Buick et al., 2020, 2021). However, the approaches applied to derive a transcriptomic BMC vary, and there is limited consensus on which is best (Farmahin et al., 2017). For the TGx-DDI biomarker, a bootstrapped median BMC, first described by Buick et al., has been shown to be an effective approach (Buick et al., 2021). This study supports that approach, with the data-poor compounds' TGx-DDI BMCs derived using the Buick et al. approach yielding ranking that is nearly identically to that observed using MicroFlow® and MultiFlow® derived BMCs. However, more studies examining different methods of calculating an overall TGx-DDI BMC, and their comparisons to apical BMCs of reference compounds, would permit a thorough assessment of regulatory utility for the TGx-DDI approach. It is a similar challenge when deriving an overall MultiFlow® BMC. Our approach selected the lowest, most conservative, BMC of the clastogen biomarkers modeled.

Theoretically, in the case of an aneugen, the lowest of the aneugenic biomarkers, would be selected. However, similar to the TGx-DDI approach, more studies comparing alternative strategies to derive a BMC (e.g., average of all biomarkers), and comparisons to those derived from apical endpoints, will need to be conducted to assess regulatory utility.

As described in Chapter 2, Avlasevich et al. applied BMC modeling in conjunction with the ToxPi tool to integrate all endpoints from the MultiFlow® assay and MicroFlow® assay to derive an overall ToxPi score for potency comparisons. We leveraged this approach to investigate how a singular potency ranking based on the ToxPi scores would compare to the three individual assay rankings. Although we did observe remarkably similar potency rankings between ToxPi and the individual assays, future works will need to investigate a broader selection of compounds to determine if this is the best approach for integrating several genotoxicity endpoint BMC values.

It is important to note that the ToxPi software is highly customizable. The slices of the toxicological profile, representing the different endpoint metrics, can be easily added or removed; moreover, differential weighting can be applied to provide more emphasis to certain endpoints. Avlasevich et al. used equal weighting for all clastogen, aneugen and pan-genotoxic endpoints; whereas, we applied differential weighting with the rationale that each assay would comprise one third of the overall profile. Thus, each of the four MultiFlow® clastogen biomarkers were 1/12 (8.3%) of the profile, while the TGx-DDI and MN endpoints were 1/3 (33.3%) of the profile. However, the question of whether each endpoint should be weighted equally or differentially is important; and should be explored in future studies. Additionally, the integration of quantitative genotoxicity data should not be limited to the ToxPi software. As

discussed in Chapter 2, there are some important limitations with this tool. Notably, that the ToxPi scores are unique to the context in which they were derived and cannot be compared between analyses; therefore, it is foreseeable that other tools, including those yet to be created, may be better suited to integration of multiplexed toxicological profiles.

Finally, it should be noted that the quantitative metrics (i.e., BMCs) generated in this study can be converted into administered equivalent doses (AEDs) by applying *in vitro* to *in vivo* extrapolation (IVIVE) based on high-throughput toxicokinetic (HTTK) models. AED values represent the estimated oral dose required to generate a steady state concentration in the plasma (i.e., *in viv*o) that is equivalent to the genotoxic concentration *in vitro*. The values can be employed to calculate margin of exposure values (e.g., bioactivity exposure ratios (BERs)) that can be used in risk assessment (Kuo et al., 2022).

To derive an AED, a POD (i.e., BMC) would need to be selected for each compound. In this study, a different BMR was applied to each assay making it difficult to directly compare the BMC values derived for each compound. Generally, the BMC values derived from the TGx-DDI and MicroFlow® assays were similar and markedly more conservative than those derived from the MultiFlow® assay. Thus, for each compound, AEDs could be determined for all PODs and used to calculate and display a range of BER values. Although, as the compounds studied are data-poor, it may be challenging to derive AEDs and BERs in this case. HTTK data would likely need to be generated from *in vitro* plasma protein binding and metabolic clearance assays to predict *in vivo* effects (Wambaugh, 2017). Moreover, it is not clear if there would be enough exposure information on these compounds to derive BERs for risk assessment activities.

3.4 Concluding Remarks

This study demonstrated that the integration a transcriptomic (i.e., TGx-DDI transcriptomic biomarker) and two flow cytometry-based assays (MultiFlow® DNA Damage Assay and *in vitro* MicroFlow®) enabled a robust assessment of genotoxicity; moreover, revealed detailed mechanistic insights for ten data-poor compounds that were prioritized for evaluation. Moreover, comparison of BMC values derived from modeling concentration-response data enabled potency ranking of these compounds for further prioritization. Ultimately, this work contributes to the establishment of a modernized approach for effective genotoxicity assessment, as well as chemical prioritization for further regulatory scrutiny. In addition, the considerable genotoxicity data generated in this study will provide regulators with crucial information regarding the hazard of these data-poor NSACB compounds. Thus, the approach effectively provides essential information to protect Canadians from potentially adverse exposures.

3.5 References

Barton-Maclaren, T. S., Westphal, M., Sarwar, E., Mattison, D., Chiu, W. A., Dix, D., et al. (2017). Challenges and opportunities in the risk assessment of existing substances in Canada: Lessons learned from the international community. *Int. J. Risk Assess. Manag.* 20, 261–283. doi: 10.1504/IJRAM.2017.082569.

Buick, J. K., Williams, A., Gagné, R., Swartz, C. D., Recio, L., Ferguson, S. S., et al. (2020). Flow cytometric micronucleus assay and TGx-DDI transcriptomic biomarker analysis of ten genotoxic and non-genotoxic chemicals in human HepaRG™ cells. *Genes Environ.* 42, 5. doi: 10.1186/s41021-019-0139-2.

Buick, J. K., Williams, A., Meier, M. J., Swartz, C. D., Recio, L., Gagné, R., et al. (2021). A Modern Genotoxicity Testing Paradigm: Integration of the High-Throughput CometChip® and the TGx-DDI Transcriptomic Biomarker in Human HepaRG™ Cell Cultures. *Front. Public Heal.* 9, 1144.

Cho, E., Rowan-Carroll, A., Williams, A., Corton, J. C., Li, H. H., Fornace, A. J., et al. (2021). Development and validation of the TGx-HDACi transcriptomic biomarker to detect histone deacetylase inhibitors in human TK6 cells. *Arch. Toxicol.* 95, 1631–1645. doi: 10.1007/s00204-021-03014-2.

Farmahin, R., Williams, A., Kuo, B., Chepelev, N. L., Thomas, R. S., Barton-Maclaren, T. S., et al. (2017). Recommended approaches in the application of toxicogenomics to derive points of departure for chemical risk assessment. *Arch. Toxicol.* 91, 2045–2065. doi: 10.1007/s00204-016-1886-5.

Harrill, J. A., Everett, L. J., Haggard, D. E., Sheffield, T., Bundy, J. L., Willis, C. M., et al. (2021). High-Throughput Transcriptomics Platform for Screening Environmental Chemicals. *Toxicol. Sci.* 181, 68–89. doi: 10.1093/toxsci/kfab009.

Kirkland, D., Pfuhler, S., Tweats, D., Aardema, M., Corvi, R., Darroudi, F., et al. (2007). How to reduce false positive results when undertaking in vitro genotoxicity testing and thus avoid unnecessary follow-up animal tests: Report of an ECVAM Workshop. *Mutat. Res. - Genet. Toxicol. Environ. Mutagen.* 628, 31–55. doi: 10.1016/j.mrgentox.2006.11.008.

Krewski, D., Acosta, D., Andersen, M., Anderson, H., Bailar, J. C., Boekelheide, K., et al. (2010). Toxicity testing in the 21st century: A vision and a strategy. *J. Toxicol. Environ. Heal. - Part B Crit. Rev.* 13, 51–138. doi: 10.1080/10937404.2010.483176.

Krewski, D., Andersen, M. E., Tyshenko, M. G., Krishnan, K., Hartung, T., Boekelheide, K., et al. (2020). Toxicity testing in the 21st century: progress in the past decade and future perspectives. *Arch. Toxicol.* 94, 3. doi: 10.1007/s00204-019-02613-4.

Kuo, B., Beal, M. A., Wills, J. W., White, P. A., Marchetti, F., Nong, A., et al. (2022). Comprehensive interpretation of in vitro micronucleus test results for 292 chemicals: from hazard identification to risk assessment application. *Arch. Toxicol.* 96, 2067–2085. doi: 10.1007/s00204-022-03286-2.

Li, H.-H., Yauk, C. L., Chen, R., Hyduke, D. R., Williams, A., Frötschl, R., et al. (2019). TGx-DDI, a Transcriptomic Biomarker for Genotoxicity Hazard Assessment of Pharmaceuticals and Environmental Chemicals. *Front. Big Data* 2, 36. doi: 10.3389/fdata.2019.00036.

Marvel, S. W., To, K., Grimm, F. A., Wright, F. A., Rusyn, I., and Reif, D. M. (2018). ToxPi Graphical User Interface 2.0: Dynamic exploration, visualization, and sharing of integrated

data models. *BMC Bioinformatics* 19, 1–7. doi: 10.1186/S12859-018-2089-2/FIGURES/3.
Mav, D., Phadke, D. P., Balik-Meisner, M. R., Merrick, B. A., Auerbach, S., Niemeijer, M., et al. (2020). Utility of Extrapolating Human S1500+ Genes to the Whole Transcriptome: Tunicamycin Case Study. *Bioinform. Biol. Insights* 14, 1177932220952742. doi: 10.1177/1177932220952742.
Mav, D., Shah, R. R., Howard, B. E., Auerbach, S. S., Bushel, P. R., Collins, J. B., et al. (2018). A hybrid gene selection approach to create the S1500+ targeted gene sets for use in high-throughput transcriptomics. *PLoS One* 13, e0191105. doi: 10.1371/journal.pone.0191105.
Nesslany, F. (2017). The current limitations of in vitro genotoxicity testing and their relevance to the in vivo situation. *Food Chem. Toxicol.* 106, 609–615. doi: https://doi.org/10.1016/j.fct.2016.08.035.
Reif, D. M., Sypa, M., Lock, E. F., Wright, F. A., Wilson, A., Cathey, T., et al. (2013). ToxPi GUI: an interactive visualization tool for transparent integration of data from diverse sources of evidence. *Bioinformatics* 29, 402. doi: 10.1093/BIOINFORMATICS/BTS686.
Thybaud, V., Aardema, M., Clements, J., Dearfield, K., Galloway, S., Hayashi, M., et al. (2007). Strategy for genotoxicity testing: Hazard identification and risk assessment in relation to in vitro testing. *Mutat. Res. - Genet. Toxicol. Environ. Mutagen.* 627, 41–58. doi: 10.1016/j.mrgentox.2006.10.003.
van der Zalm, A. J., Barroso, J., Browne, P., Casey, W., Gordon, J., Henry, T. R., et al. (2022). A framework for establishing scientific confidence in new approach methodologies. *Arch. Toxicol.* 1, 1–15. doi: 10.1007/s00204-022-03365-4.
Wambaugh, J. (2017). "httk" EPA's Tool for High Throughput Toxicokinetics. Available at: https://www.epa.gov/sites/default/files/2018-04/documents/intro-to-httk-042717.pdf.

Supplementary Material

4.1 Chapter 1

Supplementary Table I: *Observed transcriptomic responses of the 64-genes comprising the TGx-DDI transcriptomic classifier in response to genotoxic agents (from Li et al. (2015).*

Gene Symbol	Response	p53 Regulated
ACTA2	↑	Yes
AEN	↑	Yes
BTG2	↑	Yes
C12orf5	↑	Yes
CDKN1A	↑	Yes
DDB2	↑	Yes
DUSP14	↑	Yes
E2F7	↑	Yes
EI24	V	Yes
FBX022	↑	Yes
GADD45A	↑	Yes
IKBIP	↑	Yes
MDM2	↑	Yes
PHLDA3	↑	Yes
PPM1D	↑	Yes
RPS27L	↑	Yes
RRM2B	↑	Yes
TP53I3	↑	Yes
TRIAP1	↑	Yes
TRIM22	↑	Yes
ARRDC4	↑	
B3GNT2	↓	
BLOC1S2	↑	
BRMS1L	↑	
CBLB	V	
CCP110	↑	
CEBPD	V	
CENPE	↓	
COIL	V	
DAAM1	V	
DCP1B	↑	
E2F8	↑	
FAM123B	V	
GXYLT1	V	
HIST1H1E	↓	
HIST1H2BB	↓	
HIST1H2BC	↓	
HIST1H2BG	↓	
HIST1H2BI	↓	
HIST1H2BM	↓	
HIST1H2BN	↓	

HIST1H3D	↓	
ID2	V	
ITPKC	↑	
ITPR1	V	
LCE1E	↑	
LRRFIP2	V	
MEX3B	↑	
NLRX1	V	
PCDH8	↑	
PLK3	↑	
PRKAB1	↑	
PRKAB2	↑	
PTGER4	V	
RAPGEF2	↑	
RBM12B	V	
SEL1L	V	
SEMG2	↑	
SERTAD1	↑	
SMAD5	↑	
TM7SF3	↑	
TNFRSF17	↑	
TOPORS	V	
USP41	↑	

Upregulated genes are denoted by a (↑) representing a 1.5 fold increase in expression compared to untreated cells. Downregulated genes are denoted by a (↓) represented a 1.5 fold decrease in expression compared to untreated cells. Genes with variable responses are denoted with a (V). Genes that are known to be involved in the p53 signaling pathway are presented in the last column.

Supplementary Table II: *List of 35 reference chemicals selected by the Research Advisory Committee to evaluate the GeneTox21 program.*

Class	#	Acronym	Compound
Group 1: Compounds that test positive *in vitro*	1	CP	cyclophosphamide
	2	ENU	*N*-ethyl-*N*-nitrosourea
	3	MMS	methylmethanesulfonate
	4	BaP	benzo[*a*]pyrene
	5	DMBA	7,12-dimethylbenz[*a*]anthracene
	6	AAF	2-acetylaminofluorene
	7	DAT	2,4-diaminotoluene
	8	DMN	dimethylnitrosamine
	9	PhIP.HCl	1-methyl-6-phenyl-1H-imidazo[4,5-b]pyridin-2-amine hydrochloride
	10	AB1	aflatoxin B1
	11	CLA	*p*-chloroaniline (free base and HCl salt)
	12	CDDP	cisplatin
	13	EPEG	etoposide
	14	CdCl	cadmium chloride
	15	VLB	vinblastine sulfate
	16	COL	colchicine
	17	HQ	hydroquinone
Group 2: Compounds that test negative *in vitro*	18	AMP	ampicillin trihydrate
	19	MANN	D-mannitol
	20	ALO	alosetron
	21	TD	tolterodine
	22	CETMAC	(2-chloroethyl)trimethylammonium chloride
Group 3: Compounds that frequently test positive *in vitro* despite negative *in vivo*	23	ResOH	1,3-dihydroxybenzene (resorcinol)
	24	EugOH	eugenol
	25	NPOH	*p*-nitrophenol
	26	TBHQ	tertiary-butylhydroquinone
	27	EA	ethyl acrylate
	28	AA	*o*-anthranilic acid
	29	CIPM	chlorpheniramine maleate
	30	ETA	ethionamide
	31	SXZ	sulfisoxazole
Group 4: Compounds that are Ames negative & positive *in vivo* and *in vitro*	32	AM	acrylamide
	33	CHL	chlordane, analytical grade
	34	PbA	lead acetate
	35	PTX	paclitaxel

Supplementary Table III: *List of chemicals selected by the New Substances Assessment and Control Bureau (NSACB) as high priority for genotoxicity assessment using the GeneTox21 program.*

Class	#	CAS #	Compound
In Commerce List Compounds	1	719-59-5	methanone, (2-amino-5-chlorophenyl)
	2	95-84-1	2-amino-4-methylphenol
	3	85264-33-1	3,5-dimethylpyrazole-1-methanol
	4	91-68-9	3-diethylaminophenol
	5	141-86-6	2,6-diaminopyridine
	6	2835-99-6	4-amino-3-methylphenol
	7	24292-52-2	hesperidin methylchalcone
	8	3251-56-7	2-methoxy-4-nitrophenol
	9	603-85-0	2-amino-3-nitrophenol
	10	2835-98-5	2-amino-5-methylphenol
	11	68391-32-2	[8-[(4-amino-3-nitrophenyl)azo]-7-hydroxy-2-naphthyl]trimethylammonium chloride (basic brown 17)
	12	83763-47-7	2-[(3-amino-4-methoxyphenyl)amino]ethanol
	13	100418-33-5	2-[(4-methyl-2-nitrophenyl)amino]ethanol
	14	92952-81-3	4-[(3-hydroxypropyl)amino]-3-nitrophenol
New Approach Methods Substances	15	17832-28-9	1,4-butanediolmonovinylether
	16	764-99-8	di(ethyleneglycol)divinylether
	17	2752-17-2	1-amino-2-(2-amino)ethoxyethane
	18	29911-27-1	1-(1-methyl-2-propoxyethoxy)-2-propanol
	19	98-56-6	1-chloro-4-(trifluoromethyl)benzene
	20	29911-28-2	1-(2-butoxy-1-methylethoxy)propan-2-ol

4.2 Chapter 2

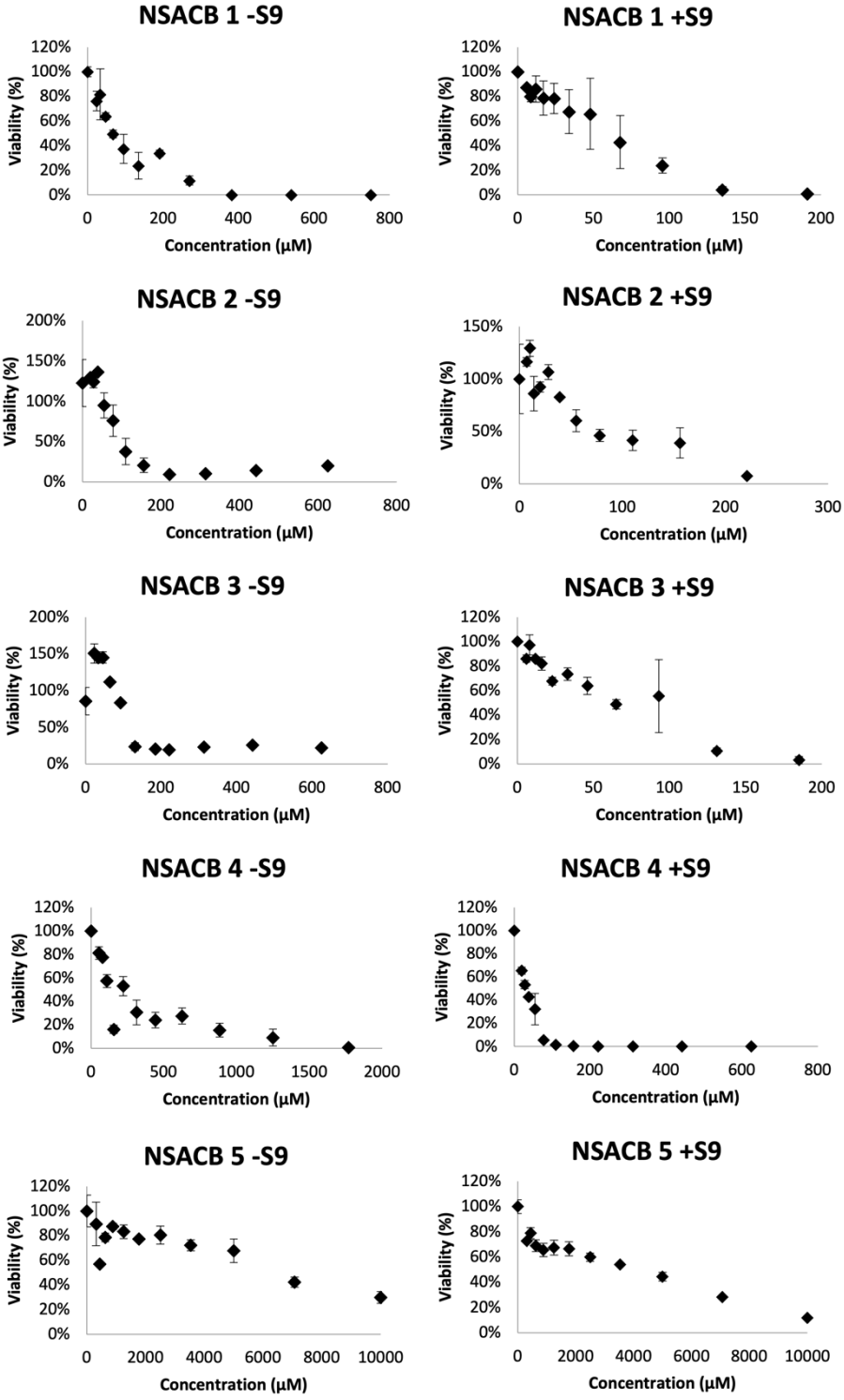
NSACB 1 -S9
Viability (%)
120%
100%
80%
60%
40%
20%
0%
0
200
400
600
800
Concentration (µM)
NSACB 1 +S9
Viability (%)
120%
100%
80%
60%
40%
20%
0%
0
50
100
150
200
Concentration (µM)
NSACB 2 -S9
Viability (%)
200%
150%
100%
50%
0%
0
200
400
600
800
Concentration (µM)
NSACB 2 +S9
Viability (%)
150%
100%
50%
0%
0
100
200
300
Concentration (µM)
NSACB 3 -S9
Viability (%)
200%
150%
100%
50%
0%
0
200
400
600
800
Concentration (µM)
NSACB 3 +S9
Viability (%)
120%
100%
80%
60%
40%
20%
0%
0
50
100
150
200
Concentration (µM)
NSACB 4 -S9
Viability (%)
120%
100%
80%
60%
40%
20%
0%
0
500
1000
1500
2000
Concentration (µM)
NSACB 4 +S9
Viability (%)
120%
100%
80%
60%
40%
20%
0%
0
200
400
600
800
Concentration (µM)
NSACB 5 -S9
Viability (%)
120%
100%
80%
60%
40%
20%
0%
0
2000
4000
6000
8000
10000
Concentration (µM)
NSACB 5 +S9
Viability (%)
120%
100%
80%
60%
40%
20%
0%
0
2000
4000
6000
8000
10000
Concentration (µM)

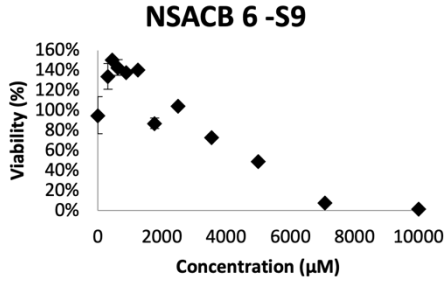
NSACB 6 -S9
Viability (%)
160%
140%
120%
100%
80%
60%
40%
20%
0%
0
2000
4000
6000
8000
10000
Concentration (µM)

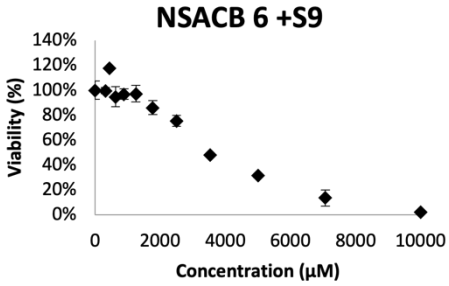
NSACB 6 +S9
Viability (%)
140%
120%
100%
80%
60%
40%
20%
0%
0
2000
4000
6000
8000
10000
Concentration (µM)

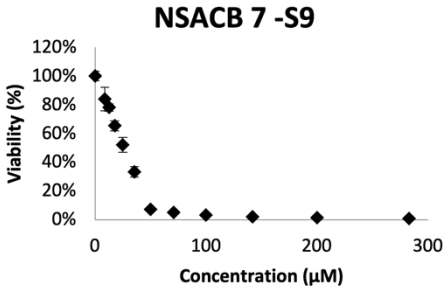
NSACB 7 -S9
Viability (%)
120%
100%
80%
60%
40%
20%
0%
0
100
200
300
Concentration (µM)

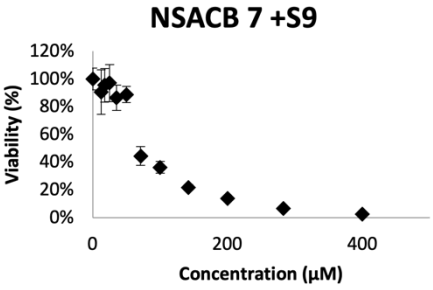
NSACB 7 +S9
Viability (%)
120%
100%
80%
60%
40%
20%
0%
0
200
400
Concentration (µM)

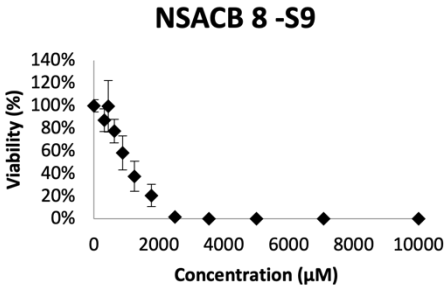
NSACB 8 -S9
Viability (%)
140%
120%
100%
80%
60%
40%
20%
0%
0
2000
4000
6000
8000
10000
Concentration (µM)

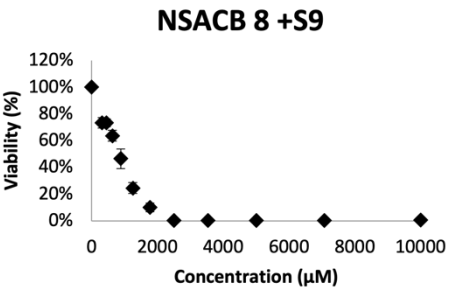
NSACB 8 +S9
Viability (%)
120%
100%
80%
60%
40%
20%
0%
0
2000
4000
6000
8000
10000
Concentration (µM)

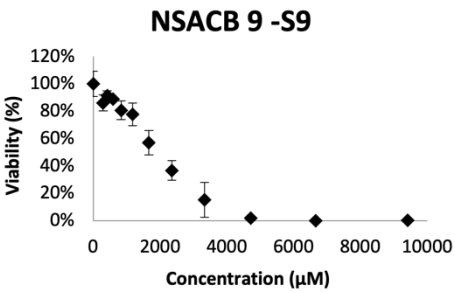
NSACB 9 -S9
Viability (%)
120%
100%
80%
60%
40%
20%
0%
0
2000
4000
6000
8000
10000
Concentration (µM)

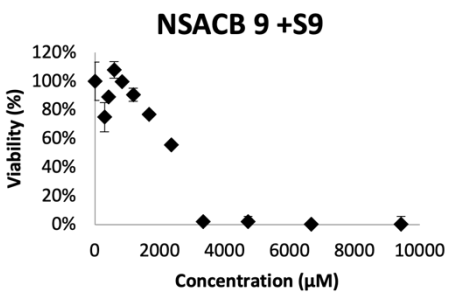
NSACB 9 +S9
Viability (%)
120%
100%
80%
60%
40%
20%
0%
0
2000
4000
6000
8000
10000
Concentration (µM)

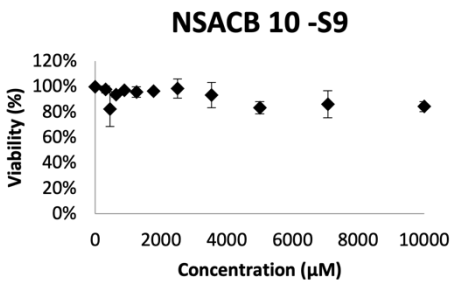
NSACB 10 -S9
Viability (%)
120%
100%
80%
60%
40%
20%
0%
0
2000
4000
6000
8000
10000
Concentration (µM)

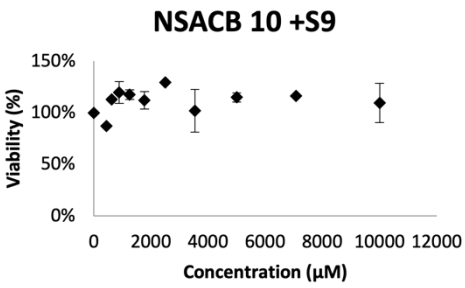
NSACB 10 +S9
Viability (%)
150%
100%
50%
0%
0
2000
4000
6000
8000
10000
12000
Concentration (µM)

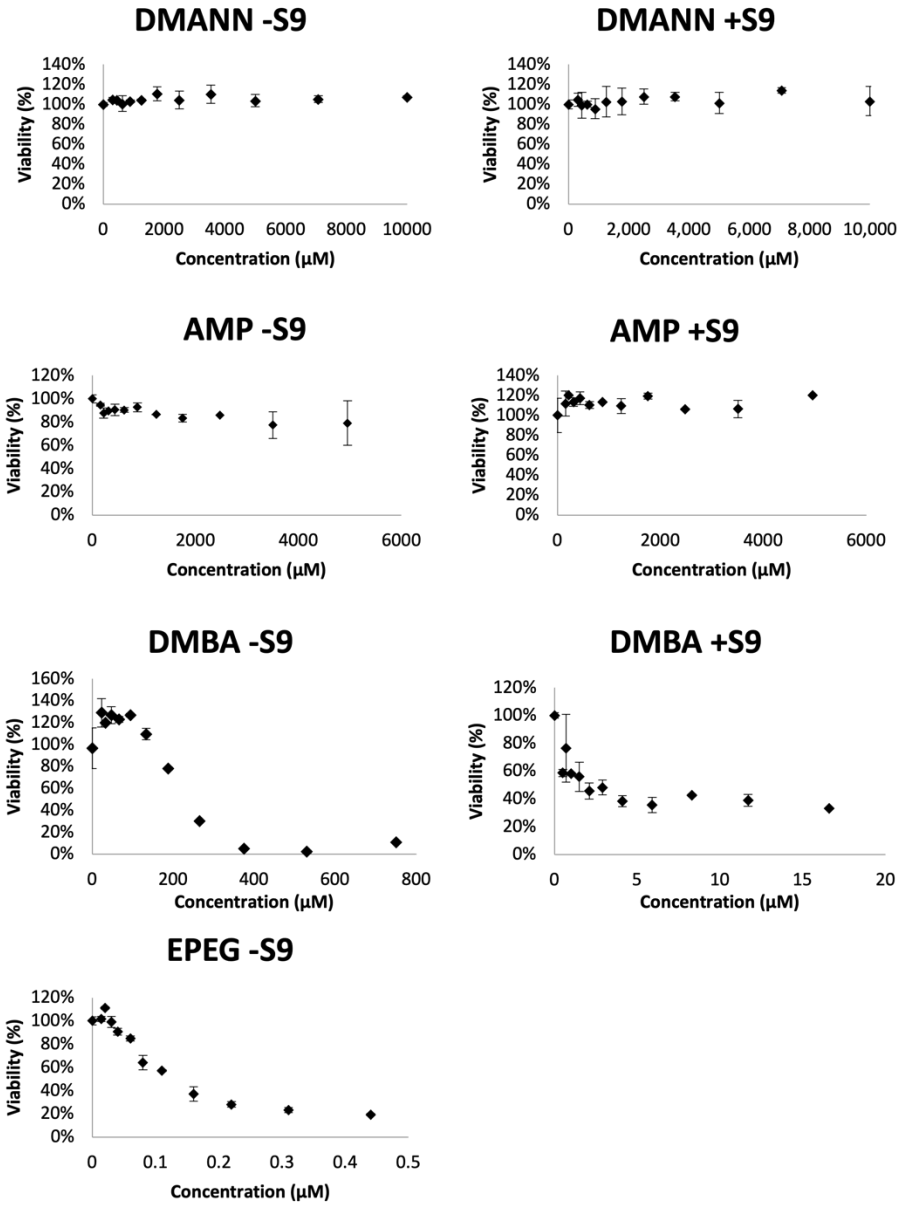

Supplementary Figure I: Viability results for the test chemicals used in this study. All chemicals (with the exception of EPEG) were tested with (+S9) and without (-S9) metabolic activation.

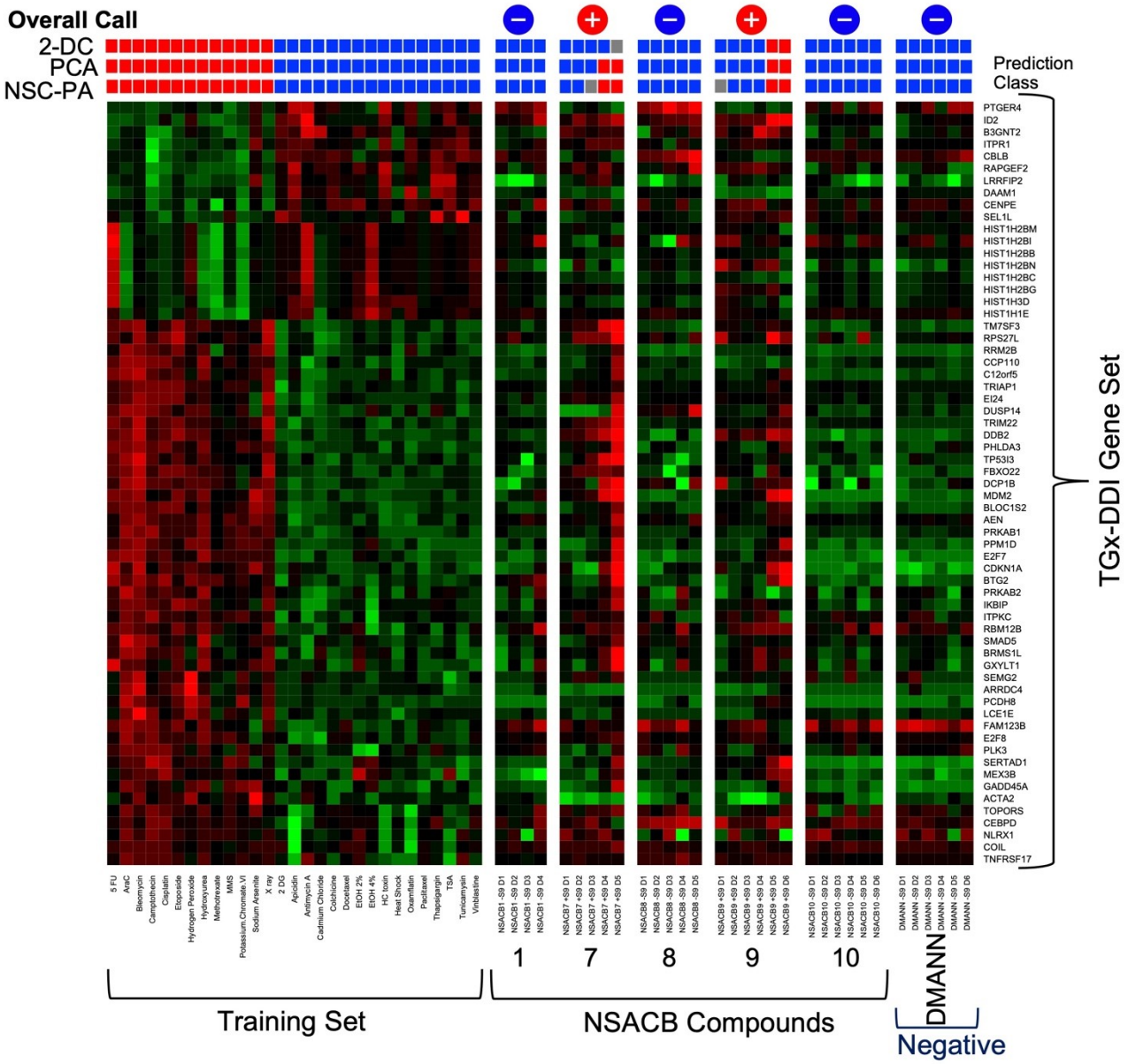

Supplementary Figure II: TGx-DDI classification of NSACB data-poor compounds. The heatmap on the left depicts the 28 reference chemicals used as a training set to generate the biomarker. The color scale indicates the average gene expression fold changes of two replicates relative to solvent control: up-regulated genes are shown in red, down-regulated genes are shown in green, genes with no change are shown in black. Three analyses: (1) 2-dimensional hierarchical clustering (2-DC), (2) principal component analysis (PCA), and (3) nearest shrunken centroid probability analysis (NSC-PA) were used to determine classification probabilities shown for all treatment conditions using red (genotoxic), blue (non-genotoxic), and grey (inconclusive) boxes. The overall calls are also shown at the top of each column: "+" signifies a positive DDI call, "-" signifies a non-DDI call. D1 represents the lowest concentration tested, D6 the highest. Cytotoxic concentrations (< 40% relative survival) were removed from the analysis. Presented -S9 condition for #1, 8, 10, DMANN. Presented +S9 condition for #7 and 9.

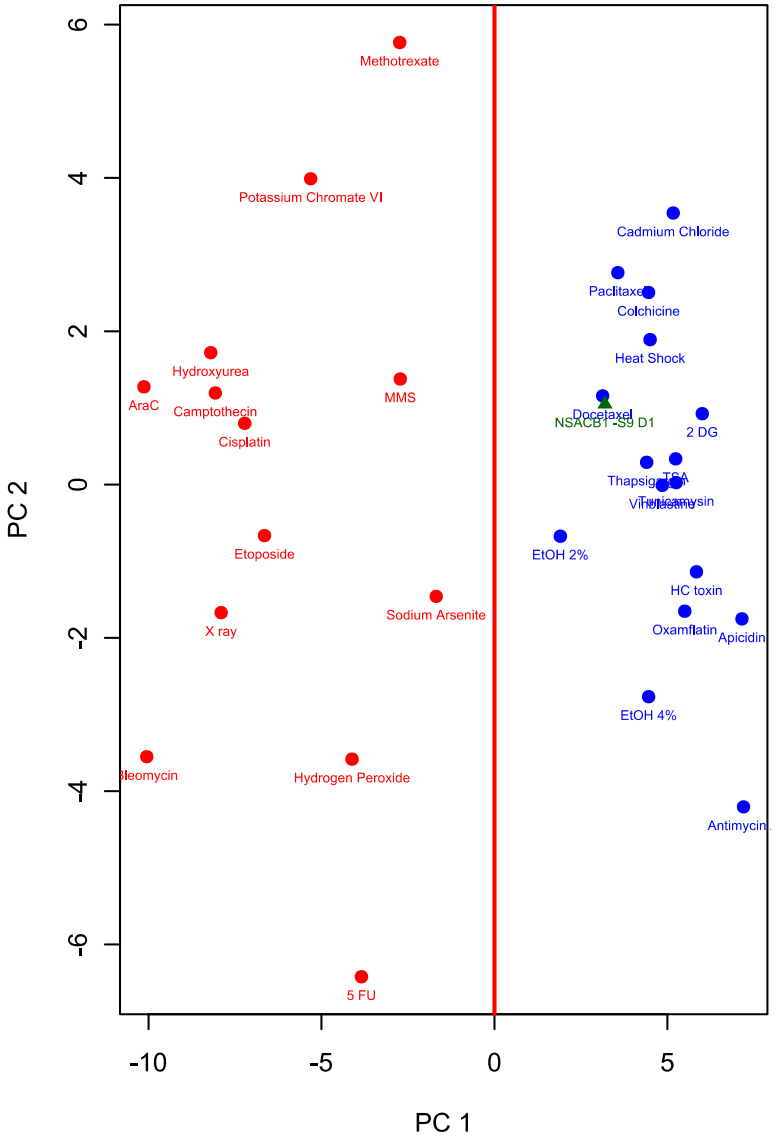
PC 2
PC 1
6
4
2
0
-2
-4
-6
-10
-5
0
5
Methotrexate
Potassium Chromate VI
Cadmium Chloride
Paclitaxel
Colchicine
Heat Shock
Hydroxyurea
AraC
Camptothecin
Cisplatin
MMS
Docetaxel
NSACB1 -S9 D1
2 DG
Thapsigargin
TSA
Tunicamycin
Vinblastine
Etoposide
EtOH 2%
HC toxin
Sodium Arsenite
X ray
Oxamflatin
Apicidin
EtOH 4%
Bleomycin
Hydrogen Peroxide
Antimycin
5 FU

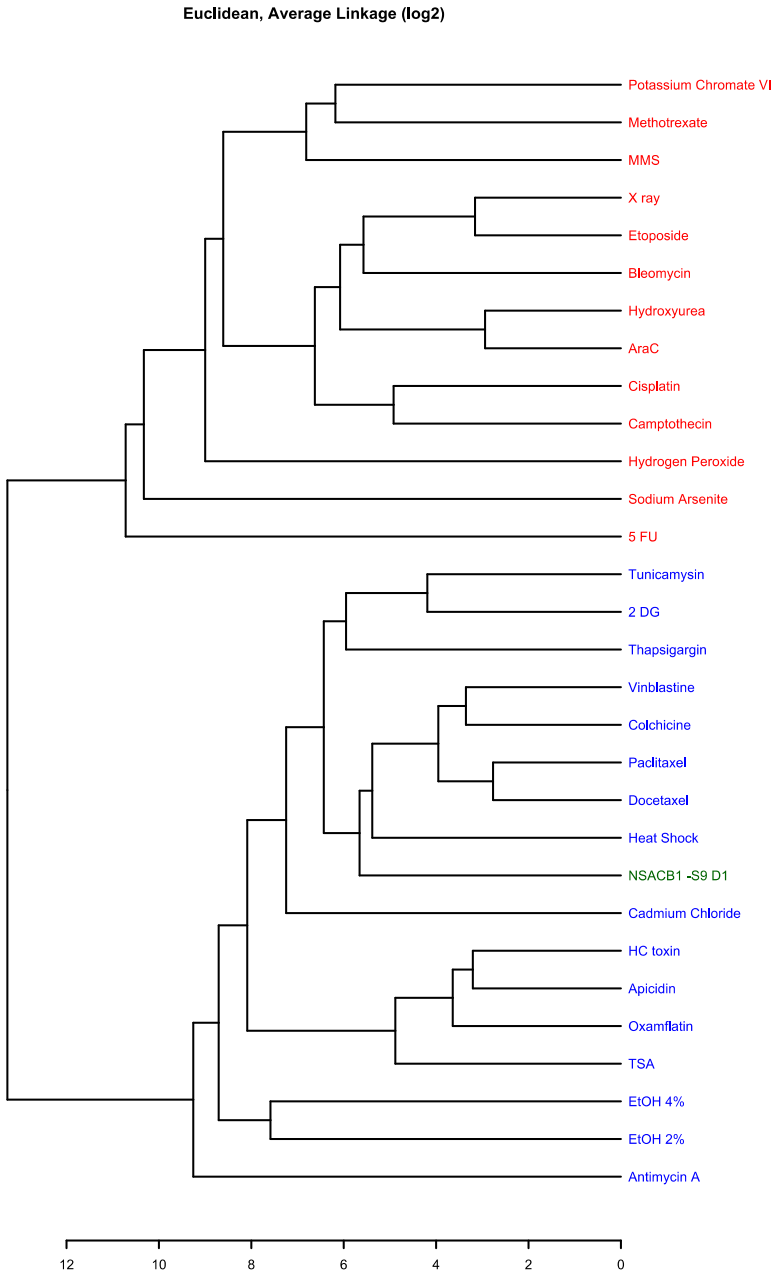
Euclidean, Average Linkage (log2)
Potassium Chromate VI
Methotrexate
MMS
X ray
Etoposide
Bleomycin
Hydroxyurea
AraC
Cisplatin
Camptothecin
Hydrogen Peroxide
Sodium Arsenite
5 FU
Tunicamycin
2 DG
Thapsigargin
Vinblastine
Colchicine
Paclitaxel
Docetaxel
Heat Shock
NSACB1 -S9 D1
Cadmium Chloride
HC toxin
Apicidin
Oxamflatin
TSA
EtOH 4%
EtOH 2%
Antimycin A
12
10
8
6
4
2
0

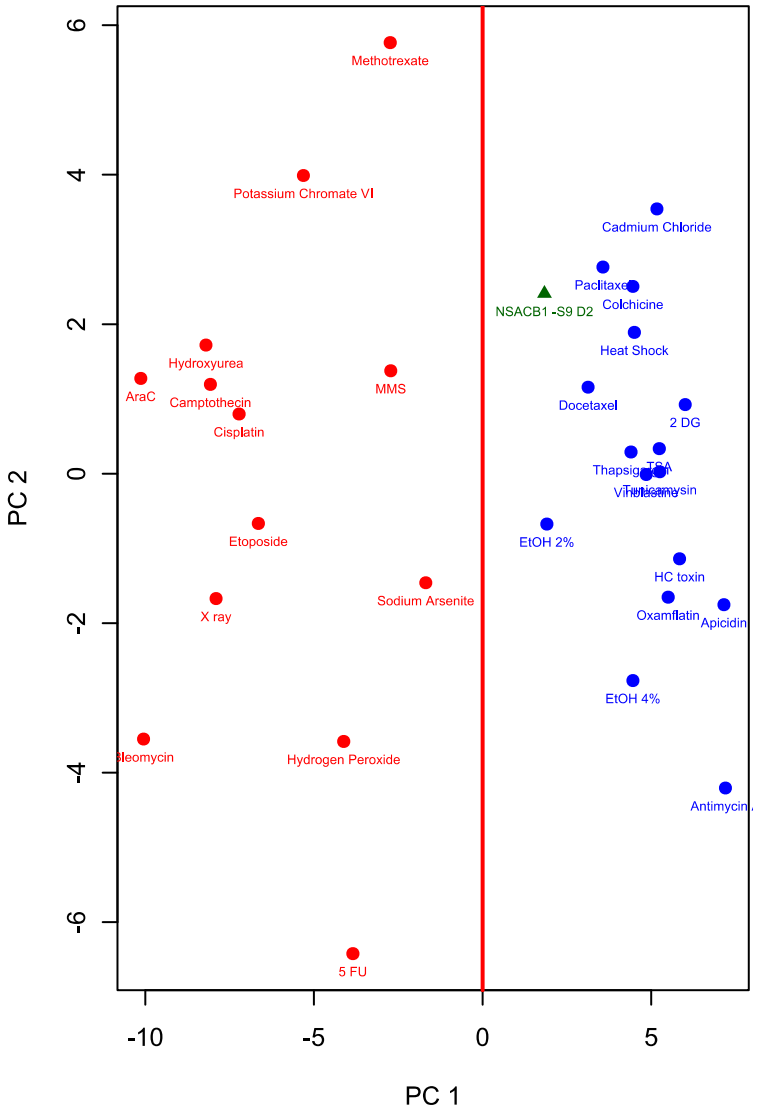
Methotrexate
Potassium Chromate VI
Cadmium Chloride
Paclitaxel
Colchicine
NSACB1 -S9 D2
Heat Shock
Hydroxyurea
AraC
Camptothecin
MMS
Docetaxel
2 DG
Cisplatin
Thapsigargin
TSA
Vinblastine
Tunicamysin
Etoposide
EtOH 2%
HC toxin
Sodium Arsenite
X ray
Oxamflatin
Apicidin
EtOH 4%
Bleomycin
Hydrogen Peroxide
Antimycin
5 FU
PC 2
PC 1
6
4
2
0
-2
-4
-6
-10
-5
0
5

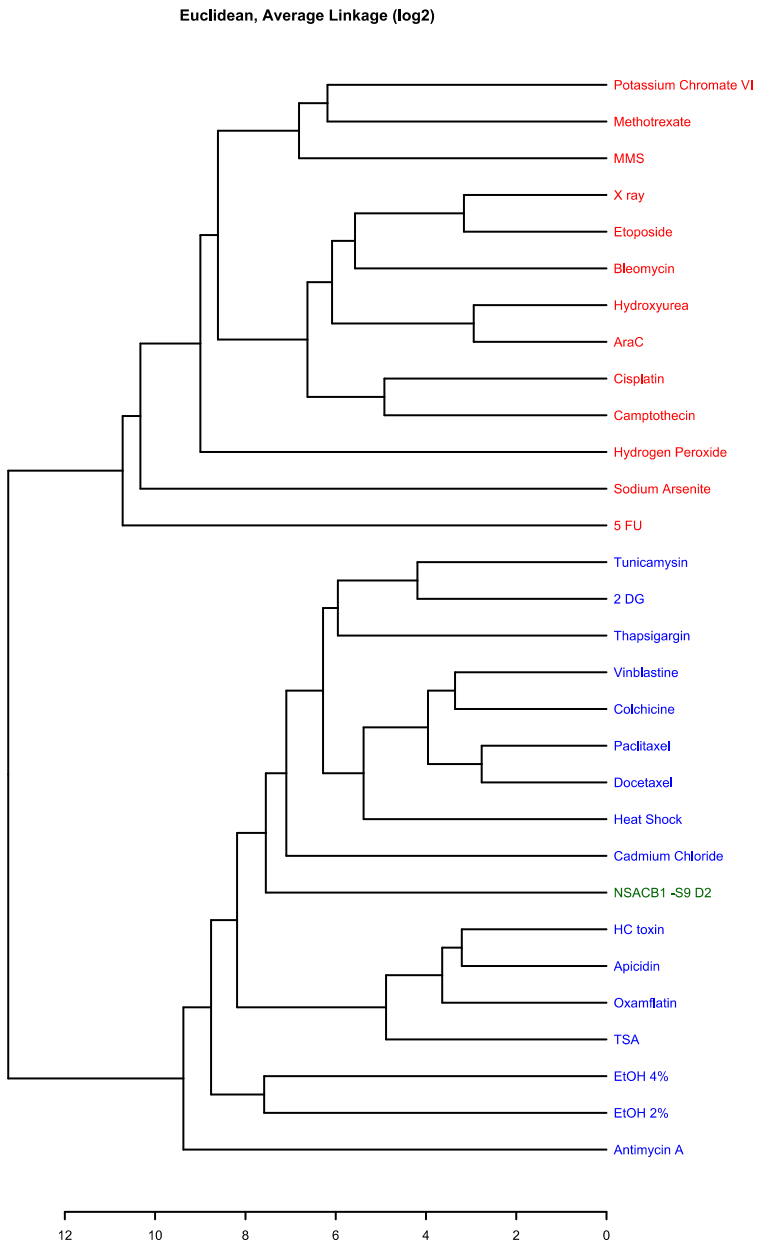
Euclidean, Average Linkage (log2)
Potassium Chromate VI
Methotrexate
MMS
X ray
Etoposide
Bleomycin
Hydroxyurea
AraC
Cisplatin
Camptothecin
Hydrogen Peroxide
Sodium Arsenite
5 FU
Tunicamysin
2 DG
Thapsigargin
Vinblastine
Colchicine
Paclitaxel
Docetaxel
Heat Shock
Cadmium Chloride
NSACB1 -S9 D2
HC toxin
Apicidin
Oxamflatin
TSA
EtOH 4%
EtOH 2%
Antimycin A
12
10
8
6
4
2
0

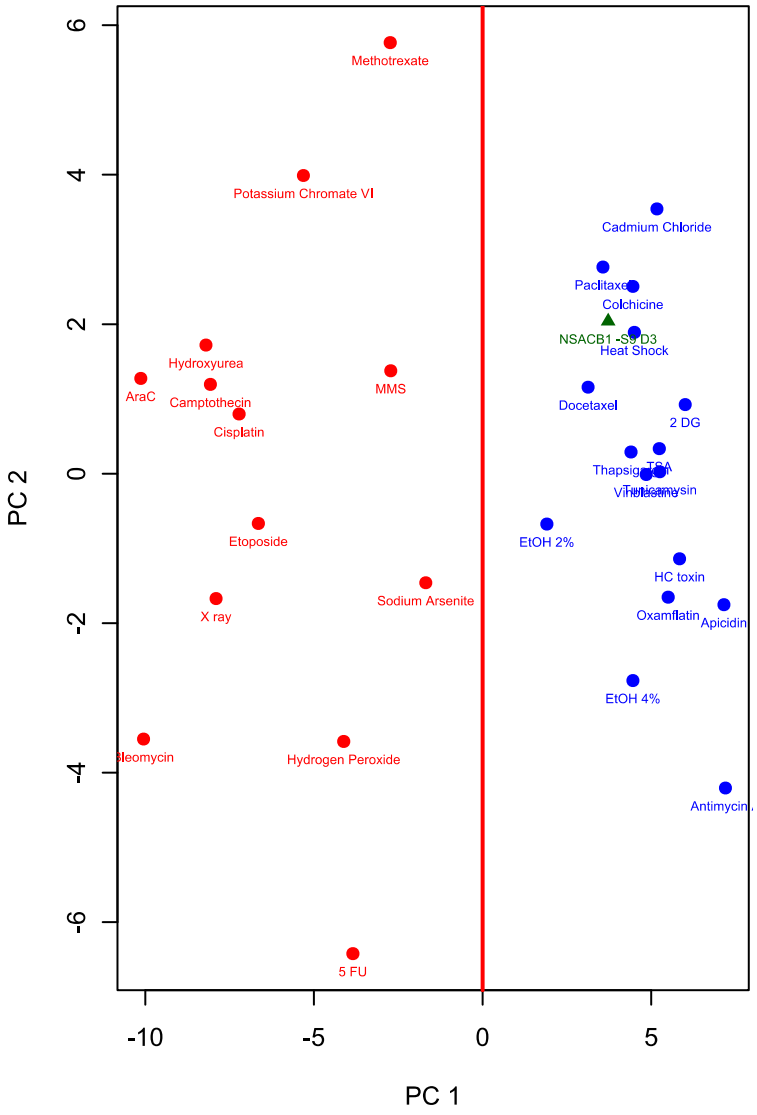
Methotrexate
Potassium Chromate VI
Cadmium Chloride
Paclitaxel
Colchicine
NSACB1 -S9 D3
Heat Shock
Hydroxyurea
AraC
Camptothecin
Cisplatin
MMS
Docetaxel
2 DG
Thapsigargin
TSA
Vinblastine
Tunicamysin
Etoposide
EtOH 2%
HC toxin
Sodium Arsenite
X ray
Oxamflatin
Apicidin
EtOH 4%
Bleomycin
Hydrogen Peroxide
Antimycin
5 FU
PC 2
PC 1
6
4
2
0
-2
-4
-6
-10
-5
0
5

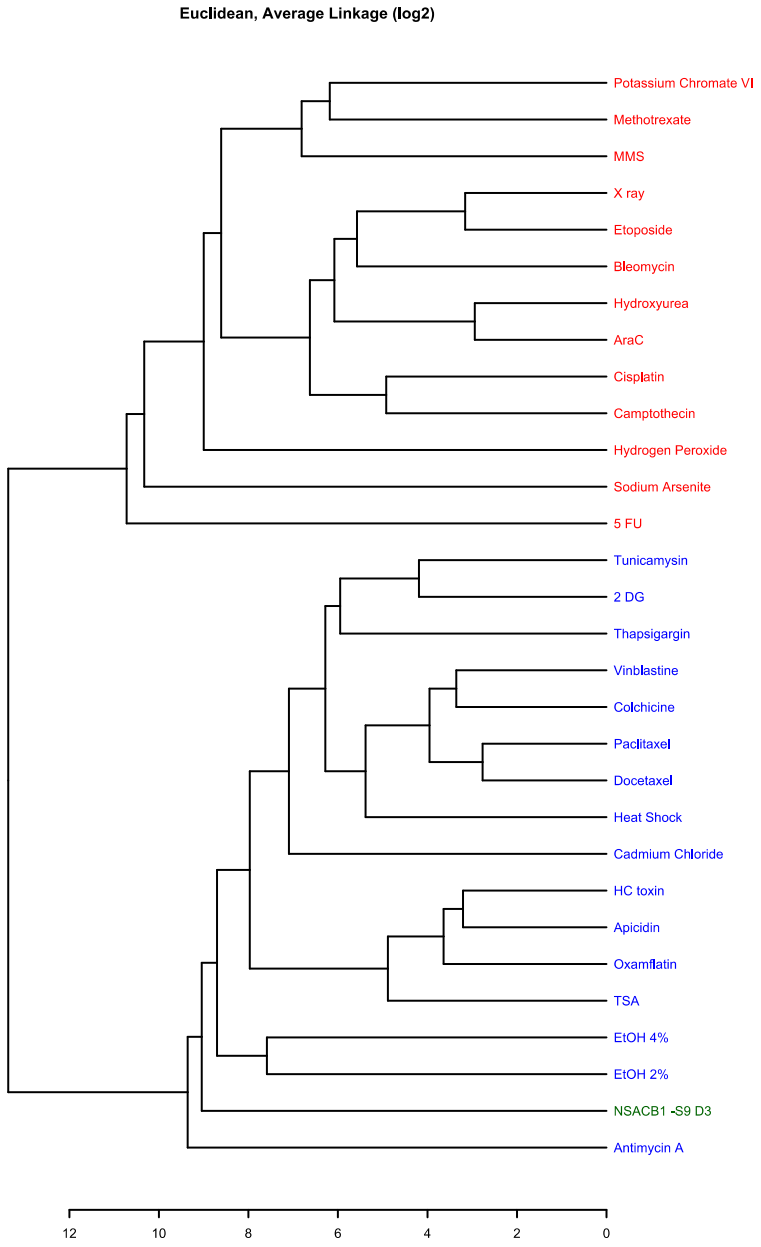
Euclidean, Average Linkage (log2)
Potassium Chromate VI
Methotrexate
MMS
X ray
Etoposide
Bleomycin
Hydroxyurea
AraC
Cisplatin
Camptothecin
Hydrogen Peroxide
Sodium Arsenite
5 FU
Tunicamysin
2 DG
Thapsigargin
Vinblastine
Colchicine
Paclitaxel
Docetaxel
Heat Shock
Cadmium Chloride
HC toxin
Apicidin
Oxamflatin
TSA
EtOH 4%
EtOH 2%
NSACB1 -S9 D3
Antimycin A
12
10
8
6
4
2
0

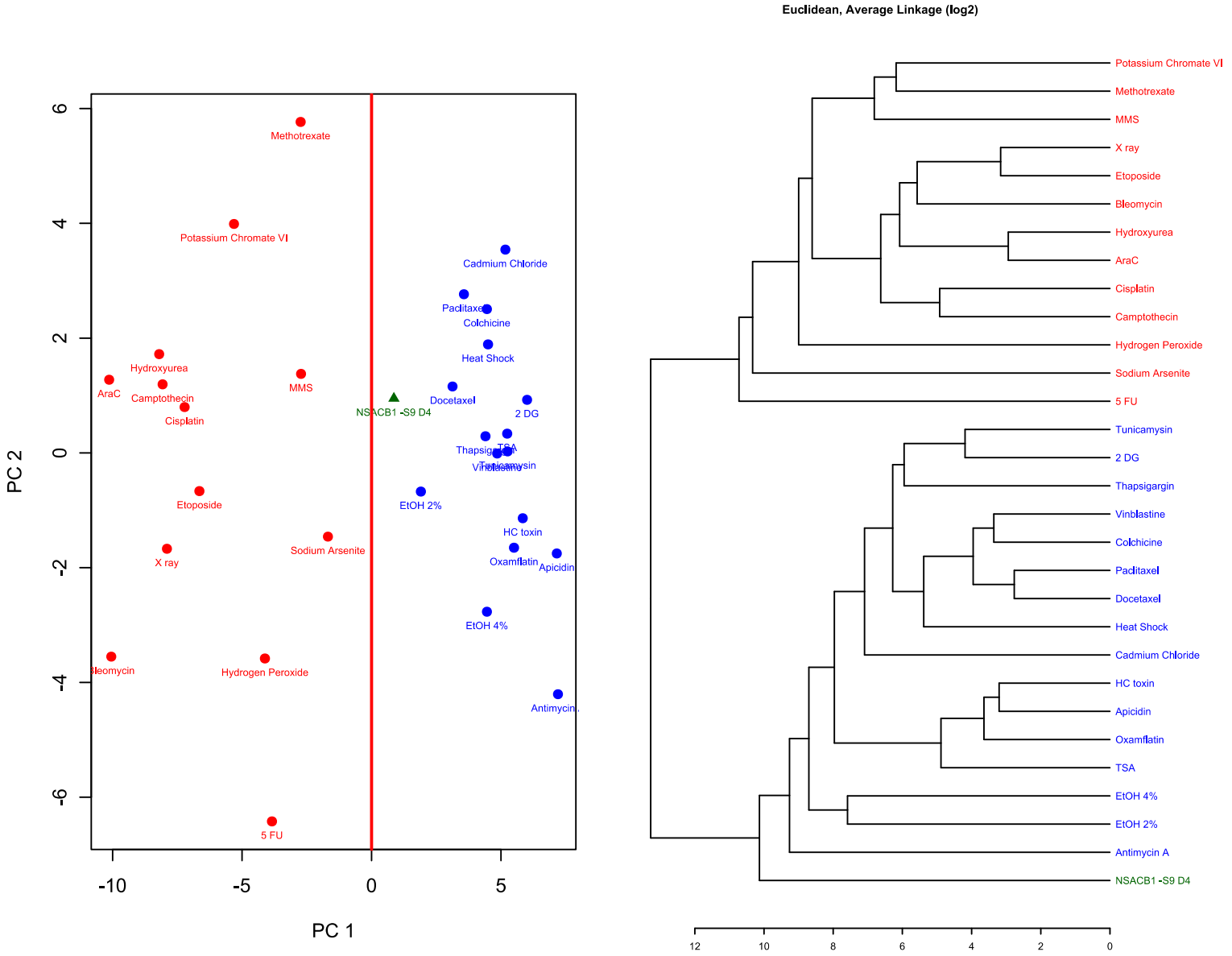

Supplementary Figure III-A: NASCB 1 (-S9) TGx-DDI biomarker classification using the Principal Component Analysis (PCA) (left) and hierarchical clustering (right) statistical analyses. Genotoxic reference chemicals are shown in red text, non-genotoxic reference chemicals are shown in blue text, and the test agent is shown in the green text. The line drawn on the PCA plot and the main branch on the dendogram divides the genotoxic and non-genotoxic agents and was used to classify the test compounds. D1 represents the lowest concentration tested, D4 the highest.

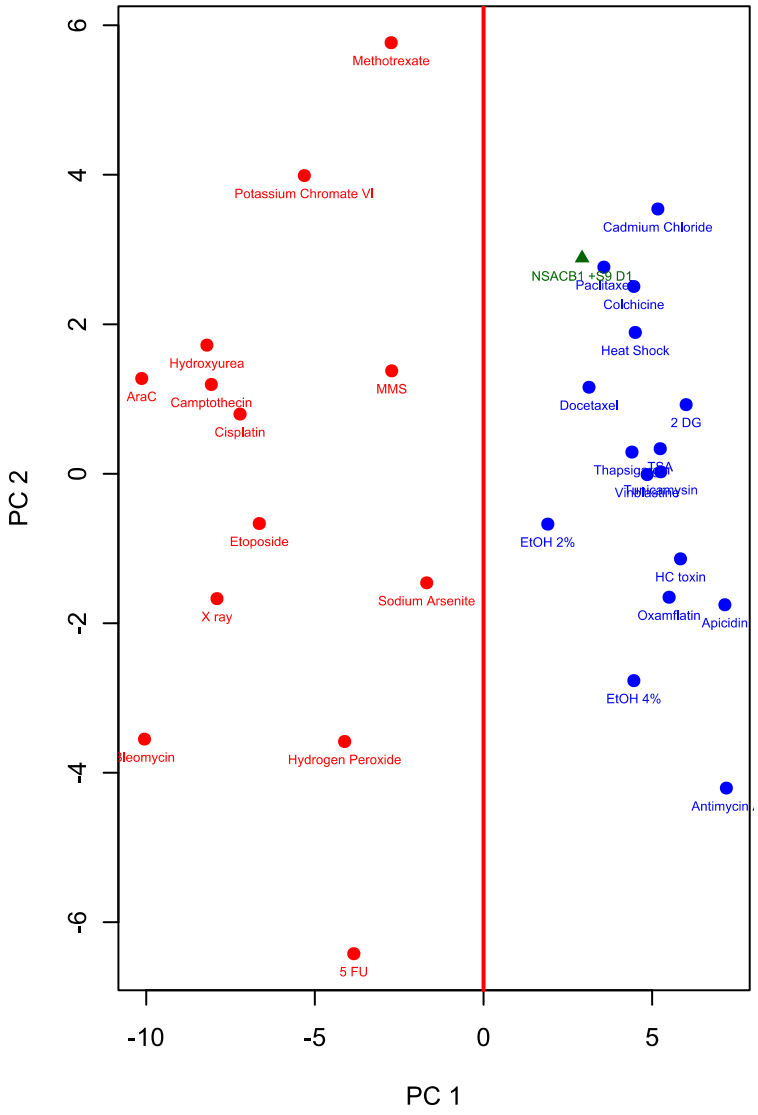
PC 2
PC 1
6
4
2
0
-2
-4
-6
-10
-5
0
5
Methotrexate
Potassium Chromate VI
Cadmium Chloride
NSACB1 +S9 D1
Paclitaxel
Colchicine
Heat Shock
Hydroxyurea
AraC
Camptothecin
Cisplatin
MMS
Docetaxel
2 DG
Thapsigargin
TSA
Tunicamysin
Vinblastine
Etoposide
EtOH 2%
HC toxin
Sodium Arsenite
X ray
Oxamflatin
Apicidin
EtOH 4%
Bleomycin
Hydrogen Peroxide
Antimycin
5 FU

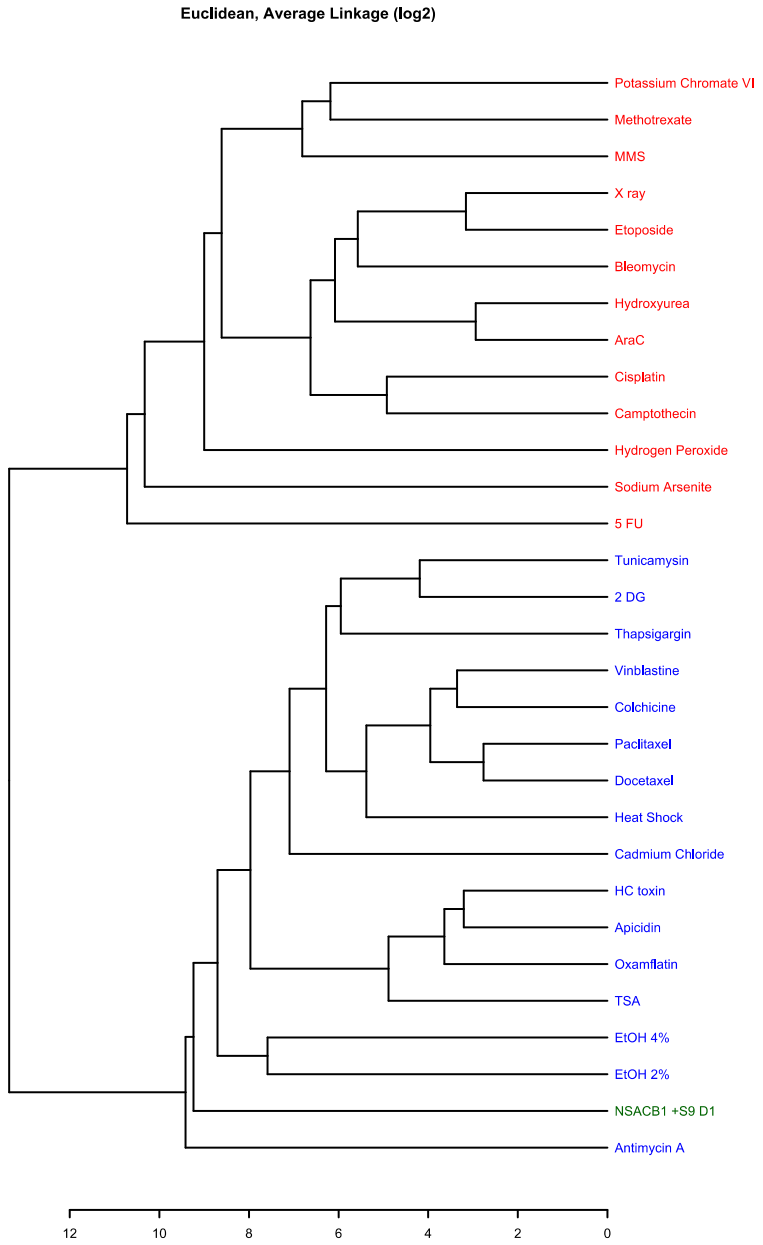
Euclidean, Average Linkage (log2)
Potassium Chromate VI
Methotrexate
MMS
X ray
Etoposide
Bleomycin
Hydroxyurea
AraC
Cisplatin
Camptothecin
Hydrogen Peroxide
Sodium Arsenite
5 FU
Tunicamysin
2 DG
Thapsigargin
Vinblastine
Colchicine
Paclitaxel
Docetaxel
Heat Shock
Cadmium Chloride
HC toxin
Apicidin
Oxamflatin
TSA
EtOH 4%
EtOH 2%
NSACB1 +S9 D1
Antimycin A
12
10
8
6
4
2
0

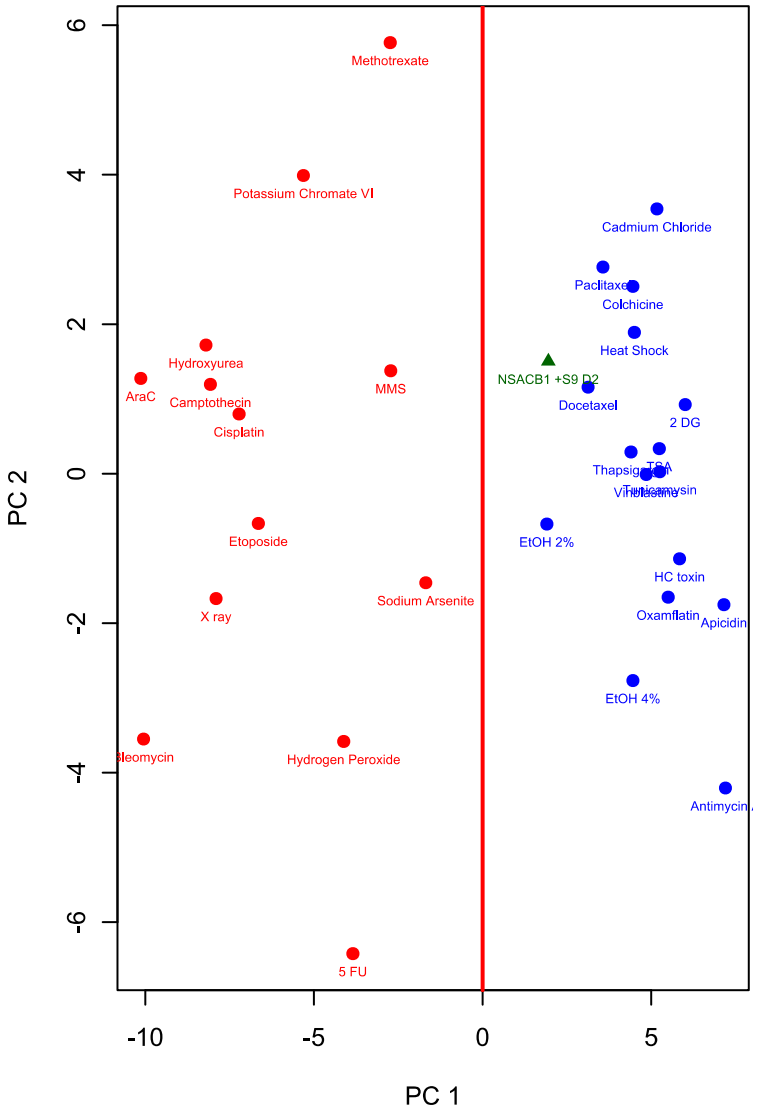
Methotrexate
Potassium Chromate VI
Cadmium Chloride
Paclitaxel
Colchicine
Heat Shock
Hydroxyurea
AraC
Camptothecin
Cisplatin
MMS
NSACB1 +S9 D2
Docetaxel
2 DG
Thapsigargin
TSA
Vinblastine
Tunicamysin
Etoposide
EtOH 2%
HC toxin
Sodium Arsenite
X ray
Oxamflatin
Apicidin
EtOH 4%
Bleomycin
Hydrogen Peroxide
Antimycin
5 FU
PC 2
PC 1
6
4
2
0
-2
-4
-6
-10
-5
0
5

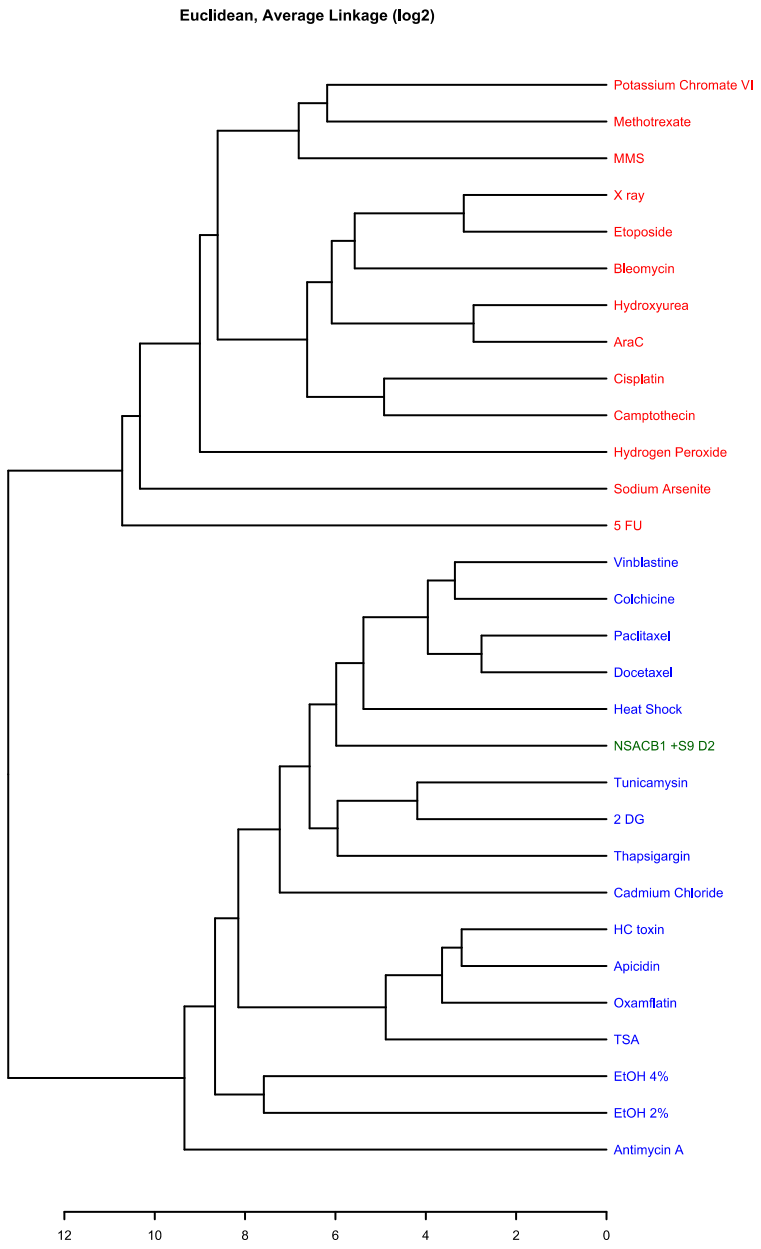
Euclidean, Average Linkage (log2)
Potassium Chromate VI
Methotrexate
MMS
X ray
Etoposide
Bleomycin
Hydroxyurea
AraC
Cisplatin
Camptothecin
Hydrogen Peroxide
Sodium Arsenite
5 FU
Vinblastine
Colchicine
Paclitaxel
Docetaxel
Heat Shock
NSACB1 +S9 D2
Tunicamysin
2 DG
Thapsigargin
Cadmium Chloride
HC toxin
Apicidin
Oxamflatin
TSA
EtOH 4%
EtOH 2%
Antimycin A
12
10
8
6
4
2
0

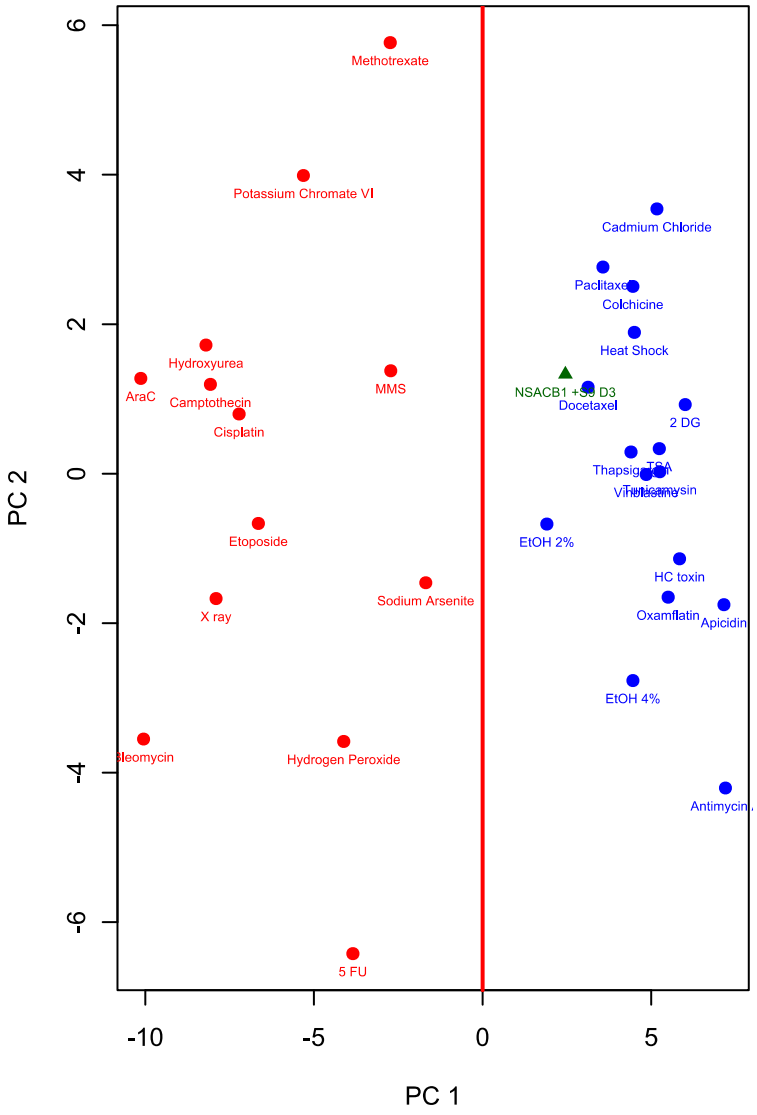
Methotrexate
Potassium Chromate VI
Cadmium Chloride
Paclitaxel
Colchicine
Heat Shock
Hydroxyurea
AraC
Camptothecin
Cisplatin
MMS
NSACB1 +S9 D3
Docetaxel
2 DG
Thapsigargin
TSA
Tunicamysin
Vinblastine
Etoposide
EtOH 2%
HC toxin
Sodium Arsenite
X ray
Oxamflatin
Apicidin
EtOH 4%
Bleomycin
Hydrogen Peroxide
Antimycin
5 FU
PC 2
PC 1
6
4
2
0
-2
-4
-6
-10
-5
0
5

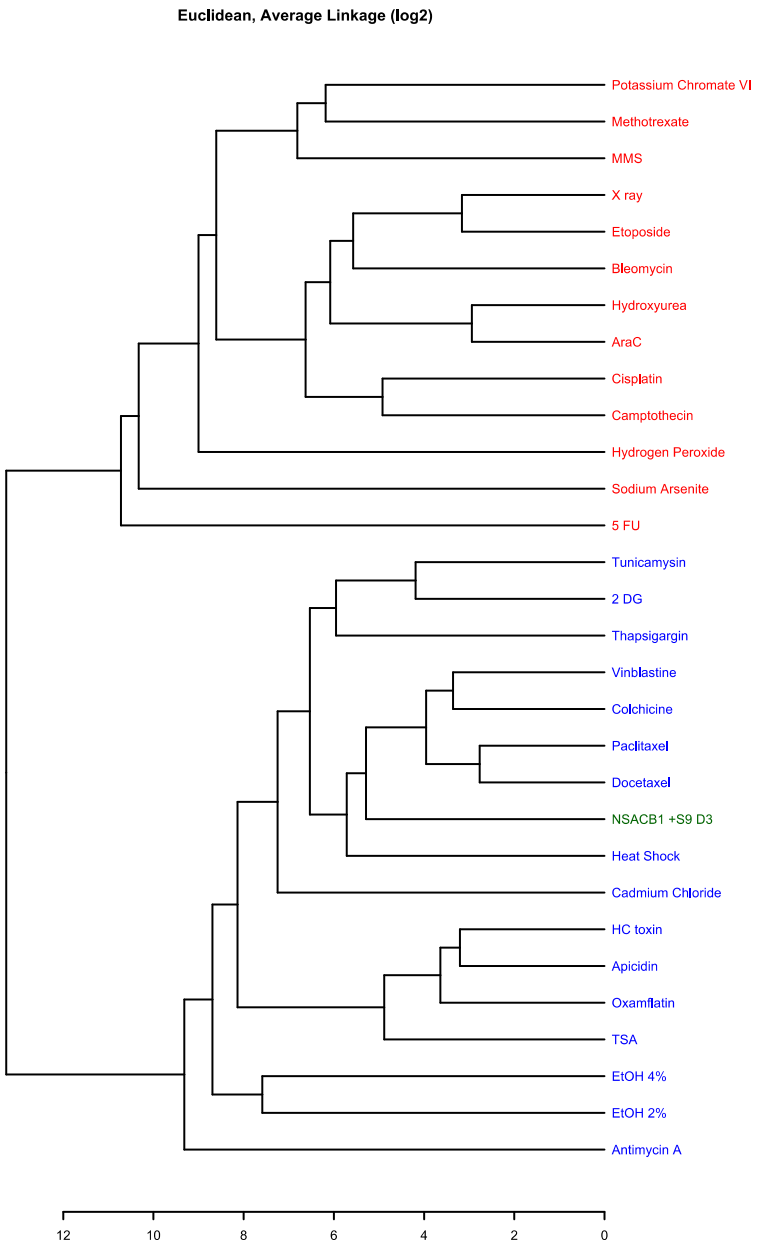
Euclidean, Average Linkage (log2)
Potassium Chromate VI
Methotrexate
MMS
X ray
Etoposide
Bleomycin
Hydroxyurea
AraC
Cisplatin
Camptothecin
Hydrogen Peroxide
Sodium Arsenite
5 FU
Tunicamysin
2 DG
Thapsigargin
Vinblastine
Colchicine
Paclitaxel
Docetaxel
NSACB1 +S9 D3
Heat Shock
Cadmium Chloride
HC toxin
Apicidin
Oxamflatin
TSA
EtOH 4%
EtOH 2%
Antimycin A
12
10
8
6
4
2
0

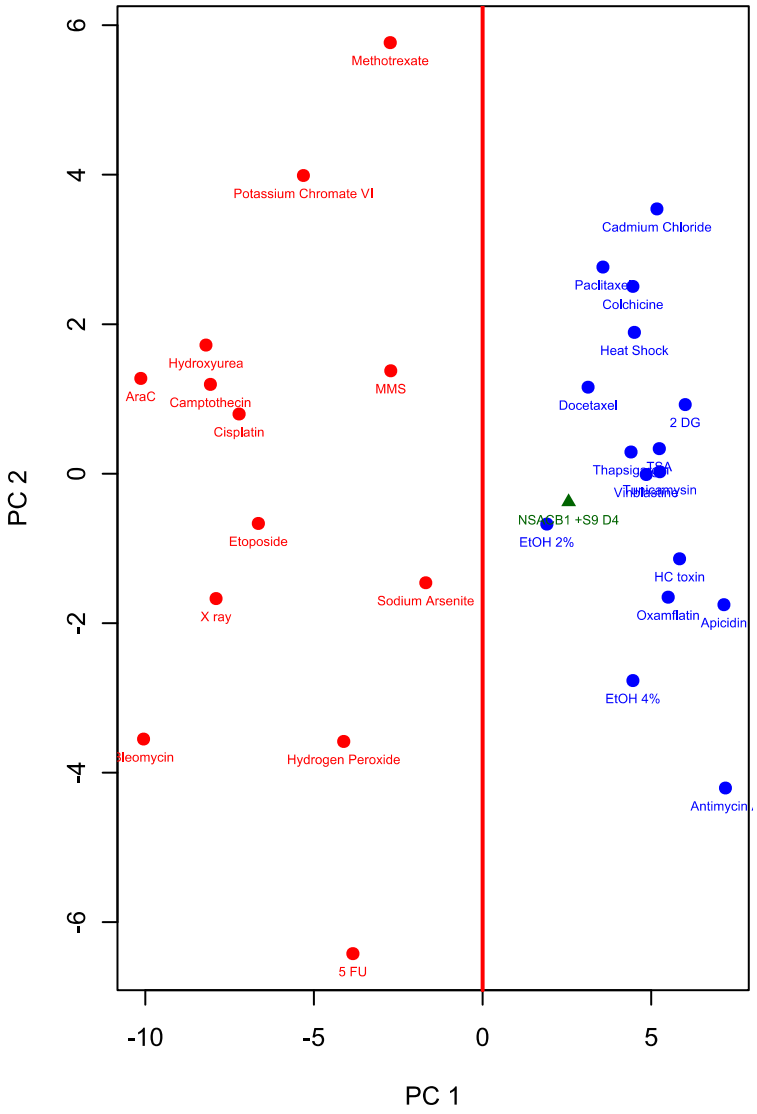
Methotrexate
Potassium Chromate VI
Cadmium Chloride
Paclitaxel
Colchicine
Heat Shock
Hydroxyurea
AraC
Camptothecin
Cisplatin
MMS
Docetaxel
2 DG
Thapsigargin
TSA
Vinblastine
Tunicamysin
NSACB1 +S9 D4
EtOH 2%
Etoposide
HC toxin
Sodium Arsenite
X ray
Oxamflatin
Apicidin
EtOH 4%
Bleomycin
Hydrogen Peroxide
Antimycin
5 FU
PC 2
PC 1
6
4
2
0
-2
-4
-6
-10
-5
0
5

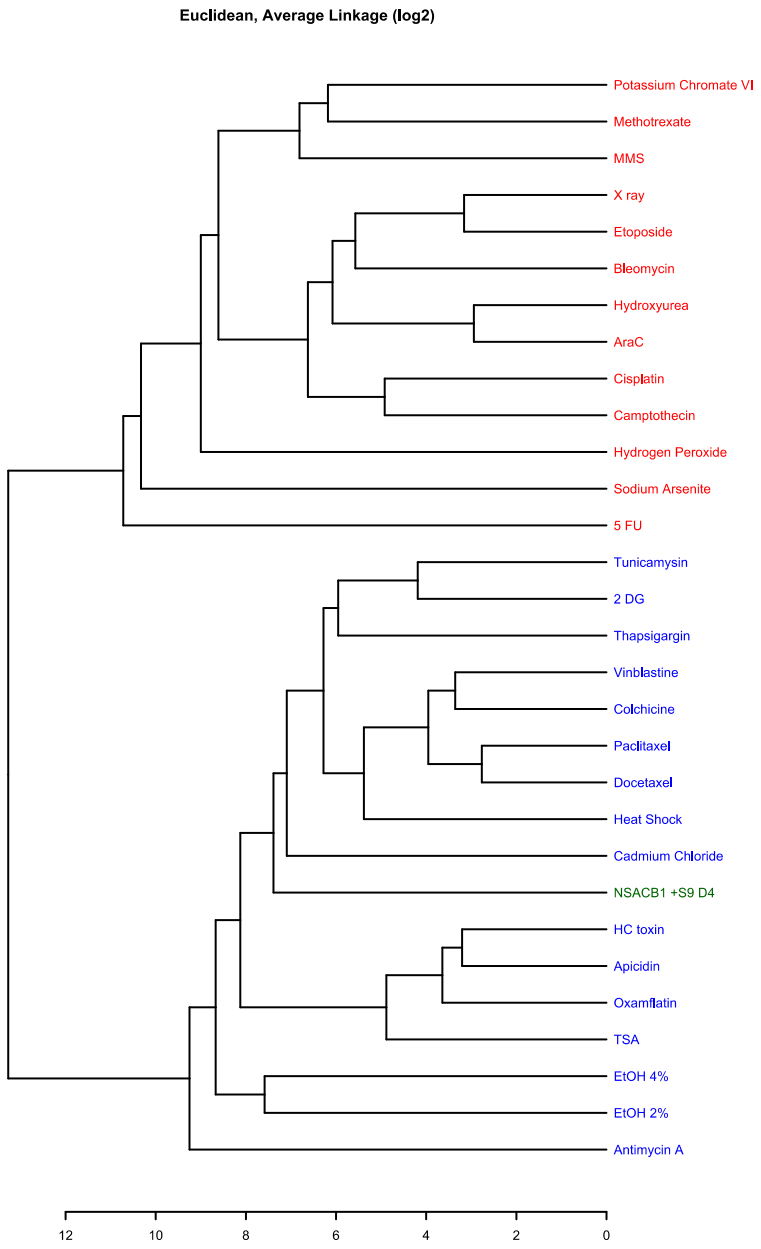
Euclidean, Average Linkage (log2)
Potassium Chromate VI
Methotrexate
MMS
X ray
Etoposide
Bleomycin
Hydroxyurea
AraC
Cisplatin
Camptothecin
Hydrogen Peroxide
Sodium Arsenite
5 FU
Tunicamysin
2 DG
Thapsigargin
Vinblastine
Colchicine
Paclitaxel
Docetaxel
Heat Shock
Cadmium Chloride
NSACB1 +S9 D4
HC toxin
Apicidin
Oxamflatin
TSA
EtOH 4%
EtOH 2%
Antimycin A
12
10
8
6
4
2
0

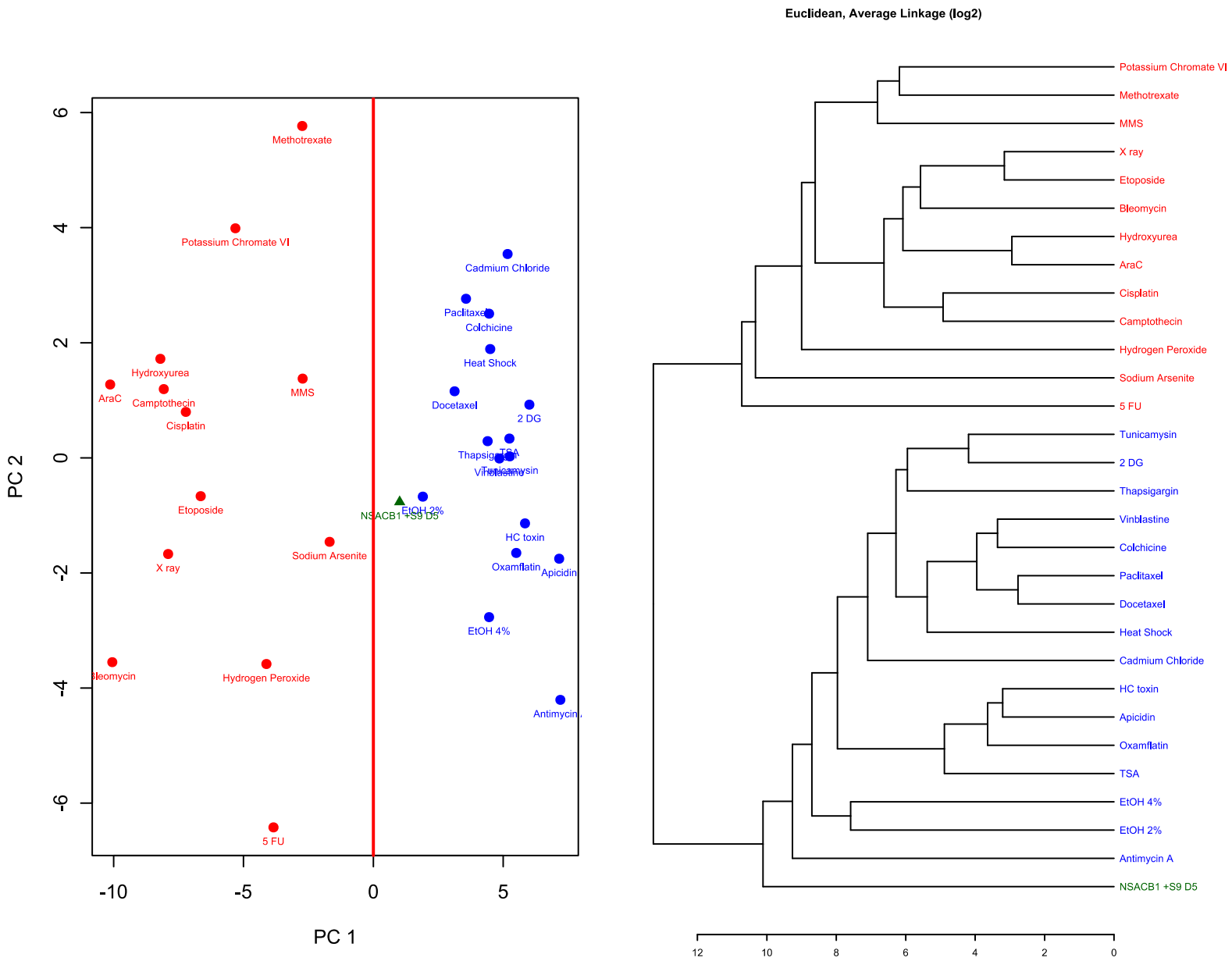

Supplementary Figure III-B: NASCB 1 (+S9) TGx-DDI biomarker classification using the Principal Component Analysis (PCA) (left) and hierarchical clustering (right) statistical analyses. Genotoxic reference chemicals are shown in red text, non-genotoxic reference chemicals are shown in blue text, and the test agent is shown in the green text. The line drawn on the PCA plot and the main branch on the dendogram divides the genotoxic and non-genotoxic agents and was used to classify the test compounds. D1 represents the lowest concentration tested, D5 the highest.

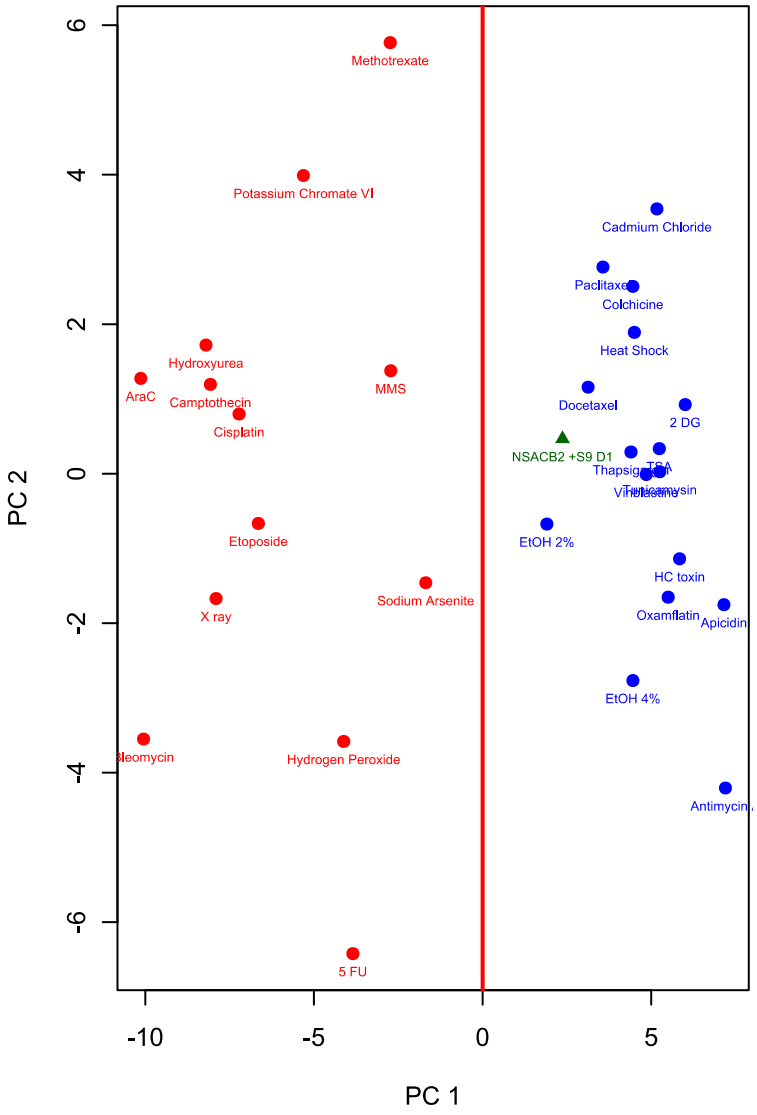
Methotrexate
Potassium Chromate VI
Cadmium Chloride
Paclitaxel
Colchicine
Heat Shock
Hydroxyurea
AraC
Camptothecin
MMS
Docetaxel
2 DG
Cisplatin
NSACB2 +S9 D1
Thapsigargin
TSA
Vinblastine
Tunicamysin
Etoposide
EtOH 2%
HC toxin
Sodium Arsenite
X ray
Oxamflatin
Apicidin
EtOH 4%
Bleomycin
Hydrogen Peroxide
Antimycin
5 FU
PC 2
PC 1
6
4
2
0
-2
-4
-6
-10
-5
0
5

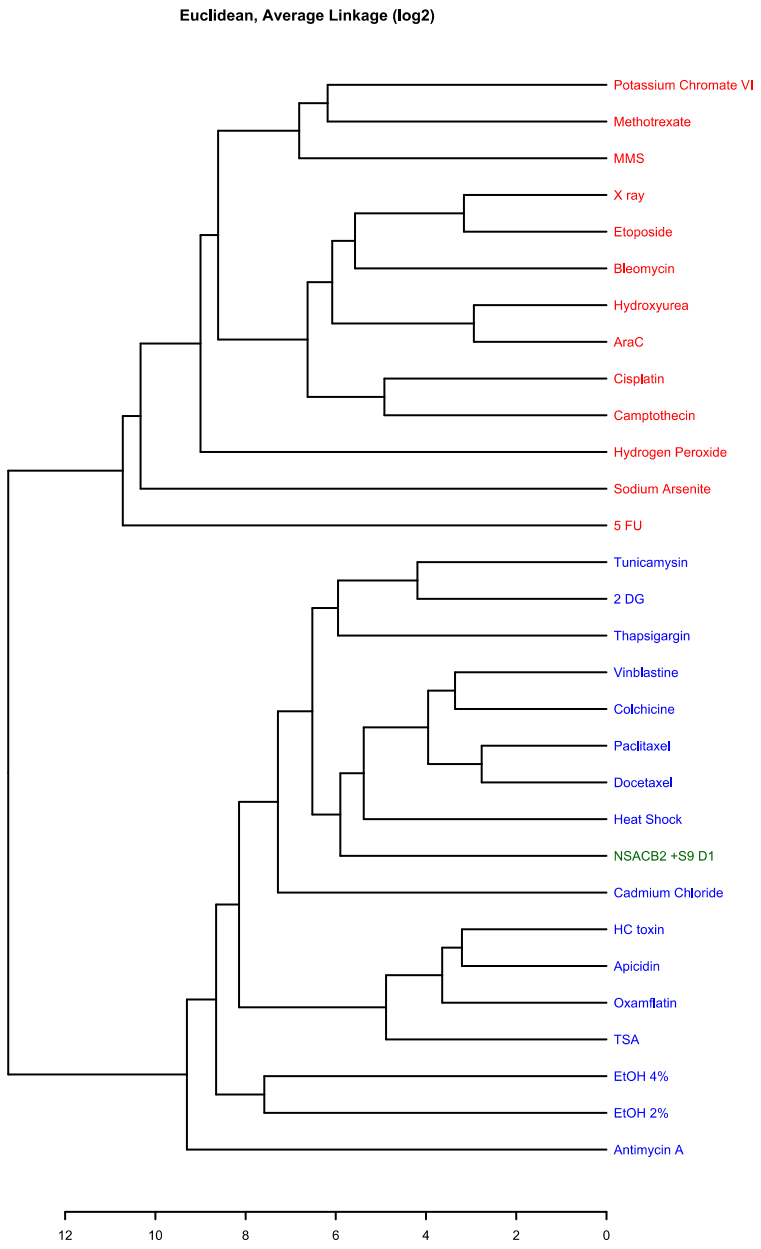
Euclidean, Average Linkage (log2)
Potassium Chromate VI
Methotrexate
MMS
X ray
Etoposide
Bleomycin
Hydroxyurea
AraC
Cisplatin
Camptothecin
Hydrogen Peroxide
Sodium Arsenite
5 FU
Tunicamysin
2 DG
Thapsigargin
Vinblastine
Colchicine
Paclitaxel
Docetaxel
Heat Shock
NSACB2 +S9 D1
Cadmium Chloride
HC toxin
Apicidin
Oxamflatin
TSA
EtOH 4%
EtOH 2%
Antimycin A
12
10
8
6
4
2
0

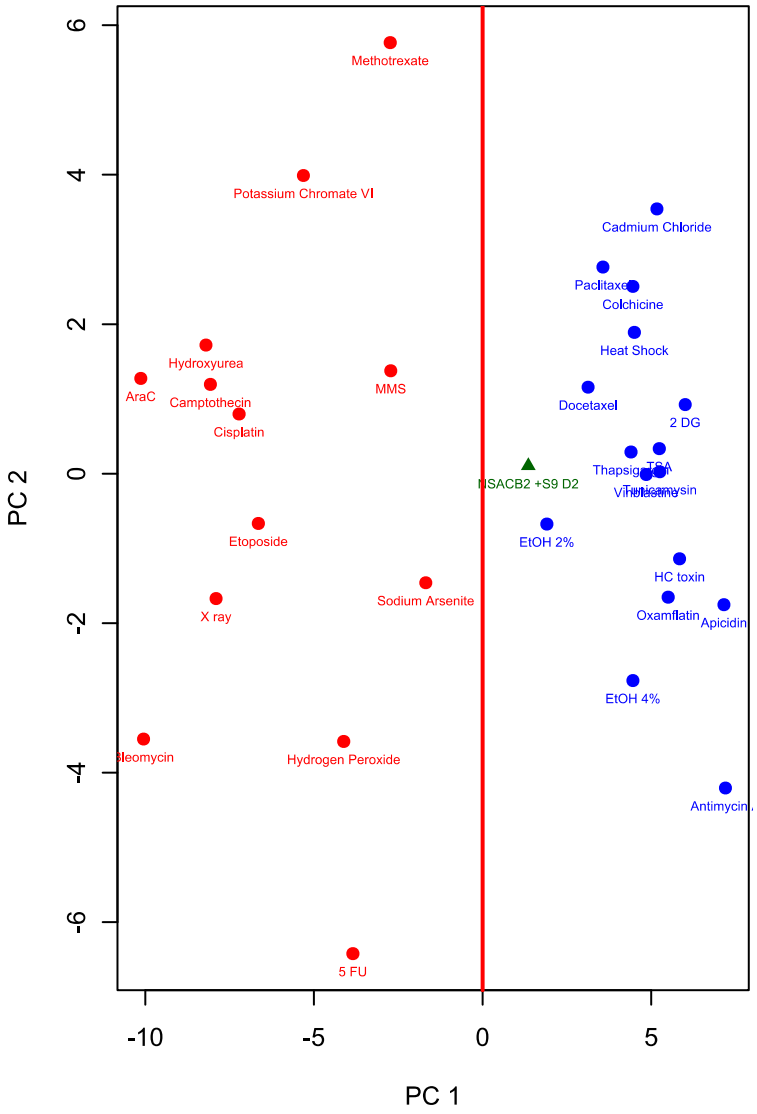
PC 2
PC 1
6
4
2
0
-2
-4
-6
-10
-5
0
5
Methotrexate
Potassium Chromate VI
Cadmium Chloride
Paclitaxel
Colchicine
Heat Shock
Hydroxyurea
AraC
Camptothecin
Cisplatin
MMS
Docetaxel
2 DG
Thapsigargin
TSA
Tunicamycin
Vinblastine
NSACB2 +S9 D2
Etoposide
EtOH 2%
HC toxin
Sodium Arsenite
X ray
Oxamflatin
Apicidin
EtOH 4%
Bleomycin
Hydrogen Peroxide
Antimycin
5 FU

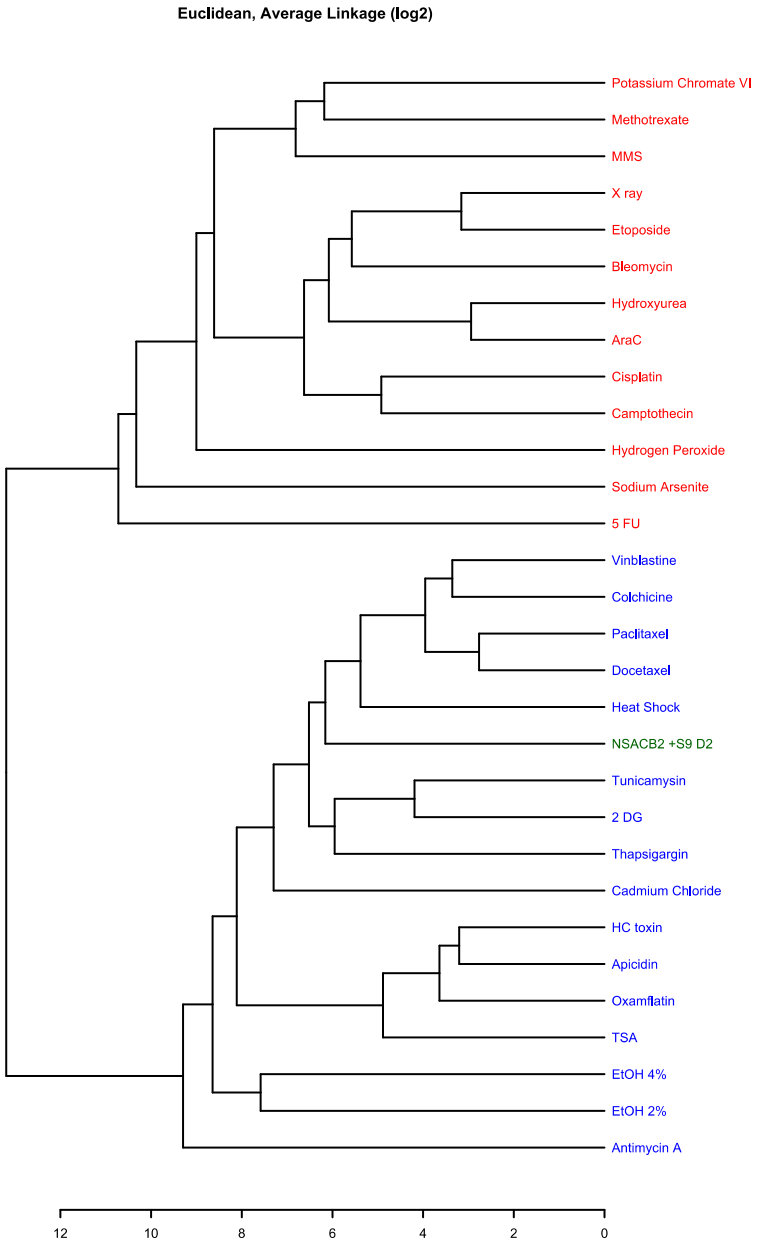
Euclidean, Average Linkage (log2)
Potassium Chromate VI
Methotrexate
MMS
X ray
Etoposide
Bleomycin
Hydroxyurea
AraC
Cisplatin
Camptothecin
Hydrogen Peroxide
Sodium Arsenite
5 FU
Vinblastine
Colchicine
Paclitaxel
Docetaxel
Heat Shock
NSACB2 +S9 D2
Tunicamycin
2 DG
Thapsigargin
Cadmium Chloride
HC toxin
Apicidin
Oxamflatin
TSA
EtOH 4%
EtOH 2%
Antimycin A
12
10
8
6
4
2
0

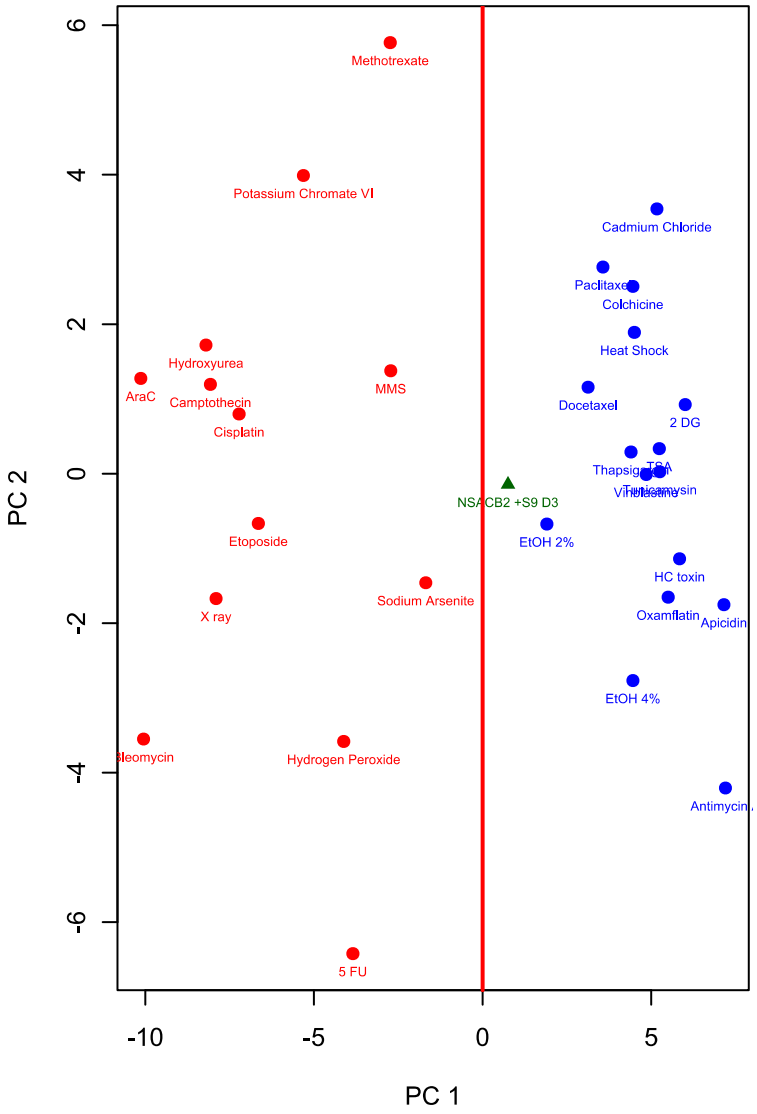
Methotrexate
Potassium Chromate VI
Cadmium Chloride
Paclitaxel
Colchicine
Heat Shock
Hydroxyurea
AraC
Camptothecin
Cisplatin
MMS
Docetaxel
2 DG
Thapsigargin
TSA
Vinblastine
Tunicamycin
NSACB2 +S9 D3
EtOH 2%
Etoposide
HC toxin
Sodium Arsenite
X ray
Oxamflatin
Apicidin
EtOH 4%
Bleomycin
Hydrogen Peroxide
Antimycin
5 FU
PC 2
PC 1
6
4
2
0
-2
-4
-6
-10
-5
0
5

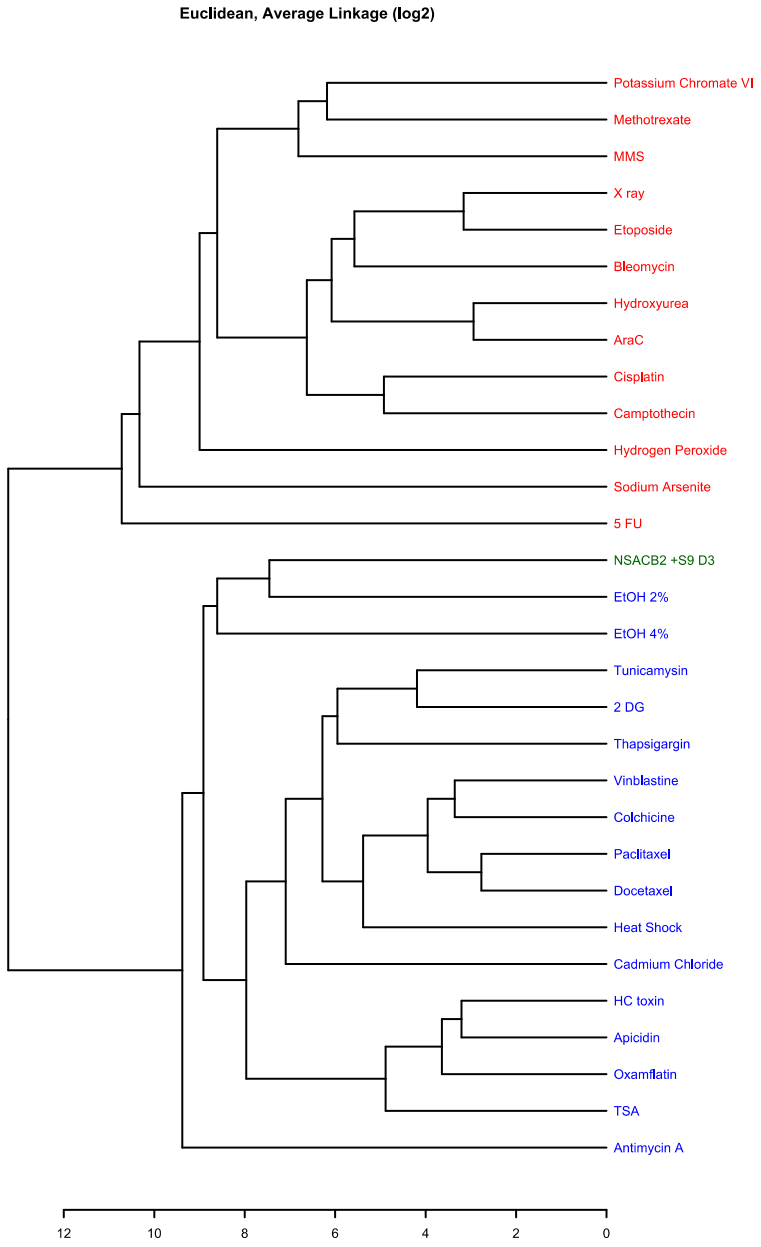
Euclidean, Average Linkage (log2)
Potassium Chromate VI
Methotrexate
MMS
X ray
Etoposide
Bleomycin
Hydroxyurea
AraC
Cisplatin
Camptothecin
Hydrogen Peroxide
Sodium Arsenite
5 FU
NSACB2 +S9 D3
EtOH 2%
EtOH 4%
Tunicamycin
2 DG
Thapsigargin
Vinblastine
Colchicine
Paclitaxel
Docetaxel
Heat Shock
Cadmium Chloride
HC toxin
Apicidin
Oxamflatin
TSA
Antimycin A
12
10
8
6
4
2
0

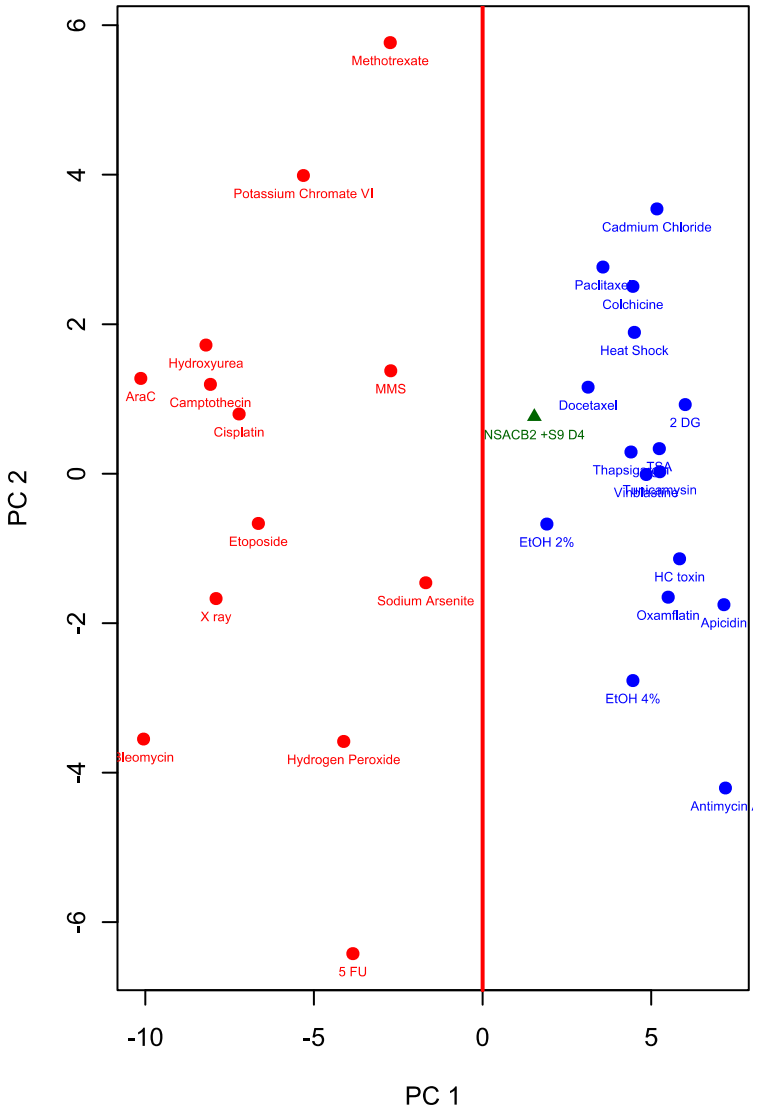
Methotrexate
Potassium Chromate VI
Cadmium Chloride
Paclitaxel
Colchicine
Heat Shock
Hydroxyurea
AraC
Camptothecin
Cisplatin
MMS
Docetaxel
2 DG
NSACB2 +S9 D4
Thapsigargin
TSA
Vinblastine
Tunicamysin
Etoposide
EtOH 2%
HC toxin
Sodium Arsenite
X ray
Oxamflatin
Apicidin
EtOH 4%
Bleomycin
Hydrogen Peroxide
Antimycin
5 FU
PC 2
PC 1
6
4
2
0
-2
-4
-6
-10
-5
0
5

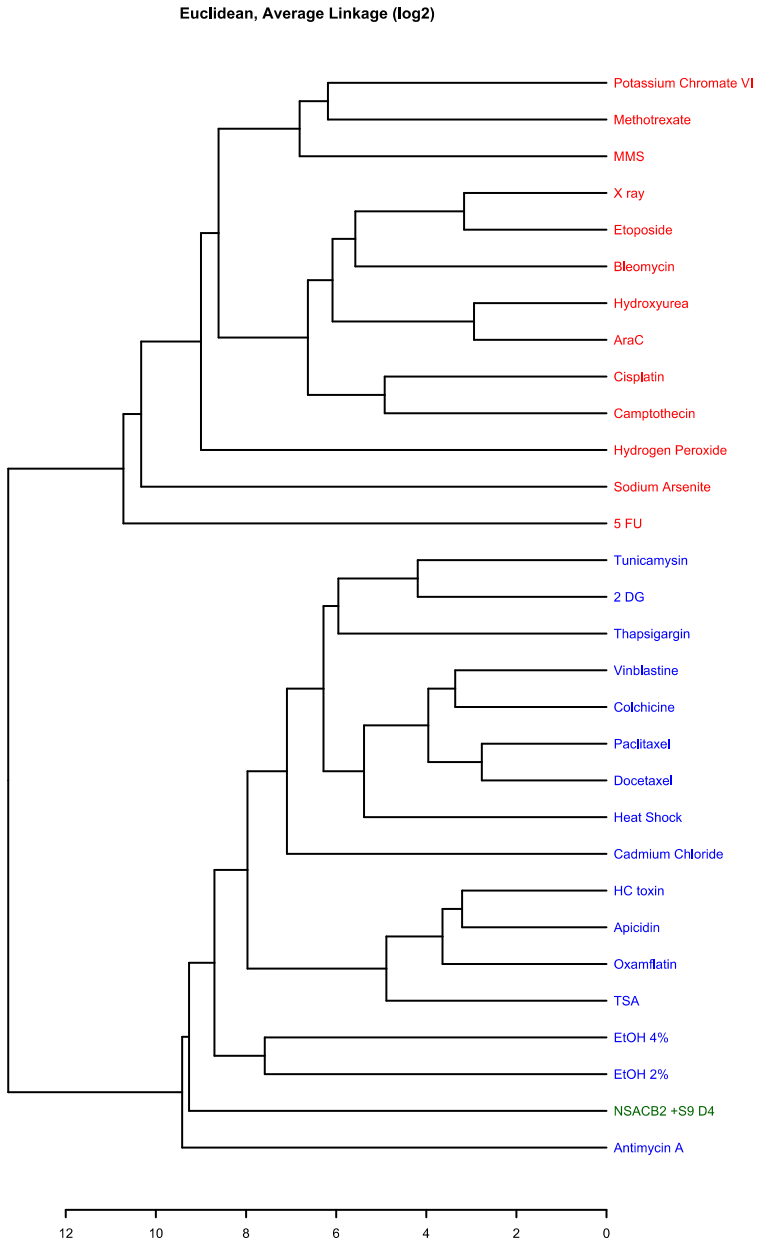
Euclidean, Average Linkage (log2)
Potassium Chromate VI
Methotrexate
MMS
X ray
Etoposide
Bleomycin
Hydroxyurea
AraC
Cisplatin
Camptothecin
Hydrogen Peroxide
Sodium Arsenite
5 FU
Tunicamysin
2 DG
Thapsigargin
Vinblastine
Colchicine
Paclitaxel
Docetaxel
Heat Shock
Cadmium Chloride
HC toxin
Apicidin
Oxamflatin
TSA
EtOH 4%
EtOH 2%
NSACB2 +S9 D4
Antimycin A
12
10
8
6
4
2
0

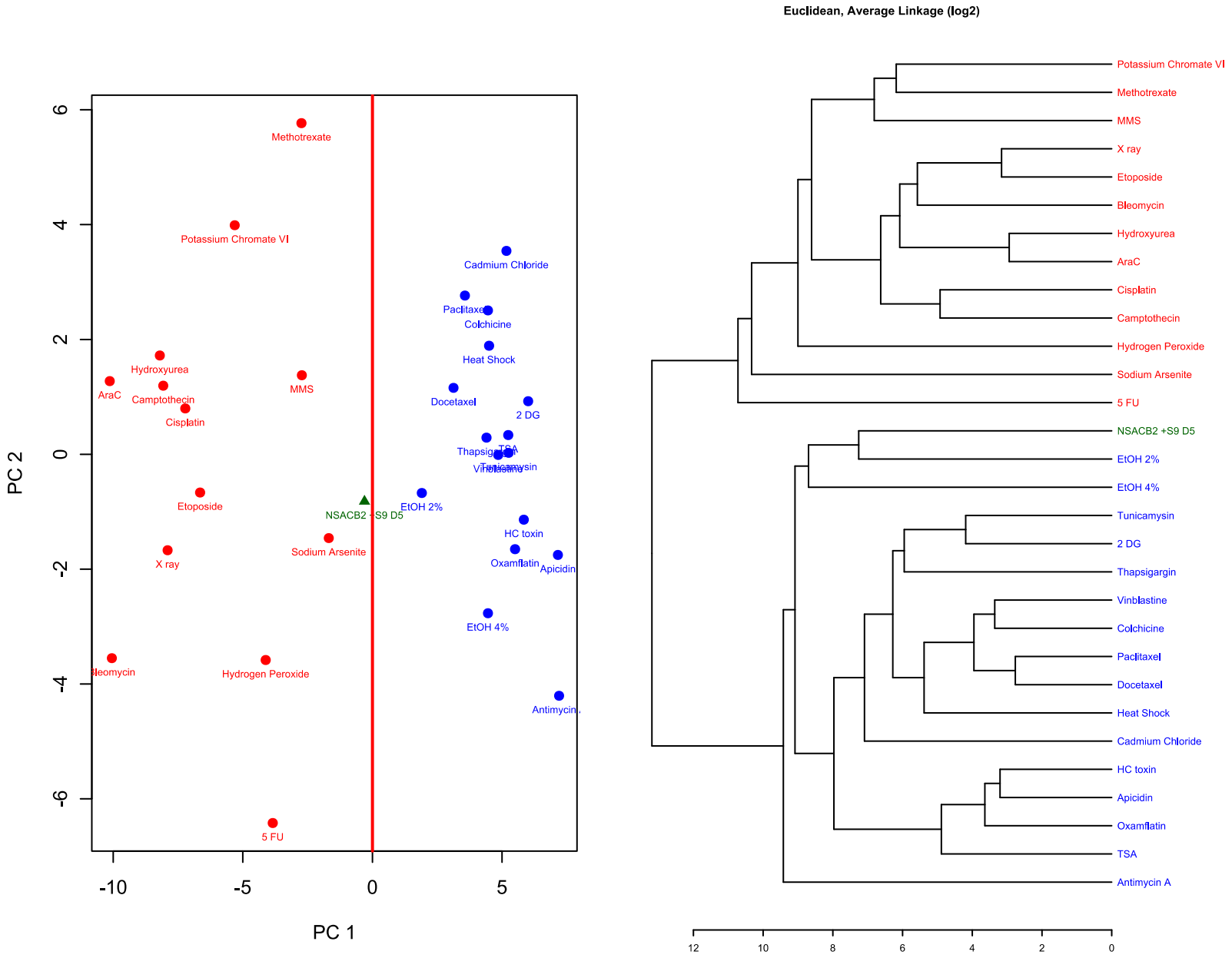

Supplementary Figure III-C: NASCB 2 (+S9) TGx-DDI biomarker classification using the Principal Component Analysis (PCA) (left) and hierarchical clustering (right) statistical analyses. Genotoxic reference chemicals are shown in red text, non-genotoxic reference chemicals are shown in blue text, and the test agent is shown in the green text. The line drawn on the PCA plot and the main branch on the dendogram divides the genotoxic and non-genotoxic agents and was used to classify the test compounds. D1 represents the lowest concentration tested, D5 the highest.

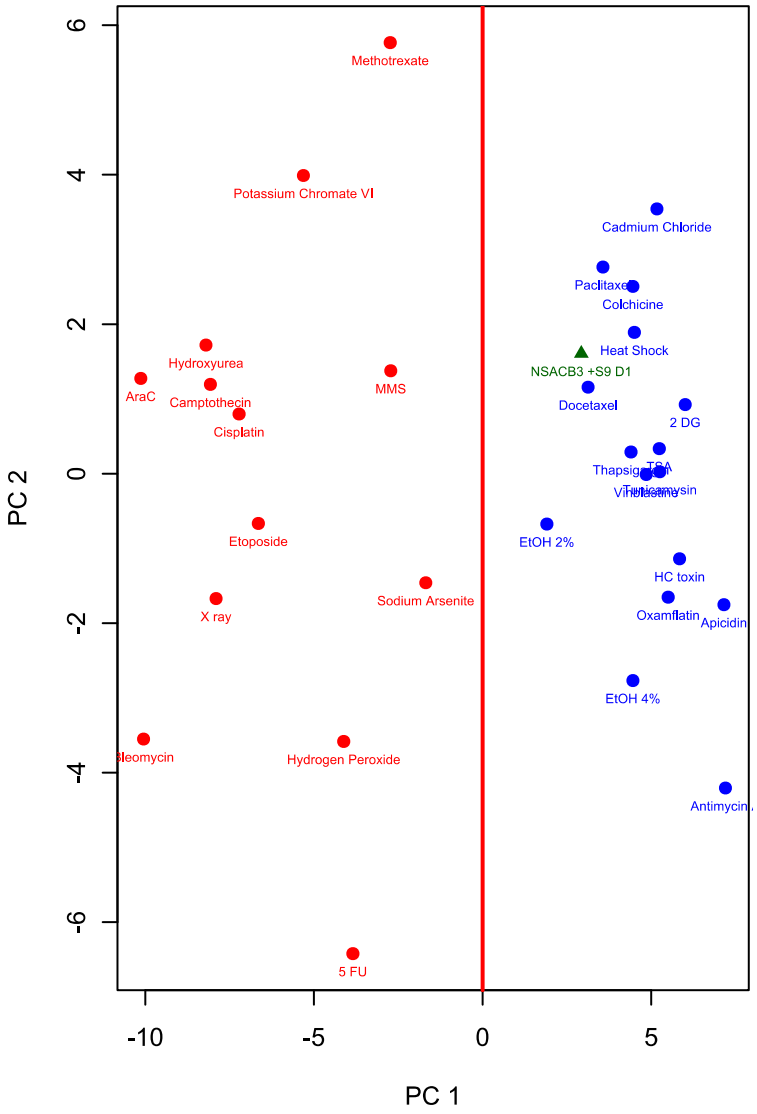
PC 2
PC 1
6
4
2
0
-2
-4
-6
-10
-5
0
5
Methotrexate
Potassium Chromate VI
Cadmium Chloride
Paclitaxel
Colchicine
Heat Shock
NSACB3 +S9 D1
Docetaxel
2 DG
Thapsigargin
TSA
Tunicamysin
Vinblastine
Hydroxyurea
AraC
Camptothecin
Cisplatin
MMS
Etoposide
EtOH 2%
HC toxin
Sodium Arsenite
X ray
Oxamflatin
Apicidin
EtOH 4%
Bleomycin
Hydrogen Peroxide
Antimycin
5 FU

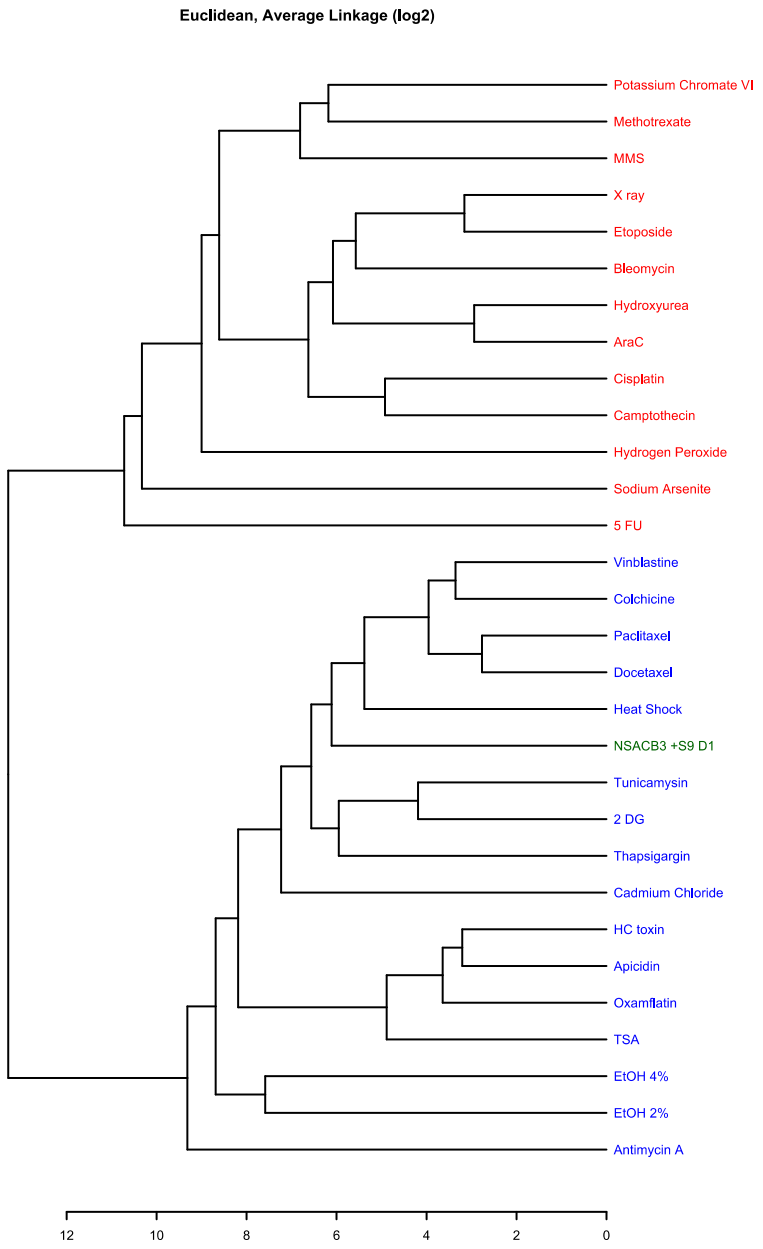
Euclidean, Average Linkage (log2)
Potassium Chromate VI
Methotrexate
MMS
X ray
Etoposide
Bleomycin
Hydroxyurea
AraC
Cisplatin
Camptothecin
Hydrogen Peroxide
Sodium Arsenite
5 FU
Vinblastine
Colchicine
Paclitaxel
Docetaxel
Heat Shock
NSACB3 +S9 D1
Tunicamysin
2 DG
Thapsigargin
Cadmium Chloride
HC toxin
Apicidin
Oxamflatin
TSA
EtOH 4%
EtOH 2%
Antimycin A
12
10
8
6
4
2
0

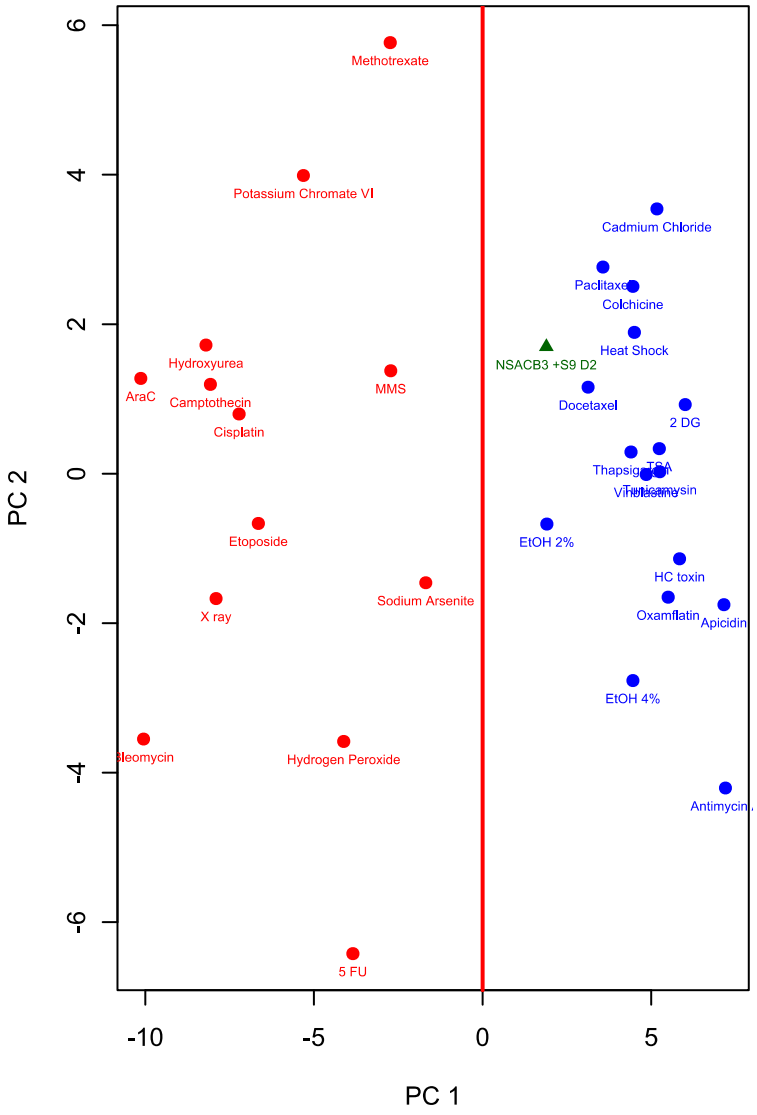
Methotrexate
Potassium Chromate VI
Cadmium Chloride
Paclitaxel
Colchicine
Heat Shock
NSACB3 +S9 D2
Hydroxyurea
AraC
Camptothecin
Cisplatin
MMS
Docetaxel
2 DG
Thapsigargin
TSA
Vinblastine
Tunicamysin
Etoposide
EtOH 2%
HC toxin
Sodium Arsenite
X ray
Oxamflatin
Apicidin
EtOH 4%
Bleomycin
Hydrogen Peroxide
Antimycin
5 FU
PC 2
PC 1
6
4
2
0
-2
-4
-6
-10
-5
0
5

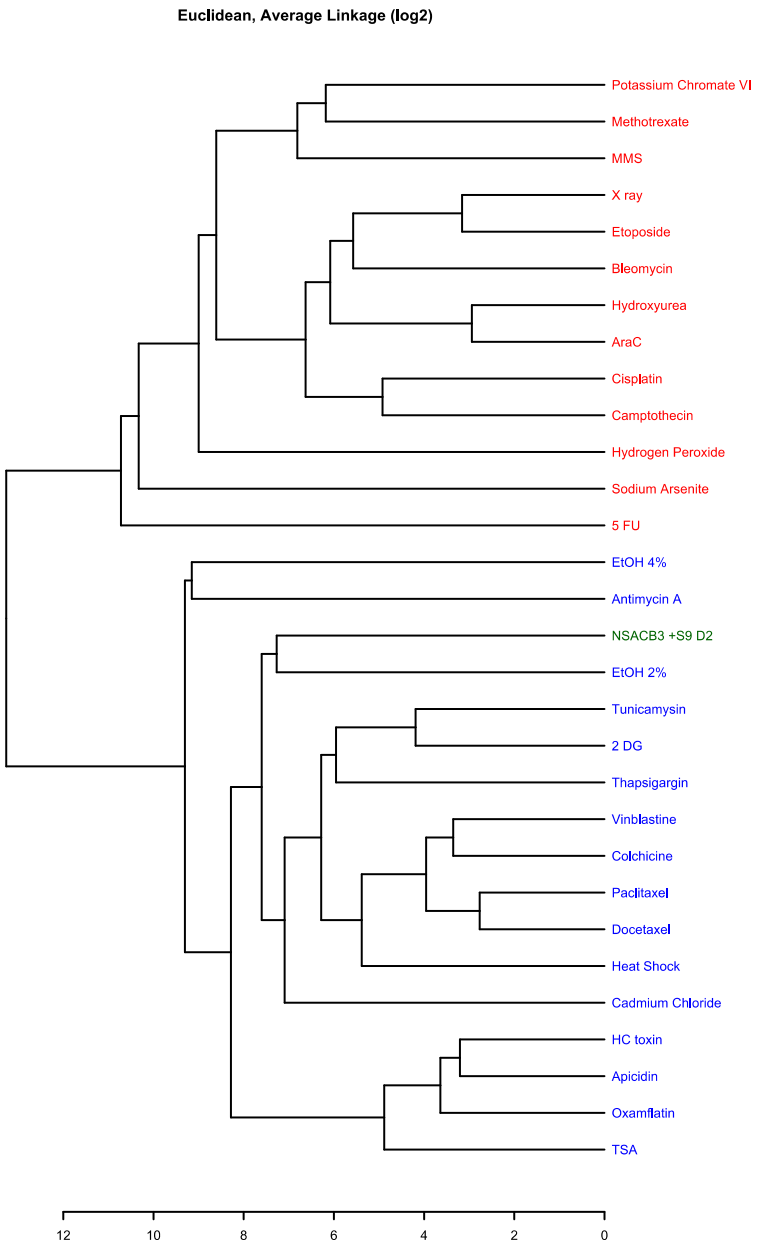
Euclidean, Average Linkage (log2)
Potassium Chromate VI
Methotrexate
MMS
X ray
Etoposide
Bleomycin
Hydroxyurea
AraC
Cisplatin
Camptothecin
Hydrogen Peroxide
Sodium Arsenite
5 FU
EtOH 4%
Antimycin A
NSACB3 +S9 D2
EtOH 2%
Tunicamysin
2 DG
Thapsigargin
Vinblastine
Colchicine
Paclitaxel
Docetaxel
Heat Shock
Cadmium Chloride
HC toxin
Apicidin
Oxamflatin
TSA
12
10
8
6
4
2
0

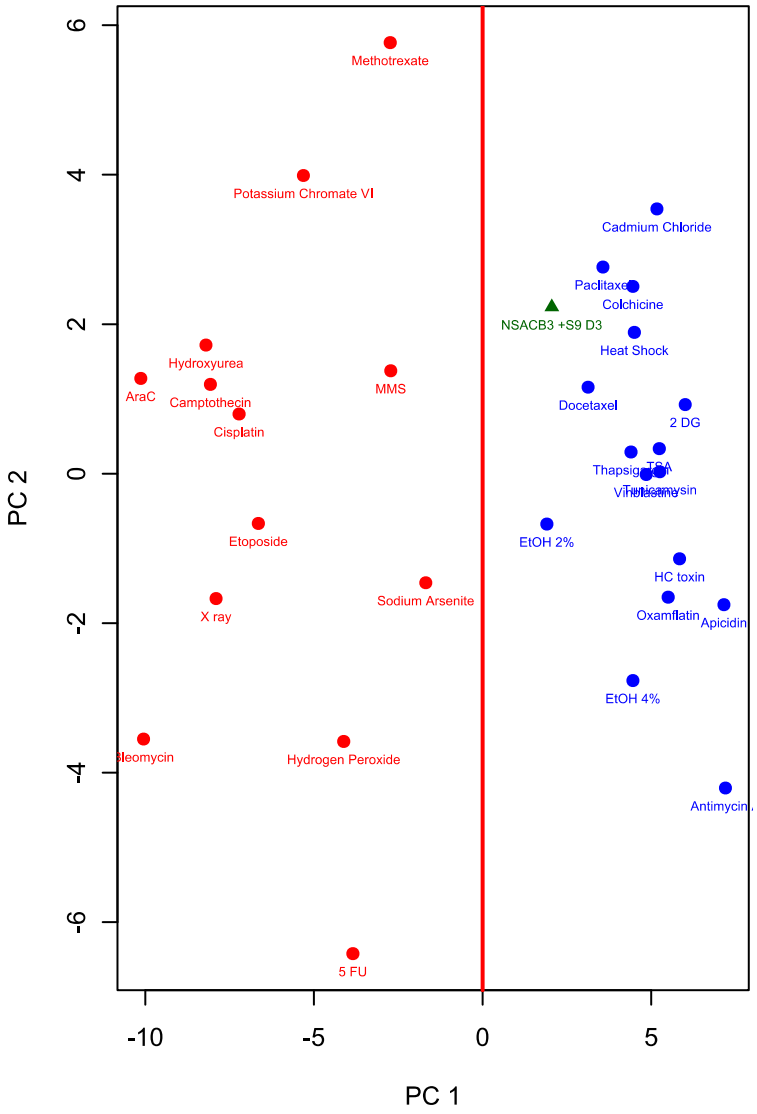
Methotrexate
Potassium Chromate VI
Cadmium Chloride
Paclitaxel
Colchicine
NSACB3 +S9 D3
Heat Shock
Hydroxyurea
AraC
Camptothecin
MMS
Docetaxel
2 DG
Cisplatin
Thapsigargin
TSA
Vinblastine
Tunicamysin
Etoposide
EtOH 2%
HC toxin
Sodium Arsenite
X ray
Oxamflatin
Apicidin
EtOH 4%
Bleomycin
Hydrogen Peroxide
Antimycin
5 FU
PC 2
PC 1
6
4
2
0
-2
-4
-6
-10
-5
0
5

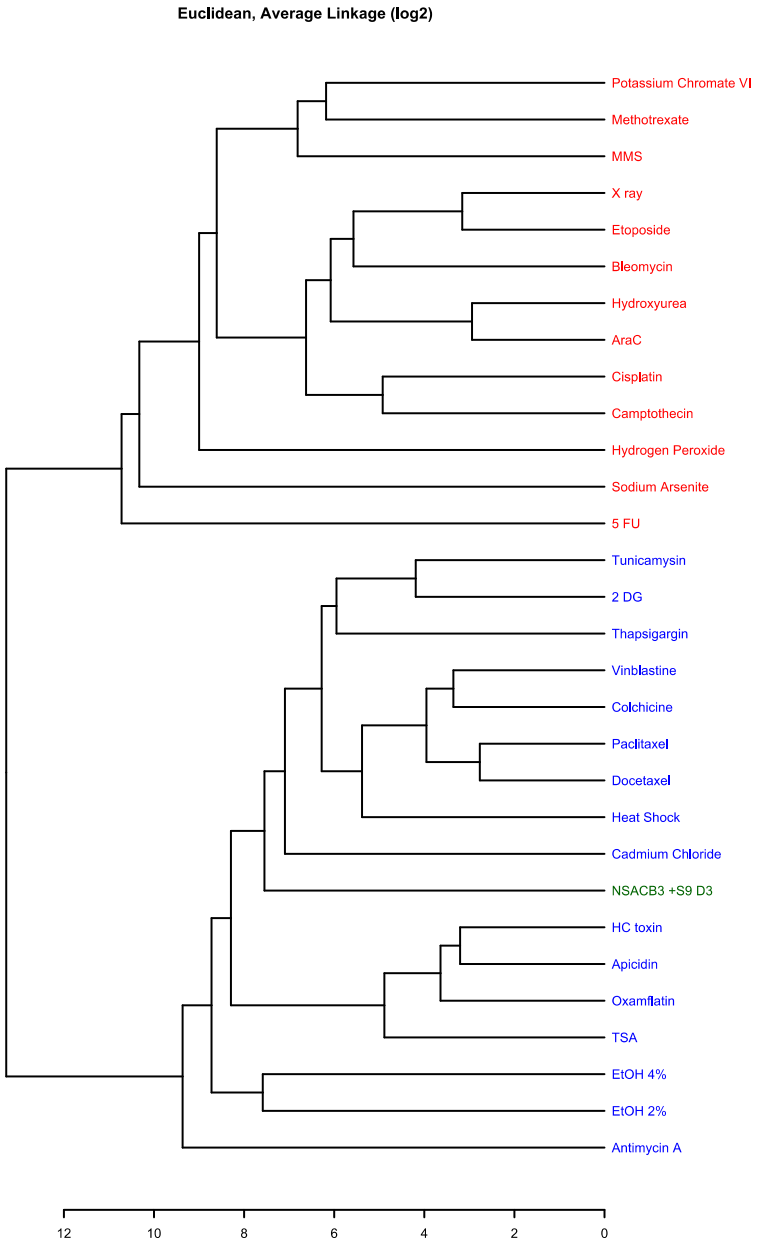
Euclidean, Average Linkage (log2)
Potassium Chromate VI
Methotrexate
MMS
X ray
Etoposide
Bleomycin
Hydroxyurea
AraC
Cisplatin
Camptothecin
Hydrogen Peroxide
Sodium Arsenite
5 FU
Tunicamysin
2 DG
Thapsigargin
Vinblastine
Colchicine
Paclitaxel
Docetaxel
Heat Shock
Cadmium Chloride
NSACB3 +S9 D3
HC toxin
Apicidin
Oxamflatin
TSA
EtOH 4%
EtOH 2%
Antimycin A
12
10
8
6
4
2
0

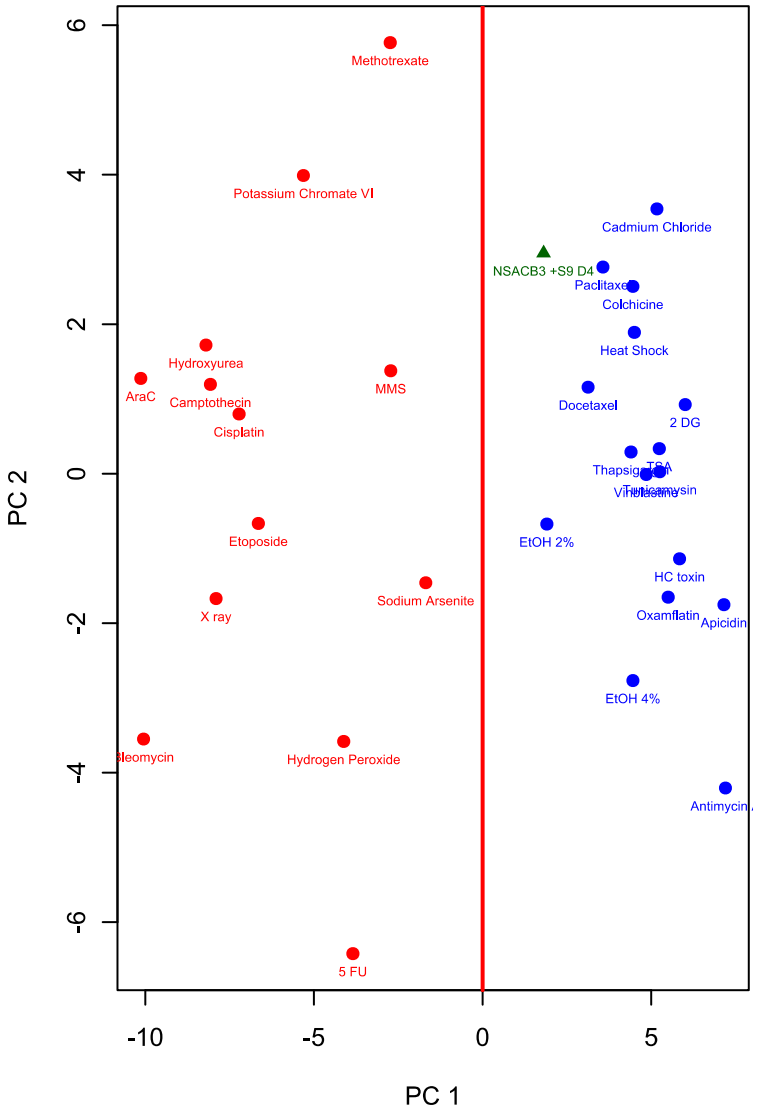
Methotrexate
Potassium Chromate VI
Cadmium Chloride
NSACB3 +S9 D4
Paclitaxel
Colchicine
Heat Shock
Hydroxyurea
AraC
Camptothecin
Cisplatin
MMS
Docetaxel
2 DG
Thapsigargin
TSA
Vinblastine
Tunicamysin
Etoposide
EtOH 2%
HC toxin
Sodium Arsenite
X ray
Oxamflatin
Apicidin
EtOH 4%
Bleomycin
Hydrogen Peroxide
Antimycin
5 FU
PC 2
PC 1
6
4
2
0
-2
-4
-6
-10
-5
0
5

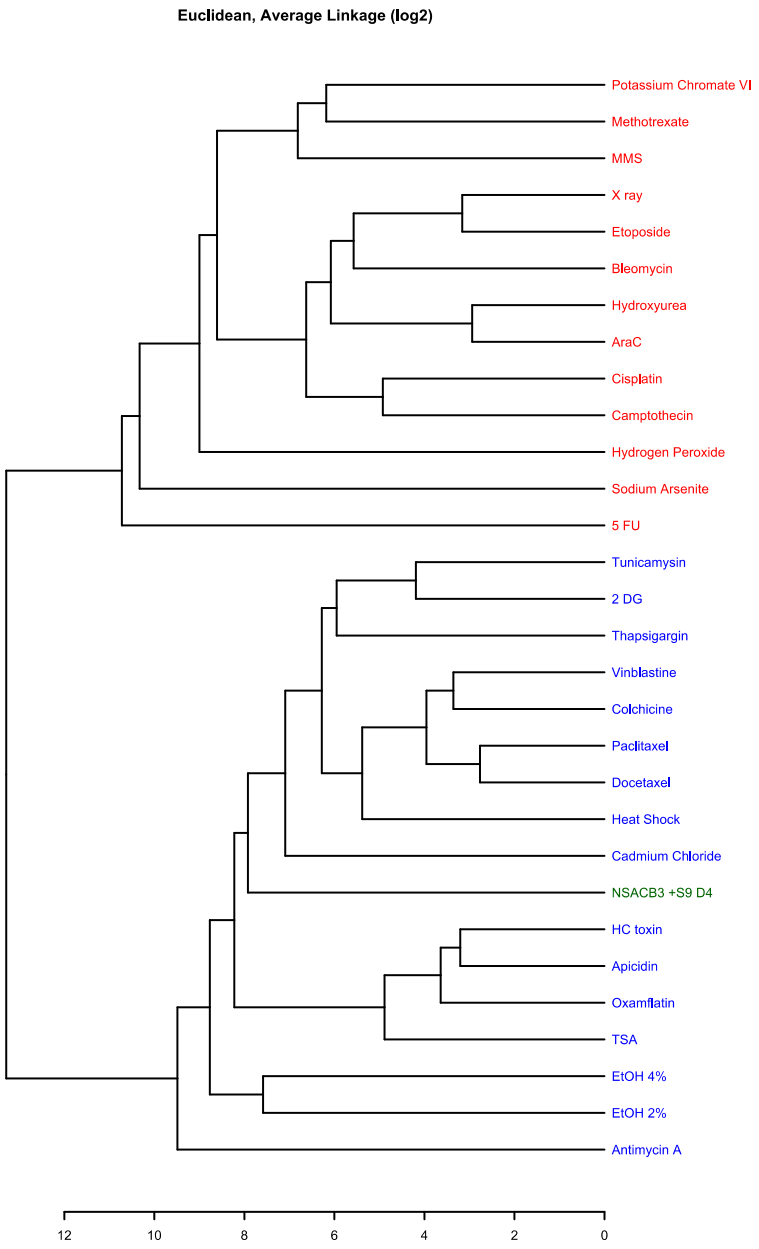
Euclidean, Average Linkage (log2)
Potassium Chromate VI
Methotrexate
MMS
X ray
Etoposide
Bleomycin
Hydroxyurea
AraC
Cisplatin
Camptothecin
Hydrogen Peroxide
Sodium Arsenite
5 FU
Tunicamysin
2 DG
Thapsigargin
Vinblastine
Colchicine
Paclitaxel
Docetaxel
Heat Shock
Cadmium Chloride
NSACB3 +S9 D4
HC toxin
Apicidin
Oxamflatin
TSA
EtOH 4%
EtOH 2%
Antimycin A
12
10
8
6
4
2
0

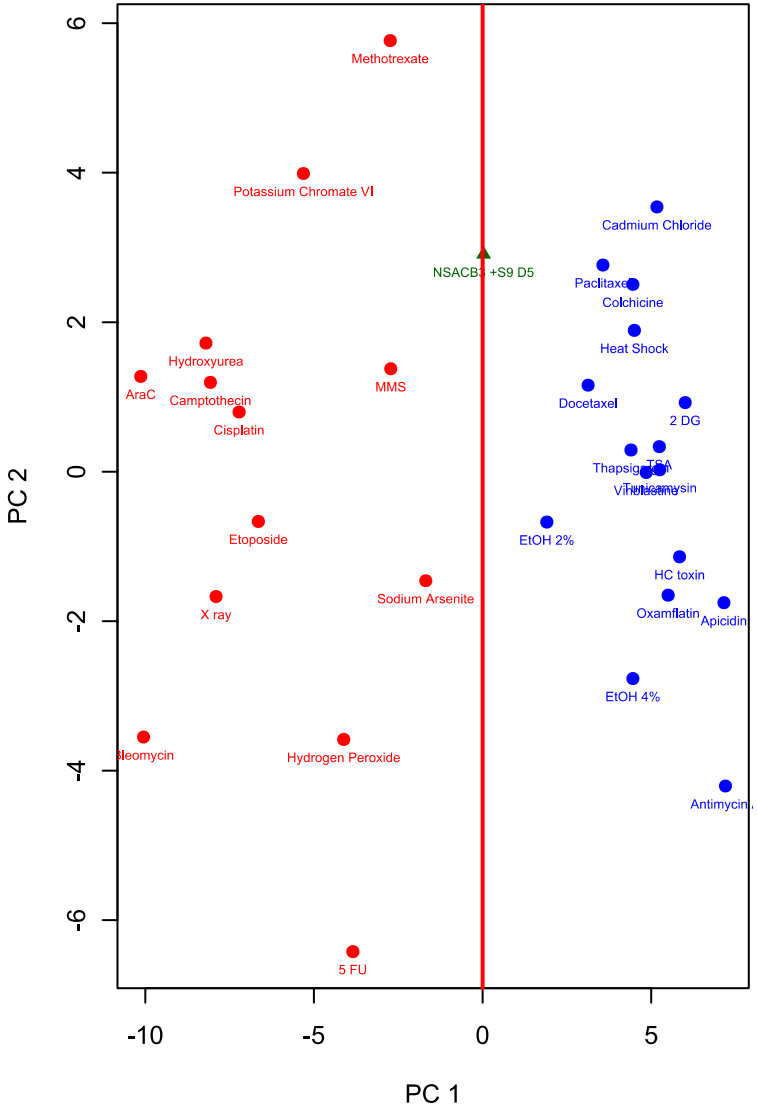
Methotrexate
Potassium Chromate VI
Cadmium Chloride
NSACB3 +S9 D5
Paclitaxel
Colchicine
Heat Shock
Hydroxyurea
AraC
Camptothecin
MMS
Docetaxel
2 DG
Cisplatin
Thapsigargin
TSA
Vinblastine
Tunicamysin
Etoposide
EtOH 2%
HC toxin
Sodium Arsenite
X ray
Oxamflatin
Apicidin
EtOH 4%
Bleomycin
Hydrogen Peroxide
Antimycin
5 FU
PC 2
PC 1
6
4
2
0
-2
-4
-6
-10
-5
0
5

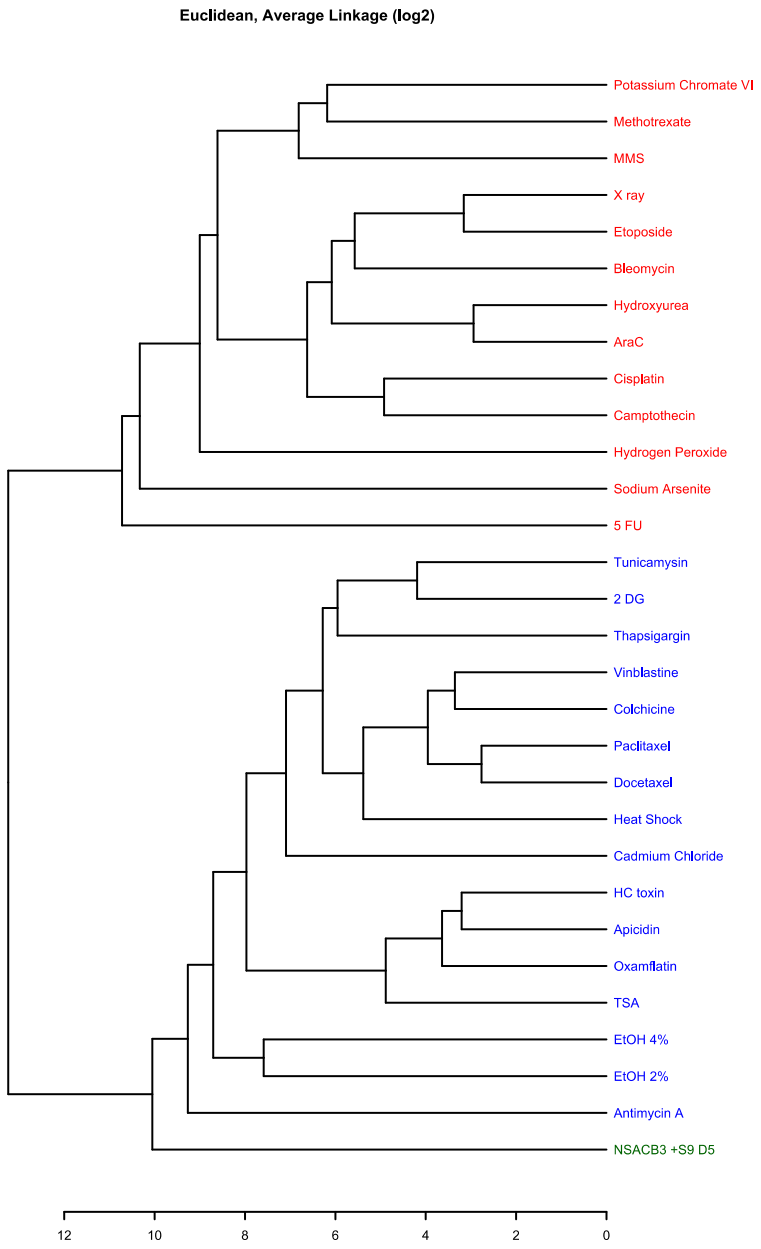
Euclidean, Average Linkage (log2)
Potassium Chromate VI
Methotrexate
MMS
X ray
Etoposide
Bleomycin
Hydroxyurea
AraC
Cisplatin
Camptothecin
Hydrogen Peroxide
Sodium Arsenite
5 FU
Tunicamysin
2 DG
Thapsigargin
Vinblastine
Colchicine
Paclitaxel
Docetaxel
Heat Shock
Cadmium Chloride
HC toxin
Apicidin
Oxamflatin
TSA
EtOH 4%
EtOH 2%
Antimycin A
NSACB3 +S9 D5
12
10
8
6
4
2
0

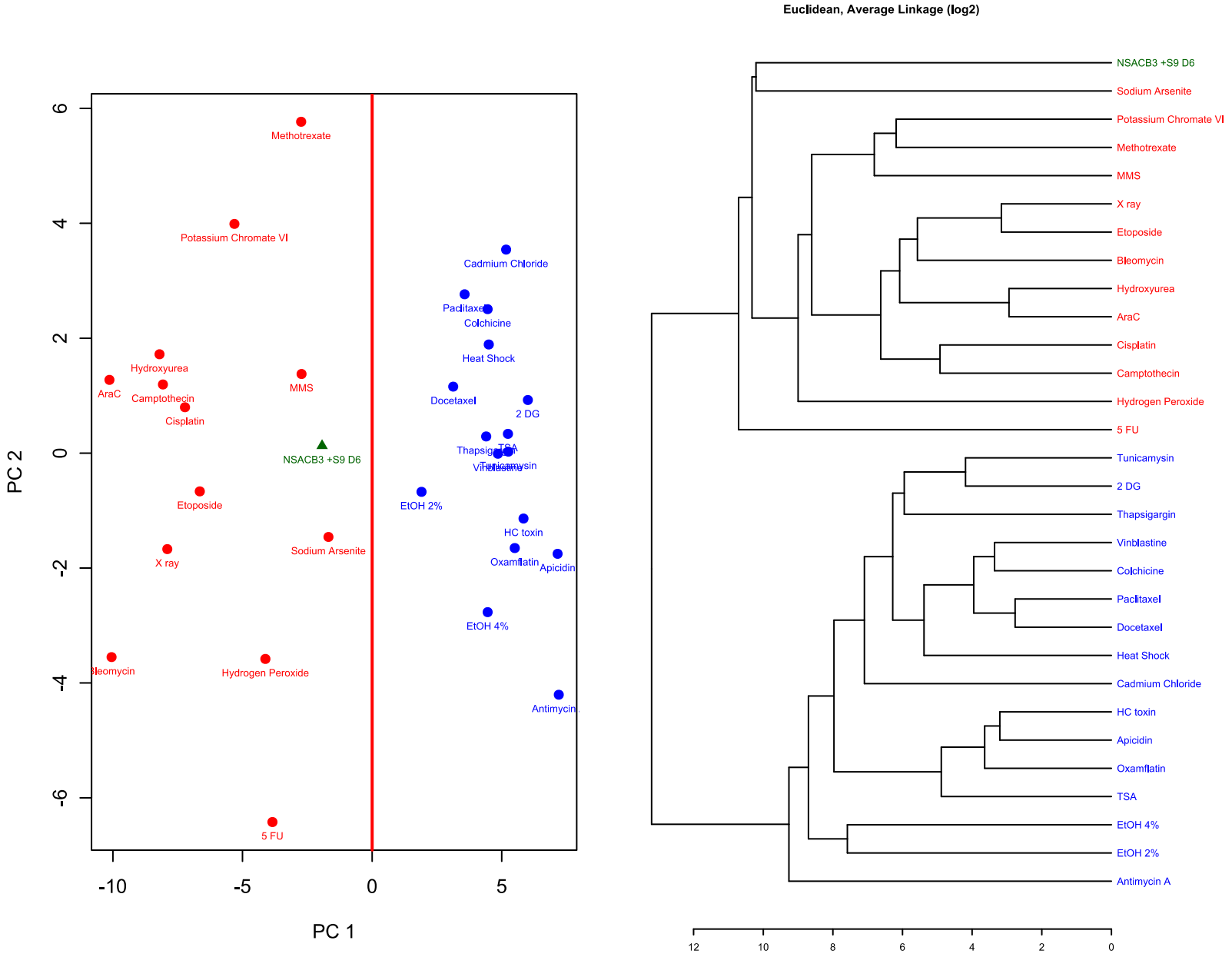

Supplementary Figure III-D: NASCB 3 (+S9) TGx-DDI biomarker classification using the Principal Component Analysis (PCA) (left) and hierarchical clustering (right) statistical analyses. Genotoxic reference chemicals are shown in red text, non-genotoxic reference chemicals are shown in blue text, and the test agent is shown in the green text. The line drawn on the PCA plot and the main branch on the dendogram divides the genotoxic and non-genotoxic agents and was used to classify the test compounds. D1 represents the lowest concentration tested, D6 the highest.

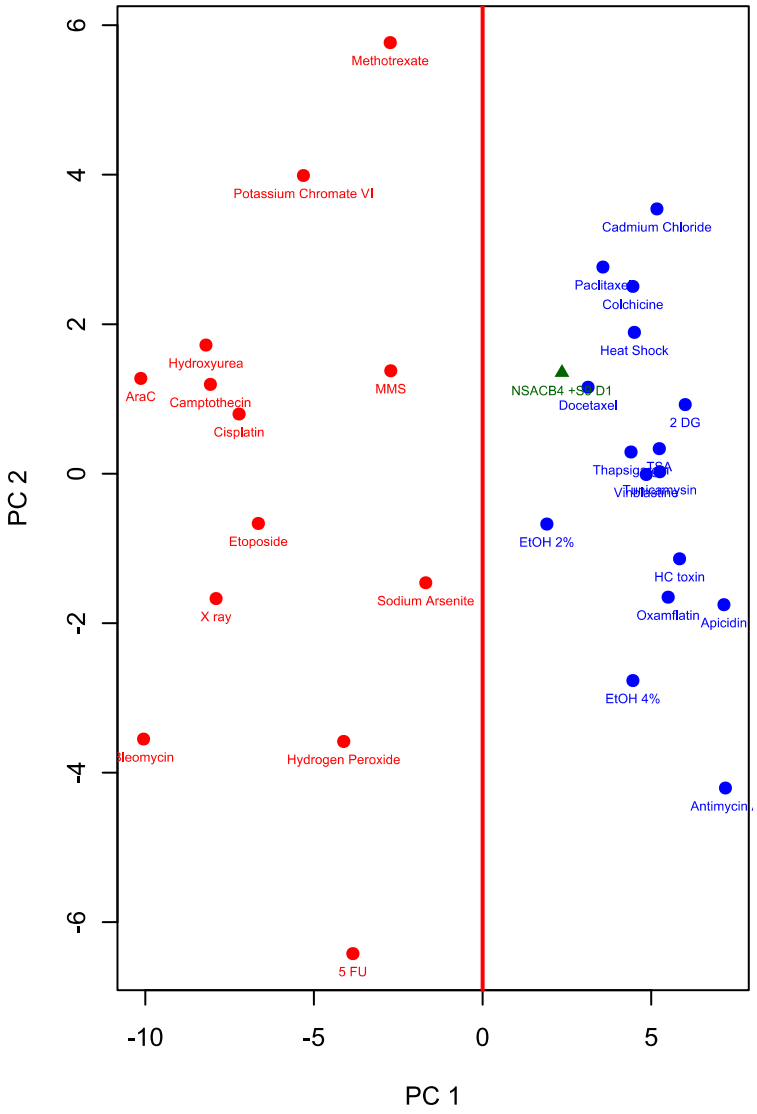
Methotrexate
Potassium Chromate VI
Cadmium Chloride
Paclitaxel
Colchicine
Heat Shock
Hydroxyurea
AraC
Camptothecin
Cisplatin
MMS
NSACB4 +S9 D1
Docetaxel
2 DG
Thapsigargin
TSA
Vinblastine
Tunicamysin
Etoposide
EtOH 2%
HC toxin
Sodium Arsenite
X ray
Oxamflatin
Apicidin
EtOH 4%
Bleomycin
Hydrogen Peroxide
Antimycin
5 FU
PC 2
PC 1
6
4
2
0
-2
-4
-6
-10
-5
0
5

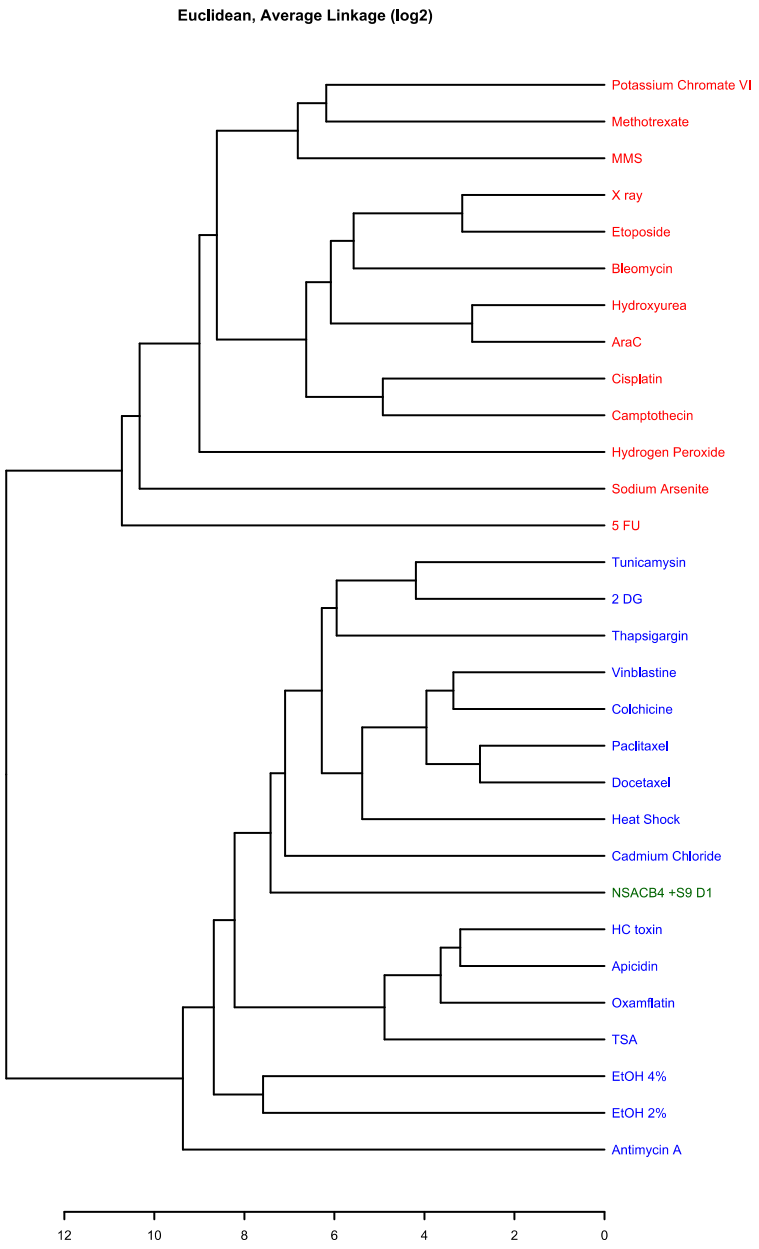
Euclidean, Average Linkage (log2)
Potassium Chromate VI
Methotrexate
MMS
X ray
Etoposide
Bleomycin
Hydroxyurea
AraC
Cisplatin
Camptothecin
Hydrogen Peroxide
Sodium Arsenite
5 FU
Tunicamysin
2 DG
Thapsigargin
Vinblastine
Colchicine
Paclitaxel
Docetaxel
Heat Shock
Cadmium Chloride
NSACB4 +S9 D1
HC toxin
Apicidin
Oxamflatin
TSA
EtOH 4%
EtOH 2%
Antimycin A
12
10
8
6
4
2
0

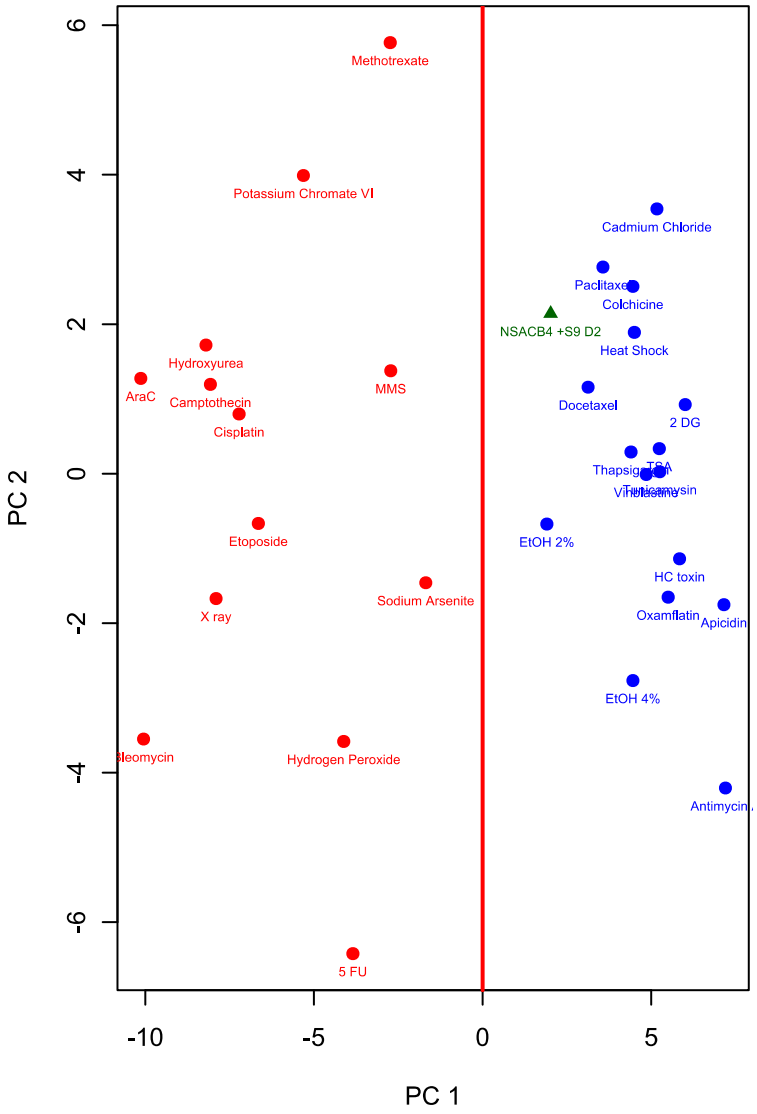
Methotrexate
Potassium Chromate VI
Cadmium Chloride
Paclitaxel
Colchicine
NSACB4 +S9 D2
Heat Shock
Hydroxyurea
AraC
Camptothecin
MMS
Docetaxel
2 DG
Cisplatin
Thapsigargin
TSA
Vinblastine
Tunicamysin
Etoposide
EtOH 2%
HC toxin
Sodium Arsenite
X ray
Oxamflatin
Apicidin
EtOH 4%
Bleomycin
Hydrogen Peroxide
Antimycin
5 FU
PC 2
PC 1
6
4
2
0
-2
-4
-6
-10
-5
0
5

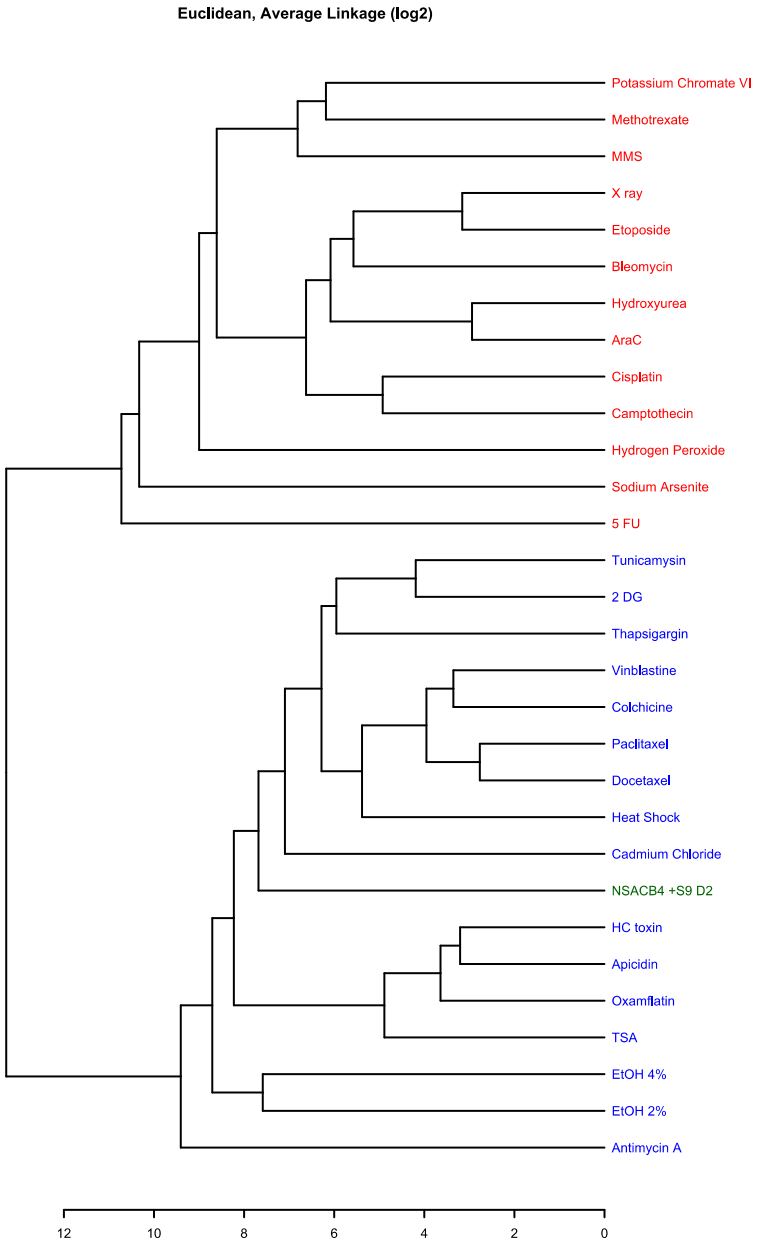
Euclidean, Average Linkage (log2)
Potassium Chromate VI
Methotrexate
MMS
X ray
Etoposide
Bleomycin
Hydroxyurea
AraC
Cisplatin
Camptothecin
Hydrogen Peroxide
Sodium Arsenite
5 FU
Tunicamysin
2 DG
Thapsigargin
Vinblastine
Colchicine
Paclitaxel
Docetaxel
Heat Shock
Cadmium Chloride
NSACB4 +S9 D2
HC toxin
Apicidin
Oxamflatin
TSA
EtOH 4%
EtOH 2%
Antimycin A
12
10
8
6
4
2
0

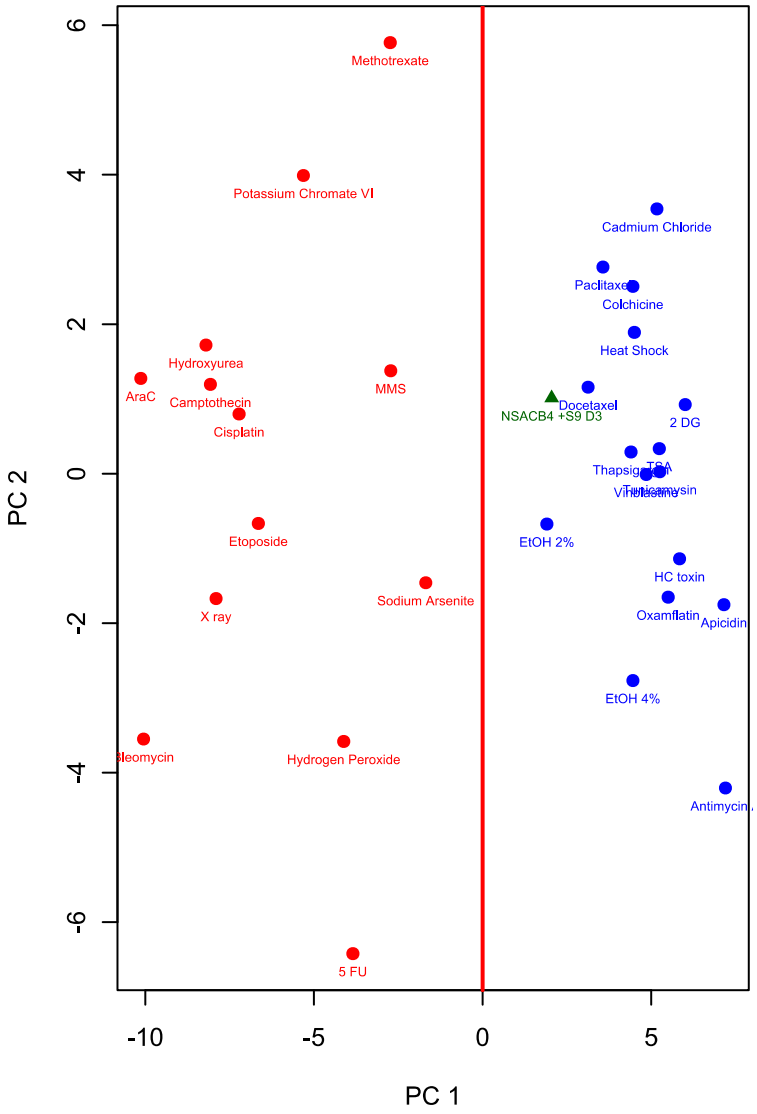
Methotrexate
Potassium Chromate VI
Cadmium Chloride
Paclitaxel
Colchicine
Heat Shock
Hydroxyurea
AraC
Camptothecin
MMS
Docetaxel
NSACB4 +S9 D3
2 DG
Cisplatin
Thapsigargin
TSA
Vinblastine
Tunicamysin
Etoposide
EtOH 2%
HC toxin
Sodium Arsenite
X ray
Oxamflatin
Apicidin
EtOH 4%
Bleomycin
Hydrogen Peroxide
Antimycin
5 FU
PC 2
PC 1
6
4
2
0
-2
-4
-6
-10
-5
0
5

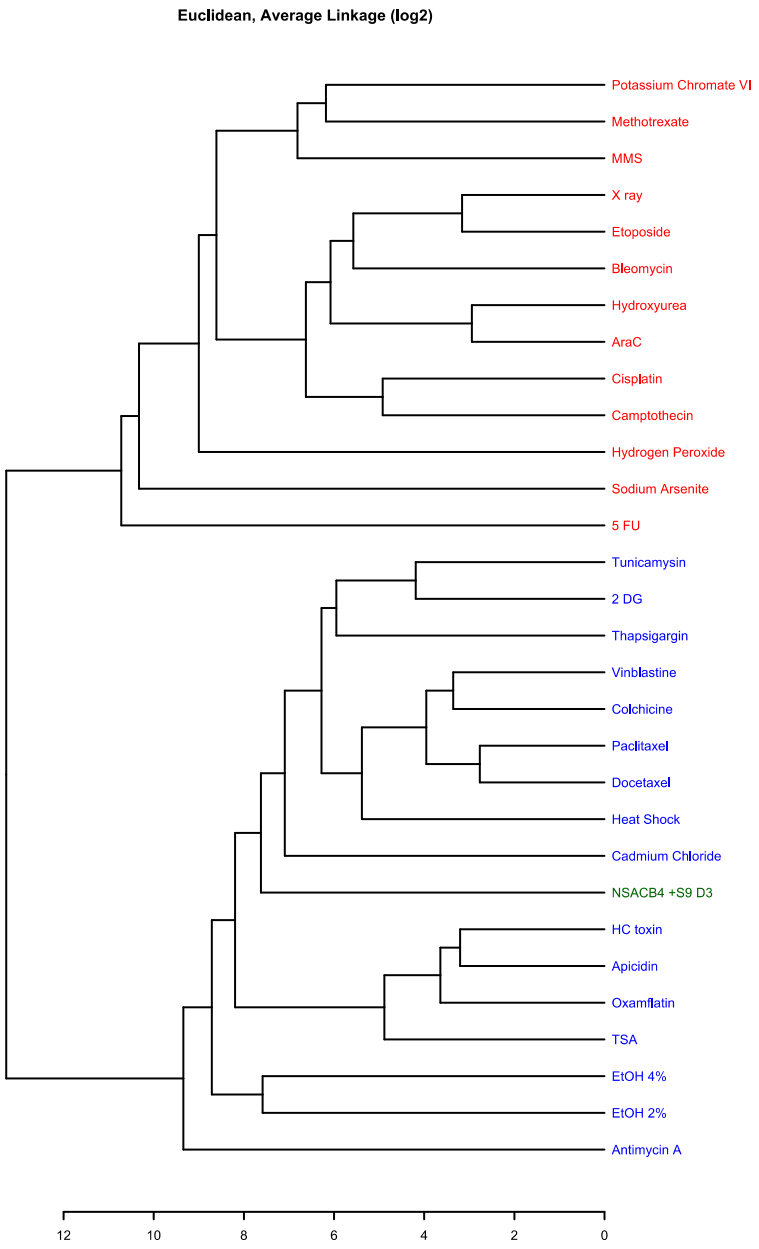
Euclidean, Average Linkage (log2)
Potassium Chromate VI
Methotrexate
MMS
X ray
Etoposide
Bleomycin
Hydroxyurea
AraC
Cisplatin
Camptothecin
Hydrogen Peroxide
Sodium Arsenite
5 FU
Tunicamysin
2 DG
Thapsigargin
Vinblastine
Colchicine
Paclitaxel
Docetaxel
Heat Shock
Cadmium Chloride
NSACB4 +S9 D3
HC toxin
Apicidin
Oxamflatin
TSA
EtOH 4%
EtOH 2%
Antimycin A
12
10
8
6
4
2
0

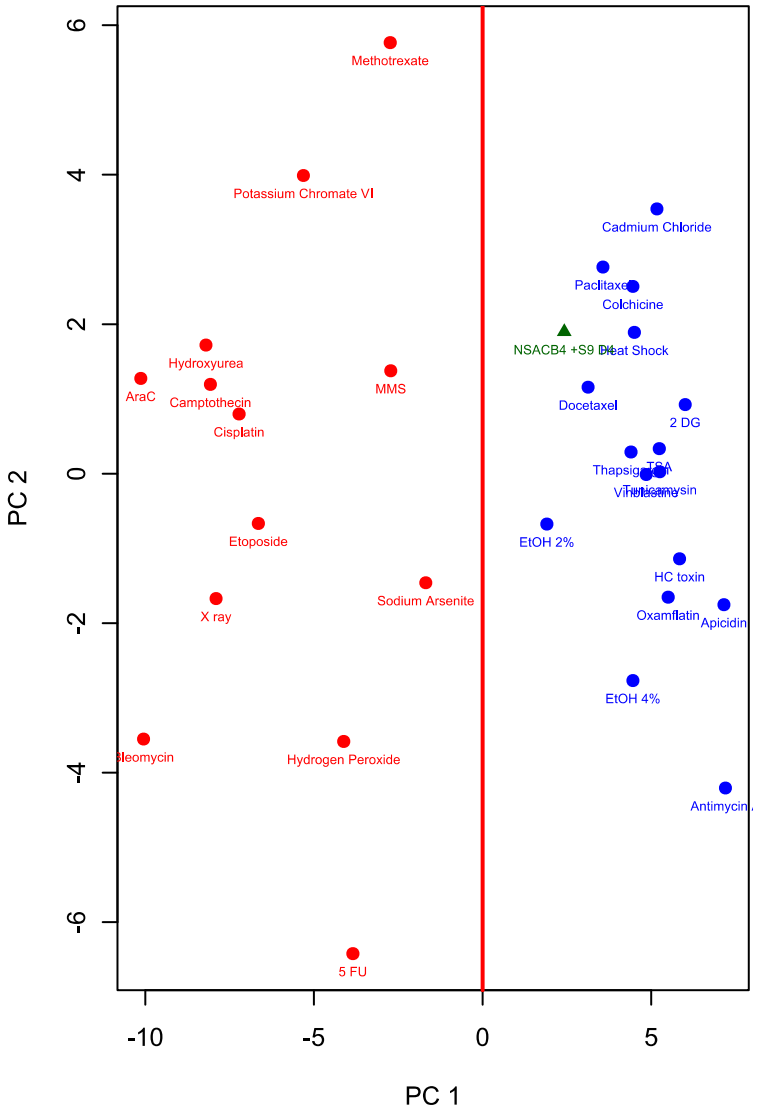
Methotrexate
Potassium Chromate VI
Cadmium Chloride
Paclitaxel
Colchicine
NSACB4 +S9 D4
Heat Shock
Hydroxyurea
AraC
Camptothecin
MMS
Docetaxel
2 DG
Cisplatin
Thapsigargin
TSA
Tunicamysin
Vinblastine
Etoposide
EtOH 2%
HC toxin
Sodium Arsenite
X ray
Oxamflatin
Apicidin
EtOH 4%
Bleomycin
Hydrogen Peroxide
Antimycin
5 FU
PC 2
PC 1
6
4
2
0
-2
-4
-6
-10
-5
0
5

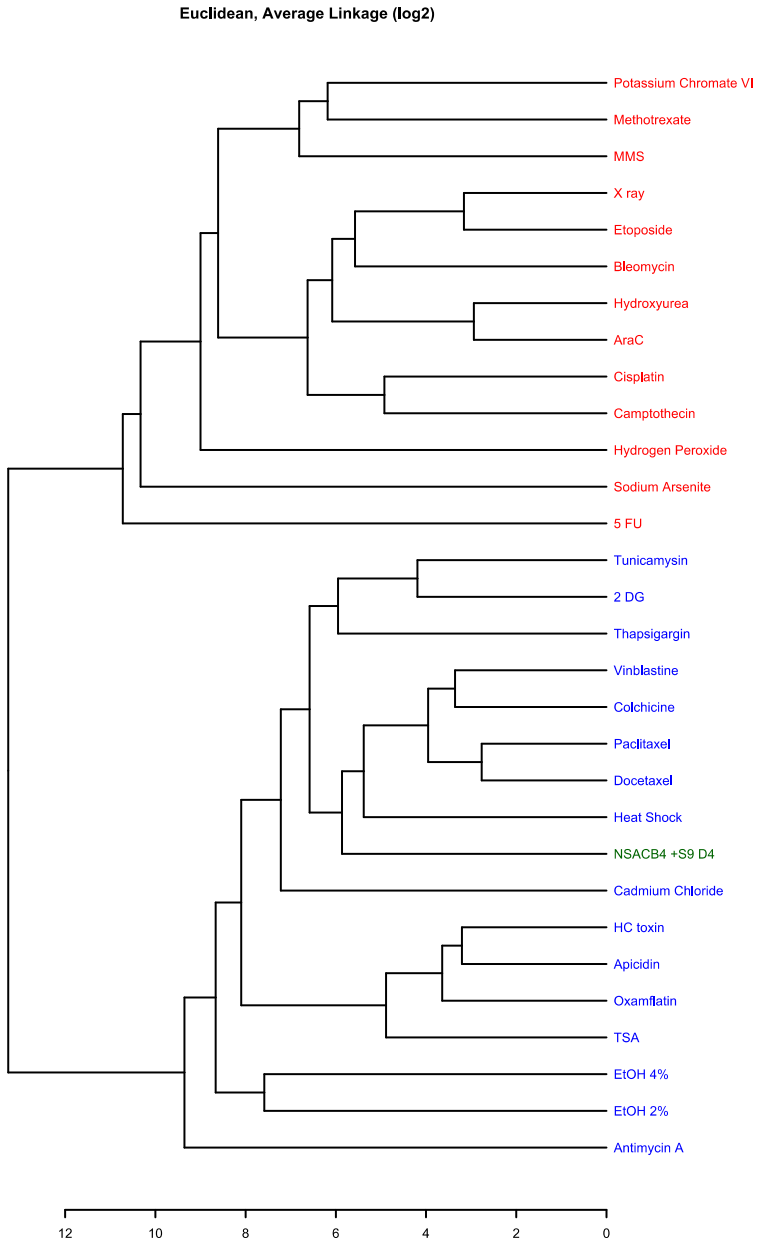
Euclidean, Average Linkage (log2)
Potassium Chromate VI
Methotrexate
MMS
X ray
Etoposide
Bleomycin
Hydroxyurea
AraC
Cisplatin
Camptothecin
Hydrogen Peroxide
Sodium Arsenite
5 FU
Tunicamysin
2 DG
Thapsigargin
Vinblastine
Colchicine
Paclitaxel
Docetaxel
Heat Shock
NSACB4 +S9 D4
Cadmium Chloride
HC toxin
Apicidin
Oxamflatin
TSA
EtOH 4%
EtOH 2%
Antimycin A
12
10
8
6
4
2
0

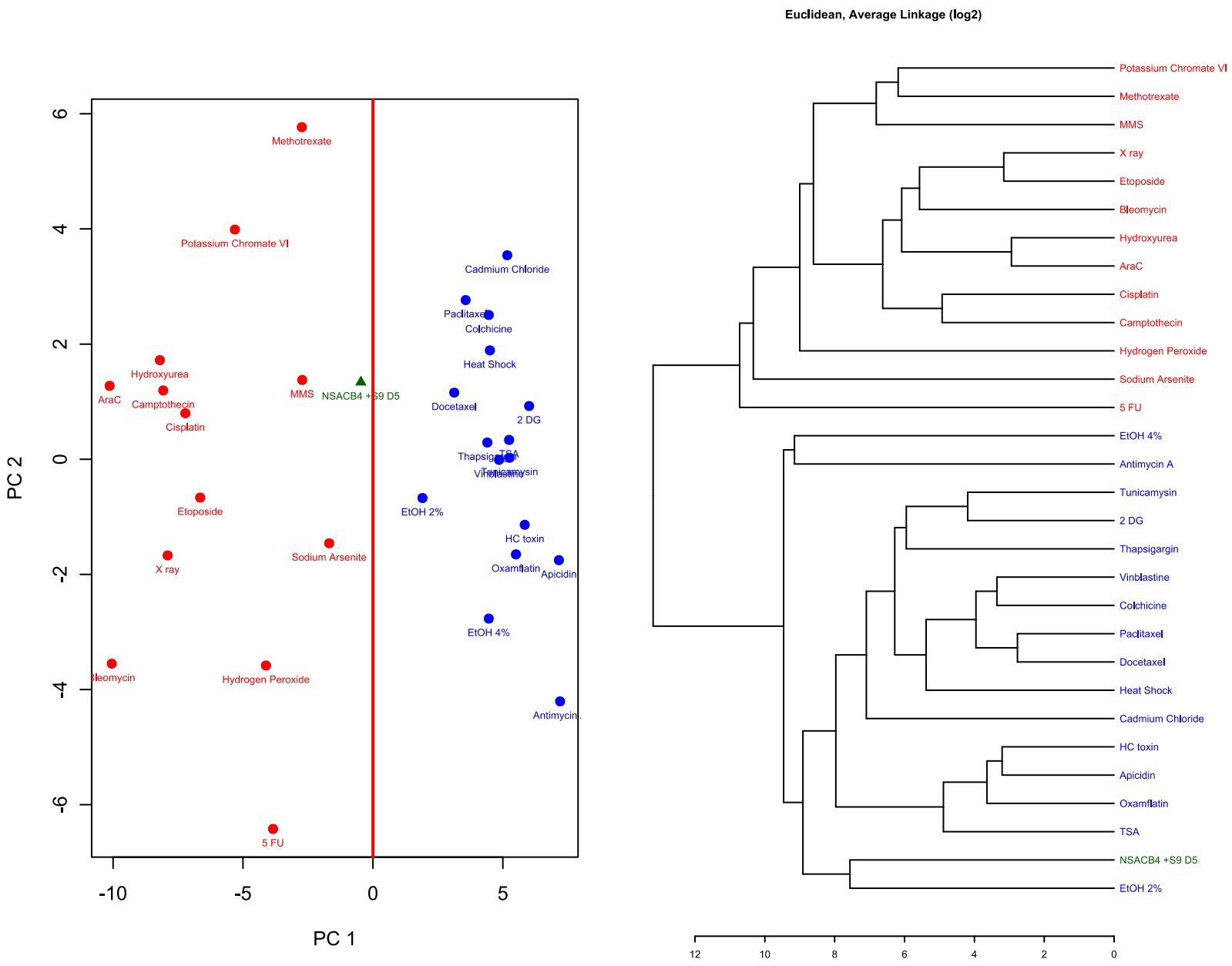

Supplementary Figure III-E: NASCB 4 (+S9) TGx-DDI biomarker classification using the Principal Component Analysis (PCA) (left) and hierarchical clustering (right) statistical analyses. Genotoxic reference chemicals are shown in red text, non-genotoxic reference chemicals are shown in blue text, and the test agent is shown in the green text. The line drawn on the PCA plot and the main branch on the dendogram divides the genotoxic and non-genotoxic agents and was used to classify the test compounds. D1 represents the lowest concentration tested, D5 the highest.

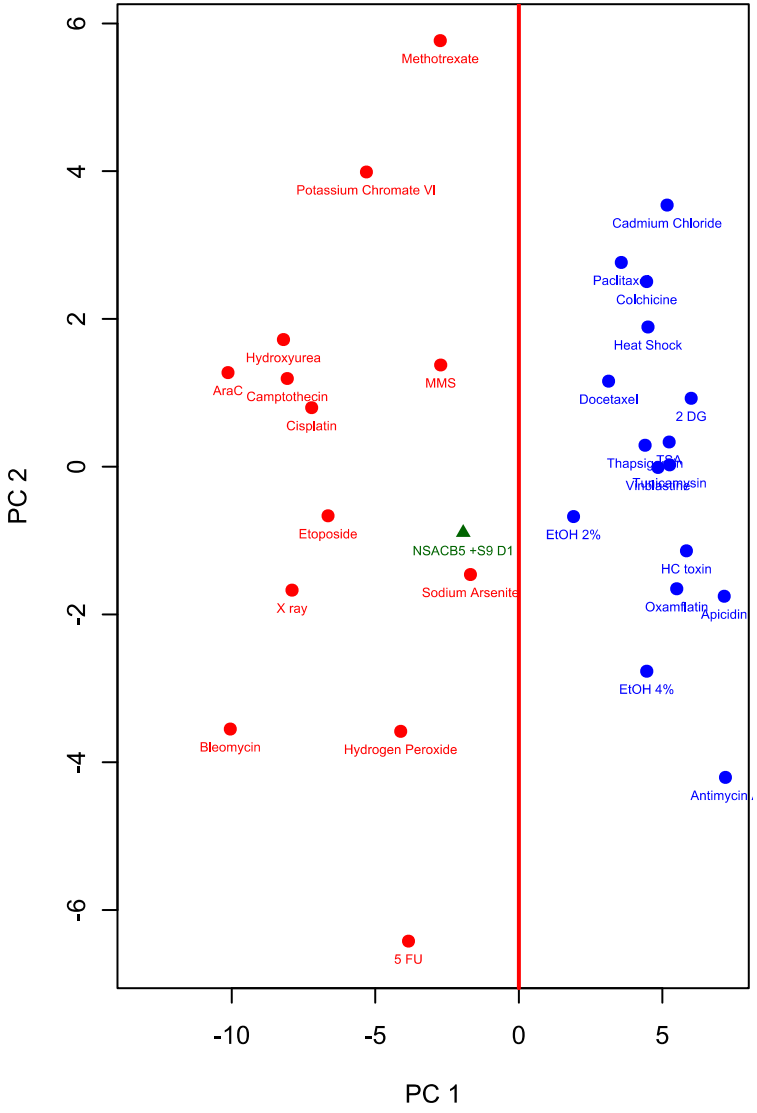
PC 2
PC 1
6
4
2
0
-2
-4
-6
-10
-5
0
5
Methotrexate
Potassium Chromate VI
Cadmium Chloride
Paclitax
Colchicine
Heat Shock
Hydroxyurea
AraC
Camptothecin
Cisplatin
MMS
Docetaxel
2 DG
Thapsig
TSA
Tunicamysin
Vinblastine
Etoposide
NSACB5 +S9 D1
EtOH 2%
HC toxin
Sodium Arsenite
X ray
Oxamflatin
Apicidin
EtOH 4%
Bleomycin
Hydrogen Peroxide
Antimycin
5 FU

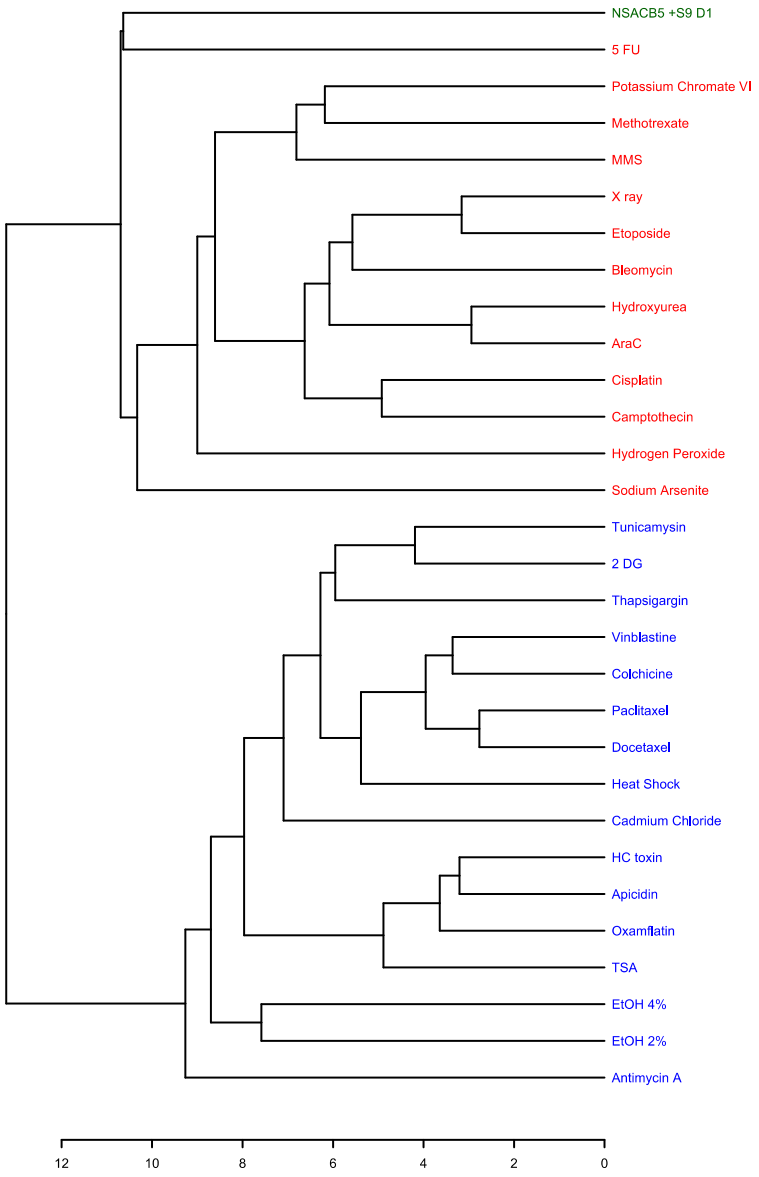
Euclidean, Average Linkage (log2)
NSACB5 +S9 D1
5 FU
Potassium Chromate VI
Methotrexate
MMS
X ray
Etoposide
Bleomycin
Hydroxyurea
AraC
Cisplatin
Camptothecin
Hydrogen Peroxide
Sodium Arsenite
Tunicamysin
2 DG
Thapsigargin
Vinblastine
Colchicine
Paclitaxel
Docetaxel
Heat Shock
Cadmium Chloride
HC toxin
Apicidin
Oxamflatin
TSA
EtOH 4%
EtOH 2%
Antimycin A
12
10
8
6
4
2
0

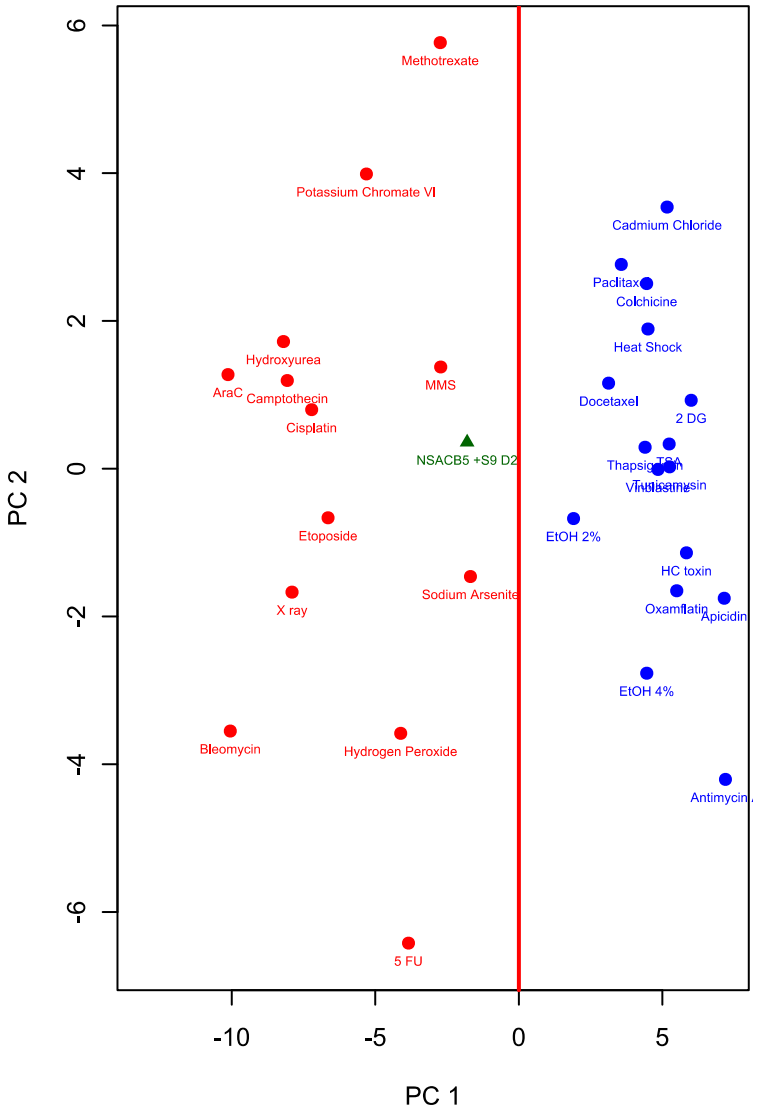
PC 2
PC 1
6
4
2
0
-2
-4
-6
-10
-5
0
5
Methotrexate
Potassium Chromate VI
Cadmium Chloride
Paclitax
Colchicine
Heat Shock
Hydroxyurea
AraC
Camptothecin
Cisplatin
MMS
Docetaxel
2 DG
NSACB5 +S9 D2
Thapsigargin
TSA
Vinblastine
Tunicamysin
Etoposide
EtOH 2%
HC toxin
Sodium Arsenite
X ray
Oxamflatin
Apicidin
EtOH 4%
Bleomycin
Hydrogen Peroxide
Antimycin.
5 FU

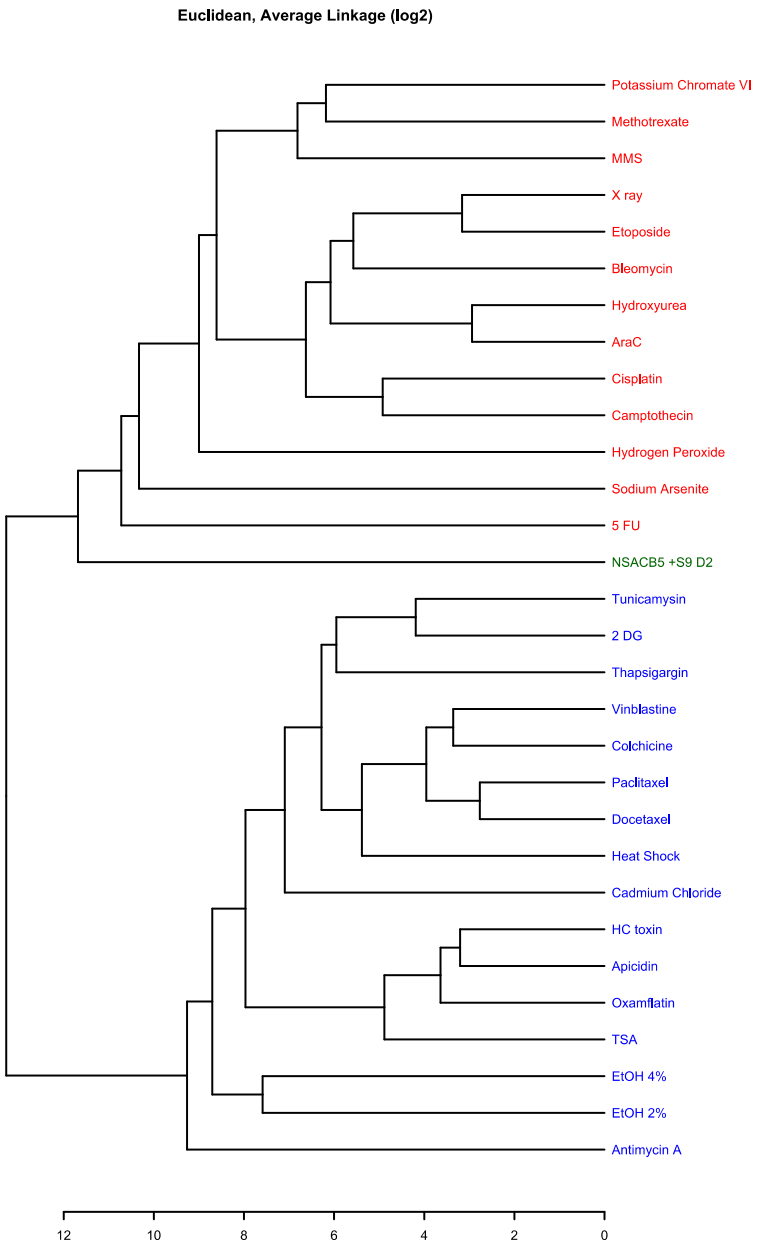
Euclidean, Average Linkage (log2)
Potassium Chromate VI
Methotrexate
MMS
X ray
Etoposide
Bleomycin
Hydroxyurea
AraC
Cisplatin
Camptothecin
Hydrogen Peroxide
Sodium Arsenite
5 FU
NSACB5 +S9 D2
Tunicamysin
2 DG
Thapsigargin
Vinblastine
Colchicine
Paclitaxel
Docetaxel
Heat Shock
Cadmium Chloride
HC toxin
Apicidin
Oxamflatin
TSA
EtOH 4%
EtOH 2%
Antimycin A
12
10
8
6
4
2
0

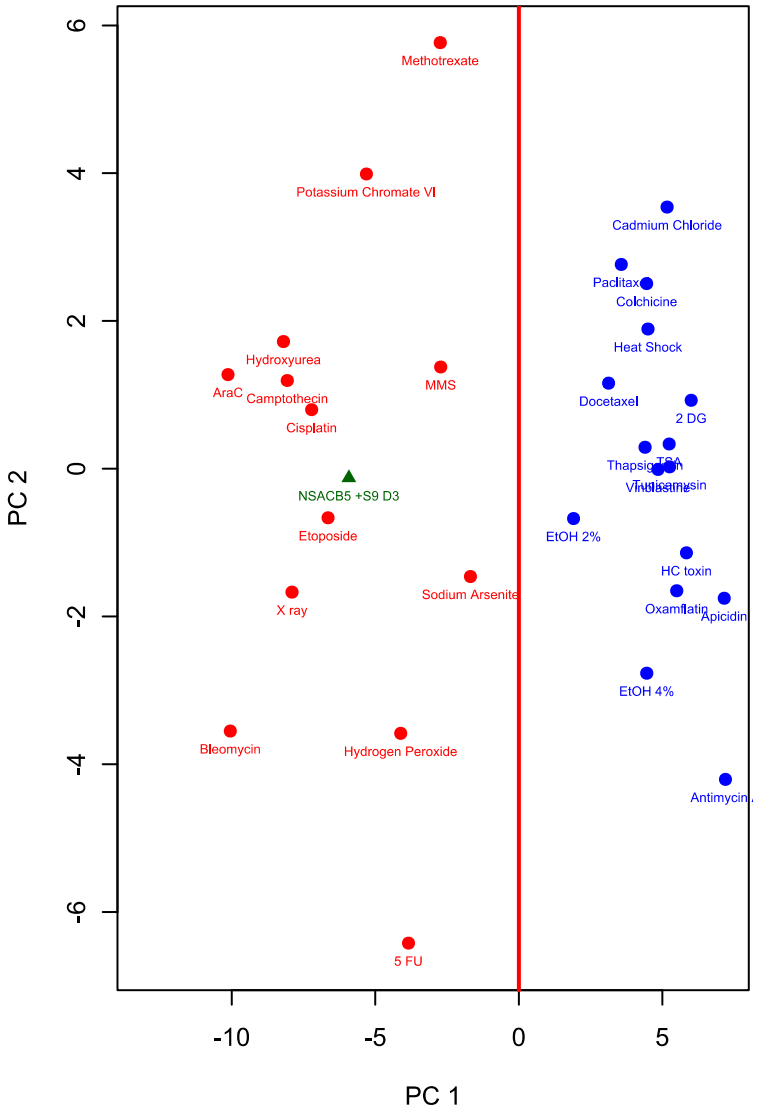
Methotrexate
Potassium Chromate VI
Cadmium Chloride
Paclitax
Colchicine
Heat Shock
Hydroxyurea
AraC
Camptothecin
MMS
Docetaxel
2 DG
Cisplatin
Thapsigargin
TSA
Tunicamysin
Vinblastine
NSACB5 +S9 D3
Etoposide
EtOH 2%
HC toxin
Sodium Arsenite
X ray
Oxamflatin
Apicidin
EtOH 4%
Bleomycin
Hydrogen Peroxide
Antimycin A
5 FU
PC 2
PC 1
6
4
2
0
-2
-4
-6
-10
-5
0
5

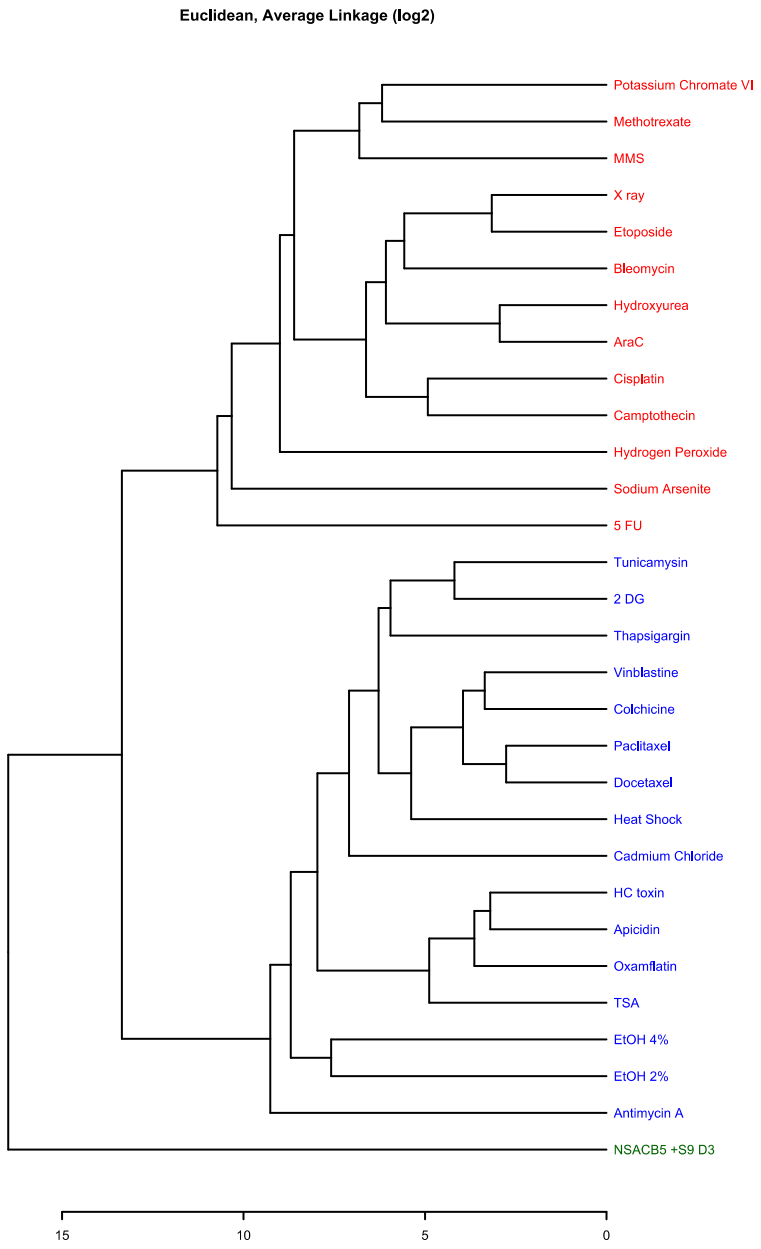
Euclidean, Average Linkage (log2)
Potassium Chromate VI
Methotrexate
MMS
X ray
Etoposide
Bleomycin
Hydroxyurea
AraC
Cisplatin
Camptothecin
Hydrogen Peroxide
Sodium Arsenite
5 FU
Tunicamysin
2 DG
Thapsigargin
Vinblastine
Colchicine
Paclitaxel
Docetaxel
Heat Shock
Cadmium Chloride
HC toxin
Apicidin
Oxamflatin
TSA
EtOH 4%
EtOH 2%
Antimycin A
NSACB5 +S9 D3
15
10
5
0

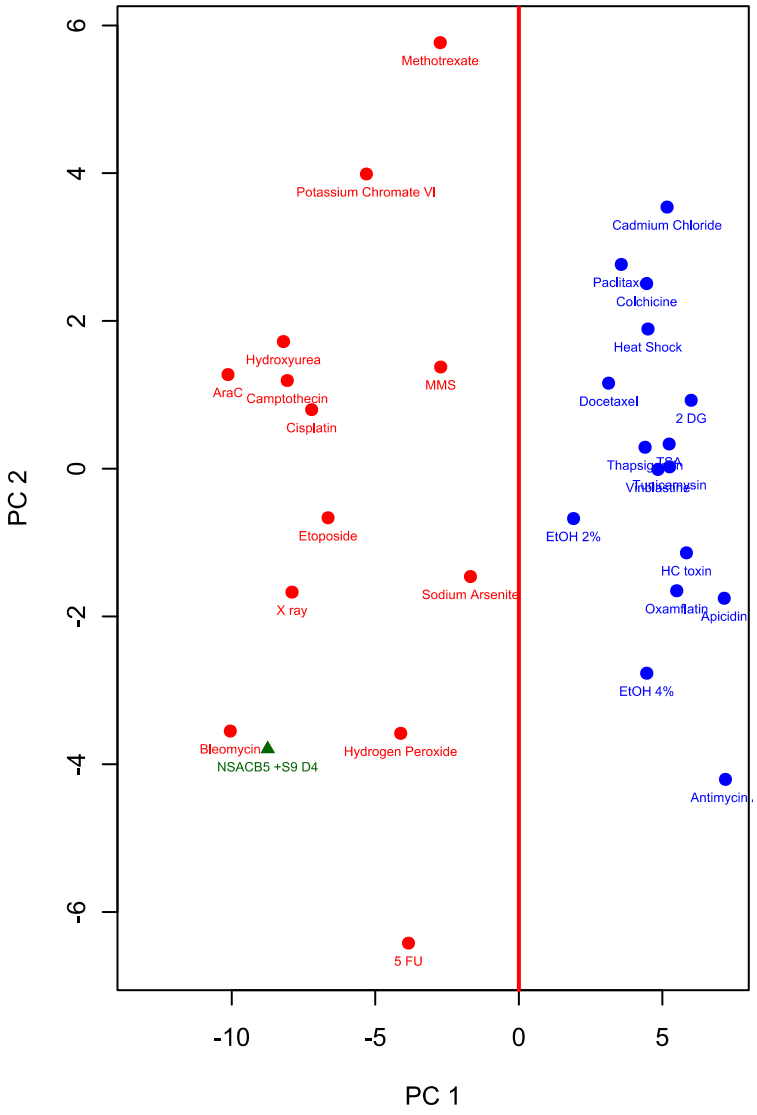
Methotrexate
Potassium Chromate VI
Cadmium Chloride
Paclitax
Colchicine
Heat Shock
Hydroxyurea
AraC
Camptothecin
Cisplatin
MMS
Docetaxel
2 DG
Thapsigargin
TSA
Tunicamysin
Vinblastine
Etoposide
EtOH 2%
HC toxin
Sodium Arsenite
X ray
Oxamflatin
Apicidin
EtOH 4%
Bleomycin
NSACB5 +S9 D4
Hydrogen Peroxide
Antimycin A
5 FU
PC 2
PC 1
6
4
2
0
-2
-4
-6
-10
-5
0
5

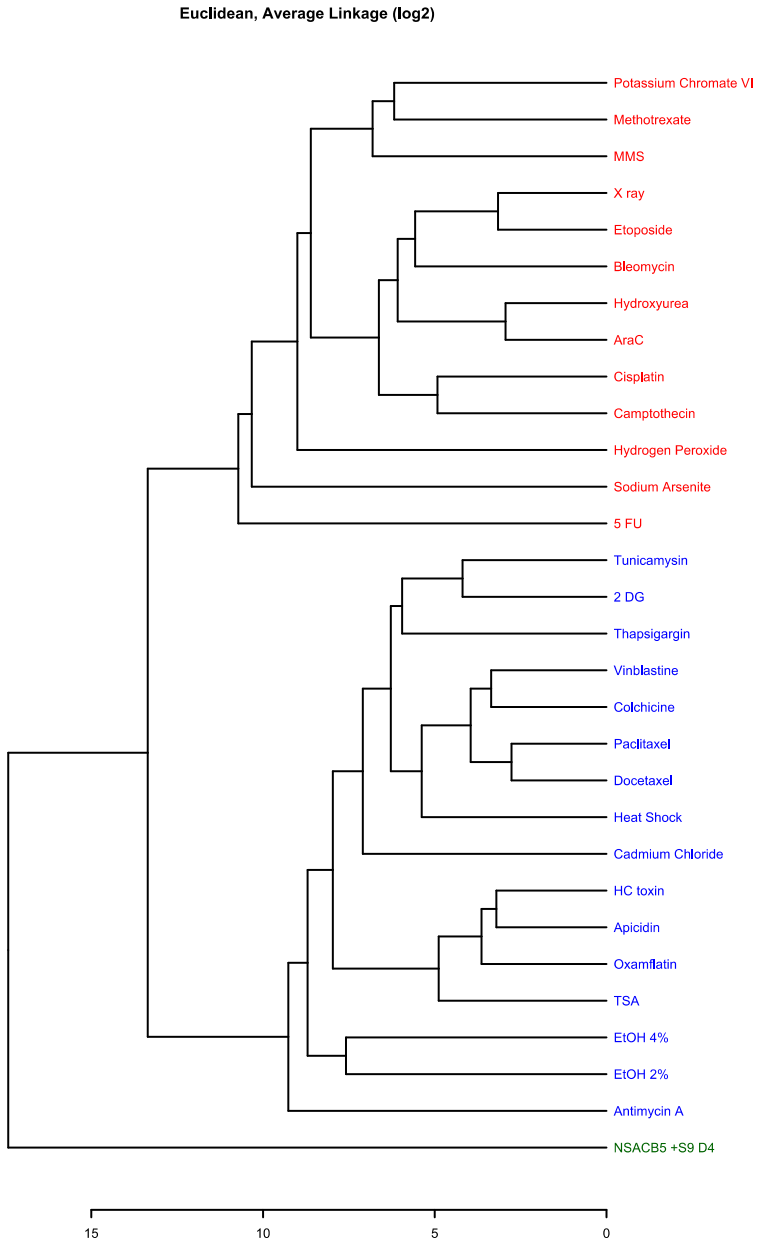
Euclidean, Average Linkage (log2)
Potassium Chromate VI
Methotrexate
MMS
X ray
Etoposide
Bleomycin
Hydroxyurea
AraC
Cisplatin
Camptothecin
Hydrogen Peroxide
Sodium Arsenite
5 FU
Tunicamysin
2 DG
Thapsigargin
Vinblastine
Colchicine
Paclitaxel
Docetaxel
Heat Shock
Cadmium Chloride
HC toxin
Apicidin
Oxamflatin
TSA
EtOH 4%
EtOH 2%
Antimycin A
NSACB5 +S9 D4
15
10
5
0

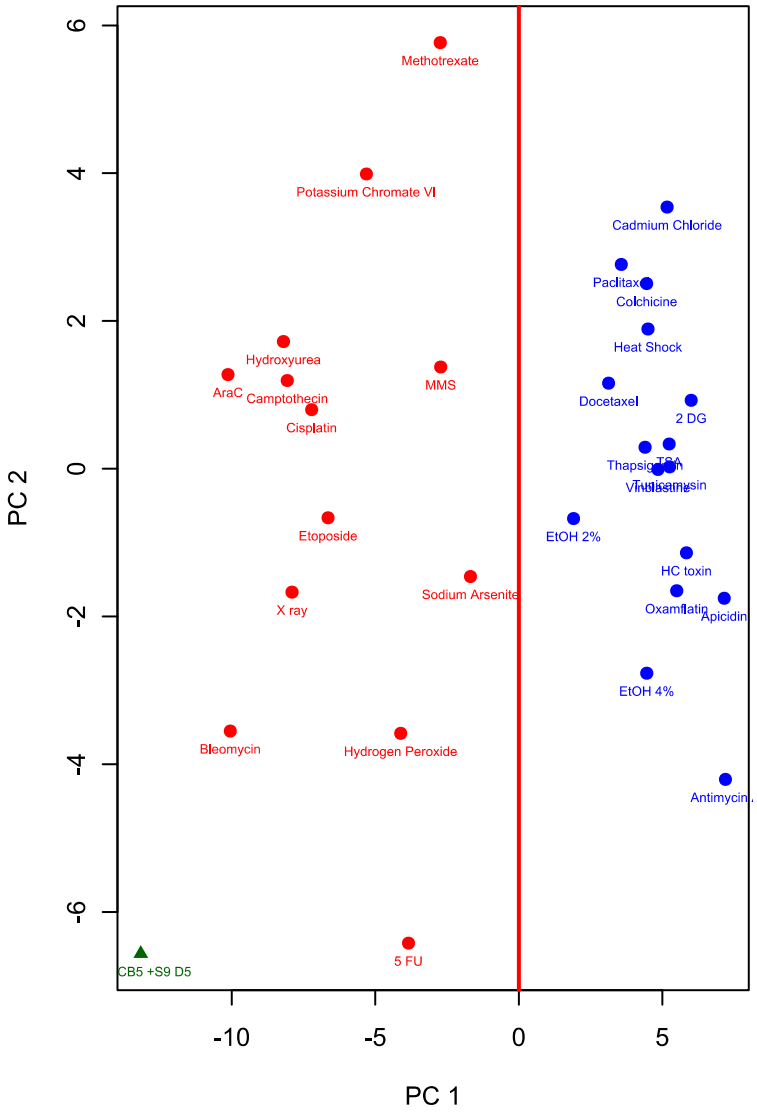
Methotrexate
Potassium Chromate VI
Cadmium Chloride
Paclitax
Colchicine
Heat Shock
Hydroxyurea
AraC
Camptothecin
Cisplatin
MMS
Docetaxel
2 DG
Thapsigargin
TSA
Tunicamysin
Vinblastine
Etoposide
EtOH 2%
HC toxin
Sodium Arsenite
X ray
Oxamflatin
Apicidin
EtOH 4%
Bleomycin
Hydrogen Peroxide
Antimycin A
CB5 +S9 D5
5 FU
PC 2
PC 1
6
4
2
0
-2
-4
-6
-10
-5
0
5

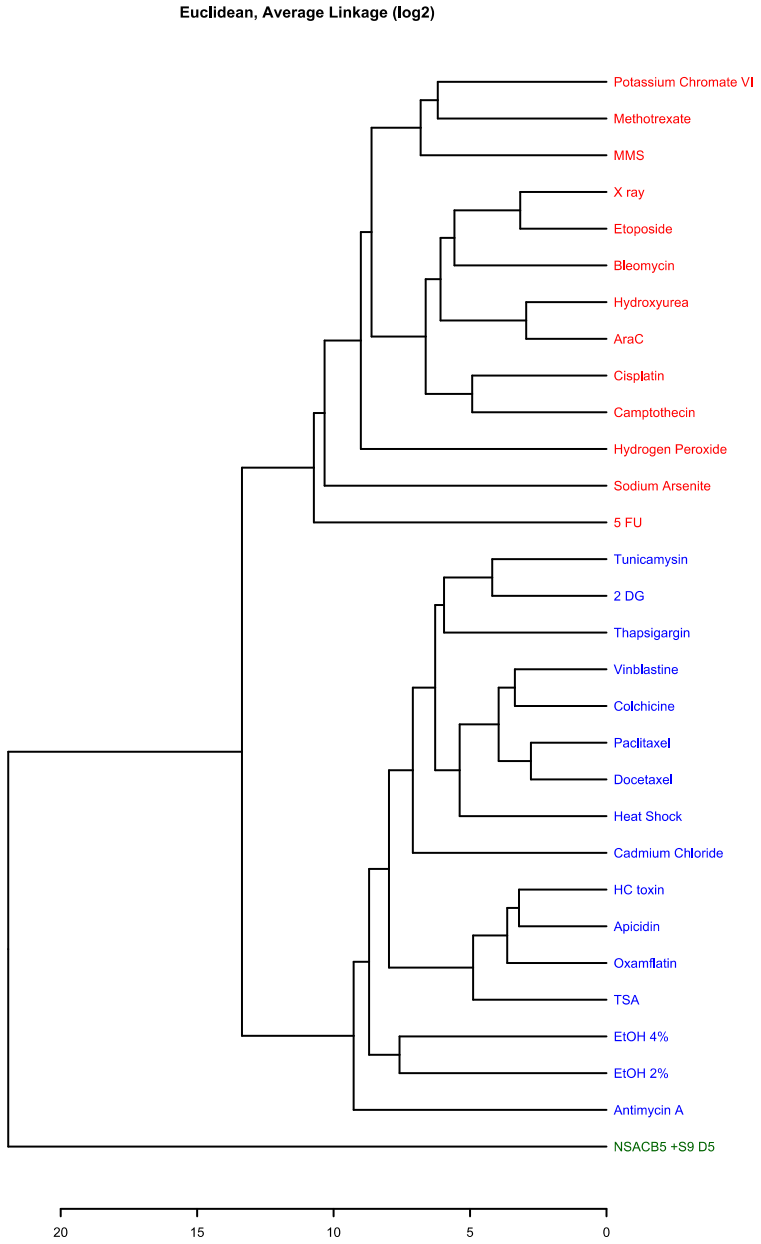
Euclidean, Average Linkage (log2)
Potassium Chromate VI
Methotrexate
MMS
X ray
Etoposide
Bleomycin
Hydroxyurea
AraC
Cisplatin
Camptothecin
Hydrogen Peroxide
Sodium Arsenite
5 FU
Tunicamysin
2 DG
Thapsigargin
Vinblastine
Colchicine
Paclitaxel
Docetaxel
Heat Shock
Cadmium Chloride
HC toxin
Apicidin
Oxamflatin
TSA
EtOH 4%
EtOH 2%
Antimycin A
NSACB5 +S9 D5
20
15
10
5
0

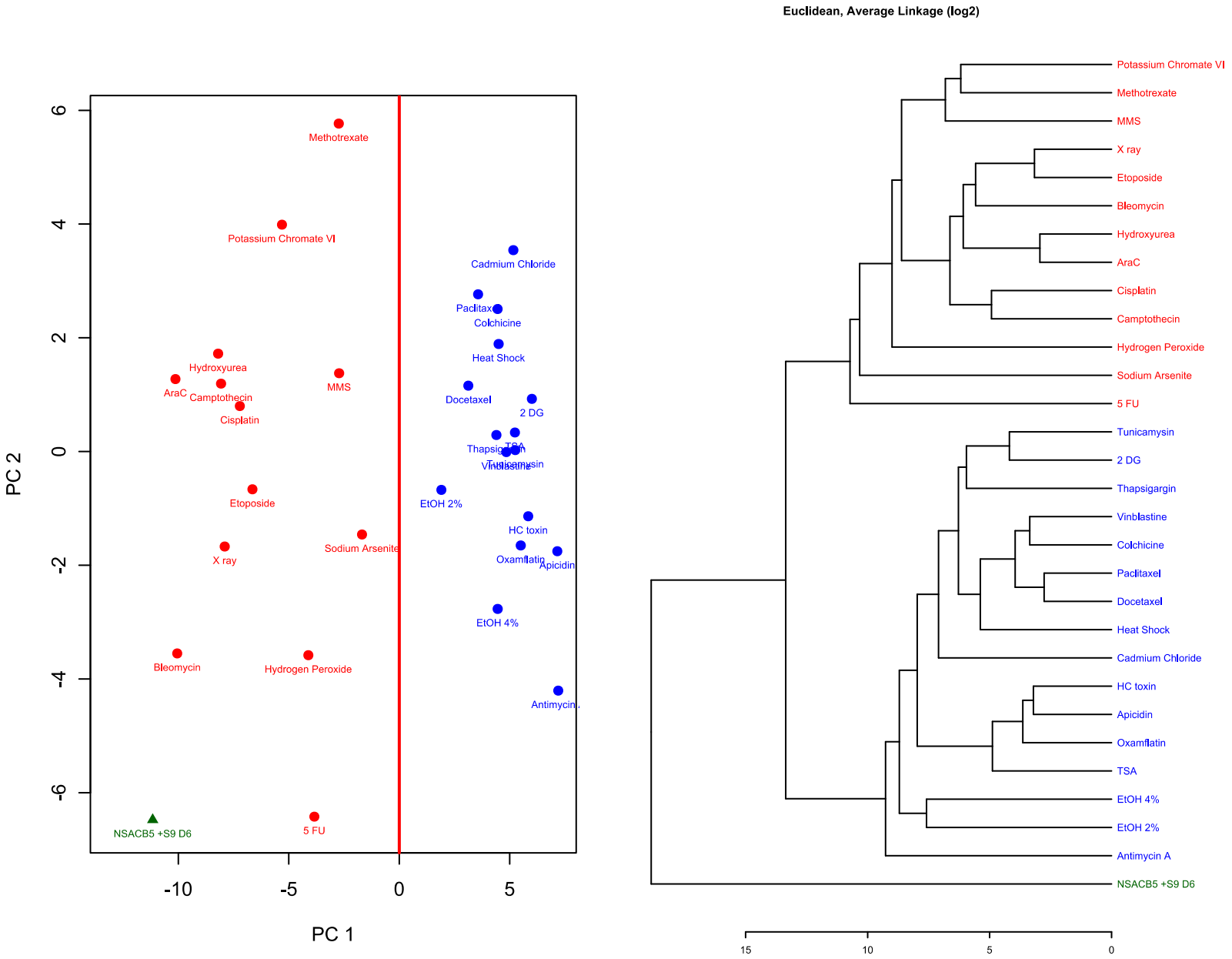

Supplementary Figure III-F: NASCB 5 (+S9) TGx-DDI biomarker classification using the Principal Component Analysis (PCA) (left) and hierarchical clustering (right) statistical analyses. Genotoxic reference chemicals are shown in red text, non-genotoxic reference chemicals are shown in blue text, and the test agent is shown in the green text. The line drawn on the PCA plot and the main branch on the dendogram divides the genotoxic and non-genotoxic agents and was used to classify the test compounds. D1 represents the lowest concentration tested, D6 the highest.

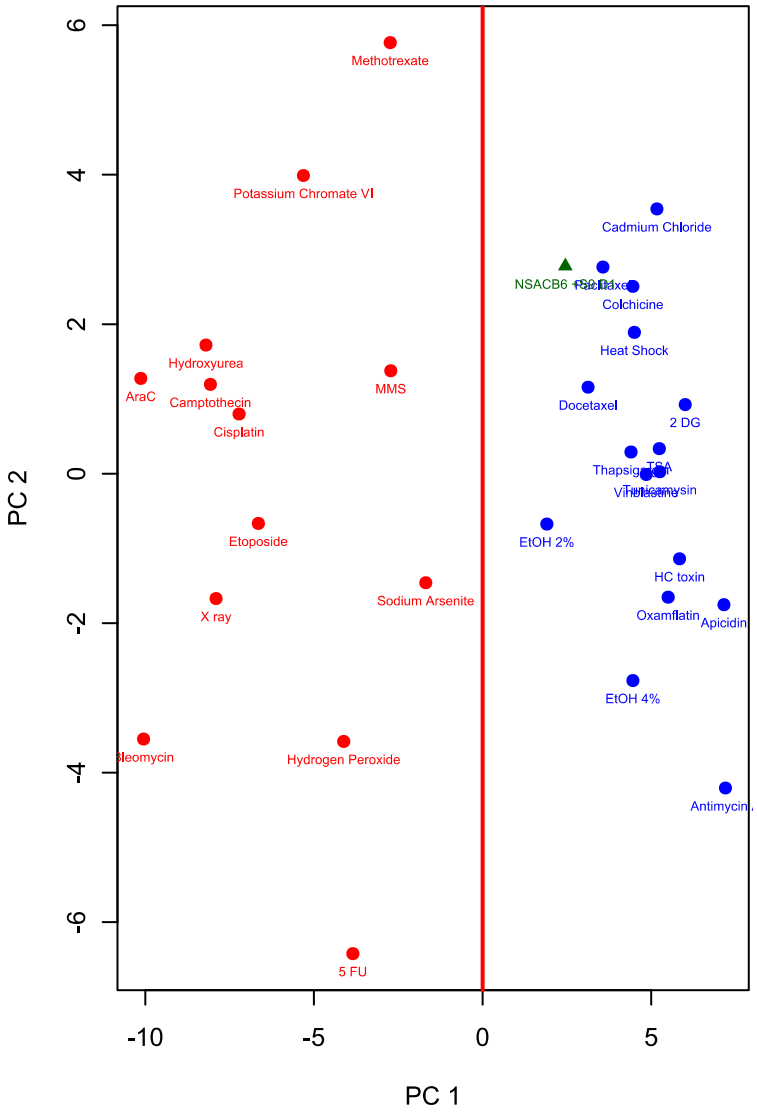
Methotrexate
Potassium Chromate VI
Cadmium Chloride
NSACB6 +S9 D1
Paclitaxel
Colchicine
Heat Shock
Hydroxyurea
AraC
Camptothecin
MMS
Docetaxel
2 DG
Cisplatin
Thapsigargin
TSA
Vinblastine
Tunicamysin
Etoposide
EtOH 2%
HC toxin
Sodium Arsenite
X ray
Oxamflatin
Apicidin
EtOH 4%
Bleomycin
Hydrogen Peroxide
Antimycin
5 FU
PC 2
PC 1
6
4
2
0
-2
-4
-6
-10
-5
0
5

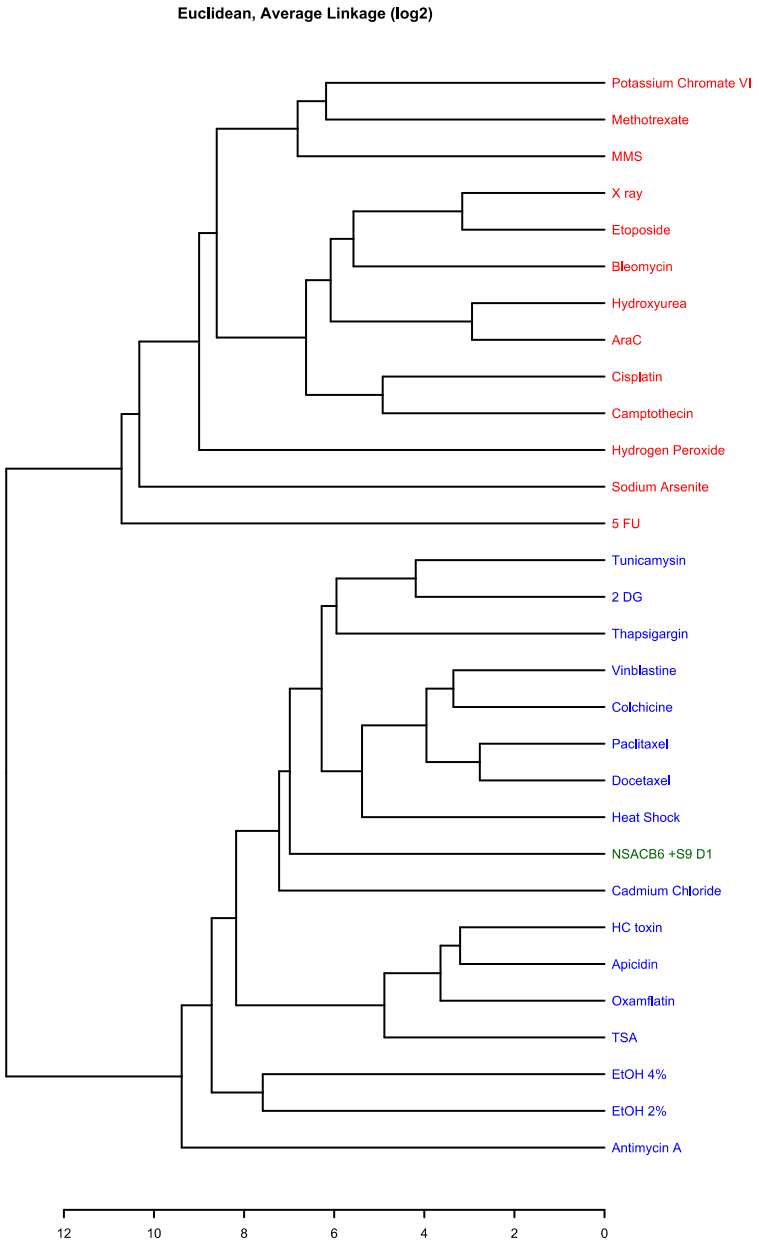
Euclidean, Average Linkage (log2)
Potassium Chromate VI
Methotrexate
MMS
X ray
Etoposide
Bleomycin
Hydroxyurea
AraC
Cisplatin
Camptothecin
Hydrogen Peroxide
Sodium Arsenite
5 FU
Tunicamysin
2 DG
Thapsigargin
Vinblastine
Colchicine
Paclitaxel
Docetaxel
Heat Shock
NSACB6 +S9 D1
Cadmium Chloride
HC toxin
Apicidin
Oxamflatin
TSA
EtOH 4%
EtOH 2%
Antimycin A
12
10
8
6
4
2
0

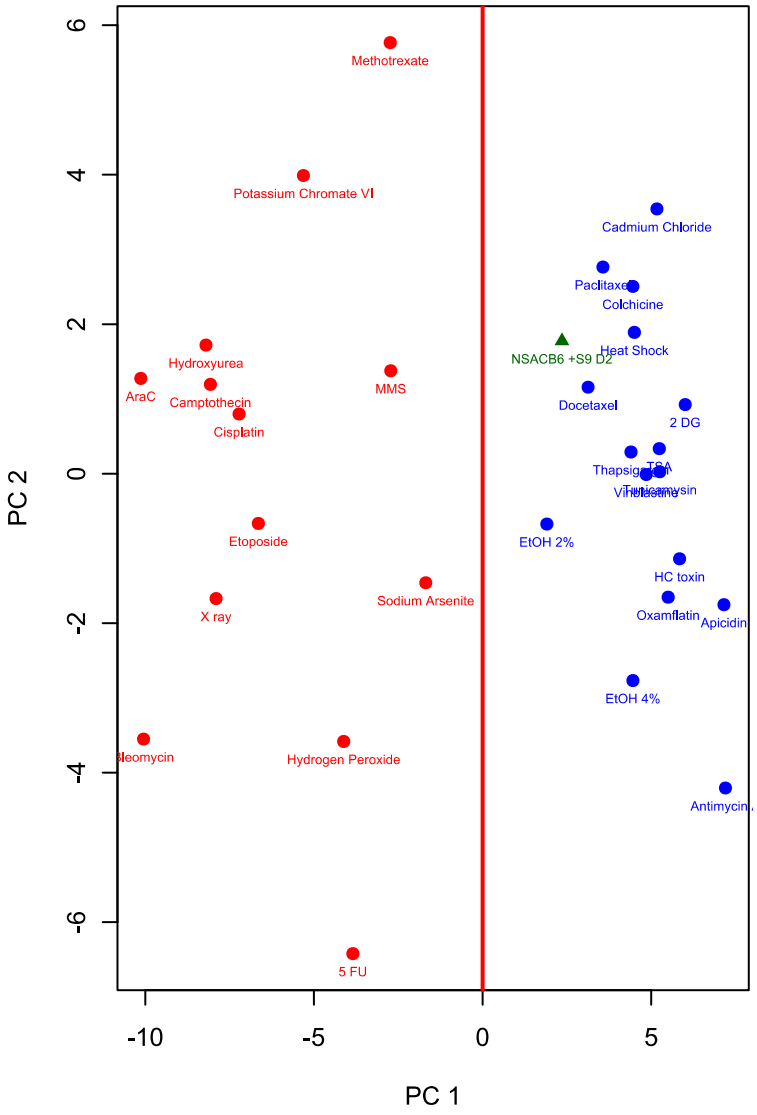
Methotrexate
Potassium Chromate VI
Cadmium Chloride
Paclitaxel
Colchicine
Heat Shock
NSACB6 +S9 D2
Hydroxyurea
AraC
Camptothecin
MMS
Docetaxel
2 DG
Cisplatin
Thapsigargin
TSA
Vinblastine
Tunicamysin
Etoposide
EtOH 2%
HC toxin
Sodium Arsenite
X ray
Oxamflatin
Apicidin
EtOH 4%
Bleomycin
Hydrogen Peroxide
Antimycin
5 FU
PC 2
PC 1
6
4
2
0
-2
-4
-6
-10
-5
0
5

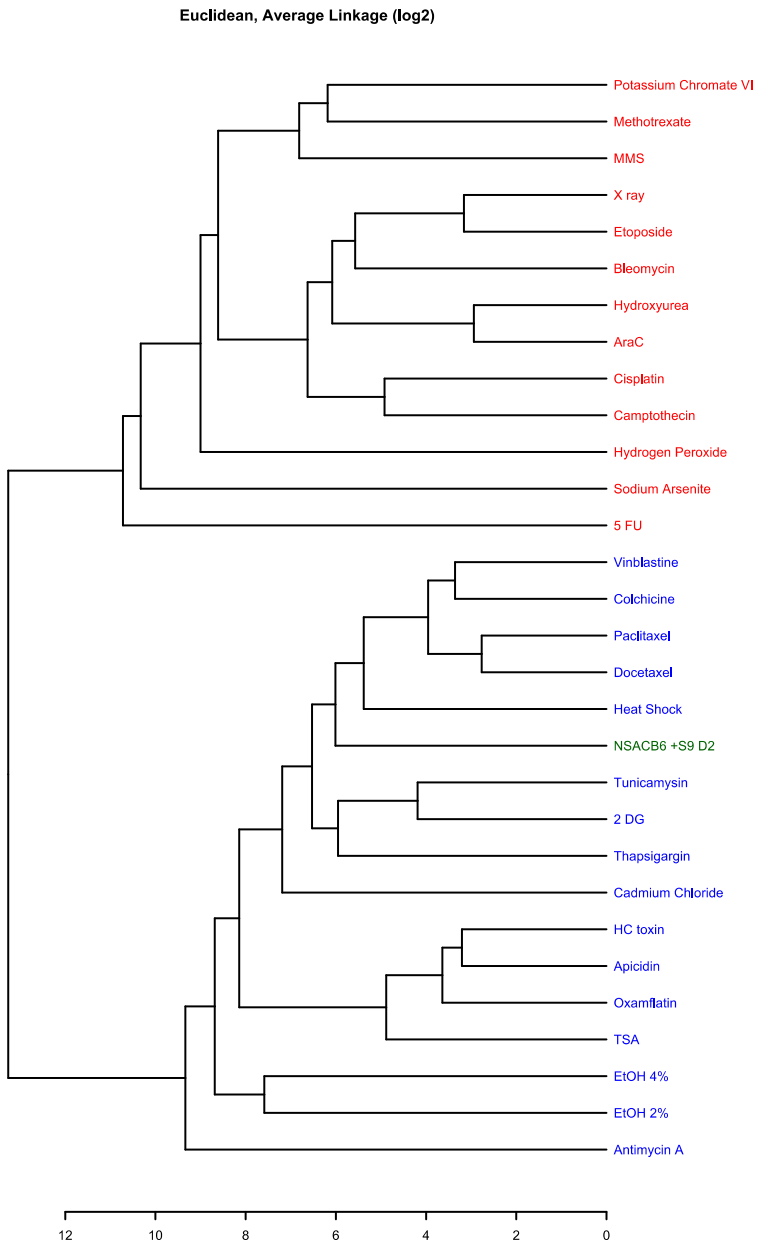
Euclidean, Average Linkage (log2)
Potassium Chromate VI
Methotrexate
MMS
X ray
Etoposide
Bleomycin
Hydroxyurea
AraC
Cisplatin
Camptothecin
Hydrogen Peroxide
Sodium Arsenite
5 FU
Vinblastine
Colchicine
Paclitaxel
Docetaxel
Heat Shock
NSACB6 +S9 D2
Tunicamysin
2 DG
Thapsigargin
Cadmium Chloride
HC toxin
Apicidin
Oxamflatin
TSA
EtOH 4%
EtOH 2%
Antimycin A
12
10
8
6
4
2
0

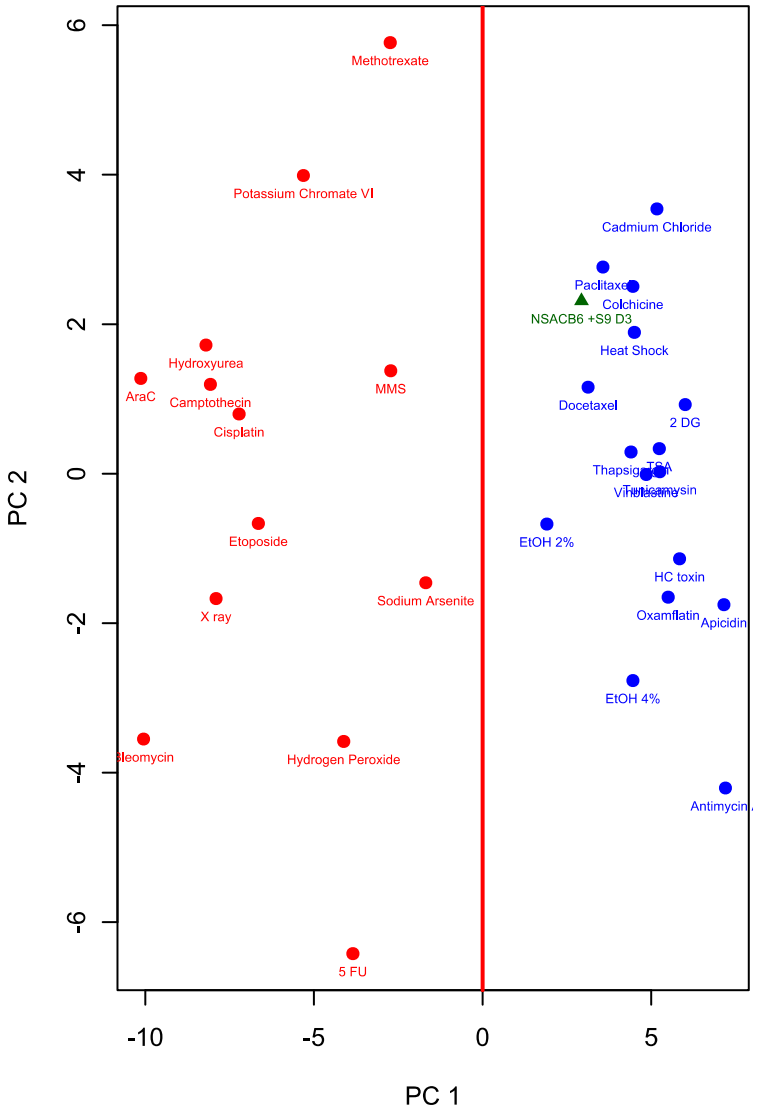
Methotrexate
Potassium Chromate VI
Cadmium Chloride
Paclitaxel
Colchicine
NSACB6 +S9 D3
Heat Shock
Hydroxyurea
AraC
Camptothecin
Cisplatin
MMS
Docetaxel
2 DG
Thapsigargin
TSA
Vinblastine
Tunicamysin
Etoposide
EtOH 2%
HC toxin
Sodium Arsenite
X ray
Oxamflatin
Apicidin
EtOH 4%
Bleomycin
Hydrogen Peroxide
Antimycin
5 FU
PC 2
PC 1
6
4
2
0
-2
-4
-6
-10
-5
0
5

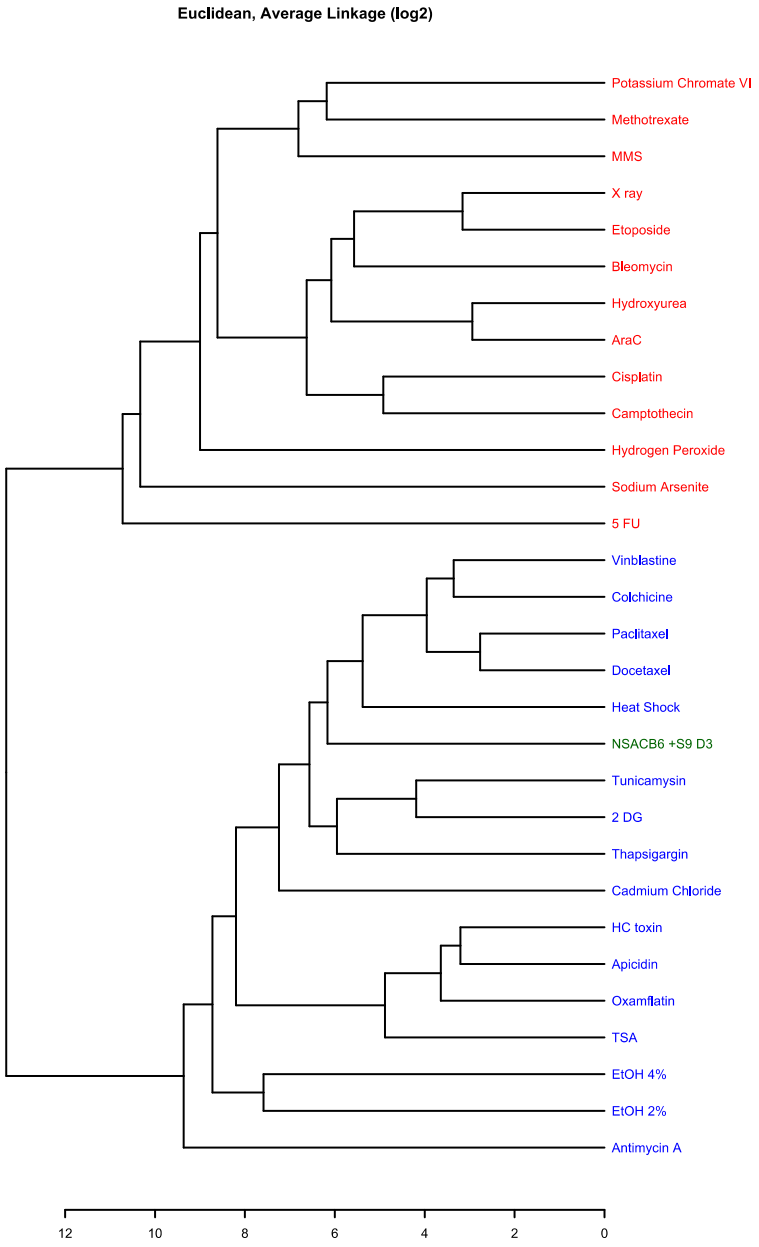
Euclidean, Average Linkage (log2)
Potassium Chromate VI
Methotrexate
MMS
X ray
Etoposide
Bleomycin
Hydroxyurea
AraC
Cisplatin
Camptothecin
Hydrogen Peroxide
Sodium Arsenite
5 FU
Vinblastine
Colchicine
Paclitaxel
Docetaxel
Heat Shock
NSACB6 +S9 D3
Tunicamysin
2 DG
Thapsigargin
Cadmium Chloride
HC toxin
Apicidin
Oxamflatin
TSA
EtOH 4%
EtOH 2%
Antimycin A
12
10
8
6
4
2
0

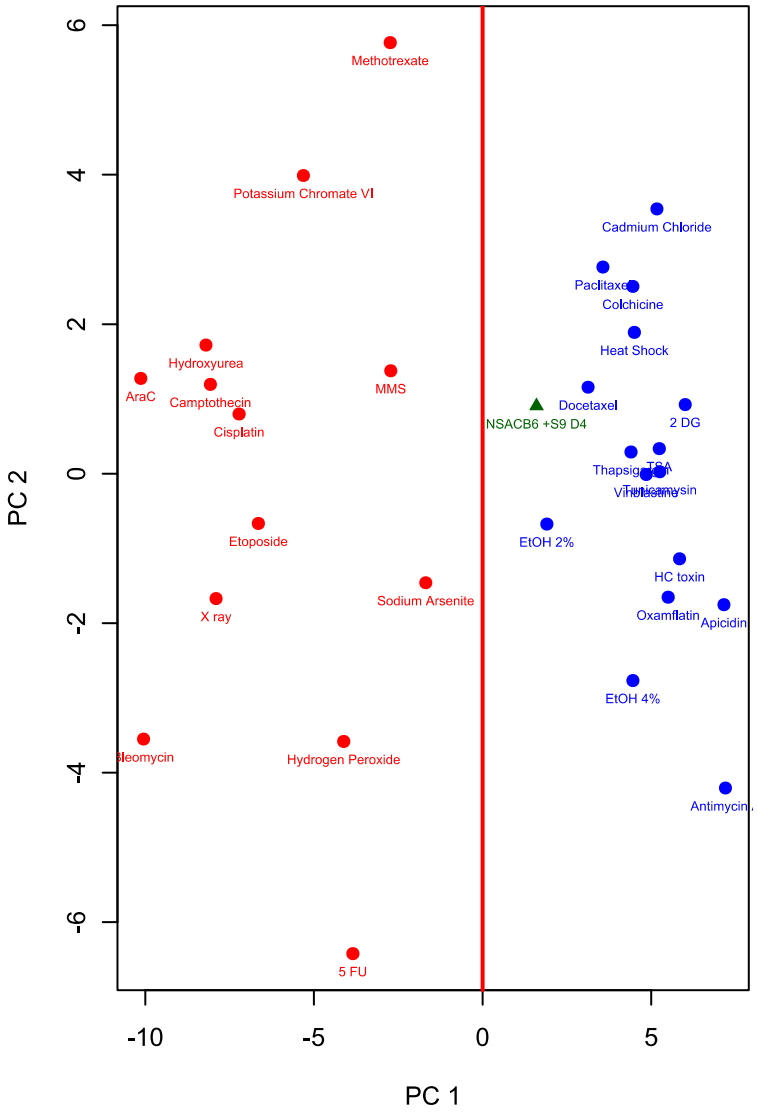
Methotrexate
Potassium Chromate VI
Cadmium Chloride
Paclitaxel
Colchicine
Heat Shock
Hydroxyurea
AraC
Camptothecin
Cisplatin
MMS
Docetaxel
NSACB6 +S9 D4
2 DG
Thapsigargin
TSA
Vinblastine
Tunicamysin
Etoposide
EtOH 2%
HC toxin
Sodium Arsenite
X ray
Oxamflatin
Apicidin
EtOH 4%
Bleomycin
Hydrogen Peroxide
Antimycin
5 FU
PC 2
PC 1
6
4
2
0
-2
-4
-6
-10
-5
0
5

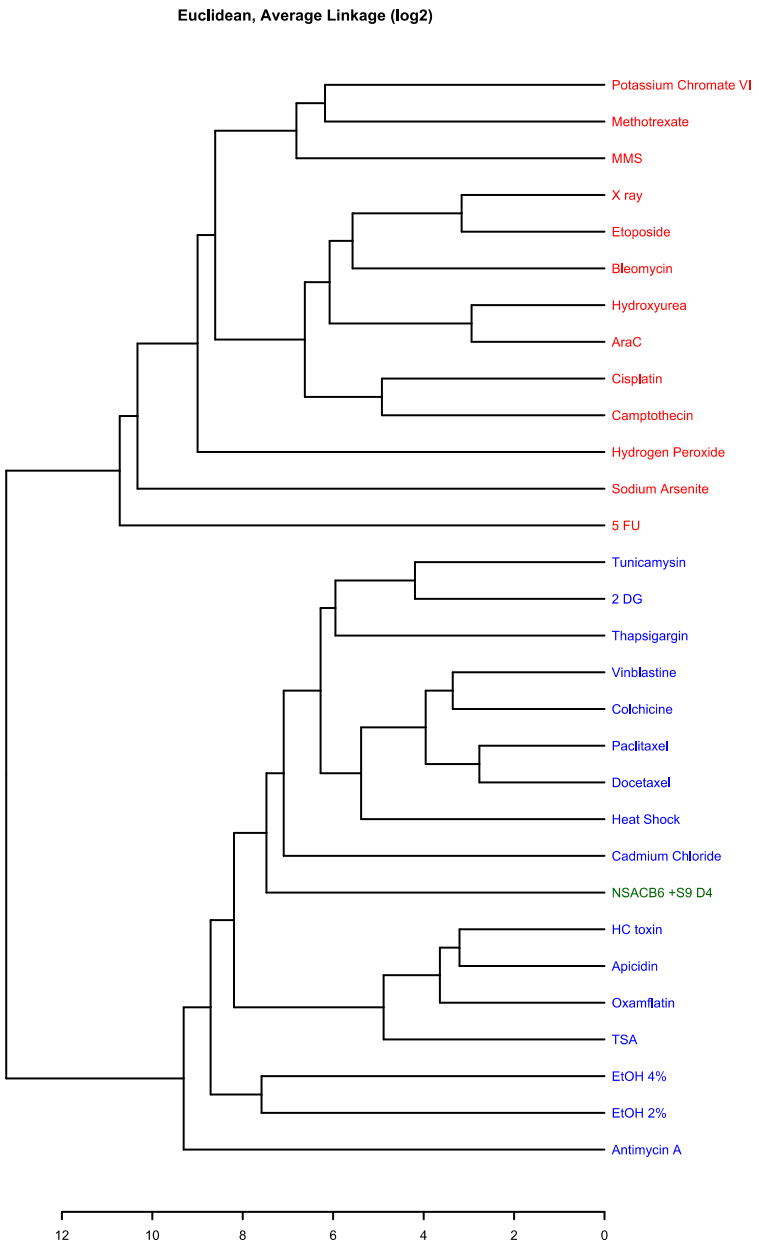
Euclidean, Average Linkage (log2)
Potassium Chromate VI
Methotrexate
MMS
X ray
Etoposide
Bleomycin
Hydroxyurea
AraC
Cisplatin
Camptothecin
Hydrogen Peroxide
Sodium Arsenite
5 FU
Tunicamysin
2 DG
Thapsigargin
Vinblastine
Colchicine
Paclitaxel
Docetaxel
Heat Shock
Cadmium Chloride
NSACB6 +S9 D4
HC toxin
Apicidin
Oxamflatin
TSA
EtOH 4%
EtOH 2%
Antimycin A
12
10
8
6
4
2
0

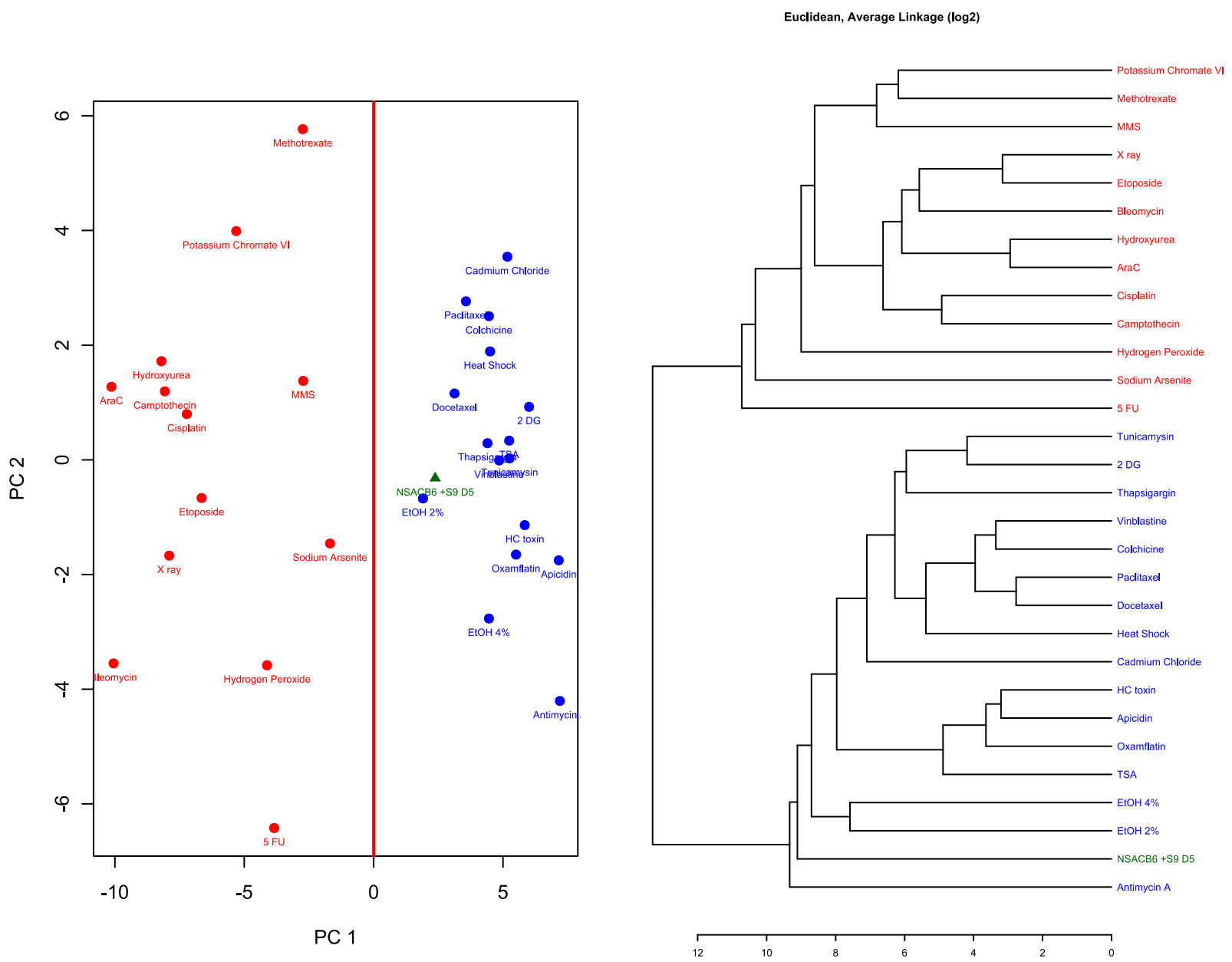

Supplementary Figure III-G: NASCB 6 (+S9) TGx-DDI biomarker classification using the Principal Component Analysis (PCA) (left) and hierarchical clustering (right) statistical analyses. Genotoxic reference chemicals are shown in red text, non-genotoxic reference chemicals are shown in blue text, and the test agent is shown in the green text. The line drawn on the PCA plot and the main branch on the dendogram divides the genotoxic and non-genotoxic agents and was used to classify the test compounds. D1 represents the lowest concentration tested, D5 the highest.

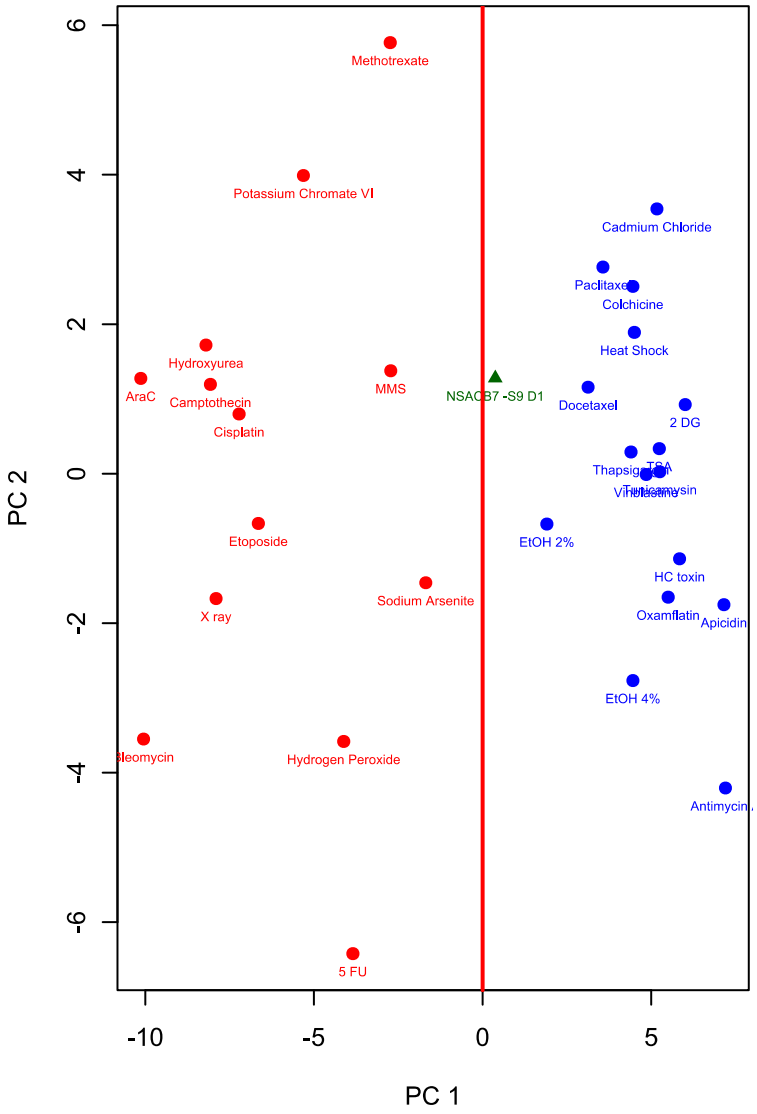
Methotrexate
Potassium Chromate VI
Cadmium Chloride
Paclitaxel
Colchicine
Heat Shock
Hydroxyurea
AraC
Camptothecin
Cisplatin
MMS
NSACB7 -S9 D1
Docetaxel
2 DG
Thapsigargin
TSA
Vinblastine
Tunicamysin
Etoposide
EtOH 2%
HC toxin
X ray
Sodium Arsenite
Oxamflatin
Apicidin
EtOH 4%
Bleomycin
Hydrogen Peroxide
Antimycin
5 FU
PC 2
PC 1
6
4
2
0
-2
-4
-6
-10
-5
0
5

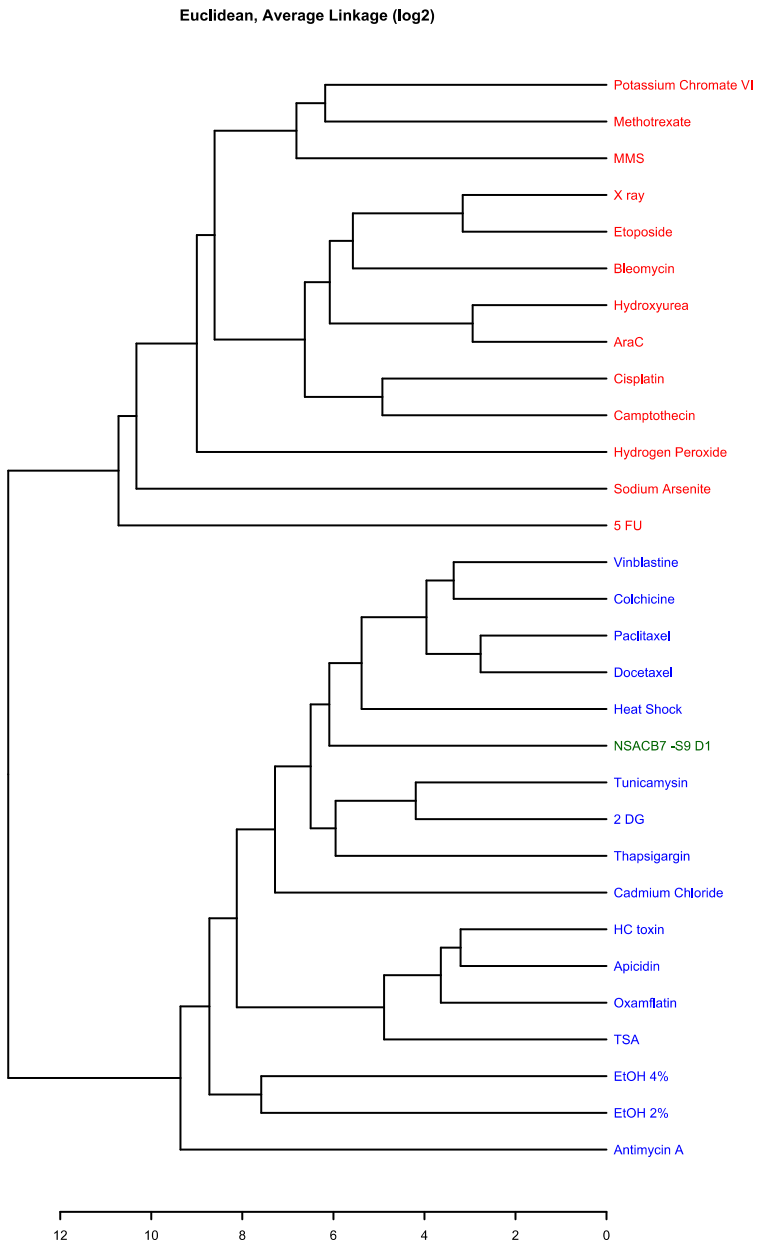
Euclidean, Average Linkage (log2)
Potassium Chromate VI
Methotrexate
MMS
X ray
Etoposide
Bleomycin
Hydroxyurea
AraC
Cisplatin
Camptothecin
Hydrogen Peroxide
Sodium Arsenite
5 FU
Vinblastine
Colchicine
Paclitaxel
Docetaxel
Heat Shock
NSACB7 -S9 D1
Tunicamysin
2 DG
Thapsigargin
Cadmium Chloride
HC toxin
Apicidin
Oxamflatin
TSA
EtOH 4%
EtOH 2%
Antimycin A
12
10
8
6
4
2
0

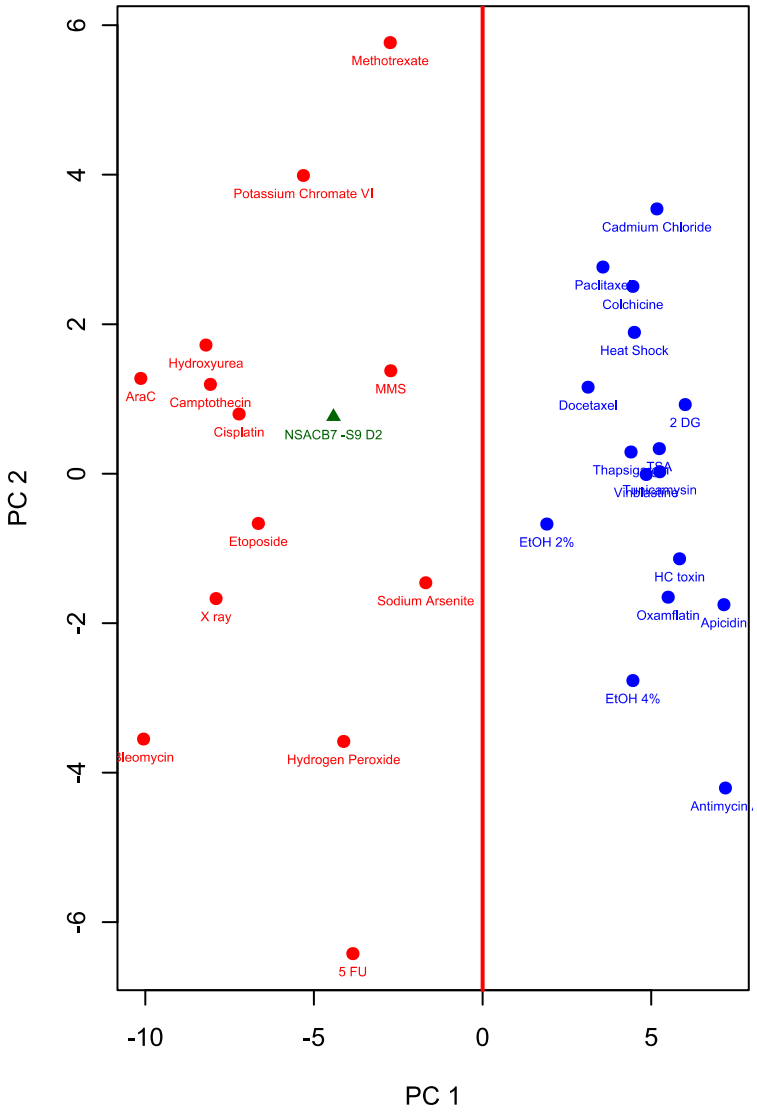
Methotrexate
Potassium Chromate VI
Cadmium Chloride
Paclitaxel
Colchicine
Heat Shock
Hydroxyurea
AraC
Camptothecin
MMS
Docetaxel
2 DG
Cisplatin
NSACB7 -S9 D2
Thapsigargin
TSA
Vinblastine
Tunicamycin
Etoposide
EtOH 2%
HC toxin
Sodium Arsenite
X ray
Oxamflatin
Apicidin
EtOH 4%
Bleomycin
Hydrogen Peroxide
Antimycin
5 FU
PC 2
PC 1
6
4
2
0
-2
-4
-6
-10
-5
0
5

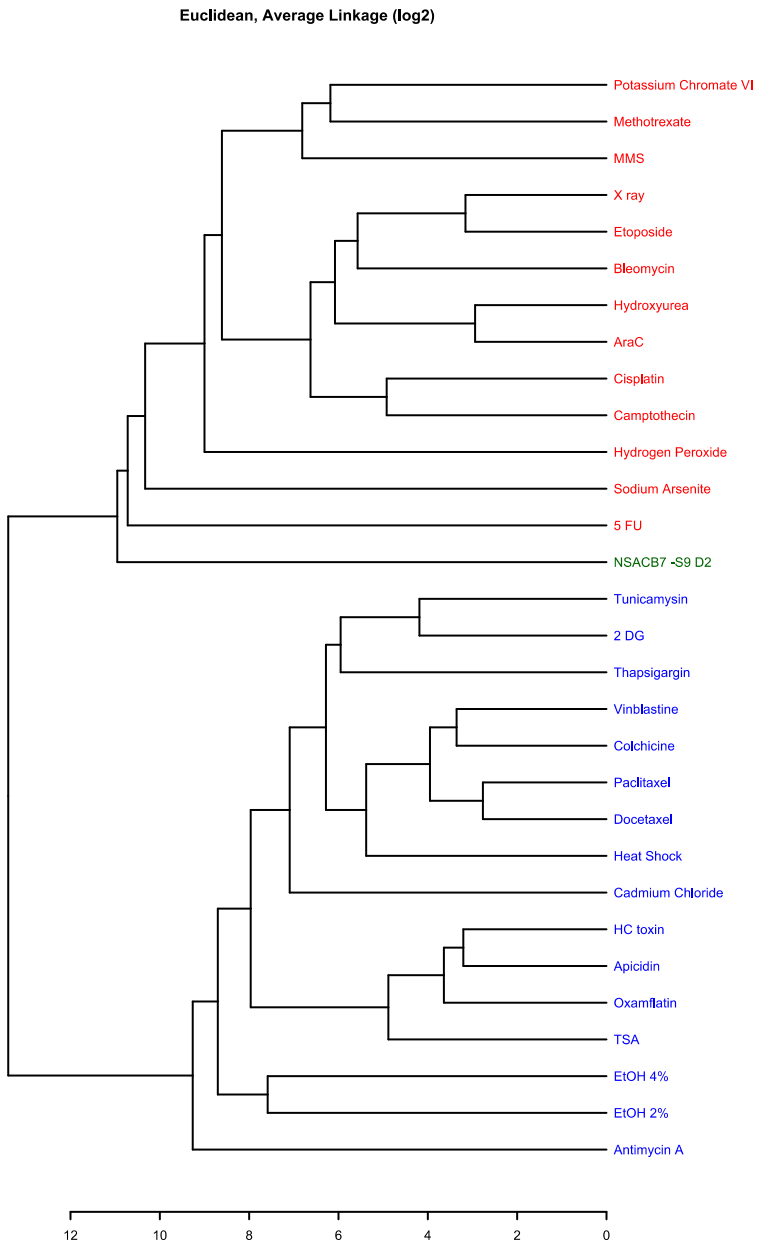
Euclidean, Average Linkage (log2)
Potassium Chromate VI
Methotrexate
MMS
X ray
Etoposide
Bleomycin
Hydroxyurea
AraC
Cisplatin
Camptothecin
Hydrogen Peroxide
Sodium Arsenite
5 FU
NSACB7 -S9 D2
Tunicamysin
2 DG
Thapsigargin
Vinblastine
Colchicine
Paclitaxel
Docetaxel
Heat Shock
Cadmium Chloride
HC toxin
Apicidin
Oxamflatin
TSA
EtOH 4%
EtOH 2%
Antimycin A
12
10
8
6
4
2
0

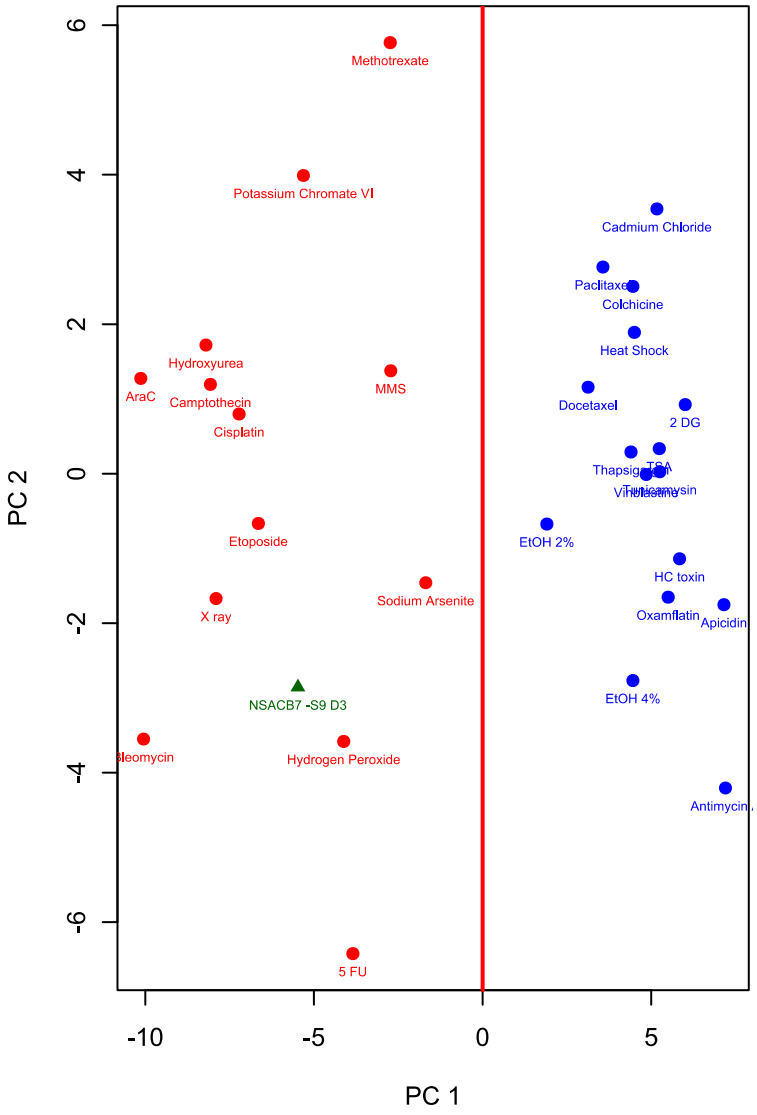
Methotrexate
Potassium Chromate VI
Cadmium Chloride
Paclitaxel
Colchicine
Heat Shock
Hydroxyurea
AraC
Camptothecin
Cisplatin
MMS
Docetaxel
2 DG
Thapsigargin
TSA
Vinblastine
Tunicamycin
Etoposide
EtOH 2%
HC toxin
Sodium Arsenite
X ray
Oxamflatin
Apicidin
NSACB7 -S9 D3
EtOH 4%
Bleomycin
Hydrogen Peroxide
Antimycin
5 FU
PC 2
PC 1
6
4
2
0
-2
-4
-6
-10
-5
0
5

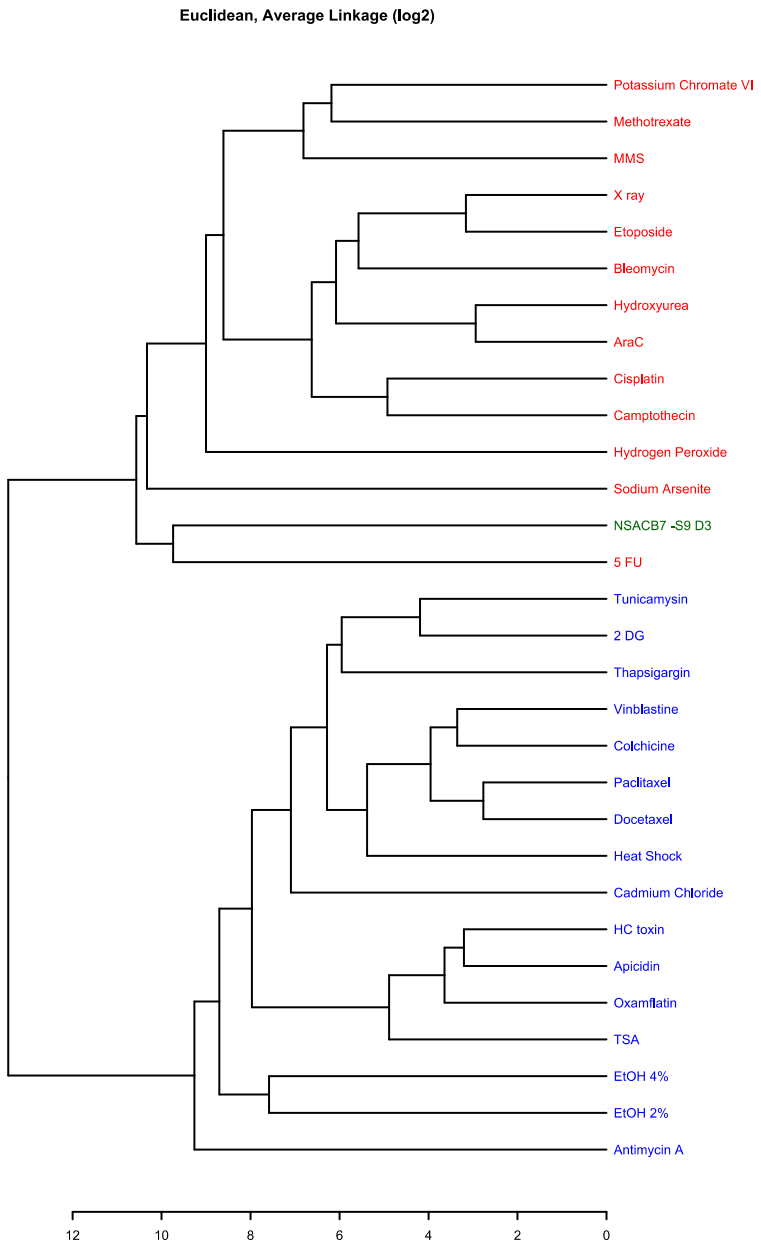
Euclidean, Average Linkage (log2)
Potassium Chromate VI
Methotrexate
MMS
X ray
Etoposide
Bleomycin
Hydroxyurea
AraC
Cisplatin
Camptothecin
Hydrogen Peroxide
Sodium Arsenite
NSACB7 -S9 D3
5 FU
Tunicamysin
2 DG
Thapsigargin
Vinblastine
Colchicine
Paclitaxel
Docetaxel
Heat Shock
Cadmium Chloride
HC toxin
Apicidin
Oxamflatin
TSA
EtOH 4%
EtOH 2%
Antimycin A
12
10
8
6
4
2
0

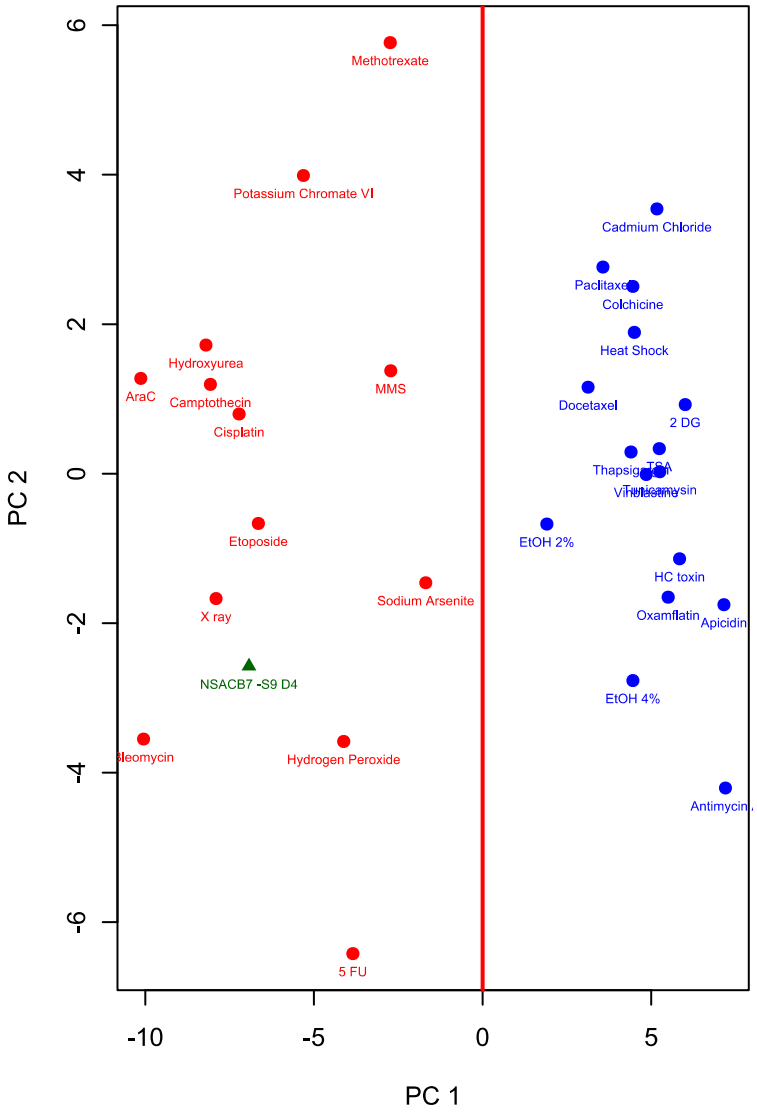
PC 2
PC 1
6
4
2
0
-2
-4
-6
-10
-5
0
5
Methotrexate
Potassium Chromate VI
Cadmium Chloride
Paclitaxel
Colchicine
Heat Shock
Hydroxyurea
AraC
Camptothecin
Cisplatin
MMS
Docetaxel
2 DG
Thapsigargin
TSA
Vinblastine
Tunicamycin
Etoposide
EtOH 2%
HC toxin
Sodium Arsenite
X ray
Oxamflatin
Apicidin
NSACB7 -S9 D4
EtOH 4%
Bleomycin
Hydrogen Peroxide
Antimycin
5 FU

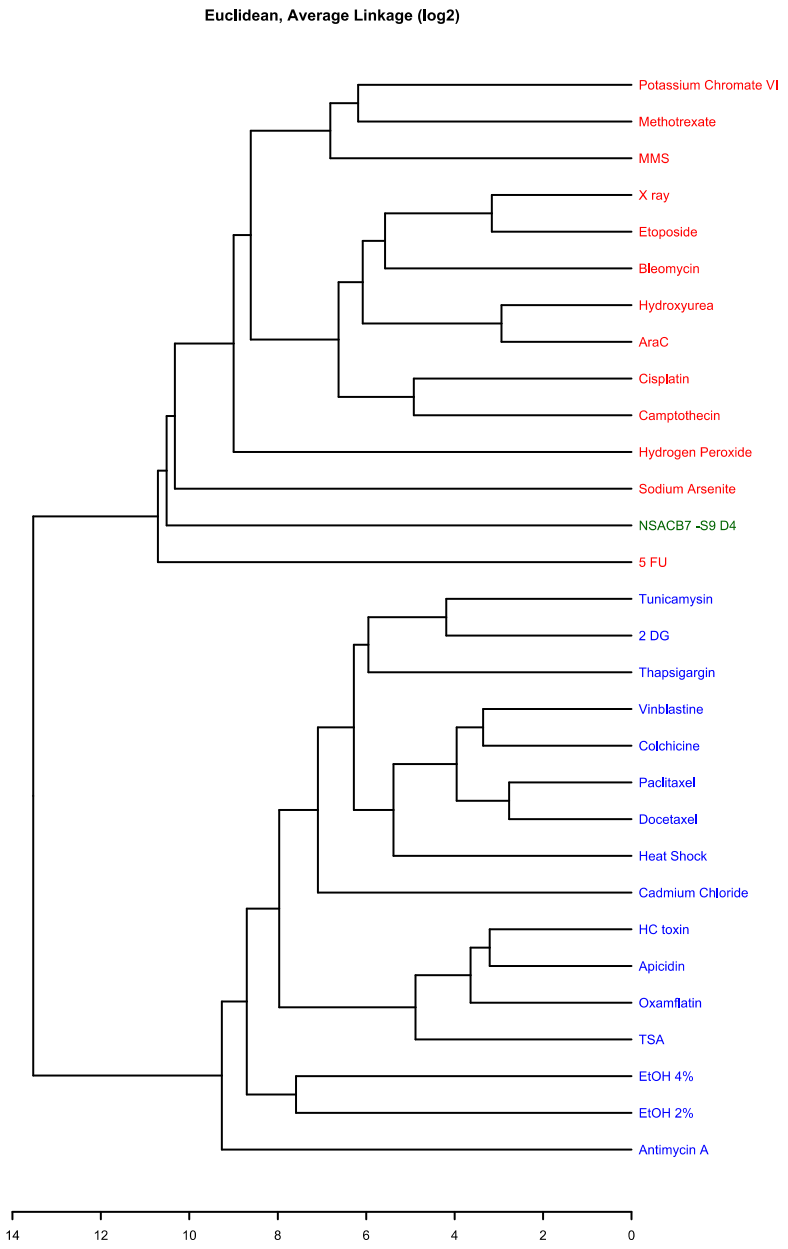
Euclidean, Average Linkage (log2)
Potassium Chromate VI
Methotrexate
MMS
X ray
Etoposide
Bleomycin
Hydroxyurea
AraC
Cisplatin
Camptothecin
Hydrogen Peroxide
Sodium Arsenite
NSACB7 -S9 D4
5 FU
Tunicamysin
2 DG
Thapsigargin
Vinblastine
Colchicine
Paclitaxel
Docetaxel
Heat Shock
Cadmium Chloride
HC toxin
Apicidin
Oxamflatin
TSA
EtOH 4%
EtOH 2%
Antimycin A
14
12
10
8
6
4
2
0

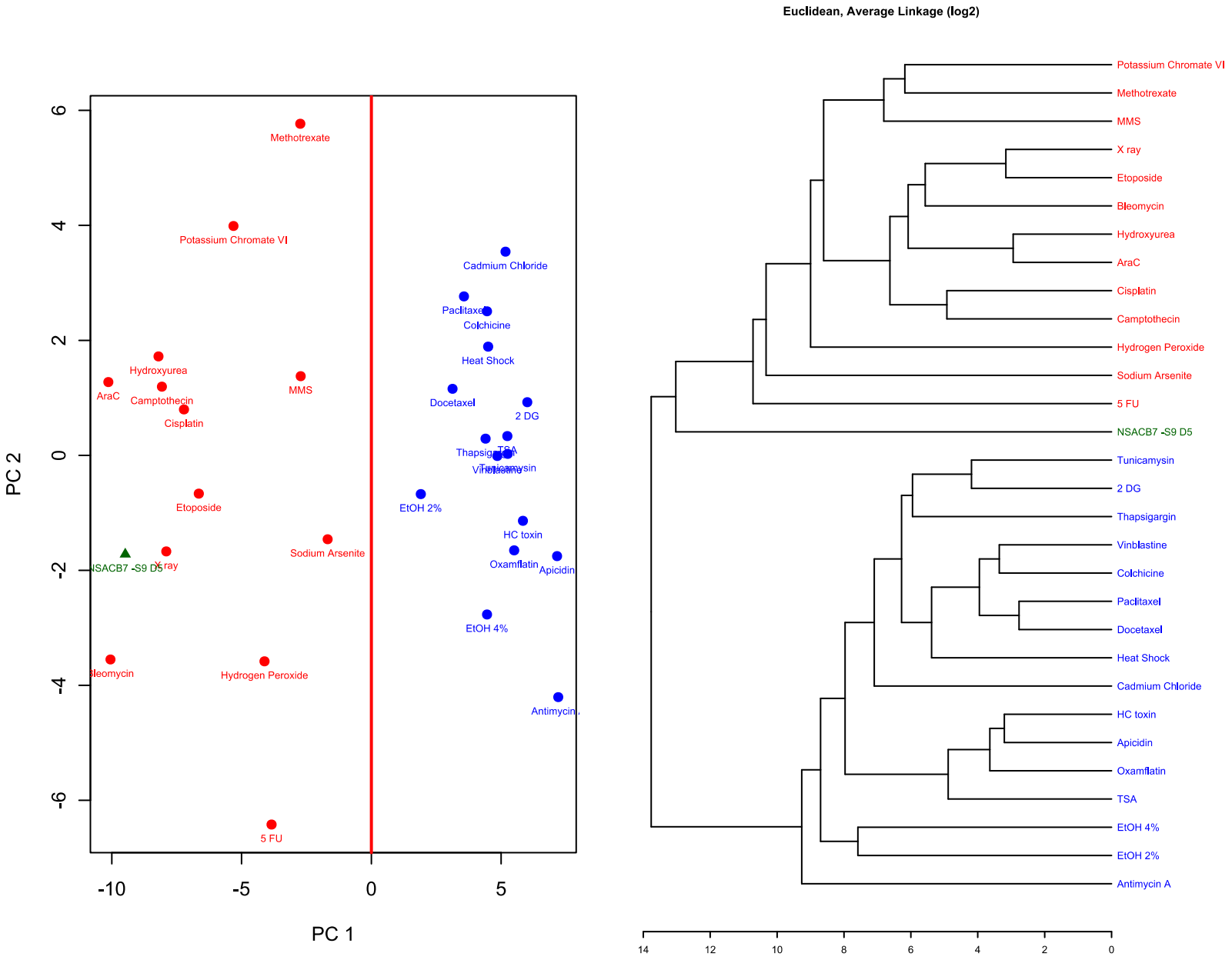

Supplementary Figure III-H: NASCB 7 (-S9) TGx-DDI biomarker classification using the Principal Component Analysis (PCA) (left) and hierarchical clustering (right) statistical analyses. Genotoxic reference chemicals are shown in red text, non-genotoxic reference chemicals are shown in blue text, and the test agent is shown in the green text. The line drawn on the PCA plot and the main branch on the dendogram divides the genotoxic and non-genotoxic agents and was used to classify the test compounds. D1 represents the lowest concentration tested, D5 the highest.

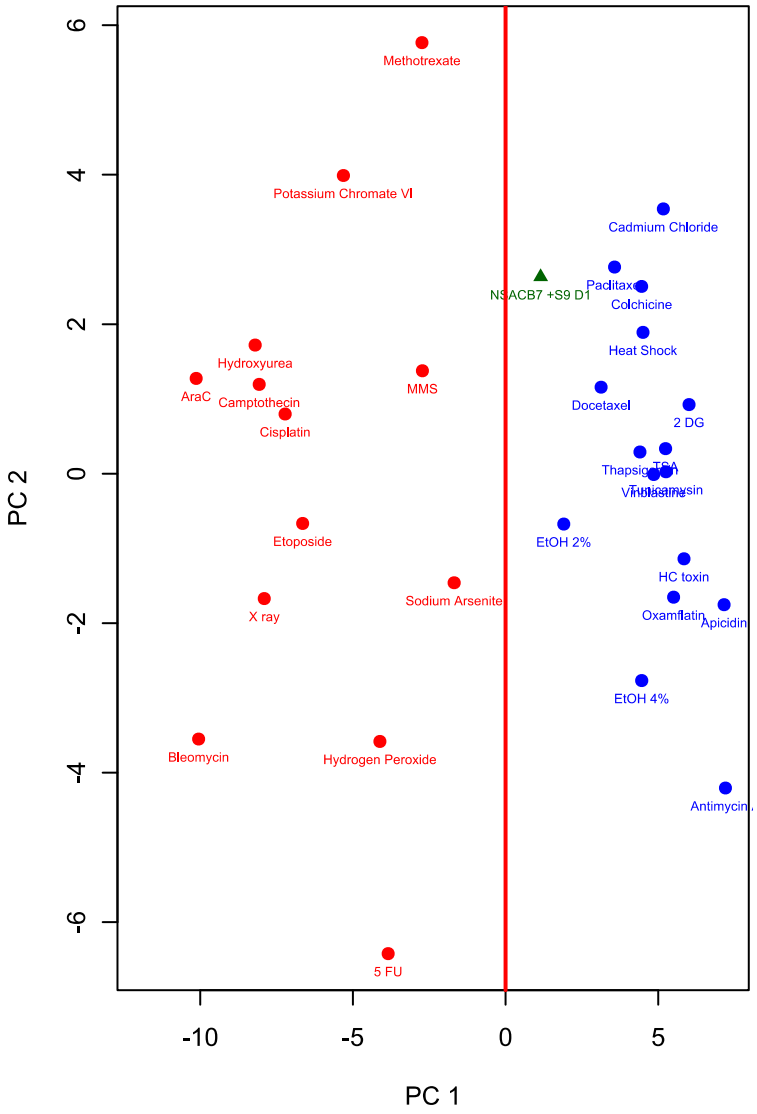
Methotrexate
Potassium Chromate VI
Cadmium Chloride
NSACB7 +S9 D1
Paclitaxel
Colchicine
Heat Shock
Hydroxyurea
AraC
Camptothecin
Cisplatin
MMS
Docetaxel
2 DG
Thapsigargin
TSA
Tunicamysin
Vinblastine
Etoposide
EtOH 2%
HC toxin
Sodium Arsenite
X ray
Oxamflatin
Apicidin
EtOH 4%
Bleomycin
Hydrogen Peroxide
Antimycin
5 FU
PC 2
PC 1
6
4
2
0
-2
-4
-6
-10
-5
0
5

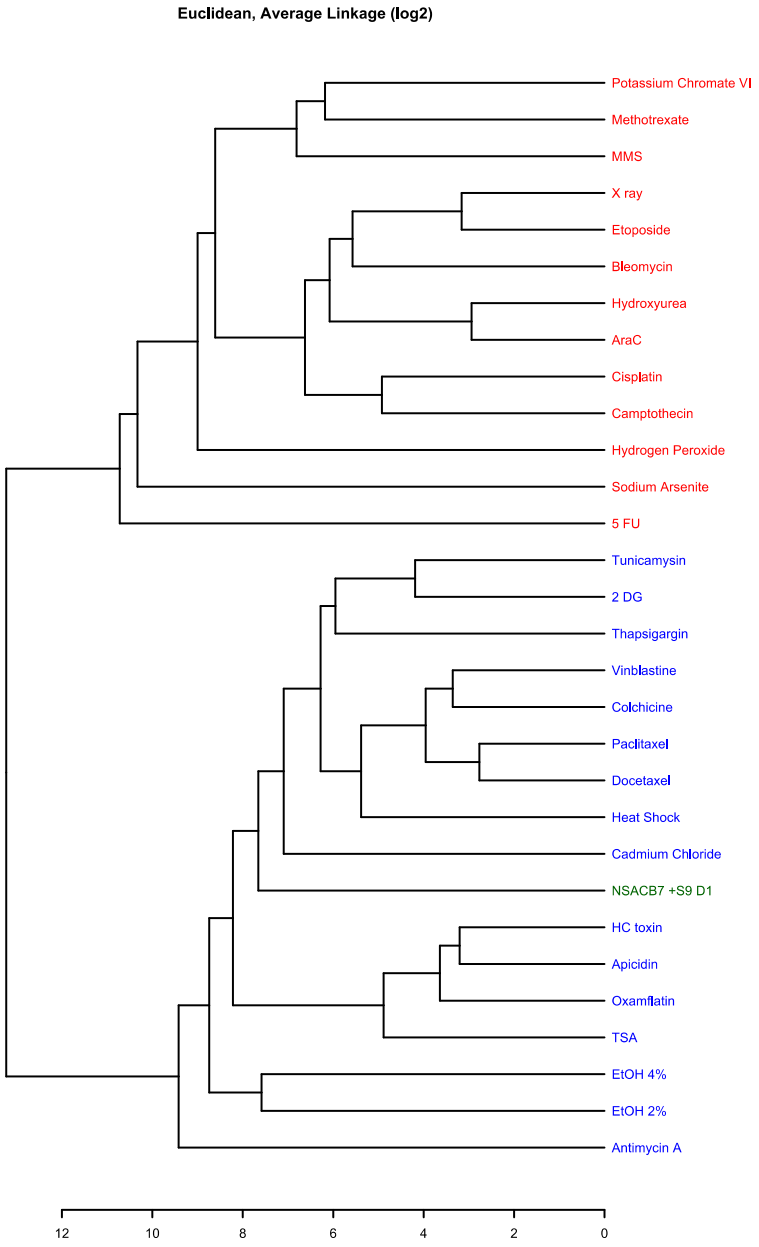
Euclidean, Average Linkage (log2)
Potassium Chromate VI
Methotrexate
MMS
X ray
Etoposide
Bleomycin
Hydroxyurea
AraC
Cisplatin
Camptothecin
Hydrogen Peroxide
Sodium Arsenite
5 FU
Tunicamysin
2 DG
Thapsigargin
Vinblastine
Colchicine
Paclitaxel
Docetaxel
Heat Shock
Cadmium Chloride
NSACB7 +S9 D1
HC toxin
Apicidin
Oxamflatin
TSA
EtOH 4%
EtOH 2%
Antimycin A
12
10
8
6
4
2
0

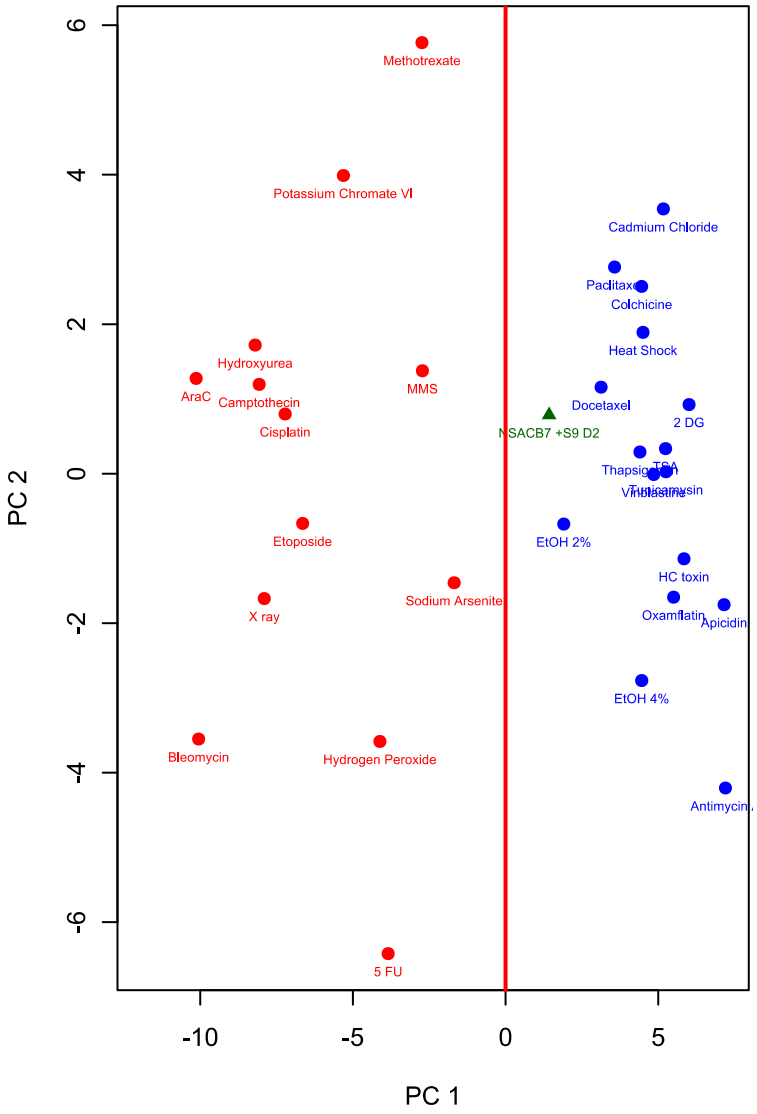
Methotrexate
Potassium Chromate VI
Cadmium Chloride
Paclitaxel
Colchicine
Heat Shock
Hydroxyurea
AraC
Camptothecin
Cisplatin
MMS
Docetaxel
2 DG
NSACB7 +S9 D2
Thapsigargin
TSA
Tunicamysin
Vinblastine
Etoposide
EtOH 2%
HC toxin
Sodium Arsenite
X ray
Oxamflatin
Apicidin
EtOH 4%
Bleomycin
Hydrogen Peroxide
Antimycin
5 FU
PC 2
PC 1
6
4
2
0
-2
-4
-6
-10
-5
0
5

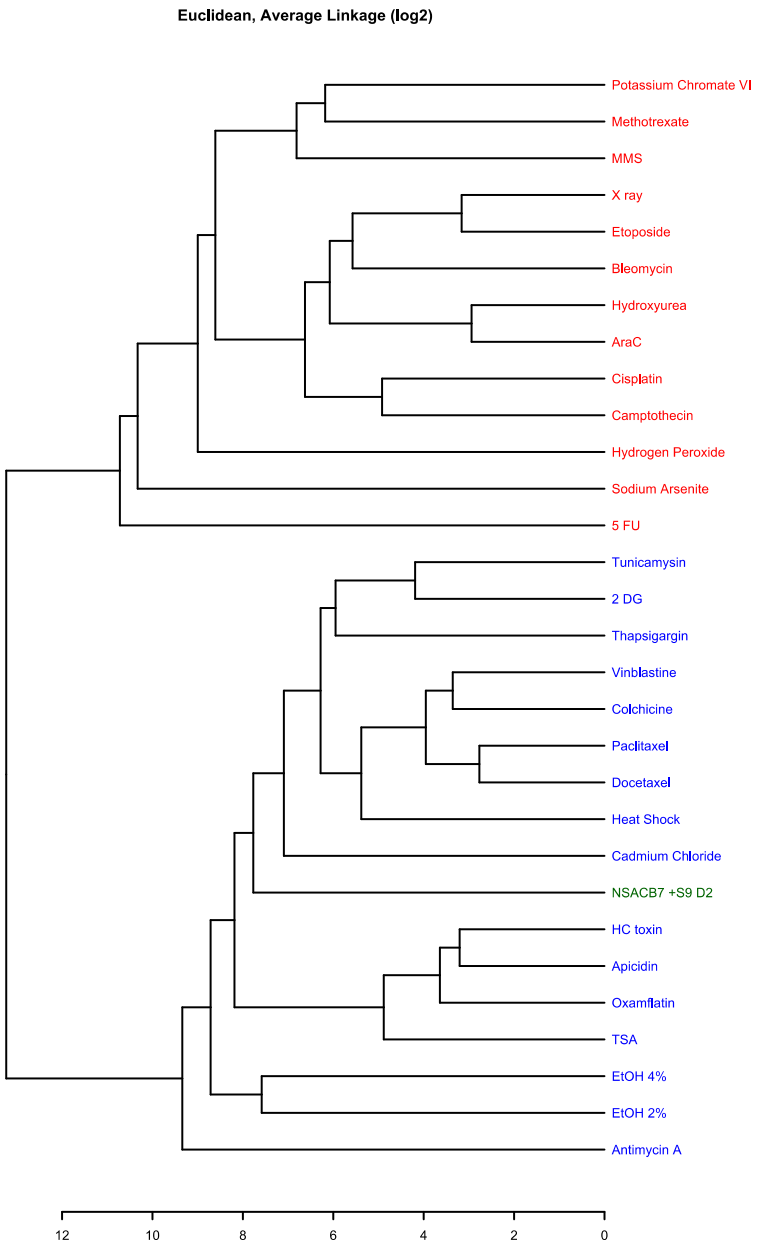
Euclidean, Average Linkage (log2)
Potassium Chromate VI
Methotrexate
MMS
X ray
Etoposide
Bleomycin
Hydroxyurea
AraC
Cisplatin
Camptothecin
Hydrogen Peroxide
Sodium Arsenite
5 FU
Tunicamysin
2 DG
Thapsigargin
Vinblastine
Colchicine
Paclitaxel
Docetaxel
Heat Shock
Cadmium Chloride
NSACB7 +S9 D2
HC toxin
Apicidin
Oxamflatin
TSA
EtOH 4%
EtOH 2%
Antimycin A
12
10
8
6
4
2
0

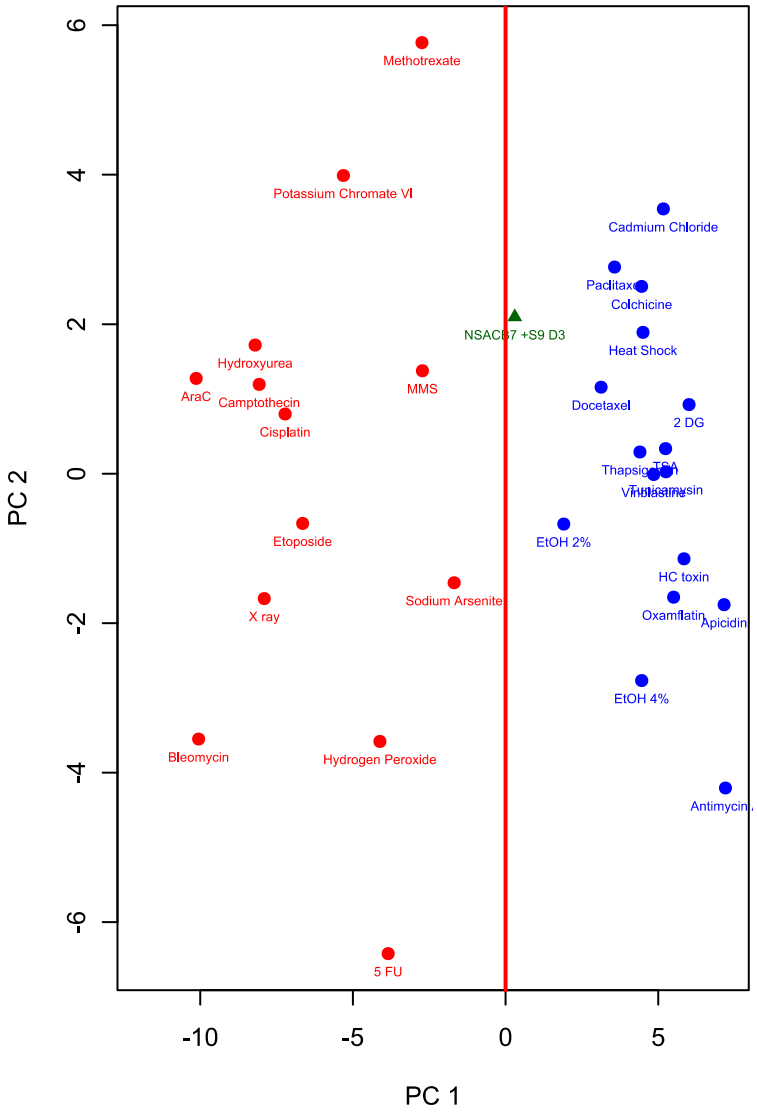
Methotrexate
Potassium Chromate VI
Cadmium Chloride
Paclitaxel
Colchicine
NSACB7 +S9 D3
Heat Shock
Hydroxyurea
AraC
Camptothecin
MMS
Docetaxel
2 DG
Cisplatin
Thapsigargin
TSA
Tunicamysin
Vinblastine
Etoposide
EtOH 2%
HC toxin
Sodium Arsenite
X ray
Oxamflatin
Apicidin
EtOH 4%
Bleomycin
Hydrogen Peroxide
Antimycin A
5 FU
PC 2
PC 1
6
4
2
0
-2
-4
-6
-10
-5
0
5

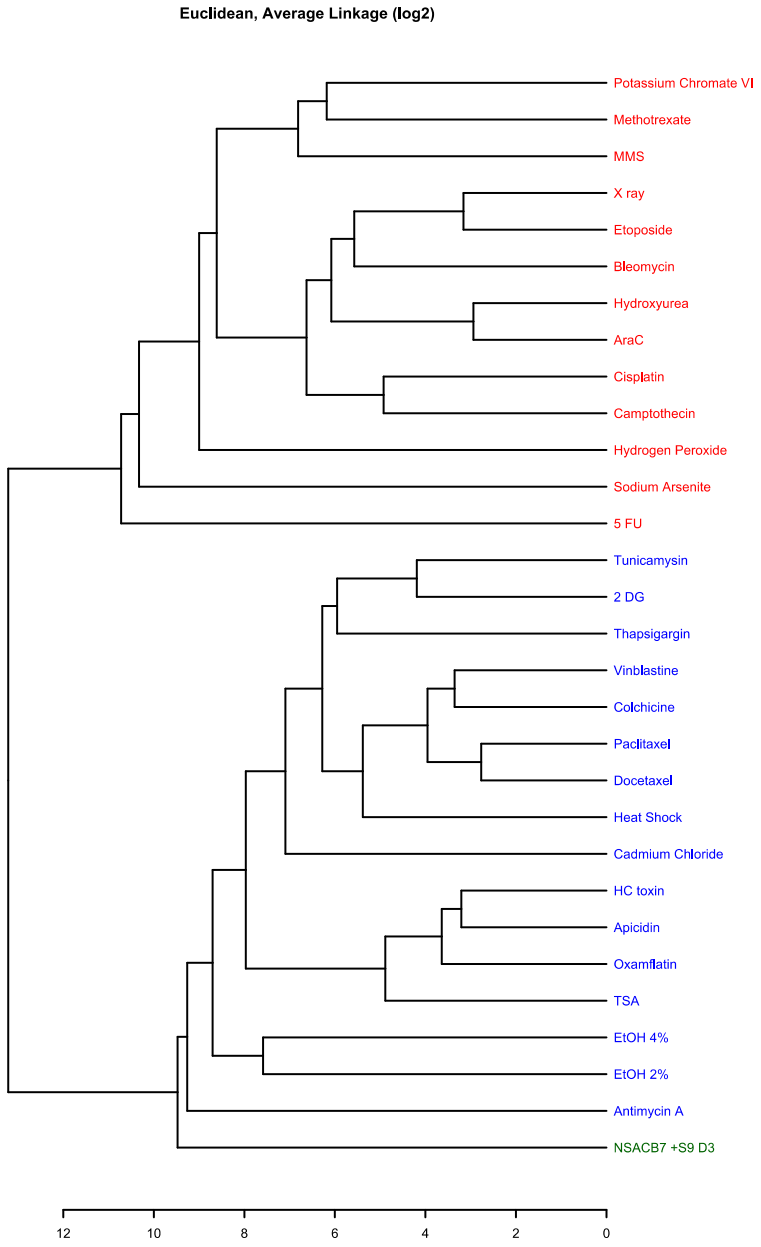
Euclidean, Average Linkage (log2)
Potassium Chromate VI
Methotrexate
MMS
X ray
Etoposide
Bleomycin
Hydroxyurea
AraC
Cisplatin
Camptothecin
Hydrogen Peroxide
Sodium Arsenite
5 FU
Tunicamysin
2 DG
Thapsigargin
Vinblastine
Colchicine
Paclitaxel
Docetaxel
Heat Shock
Cadmium Chloride
HC toxin
Apicidin
Oxamflatin
TSA
EtOH 4%
EtOH 2%
Antimycin A
NSACB7 +S9 D3
12
10
8
6
4
2
0

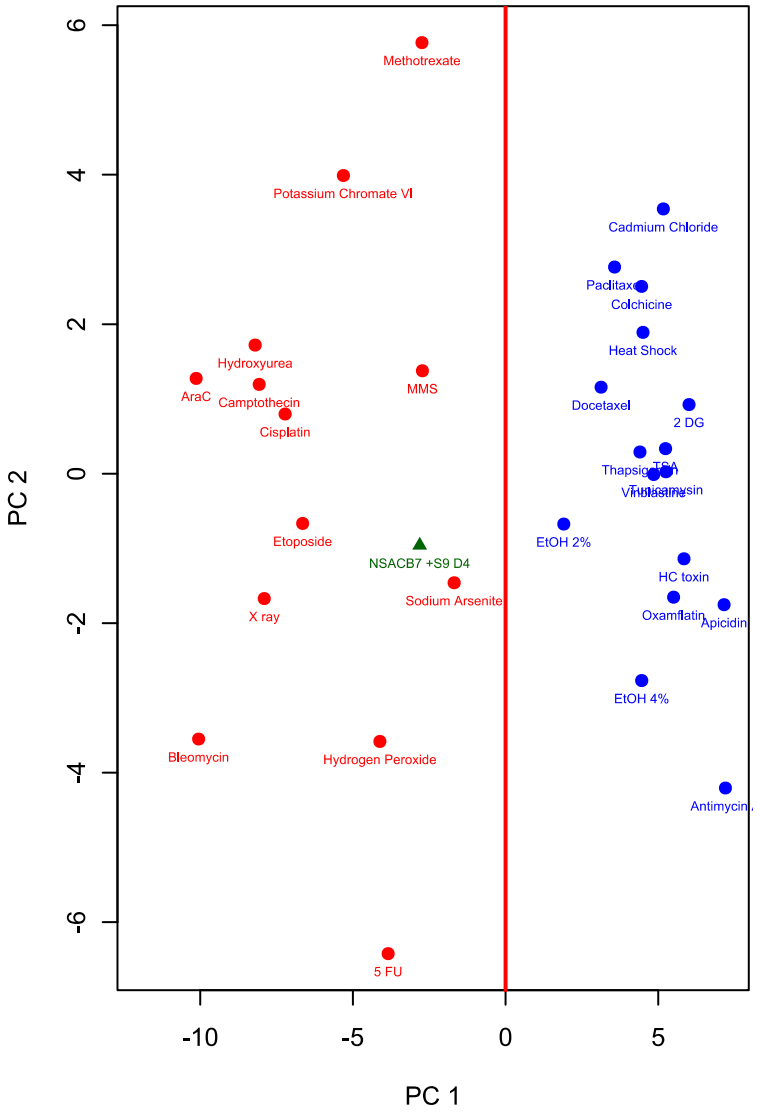
PC 2
PC 1
6
4
2
0
-2
-4
-6
-10
-5
0
5
Methotrexate
Potassium Chromate VI
Cadmium Chloride
Paclitaxel
Colchicine
Heat Shock
Hydroxyurea
AraC
Camptothecin
Cisplatin
MMS
Docetaxel
2 DG
Thapsigargin
TSA
Tunicamysin
Vinblastine
Etoposide
NSACB7 +S9 D4
EtOH 2%
HC toxin
Sodium Arsenite
X ray
Oxamflatin
Apicidin
EtOH 4%
Bleomycin
Hydrogen Peroxide
Antimycin
5 FU

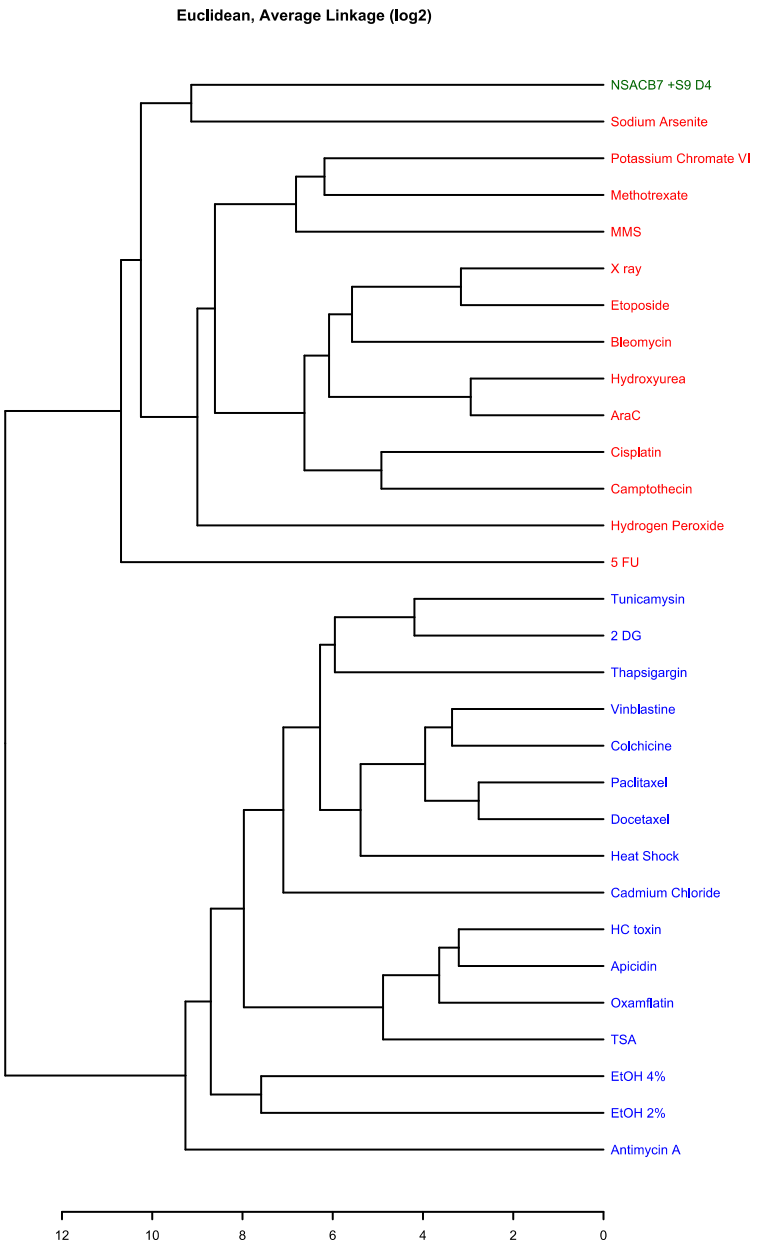
Euclidean, Average Linkage (log2)
NSACB7 +S9 D4
Sodium Arsenite
Potassium Chromate VI
Methotrexate
MMS
X ray
Etoposide
Bleomycin
Hydroxyurea
AraC
Cisplatin
Camptothecin
Hydrogen Peroxide
5 FU
Tunicamysin
2 DG
Thapsigargin
Vinblastine
Colchicine
Paclitaxel
Docetaxel
Heat Shock
Cadmium Chloride
HC toxin
Apicidin
Oxamflatin
TSA
EtOH 4%
EtOH 2%
Antimycin A
12
10
8
6
4
2
0

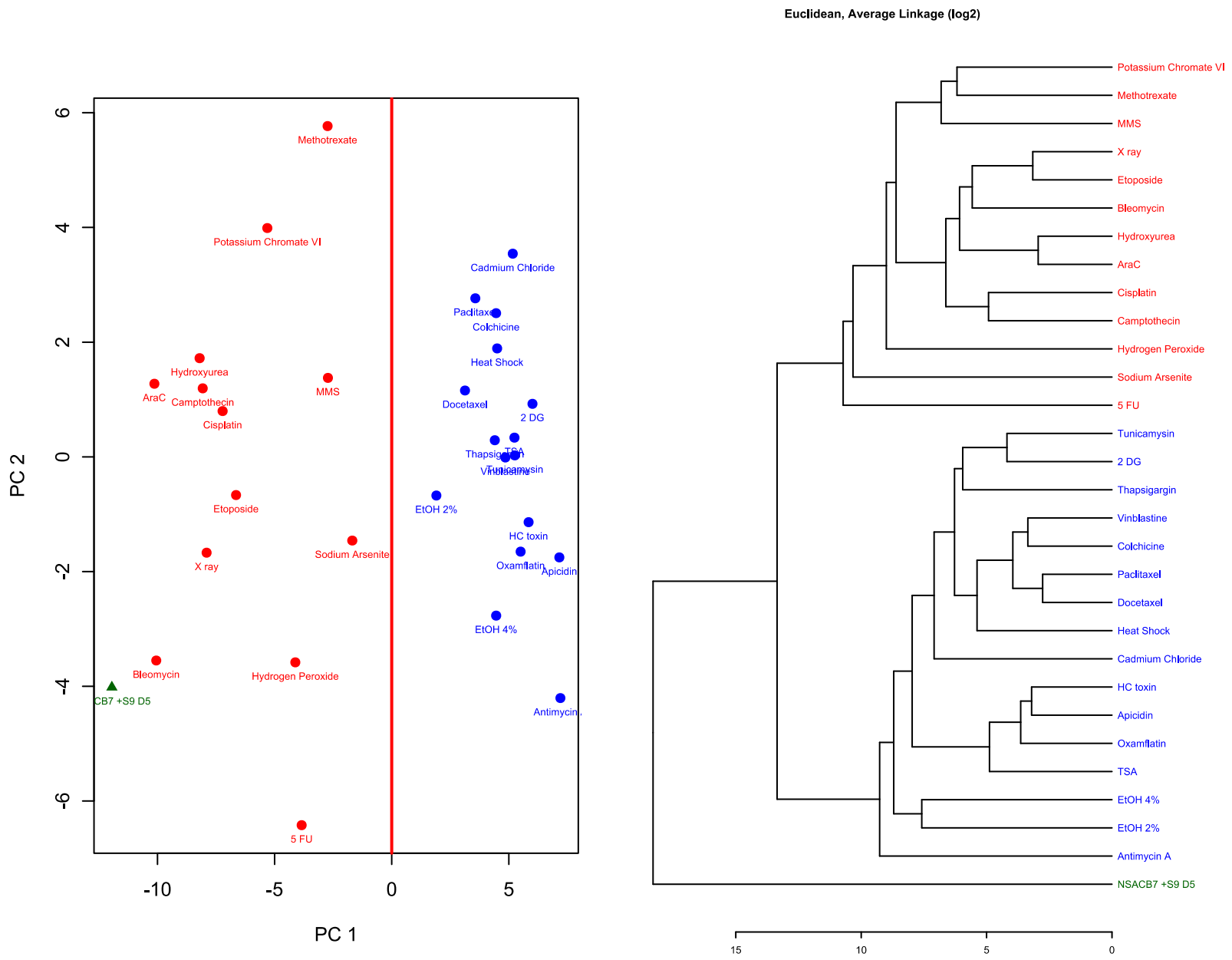

Supplementary Figure III-I: NASCB 7 (+S9) TGx-DDI biomarker classification using the Principal Component Analysis (PCA) (left) and hierarchical clustering (right) statistical analyses. Genotoxic reference chemicals are shown in red text, non-genotoxic reference chemicals are shown in blue text, and the test agent is shown in the green text. The line drawn on the PCA plot and the main branch on the dendogram divides the genotoxic and non-genotoxic agents and was used to classify the test compounds. D1 represents the lowest concentration tested, D5 the highest.

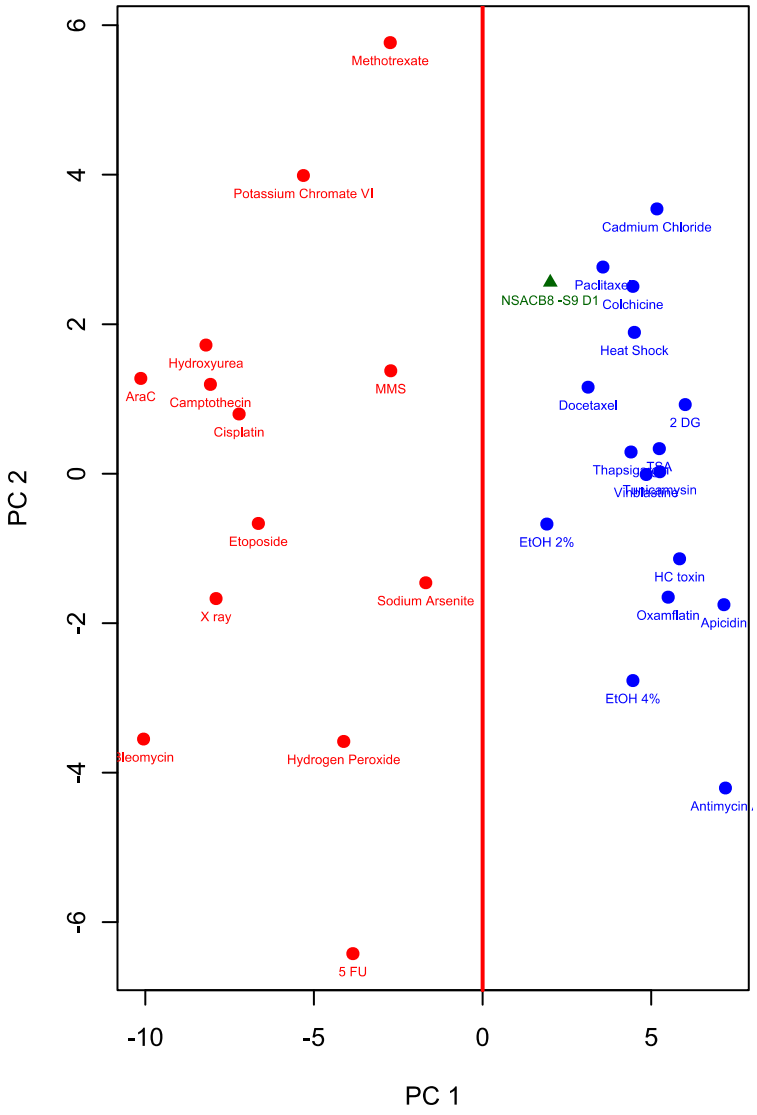
Methotrexate
Potassium Chromate VI
Cadmium Chloride
Paclitaxel
NSACB8 -S9 D1
Colchicine
Heat Shock
Hydroxyurea
AraC
Camptothecin
MMS
Docetaxel
2 DG
Cisplatin
Thapsigargin
TSA
Vinblastine
Tunicamysin
Etoposide
EtOH 2%
HC toxin
Sodium Arsenite
X ray
Oxamflatin
Apicidin
EtOH 4%
Bleomycin
Hydrogen Peroxide
Antimycin
5 FU
PC 2
PC 1
6
4
2
0
-2
-4
-6
-10
-5
0
5

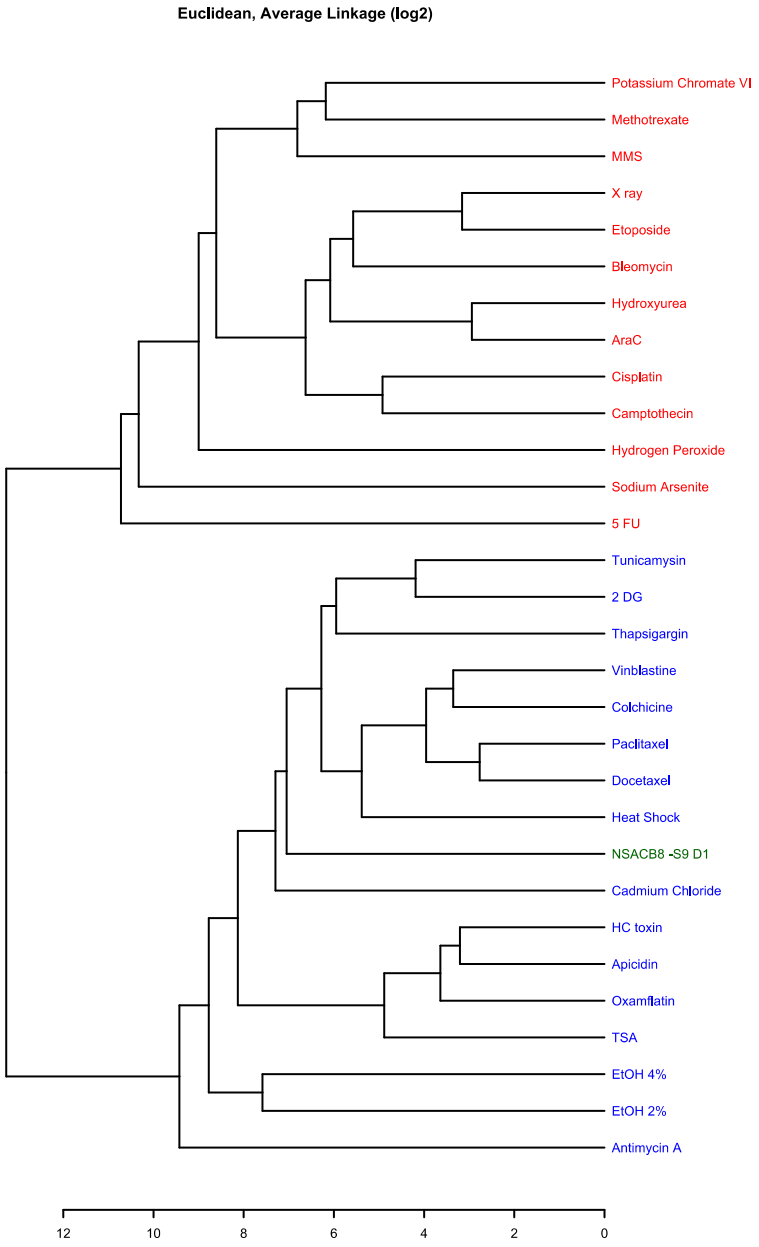
Euclidean, Average Linkage (log2)
Potassium Chromate VI
Methotrexate
MMS
X ray
Etoposide
Bleomycin
Hydroxyurea
AraC
Cisplatin
Camptothecin
Hydrogen Peroxide
Sodium Arsenite
5 FU
Tunicamysin
2 DG
Thapsigargin
Vinblastine
Colchicine
Paclitaxel
Docetaxel
Heat Shock
NSACB8 -S9 D1
Cadmium Chloride
HC toxin
Apicidin
Oxamflatin
TSA
EtOH 4%
EtOH 2%
Antimycin A
12
10
8
6
4
2
0

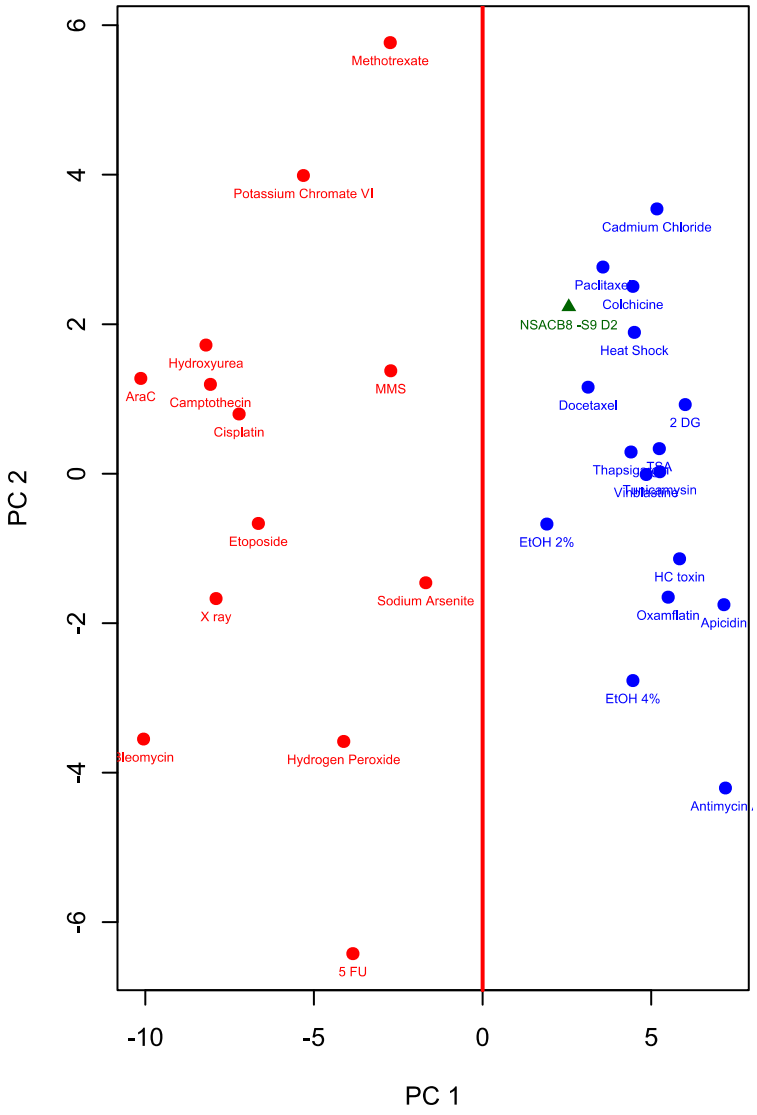
Methotrexate
Potassium Chromate VI
Cadmium Chloride
Paclitaxel
Colchicine
NSACB8 -S9 D2
Heat Shock
Hydroxyurea
AraC
Camptothecin
Cisplatin
MMS
Docetaxel
2 DG
Thapsigargin
TSA
Vinblastine
Tunicamysin
Etoposide
EtOH 2%
HC toxin
Sodium Arsenite
X ray
Oxamflatin
Apicidin
EtOH 4%
Bleomycin
Hydrogen Peroxide
Antimycin
5 FU
PC 2
PC 1
6
4
2
0
-2
-4
-6
-10
-5
0
5

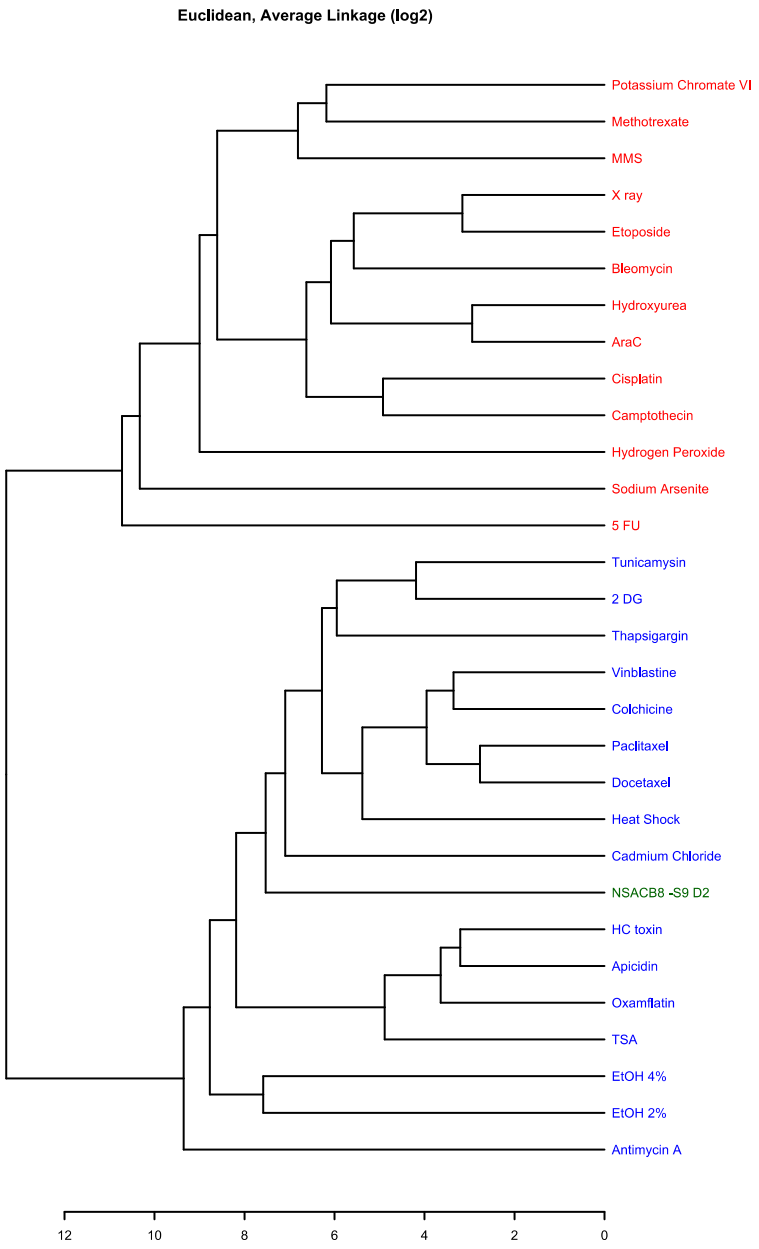
Euclidean, Average Linkage (log2)
Potassium Chromate VI
Methotrexate
MMS
X ray
Etoposide
Bleomycin
Hydroxyurea
AraC
Cisplatin
Camptothecin
Hydrogen Peroxide
Sodium Arsenite
5 FU
Tunicamysin
2 DG
Thapsigargin
Vinblastine
Colchicine
Paclitaxel
Docetaxel
Heat Shock
Cadmium Chloride
NSACB8 -S9 D2
HC toxin
Apicidin
Oxamflatin
TSA
EtOH 4%
EtOH 2%
Antimycin A
12
10
8
6
4
2
0

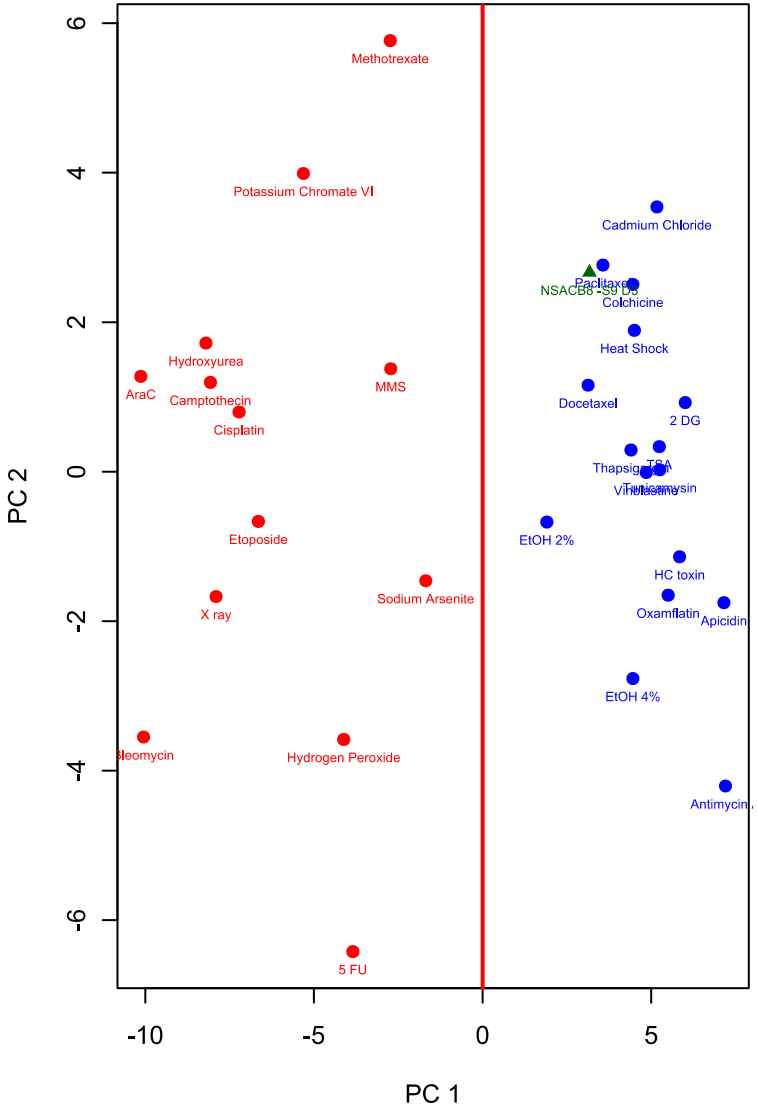
Methotrexate
Potassium Chromate VI
Cadmium Chloride
Paclitaxel
NSACB8 -S9 D3
Colchicine
Heat Shock
Hydroxyurea
AraC
Camptothecin
Cisplatin
MMS
Docetaxel
2 DG
Thapsigargin
TSA
Vinblastine
Tunicamysin
Etoposide
EtOH 2%
HC toxin
Sodium Arsenite
X ray
Oxamflatin
Apicidin
EtOH 4%
Bleomycin
Hydrogen Peroxide
Antimycin
5 FU
PC 2
PC 1
6
4
2
0
-2
-4
-6
-10
-5
0
5

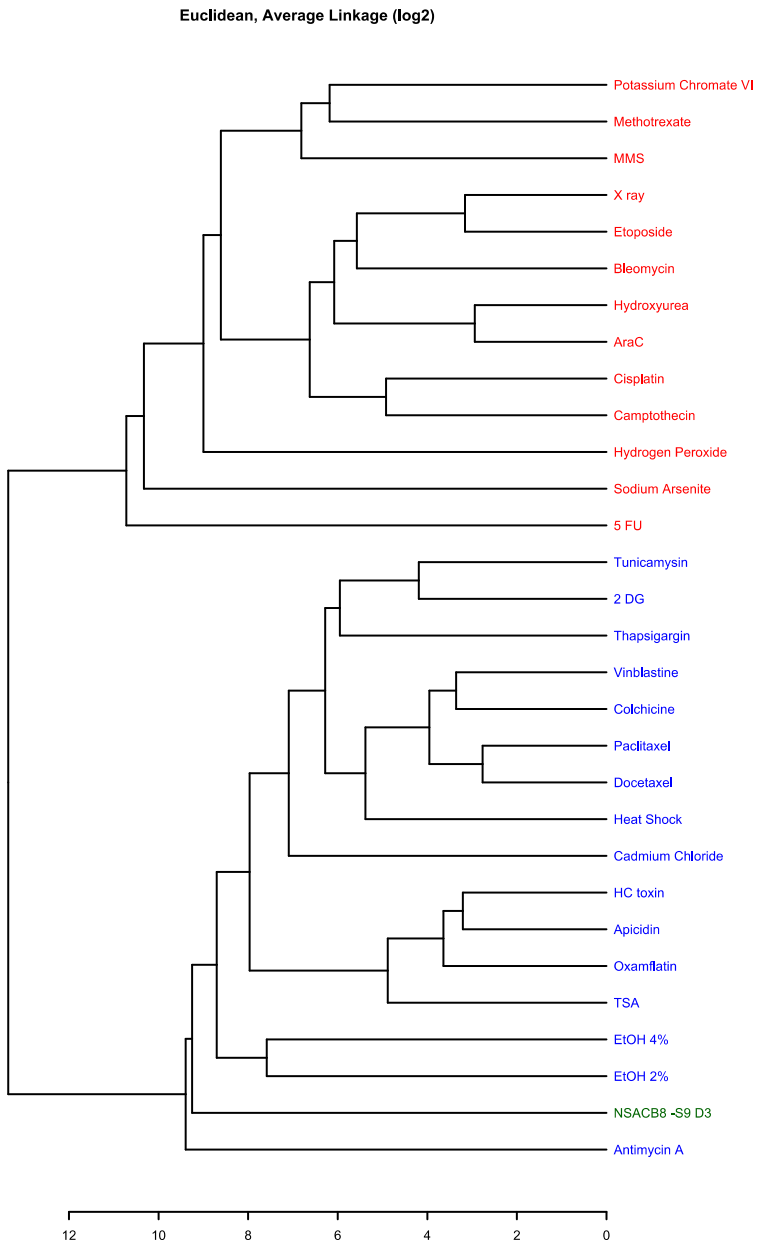
Euclidean, Average Linkage (log2)
Potassium Chromate VI
Methotrexate
MMS
X ray
Etoposide
Bleomycin
Hydroxyurea
AraC
Cisplatin
Camptothecin
Hydrogen Peroxide
Sodium Arsenite
5 FU
Tunicamysin
2 DG
Thapsigargin
Vinblastine
Colchicine
Paclitaxel
Docetaxel
Heat Shock
Cadmium Chloride
HC toxin
Apicidin
Oxamflatin
TSA
EtOH 4%
EtOH 2%
NSACB8 -S9 D3
Antimycin A
12
10
8
6
4
2
0

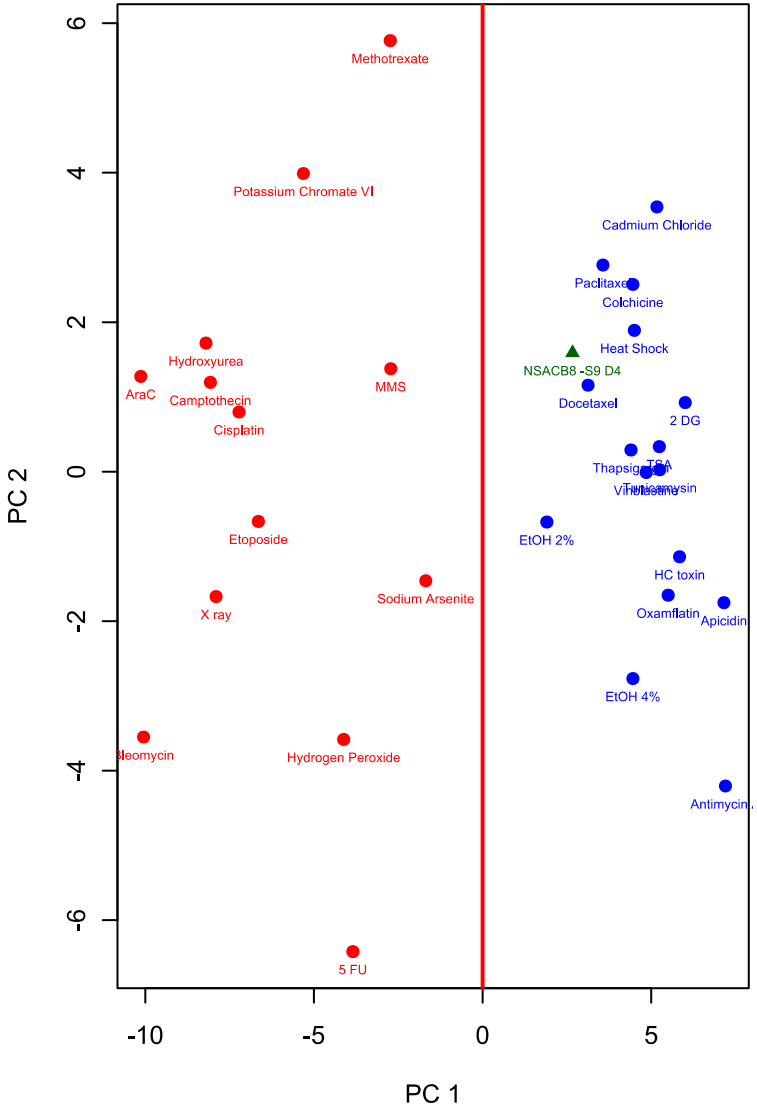
Methotrexate
Potassium Chromate VI
Cadmium Chloride
Paclitaxel
Colchicine
Heat Shock
Hydroxyurea
NSACB8 -S9 D4
AraC
MMS
Camptothecin
Docetaxel
2 DG
Cisplatin
Thapsigargin
TSA
Vinblastine
Tunicamysin
Etoposide
EtOH 2%
HC toxin
Sodium Arsenite
X ray
Oxamflatin
Apicidin
EtOH 4%
Bleomycin
Hydrogen Peroxide
Antimycin
5 FU
PC 2
PC 1
6
4
2
0
-2
-4
-6
-10
-5
0
5

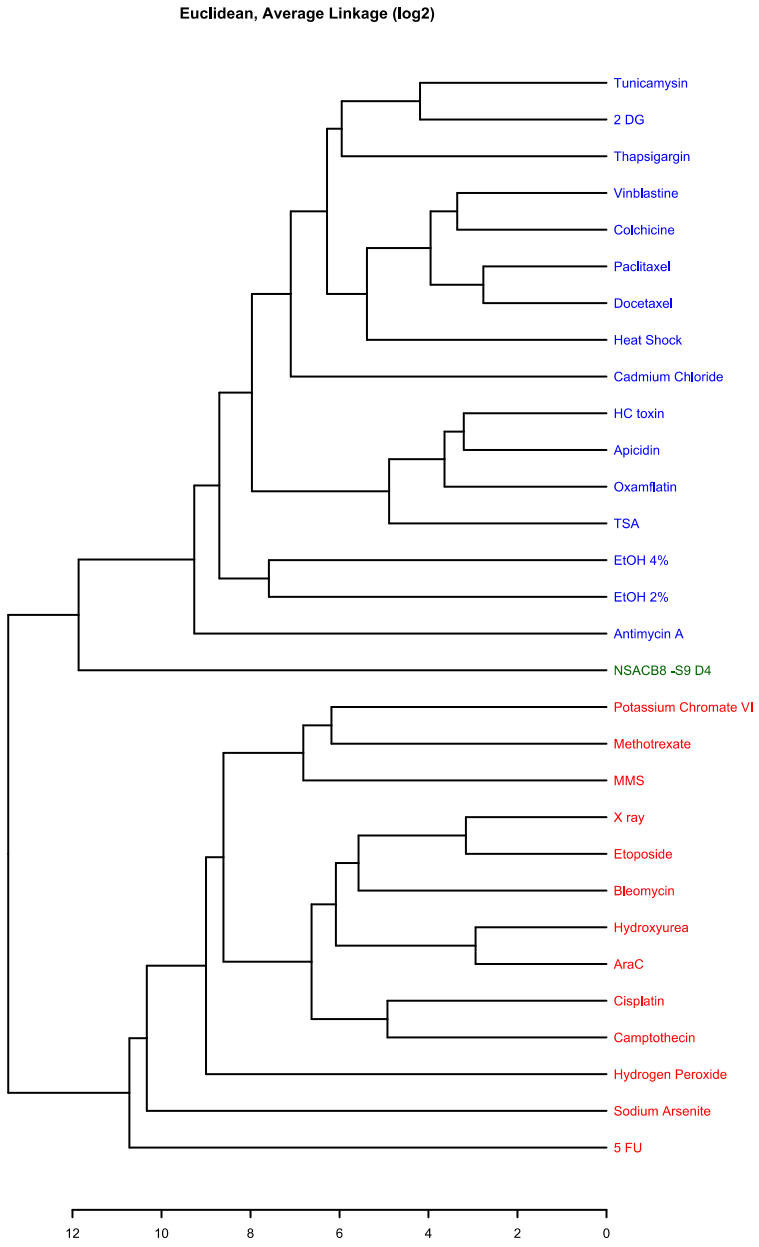
Euclidean, Average Linkage (log2)
Tunicamysin
2 DG
Thapsigargin
Vinblastine
Colchicine
Paclitaxel
Docetaxel
Heat Shock
Cadmium Chloride
HC toxin
Apicidin
Oxamflatin
TSA
EtOH 4%
EtOH 2%
Antimycin A
NSACB8 -S9 D4
Potassium Chromate VI
Methotrexate
MMS
X ray
Etoposide
Bleomycin
Hydroxyurea
AraC
Cisplatin
Camptothecin
Hydrogen Peroxide
Sodium Arsenite
5 FU
12
10
8
6
4
2
0

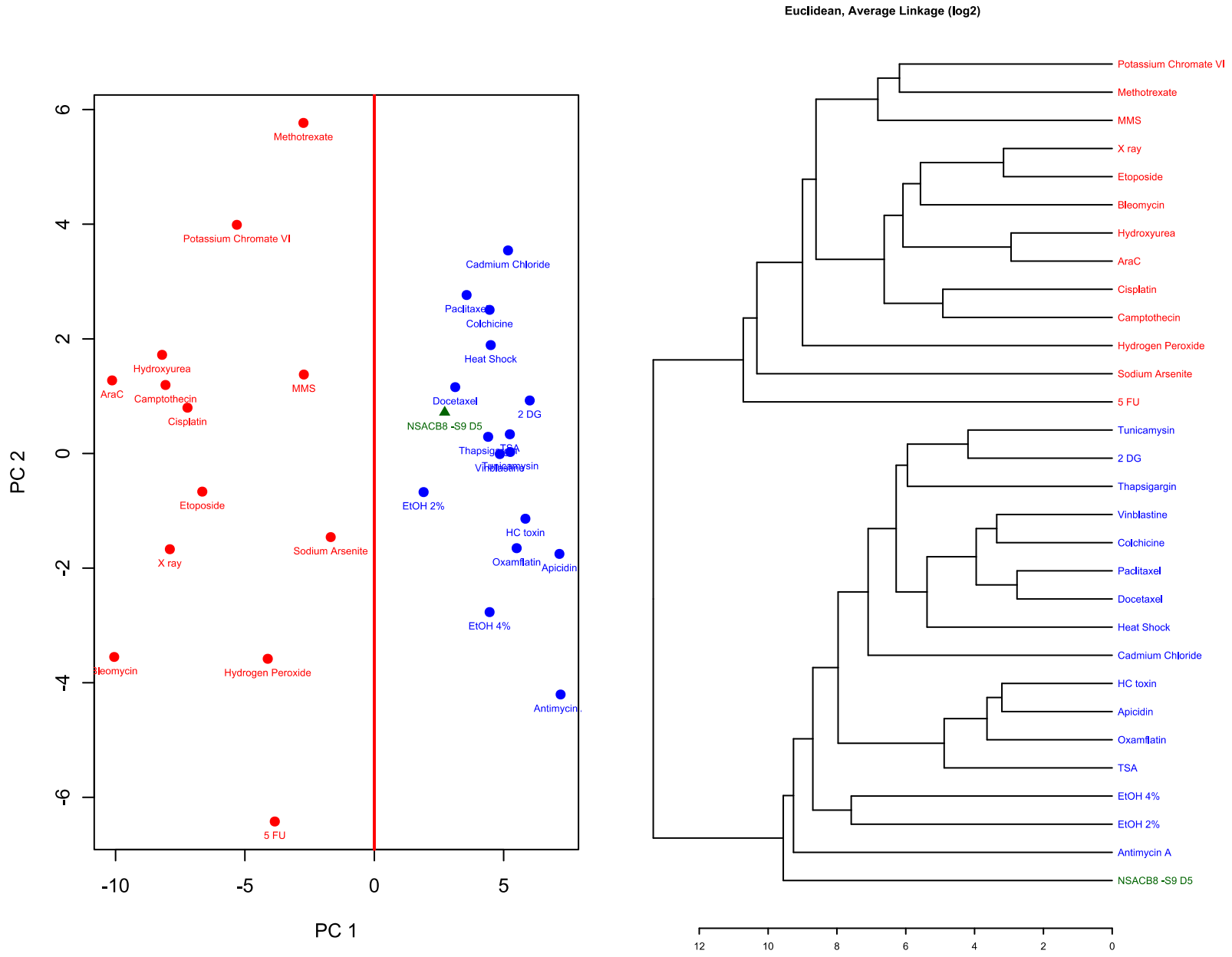

Supplementary Figure III-J: NASCB 8 (-S9) TGx-DDI biomarker classification using the Principal Component Analysis (PCA) (left) and hierarchical clustering (right) statistical analyses. Genotoxic reference chemicals are shown in red text, non-genotoxic reference chemicals are shown in blue text, and the test agent is shown in the green text. The line drawn on the PCA plot and the main branch on the dendogram divides the genotoxic and non-genotoxic agents and was used to classify the test compounds. D1 represents the lowest concentration tested, D5 the highest.

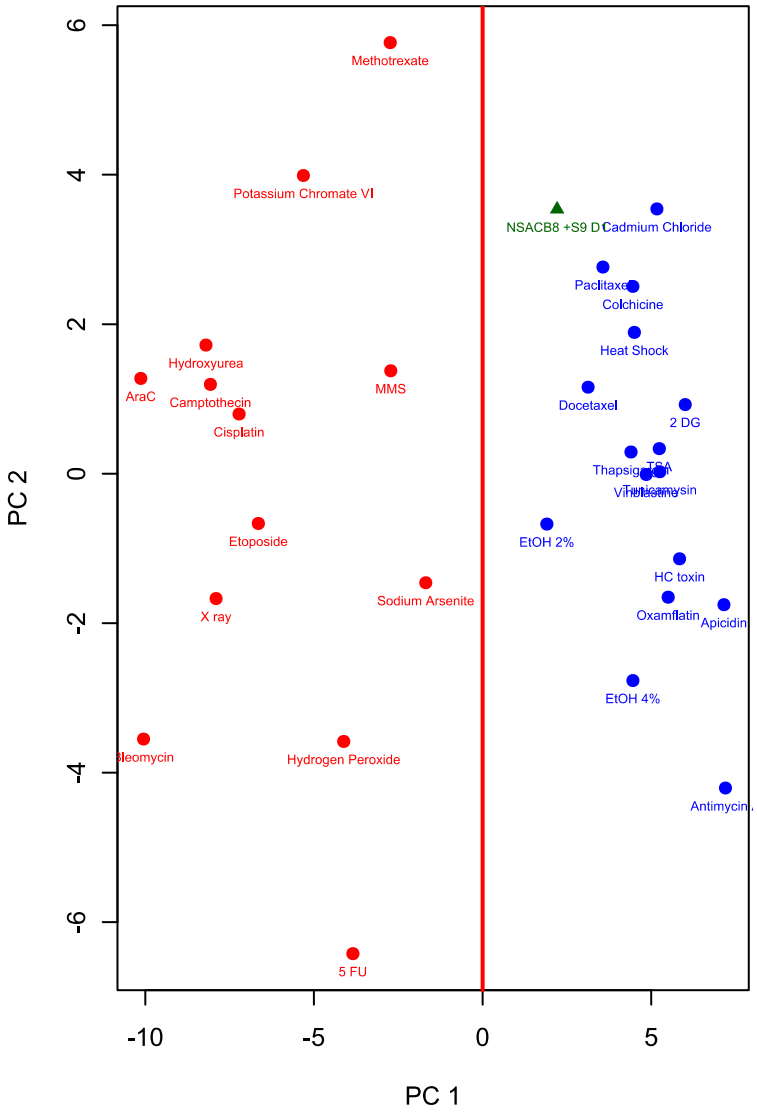
Methotrexate
Potassium Chromate VI
NSACB8 +S9 D1
Cadmium Chloride
Paclitaxel
Colchicine
Heat Shock
Hydroxyurea
AraC
Camptothecin
Cisplatin
MMS
Docetaxel
2 DG
Thapsigargin
TSA
Vinblastine
Tunicamysin
Etoposide
EtOH 2%
HC toxin
Sodium Arsenite
X ray
Oxamflatin
Apicidin
EtOH 4%
Bleomycin
Hydrogen Peroxide
Antimycin
5 FU
PC 2
PC 1
6
4
2
0
-2
-4
-6
-10
-5
0
5

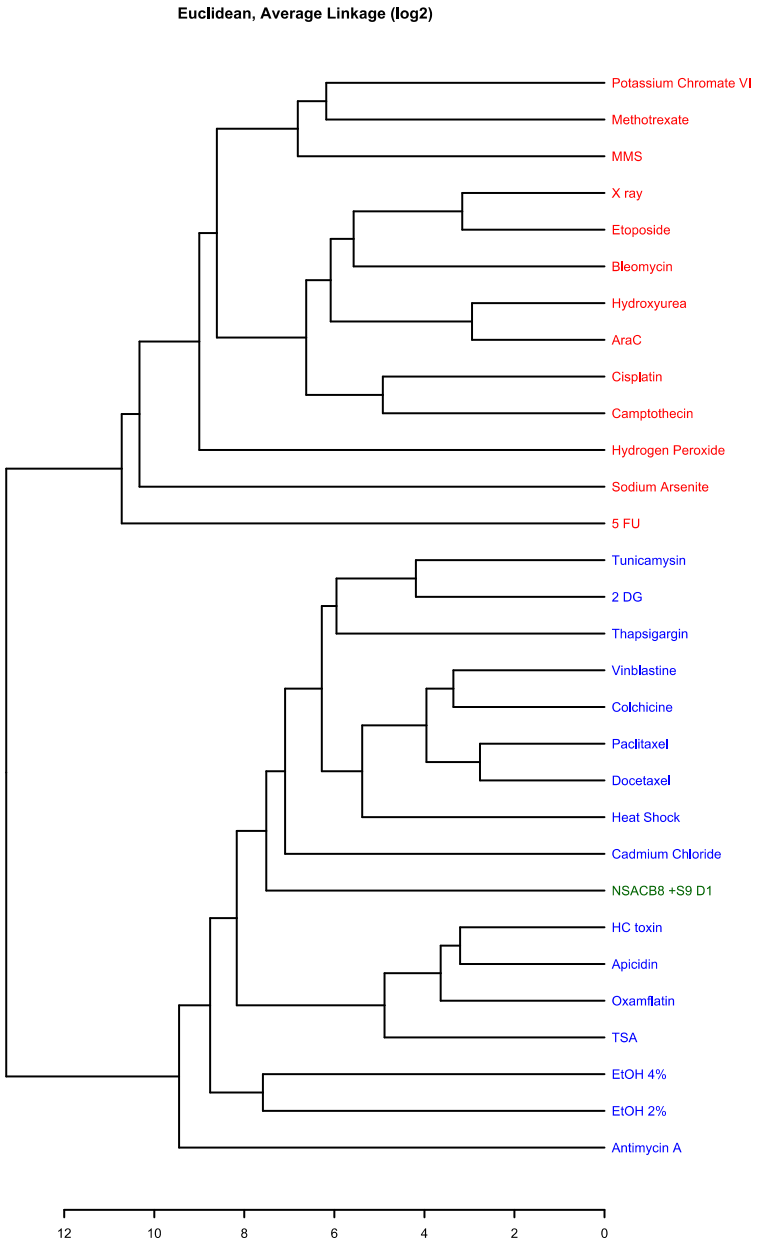
Euclidean, Average Linkage (log2)
Potassium Chromate VI
Methotrexate
MMS
X ray
Etoposide
Bleomycin
Hydroxyurea
AraC
Cisplatin
Camptothecin
Hydrogen Peroxide
Sodium Arsenite
5 FU
Tunicamysin
2 DG
Thapsigargin
Vinblastine
Colchicine
Paclitaxel
Docetaxel
Heat Shock
Cadmium Chloride
NSACB8 +S9 D1
HC toxin
Apicidin
Oxamflatin
TSA
EtOH 4%
EtOH 2%
Antimycin A
12
10
8
6
4
2
0

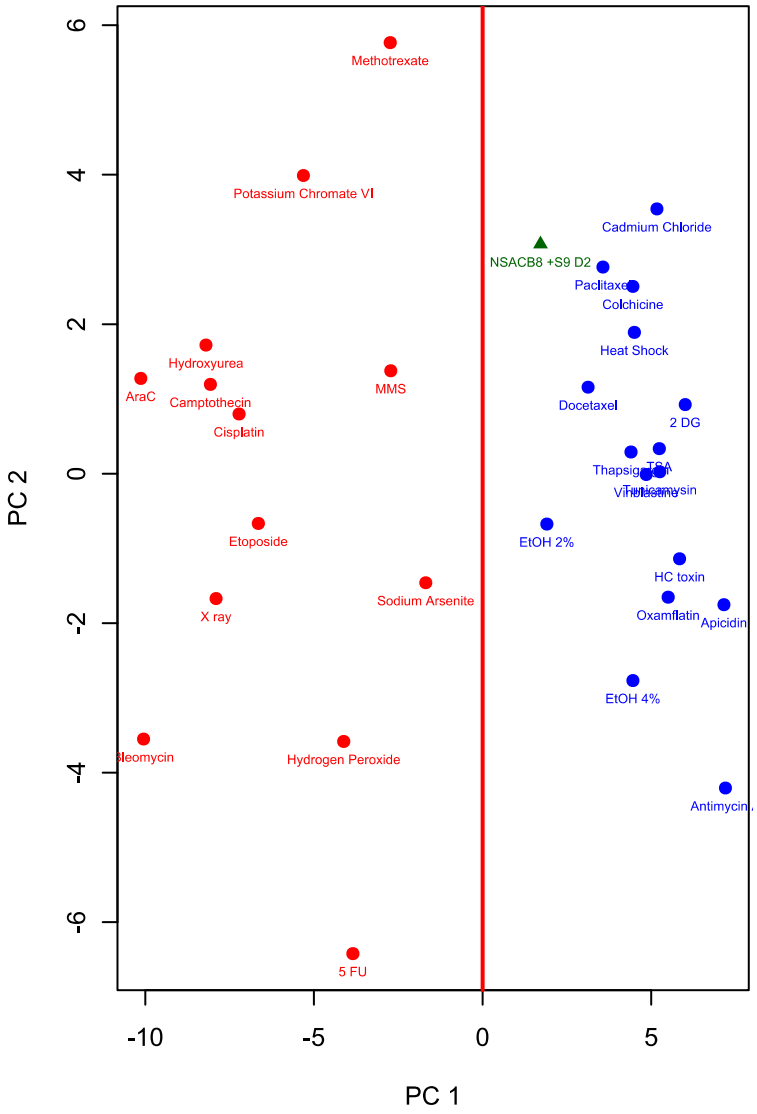
Methotrexate
Potassium Chromate VI
Cadmium Chloride
NSACB8 +S9 D2
Paclitaxel
Colchicine
Heat Shock
Hydroxyurea
AraC
Camptothecin
Cisplatin
MMS
Docetaxel
2 DG
Thapsigargin
TSA
Vinblastine
Tunicamysin
Etoposide
EtOH 2%
HC toxin
Sodium Arsenite
X ray
Oxamflatin
Apicidin
EtOH 4%
Bleomycin
Hydrogen Peroxide
Antimycin
5 FU
PC 2
PC 1
6
4
2
0
-2
-4
-6
-10
-5
0
5

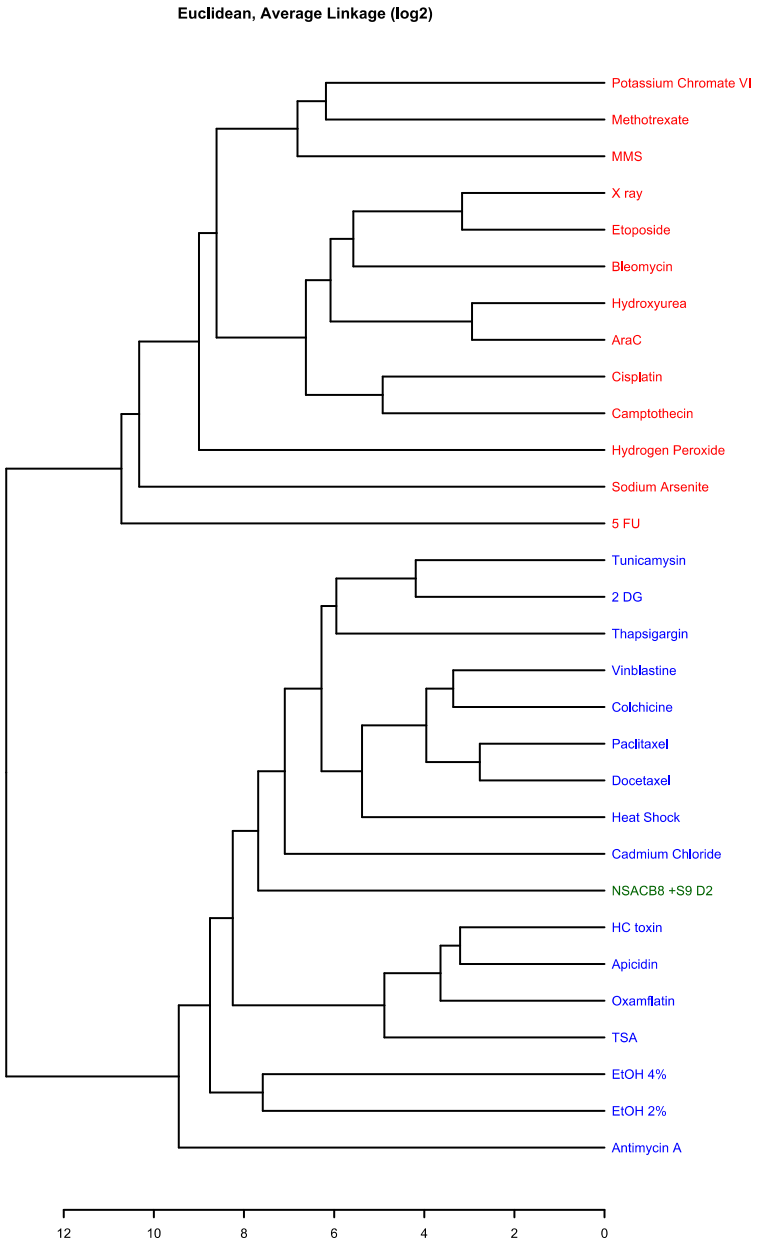
Euclidean, Average Linkage (log2)
Potassium Chromate VI
Methotrexate
MMS
X ray
Etoposide
Bleomycin
Hydroxyurea
AraC
Cisplatin
Camptothecin
Hydrogen Peroxide
Sodium Arsenite
5 FU
Tunicamysin
2 DG
Thapsigargin
Vinblastine
Colchicine
Paclitaxel
Docetaxel
Heat Shock
Cadmium Chloride
NSACB8 +S9 D2
HC toxin
Apicidin
Oxamflatin
TSA
EtOH 4%
EtOH 2%
Antimycin A
12
10
8
6
4
2
0

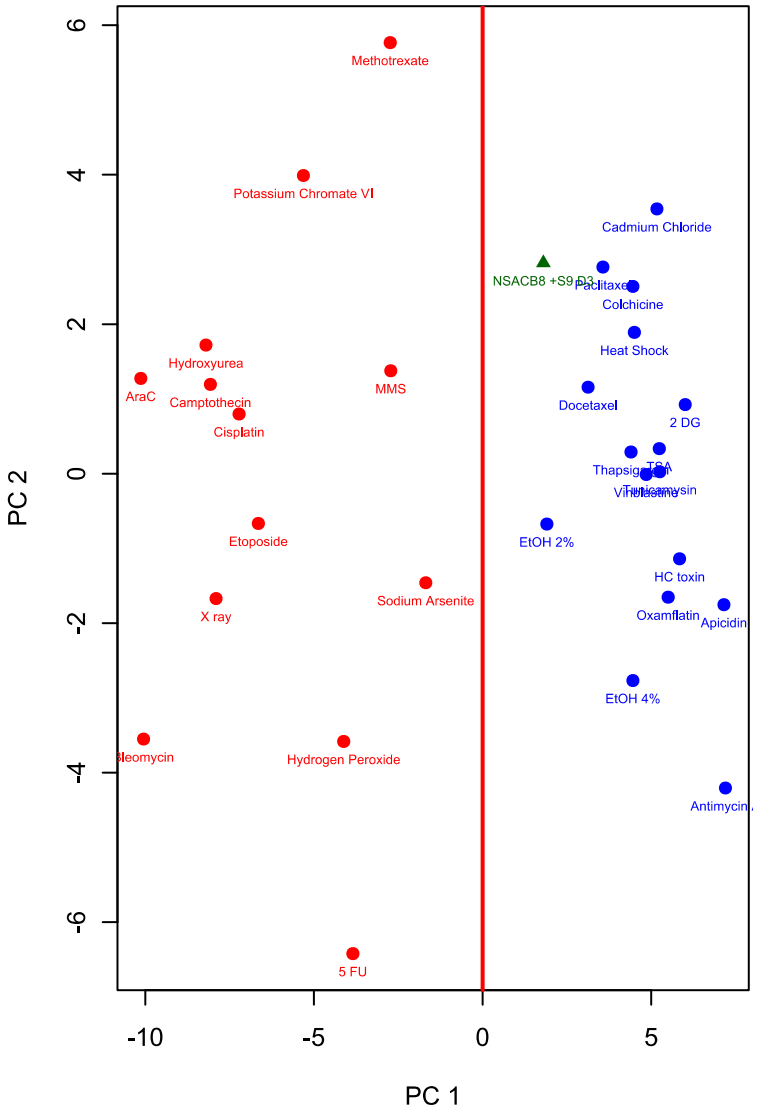
Methotrexate
Potassium Chromate VI
Cadmium Chloride
NSACB8 +S9 D3
Paclitaxel
Colchicine
Heat Shock
Hydroxyurea
AraC
Camptothecin
MMS
Docetaxel
2 DG
Cisplatin
Thapsigargin
TSA
Vinblastine
Tunicamysin
Etoposide
EtOH 2%
HC toxin
Sodium Arsenite
X ray
Oxamflatin
Apicidin
EtOH 4%
Bleomycin
Hydrogen Peroxide
Antimycin
5 FU
PC 2
PC 1
6
4
2
0
-2
-4
-6
-10
-5
0
5

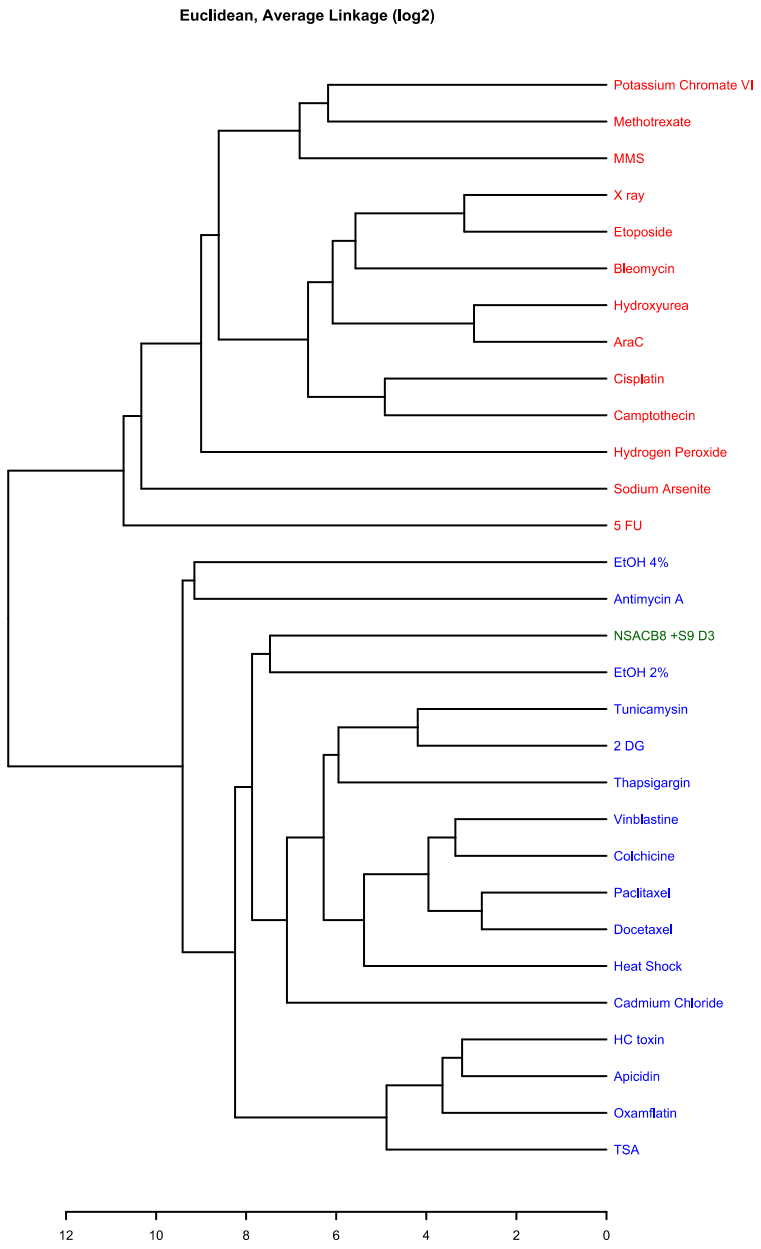
Euclidean, Average Linkage (log2)
Potassium Chromate VI
Methotrexate
MMS
X ray
Etoposide
Bleomycin
Hydroxyurea
AraC
Cisplatin
Camptothecin
Hydrogen Peroxide
Sodium Arsenite
5 FU
EtOH 4%
Antimycin A
NSACB8 +S9 D3
EtOH 2%
Tunicamysin
2 DG
Thapsigargin
Vinblastine
Colchicine
Paclitaxel
Docetaxel
Heat Shock
Cadmium Chloride
HC toxin
Apicidin
Oxamflatin
TSA
12
10
8
6
4
2
0

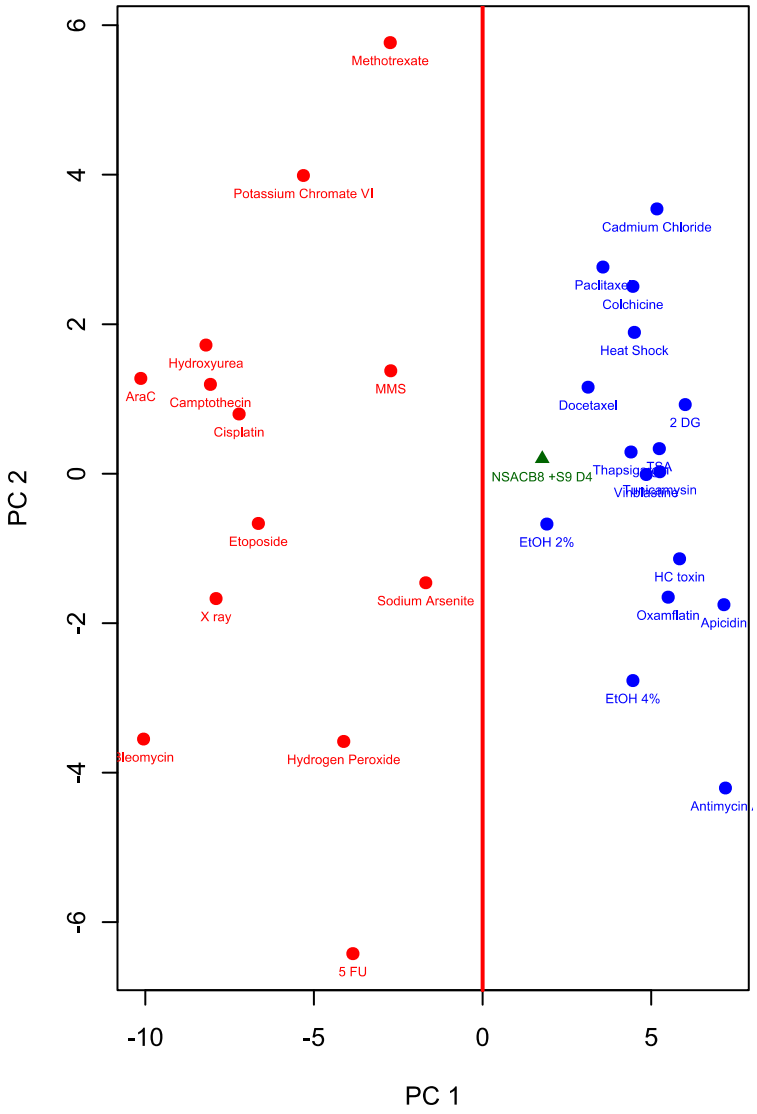
Methotrexate
Potassium Chromate VI
Cadmium Chloride
Paclitaxel
Colchicine
Heat Shock
Hydroxyurea
AraC
Camptothecin
Cisplatin
MMS
Docetaxel
2 DG
NSACB8 +S9 D4
Thapsigargin
TSA
Vinblastine
Tunicamysin
Etoposide
EtOH 2%
HC toxin
Sodium Arsenite
X ray
Oxamflatin
Apicidin
EtOH 4%
Bleomycin
Hydrogen Peroxide
Antimycin
5 FU
PC 2
PC 1
6
4
2
0
-2
-4
-6
-10
-5
0
5

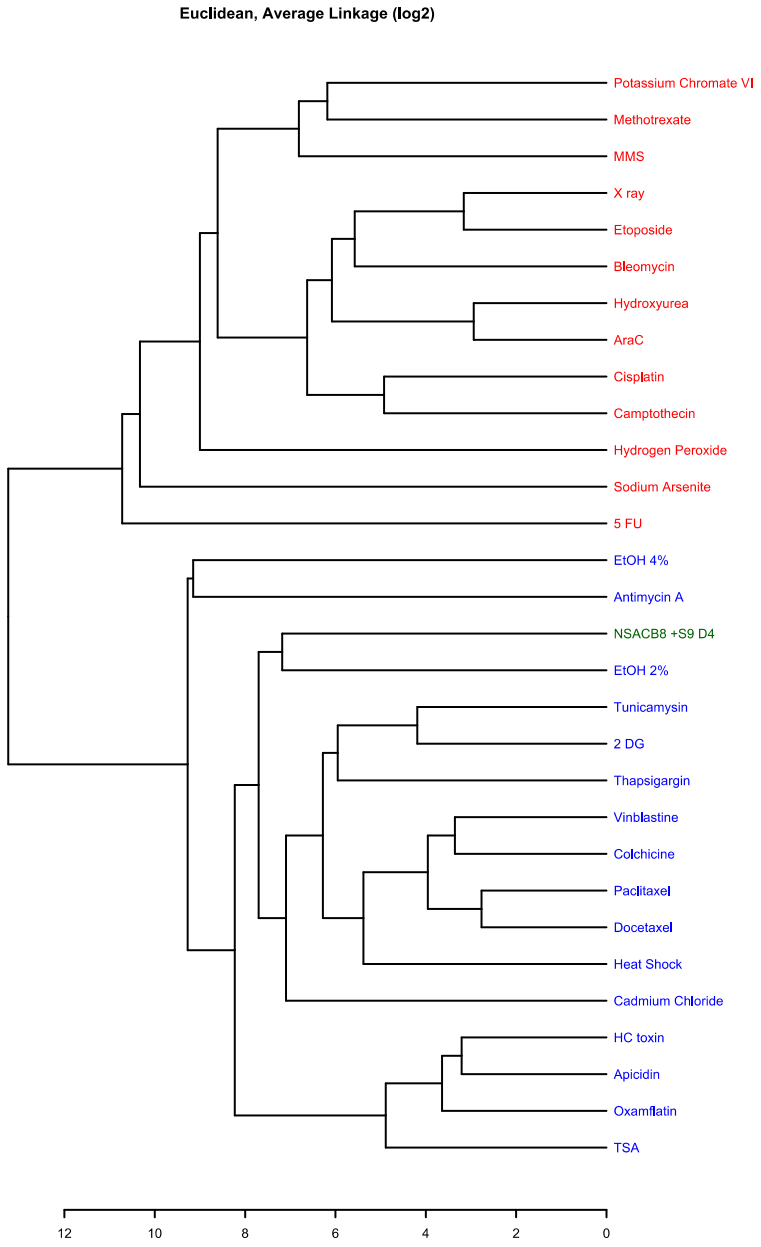
Euclidean, Average Linkage (log2)
Potassium Chromate VI
Methotrexate
MMS
X ray
Etoposide
Bleomycin
Hydroxyurea
AraC
Cisplatin
Camptothecin
Hydrogen Peroxide
Sodium Arsenite
5 FU
EtOH 4%
Antimycin A
NSACB8 +S9 D4
EtOH 2%
Tunicamysin
2 DG
Thapsigargin
Vinblastine
Colchicine
Paclitaxel
Docetaxel
Heat Shock
Cadmium Chloride
HC toxin
Apicidin
Oxamflatin
TSA
12
10
8
6
4
2
0

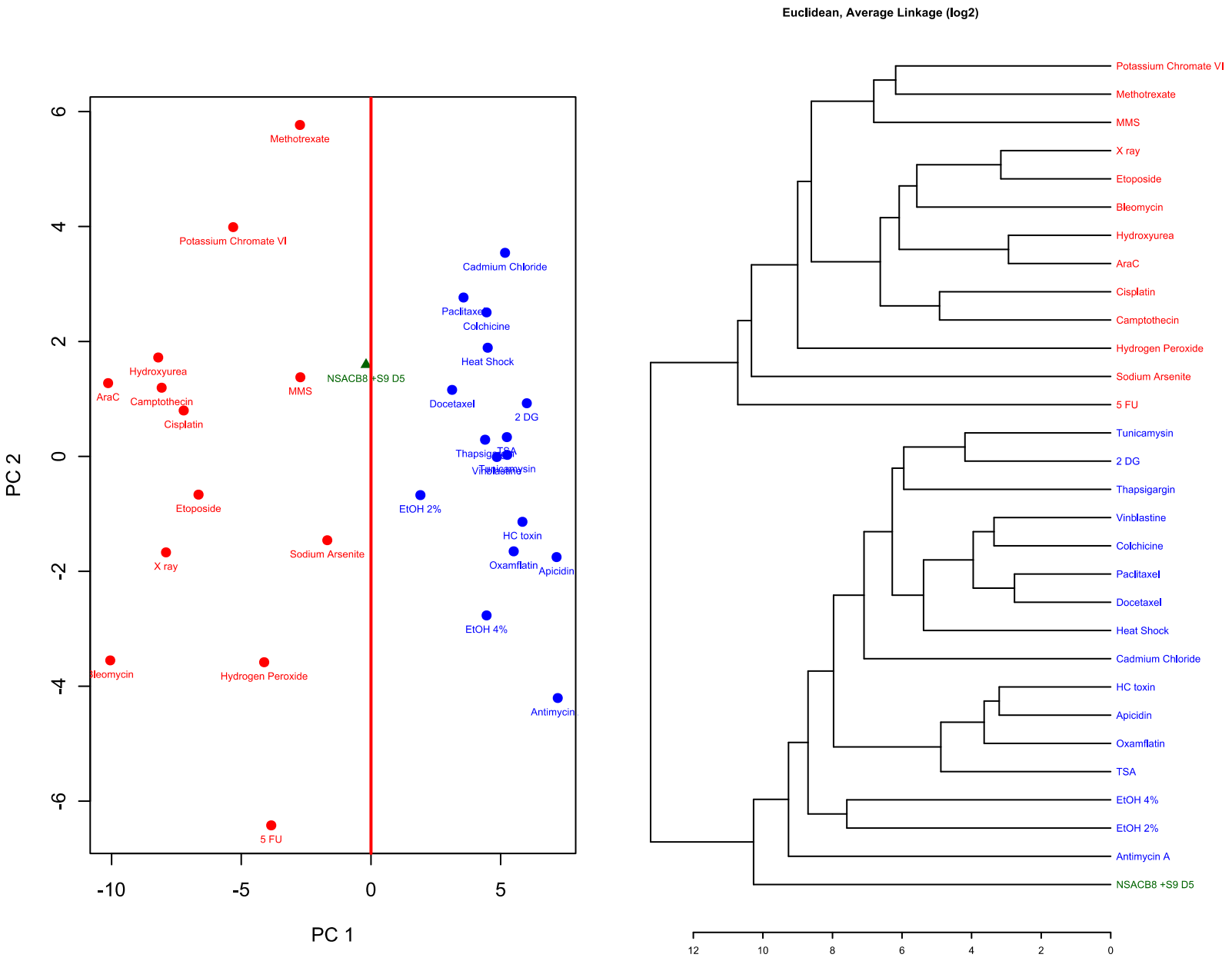

Supplementary Figure III-K: NASCB 8 (+S9) TGx-DDI biomarker classification using the Principal Component Analysis (PCA) (left) and hierarchical clustering (right) statistical analyses. Genotoxic reference chemicals are shown in red text, non-genotoxic reference chemicals are shown in blue text, and the test agent is shown in the green text. The line drawn on the PCA plot and the main branch on the dendogram divides the genotoxic and non-genotoxic agents and was used to classify the test compounds. D1 represents the lowest concentration tested, D5 the highest.

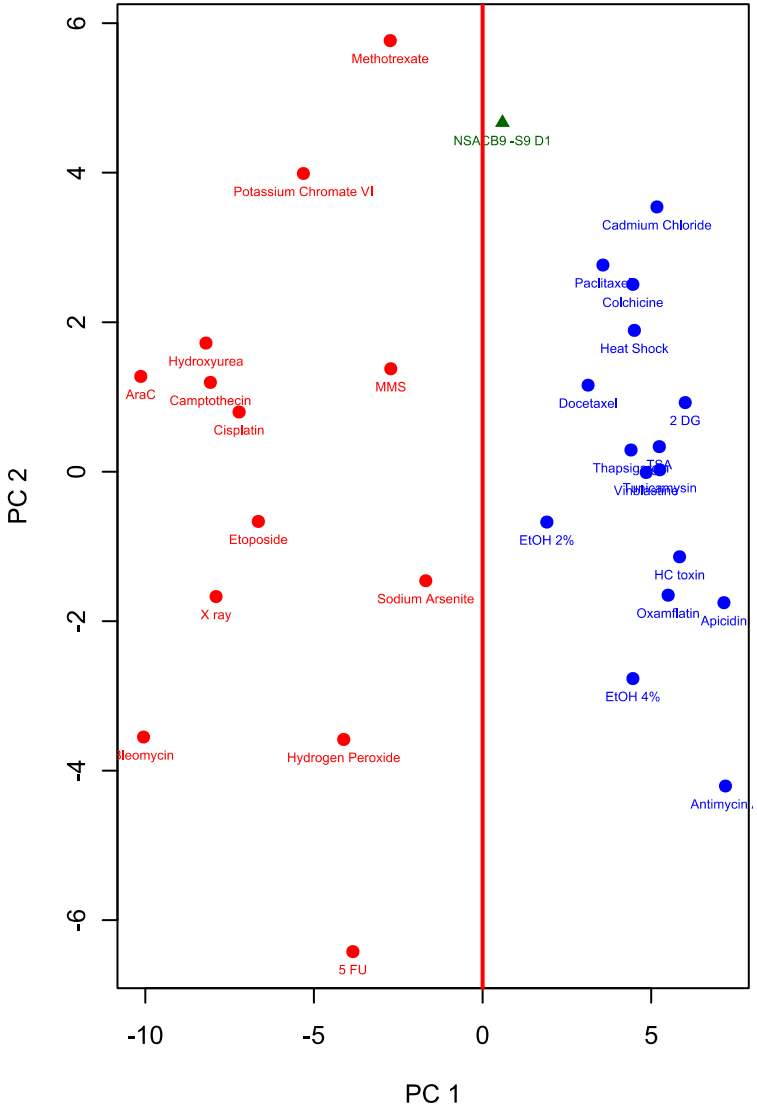
Methotrexate
NSACB9 -S9 D1
Potassium Chromate VI
Cadmium Chloride
Paclitaxel
Colchicine
Heat Shock
Hydroxyurea
AraC
Camptothecin
Cisplatin
MMS
Docetaxel
2 DG
Thapsigargin
TSA
Tunicamycin
Vinblastine
Etoposide
EtOH 2%
HC toxin
Sodium Arsenite
X ray
Oxamflatin
Apicidin
EtOH 4%
Bleomycin
Hydrogen Peroxide
Antimycin
5 FU
PC 2
PC 1
6
4
2
0
-2
-4
-6
-10
-5
0
5

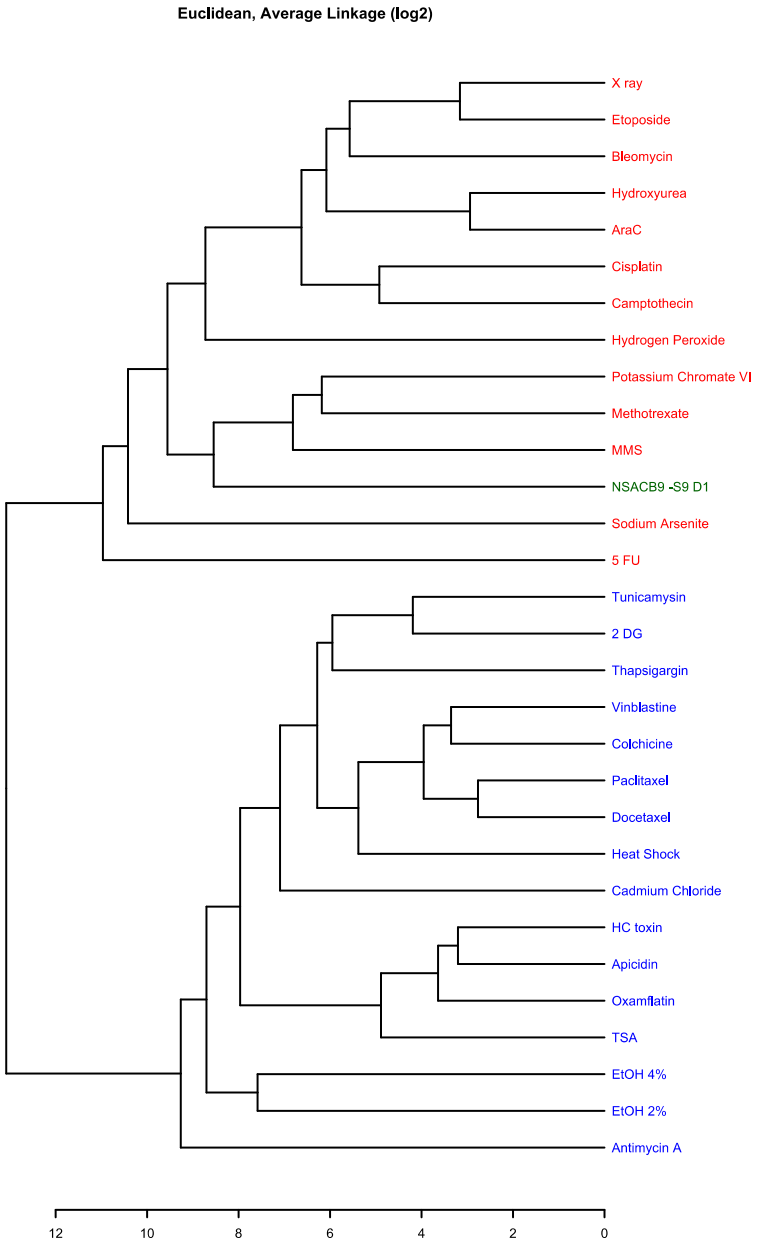
Euclidean, Average Linkage (log2)
X ray
Etoposide
Bleomycin
Hydroxyurea
AraC
Cisplatin
Camptothecin
Hydrogen Peroxide
Potassium Chromate VI
Methotrexate
MMS
NSACB9 -S9 D1
Sodium Arsenite
5 FU
Tunicamycin
2 DG
Thapsigargin
Vinblastine
Colchicine
Paclitaxel
Docetaxel
Heat Shock
Cadmium Chloride
HC toxin
Apicidin
Oxamflatin
TSA
EtOH 4%
EtOH 2%
Antimycin A
12
10
8
6
4
2
0

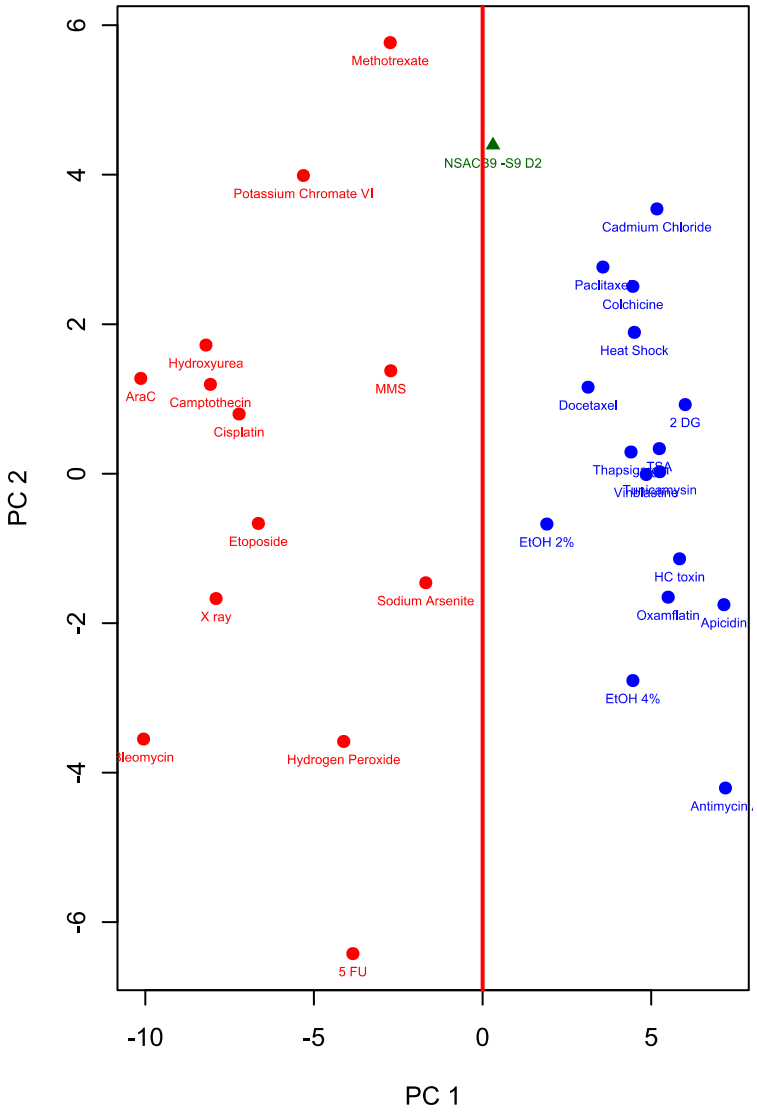
Methotrexate
NSACB9 -S9 D2
Potassium Chromate VI
Cadmium Chloride
Paclitaxel
Colchicine
Heat Shock
Hydroxyurea
AraC
Camptothecin
Cisplatin
MMS
Docetaxel
2 DG
Thapsigargin
TSA
Vinblastine
Tunicamycin
Etoposide
EtOH 2%
HC toxin
Sodium Arsenite
X ray
Oxamflatin
Apicidin
EtOH 4%
Bleomycin
Hydrogen Peroxide
Antimycin
5 FU
PC 2
PC 1
6
4
2
0
-2
-4
-6
-10
-5
0
5

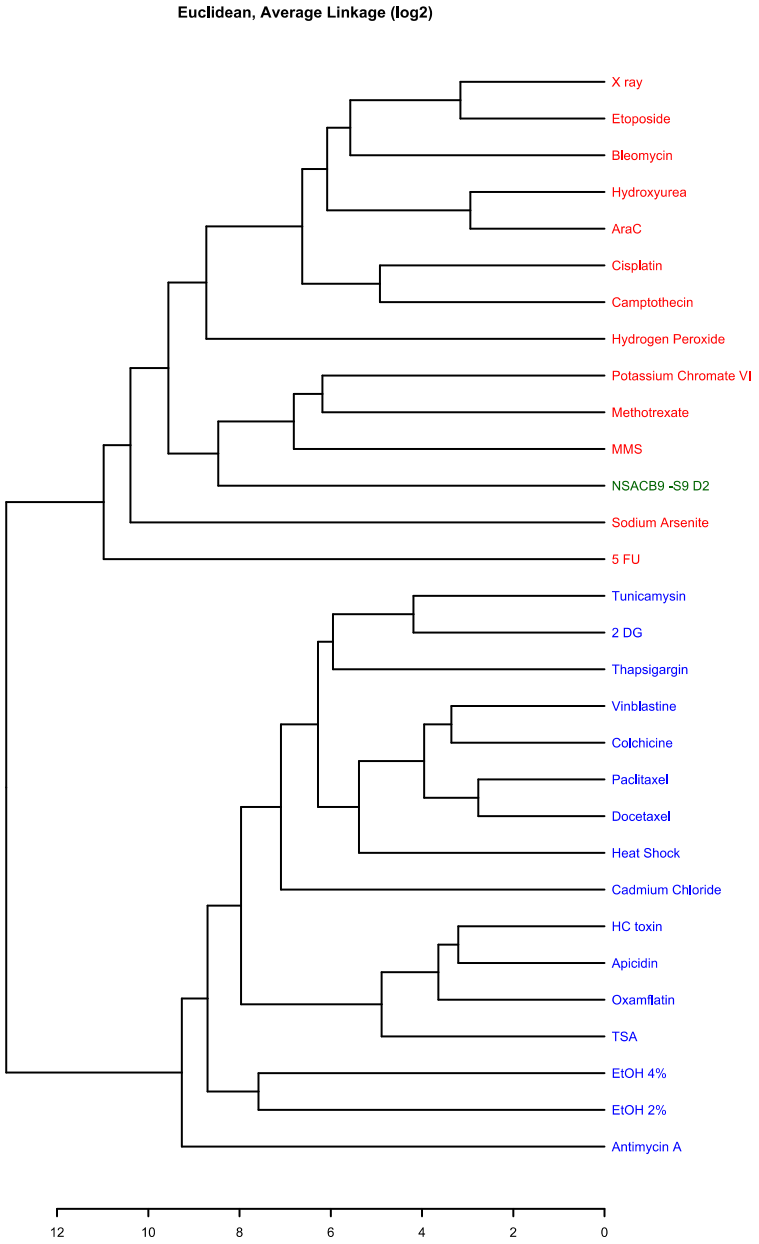
Euclidean, Average Linkage (log2)
X ray
Etoposide
Bleomycin
Hydroxyurea
AraC
Cisplatin
Camptothecin
Hydrogen Peroxide
Potassium Chromate VI
Methotrexate
MMS
NSACB9 -S9 D2
Sodium Arsenite
5 FU
Tunicamycin
2 DG
Thapsigargin
Vinblastine
Colchicine
Paclitaxel
Docetaxel
Heat Shock
Cadmium Chloride
HC toxin
Apicidin
Oxamflatin
TSA
EtOH 4%
EtOH 2%
Antimycin A
12
10
8
6
4
2
0

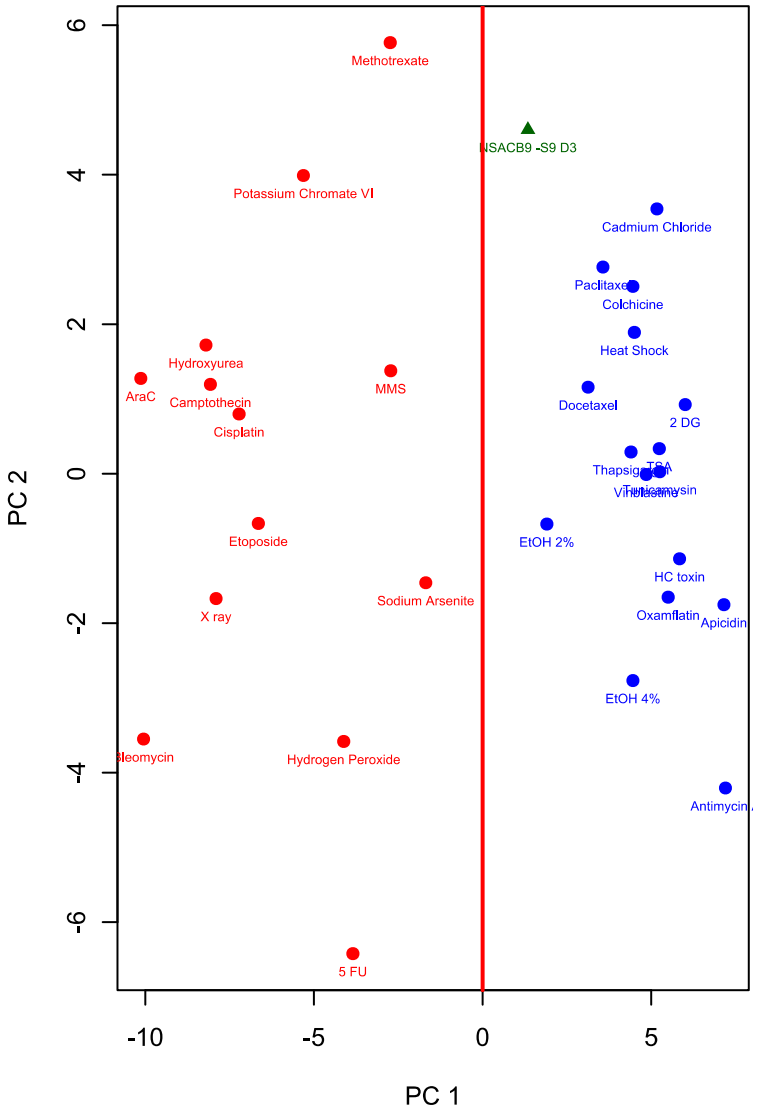
Methotrexate
NSACB9 -S9 D3
Potassium Chromate VI
Cadmium Chloride
Paclitaxel
Colchicine
Heat Shock
Hydroxyurea
AraC
Camptothecin
Cisplatin
MMS
Docetaxel
2 DG
Thapsigargin
TSA
Vinblastine
Tunicamysin
Etoposide
EtOH 2%
HC toxin
Sodium Arsenite
X ray
Oxamflatin
Apicidin
EtOH 4%
Bleomycin
Hydrogen Peroxide
Antimycin
5 FU
PC 2
PC 1
6
4
2
0
-2
-4
-6
-10
-5
0
5

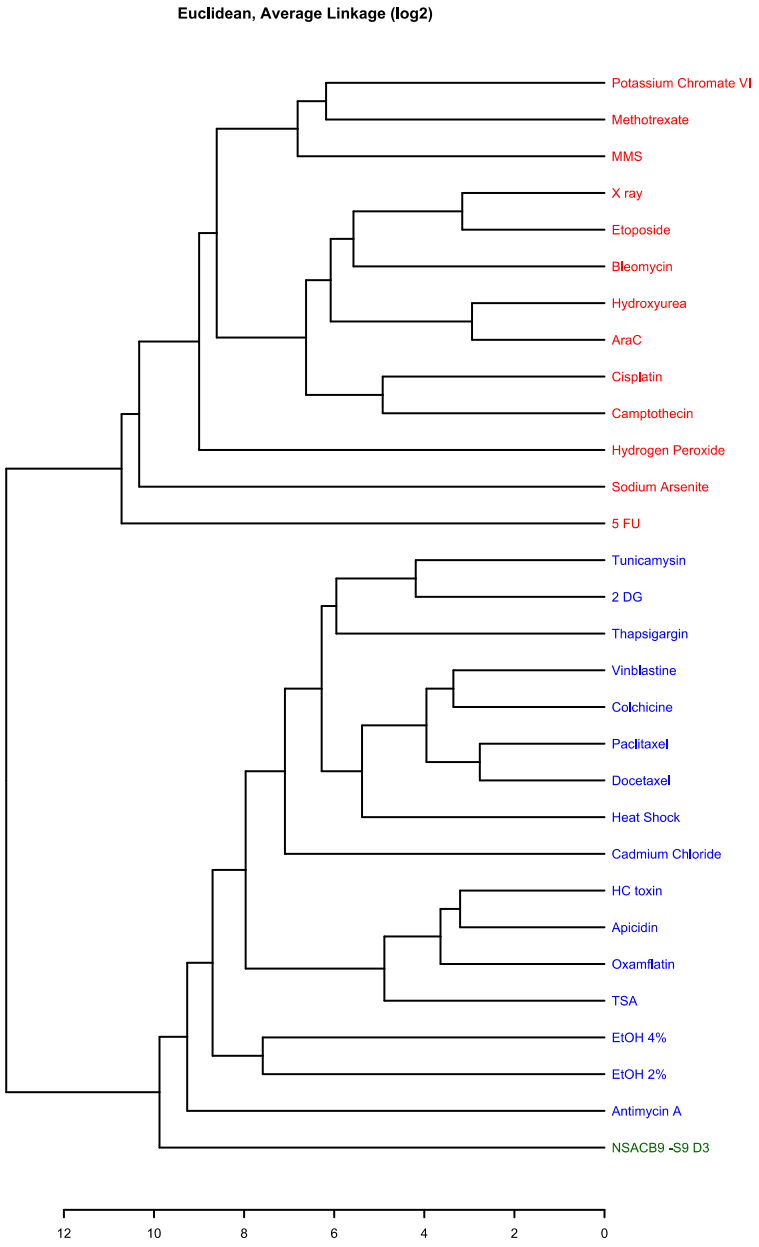
Euclidean, Average Linkage (log2)
Potassium Chromate VI
Methotrexate
MMS
X ray
Etoposide
Bleomycin
Hydroxyurea
AraC
Cisplatin
Camptothecin
Hydrogen Peroxide
Sodium Arsenite
5 FU
Tunicamysin
2 DG
Thapsigargin
Vinblastine
Colchicine
Paclitaxel
Docetaxel
Heat Shock
Cadmium Chloride
HC toxin
Apicidin
Oxamflatin
TSA
EtOH 4%
EtOH 2%
Antimycin A
NSACB9 -S9 D3
12
10
8
6
4
2
0

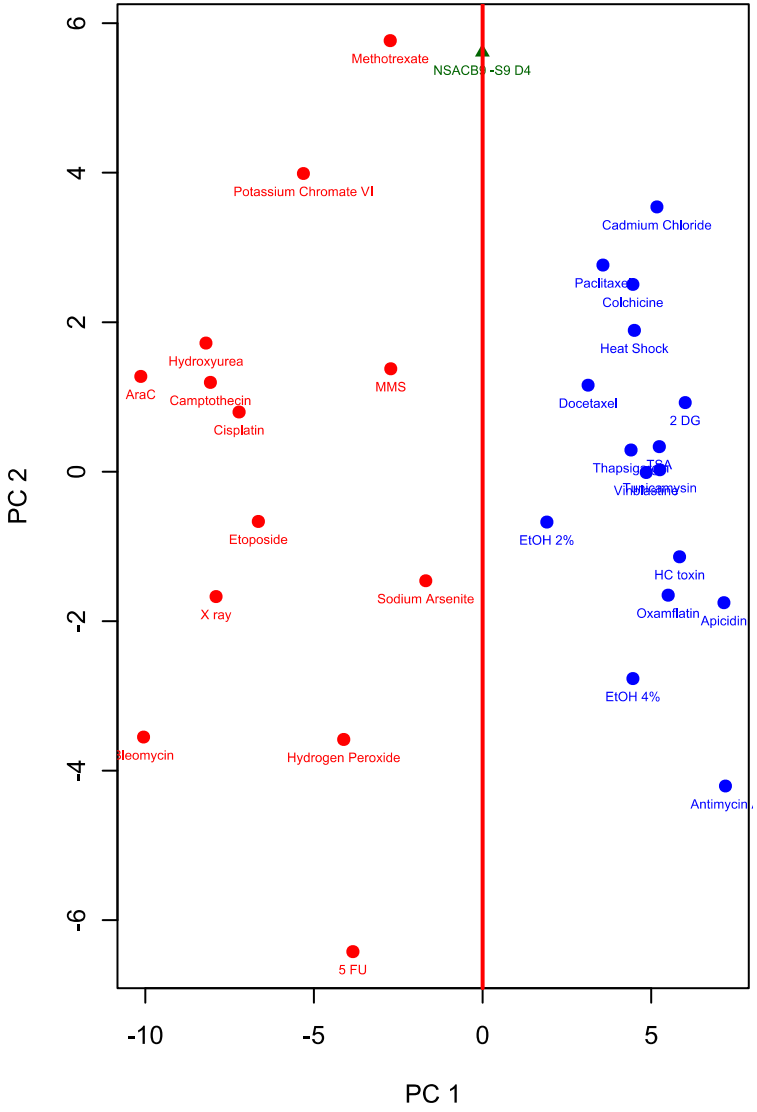
Methotrexate
NSACB9 -S9 D4
Potassium Chromate VI
Cadmium Chloride
Paclitaxel
Colchicine
Heat Shock
Hydroxyurea
AraC
Camptothecin
Cisplatin
MMS
Docetaxel
2 DG
Thapsigargin
TSA
Tunicamycin
Vinblastine
Etoposide
EtOH 2%
HC toxin
Sodium Arsenite
X ray
Oxamflatin
Apicidin
EtOH 4%
Bleomycin
Hydrogen Peroxide
Antimycin
5 FU
PC 2
PC 1
6
4
2
0
-2
-4
-6
-10
-5
0
5

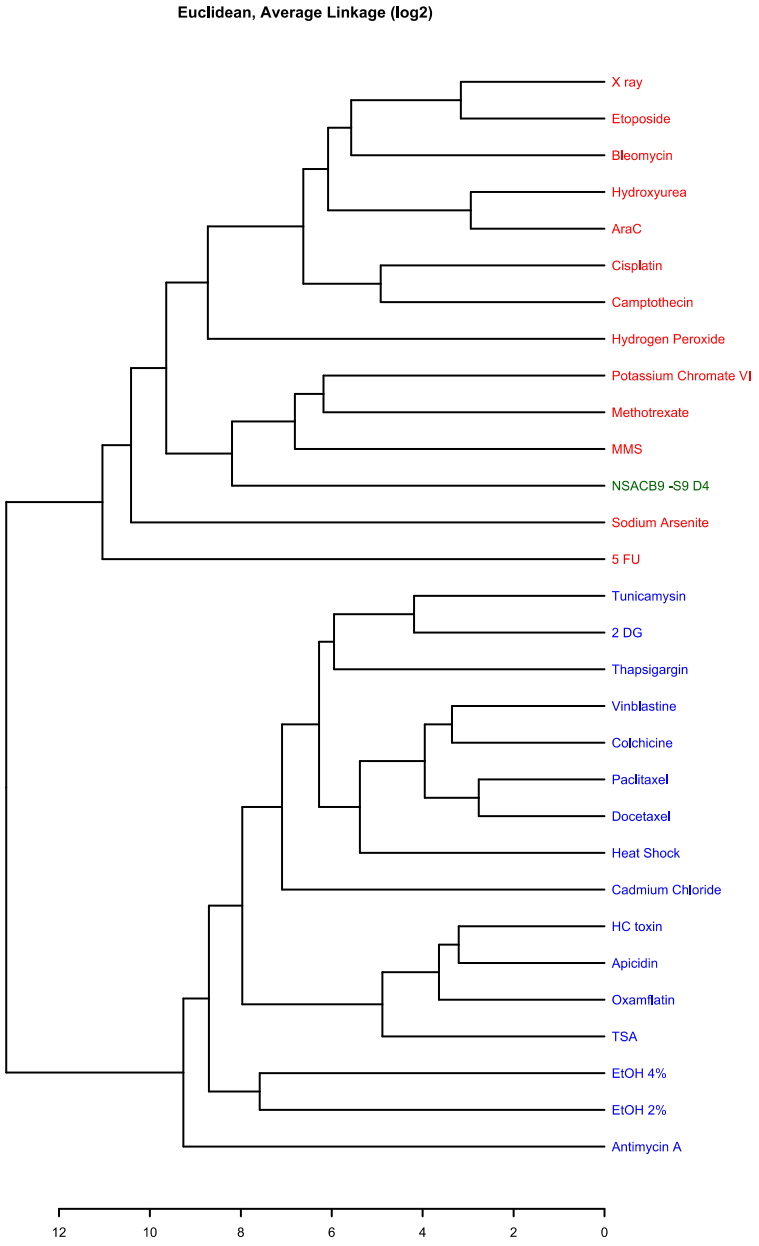
Euclidean, Average Linkage (log2)
X ray
Etoposide
Bleomycin
Hydroxyurea
AraC
Cisplatin
Camptothecin
Hydrogen Peroxide
Potassium Chromate VI
Methotrexate
MMS
NSACB9 -S9 D4
Sodium Arsenite
5 FU
Tunicamycin
2 DG
Thapsigargin
Vinblastine
Colchicine
Paclitaxel
Docetaxel
Heat Shock
Cadmium Chloride
HC toxin
Apicidin
Oxamflatin
TSA
EtOH 4%
EtOH 2%
Antimycin A
12
10
8
6
4
2
0

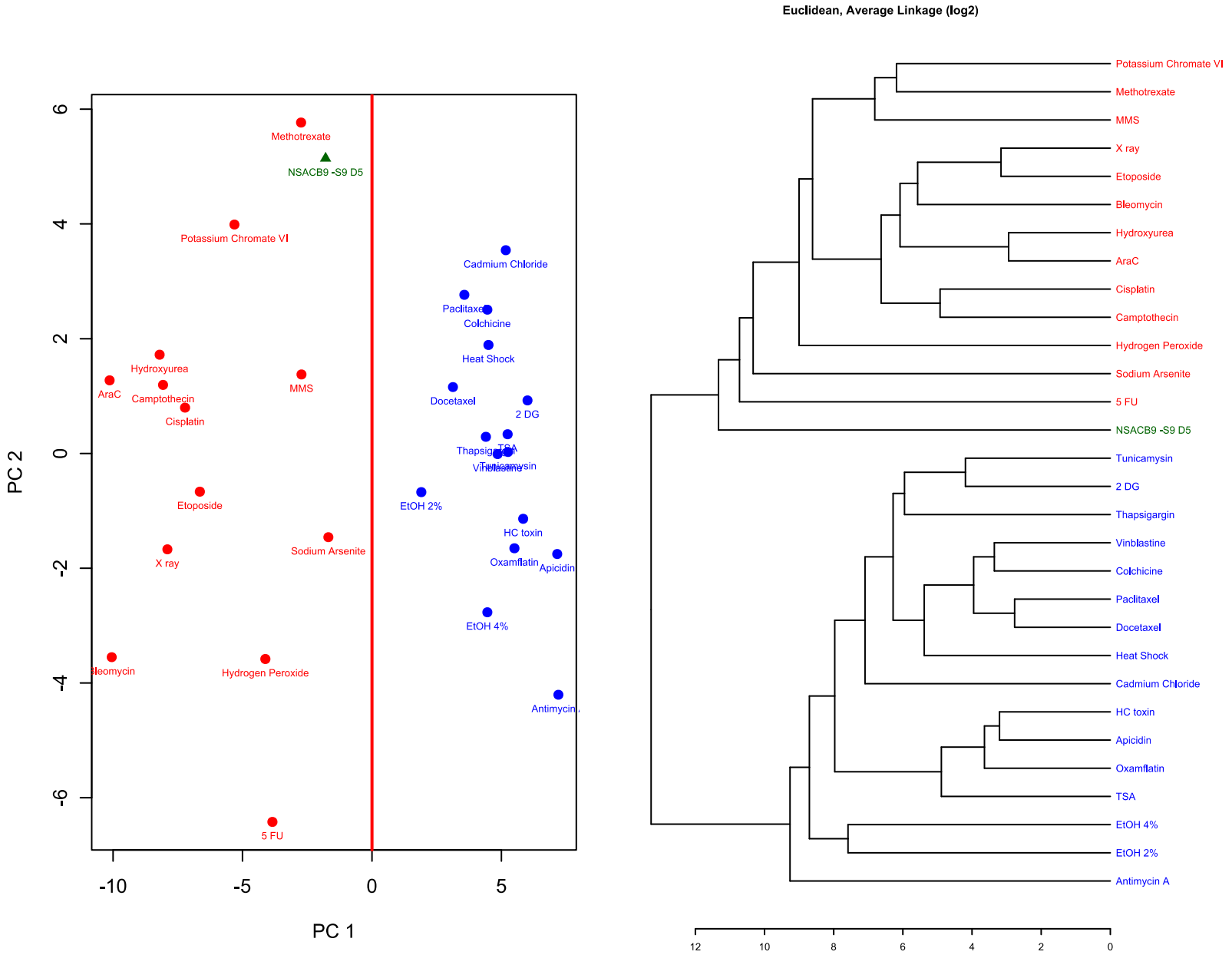

Supplementary Figure III-L: NASCB 9 (-S9) TGx-DDI biomarker classification using the Principal Component Analysis (PCA) (left) and hierarchical clustering (right) statistical analyses. Genotoxic reference chemicals are shown in red text, non-genotoxic reference chemicals are shown in blue text, and the test agent is shown in the green text. The line drawn on the PCA plot and the main branch on the dendogram divides the genotoxic and non-genotoxic agents and was used to classify the test compounds. D1 represents the lowest concentration tested, D5 the highest.

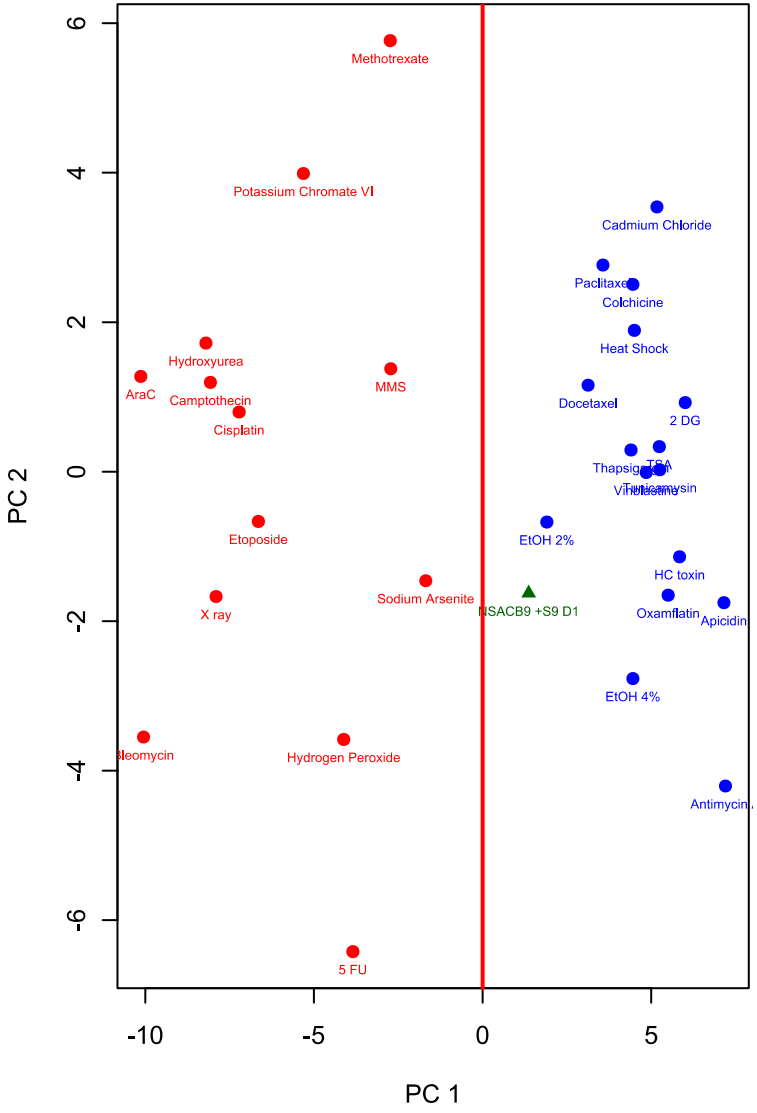
Methotrexate
Potassium Chromate VI
Cadmium Chloride
Paclitaxel
Colchicine
Heat Shock
Hydroxyurea
AraC
Camptothecin
Cisplatin
MMS
Docetaxel
2 DG
Thapsigargin
TSA
Vinblastine
Tunicamysin
Etoposide
EtOH 2%
HC toxin
Sodium Arsenite
X ray
NSACB9 +S9 D1
Oxamflatin
Apicidin
EtOH 4%
Bleomycin
Hydrogen Peroxide
Antimycin
5 FU
PC 2
PC 1
6
4
2
0
-2
-4
-6
-10
-5
0
5

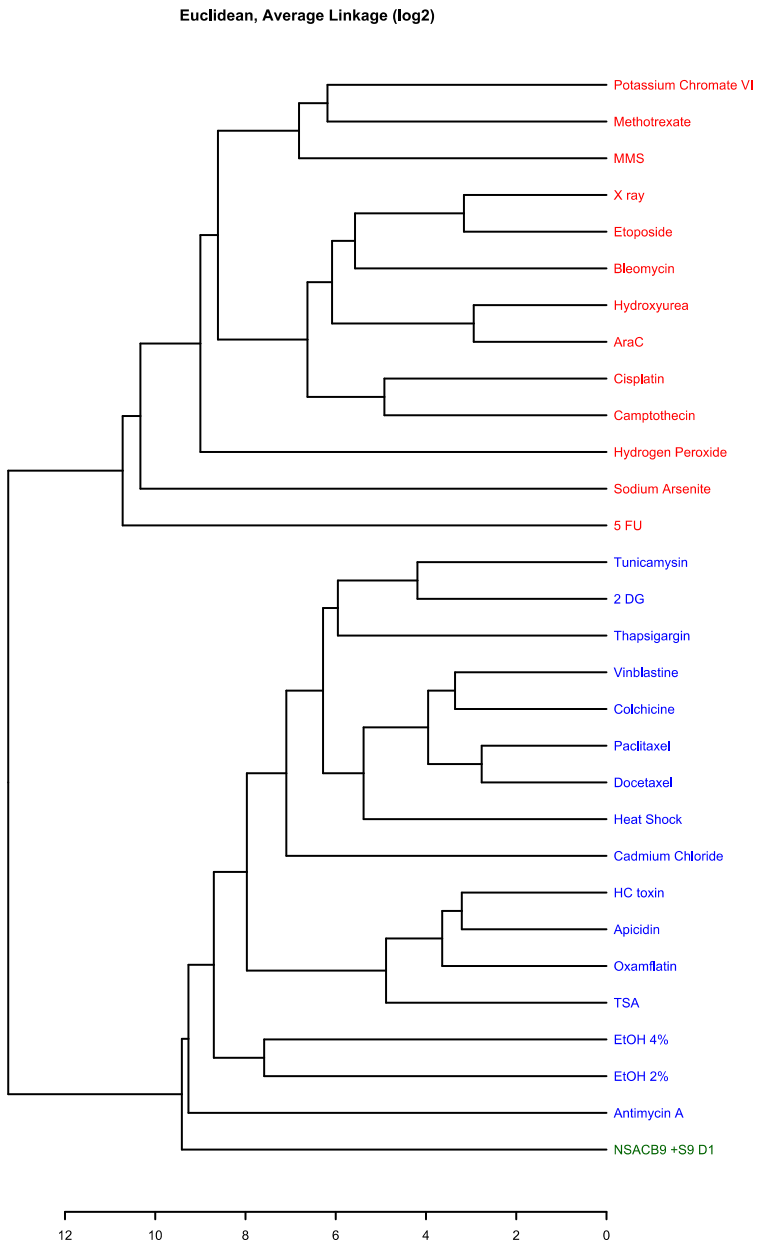
Euclidean, Average Linkage (log2)
Potassium Chromate VI
Methotrexate
MMS
X ray
Etoposide
Bleomycin
Hydroxyurea
AraC
Cisplatin
Camptothecin
Hydrogen Peroxide
Sodium Arsenite
5 FU
Tunicamysin
2 DG
Thapsigargin
Vinblastine
Colchicine
Paclitaxel
Docetaxel
Heat Shock
Cadmium Chloride
HC toxin
Apicidin
Oxamflatin
TSA
EtOH 4%
EtOH 2%
Antimycin A
NSACB9 +S9 D1
12
10
8
6
4
2
0

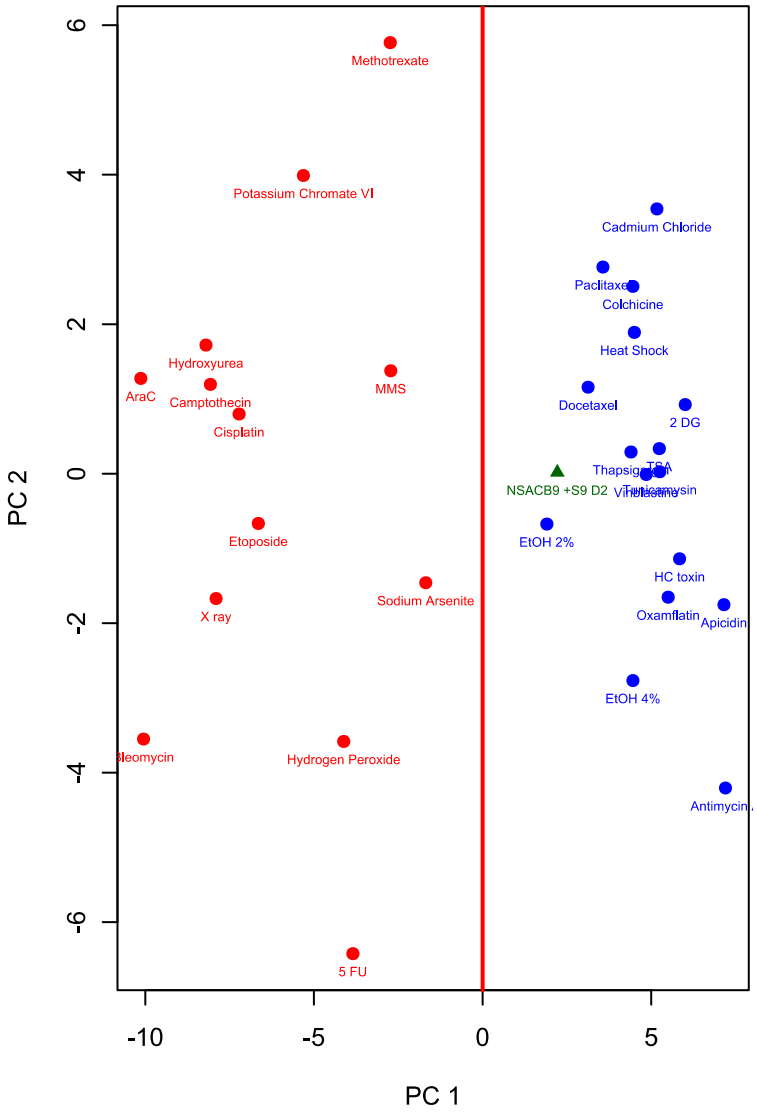
Methotrexate
Potassium Chromate VI
Cadmium Chloride
Paclitaxel
Colchicine
Heat Shock
Hydroxyurea
AraC
Camptothecin
Cisplatin
MMS
Docetaxel
2 DG
Thapsigargin
TSA
NSACB9 +S9 D2
Vinblastine
Tunicamysin
Etoposide
EtOH 2%
HC toxin
Sodium Arsenite
X ray
Oxamflatin
Apicidin
EtOH 4%
Bleomycin
Hydrogen Peroxide
Antimycin
5 FU
PC 2
PC 1
6
4
2
0
-2
-4
-6
-10
-5
0
5

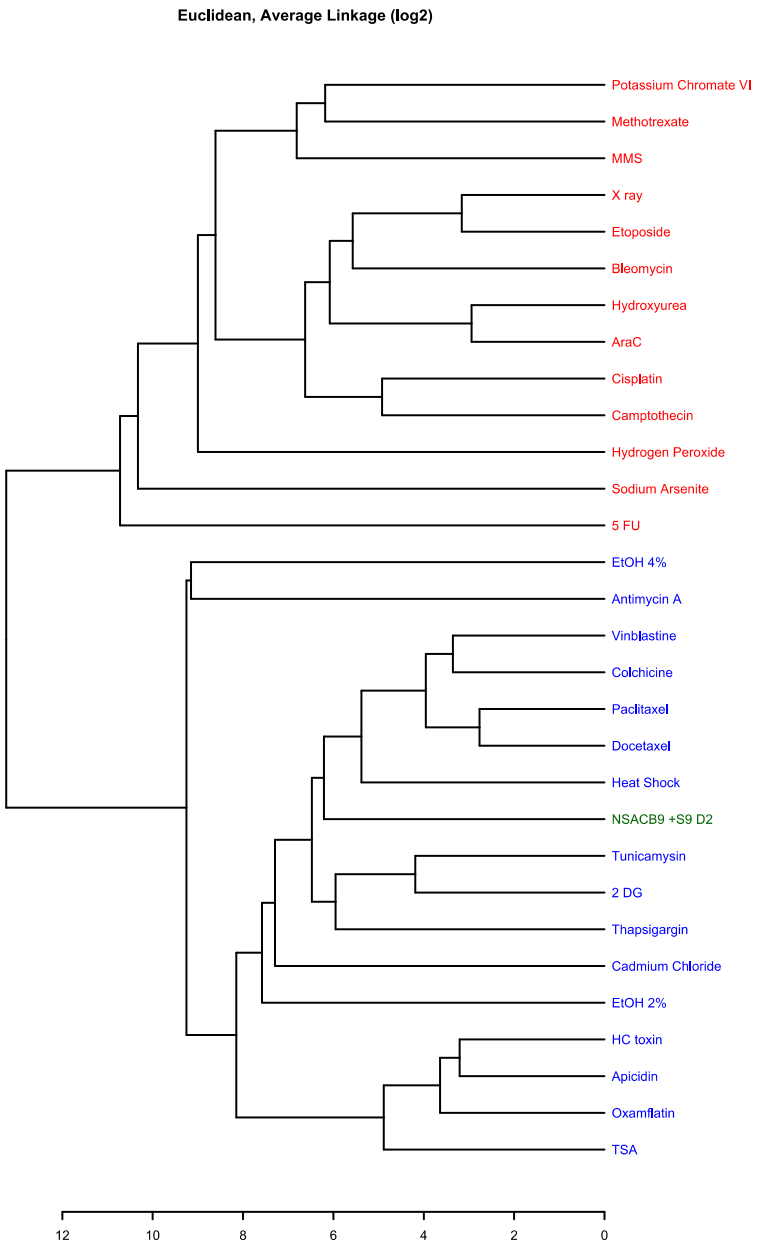
Euclidean, Average Linkage (log2)
Potassium Chromate VI
Methotrexate
MMS
X ray
Etoposide
Bleomycin
Hydroxyurea
AraC
Cisplatin
Camptothecin
Hydrogen Peroxide
Sodium Arsenite
5 FU
EtOH 4%
Antimycin A
Vinblastine
Colchicine
Paclitaxel
Docetaxel
Heat Shock
NSACB9 +S9 D2
Tunicamysin
2 DG
Thapsigargin
Cadmium Chloride
EtOH 2%
HC toxin
Apicidin
Oxamflatin
TSA
12
10
8
6
4
2
0

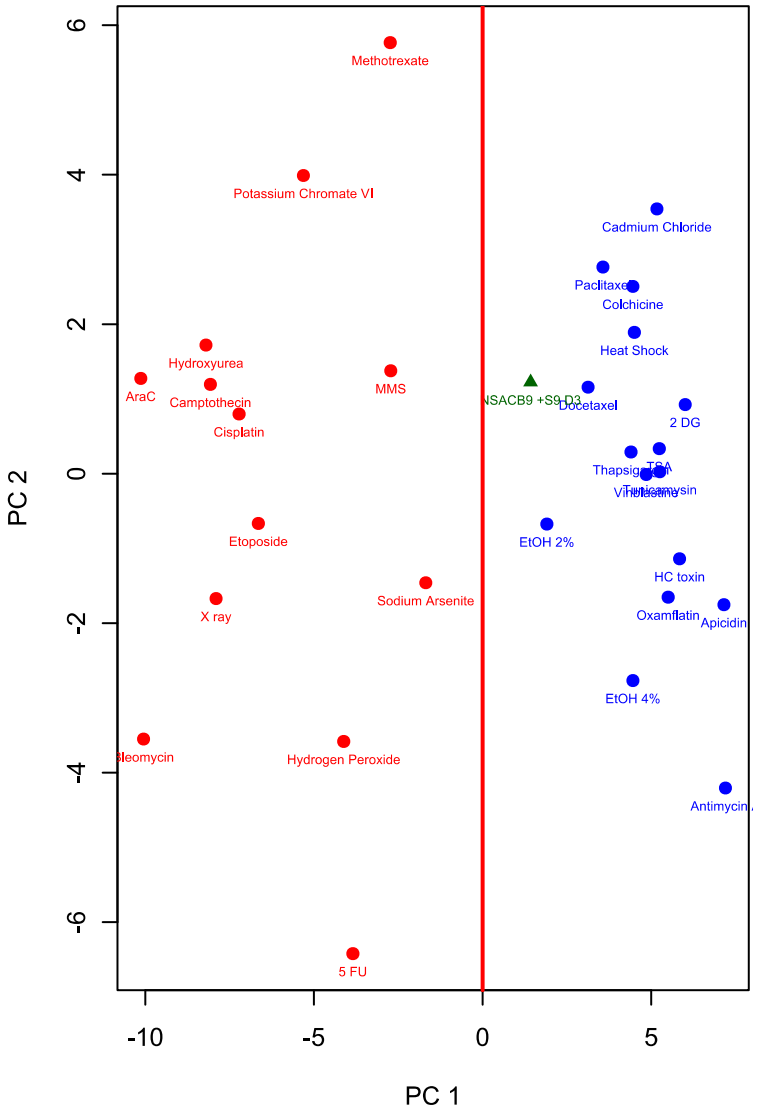
Methotrexate
Potassium Chromate VI
Cadmium Chloride
Paclitaxel
Colchicine
Heat Shock
Hydroxyurea
AraC
Camptothecin
Cisplatin
MMS
NSACB9 +S9 D3
Docetaxel
2 DG
Thapsigargin
TSA
Vinblastine
Tunicamysin
Etoposide
EtOH 2%
HC toxin
Sodium Arsenite
X ray
Oxamflatin
Apicidin
EtOH 4%
Bleomycin
Hydrogen Peroxide
Antimycin
5 FU
PC 2
PC 1
6
4
2
0
-2
-4
-6
-10
-5
0
5

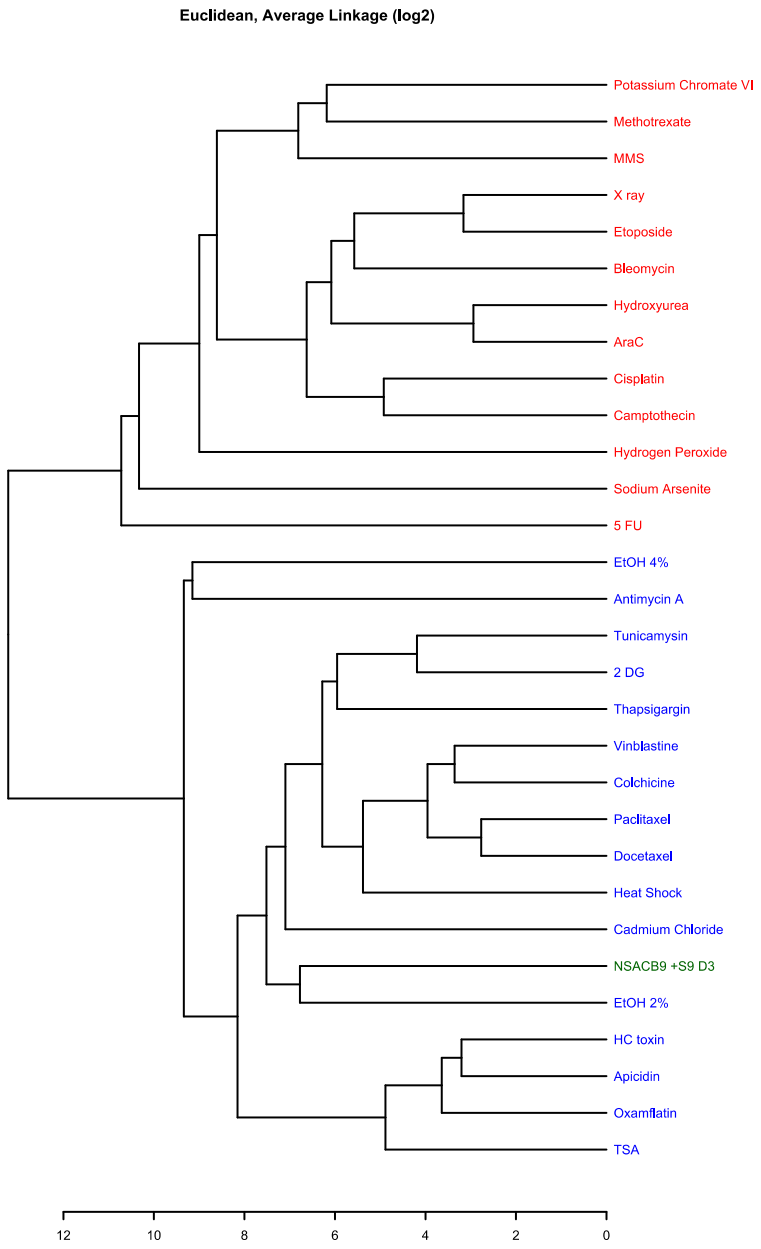
Euclidean, Average Linkage (log2)
Potassium Chromate VI
Methotrexate
MMS
X ray
Etoposide
Bleomycin
Hydroxyurea
AraC
Cisplatin
Camptothecin
Hydrogen Peroxide
Sodium Arsenite
5 FU
EtOH 4%
Antimycin A
Tunicamysin
2 DG
Thapsigargin
Vinblastine
Colchicine
Paclitaxel
Docetaxel
Heat Shock
Cadmium Chloride
NSACB9 +S9 D3
EtOH 2%
HC toxin
Apicidin
Oxamflatin
TSA
12
10
8
6
4
2
0

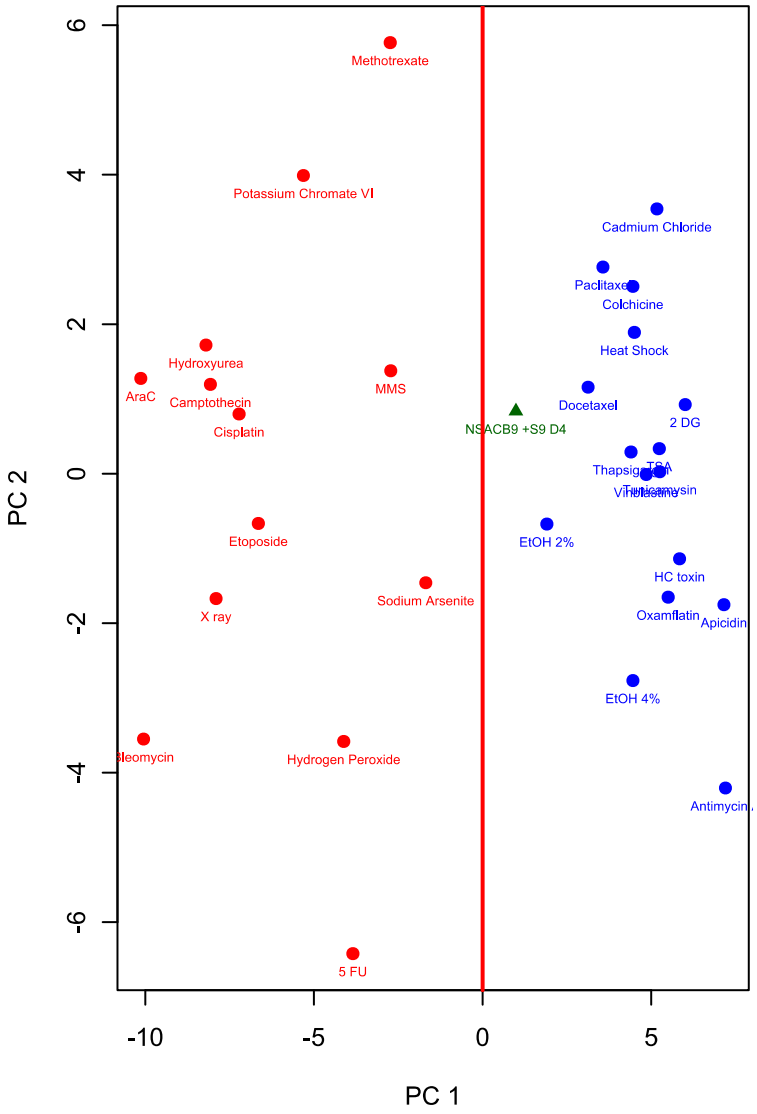
Methotrexate
Potassium Chromate VI
Cadmium Chloride
Paclitaxel
Colchicine
Heat Shock
Hydroxyurea
AraC
Camptothecin
Cisplatin
MMS
Docetaxel
2 DG
NSACB9 +S9 D4
Thapsigargin
TSA
Vinblastine
Tunicamysin
Etoposide
EtOH 2%
HC toxin
Sodium Arsenite
X ray
Oxamflatin
Apicidin
EtOH 4%
Bleomycin
Hydrogen Peroxide
Antimycin
5 FU
PC 2
PC 1
6
4
2
0
-2
-4
-6
-10
-5
0
5

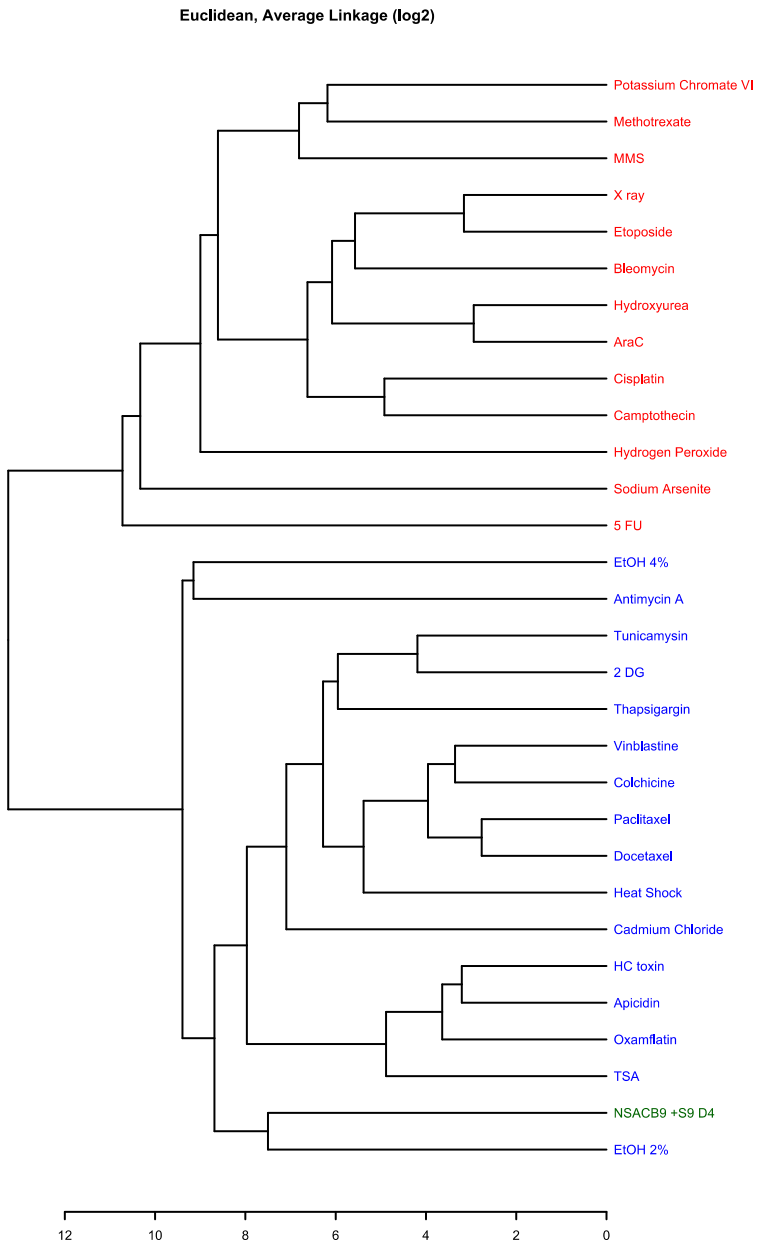
Euclidean, Average Linkage (log2)
Potassium Chromate VI
Methotrexate
MMS
X ray
Etoposide
Bleomycin
Hydroxyurea
AraC
Cisplatin
Camptothecin
Hydrogen Peroxide
Sodium Arsenite
5 FU
EtOH 4%
Antimycin A
Tunicamysin
2 DG
Thapsigargin
Vinblastine
Colchicine
Paclitaxel
Docetaxel
Heat Shock
Cadmium Chloride
HC toxin
Apicidin
Oxamflatin
TSA
NSACB9 +S9 D4
EtOH 2%
12
10
8
6
4
2
0

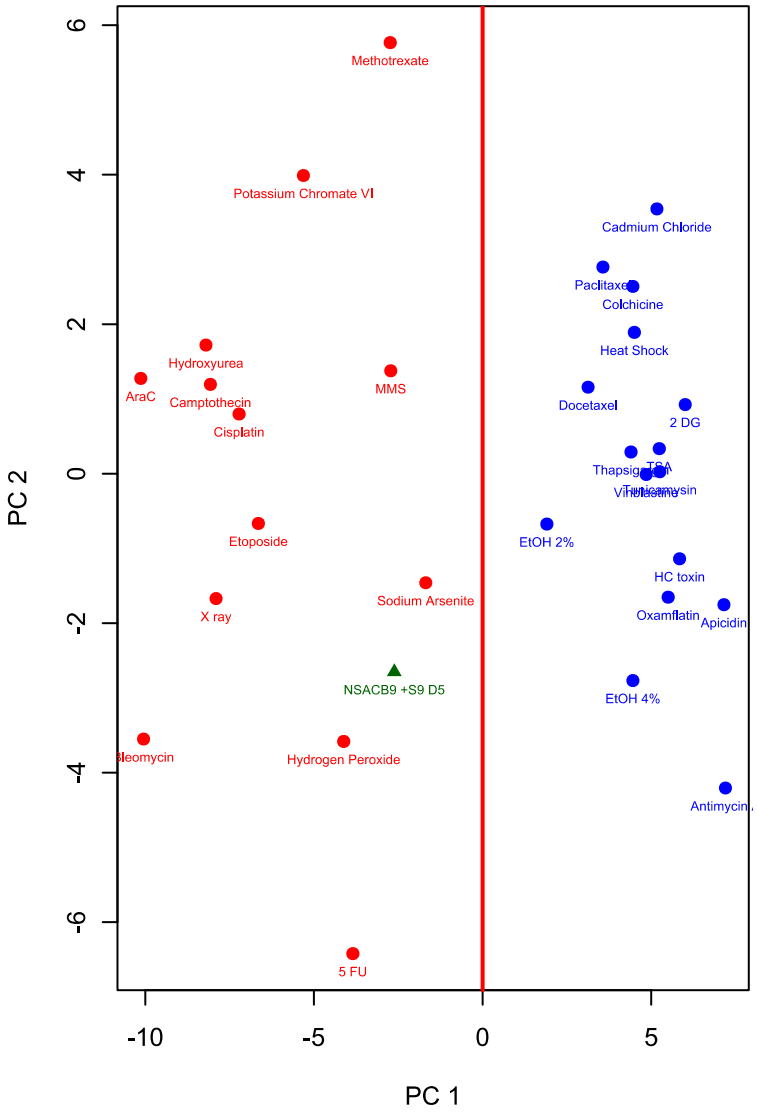
Methotrexate
Potassium Chromate VI
Cadmium Chloride
Paclitaxel
Colchicine
Heat Shock
Hydroxyurea
AraC
Camptothecin
Cisplatin
MMS
Docetaxel
2 DG
Thapsigargin
TSA
Vinblastine
Tunicamycin
Etoposide
EtOH 2%
HC toxin
Sodium Arsenite
X ray
Oxamflatin
Apicidin
NSACB9 +S9 D5
EtOH 4%
Bleomycin
Hydrogen Peroxide
Antimycin
5 FU
PC 2
PC 1
6
4
2
0
-2
-4
-6
-10
-5
0
5

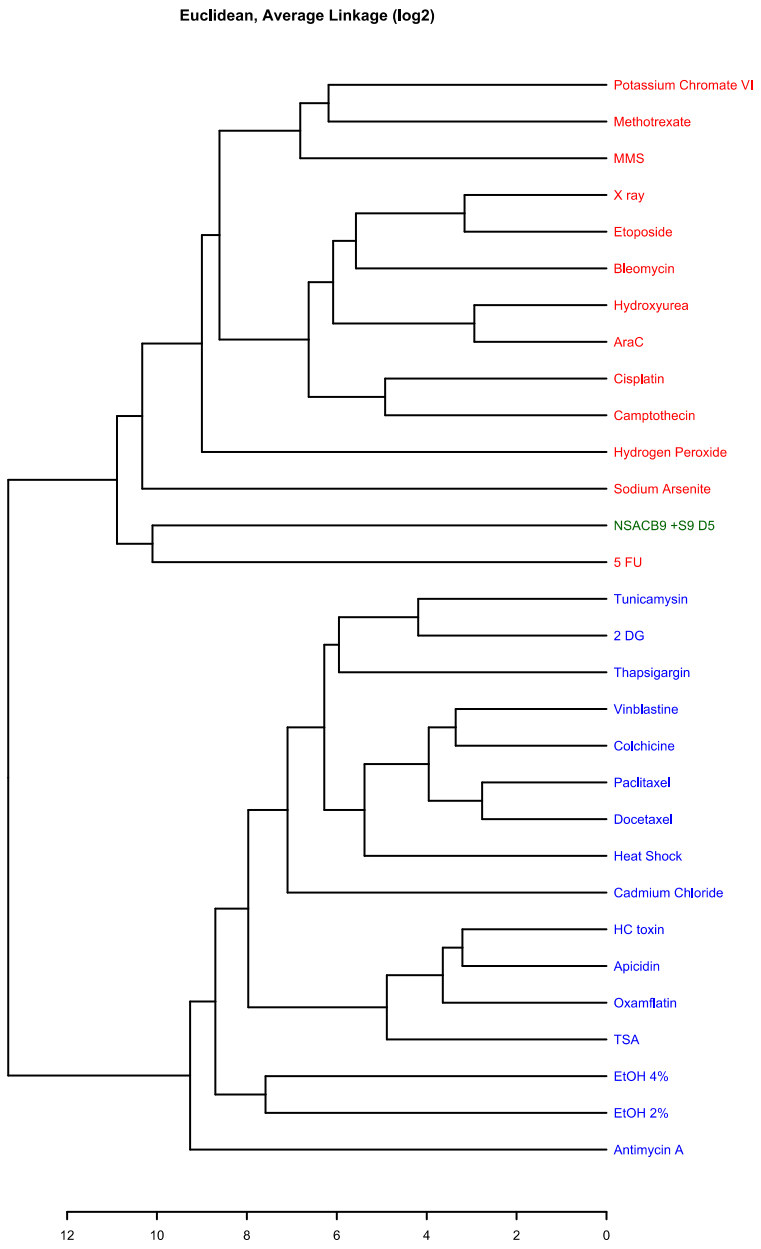
Euclidean, Average Linkage (log2)
Potassium Chromate VI
Methotrexate
MMS
X ray
Etoposide
Bleomycin
Hydroxyurea
AraC
Cisplatin
Camptothecin
Hydrogen Peroxide
Sodium Arsenite
NSACB9 +S9 D5
5 FU
Tunicamysin
2 DG
Thapsigargin
Vinblastine
Colchicine
Paclitaxel
Docetaxel
Heat Shock
Cadmium Chloride
HC toxin
Apicidin
Oxamflatin
TSA
EtOH 4%
EtOH 2%
Antimycin A
12
10
8
6
4
2
0

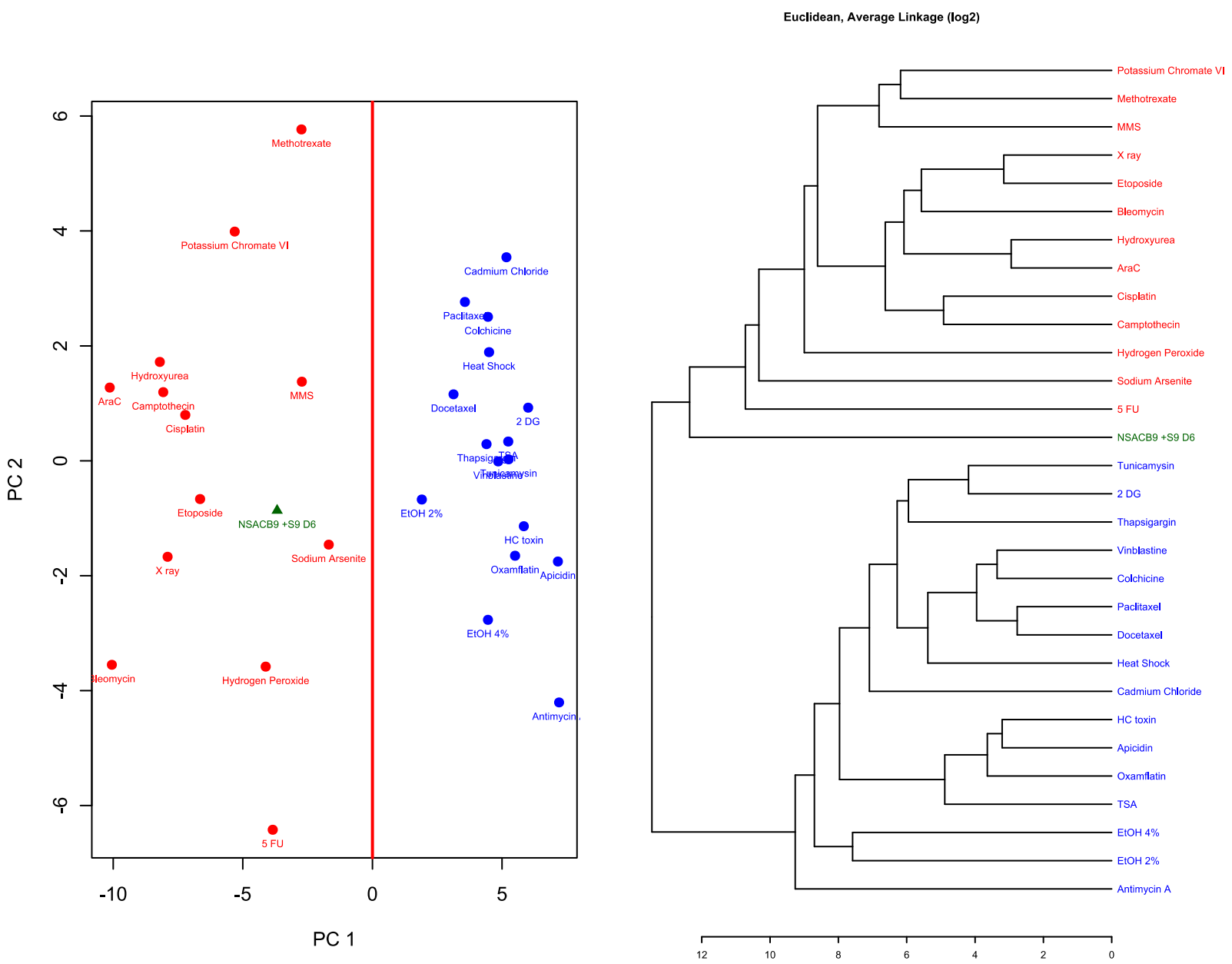

Supplementary Figure III-M: NASCB 9 (+S9) TGx-DDI biomarker classification using the Principal Component Analysis (PCA) (left) and hierarchical clustering (right) statistical analyses. Genotoxic reference chemicals are shown in red text, non-genotoxic reference chemicals are shown in blue text, and the test agent is shown in the green text. The line drawn on the PCA plot and the main branch on the dendogram divides the genotoxic and non-genotoxic agents and was used to classify the test compounds. D1 represents the lowest concentration tested, D6 the highest.

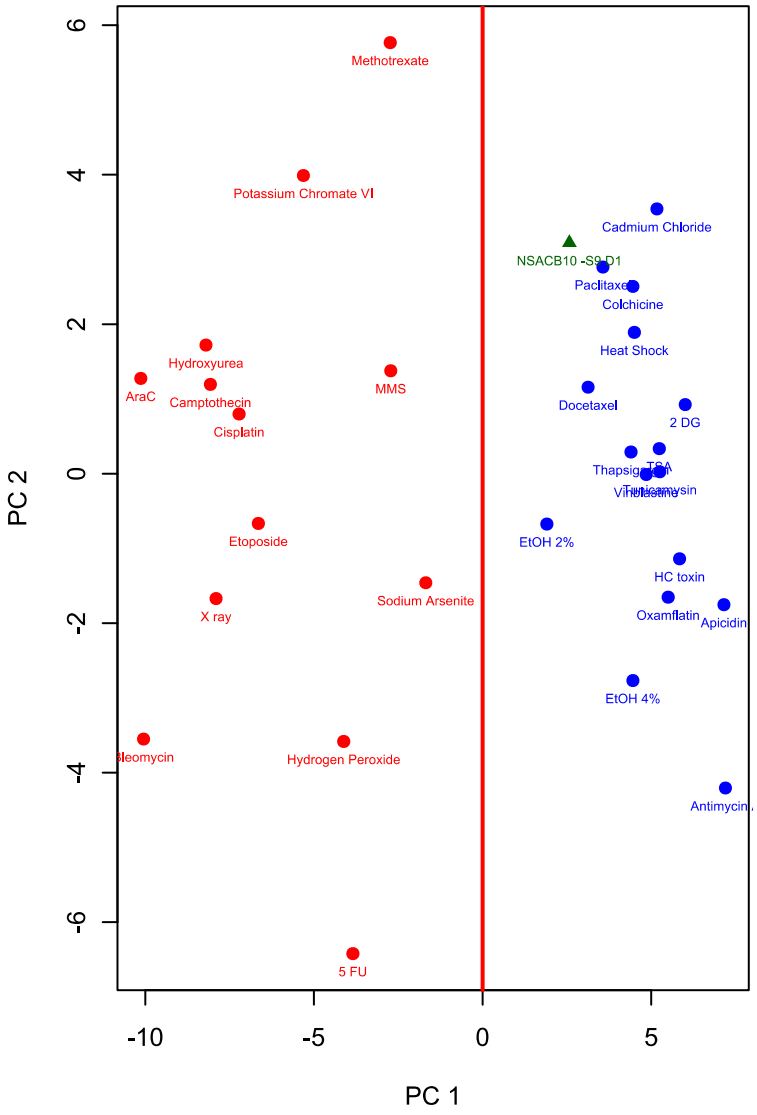
Methotrexate
Potassium Chromate VI
Cadmium Chloride
NSACB10 -S9 D1
Paclitaxel
Colchicine
Heat Shock
Hydroxyurea
AraC
Camptothecin
MMS
Docetaxel
2 DG
Cisplatin
Thapsigargin
TSA
Vinblastine
Tunicamysin
Etoposide
EtOH 2%
HC toxin
Sodium Arsenite
X ray
Oxamflatin
Apicidin
EtOH 4%
Bleomycin
Hydrogen Peroxide
Antimycin
5 FU
PC 2
PC 1
6
4
2
0
-2
-4
-6
-10
-5
0
5

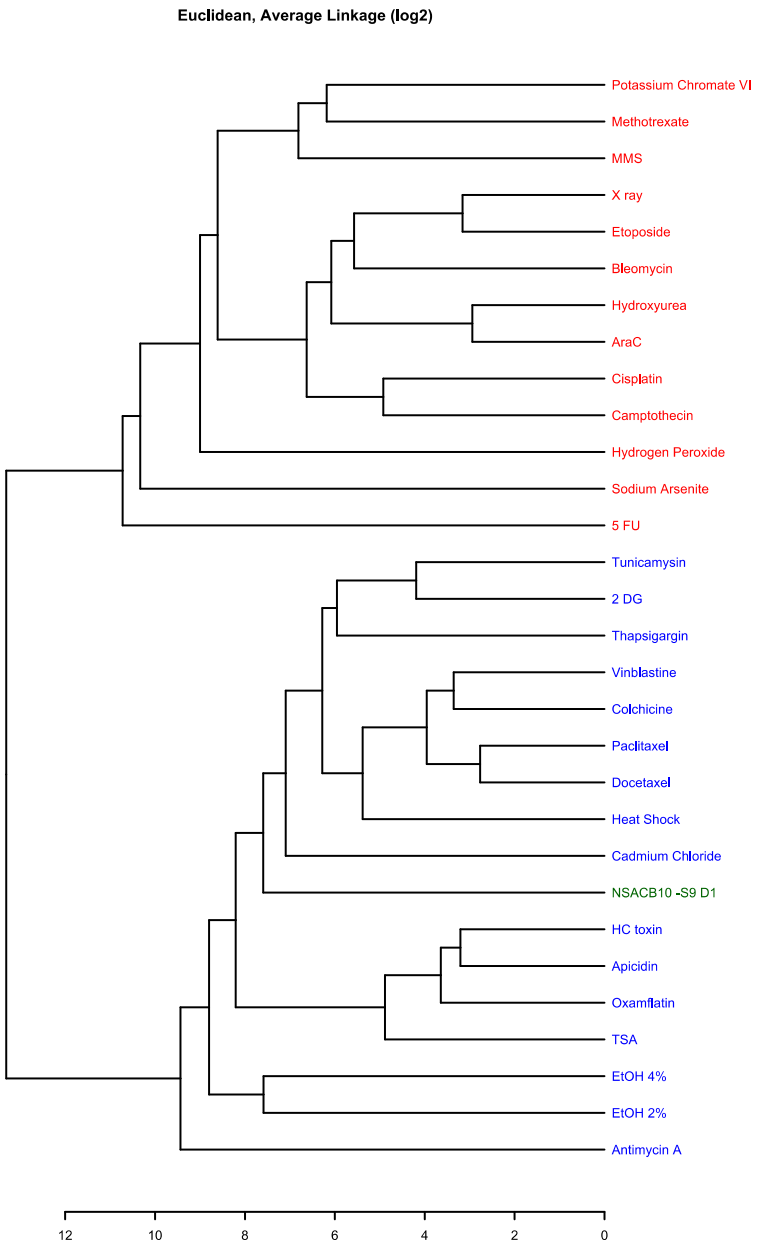
Euclidean, Average Linkage (log2)
Potassium Chromate VI
Methotrexate
MMS
X ray
Etoposide
Bleomycin
Hydroxyurea
AraC
Cisplatin
Camptothecin
Hydrogen Peroxide
Sodium Arsenite
5 FU
Tunicamysin
2 DG
Thapsigargin
Vinblastine
Colchicine
Paclitaxel
Docetaxel
Heat Shock
Cadmium Chloride
NSACB10 -S9 D1
HC toxin
Apicidin
Oxamflatin
TSA
EtOH 4%
EtOH 2%
Antimycin A
12
10
8
6
4
2
0

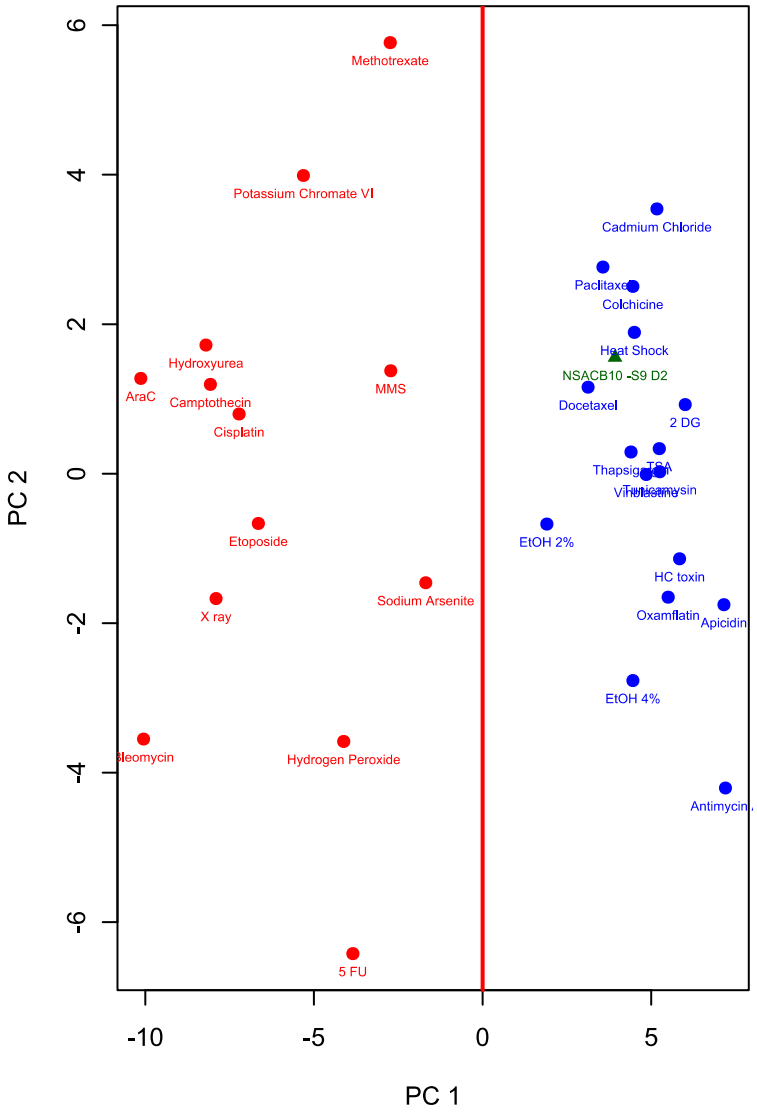
Methotrexate
Potassium Chromate VI
Cadmium Chloride
Paclitaxel
Colchicine
Heat Shock
Hydroxyurea
NSACB10 -S9 D2
AraC
Camptothecin
MMS
Docetaxel
2 DG
Cisplatin
Thapsigargin
TSA
Vinblastine
Tunicamysin
Etoposide
EtOH 2%
HC toxin
Sodium Arsenite
X ray
Oxamflatin
Apicidin
EtOH 4%
Bleomycin
Hydrogen Peroxide
Antimycin
5 FU
PC 2
PC 1
6
4
2
0
-2
-4
-6
-10
-5
0
5

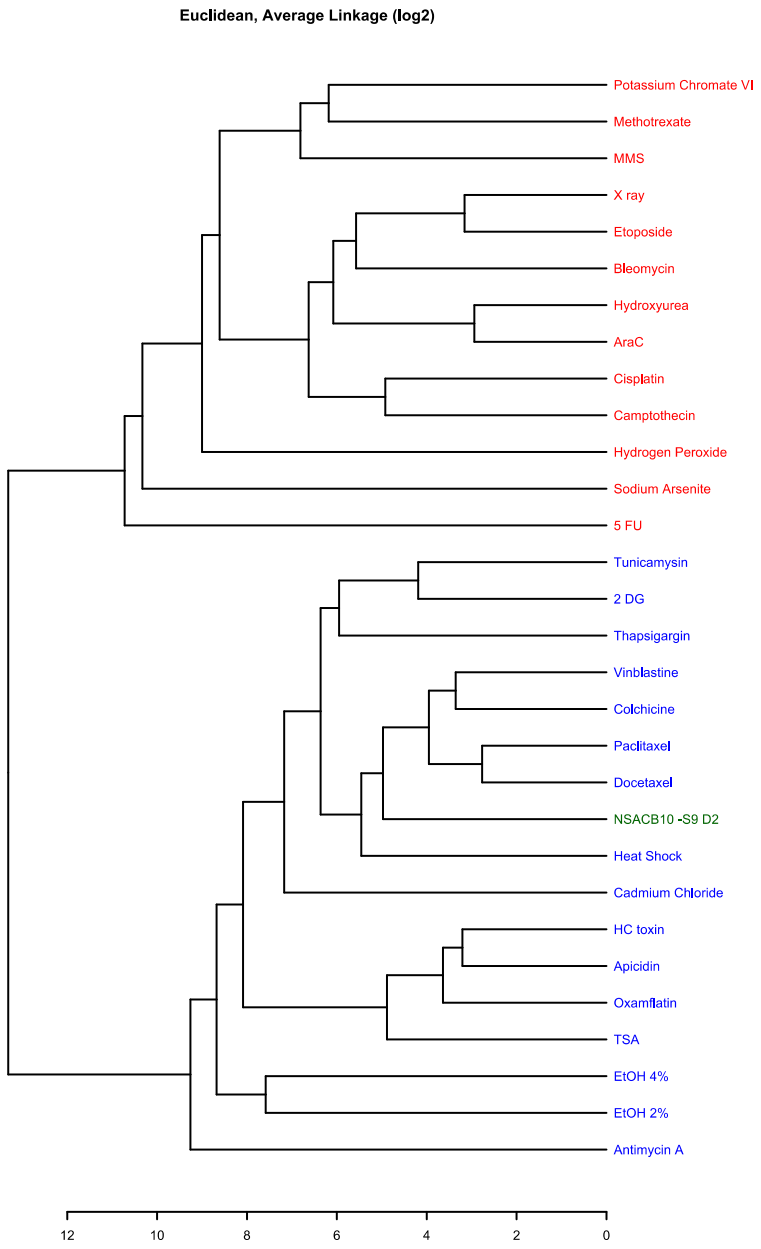
Euclidean, Average Linkage (log2)
Potassium Chromate VI
Methotrexate
MMS
X ray
Etoposide
Bleomycin
Hydroxyurea
AraC
Cisplatin
Camptothecin
Hydrogen Peroxide
Sodium Arsenite
5 FU
Tunicamysin
2 DG
Thapsigargin
Vinblastine
Colchicine
Paclitaxel
Docetaxel
NSACB10 -S9 D2
Heat Shock
Cadmium Chloride
HC toxin
Apicidin
Oxamflatin
TSA
EtOH 4%
EtOH 2%
Antimycin A
12
10
8
6
4
2
0

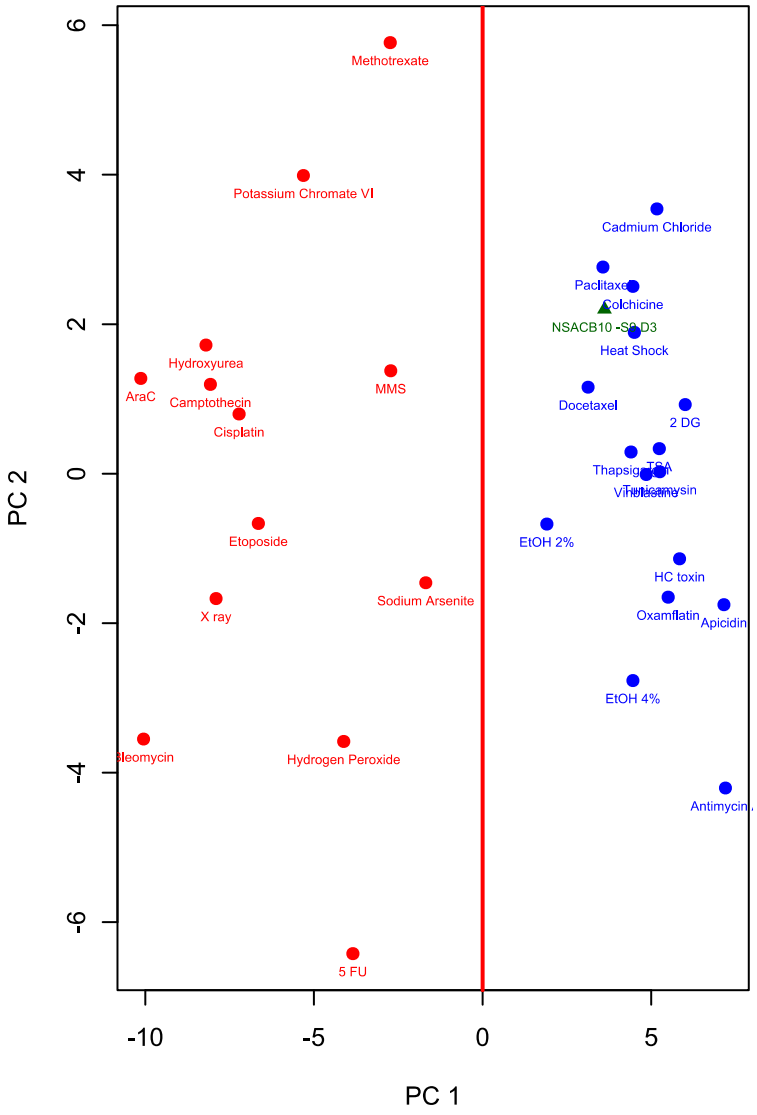
Methotrexate
Potassium Chromate VI
Cadmium Chloride
Paclitaxel
Colchicine
NSACB10 -S9 D3
Heat Shock
Hydroxyurea
AraC
Camptothecin
MMS
Docetaxel
2 DG
Cisplatin
Thapsigargin
TSA
Tunicamysin
Vinblastine
Etoposide
EtOH 2%
HC toxin
Sodium Arsenite
X ray
Oxamflatin
Apicidin
EtOH 4%
Bleomycin
Hydrogen Peroxide
Antimycin
5 FU
PC 2
PC 1
6
4
2
0
-2
-4
-6
-10
-5
0
5

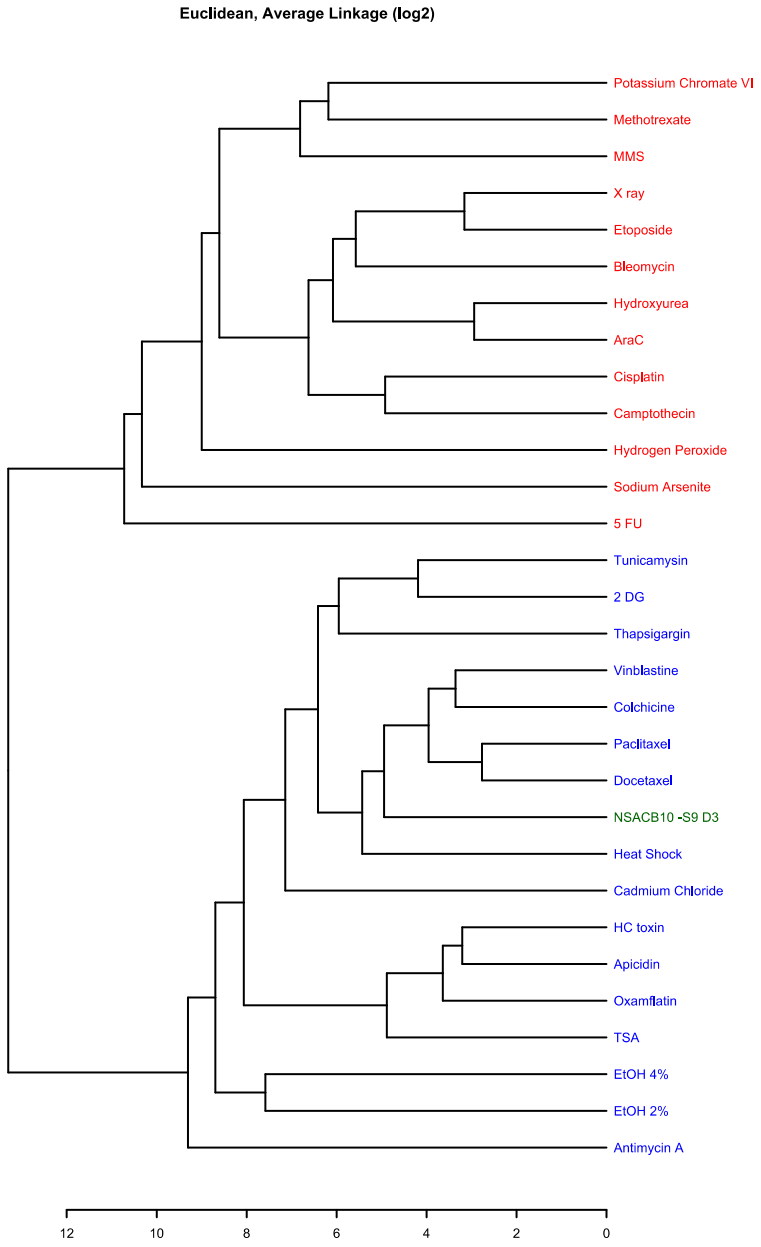
Euclidean, Average Linkage (log2)
Potassium Chromate VI
Methotrexate
MMS
X ray
Etoposide
Bleomycin
Hydroxyurea
AraC
Cisplatin
Camptothecin
Hydrogen Peroxide
Sodium Arsenite
5 FU
Tunicamysin
2 DG
Thapsigargin
Vinblastine
Colchicine
Paclitaxel
Docetaxel
NSACB10 -S9 D3
Heat Shock
Cadmium Chloride
HC toxin
Apicidin
Oxamflatin
TSA
EtOH 4%
EtOH 2%
Antimycin A
12
10
8
6
4
2
0

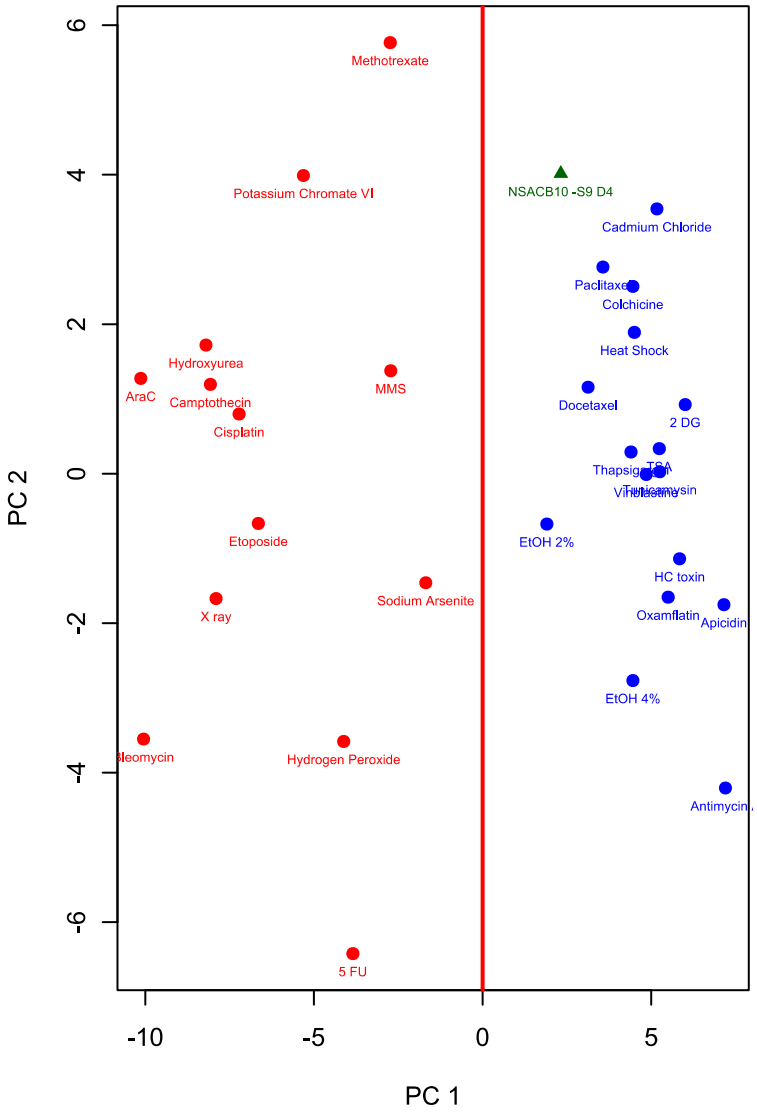
Methotrexate
Potassium Chromate VI
NSACB10 -S9 D4
Cadmium Chloride
Paclitaxel
Colchicine
Heat Shock
Hydroxyurea
AraC
Camptothecin
Cisplatin
MMS
Docetaxel
2 DG
Thapsigargin
TSA
Vinblastine
Tunicamysin
Etoposide
EtOH 2%
HC toxin
Sodium Arsenite
X ray
Oxamflatin
Apicidin
EtOH 4%
Bleomycin
Hydrogen Peroxide
Antimycin
5 FU
PC 2
PC 1
6
4
2
0
-2
-4
-6
-10
-5
0
5

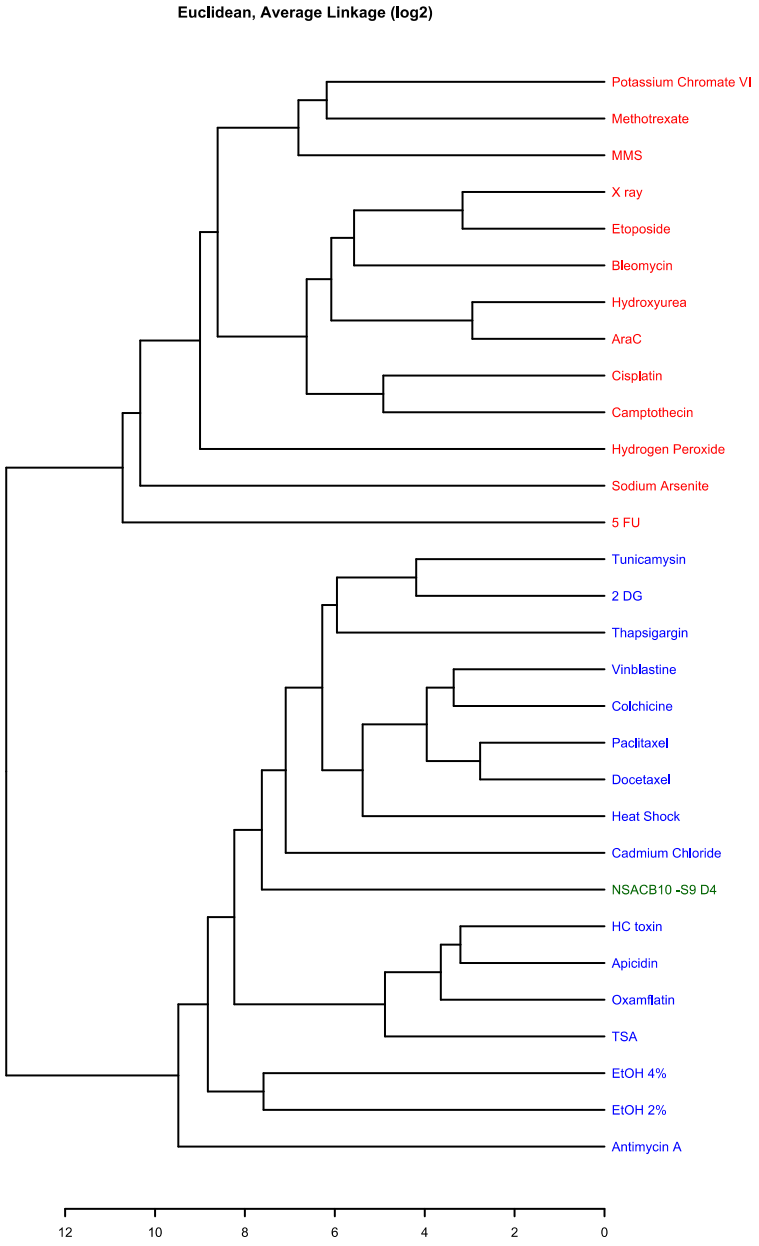
Euclidean, Average Linkage (log2)
Potassium Chromate VI
Methotrexate
MMS
X ray
Etoposide
Bleomycin
Hydroxyurea
AraC
Cisplatin
Camptothecin
Hydrogen Peroxide
Sodium Arsenite
5 FU
Tunicamysin
2 DG
Thapsigargin
Vinblastine
Colchicine
Paclitaxel
Docetaxel
Heat Shock
Cadmium Chloride
NSACB10 -S9 D4
HC toxin
Apicidin
Oxamflatin
TSA
EtOH 4%
EtOH 2%
Antimycin A
12
10
8
6
4
2
0

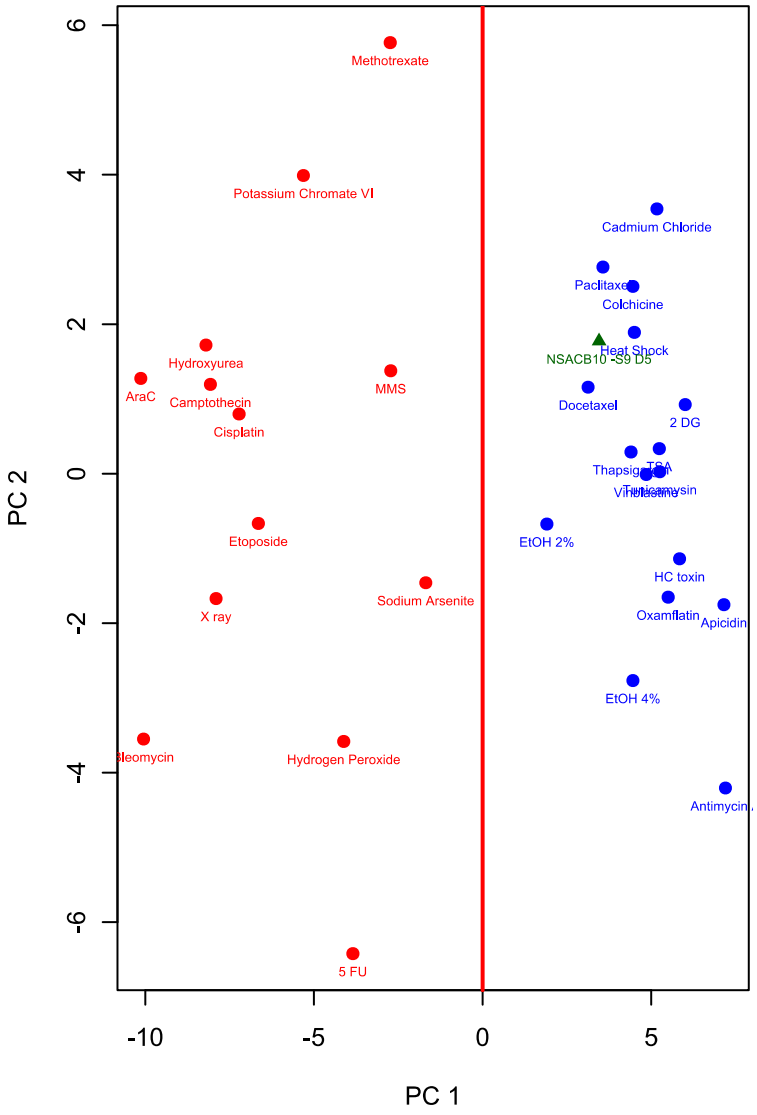
Methotrexate
Potassium Chromate VI
Cadmium Chloride
Paclitaxel
Colchicine
Heat Shock
NSACB10 -S9 D5
Hydroxyurea
AraC
Camptothecin
Cisplatin
MMS
Docetaxel
2 DG
Thapsigargin
TSA
Vinblastine
Tunicamysin
Etoposide
EtOH 2%
HC toxin
Sodium Arsenite
X ray
Oxamflatin
Apicidin
EtOH 4%
Bleomycin
Hydrogen Peroxide
Antimycin
5 FU
PC 2
PC 1
6
4
2
0
-2
-4
-6
-10
-5
0
5

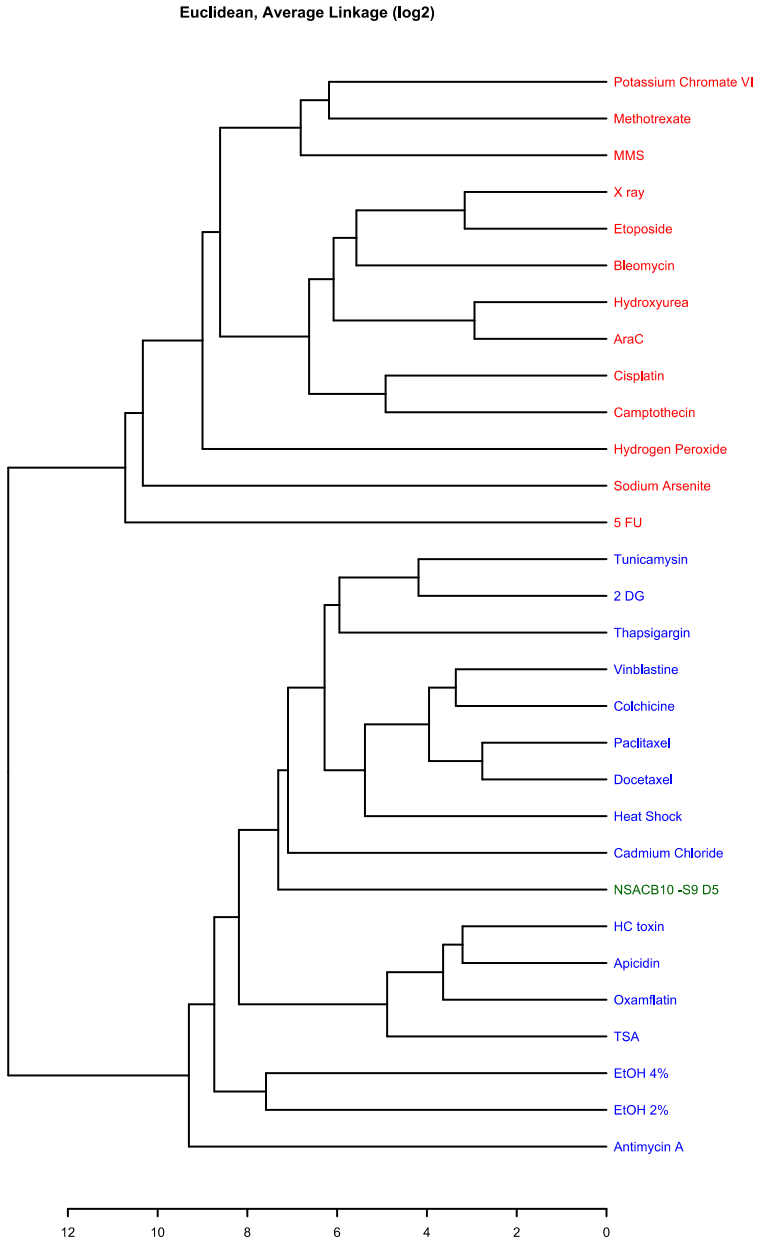
Euclidean, Average Linkage (log2)
Potassium Chromate VI
Methotrexate
MMS
X ray
Etoposide
Bleomycin
Hydroxyurea
AraC
Cisplatin
Camptothecin
Hydrogen Peroxide
Sodium Arsenite
5 FU
Tunicamysin
2 DG
Thapsigargin
Vinblastine
Colchicine
Paclitaxel
Docetaxel
Heat Shock
Cadmium Chloride
NSACB10 -S9 D5
HC toxin
Apicidin
Oxamflatin
TSA
EtOH 4%
EtOH 2%
Antimycin A
12
10
8
6
4
2
0

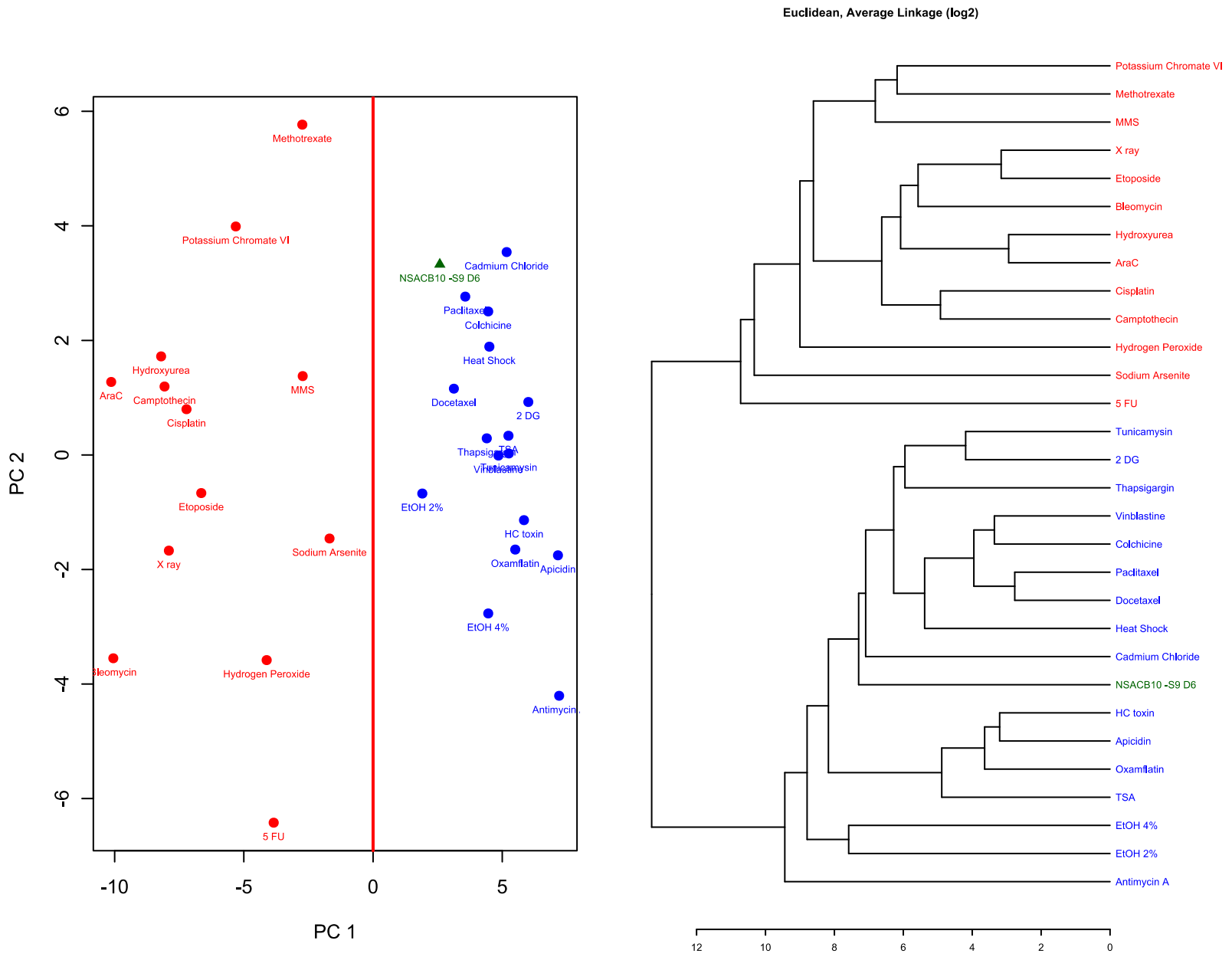

Supplementary Figure III-N: NASCB 10 (-S9) TGx-DDI biomarker classification using the Principal Component Analysis (PCA) (left) and hierarchical clustering (right) statistical analyses. Genotoxic reference chemicals are shown in red text, non-genotoxic reference chemicals are shown in blue text, and the test agent is shown in the green text. The line drawn on the PCA plot and the main branch on the dendogram divides the genotoxic and non-genotoxic agents and was used to classify the test compounds. D1 represents the lowest concentration tested, D6 the highest.

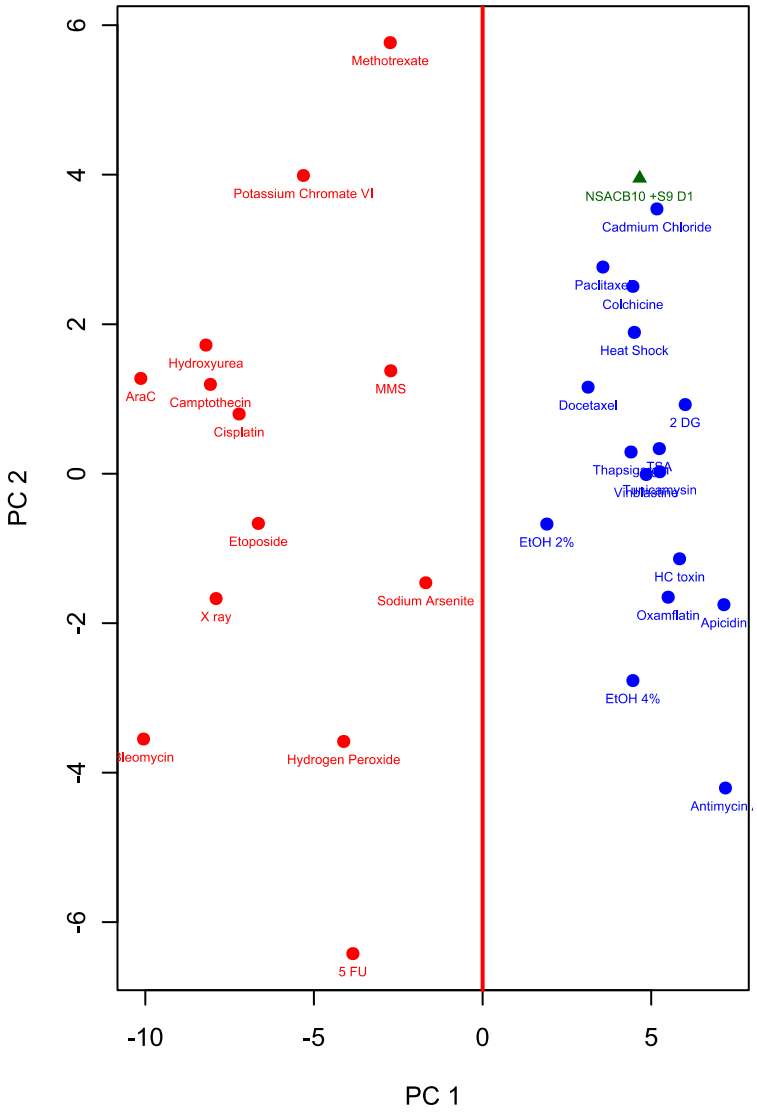
Methotrexate
Potassium Chromate VI
Hydroxyurea
AraC
Camptothecin
Cisplatin
MMS
Etoposide
X ray
Sodium Arsenite
Bleomycin
Hydrogen Peroxide
5 FU
NSACB10 +S9 D1
Cadmium Chloride
Paclitaxel
Colchicine
Heat Shock
Docetaxel
2 DG
Thapsigargin
TSA
Tunicamysin
Vinblastine
EtOH 2%
HC toxin
Oxamflatin
Apicidin
EtOH 4%
Antimycin
PC 2
PC 1
6
4
2
0
-2
-4
-6
-10
-5
0
5

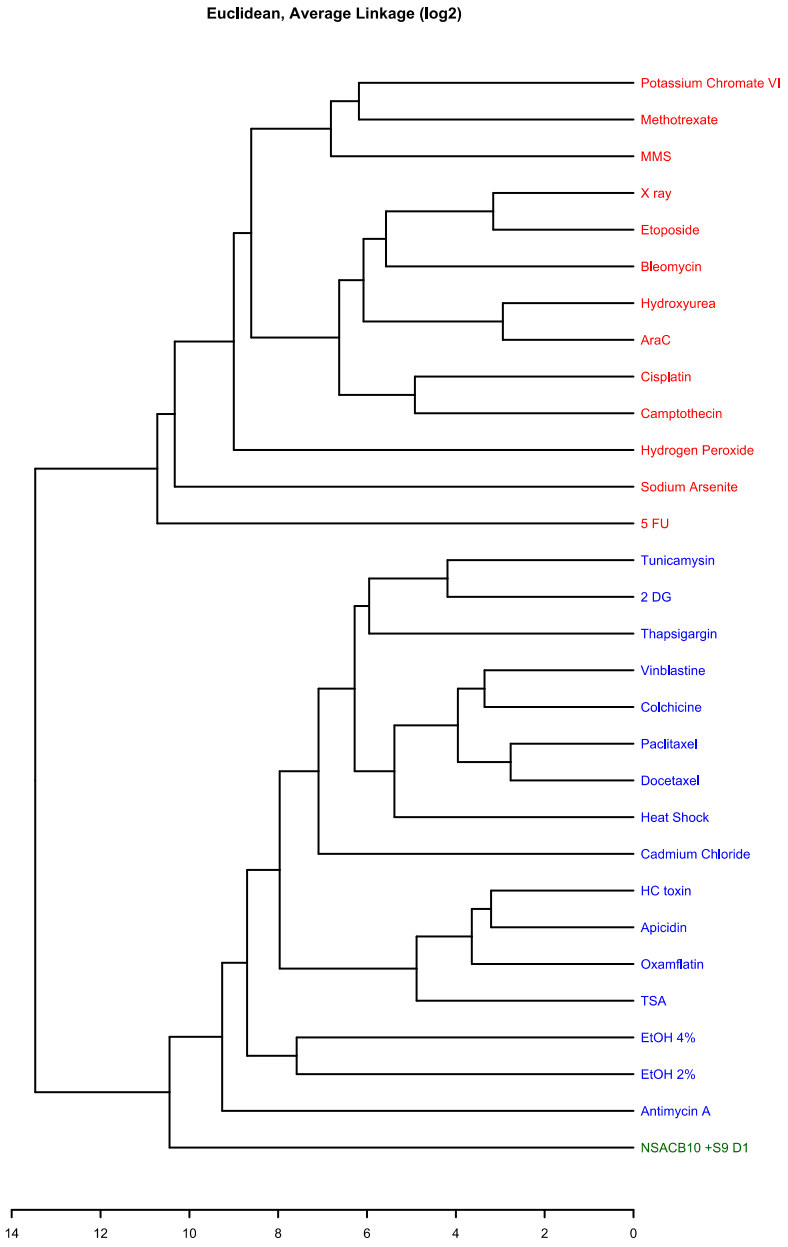
Euclidean, Average Linkage (log2)
Potassium Chromate VI
Methotrexate
MMS
X ray
Etoposide
Bleomycin
Hydroxyurea
AraC
Cisplatin
Camptothecin
Hydrogen Peroxide
Sodium Arsenite
5 FU
Tunicamysin
2 DG
Thapsigargin
Vinblastine
Colchicine
Paclitaxel
Docetaxel
Heat Shock
Cadmium Chloride
HC toxin
Apicidin
Oxamflatin
TSA
EtOH 4%
EtOH 2%
Antimycin A
NSACB10 +S9 D1
14
12
10
8
6
4
2
0

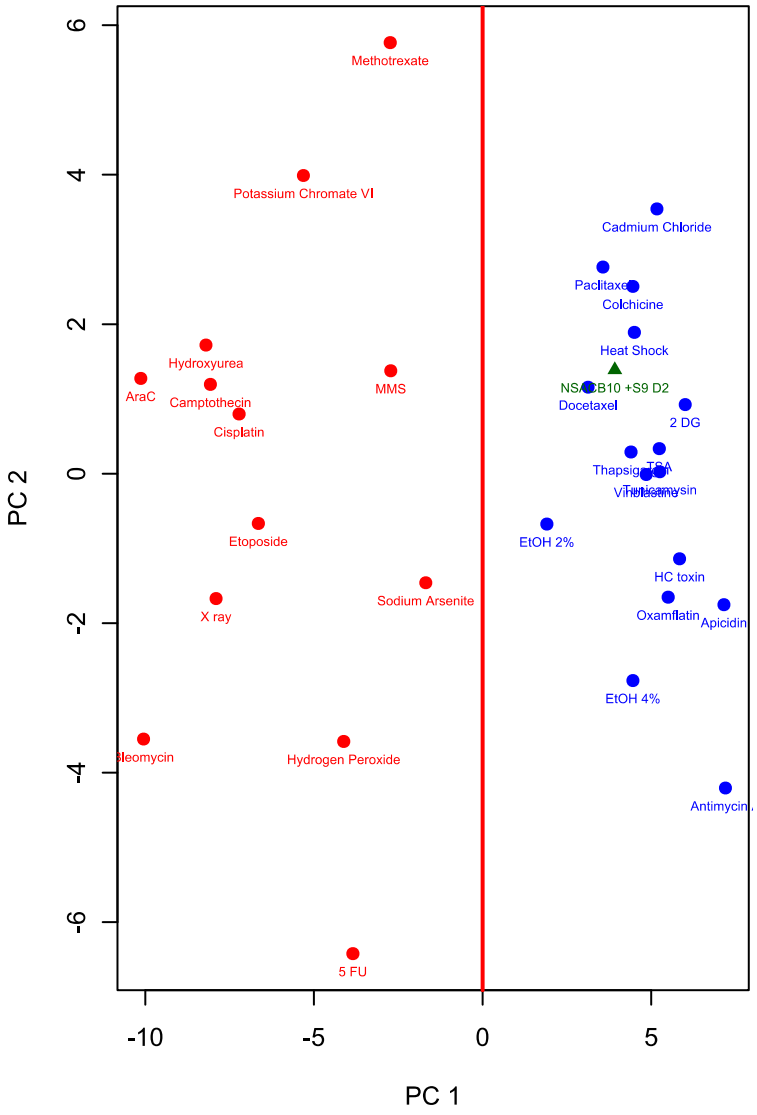
Methotrexate
Potassium Chromate VI
Cadmium Chloride
Paclitaxel
Colchicine
Heat Shock
Hydroxyurea
AraC
Camptothecin
MMS
NSACB10 +S9 D2
Docetaxel
2 DG
Cisplatin
Thapsigargin
TSA
Tunicamysin
Vinblastine
Etoposide
EtOH 2%
HC toxin
Sodium Arsenite
X ray
Oxamflatin
Apicidin
EtOH 4%
Bleomycin
Hydrogen Peroxide
Antimycin
5 FU
PC 2
PC 1
6
4
2
0
-2
-4
-6
-10
-5
0
5

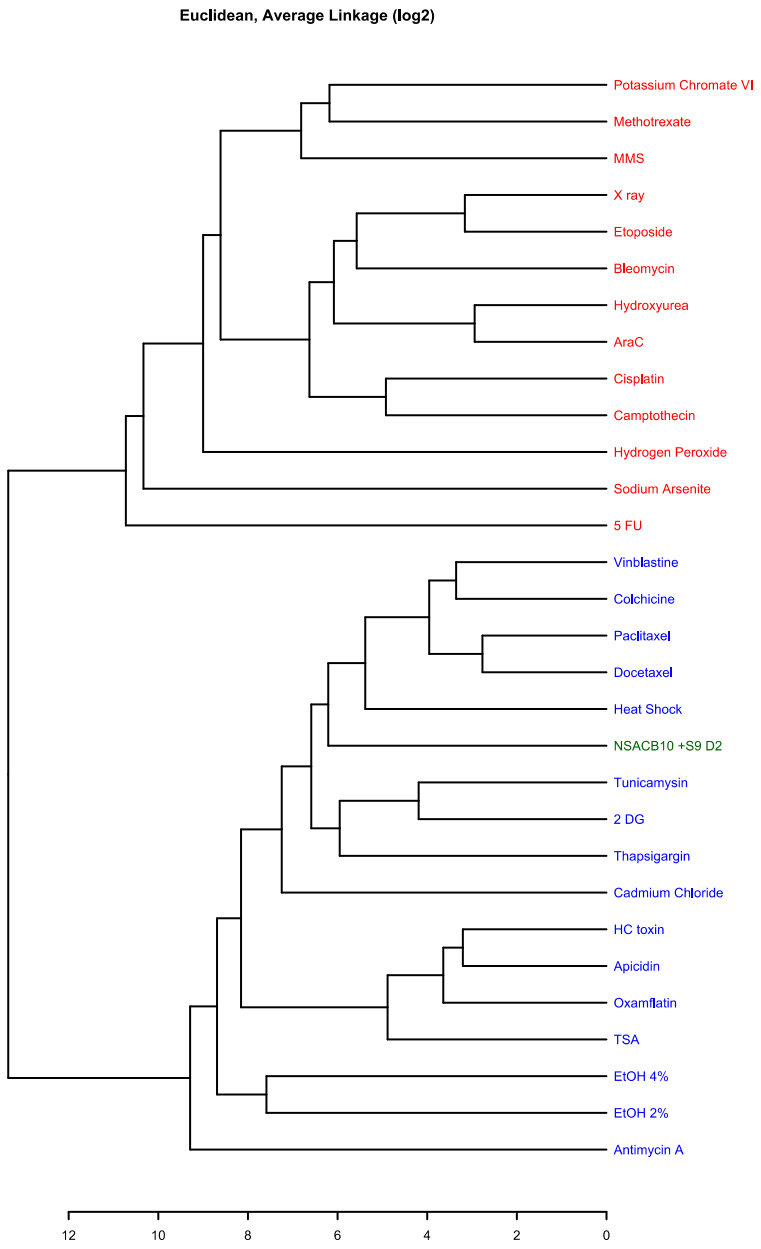
Euclidean, Average Linkage (log2)
Potassium Chromate VI
Methotrexate
MMS
X ray
Etoposide
Bleomycin
Hydroxyurea
AraC
Cisplatin
Camptothecin
Hydrogen Peroxide
Sodium Arsenite
5 FU
Vinblastine
Colchicine
Paclitaxel
Docetaxel
Heat Shock
NSACB10 +S9 D2
Tunicamysin
2 DG
Thapsigargin
Cadmium Chloride
HC toxin
Apicidin
Oxamflatin
TSA
EtOH 4%
EtOH 2%
Antimycin A
12
10
8
6
4
2
0

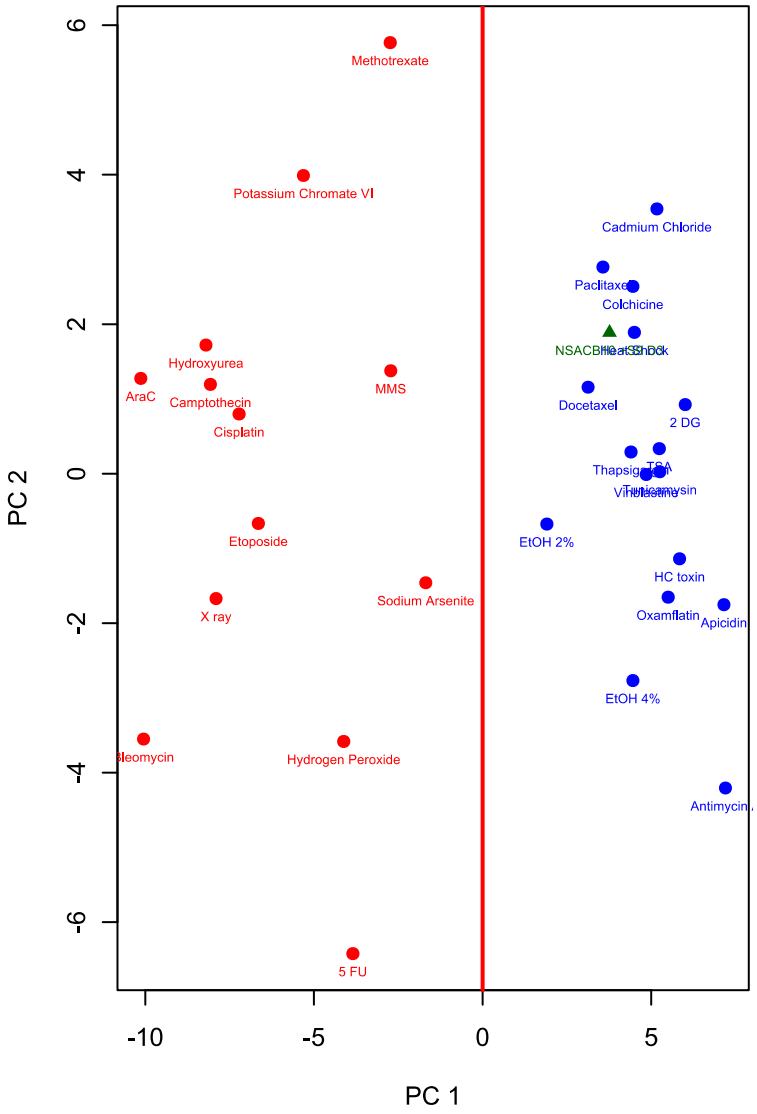
Methotrexate
Potassium Chromate VI
Cadmium Chloride
Paclitaxel
Colchicine
Hydroxyurea
AraC
Camptothecin
Cisplatin
MMS
Docetaxel
2 DG
Etoposide
EtOH 2%
HC toxin
Sodium Arsenite
X ray
Oxamflatin
Apicidin
EtOH 4%
Hydrogen Peroxide
Antimycin
5 FU
PC 2
PC 1
6
4
2
0
-2
-4
-6
-10
-5
0
5

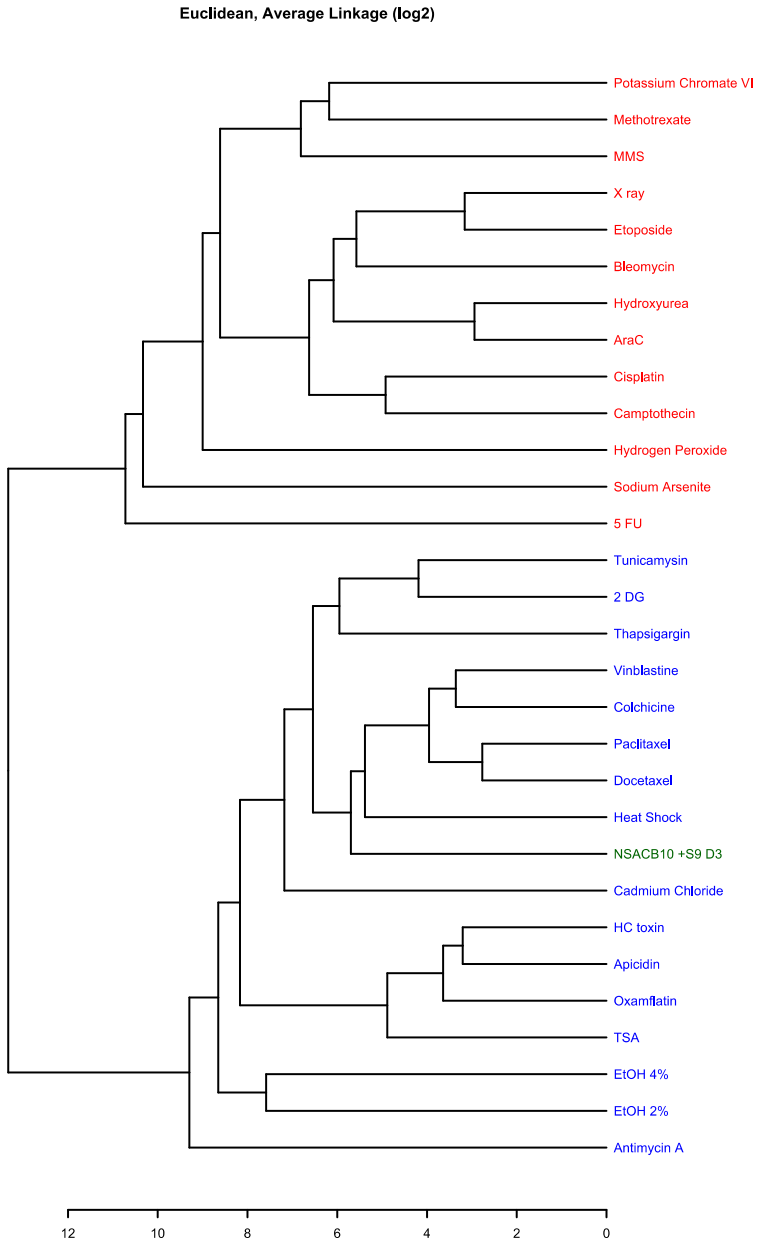
Euclidean, Average Linkage (log2)
Potassium Chromate VI
Methotrexate
MMS
X ray
Etoposide
Bleomycin
Hydroxyurea
AraC
Cisplatin
Camptothecin
Hydrogen Peroxide
Sodium Arsenite
5 FU
Tunicamysin
2 DG
Thapsigargin
Vinblastine
Colchicine
Paclitaxel
Docetaxel
Heat Shock
NSACB10 +S9 D3
Cadmium Chloride
HC toxin
Apicidin
Oxamflatin
TSA
EtOH 4%
EtOH 2%
Antimycin A
12
10
8
6
4
2
0

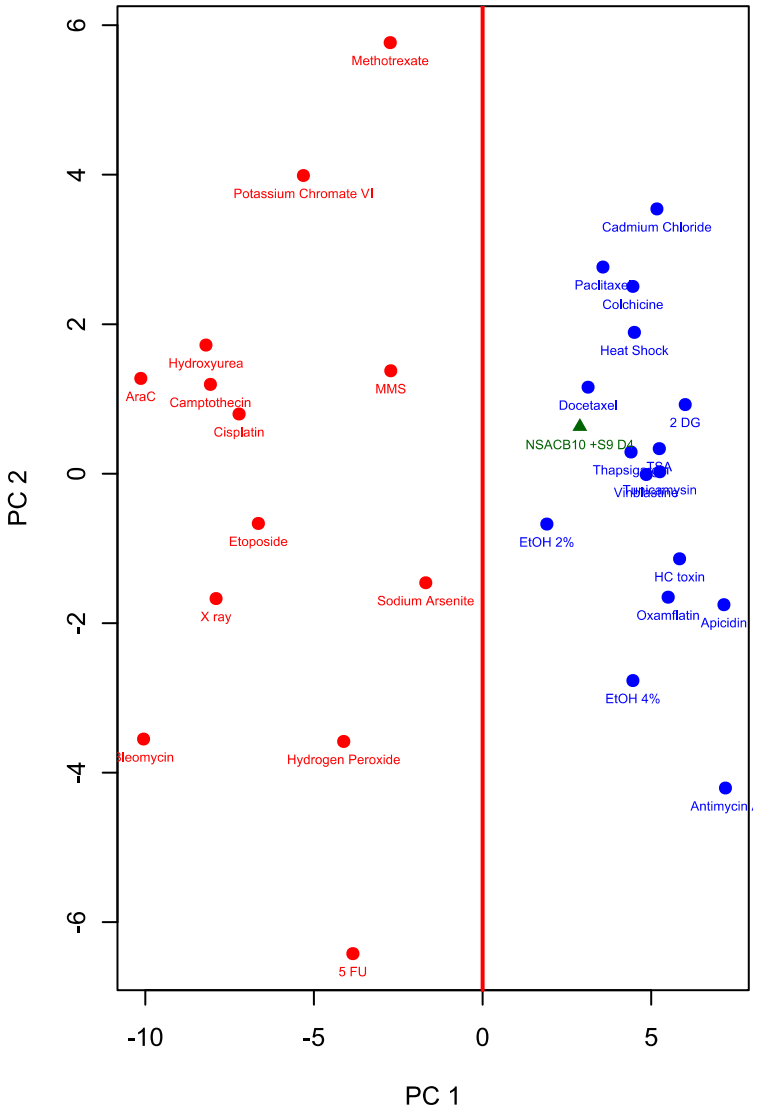
Methotrexate
Potassium Chromate VI
Cadmium Chloride
Paclitaxel
Colchicine
Heat Shock
Hydroxyurea
AraC
Camptothecin
MMS
Docetaxel
2 DG
Cisplatin
NSACB10 +S9 D4
Thapsigargin
TSA
Tunicamysin
Vinblastine
Etoposide
EtOH 2%
HC toxin
Sodium Arsenite
X ray
Oxamflatin
Apicidin
EtOH 4%
Bleomycin
Hydrogen Peroxide
Antimycin
5 FU
PC 2
PC 1
6
4
2
0
-2
-4
-6
-10
-5
0
5

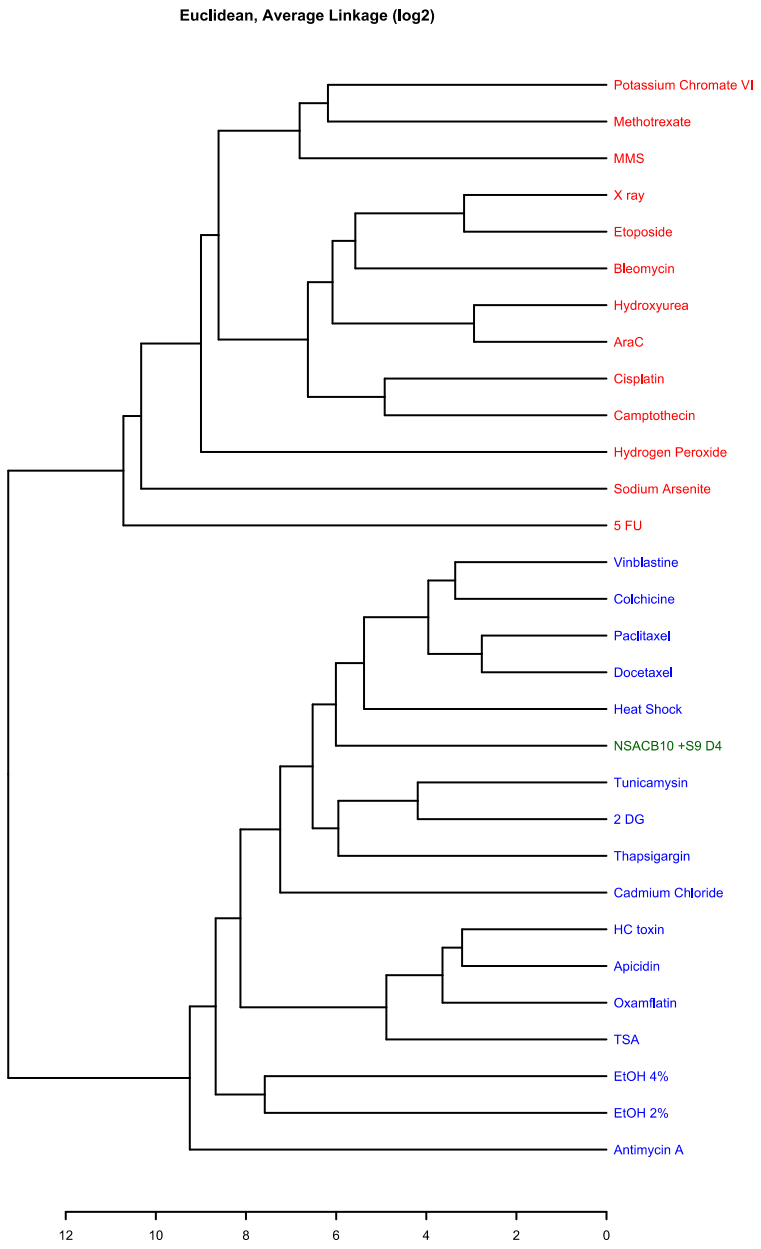
Euclidean, Average Linkage (log2)
Potassium Chromate VI
Methotrexate
MMS
X ray
Etoposide
Bleomycin
Hydroxyurea
AraC
Cisplatin
Camptothecin
Hydrogen Peroxide
Sodium Arsenite
5 FU
Vinblastine
Colchicine
Paclitaxel
Docetaxel
Heat Shock
NSACB10 +S9 D4
Tunicamysin
2 DG
Thapsigargin
Cadmium Chloride
HC toxin
Apicidin
Oxamflatin
TSA
EtOH 4%
EtOH 2%
Antimycin A
12
10
8
6
4
2
0

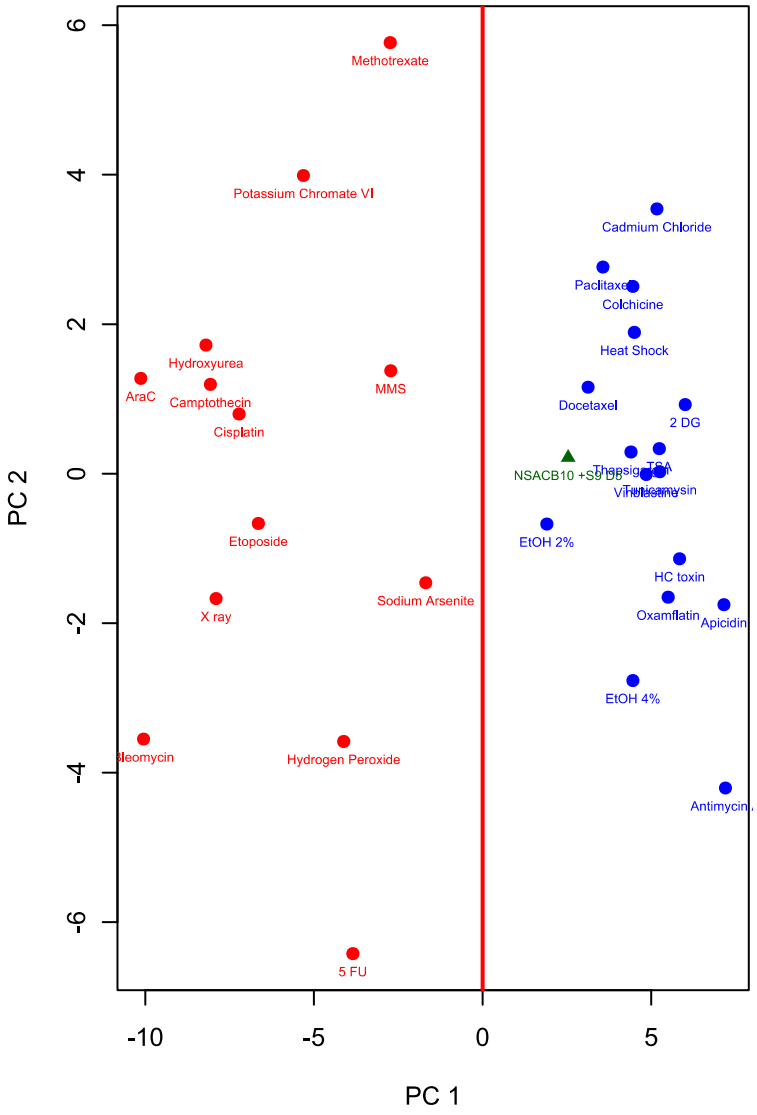
Methotrexate
Potassium Chromate VI
Cadmium Chloride
Paclitaxel
Colchicine
Heat Shock
Hydroxyurea
AraC
Camptothecin
Cisplatin
MMS
Docetaxel
2 DG
NSACB10 +S9 D5
TSA
Vinblastine
Tunicamysin
Etoposide
EtOH 2%
HC toxin
Sodium Arsenite
X ray
Oxamflatin
Apicidin
EtOH 4%
Bleomycin
Hydrogen Peroxide
Antimycin
5 FU
PC 2
PC 1
6
4
2
0
-2
-4
-6
-10
-5
0
5

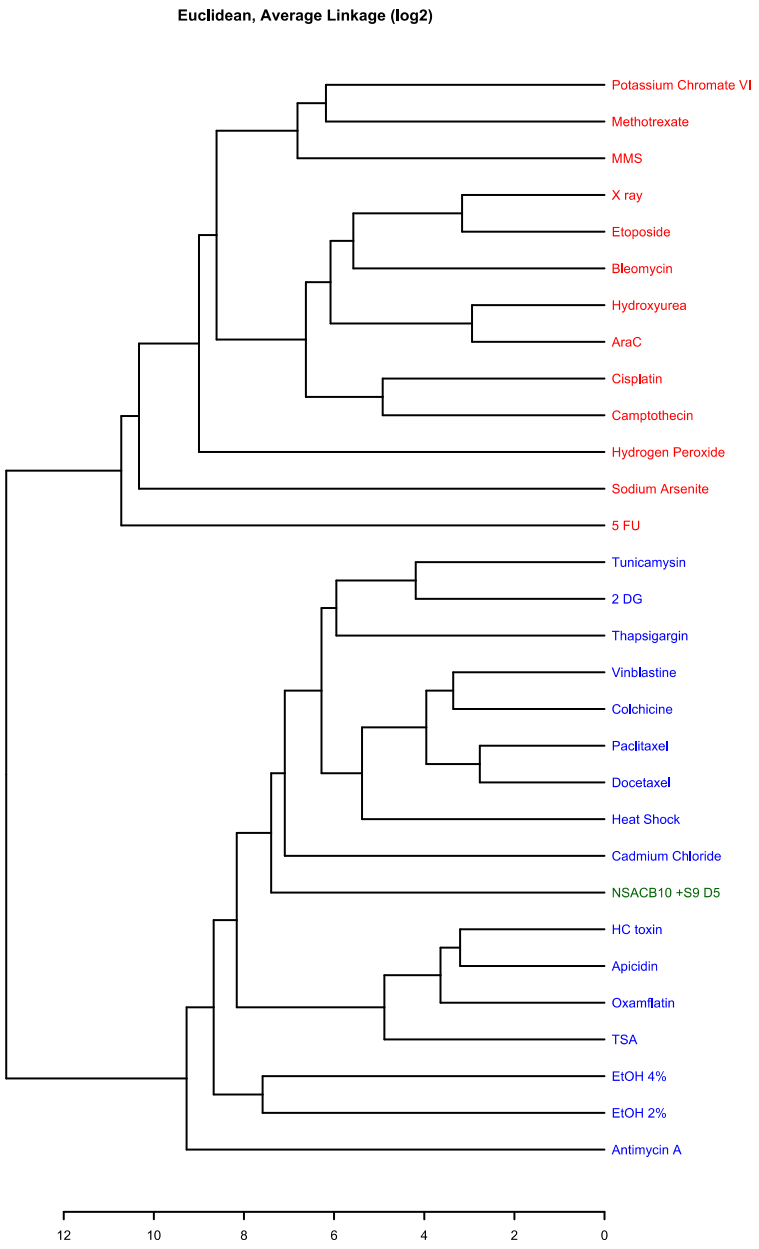
Euclidean, Average Linkage (log2)
Potassium Chromate VI
Methotrexate
MMS
X ray
Etoposide
Bleomycin
Hydroxyurea
AraC
Cisplatin
Camptothecin
Hydrogen Peroxide
Sodium Arsenite
5 FU
Tunicamysin
2 DG
Thapsigargin
Vinblastine
Colchicine
Paclitaxel
Docetaxel
Heat Shock
Cadmium Chloride
NSACB10 +S9 D5
HC toxin
Apicidin
Oxamflatin
TSA
EtOH 4%
EtOH 2%
Antimycin A
12
10
8
6
4
2
0

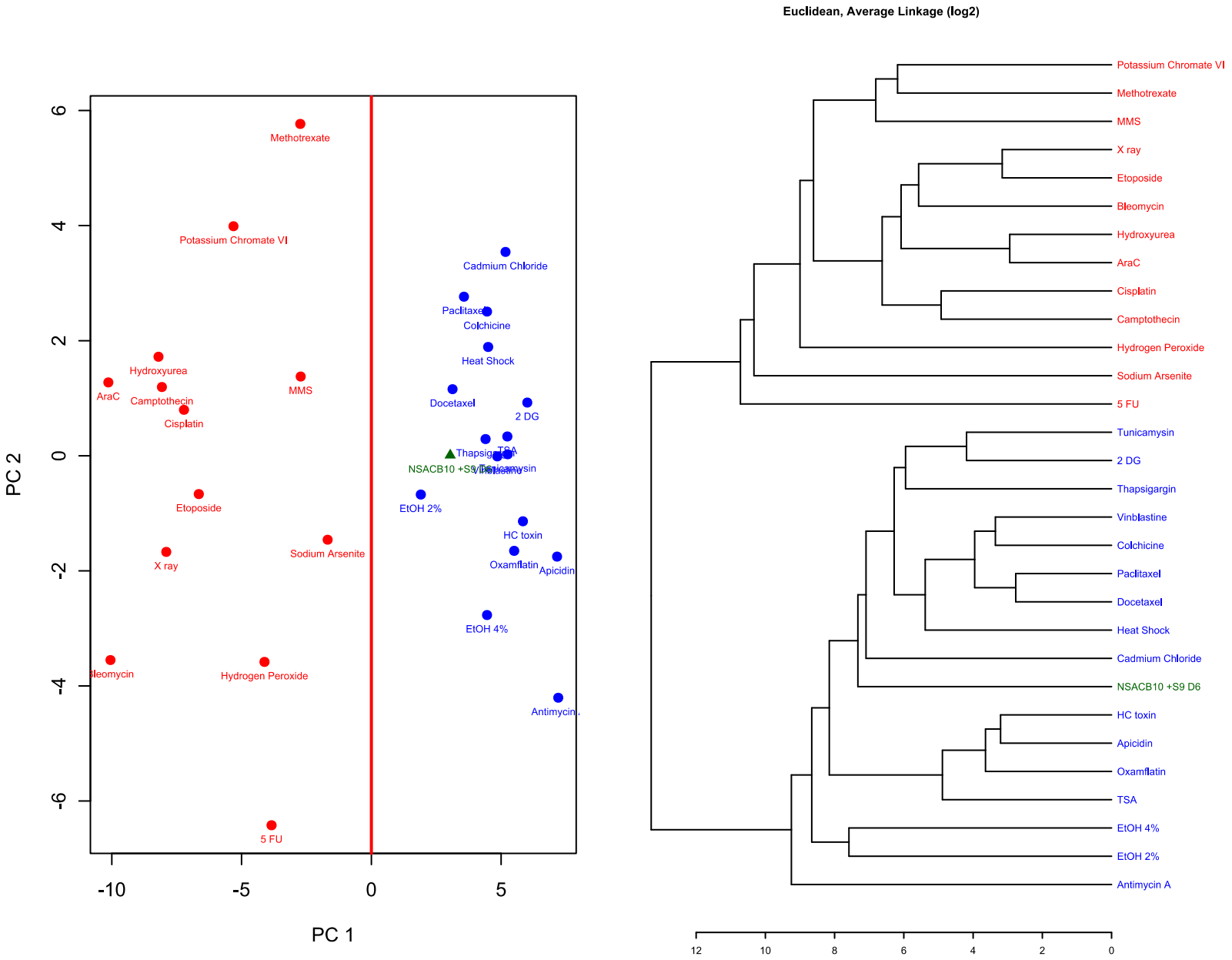

Supplementary Figure III-O: NASCB 10 (+S9) TGx-DDI biomarker classification using the Principal Component Analysis (PCA) (left) and hierarchical clustering (right) statistical analyses. Genotoxic reference chemicals are shown in red text, non-genotoxic reference chemicals are shown in blue text, and the test agent is shown in the green text. The line drawn on the PCA plot and the main branch on the dendogram divides the genotoxic and non-genotoxic agents and was used to classify the test compounds. D1 represents the lowest concentration tested, D6 the highest.

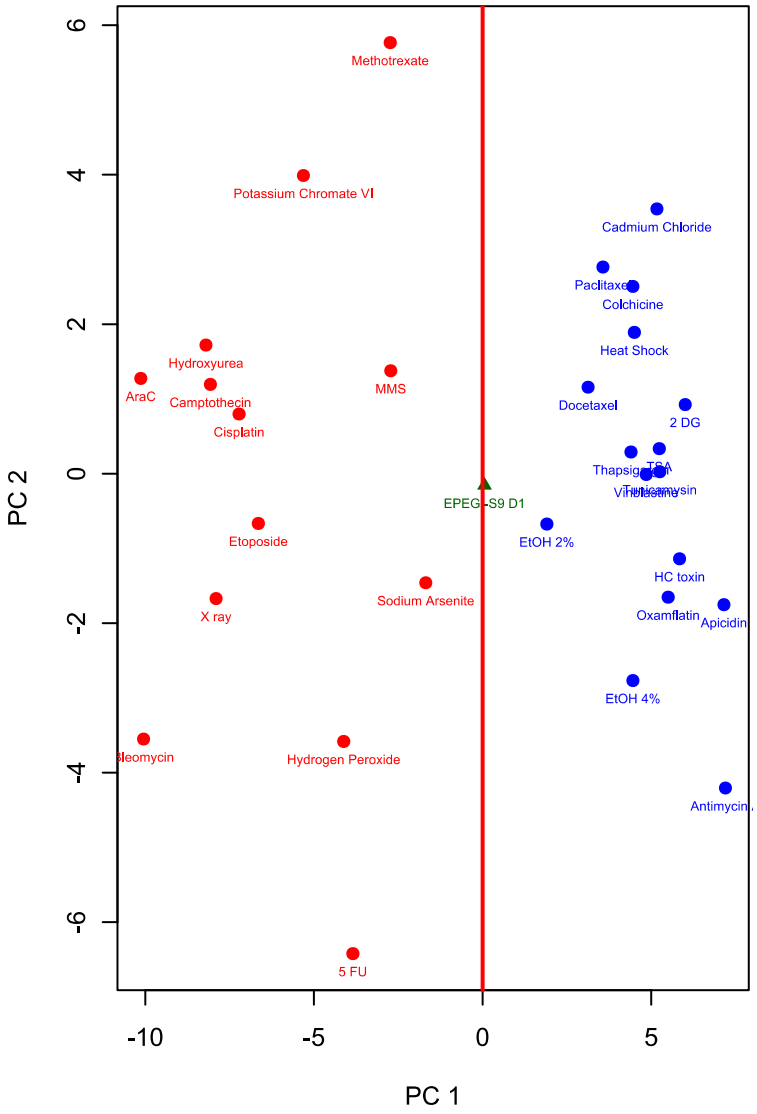
Methotrexate
Potassium Chromate VI
Cadmium Chloride
Paclitaxel
Colchicine
Heat Shock
Hydroxyurea
AraC
Camptothecin
Cisplatin
MMS
Docetaxel
2 DG
Thapsigargin
TSA
Tunicamysin
Vinblastine
EPEG -S9 D1
EtOH 2%
Etoposide
HC toxin
Sodium Arsenite
X ray
Oxamflatin
Apicidin
EtOH 4%
Bleomycin
Hydrogen Peroxide
Antimycin
5 FU
PC 2
PC 1
6
4
2
0
-2
-4
-6
-10
-5
0
5

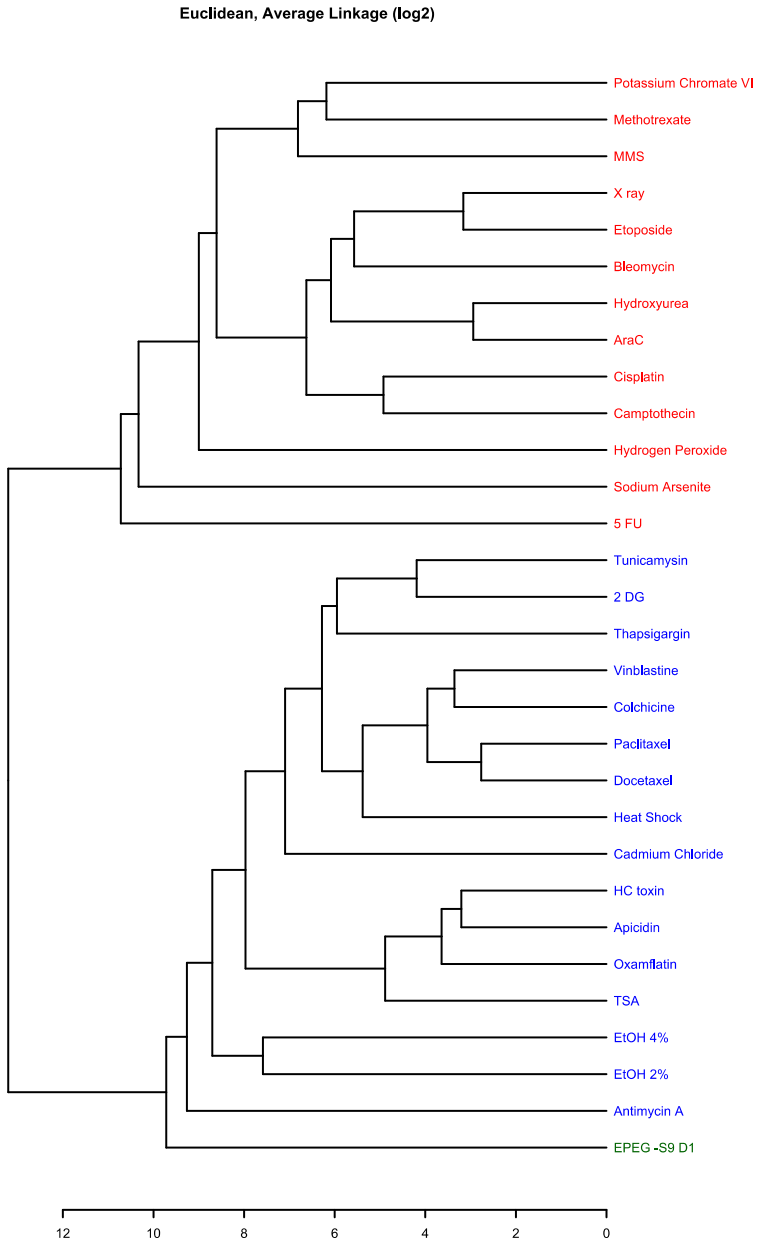
Euclidean, Average Linkage (log2)
Potassium Chromate VI
Methotrexate
MMS
X ray
Etoposide
Bleomycin
Hydroxyurea
AraC
Cisplatin
Camptothecin
Hydrogen Peroxide
Sodium Arsenite
5 FU
Tunicamysin
2 DG
Thapsigargin
Vinblastine
Colchicine
Paclitaxel
Docetaxel
Heat Shock
Cadmium Chloride
HC toxin
Apicidin
Oxamflatin
TSA
EtOH 4%
EtOH 2%
Antimycin A
EPEG -S9 D1
12
10
8
6
4
2
0

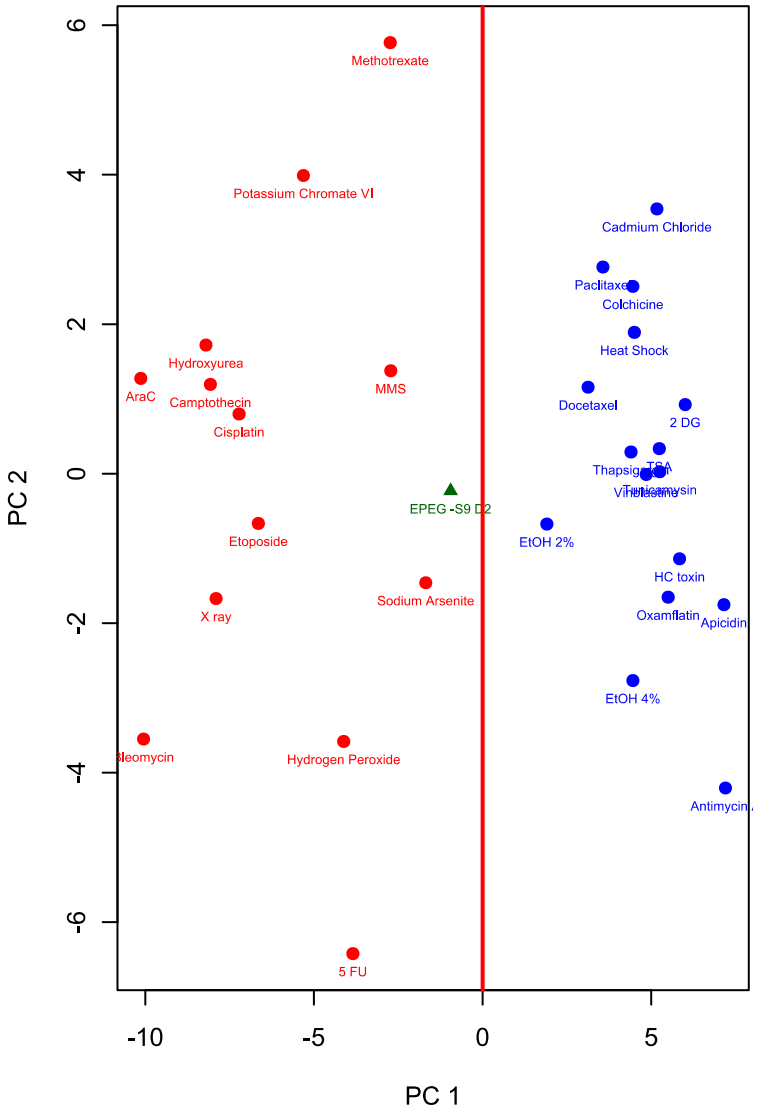
Methotrexate
Potassium Chromate VI
Cadmium Chloride
Paclitaxel
Colchicine
Heat Shock
Hydroxyurea
AraC
Camptothecin
Cisplatin
MMS
Docetaxel
2 DG
Thapsigargin
TSA
Vinblastine
Tunicamysin
EPEG -S9 D2
Etoposide
EtOH 2%
HC toxin
Sodium Arsenite
X ray
Oxamflatin
Apicidin
EtOH 4%
Bleomycin
Hydrogen Peroxide
Antimycin
5 FU
PC 2
PC 1
6
4
2
0
-2
-4
-6
-10
-5
0
5

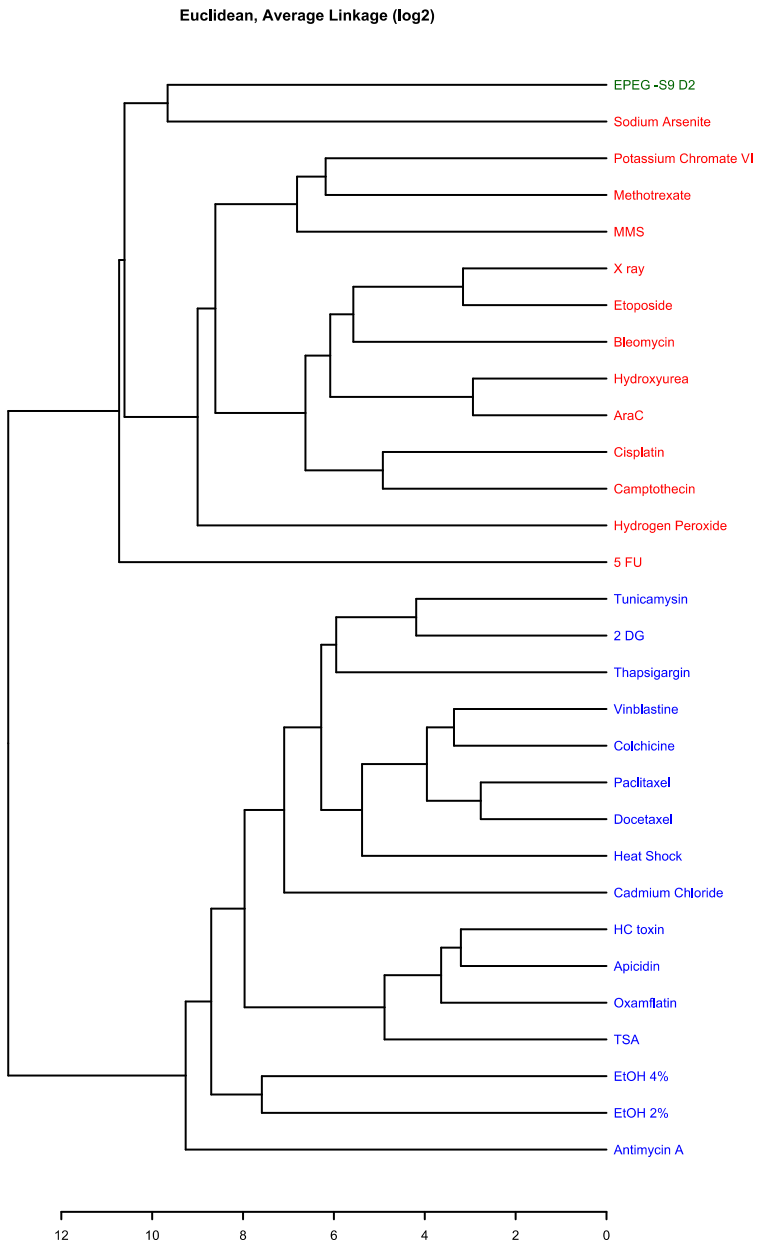
Euclidean, Average Linkage (log2)
EPEG -S9 D2
Sodium Arsenite
Potassium Chromate VI
Methotrexate
MMS
X ray
Etoposide
Bleomycin
Hydroxyurea
AraC
Cisplatin
Camptothecin
Hydrogen Peroxide
5 FU
Tunicamysin
2 DG
Thapsigargin
Vinblastine
Colchicine
Paclitaxel
Docetaxel
Heat Shock
Cadmium Chloride
HC toxin
Apicidin
Oxamflatin
TSA
EtOH 4%
EtOH 2%
Antimycin A
12
10
8
6
4
2
0

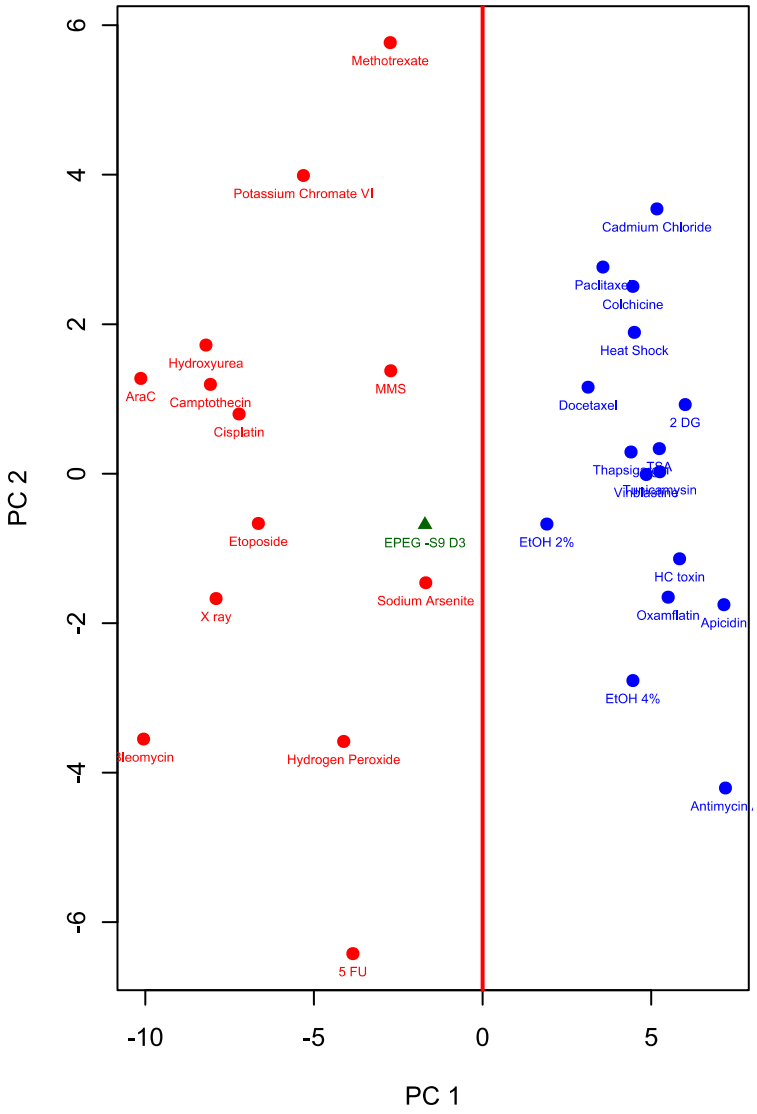
PC 2
PC 1
6
4
2
0
-2
-4
-6
-10
-5
0
5
Methotrexate
Potassium Chromate VI
Cadmium Chloride
Paclitaxel
Colchicine
Heat Shock
Hydroxyurea
AraC
Camptothecin
Cisplatin
MMS
Docetaxel
2 DG
Thapsigargin
TSA
Vinblastine
Tunicamycin
Etoposide
EPEG -S9 D3
EtOH 2%
HC toxin
Sodium Arsenite
X ray
Oxamflatin
Apicidin
EtOH 4%
Bleomycin
Hydrogen Peroxide
Antimycin
5 FU

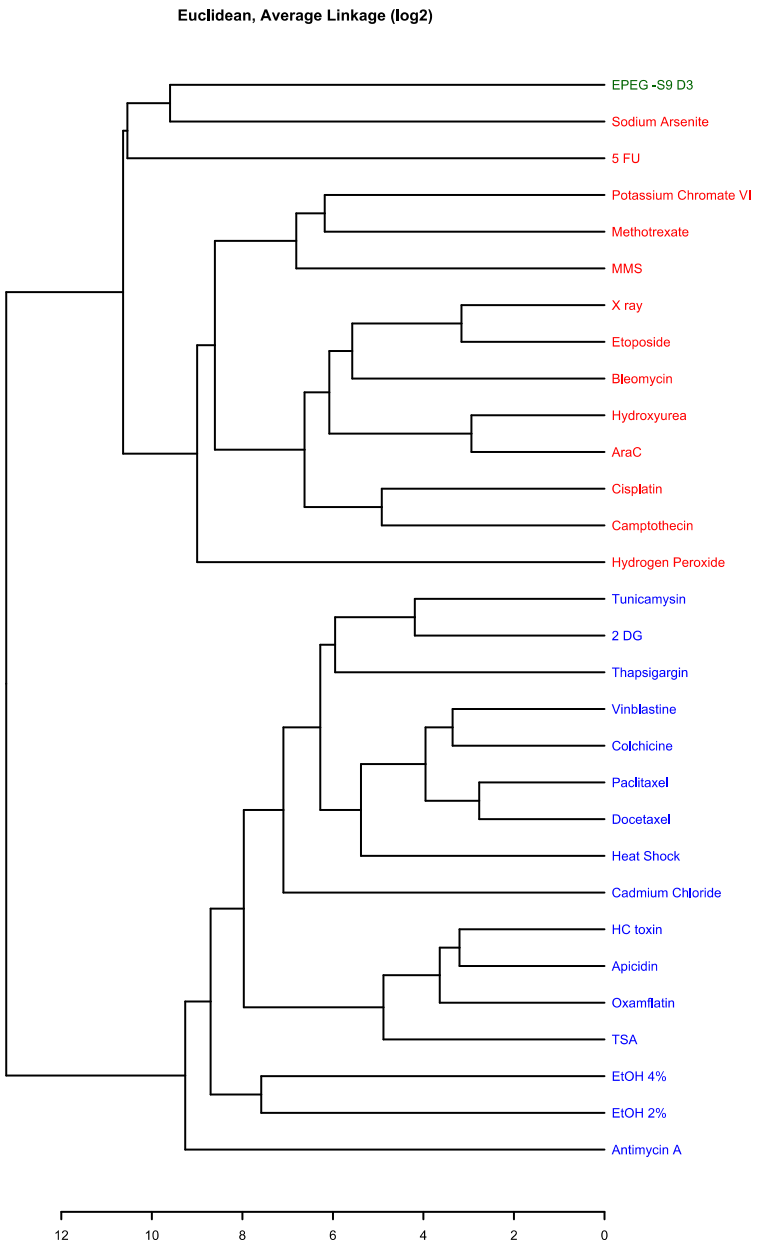
Euclidean, Average Linkage (log2)
EPEG -S9 D3
Sodium Arsenite
5 FU
Potassium Chromate VI
Methotrexate
MMS
X ray
Etoposide
Bleomycin
Hydroxyurea
AraC
Cisplatin
Camptothecin
Hydrogen Peroxide
Tunicamycin
2 DG
Thapsigargin
Vinblastine
Colchicine
Paclitaxel
Docetaxel
Heat Shock
Cadmium Chloride
HC toxin
Apicidin
Oxamflatin
TSA
EtOH 4%
EtOH 2%
Antimycin A
12
10
8
6
4
2
0

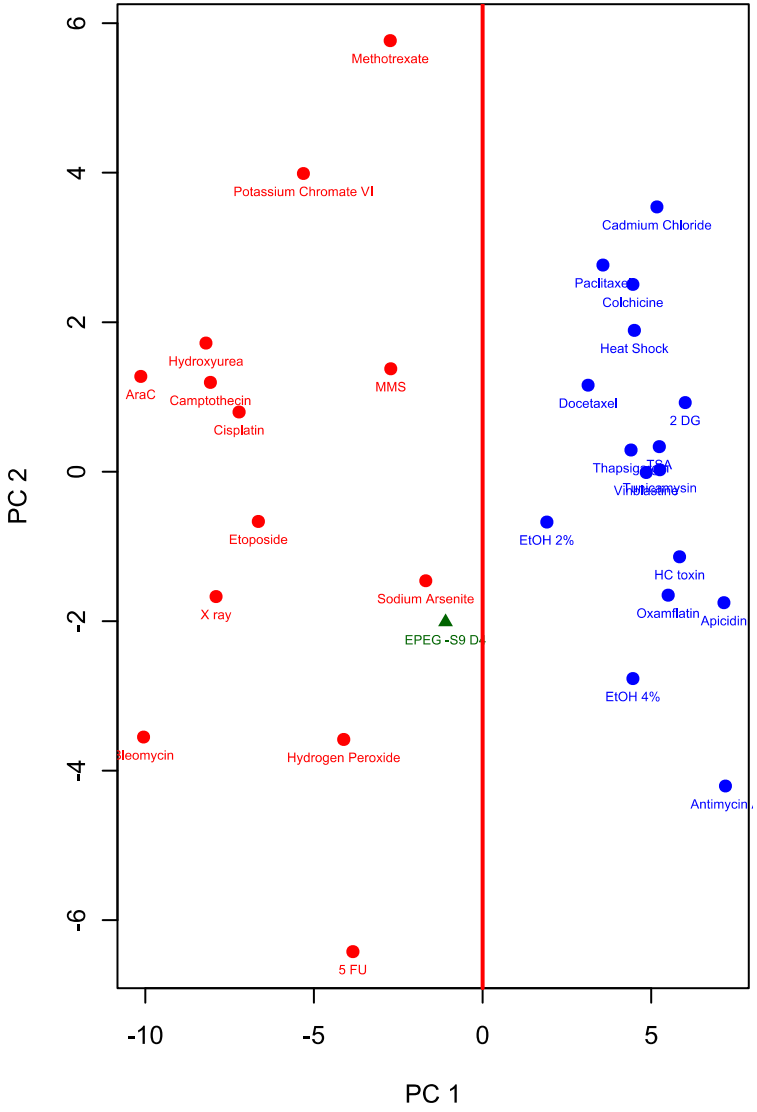
Methotrexate
Potassium Chromate VI
Cadmium Chloride
Paclitaxel
Colchicine
Heat Shock
Hydroxyurea
AraC
Camptothecin
Cisplatin
MMS
Docetaxel
2 DG
Thapsigargin
TSA
Vinblastine
Tunicamycin
Etoposide
EtOH 2%
HC toxin
Sodium Arsenite
X ray
Oxamflatin
Apicidin
EPEG -S9 D4
EtOH 4%
Bleomycin
Hydrogen Peroxide
Antimycin
5 FU
PC 2
PC 1
6
4
2
0
-2
-4
-6
-10
-5
0
5

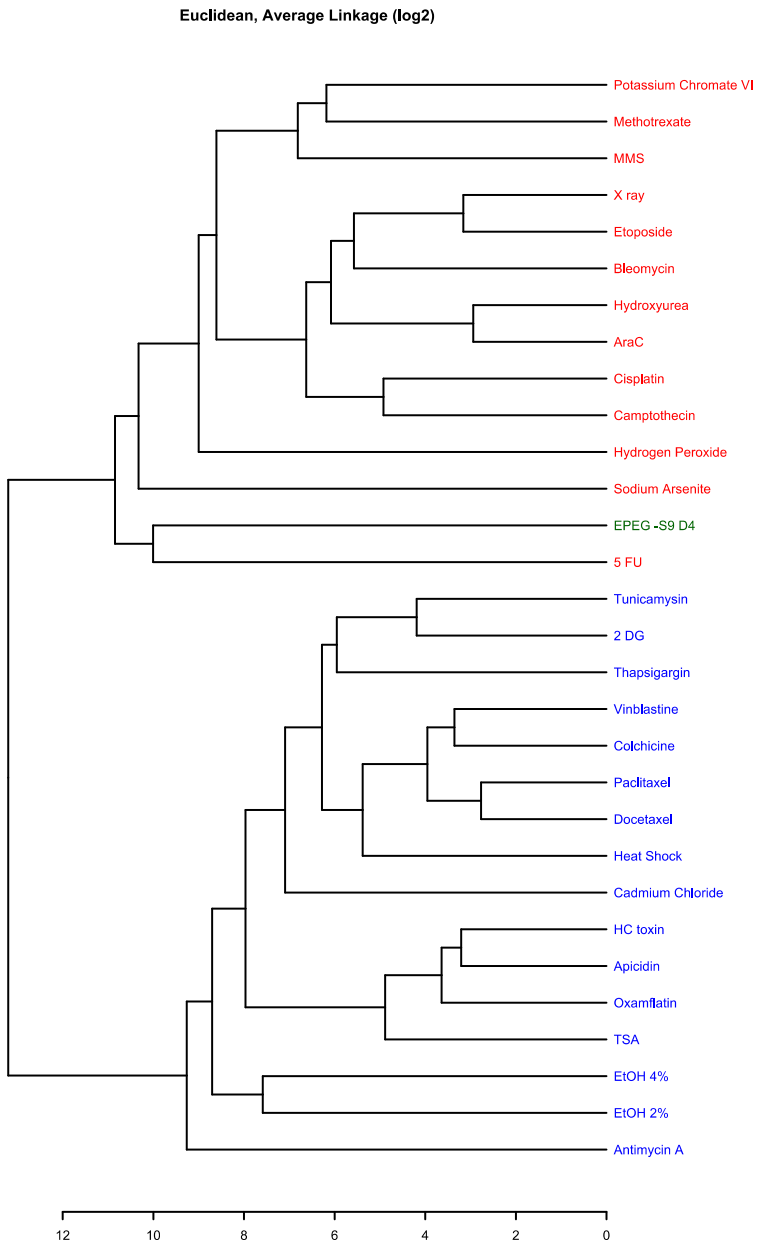
Euclidean, Average Linkage (log2)
Potassium Chromate VI
Methotrexate
MMS
X ray
Etoposide
Bleomycin
Hydroxyurea
AraC
Cisplatin
Camptothecin
Hydrogen Peroxide
Sodium Arsenite
EPEG -S9 D4
5 FU
Tunicamycin
2 DG
Thapsigargin
Vinblastine
Colchicine
Paclitaxel
Docetaxel
Heat Shock
Cadmium Chloride
HC toxin
Apicidin
Oxamflatin
TSA
EtOH 4%
EtOH 2%
Antimycin A
12
10
8
6
4
2
0

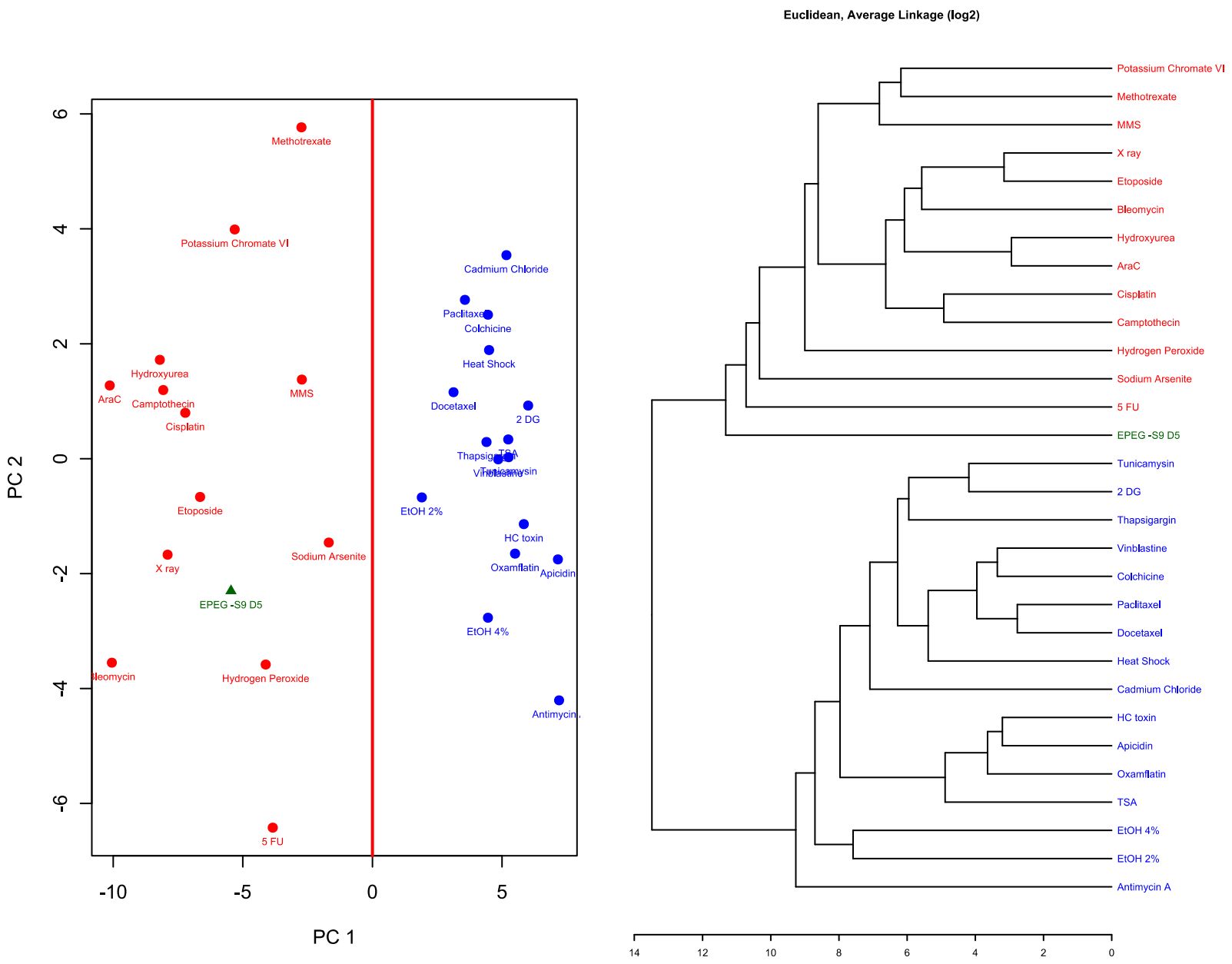

Supplementary Figure III-P: EPEG (-S9) TGx-DDI biomarker classification using the Principal Component Analysis (PCA) (left) and hierarchical clustering (right) statistical analyses. Genotoxic reference chemicals are shown in red text, non-genotoxic reference chemicals are shown in blue text, and the test agent is shown in the green text. The line drawn on the PCA plot and the main branch on the dendogram divides the genotoxic and non-genotoxic agents and was used to classify the test compounds. D1 represents the lowest concentration tested, D5 the highest.

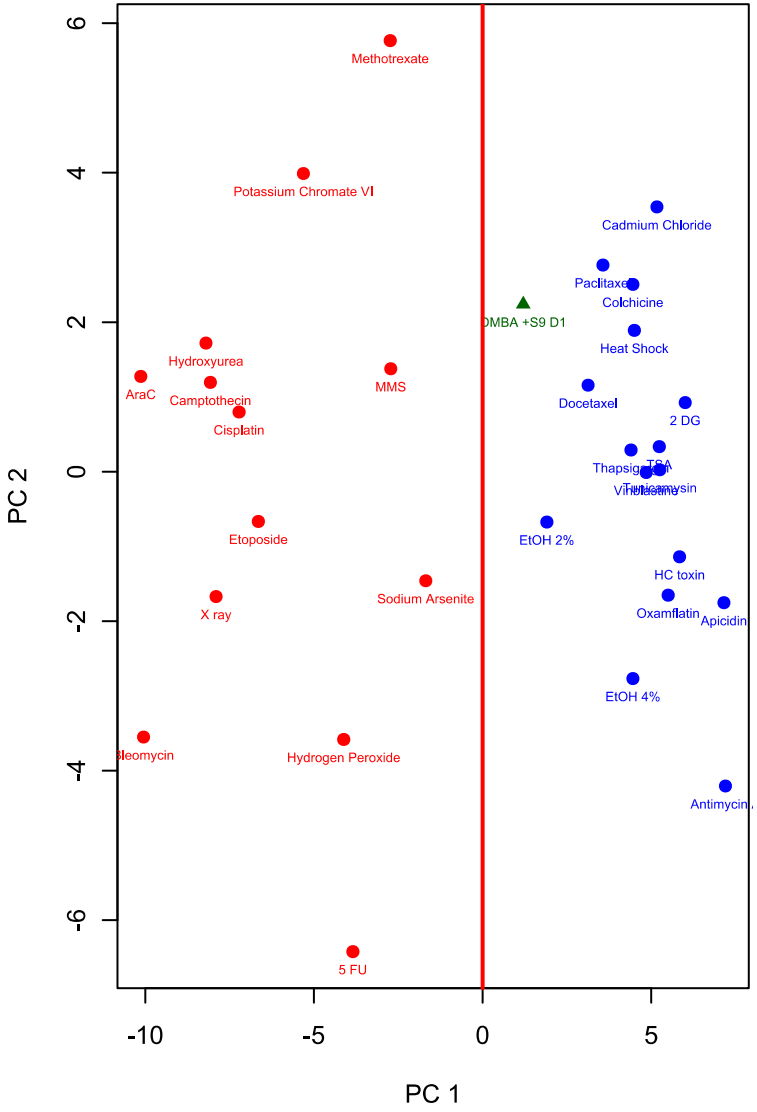
Methotrexate
Potassium Chromate VI
Cadmium Chloride
Paclitaxel
Colchicine
DMBA +S9 D1
Heat Shock
Hydroxyurea
AraC
Camptothecin
MMS
Docetaxel
2 DG
Cisplatin
Thapsigargin
TSA
Vinblastine
Tunicamysin
Etoposide
EtOH 2%
HC toxin
Sodium Arsenite
X ray
Oxamflatin
Apicidin
EtOH 4%
Bleomycin
Hydrogen Peroxide
Antimycin
5 FU
PC 2
PC 1
6
4
2
0
-2
-4
-6
-10
-5
0
5

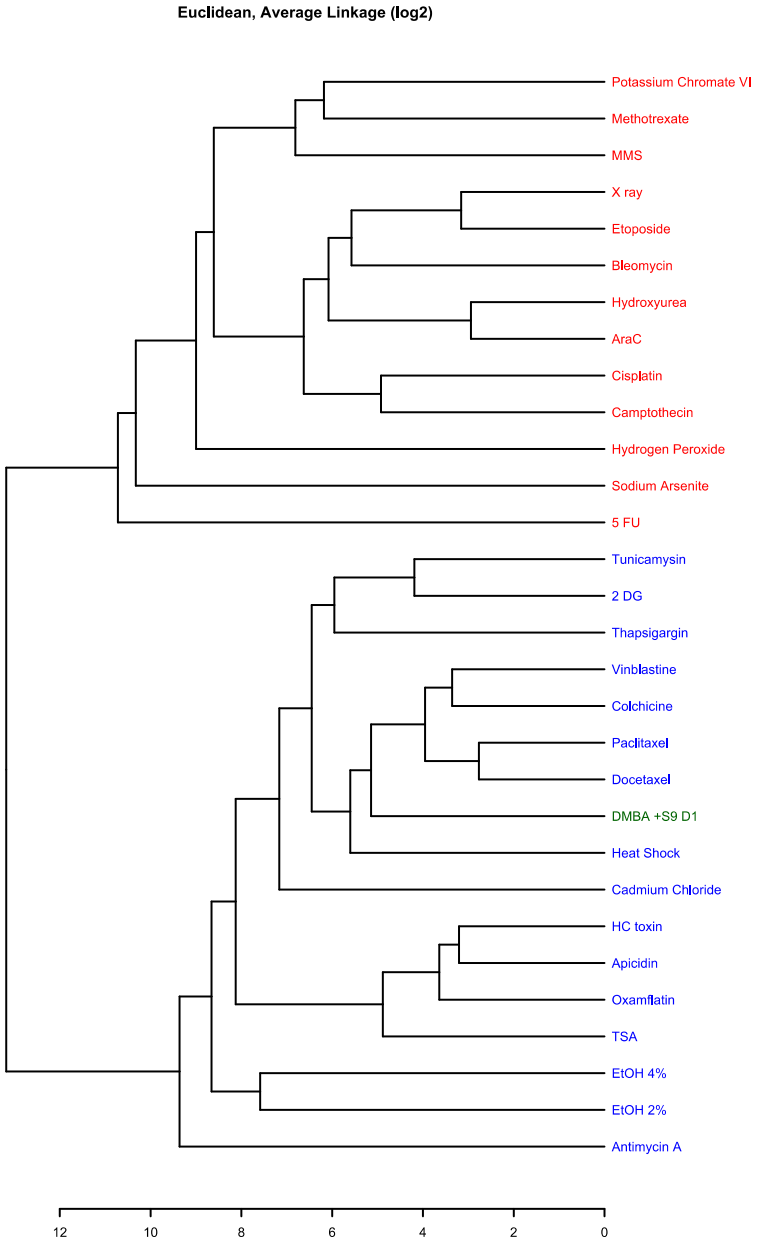
Euclidean, Average Linkage (log2)
Potassium Chromate VI
Methotrexate
MMS
X ray
Etoposide
Bleomycin
Hydroxyurea
AraC
Cisplatin
Camptothecin
Hydrogen Peroxide
Sodium Arsenite
5 FU
Tunicamysin
2 DG
Thapsigargin
Vinblastine
Colchicine
Paclitaxel
Docetaxel
DMBA +S9 D1
Heat Shock
Cadmium Chloride
HC toxin
Apicidin
Oxamflatin
TSA
EtOH 4%
EtOH 2%
Antimycin A
12
10
8
6
4
2
0

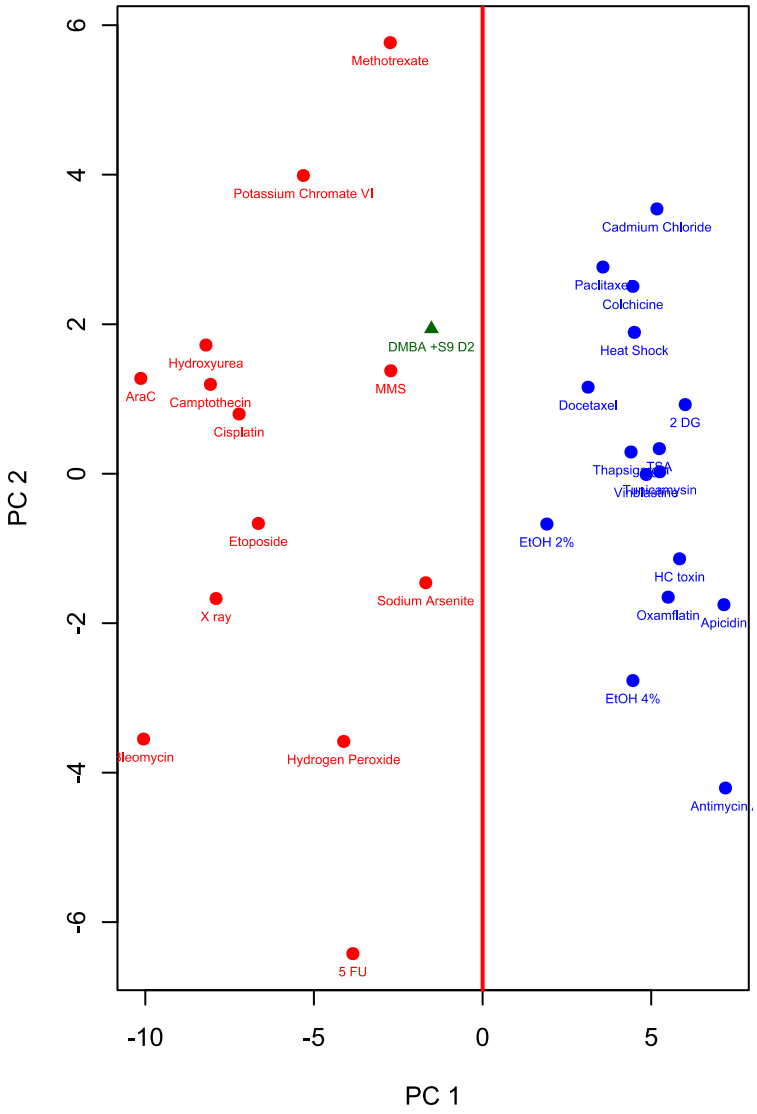
Methotrexate
Potassium Chromate VI
Cadmium Chloride
Paclitaxel
Colchicine
DMBA +S9 D2
Heat Shock
Hydroxyurea
AraC
MMS
Camptothecin
Docetaxel
2 DG
Cisplatin
Thapsigargin
TSA
Tunicamysin
Vinblastine
Etoposide
EtOH 2%
HC toxin
Sodium Arsenite
X ray
Oxamflatin
Apicidin
EtOH 4%
Bleomycin
Hydrogen Peroxide
Antimycin
5 FU
PC 2
PC 1
6
4
2
0
-2
-4
-6
-10
-5
0
5

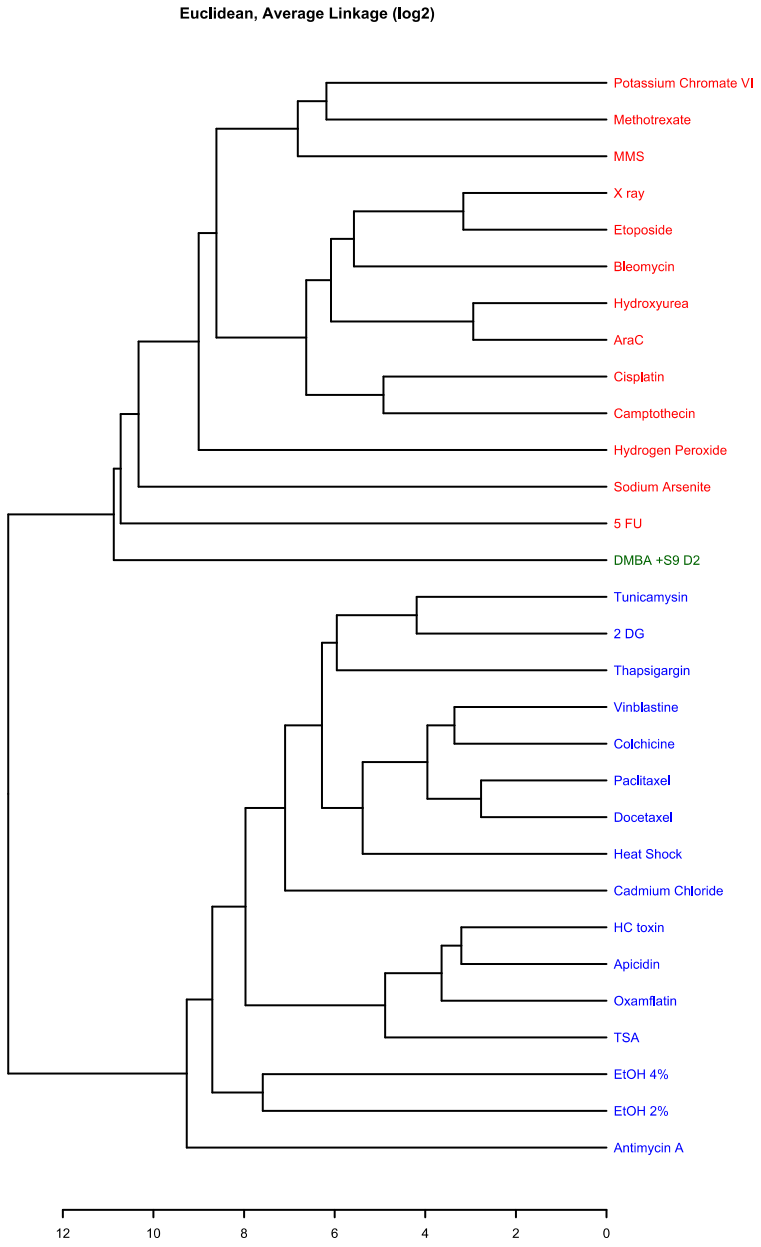
Euclidean, Average Linkage (log2)
Potassium Chromate VI
Methotrexate
MMS
X ray
Etoposide
Bleomycin
Hydroxyurea
AraC
Cisplatin
Camptothecin
Hydrogen Peroxide
Sodium Arsenite
5 FU
DMBA +S9 D2
Tunicamysin
2 DG
Thapsigargin
Vinblastine
Colchicine
Paclitaxel
Docetaxel
Heat Shock
Cadmium Chloride
HC toxin
Apicidin
Oxamflatin
TSA
EtOH 4%
EtOH 2%
Antimycin A
12
10
8
6
4
2
0

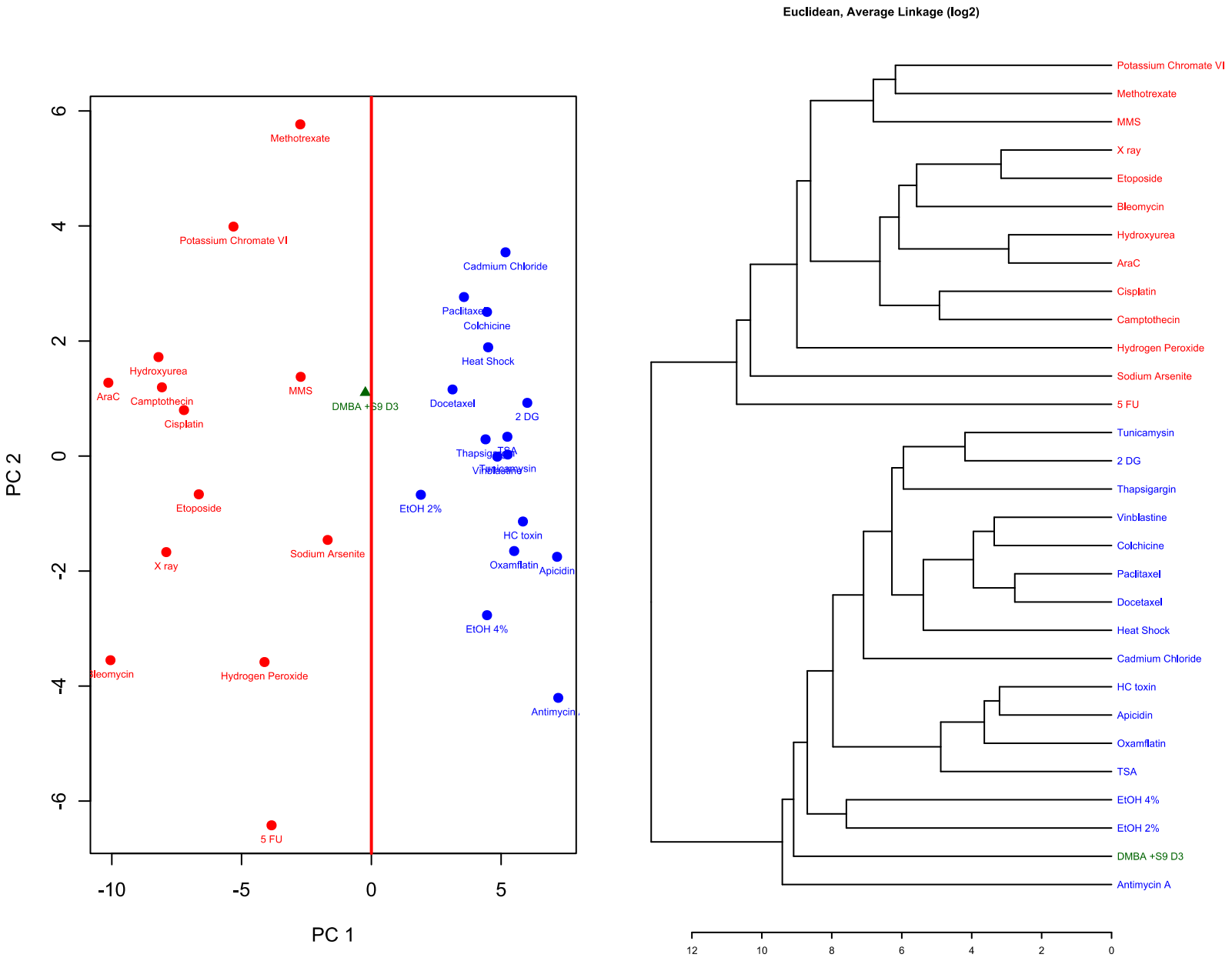
Euclidean, Average Linkage (log2)
Methotrexate
Potassium Chromate VI
Cadmium Chloride
Paclitaxel
Colchicine
Heat Shock
Hydroxyurea
AraC
Camptothecin
Cisplatin
MMS
DMBA +S9 D3
Docetaxel
2 DG
Thapsigargin
TSA
Tunicamysin
Vinblastine
Etoposide
EtOH 2%
HC toxin
Sodium Arsenite
X ray
Oxamflatin
Apicidin
EtOH 4%
Bleomycin
Hydrogen Peroxide
Antimycin A
5 FU
PC 1
PC 2
-10
-5
0
5
6
4
2
0
-2
-4
-6
12
10
8
6
4
2
0

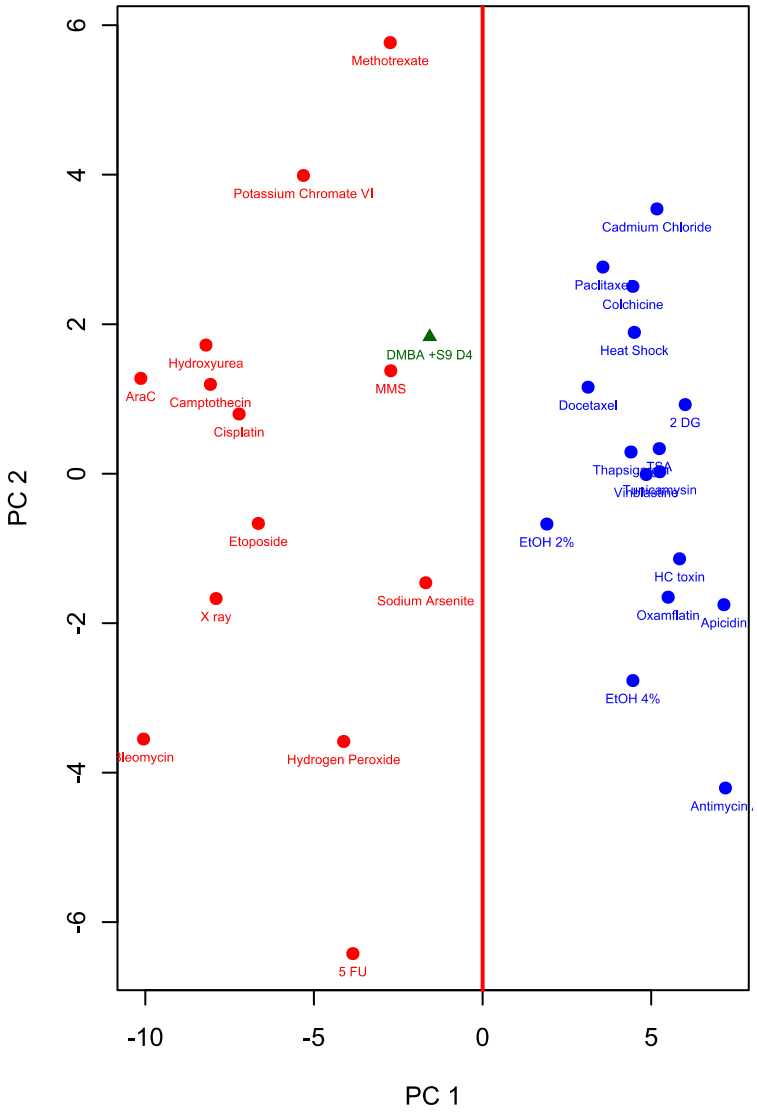
Methotrexate
Potassium Chromate VI
Cadmium Chloride
Paclitaxel
Colchicine
Heat Shock
DMBA +S9 D4
Hydroxyurea
AraC
Camptothecin
MMS
Docetaxel
2 DG
Cisplatin
Thapsigargin
TSA
Tunicamycin
Vinblastine
Etoposide
EtOH 2%
HC toxin
Sodium Arsenite
X ray
Oxamflatin
Apicidin
EtOH 4%
Bleomycin
Hydrogen Peroxide
Antimycin
5 FU
PC 2
PC 1
6
4
2
0
-2
-4
-6
-10
-5
0
5

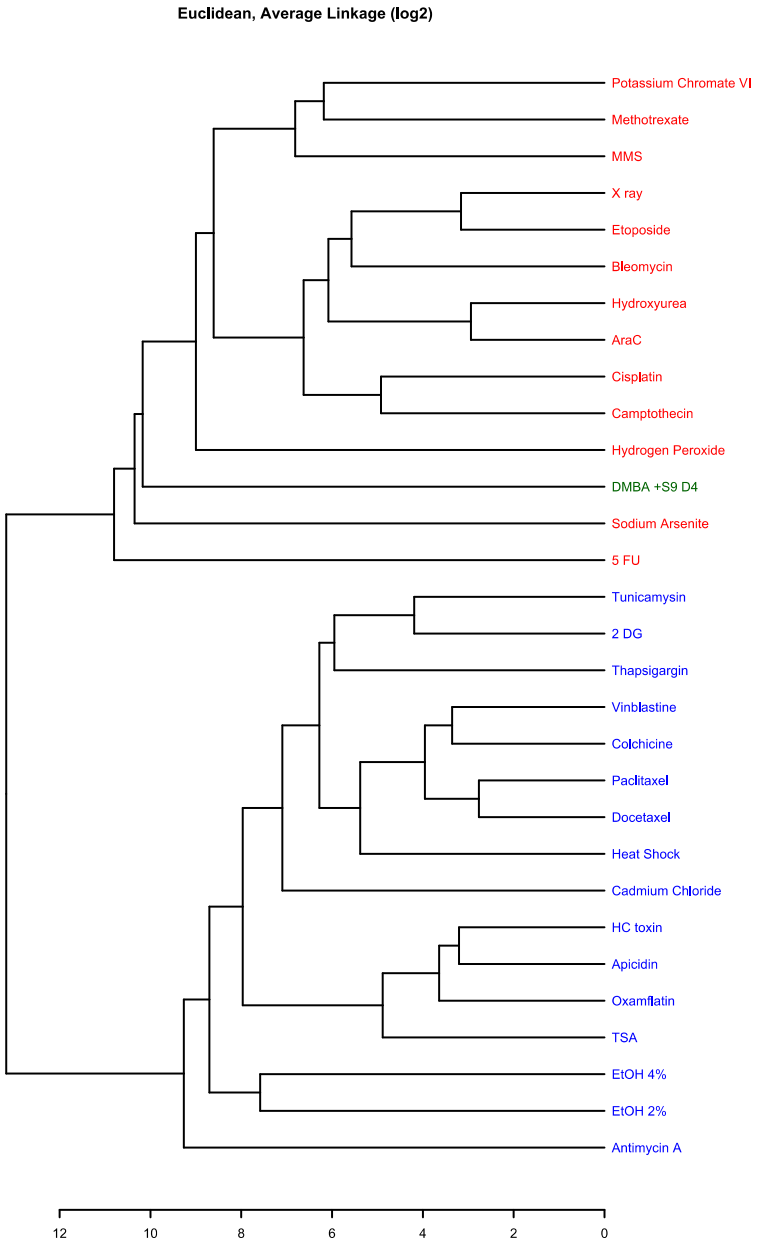
Euclidean, Average Linkage (log2)
Potassium Chromate VI
Methotrexate
MMS
X ray
Etoposide
Bleomycin
Hydroxyurea
AraC
Cisplatin
Camptothecin
Hydrogen Peroxide
DMBA +S9 D4
Sodium Arsenite
5 FU
Tunicamycin
2 DG
Thapsigargin
Vinblastine
Colchicine
Paclitaxel
Docetaxel
Heat Shock
Cadmium Chloride
HC toxin
Apicidin
Oxamflatin
TSA
EtOH 4%
EtOH 2%
Antimycin A
12
10
8
6
4
2
0

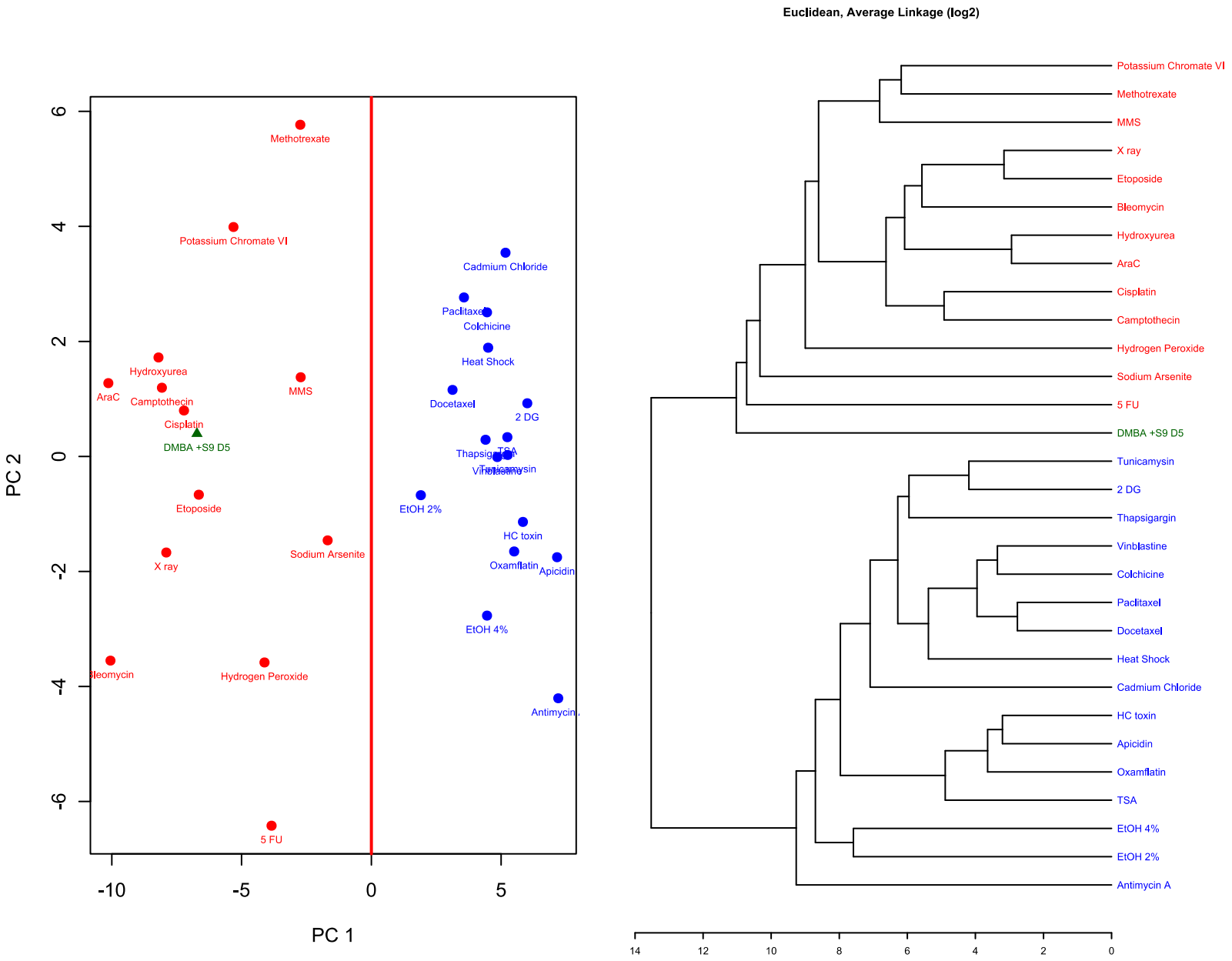

Supplementary Figure III-Q: DMBA (+S9) TGx-DDI biomarker classification using the Principal Component Analysis (PCA) (left) and hierarchical clustering (right) statistical analyses. Genotoxic reference chemicals are shown in red text, non-genotoxic reference chemicals are shown in blue text, and the test agent is shown in the green text. The line drawn on the PCA plot and the main branch on the dendogram divides the genotoxic and non-genotoxic agents and was used to classify the test compounds. D1 represents the lowest concentration tested, D5 the highest.

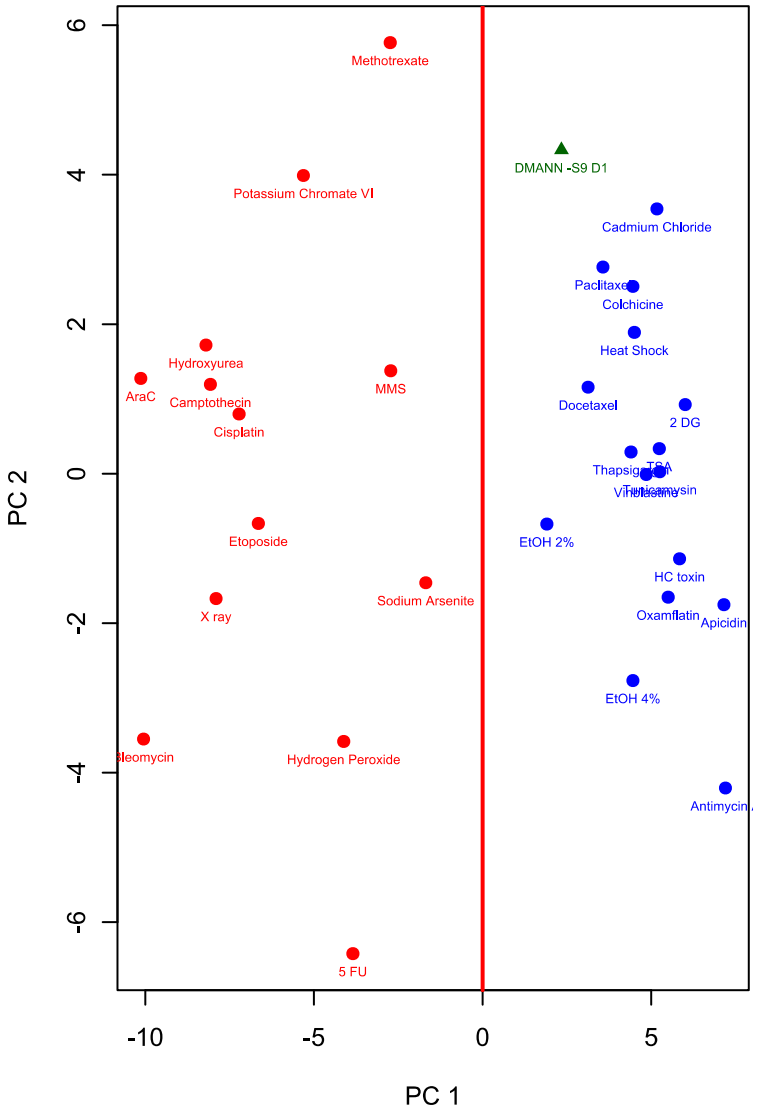
Methotrexate
Potassium Chromate VI
Hydroxyurea
AraC
Camptothecin
Cisplatin
MMS
Etoposide
X ray
Sodium Arsenite
Bleomycin
Hydrogen Peroxide
5 FU
DMANN -S9 D1
Cadmium Chloride
Paclitaxel
Colchicine
Heat Shock
Docetaxel
2 DG
Thapsigargin
TSA
Vinblastine
Tunicamysin
EtOH 2%
HC toxin
Oxamflatin
Apicidin
EtOH 4%
Antimycin
PC 2
PC 1
6
4
2
0
-2
-4
-6
-10
-5
0
5

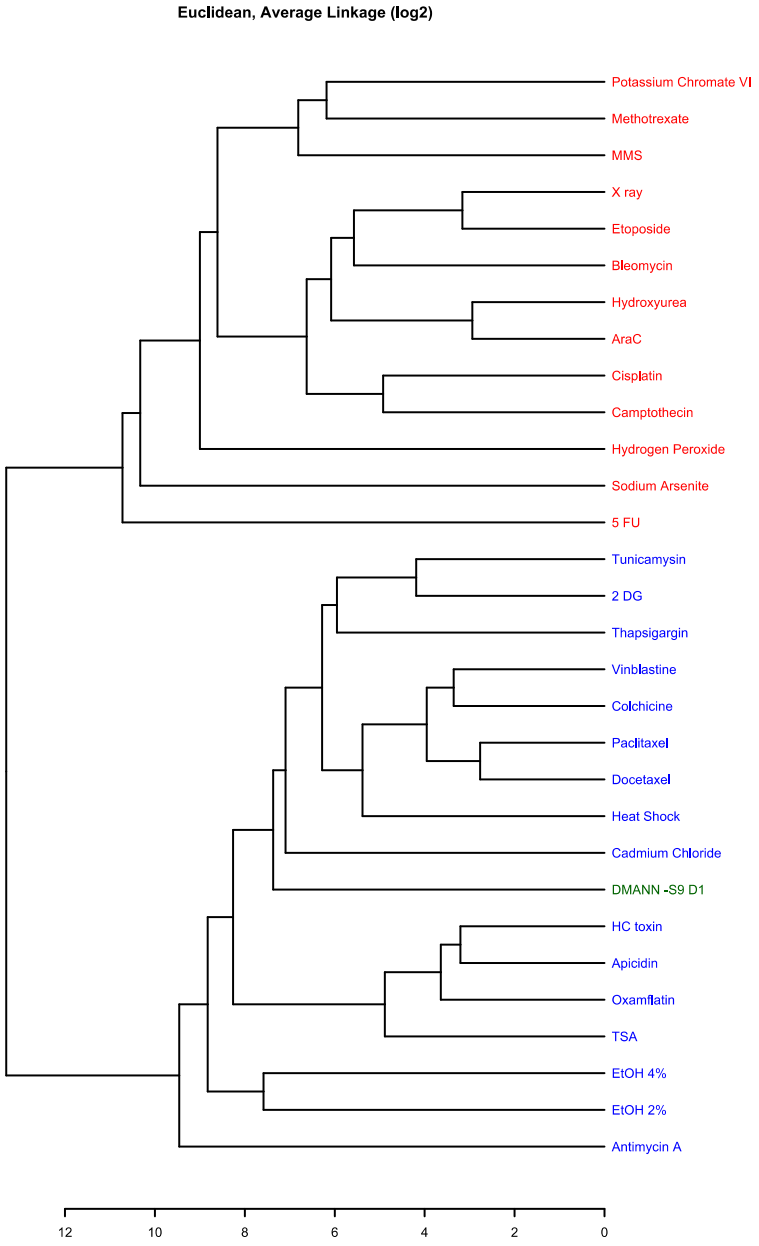
Euclidean, Average Linkage (log2)
Potassium Chromate VI
Methotrexate
MMS
X ray
Etoposide
Bleomycin
Hydroxyurea
AraC
Cisplatin
Camptothecin
Hydrogen Peroxide
Sodium Arsenite
5 FU
Tunicamysin
2 DG
Thapsigargin
Vinblastine
Colchicine
Paclitaxel
Docetaxel
Heat Shock
Cadmium Chloride
DMANN -S9 D1
HC toxin
Apicidin
Oxamflatin
TSA
EtOH 4%
EtOH 2%
Antimycin A
12
10
8
6
4
2
0

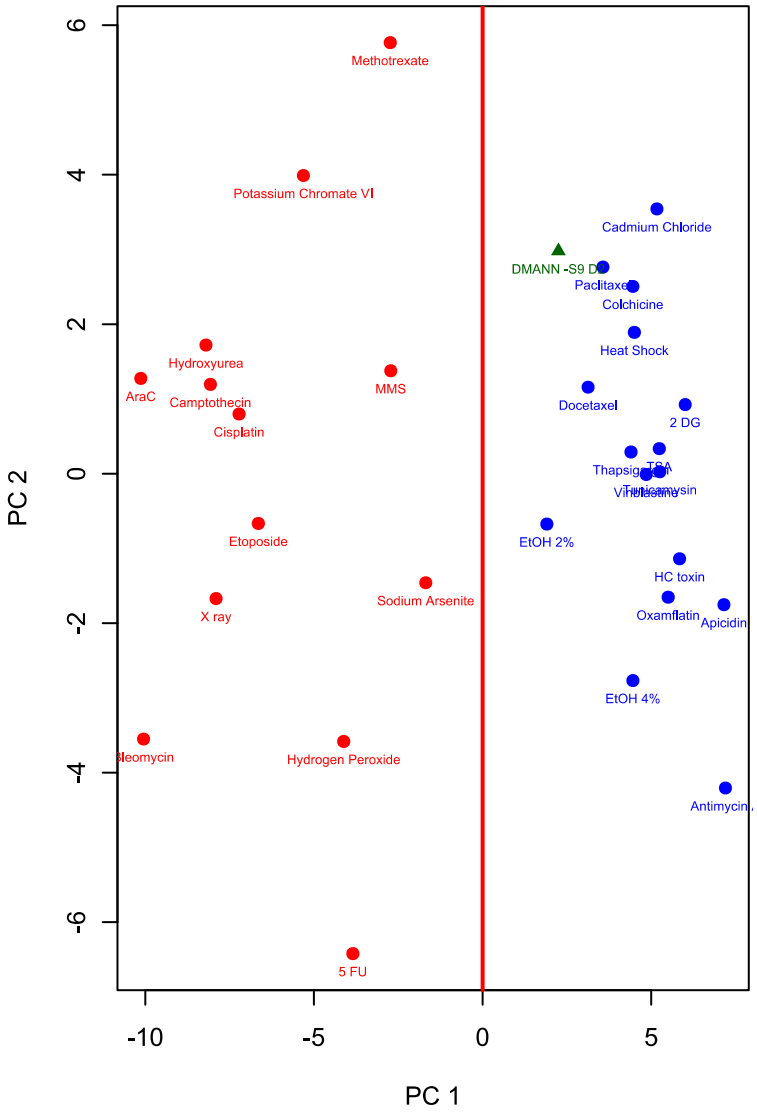
Methotrexate
Potassium Chromate VI
Cadmium Chloride
DMANN -S9 D2
Paclitaxel
Colchicine
Heat Shock
Hydroxyurea
AraC
Camptothecin
Cisplatin
MMS
Docetaxel
2 DG
Thapsigargin
TSA
Vinblastine
Tunicamysin
Etoposide
EtOH 2%
HC toxin
Sodium Arsenite
X ray
Oxamflatin
Apicidin
EtOH 4%
Bleomycin
Hydrogen Peroxide
Antimycin
5 FU
PC 2
PC 1
6
4
2
0
-2
-4
-6
-10
-5
0
5

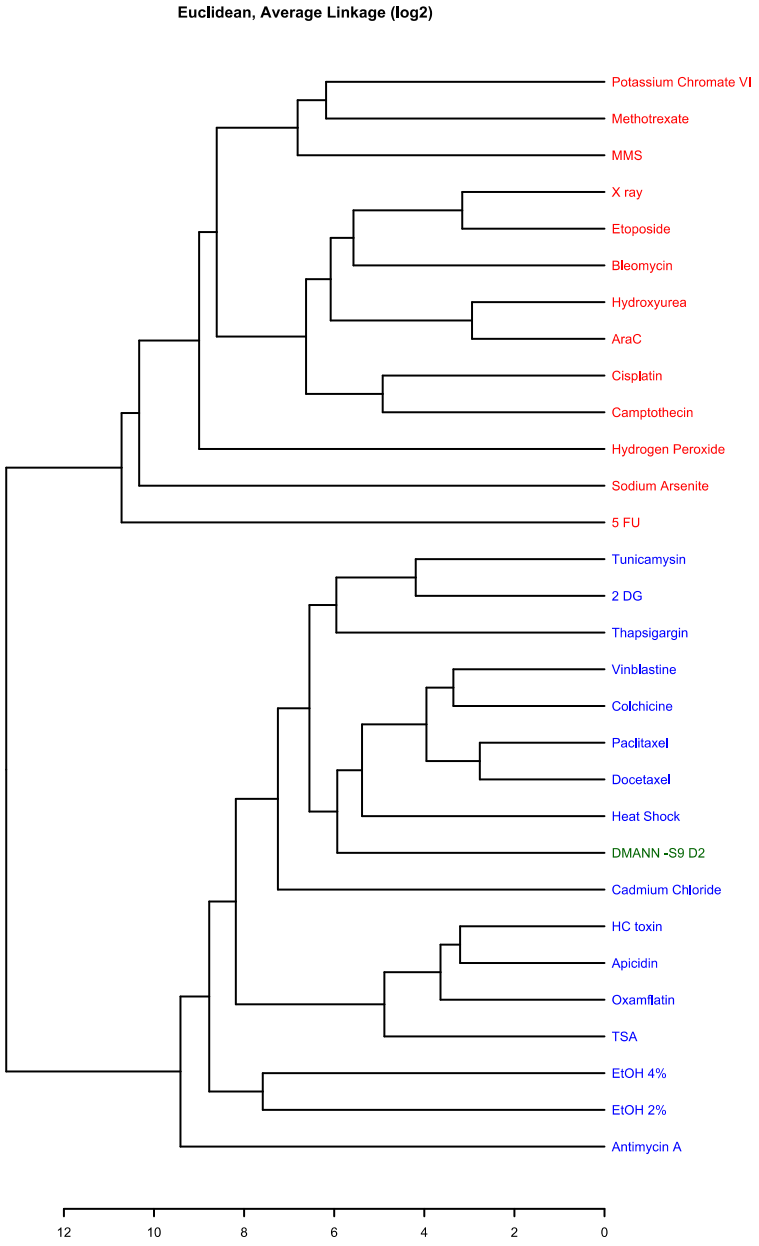
Euclidean, Average Linkage (log2)
Potassium Chromate VI
Methotrexate
MMS
X ray
Etoposide
Bleomycin
Hydroxyurea
AraC
Cisplatin
Camptothecin
Hydrogen Peroxide
Sodium Arsenite
5 FU
Tunicamysin
2 DG
Thapsigargin
Vinblastine
Colchicine
Paclitaxel
Docetaxel
Heat Shock
DMANN -S9 D2
Cadmium Chloride
HC toxin
Apicidin
Oxamflatin
TSA
EtOH 4%
EtOH 2%
Antimycin A
12
10
8
6
4
2
0

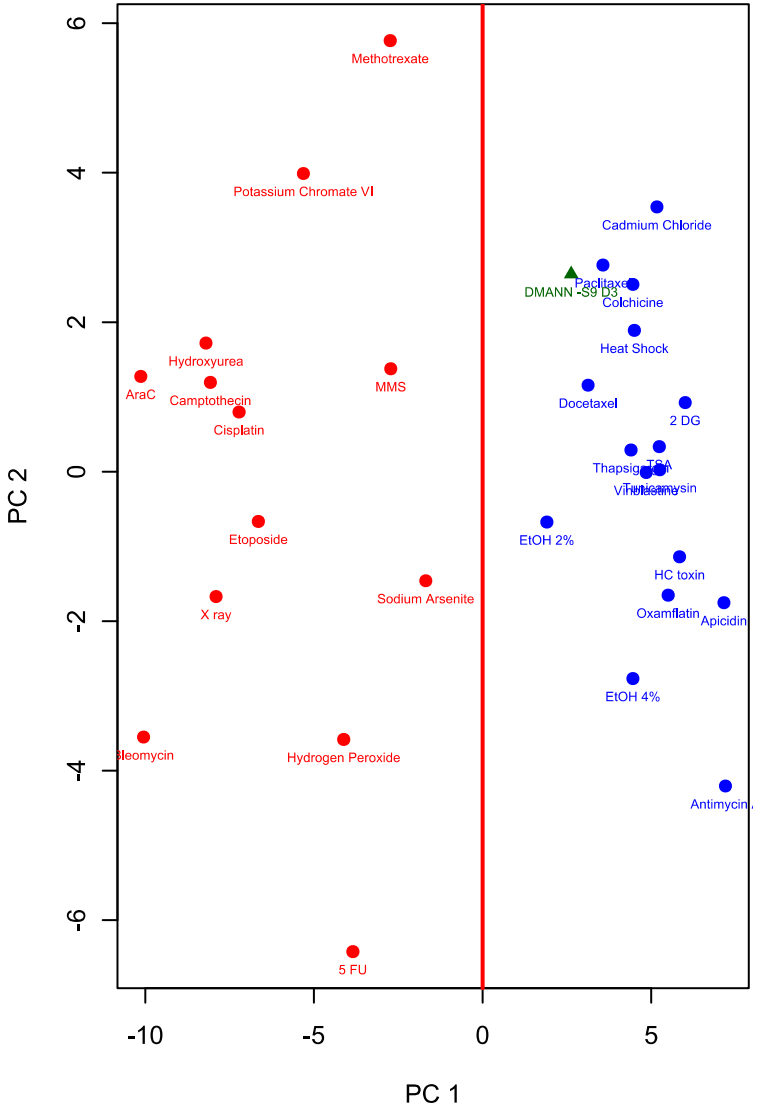
Methotrexate
Potassium Chromate VI
Cadmium Chloride
DMANN -S9 D3
Paclitaxel
Colchicine
Heat Shock
Hydroxyurea
AraC
Camptothecin
MMS
Docetaxel
2 DG
Cisplatin
Thapsigargin
TSA
Vinblastine
Tunicamysin
Etoposide
EtOH 2%
HC toxin
Sodium Arsenite
X ray
Oxamflatin
Apicidin
EtOH 4%
Bleomycin
Hydrogen Peroxide
Antimycin
5 FU
PC 2
PC 1
6
4
2
0
-2
-4
-6
-10
-5
0
5

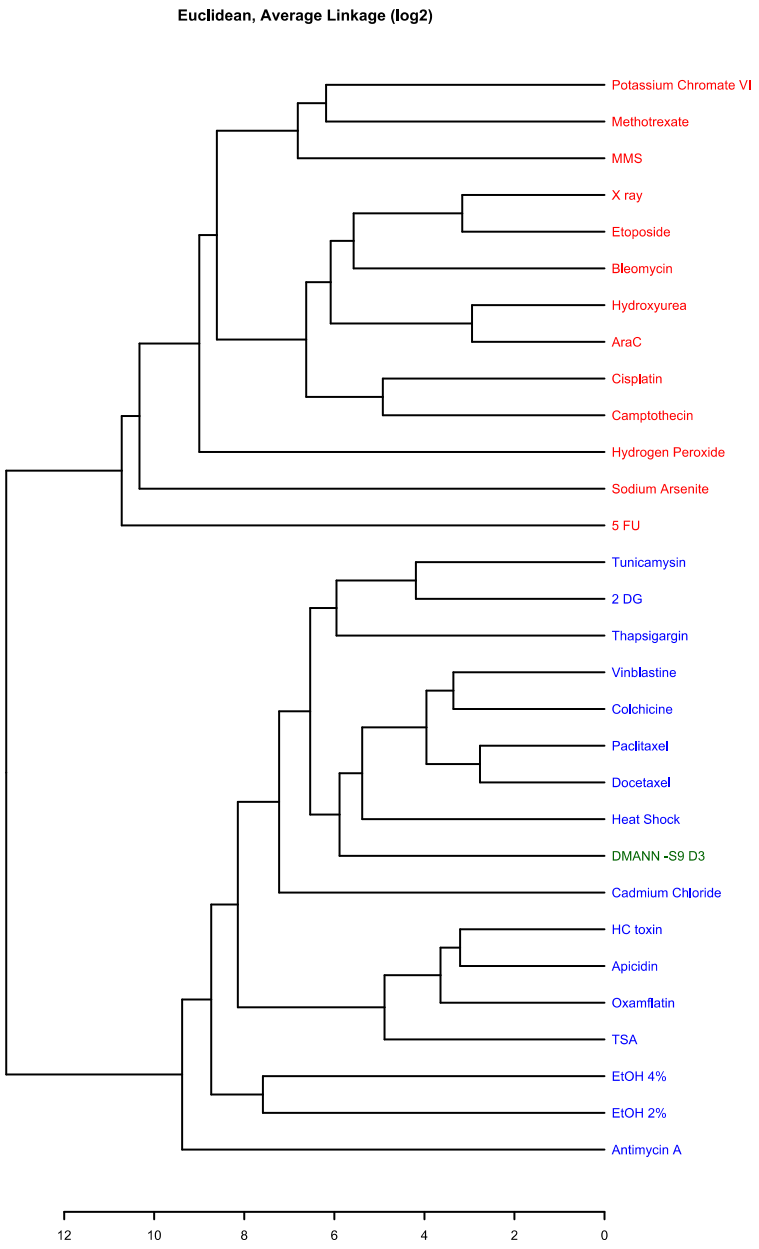
Euclidean, Average Linkage (log2)
Potassium Chromate VI
Methotrexate
MMS
X ray
Etoposide
Bleomycin
Hydroxyurea
AraC
Cisplatin
Camptothecin
Hydrogen Peroxide
Sodium Arsenite
5 FU
Tunicamysin
2 DG
Thapsigargin
Vinblastine
Colchicine
Paclitaxel
Docetaxel
Heat Shock
DMANN -S9 D3
Cadmium Chloride
HC toxin
Apicidin
Oxamflatin
TSA
EtOH 4%
EtOH 2%
Antimycin A
12
10
8
6
4
2
0

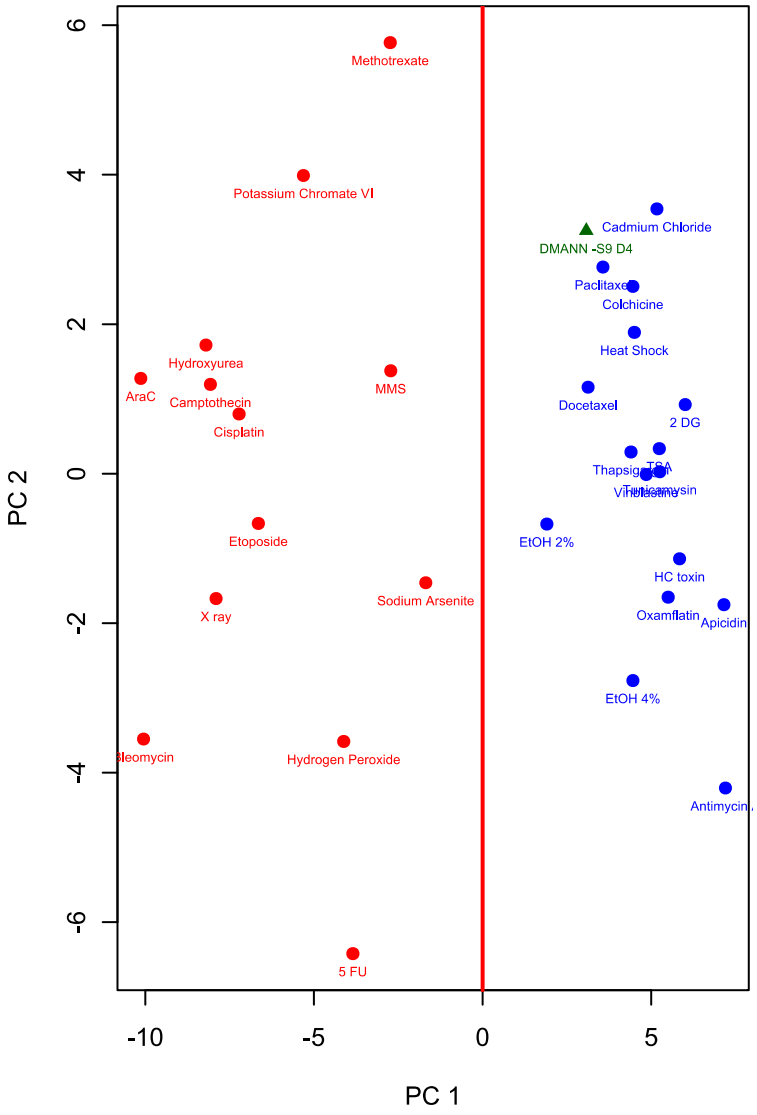
Methotrexate
Potassium Chromate VI
Hydroxyurea
AraC
Camptothecin
Cisplatin
MMS
Etoposide
X ray
Sodium Arsenite
Bleomycin
Hydrogen Peroxide
5 FU
Cadmium Chloride
DMANN -S9 D4
Paclitaxel
Colchicine
Heat Shock
Docetaxel
2 DG
Thapsigargin
TSA
Tunicamysin
Vinblastine
EtOH 2%
HC toxin
Oxamflatin
Apicidin
EtOH 4%
Antimycin
PC 2
PC 1
6
4
2
0
-2
-4
-6
-10
-5
0
5

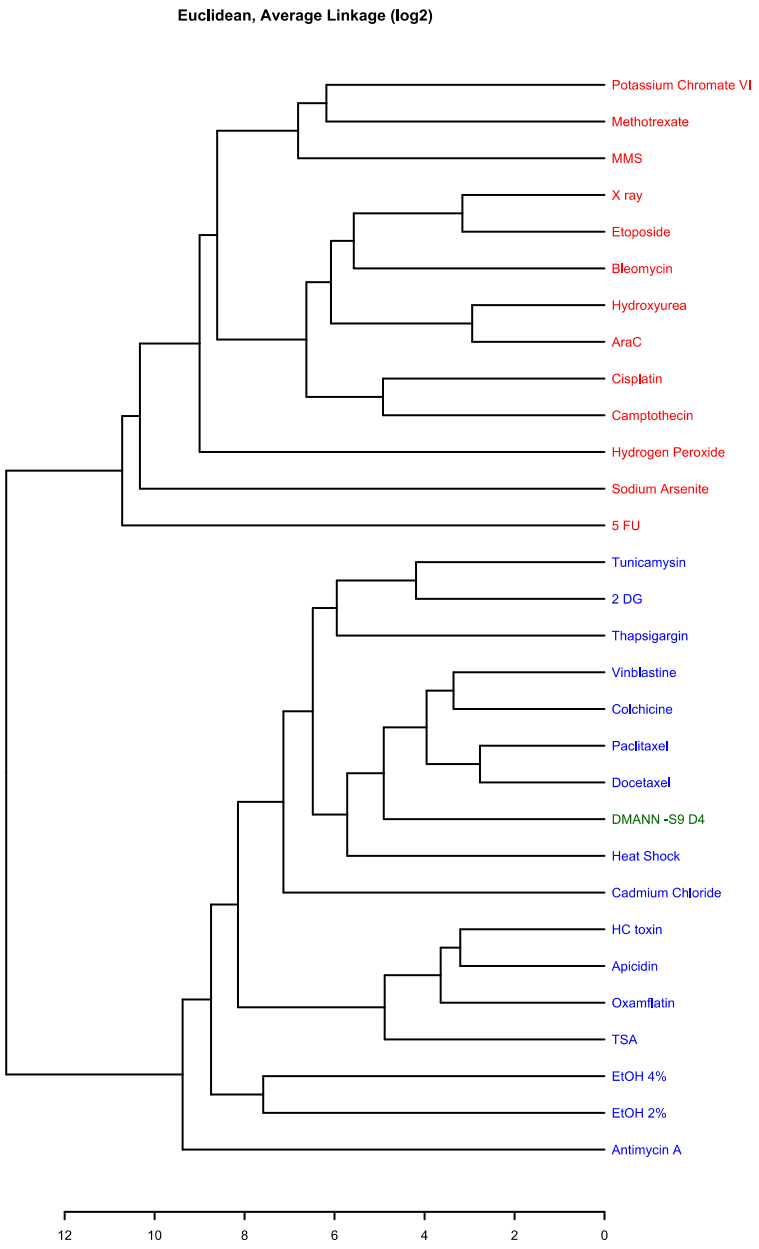
Euclidean, Average Linkage (log2)
Potassium Chromate VI
Methotrexate
MMS
X ray
Etoposide
Bleomycin
Hydroxyurea
AraC
Cisplatin
Camptothecin
Hydrogen Peroxide
Sodium Arsenite
5 FU
Tunicamysin
2 DG
Thapsigargin
Vinblastine
Colchicine
Paclitaxel
Docetaxel
DMANN -S9 D4
Heat Shock
Cadmium Chloride
HC toxin
Apicidin
Oxamflatin
TSA
EtOH 4%
EtOH 2%
Antimycin A
12
10
8
6
4
2
0

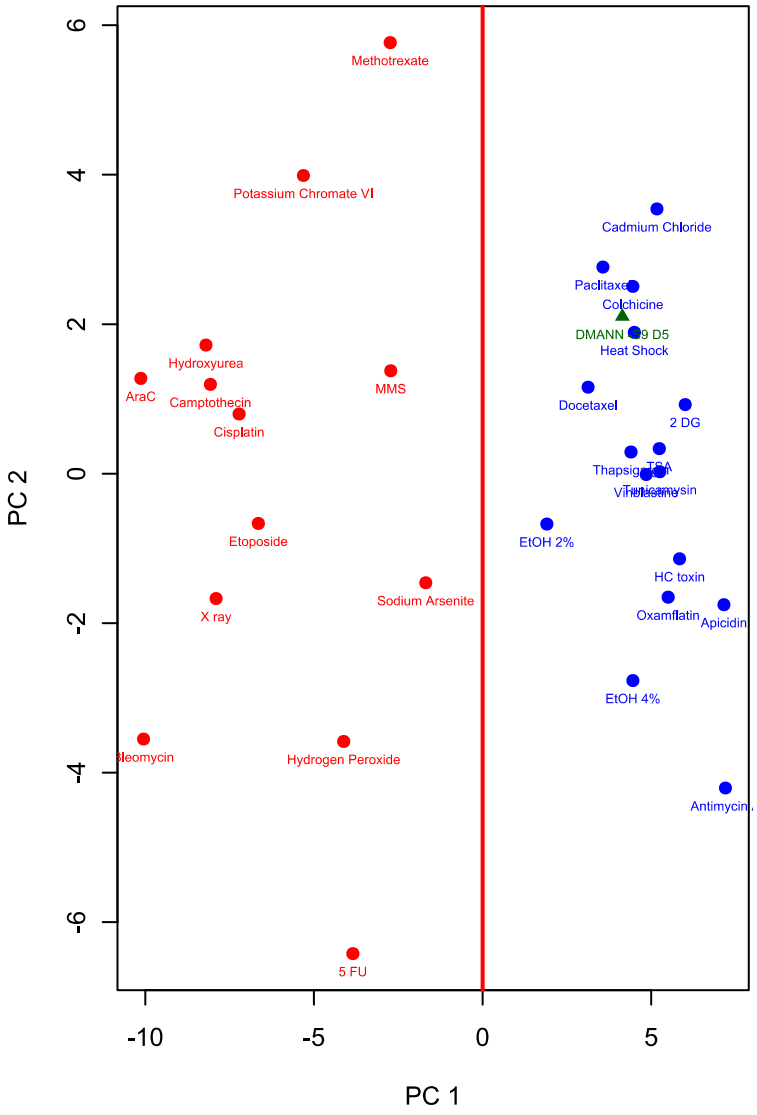
Methotrexate
Potassium Chromate VI
Cadmium Chloride
Paclitaxel
Colchicine
DMANN -S9 D5
Heat Shock
Hydroxyurea
AraC
Camptothecin
Cisplatin
MMS
Docetaxel
2 DG
Thapsigargin
TSA
Vinblastine
Tunicamysin
Etoposide
EtOH 2%
HC toxin
Sodium Arsenite
X ray
Oxamflatin
Apicidin
EtOH 4%
Bleomycin
Hydrogen Peroxide
Antimycin
5 FU
PC 2
PC 1
6
4
2
0
-2
-4
-6
-10
-5
0
5

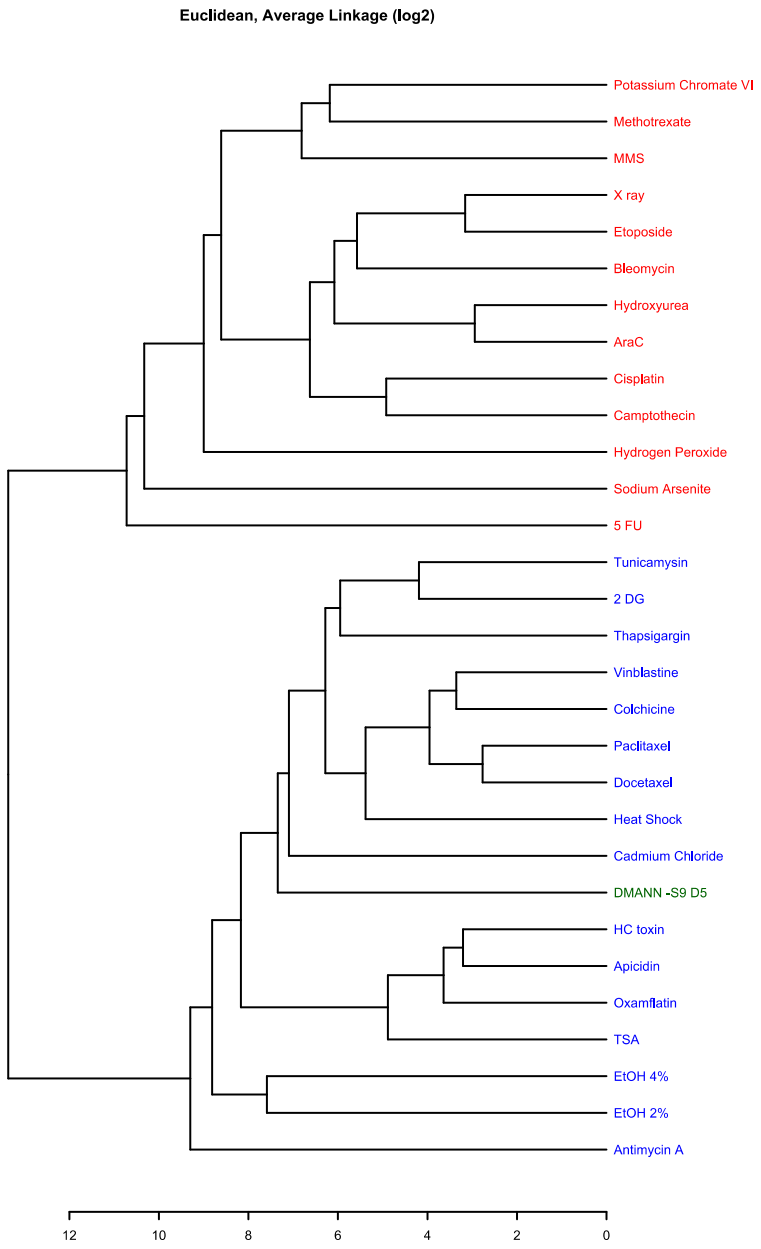
Euclidean, Average Linkage (log2)
Potassium Chromate VI
Methotrexate
MMS
X ray
Etoposide
Bleomycin
Hydroxyurea
AraC
Cisplatin
Camptothecin
Hydrogen Peroxide
Sodium Arsenite
5 FU
Tunicamysin
2 DG
Thapsigargin
Vinblastine
Colchicine
Paclitaxel
Docetaxel
Heat Shock
Cadmium Chloride
DMANN -S9 D5
HC toxin
Apicidin
Oxamflatin
TSA
EtOH 4%
EtOH 2%
Antimycin A
12
10
8
6
4
2
0

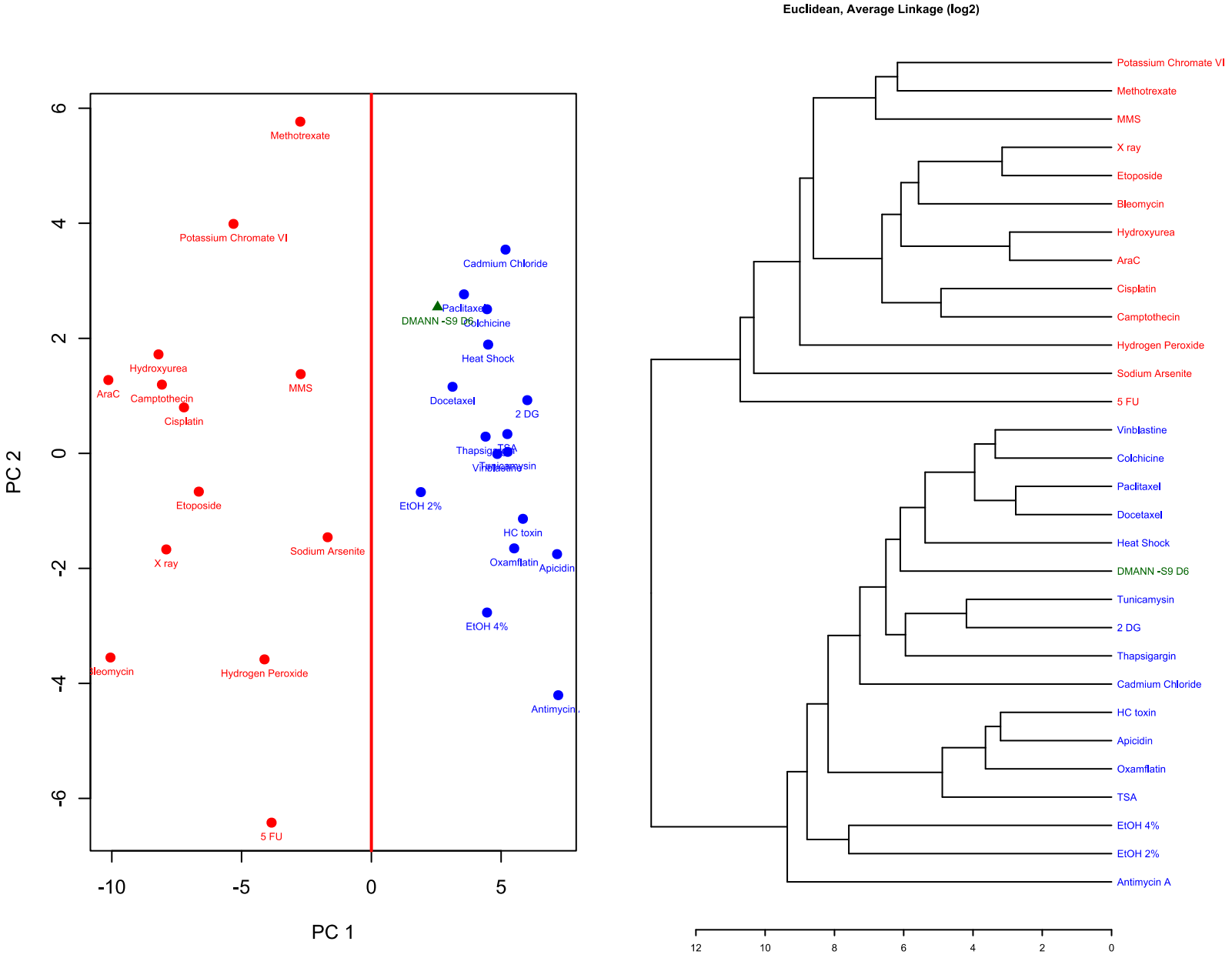

Supplementary Figure III-R: DMANN (-S9) TGx-DDI biomarker classification using the Principal Component Analysis (PCA) (left) and hierarchical clustering (right) statistical analyses. Genotoxic reference chemicals are shown in red text, non-genotoxic reference chemicals are shown in blue text, and the test agent is shown in the green text. The line drawn on the PCA plot and the main branch on the dendogram divides the genotoxic and non-genotoxic agents and was used to classify the test compounds. D1 represents the lowest concentration tested, D6 the highest.

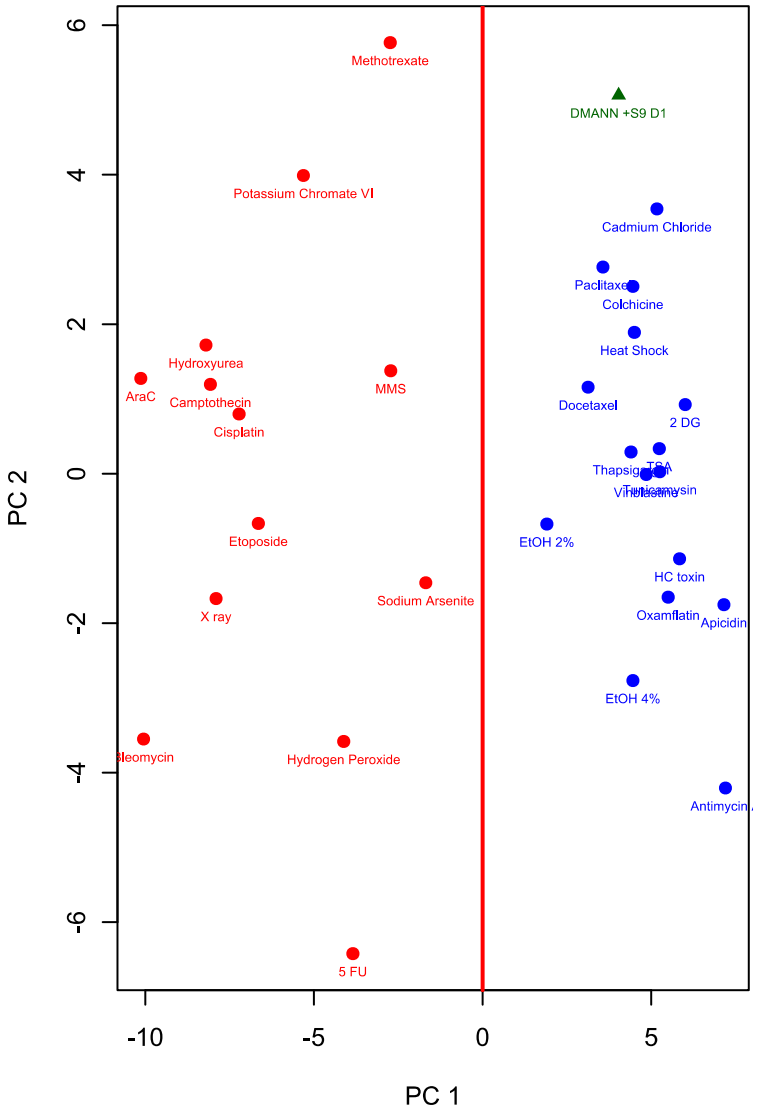
Methotrexate
DMANN +S9 D1
Potassium Chromate VI
Cadmium Chloride
Paclitaxel
Colchicine
Heat Shock
Hydroxyurea
AraC
Camptothecin
Cisplatin
MMS
Docetaxel
2 DG
Thapsigargin
TSA
Tunicamysin
Vinblastine
Etoposide
EtOH 2%
HC toxin
Sodium Arsenite
X ray
Oxamflatin
Apicidin
EtOH 4%
Bleomycin
Hydrogen Peroxide
Antimycin
5 FU
PC 2
PC 1
6
4
2
0
-2
-4
-6
-10
-5
0
5

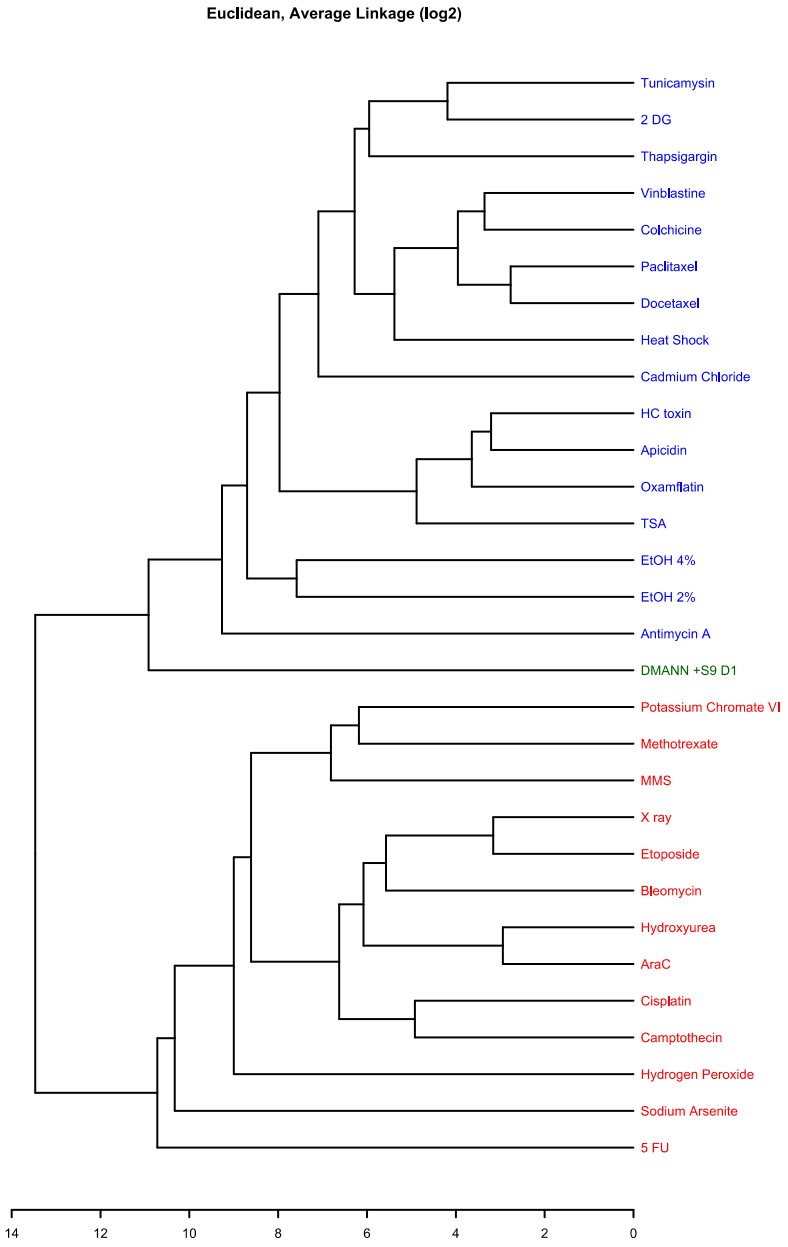
Euclidean, Average Linkage (log2)
Tunicamysin
2 DG
Thapsigargin
Vinblastine
Colchicine
Paclitaxel
Docetaxel
Heat Shock
Cadmium Chloride
HC toxin
Apicidin
Oxamflatin
TSA
EtOH 4%
EtOH 2%
Antimycin A
DMANN +S9 D1
Potassium Chromate VI
Methotrexate
MMS
X ray
Etoposide
Bleomycin
Hydroxyurea
AraC
Cisplatin
Camptothecin
Hydrogen Peroxide
Sodium Arsenite
5 FU
14
12
10
8
6
4
2
0

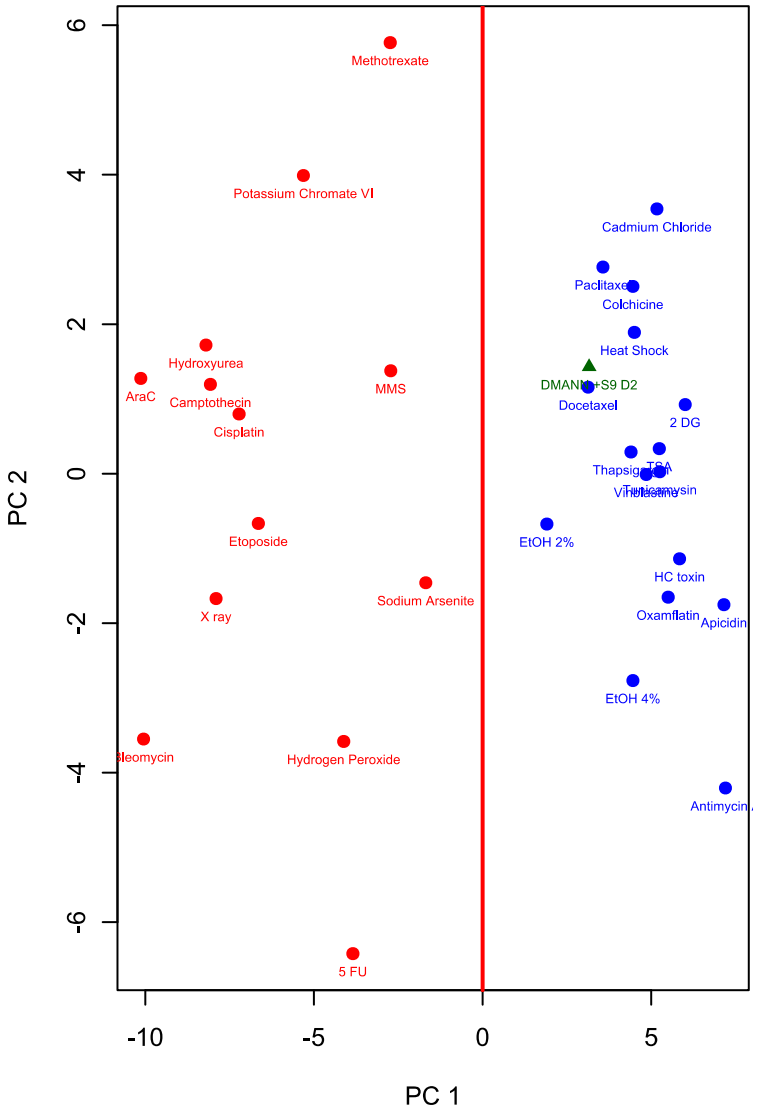
Methotrexate
Potassium Chromate VI
Cadmium Chloride
Paclitaxel
Colchicine
Heat Shock
Hydroxyurea
AraC
Camptothecin
Cisplatin
MMS
DMANN +S9 D2
Docetaxel
2 DG
Thapsigargin
TSA
Tunicamysin
Vinblastine
Etoposide
EtOH 2%
HC toxin
Sodium Arsenite
X ray
Oxamflatin
Apicidin
EtOH 4%
Bleomycin
Hydrogen Peroxide
Antimycin
5 FU
PC 1
PC 2
-10
-5
0
5
6
4
2
0
-2
-4
-6

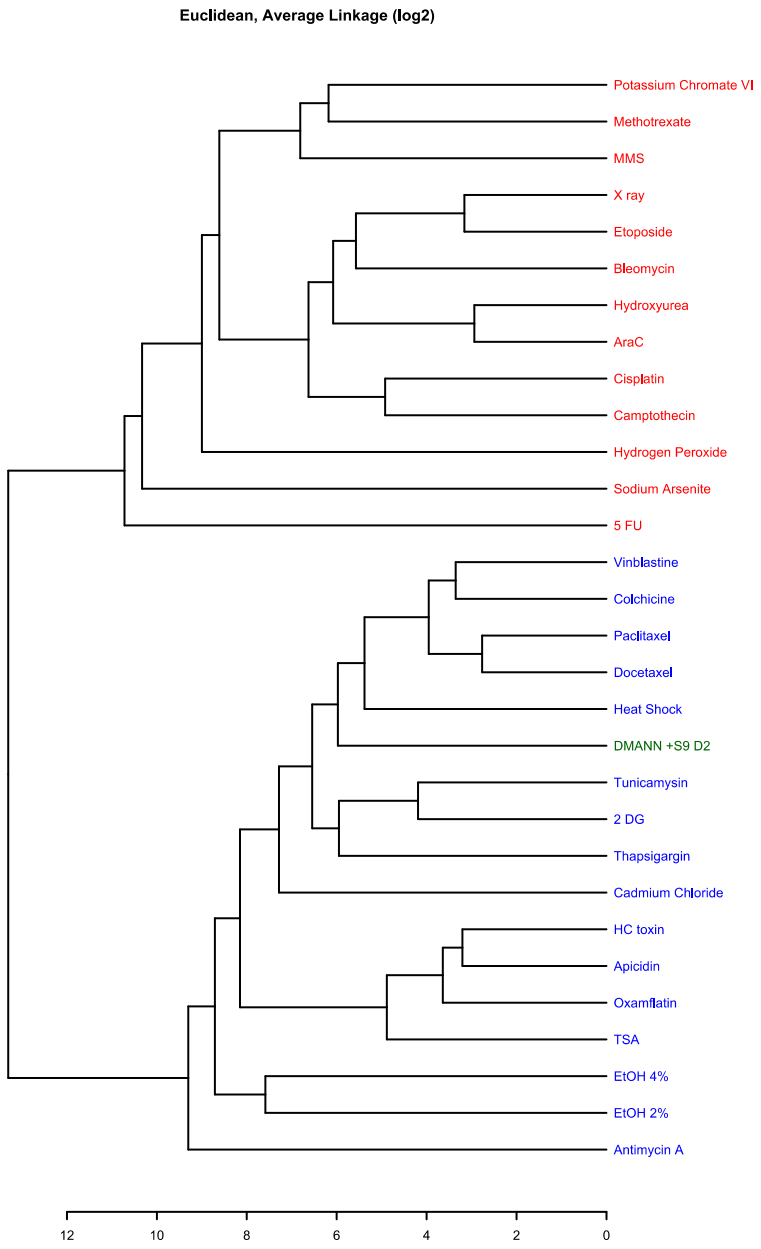
Euclidean, Average Linkage (log2)
Potassium Chromate VI
Methotrexate
MMS
X ray
Etoposide
Bleomycin
Hydroxyurea
AraC
Cisplatin
Camptothecin
Hydrogen Peroxide
Sodium Arsenite
5 FU
Vinblastine
Colchicine
Paclitaxel
Docetaxel
Heat Shock
DMANN +S9 D2
Tunicamysin
2 DG
Thapsigargin
Cadmium Chloride
HC toxin
Apicidin
Oxamflatin
TSA
EtOH 4%
EtOH 2%
Antimycin A
12
10
8
6
4
2
0

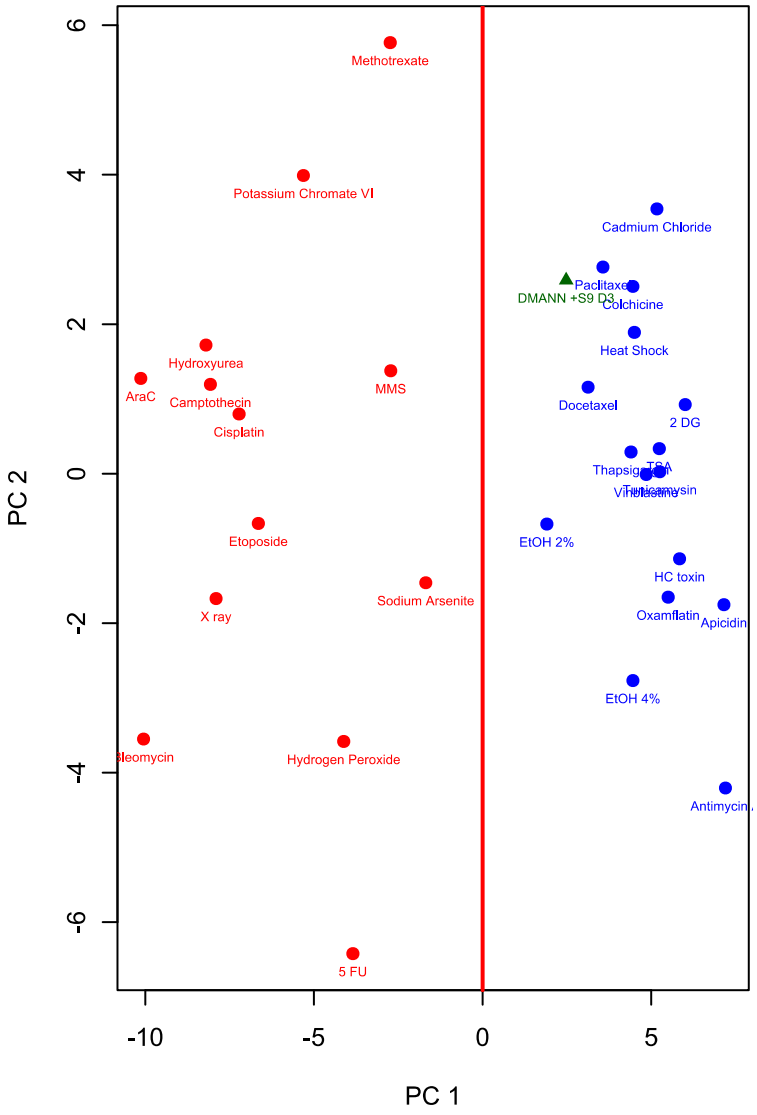
Methotrexate
Potassium Chromate VI
Cadmium Chloride
Paclitaxel
DMANN +S9 D3
Colchicine
Heat Shock
Hydroxyurea
AraC
Camptothecin
MMS
Docetaxel
2 DG
Cisplatin
Thapsigargin
TSA
Vinblastine
Tunicamysin
Etoposide
EtOH 2%
HC toxin
Sodium Arsenite
X ray
Oxamflatin
Apicidin
EtOH 4%
Bleomycin
Hydrogen Peroxide
Antimycin
5 FU
PC 2
PC 1
6
4
2
0
-2
-4
-6
-10
-5
0
5

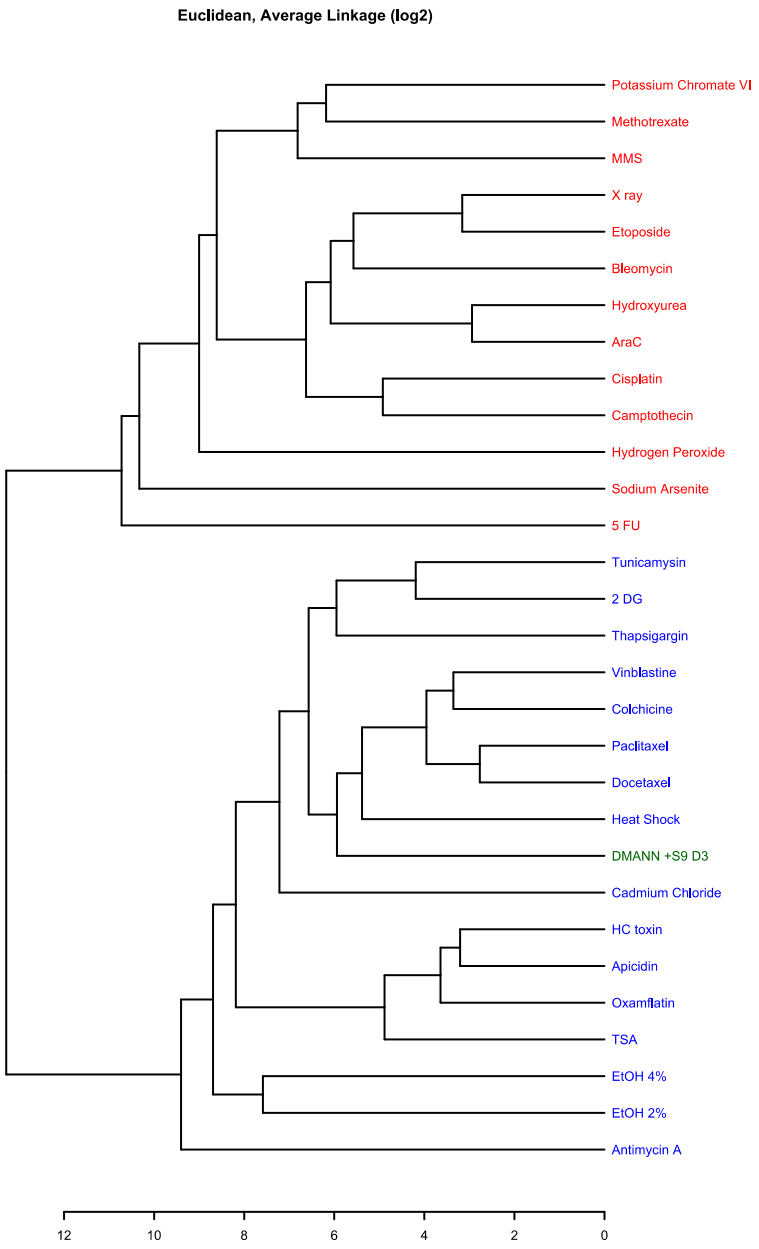
Euclidean, Average Linkage (log2)
Potassium Chromate VI
Methotrexate
MMS
X ray
Etoposide
Bleomycin
Hydroxyurea
AraC
Cisplatin
Camptothecin
Hydrogen Peroxide
Sodium Arsenite
5 FU
Tunicamysin
2 DG
Thapsigargin
Vinblastine
Colchicine
Paclitaxel
Docetaxel
Heat Shock
DMANN +S9 D3
Cadmium Chloride
HC toxin
Apicidin
Oxamflatin
TSA
EtOH 4%
EtOH 2%
Antimycin A
12
10
8
6
4
2
0

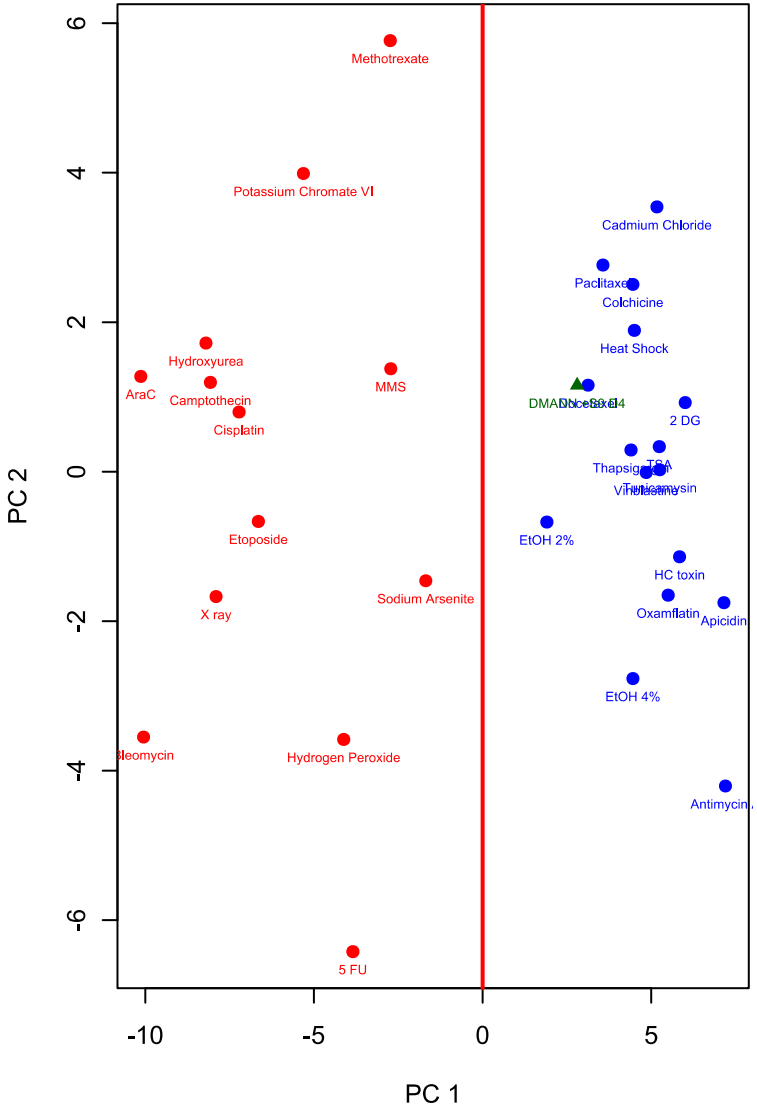
Methotrexate
Potassium Chromate VI
Cadmium Chloride
Paclitaxel
Colchicine
Heat Shock
Hydroxyurea
AraC
Camptothecin
MMS
Cisplatin
2 DG
Thapsigargin
TSA
Tunicamysin
Vinblastine
Etoposide
EtOH 2%
HC toxin
Sodium Arsenite
X ray
Oxamflatin
Apicidin
EtOH 4%
Bleomycin
Hydrogen Peroxide
Antimycin
5 FU
PC 2
PC 1
6
4
2
0
-2
-4
-6
-10
-5
0
5

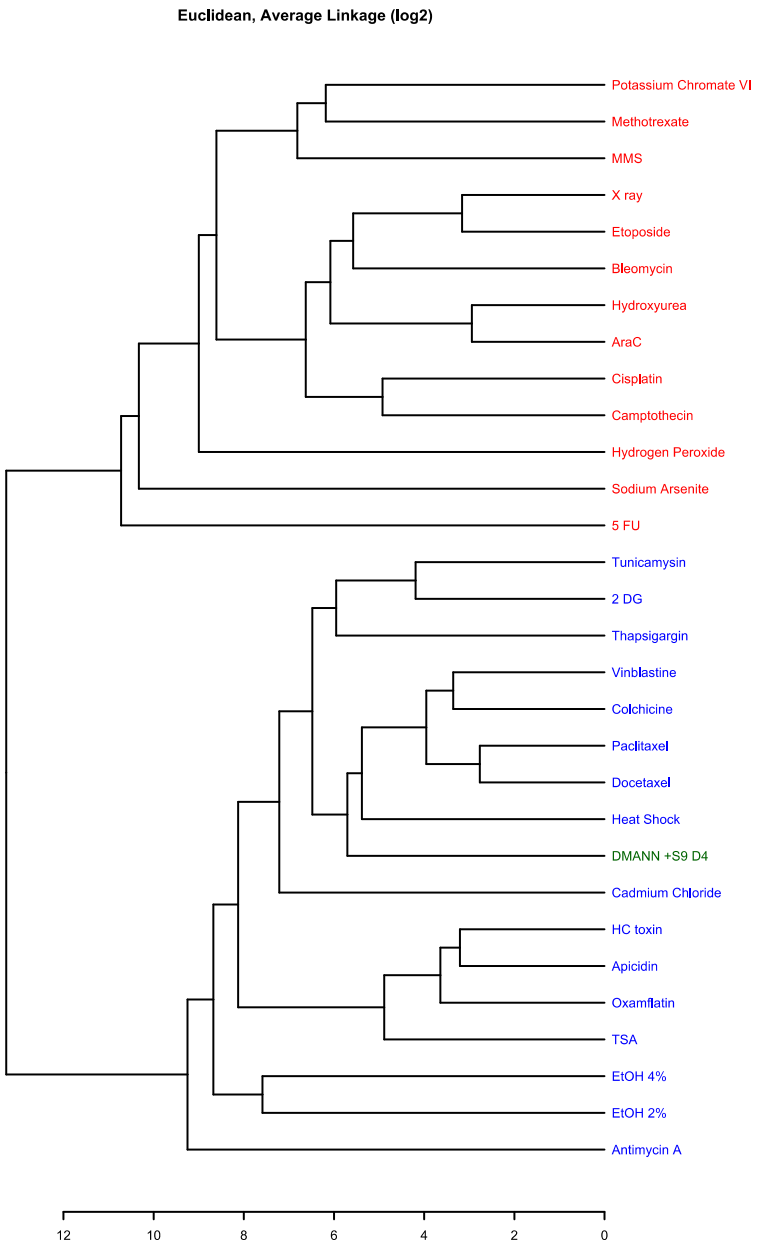
Euclidean, Average Linkage (log2)
Potassium Chromate VI
Methotrexate
MMS
X ray
Etoposide
Bleomycin
Hydroxyurea
AraC
Cisplatin
Camptothecin
Hydrogen Peroxide
Sodium Arsenite
5 FU
Tunicamysin
2 DG
Thapsigargin
Vinblastine
Colchicine
Paclitaxel
Docetaxel
Heat Shock
DMANN +S9 D4
Cadmium Chloride
HC toxin
Apicidin
Oxamflatin
TSA
EtOH 4%
EtOH 2%
Antimycin A
12
10
8
6
4
2
0

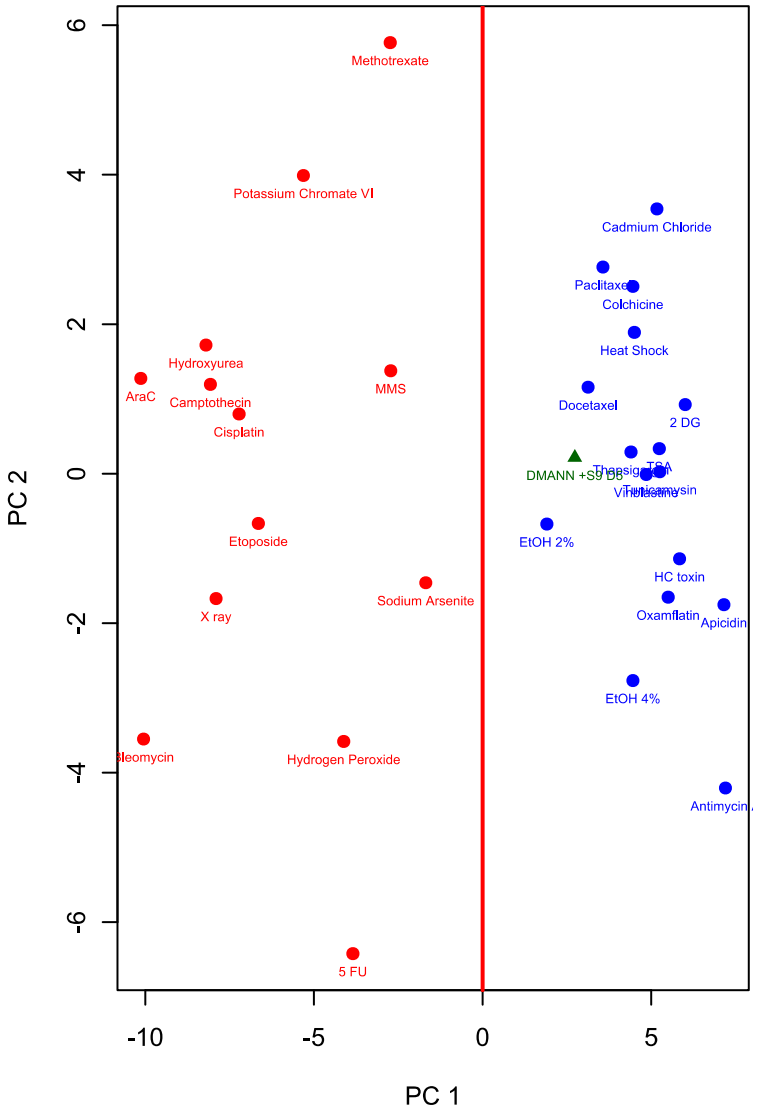
Methotrexate
Potassium Chromate VI
Cadmium Chloride
Paclitaxel
Colchicine
Heat Shock
Hydroxyurea
AraC
Camptothecin
Cisplatin
MMS
Docetaxel
2 DG
DMANN +S9 D5
Thapsigargin
TSA
Tunicamysin
Vinblastine
Etoposide
EtOH 2%
HC toxin
Sodium Arsenite
X ray
Oxamflatin
Apicidin
EtOH 4%
Bleomycin
Hydrogen Peroxide
Antimycin
5 FU
PC 2
PC 1
6
4
2
0
-2
-4
-6
-10
-5
0
5

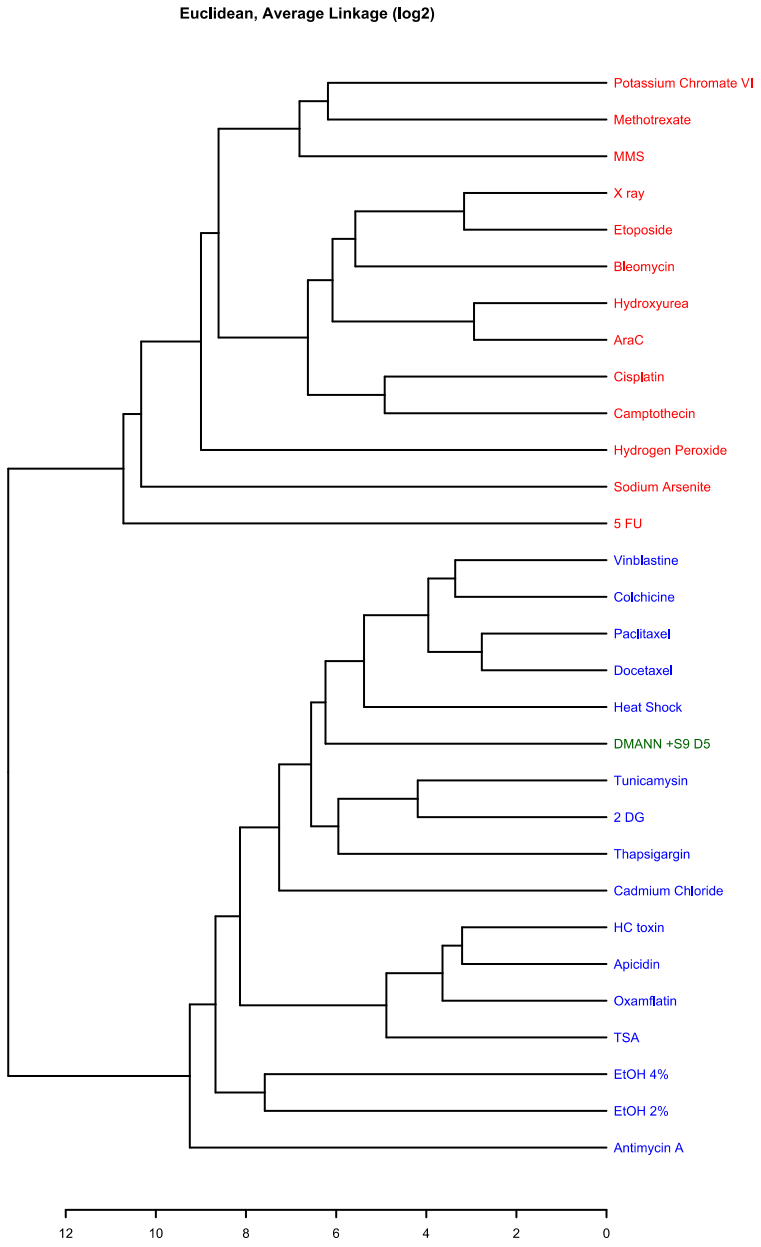
Euclidean, Average Linkage (log2)
Potassium Chromate VI
Methotrexate
MMS
X ray
Etoposide
Bleomycin
Hydroxyurea
AraC
Cisplatin
Camptothecin
Hydrogen Peroxide
Sodium Arsenite
5 FU
Vinblastine
Colchicine
Paclitaxel
Docetaxel
Heat Shock
DMANN +S9 D5
Tunicamysin
2 DG
Thapsigargin
Cadmium Chloride
HC toxin
Apicidin
Oxamflatin
TSA
EtOH 4%
EtOH 2%
Antimycin A
12
10
8
6
4
2
0

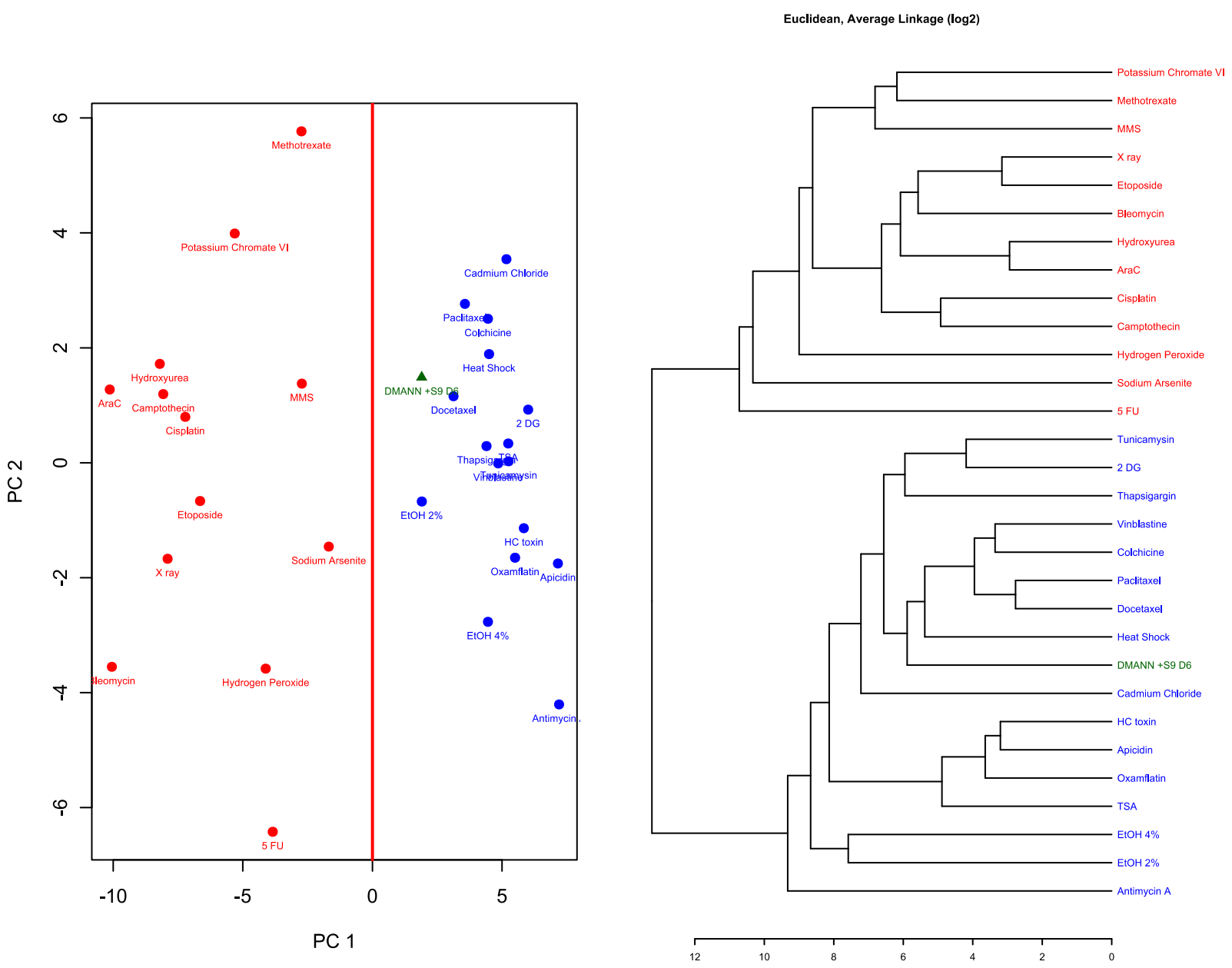

Supplementary Figure III-S: DMANN (+S9) TGx-DDI biomarker classification using the Principal Component Analysis (PCA) (left) and hierarchical clustering (right) statistical analyses. Genotoxic reference chemicals are shown in red text, non-genotoxic reference chemicals are shown in blue text, and the test agent is shown in the green text. The line drawn on the PCA plot and the main branch on the dendogram divides the genotoxic and non-genotoxic agents and was used to classify the test compounds. D1 represents the lowest concentration tested, D6 the highest.

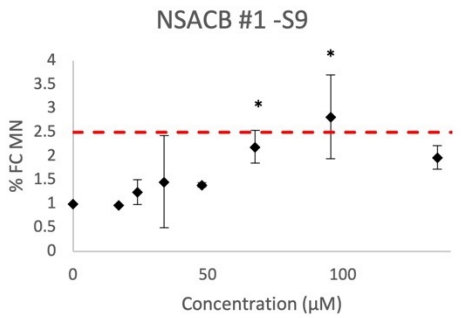
NSACB #1 -S9
% FC MN
Concentration (μM)

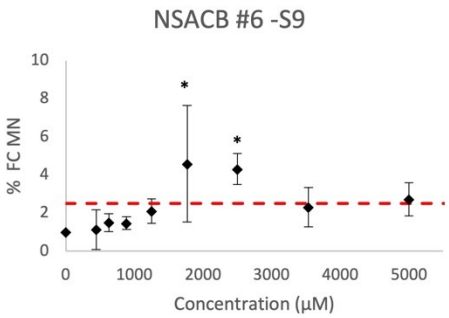
NSACB #6 -S9
% FC MN
Concentration (μM)

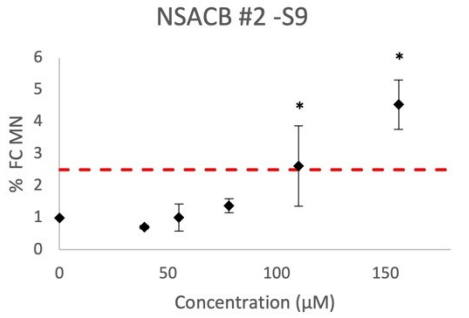
NSACB #2 -S9
% FC MN
Concentration (μM)

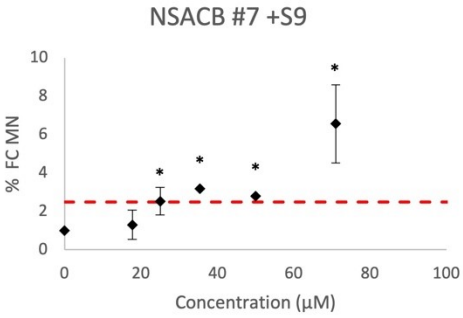
NSACB #7 +S9
% FC MN
Concentration (μM)

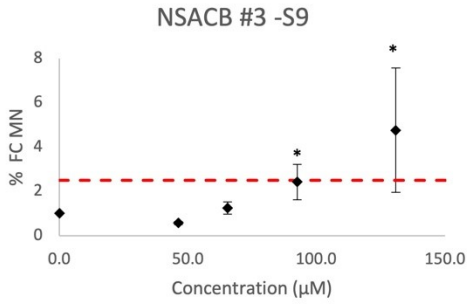
NSACB #3 -S9
% FC MN
Concentration (μM)

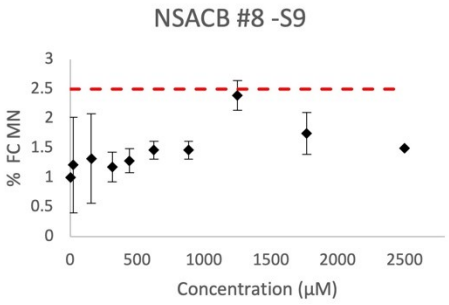
NSACB #8 -S9
% FC MN
Concentration (μM)

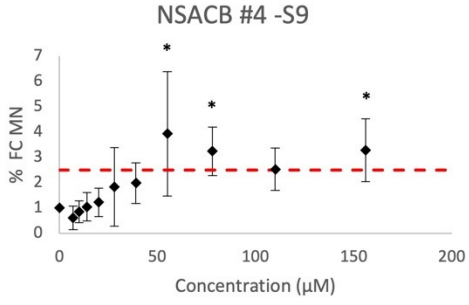
NSACB #4 -S9
% FC MN
Concentration (μM)

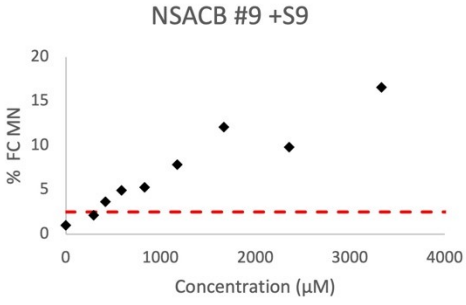
NSACB #9 +S9
% FC MN
Concentration (μM)

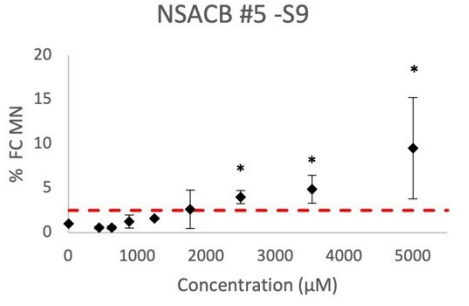
NSACB #5 -S9
% FC MN
Concentration (μM)

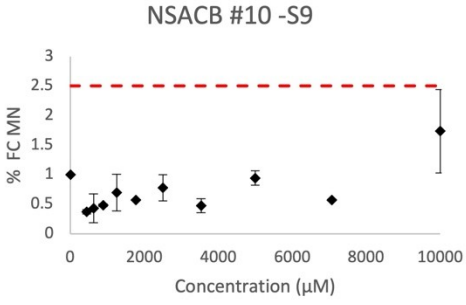
NSACB #10 -S9
% FC MN
Concentration (μM)

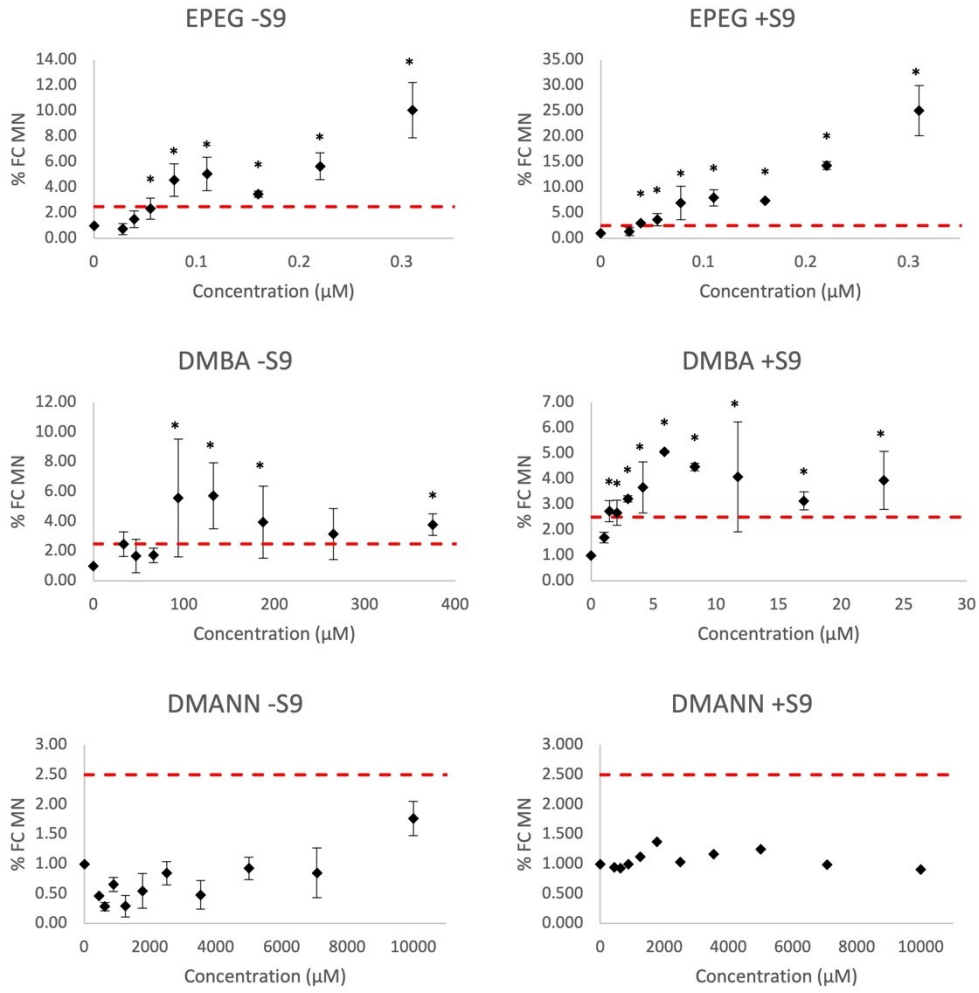

Supplementary Figure IV: In vitro MicroFlow® assay results for ten NSACB data-poor substances (#1-10) and control chemicals. Fold-increase in % micronucleus (MN) compared to vehicle control is depicted by black diamonds. The dashed red line shows the 2.5-fold threshold required in %MN to yield a positive classification. Statistically significant increases ($p < 0.05$) are designated by an asterisk (*). Cytotoxic concentrations (<40% viability) were removed from the analysis. Error bars denote standard deviation from mean. N=2.

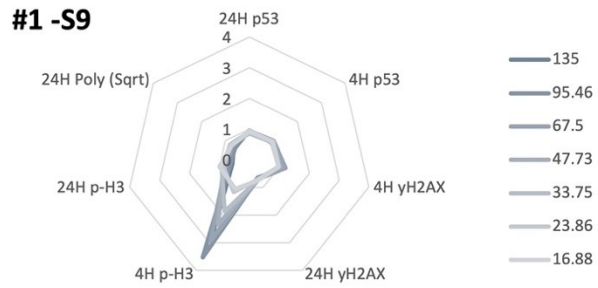
#1 -S9
24H p53
4H p53
4H yH2AX
24H yH2AX
4H p-H3
24H p-H3
24H Poly (Sqrt)
135
95.46
67.5
47.73
33.75
23.86
16.88


#6 -S9
24H p53
4H p53
4H yH2AX
24H yH2AX
4H p-H3
24H p-H3
24H Poly (Sqrt)
5,000.0
3,535.5
2,500.0
1,767.8
1,250.0
883.9
625.0
441.9

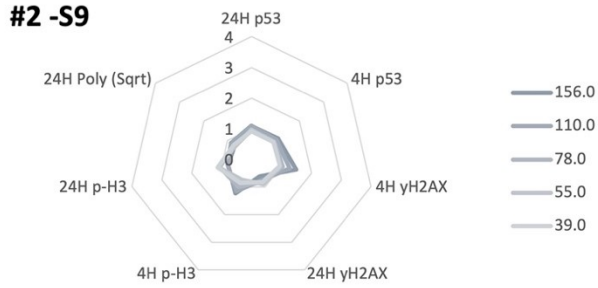
#2 -S9
24H p53
4H p53
4H yH2AX
24H yH2AX
4H p-H3
24H p-H3
24H Poly (Sqrt)
156.0
110.0
78.0
55.0
39.0

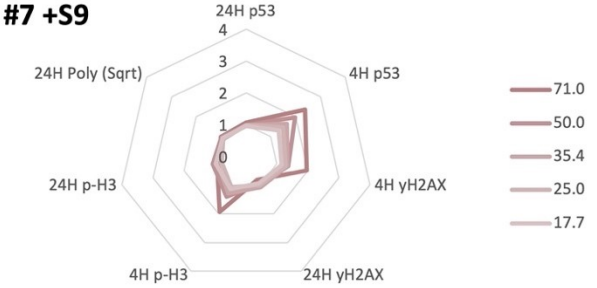
#7 +S9
24H p53
4H p53
4H yH2AX
24H yH2AX
4H p-H3
24H p-H3
24H Poly (Sqrt)
71.0
50.0
35.4
25.0
17.7

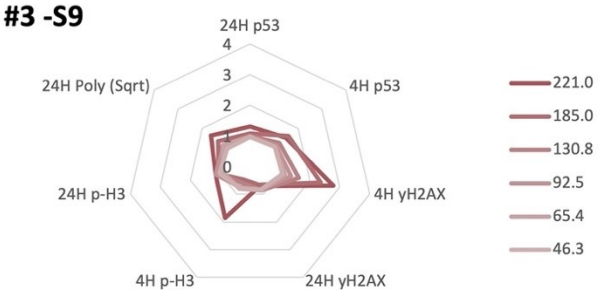
#3 -S9
24H p53
4H p53
4H yH2AX
24H yH2AX
4H p-H3
24H p-H3
24H Poly (Sqrt)
221.0
185.0
130.8
92.5
65.4
46.3


#8 -S9
24H p53
4H p53
4H yH2AX
24H yH2AX
4H p-H3
24H p-H3
24H Poly (Sqrt)
2500
1768
1250
884
625
442
313
221
156.3

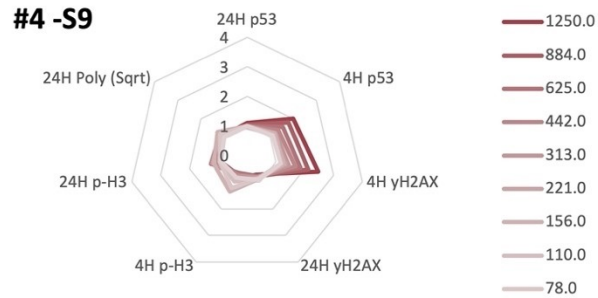
#4 -S9
24H p53
4H p53
4H yH2AX
24H yH2AX
4H p-H3
24H p-H3
24H Poly (Sqrt)
1250.0
884.0
625.0
442.0
313.0
221.0
156.0
110.0
78.0

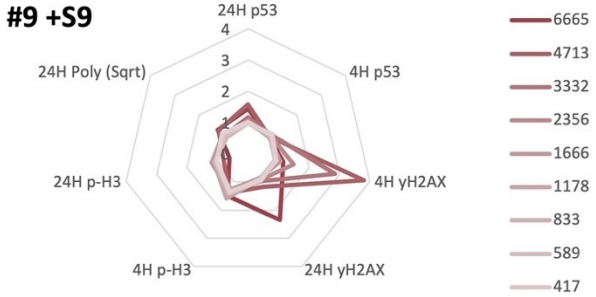
#9 +S9
24H p53
4H p53
4H yH2AX
24H yH2AX
4H p-H3
24H p-H3
24H Poly (Sqrt)
6665
4713
3332
2356
1666
1178
833
589
417

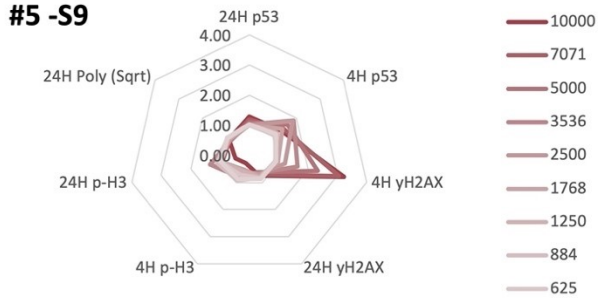
#5 -S9
24H p53
4H p53
4H yH2AX
24H yH2AX
4H p-H3
24H p-H3
24H Poly (Sqrt)
10000
7071
5000
3536
2500
1768
1250
884
625

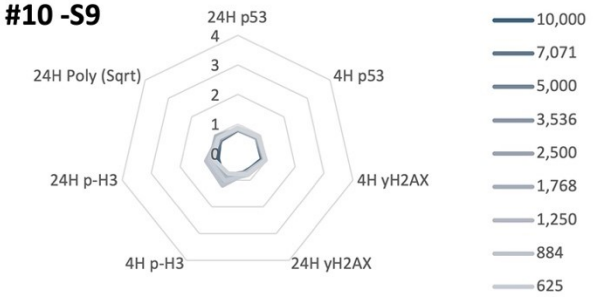
#10 -S9
24H p53
4H p53
4H yH2AX
24H yH2AX
4H p-H3
24H p-H3
24H Poly (Sqrt)
10,000
7,071
5,000
3,536
2,500
1,768
1,250
884
625

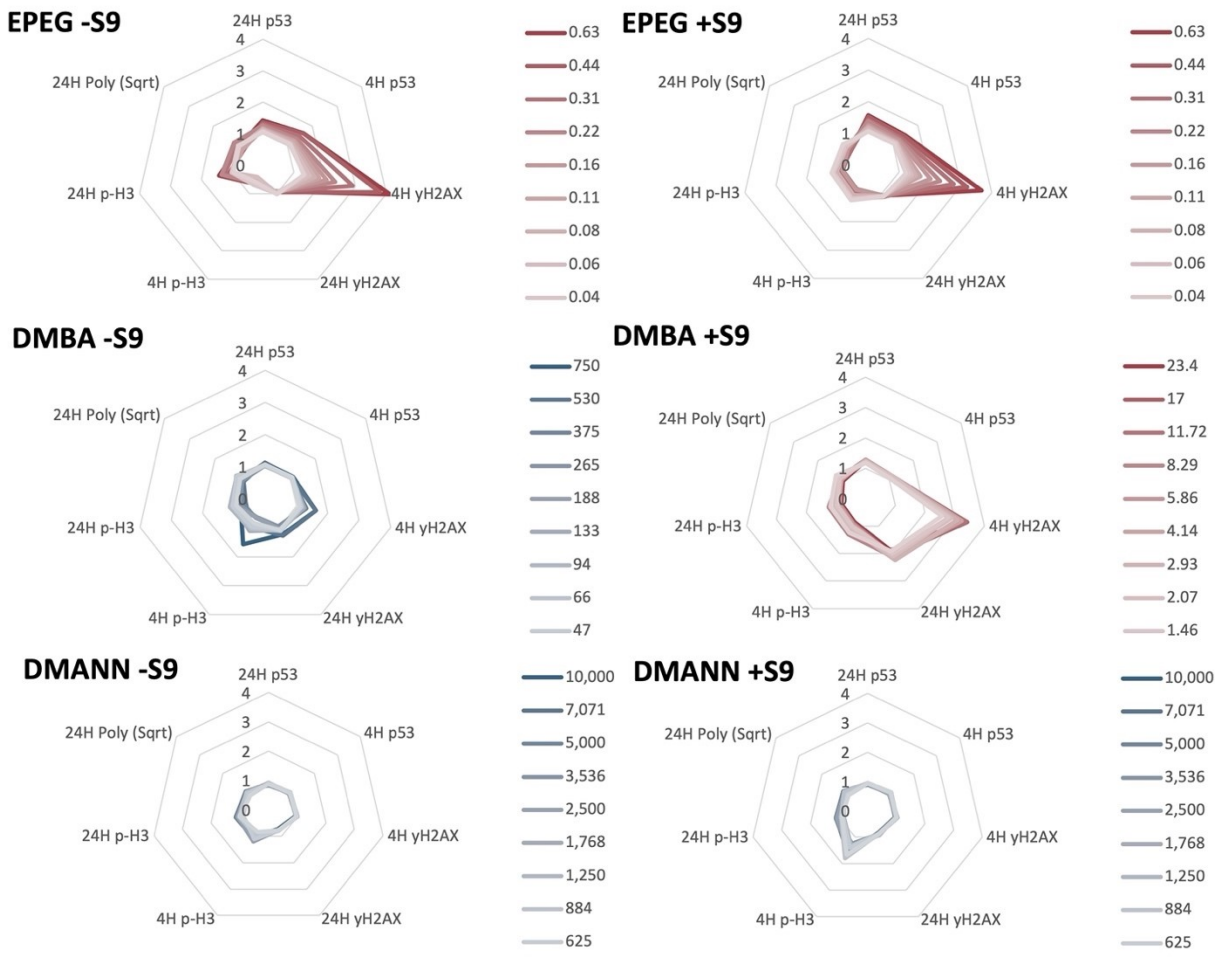

Supplementary Figure V: MultiFlow® DNA Damage assay classification results for ten NSACB data-poor substances (#1-10) and control chemicals. Each radar plot shows the seven biomarkers predicting the predominant mode of action (MoA) for each chemical. Clastogen MoA biomarkers are on the right: 4H p53, 4H γH2AX, 24H p53, and 24H γH2AX. Aneugen MoA biomarkers are on the left: 4H p-H3, 24H p-H3, 24H Polyploidy, and 24H p53. The biomarker data are expressed as a fold-increase over the mean solvent control for each non-cytotoxic concentration (<20% viability) represented by lines with different colour intensities (as shown in the legend). The line colour in each plot represents the classification call: clastogens are red, non-genotoxicants are blue, and pan-genotoxicants are orange. Chemicals meeting or exceeding the Global Evaluation Factors (GEFs) in at least one concentration in two MoA-specific biomarkers were classified as aneugenic or clastogenic, or classified as pan-genotoxic if both the aneugen and clastogen criteria were met.

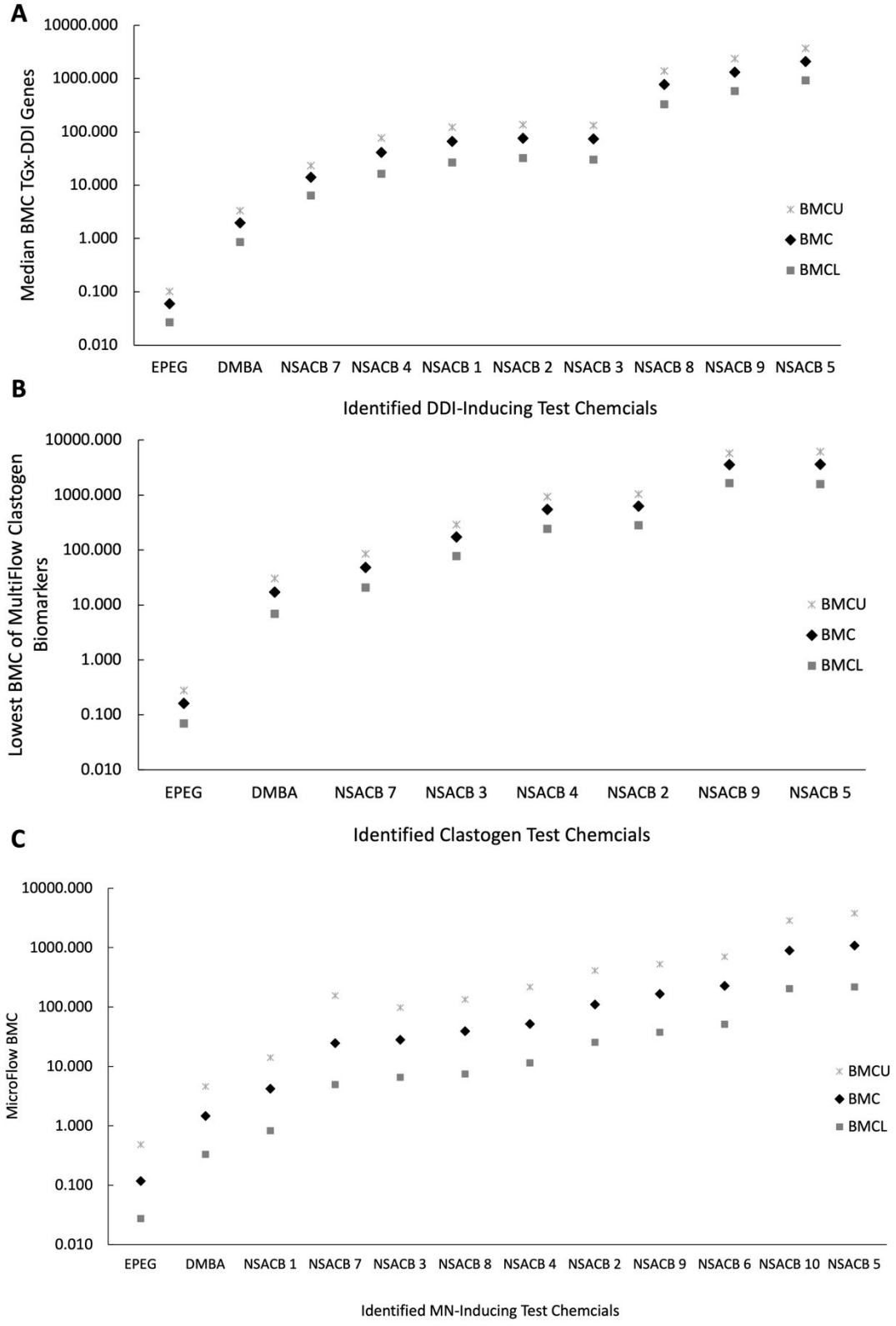

Supplementary Figure VI: Comparison of potency ranking for the positive NSACB compounds from each assay based on their respective Benchmark Concentrations (BMCs). (A) The potency ranking from the TGx-DDI transcriptomic biomarker based on median gene BMC, (B) the potency ranking from MultiFlow® assay based on the lowest clastogen biomarker BMC, and (C) the ranking from the *in vitro* MicroFlow® assay.

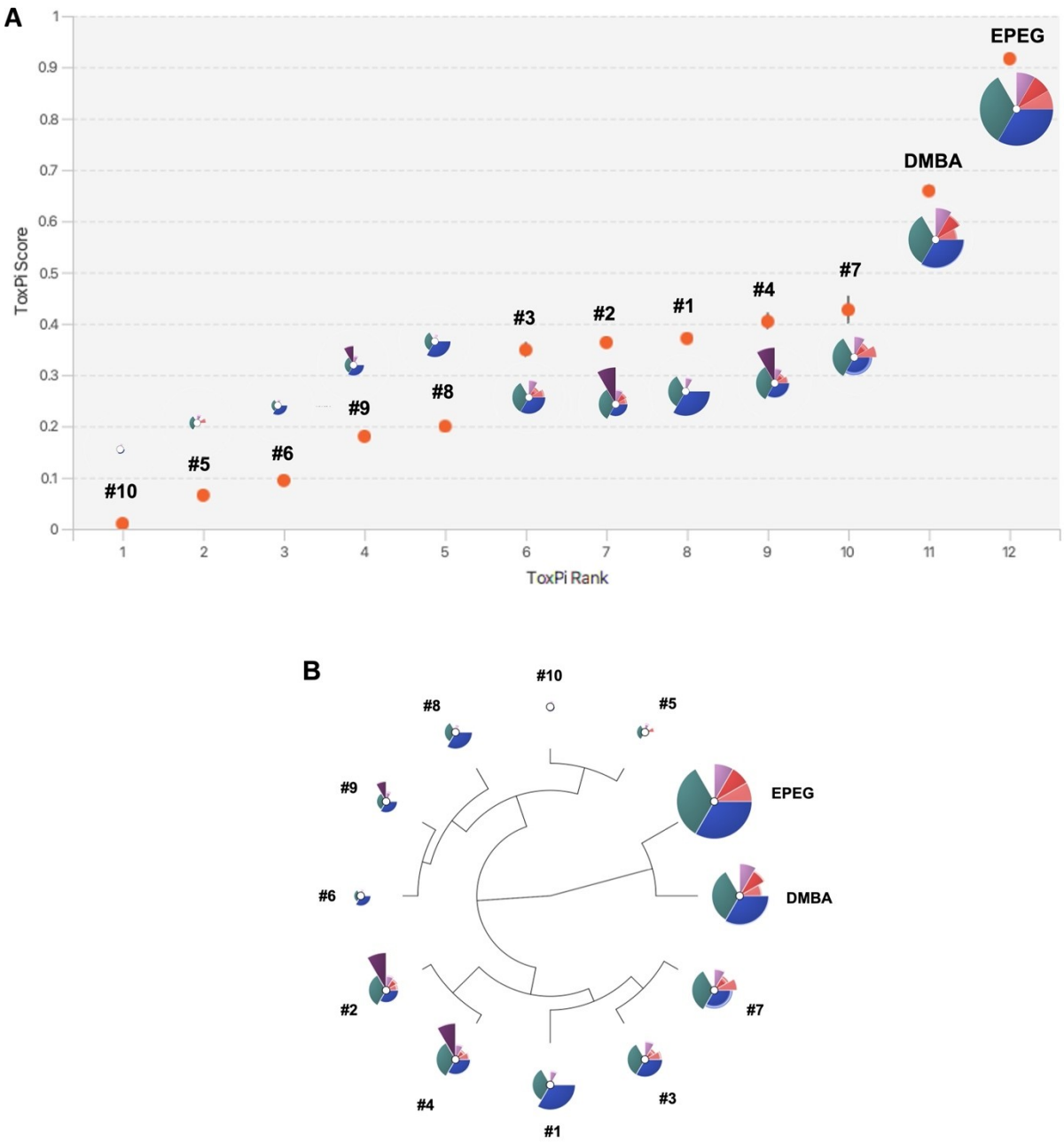

Supplementary Figure VII: ToxPi visualization of multiplexed BMCs for the integrated test strategy. (A) ToxPi score rankings and profiles for the data-poor compounds. For the ToxPi profiles, the distance of each slice from the origin indicates the slice score and endpoint potency (i.e., -log10 BMC). Slices represent the following endpoints: teal is TGx-DDI BMC, blue is MicroFlow® BMC, pink and purple are the MultiFlow® BMCs (i.e., dark pink is 24H p53, light pink is 4H p53, dark purple is 24H γH2AX, light purple is 4H γH2AX). Lower and upper bound confidence intervals are indicated by lighter shaded areas at the periphery of each slice. The width of each slice indicates the assigned endpoint weight. The TGx-DDI, MicroFlow®, and combined MultiFlow® endpoints each represent 1/3 of the profile. (B) Hierarchical clustering of the ToxPi profiles. The ToxPi algorithm groups substances with similar toxicological profiles.